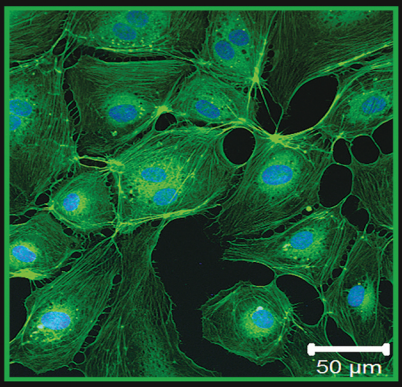
WOODHEAD PUBLISHING SERIES IN BIOMATERIALS



Hemocompatibility of Biomaterials for Clinical Applications

Blood-Biomaterials Interactions

Edited by Christopher A. Siedlecki

WP
WOODHEAD PUBLISHING

Hemocompatibility of Biomaterials for Clinical Applications

This page intentionally left blank

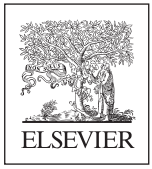
Woodhead publishing series in biomaterials

Hemocompatibility of Biomaterials for Clinical Applications

Blood-Biomaterials Interactions

Edited by

Christopher A. Siedlecki



WP
WOODHEAD
PUBLISHING
An imprint of Elsevier

Woodhead Publishing is an imprint of Elsevier
The Officers' Mess Business Centre, Royston Road, Duxford, CB22 4QH, United Kingdom
50 Hampshire Street, 5th Floor, Cambridge, MA 02139, United States
The Boulevard, Langford Lane, Kidlington, OX5 1GB, United Kingdom

© 2018 Elsevier Ltd. All rights reserved.

No part of this publication may be reproduced or transmitted in any form or by any means, electronic or mechanical, including photocopying, recording, or any information storage and retrieval system, without permission in writing from the publisher. Details on how to seek permission, further information about the Publisher's permissions policies and our arrangements with organizations such as the Copyright Clearance Center and the Copyright Licensing Agency, can be found at our website: www.elsevier.com/permissions.

This book and the individual contributions contained in it are protected under copyright by the Publisher (other than as may be noted herein).

Notices
Knowledge and best practice in this field are constantly changing. As new research and experience broaden our understanding, changes in research methods, professional practices, or medical treatment may become necessary.

Practitioners and researchers must always rely on their own experience and knowledge in evaluating and using any information, methods, compounds, or experiments described herein. In using such information or methods they should be mindful of their own safety and the safety of others, including parties for whom they have a professional responsibility.

To the fullest extent of the law, neither the Publisher nor the authors, contributors, or editors, assume any liability for any injury and/or damage to persons or property as a matter of products liability, negligence or otherwise, or from any use or operation of any methods, products, instructions, or ideas contained in the material herein.

Library of Congress Cataloging-in-Publication Data
A catalog record for this book is available from the Library of Congress

British Library Cataloguing-in-Publication Data
A catalogue record for this book is available from the British Library

ISBN: 978-0-08-100497-5 (print)
ISBN: 978-0-08-100499-9 (online)

For information on all Woodhead publications
visit our website at https://www.elsevier.com/books-and-journals



Publisher: Mathew Deans
Acquisition Editor: Laura Overend
Editorial Project Manager: Natasha Welford
Production Project Manager: Surya Narayanan Jayachandran
Cover Designer: Victoria Pearson

Typeset by SPi Global, India

Contents

Contributors **xi**

Part One Fundamentals and testing methods for the hemocompatiblity of biomaterials **1**

1 Contact activation by the intrinsic pathway of blood plasma coagulation **3**
Y. Yan, L.-C. Xu, E.A. Vogler, C.A. Siedlecki
1.1 Introduction **3**
1.2 Structural analysis of FXII **5**
1.3 Contact activation of blood plasma **7**
1.4 Contact activation of FXII in neat-buffer **9**
1.5 Influences of plasma proteins on FXII autoactivation **15**
1.6 Role of platelets in FXII contact activation **17**
1.7 Summary and future perspectives **23**
References **24**

2 Mechanisms of blood coagulation in response to biomaterials: Extrinsic factors **29**
M.T. Kalathottukaren, J.N. Kizhakkedathu
2.1 Introduction **29**
2.2 The blood coagulation cascade and physiological inhibitors **30**
2.3 Mechanisms by which clinically used biomaterials induce blood clotting (thrombosis) **36**
2.4 Summary and concluding remarks **41**
Acknowledgments **42**
References **43**

3 Developing standards and test protocols for testing the hemocompatibility of biomaterials **51**
S. Braune, A. Lendlein, F. Jung
3.1 Introduction **51**
3.2 Requirements for a reproducible and standardized in vitro testing **52**
3.3 Test protocols **59**
3.4 Summary **65**
References **65**

4 Test methods for hemocompatibility of biomaterials **77**
C. Sperling, M.F. Maitz, C. Werner
4.1 Introduction **77**
4.2 Incubation of whole blood versus blood fractions **78**
4.3 Incubation settings **82**
4.4 Analytical parameters **89**
4.5 Future trends and open problems **96**
References **97**

Part Two Improving the hemocompatibility of biomaterial surfaces **105**

5 Analyzing biomaterial surfaces and blood-surface interactions **107**
M. Nezafati
5.1 Flow dynamics **108**
5.2 Chandler's loop **110**
5.3 Current design **110**
5.4 Method and materials **112**
5.5 Static hemocompatibility experiment **113**
5.6 Dynamic hemocompatibllity experiments **114**
5.7 Summary **116**
References **116**

6 Surface analysis technique for assessing hemocompatibility of biomaterials **119**
V. Kumar, P. Gopinath, V.-K. Lakshmanan, K. Navaneetha Pandiyaraj
6.1 Introduction **119**
6.2 Biomaterials **120**
6.3 Nano-biomaterials **123**
6.4 Surface characterization of biomaterials **142**
6.5 Conclusion **156**
Acknowledgment **156**
References **156**
Further reading **161**

7 Coatings for biomaterials to improve hemocompatibility **163**
M. Fischer, M.F. Maitz, C. Werner
7.1 Introduction **163**
7.2 Main **165**
7.3 Future trends **178**
7.4 Conclusion **178**
Acknowledgment **179**
References **179**

8 Techniques for modifying biomaterials to improve hemocompatibility 191
N. Kasoju, L.T.B. Nguyen, A.R. Padalhin, J.F. Dye, Z. Cui, H. Ye
8.1 Introduction **191**
8.2 Blood and its interactions with interfaces **193**
8.3 Biomaterials modification techniques **197**
8.4 Summary and future prospects **211**
Acknowledgments **213**
References **213**

Part Three Improving the hemocompatibility of types of biomaterial 221

9 Improving the hemocompatibility of biomedical polymers 223
K. Amoako, R. Gbyli
9.1 Prelude **223**
9.2 Usage of blood-contacting devices **223**
9.3 Biomaterial surface and blood interaction **225**
9.4 Biomaterial surface properties and their influence on coagulation **230**
9.5 Surface anticoagulation approaches **231**
9.6 Current state of systemic anticoagulation usage **236**
9.7 Keys to achieving totally local surface anticoagulation **239**
9.8 Standardization of in vitro and in vivo test protocols **243**
9.9 Highlights of promising anticoagulation works **247**
9.10 Conclusion **247**
Acknowledgments **248**
References **248**

10 Strategies to improve the hemocompatibility of biodegradable biomaterials 253
P. Mulinti, J.E. Brooks, B. Lervick, J.E. Pullan, A.E. Brooks
10.1 Introduction **253**
10.2 Biomaterial hemocompatibility **254**
10.3 Biodegradable polymeric materials **254**
10.4 Hybrid biodegradable biomaterials **264**
10.5 Hemocompatible surface coatings and modifications **268**
10.6 Conclusion **270**
Acknowledgment **271**
References **271**

11 Surface treatment of metallic biomaterials in contact with blood to enhance hemocompatibility 279
J.P. Allain, M. Echeverry-Rendón
11.1 Multiscale interaction of blood and metals **279**
11.2 Evaluation of hemocompatibility of metallic systems **283**

11.3 Irradiation-driven synthesis and modification to improve the hemo-compatibility behavior of metallic systems **286**
11.4 Advanced hydrogels integrated with metallic nanoparticles and their hemocompatibility **301**
11.5 Advanced in situ characterization of bioactive hemocompatible metallic surfaces **304**
References **319**

12 Bioinspired thin film materials designed for blood contact **327**
R. Major, M. Sanak, J.M. Lackner, F. Bruckert, J. Marczak, B. Major
12.1 Introduction **327**
12.2 Materials and methods **327**
12.3 Concluding remarks **350**
Acknowledgments **352**
References **353**

13 Improving the hemocompatibility of biomedical composites **357**
G. Voskerician
13.1 Introduction **357**
13.2 Design criteria of blood contacting devices **358**
13.3 Heart valves **360**
13.4 Vascular grafts **363**
13.5 Stents **367**
13.6 Conclusion **369**
References **369**

Part Four Biomedical applications of hemocompatible biomaterials **377**

14 Improving the hemocompatibility of stents **379**
H.Q. Liu
14.1 Introduction **379**
14.2 Stent materials **379**
14.3 The consequence induced by hemocompatibility **381**
14.4 The assess method of hemocompatibility **382**
14.5 The improving approach of hemocompatibility **383**
14.6 Summary **391**
Acknowledgments **391**
References **391**

15 Improving the hemocompatibility of heart valves **395**
T. Gourlay, M. Rozeik
15.1 Introduction **396**
15.2 Valve pioneering era **397**

15.3 Advancements in valve development **405**
15.4 Future **416**
References **417**

16 Improving the hemocompatibility of catheters via NO release/generation **431**
Y. Wo, E.J. Brisbois, R.H. Bartlett, M.E. Meyerhoff
16.1 The need for hemocompatible polymeric surfaces **431**
16.2 Catheter lock solutions **433**
16.3 Thromboresistant catheters **434**
16.4 Antibacterial catheters **436**
16.5 Antithrombotic and antibacterial nitric oxide releasing/generating catheters **438**
16.6 Conclusion **447**
References **447**

Index **457**

This page intentionally left blank

Contributors

J.P. Allain University of Illinois at Urbana-Champaign, Champaign, IL, United States

K. Amoako University of New Haven, West Haven, CT, United States

R.H. Bartlett University of Michigan, Ann Arbor, MI, United States

S. Braune Institute of Biomaterial Science and Berlin-Brandenburg Center for Regenerative Therapies, Teltow, Germany

E.J. Brisbois University of Michigan, Ann Arbor, MI, United States

J.E. Brooks Southern Utah University, Cedar City, UT, United States

A.E. Brooks North Dakota State University, Fargo, ND, United States

F. Bruckert Grenoble Institute of Technology, Grenoble, France

Z. Cui University of Oxford, Oxford, United Kingdom

J.F. Dye University of Oxford, Oxford, United Kingdom

M. Echeverry-Rendón University of Groningen, Groningen, Netherlands

M. Fischer Leibniz Institute of Polymer Research Dresden, Dresden, Germany

R. Gbyli University of New Haven, West Haven, CT, United States

P. Gopinath Indian Institute of Technology Roorkee, Roorkee, India

T. Gourlay University of Strathclyde, Glasgow, United Kingdom

F. Jung Institute of Biomaterial Science and Berlin-Brandenburg Center for Regenerative Therapies, Teltow, Germany

M.T. Kalathottukaren University of British Columbia, Vancouver, BC, Canada

N. Kasoju Sree Chitra Tirunal Institute for Medical Sciences and Technology (SCTIMST), Thiruvananthapuram, India

J.N. Kizhakkedathu University of British Columbia, Vancouver, BC, Canada

V. Kumar Indian Institute of Technology Roorkee, Roorkee, India

J.M. Lackner Institute of Surface Technologies and Photonics, Functional Surfaces, Niklasdorf, Austria

V.-K. Lakshmanan Chonnam National University Medical School, Gwangju, South Korea

A. Lendlein Institute of Biomaterial Science and Berlin-Brandenburg Center for Regenerative Therapies, Teltow, Germany

B. Lervick North Dakota State University, Fargo, ND, United States

H.Q. Liu Chengdu University of Technology, Chengdu, China

M.F. Maitz Max Bergmann Center of Biomaterials Dresden; Leibniz Institute of Polymer Research Dresden, Dresden, Germany

R. Major Institute of Metallurgy and Materials Science, Polish Academy of Sciences, Krakow, Poland

B. Major Institute of Metallurgy and Materials Science, Polish Academy of Sciences, Krakow, Poland

J. Marczak Military University of Technology, Warsaw, Poland

M.E. Meyerhoff University of Michigan, Ann Arbor, MI, United States

P. Mulinti North Dakota State University, Fargo, ND, United States

K. Navaneetha Pandiyaraj Sri Shakthi Institute of Engineering and Technology, Coimbatore, India

M. Nezafati Emory University, Atlanta, GA, United States

L.T.B. Nguyen University of Oxford, Oxford, United Kingdom

A.R. Padalhin Soonchunhyang University, Asan, South Korea

J.E. Pullan North Dakota State University, Fargo, ND, United States

M. Rozeik University of Strathclyde, Glasgow, United Kingdom

M. Sanak Jagiellonian University Medical College, Cracow, Poland

C.A. Siedlecki The Pennsylvania State University, Hershey, PA, United States

C. Sperling Max Bergmann Center of Biomaterials Dresden, Dresden, Germany

E.A. Vogler The Pennsylvania State University, Hershey, PA, United States

G. Voskerician Case Western Reserve University, Cleveland, OH, United States

C. Werner Max Bergmann Center of Biomaterials Dresden; Leibniz Institute of Polymer Research Dresden, Dresden, Germany

Y. Wo University of Michigan, Ann Arbor, MI, United States

L.-C. Xu The Pennsylvania State University, Hershey, PA, United States

Y. Yan The Pennsylvania State University, Hershey, PA, United States

H. Ye University of Oxford, Oxford, United Kingdom

This page intentionally left blank

Part One

Fundamentals and testing methods for the hemocompatiblity of biomaterials

This page intentionally left blank

Contact activation by the intrinsic pathway of blood plasma coagulation

1

Y. Yan, L.-C. Xu, E.A. Vogler[1]*, C.A. Siedlecki*
The Pennsylvania State University, Hershey, PA, United States

1.1 Introduction

Biomaterial surfaces initiate blood coagulation. This poses a significant challenge to the development of blood-contacting devices used in human beings and especially for the implementation of cardiovascular devices. The performance of medical products such as catheters, blood vessel grafts, vascular stents, extracorporeal oxygenator membranes, and left ventricular assistant device are significantly impaired by thrombosis problems [1]. A thrombus is composed of cross-linked fibrin clots and aggregated platelets connected by fibrinogen. When thrombi come off the site as emboli and travel through the blood stream, they may block small vessels downstream leading to stroke or tissue death. With the increasing demand for cardiovascular healthcare worldwide, it is imperative to understand the mechanisms leading to thrombus formation on biomaterial surfaces in order to develop strategies for improved hemocompatibility.

Blood coagulation can be potentiated by plasma-phase coagulation and/or platelet-mediated reactions [2]. When a biomaterial is implanted and/or blood vessel is injured, a variety of biological responses are initiated triggering processes of platelet activation/aggregation and plasma coagulation. The mechanism of platelet aggregation involves the adhesion, activation, and aggregation of platelets at the site of injured wall or on implanted biomaterial surfaces [3]. Plasma coagulation is a series of zymogen-to-enzyme conversions that occur as a cascade, in which the enzyme produced in one reaction catalyzes the next reaction. It penultimately produces thrombin (FIIa), a powerful serine protease, which hydrolyzes fibrinogen into fibrin monomers [2]. Fibrin monomers then oligomerize and cross-link into a mesh on and between aggregated platelets to form a mechanically stabilized aggregate. Platelet activation/aggregation and blood plasma coagulation are seemingly independent events, but in reality, there are strong interactions between the processes. The surface membrane of activated platelets promotes certain coagulation reactions, and FIIa itself is a potent platelet activator [3].

The plasma coagulation cascade is usually divided into two branches, termed the extrinsic and intrinsic pathways, that are dependent on the initial trigger. The extrinsic pathway is primarily responsible for hemostasis following vascular injury. Tissue factor (TF) embedded in the vessel walls is exposed after blood vessel injury and

1 Deceased April 3, 2017

Hemocompatibility of Biomaterials for Clinical Applications. https://doi.org/10.1016/B978-0-08-100497-5.00001-X
© 2018 Elsevier Ltd. All rights reserved.

binds activated plasma coagulation factor VII (FVIIa). This surface-bound complex potentiates the blood coagulation by activating FIX and FX to FIXa and FXa, respectively [3]. Understanding of the intrinsic pathway dates back to the pioneering work of Oscar Ratnoff who discovered the indispensable role of Hageman factor (HF, otherwise known as factor XII, FXII) in promoting glass-induced blood coagulation in the 1950s [4]. The intrinsic pathway is initiated by biomaterial surface contact-induced activation of FXII to FXIIa (a.k.a. contact activation). This leads to the formation of a pathological thrombus in response to blood contact with foreign surfaces. Contact activation has been implicated as one of the causes for poor hemocompatibility of cardiovascular biomaterials. Both the intrinsic and extrinsic pathways eventually merge into the common pathway, leading to the formation of thrombin (FIIa), followed by fibrin monomer formation and oligomerization (Fig. 1.1). Note that plasma coagulation also involves feedforward or feedback loops in which an enzyme produced in one step acts as an inhibitor or activator in other reactions, which are not shown in Fig. 1.1 for simplicity.

It has been widely accepted that FXII activation is specific only to negatively charged surfaces or compounds such as kaolin, glass, and ellagic acid. Recent studies revealed that FXII is activated in neat buffer solution at equal efficiency by contact with either hydrophobic or hydrophilic surfaces [5]. In addition, several "natural" surfaces have been identified to activate FXII in vivo, such as platelet polyphosphate, microparticles (MPs) derived from platelets and erythrocytes, RNA, amyloid β aggregates, misfolded proteins, collagen, and mast cell heparin [6–13]. Evidence shows that the presence of few platelets was enough to propagate coagulation substantially

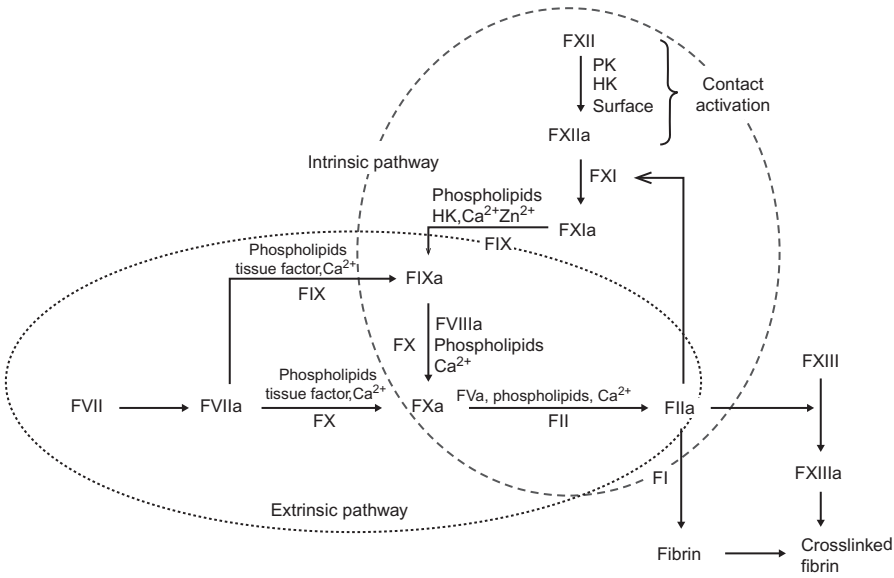


Fig. 1.1 Simplified diagrams of plasma coagulation cascade with emphasis on the intersections of intrinsic and extrinsic pathways. Mediators, cofactors, inhibitors, and amplification loops are not shown for simplicity [2].

if contact activation was simultaneously initiated, indicating that plasma contact activation and platelet adhesion had a strong synergetic effect on thrombosis in blood-contacting materials [14].

It is proposed that extent of FXII activation is related to the plasma coagulation. Previous studies suggested that activated FXII can be produced via at least three different biochemical pathways: autoactivation produces FXIIa by contact of FXII with an activating surface (FXII → FXIIa), reciprocal activation of FXII and prekallikrein (PK) (FXII is enzymatically cleaved by kallikrein presumably generated by FXIIa-mediated hydrolysis of PK), and autohydrolysis of FXII by (FXII + FXIIa → 2FXIIa) [15]. In this chapter, we will review the current understanding of FXII contact activation and recent insights into the process and introduce some new perspectives on FXII activation.

The efficiency of FXII activation is conventionally measured by functional assays in terms of enzymatic activities of FXII-derived products, generally referred to as procoagulant activity and amidolytic activity. Procoagulant activity is measured by simple plasma clotting assays (related to whole blood clotting tests) for the potential of FXII-derived products to induce clot formation (procoagulant activity). Procoagulant activity can be determined by comparing with a standard curve relating exogenously added αFXIIa, synthetic material surfaces, or other known activators to the clotting time. Amidolytic activity is assessed using various chromogenic assays as the ability to cleave a commercial chromogenic peptide in response to the presence of enzyme. Quantification of amidolytic activity is carried out by monitoring the color development due to proteolytic cleavage of the chromogen by FXIIa or other FXII-derived products. Both assays measure the net activity of the total FXII-derived proteins following activation without differentiating various proteins [16].

1.2 Structural analysis of FXII

FXII is an 80 KD single-chain polypeptide glycoprotein circulating in the blood as an inactive zymogen form [17]. The concentration of HF in normal human plasma is ~29 μg/mL with variations between individuals ranging from 15 to 47 μg/mL [18]. FXII shares the same gene ancestor with hepatocyte growth factor. Both of them are mosaic proteins sharing a similar domain organization from N to C terminal consisting of a fibronectin type II domain (FnII), an epidermal growth factor (EGF)-like 1 domain, a fibronectin type I domain (FnI), an EGF2 domain, a kringle domain with three disulfide cross-linkages, and a serine protease domain with an additional proline-rich domain unique to FXII (Fig. 1.2A) [20,21].

Various domains on the FXII protein chain are involved in contact activation. Experimental evidence demonstrates that the FnI, FnII, and/or the kringle domains have been implicated in binding of FXII to negatively charged surfaces [22]. Recombinant proteins lacking some N-terminal domains displayed inhibited capacity in binding to negatively charged solid surfaces and correspondingly decreased procoagulant efficiency compared with those of full-length FXII. Monoclonal antibody KOK5, designed against the heavy chain region of FXII, was found to inhibit kaolin-induced

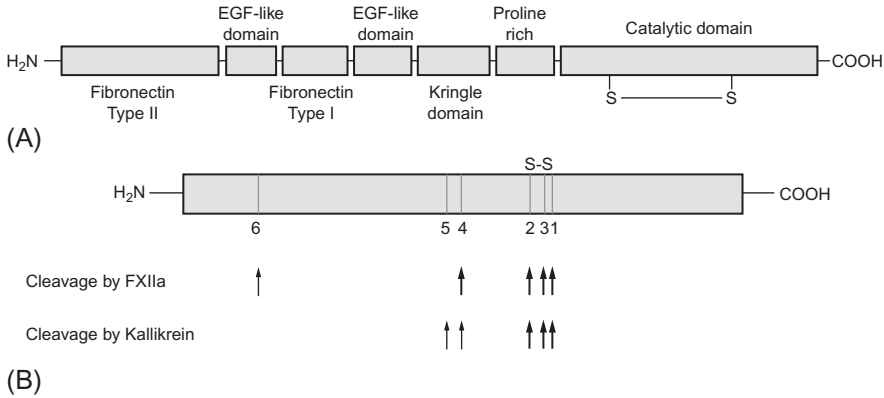


Fig. 1.2 (A) Schematic diagram of the structure FXII and (B) proposed proteolytic cleavage sites by plasma proteins adapted from [16,19]. The *heavy arrows* indicate the most frequent cleavages and the lighter ones less frequently.

clotting by preventing binding of FXII to kaolin but enhanced kallikrein-mediated FXII activation and supported FXII autoactivation [23]. This result suggested that mAb KOK5 recognized a discontinuous epitope on the FnII domain, which contributes to FXII binding sites for negatively charged surfaces. Recent structural analyses revealed continuous patches of positive potential on the surface of FXII-FnI-EGF2 involving FnI residues Lys127, Arg141, Lys145, His150, and Arg153, which might explain interaction of FXII-FnI with cross-β structure found in amyloid and misfolded proteins [24,25]. Negatively charged amino acid clusters surrounding the S1 pocket have been observed from crystal structures of FXII protease domain, which could potentially contribute to its interaction with substrates and inhibitors of overall net positive charges like FXI [21].

Evidence shows that FXII activation by enzymatic cleavage produces an inventory of FXII-derived fragments [19,26–28]. Fig. 1.2B demonstrates the proposed cleavage sites by kallikrein and FXIIa, which account for PK-involved activation and autohydrolysis. In each case, an initial cleavage of FXII at Arg353-Val354 peptide bond (site 1) was observed to yield a two-chain serine protease αFXIIa consisting of a heavy chain (52 kDa) disulfide linked to a light chain (28 kDa). However, the rate of FXII activation by kallikrein is much faster than the rate of autohydrolysis. Sequential cleavages of αFXIIa form active fragments with diminishing molecular weights including a 40 kDa activated enzyme (site 4) and βFXIIa as a doublet with molecular weight of 30 kDa (site 2) and 28.5 kDa (site 3) [19,26,29]. Structural analyses showed that all these active fragments share a 28 kDa chain that appears to be derived from the light chain of αFXIIa [19,30]. A minor fragment of 70 kDa (site 6) was also seen as autohydrolysis proceeds, while a 36 kDa fragment (site 5) appeared in the presence of kallikrein. Previous studies have identified αFXIIa and βFXIIa in terms of their enzymatic activities. There is evidence that βFXIIa is unable to bind to surfaces and activate FXI due to loss of the 50 kDa heavy chain from αFXIIa, which may account for its very weak procoagulant activity compared with αFXIIa [30,31]. In addition, it was

reported that βFXIIa activates PK at only 2%–4% of the coagulant activity of αFXIIa [16]. Experiments have demonstrated that both αFXIIa and βFXIIa keep the protease catalytic domain from FXII, rendering to them the amidolytic activity to hydrolyze a chromogenic substrate [5,32].

1.3 Contact activation of blood plasma

Contact activation studies in vitro are often performed by incubation of blood or platelet-poor plasma (PPP) with activators. In biomaterial studies, these activators may be glass particles or solid substrates modified by surface-modifying agents, polymers, or other model materials. Contact activation of blood plasma exhibits a dependence on both surface area and surface energy/chemistry as illustrated in surface area titration curves (SAT, Fig. 1.3) [33]. A typical SAT shows that coagulation time (CT) asymptotically decreases with the increasing surface area until a surface water wettability-dependent minimum is reached and that minimum CT appears to increase with increasing activator hydrophobicity. Note that incremental increases in surface area cause rapid decreases in CT initially, followed by a decreasing rate of change in CT with increasing surface area until addition of additional surface area no longer leads to a decrease in CT. Note that actual measurement of surface-induced FXII activation in plasma is difficult to carry out due to the complexity of the plasma proteome and the presence of numerous proteolytic enzymes in activated plasma [32,34–36].

The asymptotic trends observed in plasma SAT with increasing surface area are unanticipated in that the continuous presence of procoagulant stimulus (activator surface

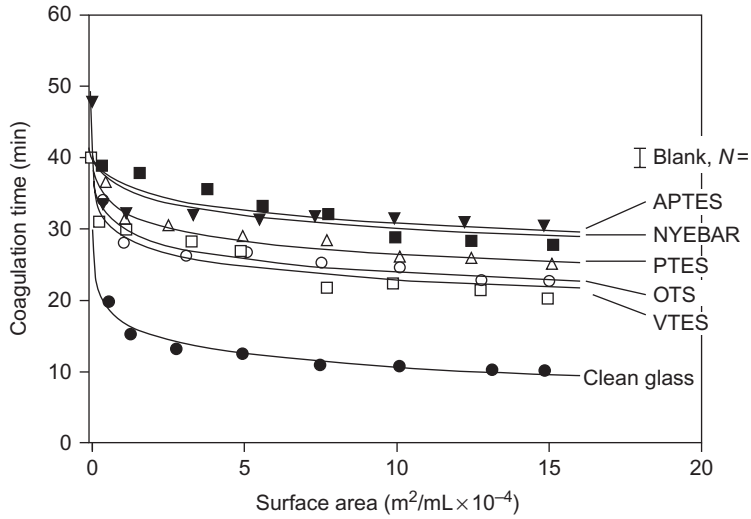


Fig. 1.3 Surface area titration of human plasma using activators with varying water wettability. Error bar annotated "blank" represents mean and standard deviations of seven measurements of plasma coagulation time in the absence of activator particles [33].

area) does not result in continuously lowering CT. Experimental evidence shows that the procoagulant surface remains active even after repeated applications, discounting the possibility of procoagulant poisoning or deactivation by plasma proteins [37]. It was observed that potentiation of plasma coagulation by surface contact leads to a bolus release of FIIa at a nearly constant concentration throughout coagulation [37–39]. Considering that coagulation is the result of fibrin oligomerization to a certain density to cause the phase transition from liquid to solid, it is reasonable to suspect that CT is controlled by FIIa-induced hydrolysis of fibrinogen to fibrin, which in turn depends on the procoagulant stimulus propagating down the intrinsic pathway [32,38,40]. Studies demonstrate that bolus production of FII is proportional to the intensity of contact activation as measured by both procoagulant surface area and surface energy, accounting for the proportional relationship between contact activation of plasma and surface properties [37]. How contact activation-induced procoagulant stimulus affects the plasma coagulation and is yet to be fully understood. In fact, CT induced by high surface area of hydrophilic surfaces (~10 min) is much higher than the lowest possible CT by FIIa (<1 min) (thrombin time), suggesting some unidentified factors delay the procoagulant stimulus processing along the intrinsic pathway [32]. FXII is self-terminated by FXIIa, thus sending a discontinuation signal down the coagulation cascade, acting as one contributing factor to discontinuously lower CT with increasing procoagulant stimulus [37,41].

We have developed relationships linking procoagulant surface properties (dose) and blood plasma coagulation time (response) that can be quantified using mathematical models derived from Michaelis-Menten enzyme kinetics [42]. The application of this model SAT allows extraction of K_{act}, a parameter of procoagulant catalytic potential for different activators (Table 1.1). It appears that the potential of activators in inducing plasma coagulation scales nearly exponentially with increasing surface hydrophilicity, showing values near zero for hydrophobic activators and increasingly higher for hydrophilic activators [32,37,40]. This is in good agreement with the conventional hematology observation that fully water wettable surfaces tend to be more efficient in blood coagulation activation. Note that the surface wettability is not the only property determining

Table 1.1 Procoagulant catalytic potential to induce plasma coagulation by activators with varying wettability

Procoagulant	Advancing contact angle (θ, degrees)	τ° (dyne/cm)	K_{act} (mL/m^2)	R^2 (%)
Nyebar	110.5 ± 2.76	−25.2 ± 3.06	0.009 ± 0.002	86.1
OTS	102.3 ± 2.56	−15.33 ± 3.14	0.13 ± 0.02	97.0
PTES	93.41 ± 1.51	−4.28 ± 1.89	0.05 ± 0.01	97.2
VTES	85.12 ± 1.70	6.12 ± 2.12	0.19 ± 0.04	93.4
APTES	54.6 ± 0.42	41.69 ± 2.63	0.01 ± 0.01	58.2
Clean glass	0	72	19.2 ± 1.9	99.4

Adapted from A. Golas, P. Parhi, Z. Dimachkie, C. Siedlecki, E. Vogler, Surface-energy dependent contact activation of blood factor XII, Biomaterials 31 (2010) 1068–1079.

the potential of plasma coagulation. Biomaterial surfaces bearing quaternary ammonium groups do not seem to induce plasma coagulation although these materials exhibit relatively higher hydrophilicity compared with clean glass [2,40,43,44].

The intensity of plasma coagulation depends on both the catalytic potential K_{act} and surface area [32]. Zhuo et al. showed that FIIa production is exponentially related with K_{act} but related to activator surface area [37]. Plasma SAT establishes a general understanding of the relationships among biomaterial surface chemistry, area, and the propensity to activate plasma coagulation cascade. However, details on the nature of contact activation are difficult to discern due to the complexity of the blood plasma proteome [35,36]. Thus, mechanisms of how FXII is activated in response to different types of activators and how activated FXII is amplified and propagates down the intrinsic pathway thus affecting the final coagulation remain unclear.

1.4 Contact activation of FXII in neat-buffer

Contact activation of FXII in neat buffer is the simplest example of surface-mediated FXII activation and allows for close examination of FXII/surface interactions without the interference of other plasma proteins. Experimental evidence suggests that autoactivation in neat buffer occurs upon contact with activators of varying surface chemistry, giving rise to a suite of FXII-derived fragments, represented by the symbol $FXII_{act}$, depending on activator surface properties [16,32,33,45]. At least three categories of activated fragments have been proposed. One category contains procoagulant fragments that exhibit potential to induce plasma coagulation, termed as procoagulant activity; a second category includes amidolytic fragments that display proteolytic activity toward chromogen Pefa-5963, termed as amidolytic activity; a third category contains fragments that suppress autoactivation. Procoagulant and amidolytic yields can be quantified by functional assays, plasma coagulation time assay, and amidolytic assay, respectively. Suppressive effects were demonstrated by specially designed autoactivation assays discussed further below. All above assays measure the net activity of any number of proteins produced by autoactivation without discrimination of FXII-derived fragments of different activities. It is still uncertain about whether there is any overlapping between each category of fragments.

1.4.1 Autoactivation of FXII is a sharp function of solid activator surface energy

Surface energy influences contact activation of FXII. The contact activation of FXII in neat buffer exhibits a parabolic profile in terms of both procoagulant and amidolytic yields as a function of activator surface energy [33]. Nearly equal autoactivation is observed at the hydrophilic and hydrophobic extremes of water wetting properties ($-36 < \tau^\circ < 72$ dyne/cm and $0 \leq \theta < 120^\circ$), with minimal activation at activators displaying surface water wettability falling between ($20 < \tau^\circ < 40$ dyne/cm and $55 \leq \theta < 75^\circ$) [33] (Fig. 1.4). In addition, no matter how long the contact time is, <3.5% of FXII available in solution is activated in all cases [32,33].

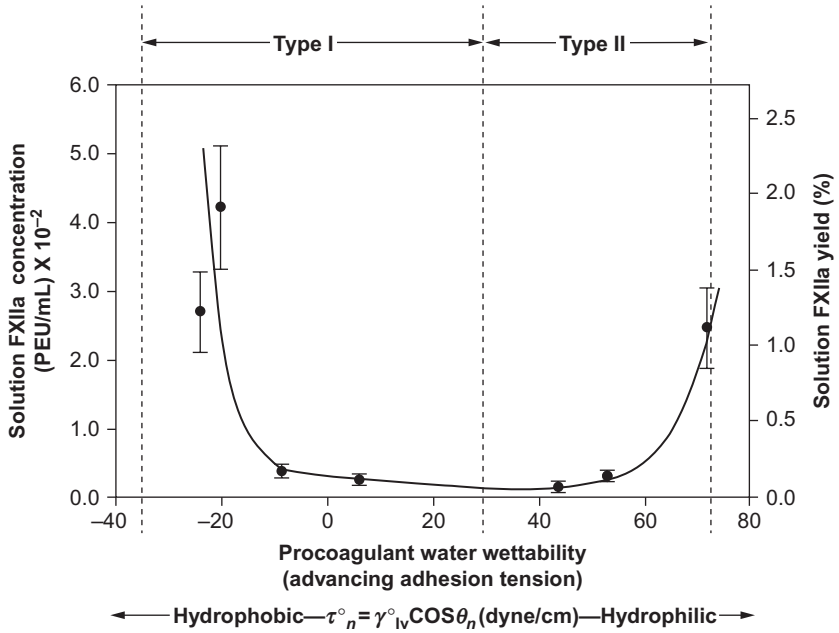


Fig. 1.4 Yields of FXII (30 µg/mL) autoactivation in neat buffer solution by contact with glass-based particles of different surface energy expressed as water adhesion tension [33].

These findings are quite contrary to expectations based on the traditional observations of contact activation in blood plasma, in which hydrophilic activator is more efficient in inducing plasma coagulation than hydrophobic one. The discrepancy between the dependence on procoagulant surface energy by FXII activation in neat buffer and whole plasma can be explained on the basis of adsorption-dilution effect [33]. The presence of numerous plasma proteins competes with FXII in adsorption to hydrophobic surfaces, which results in a significant decrease in FXII contacts, and thus reducing FXIIa production [5,33]. In other words, FXII contact activation is not specific to anionic surfaces; instead, competitive adsorption of plasma proteins leads to a seeming preference for hydrophilic surfaces that is actually due to a relative decrease in FXII → FXIIa reaction at hydrophobic surfaces [5]. One study demonstrated that FXIIa titration of plasma using exogenous FXIIa dissolved in protein cocktail and heat-denatured serum led to different relationship between CT and FXIIa concentration, suggesting again that plasma proteins affect the stoichiometry of contact activation in response to procoagulant stimulus [32]. In all, different activation properties in neat buffer and whole plasma may be attributed to not only surface-mediated competitive adsorption but also unidentified mechanisms related to protein compositions of fluid phase.

Influences of surface wettability on FXII autoactivation efficiency are not yet fully understood. It is proposed that properties of vicinal water profoundly affect contact activation in response to materials with different water wettability [46]. For more hydrophobic surfaces with a water tension $\tau^{0} < 30$ dyne/cm (pivot point for type I surfaces),

displacement of vicinal water by proteins is energetically favored, allowing more proteins to be concentrated in the interphase region which promotes the frequency of FXII autoactivation [33]. For more hydrophilic surfaces with water tension larger than 30 dyne/cm (type II surfaces), interfacial water is so tightly surface bound that displacement is energetically prohibitive [47], and FXII encounters the hydrophilic interphase region by random diffusion/thermal motion [33]. Within the region of the wetting continuum near $\tau^0 = 30$ dyne/cm (type 0 surfaces), it is proposed that vicinal water retains bulk water-like properties, thus rendering minimum activation of FXII [33].

1.4.2 Surface area dependence of FXII autoactivation

FXII contact activation in neat buffer exhibits different surface area dependence by different types of activators (Fig. 1.5). Increased surface area of hydrophilic glass resulted in more FXII activation, with FXIIa yield rising from 0.01 PEU/mL to 0.28 PEU/mL by increasing surface area from 0.25 to 25×10^{-4} m^2/mL (Fig. 1.5). However, autoactivation yields by OTS and APTES were not significantly affected by increased surface area. It is likely that increased surface area of hydrophilic glass offers more "activation sites" for FXII, thus producing more activated FXII. Increased surface area of relative hydrophobic activators (OTS and APTES) theoretically attracted more proteins to the interphase area but did not appear to activate more FXII. It is possible that suppressive fragments produced during FXII activation offset the effects of increased surface area [16]. Recent studies revealed that FXII activation by Type 0 silanized-glass activators

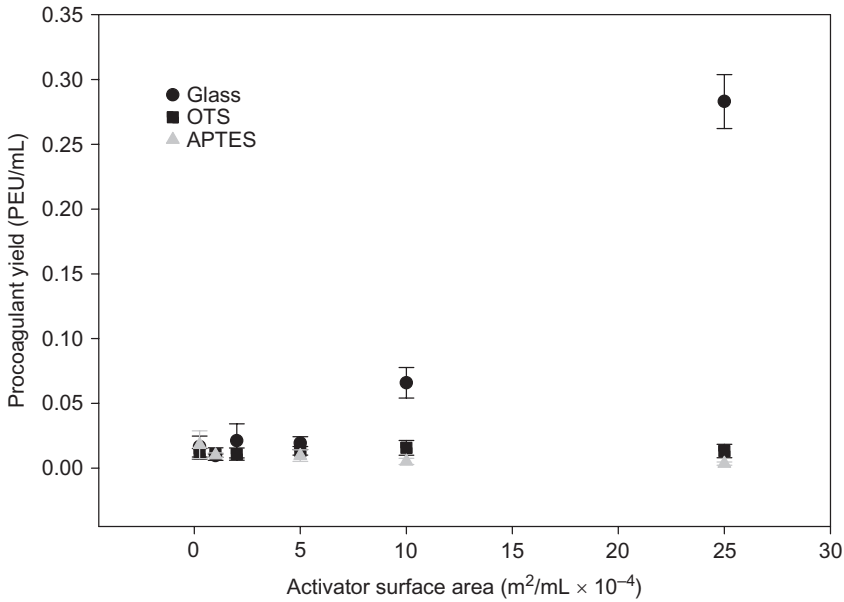


Fig. 1.5 Yields of FXII (30 µg/mL) autoactivation in neat buffer solution following contact with solid activators of varying surface wettability. Data and error bars represent mean and standard deviation of $n = 3$ measurements.

produced proteins that were capable of suppressing autoactivation by Type II hydrophilic glass particles [16]. It is thus proposed that FXII autoactivation is self-limited by some kind of suppressive proteins which are coproduced with procoagulant proteins initially but "turn off" activation of FXII afterward by unknown chemistry [32].

1.4.3 Influences of surface charge on FXII autoactivation

Ionic interactions are relevant in the binding of FXII to negatively charged surfaces and affect the efficiency of FXII activation in the presences of negatively charged surfaces [48]. Sepharose-based resins bearing strong Lewis acid/base functional groups (iminodiacetic acid (CH), sulfopropyl (SP), and quaternary ammonium (Q)) appear to more efficiently activate FXII in neat buffer than in hydrophilic clean glass (Fig. 1.6) [44]. Resins with higher ion-exchange capacities demonstrate higher potential for FXII activation regardless of whether they are cationic or anionic [44], with the exceptions of carboxymethyl (CM) and dimethyl aminoethyl (DEAE), which seems to be less efficient in activation of FXII in terms of FXIIa yield in solution. In fact, a significant amount of FXIIa is found to be bound to CM and DEAE surface and is detected only after addition of lysozyme to displace FXIIa off the surfaces. It is known that ion-exchange surfaces typically exhibit higher adsorbent capacity for blood protein even to hydrophobic surfaces [49]. It is likely that strong FXII/surface interactions as the result of electric field surrounding ion-exchange resins allow them to be potent FXII activators [50]. On the other hand, wholesale adsorption of plasma proteins could

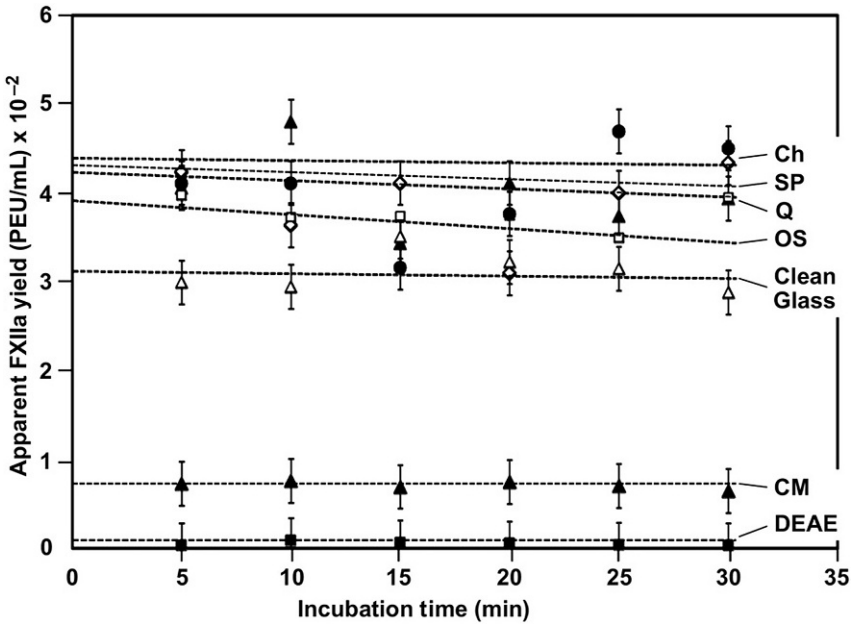


Fig. 1.6 Autoactivation of FXII in neat buffer by Sepharose-based ion-exchange resin particle. *Dashed lines* through the data are guides to the eyes [44].

compete with FXII/surface contacts, which explained why these resin activators are not as efficient in activating plasma coagulation as activators like hydrophilic clean glass even hydrophobic OTS [44].

1.4.4 Relative yields of FXII-derived products in terms of surface energy and surface area

Both procoagulant and amidolytic assays measure the efficiency of contact activation in terms of activated FXII. As mentioned before, procoagulant activity represents the capacity of activated FXII propagating down the intrinsic pathway and ultimately inducing plasma coagulation. However, the amidolytic assay is used to measure the cleavage ability of FXIIa toward a specific peptide substrate. Recent studies suggested that procoagulant and amidolytic yield may represent different groups of activated FXII that have some overlap with each other [45]. Autohydrolysis of FXII by activated FXII seems to produce greater amounts of amidolytic proteins as opposed to procoagulant ones [16,32]. Quantification of relative yields of procoagulant and amidolytic fragments in response to different surface activators helps explain the different catalytic potentials of solid activators. Table 1.2 summarizes the ratios of procoagulant and amidolytic yields following contact activation by different types of activators of varying surface areas. The ratio of procoagulant to amidolytic yield is surface energy dependent with highest P/A (procoagulant/amidolytic) seen for hydrophilic clean glass, followed by OTS and APTES. Notably, the P/A ratio for glass increased from 0.1 to 2.0 with increasing surface area from 1.0×10^{-3} to 5.0×10^{-3} m^2/mL, suggesting that increasing the amount of hydrophilic surface area tends to produce fragments exhibiting greater procoagulant activity than amidolytic. A decrease of P/A was observed when adding more OTS or APTES, although the absolute yields of both procoagulant and amidolytic activities did not change significantly as increasing surface area up to 5.0×10^{-3} m^2/mL. In all, relative proportions of procoagulant and amidolytic

Table 1.2 Summary of FXII autoactivation products induced by activators of varying surface energy and surface areas

Activator	Surface area (m^2/mL$\times10^{-4}$)	Procoagulant activity (PEU/mL)	Amidolytic activity (PEU/mL)	Ratio (procoagulant/amidolytic)	Error of propagation
Glass	10	9.06E−03	8.46E−02	0.11	9.96E−03
	25	1.81E−01	2.23E−01	0.81	3.73E−02
	50	5.86E−01	2.98E−01	1.96	1.32E−01
OTS	10	7.80E−05	7.90E−04	0.10	4.69E−02
	25	8.94E−05	7.90E−04	0.11	8.82E−02
	50	2.47E−05	9.88E−04	0.025	1.17E−02
APTES	10	7.16E−06	7.90E−04	0.0091	5.06E−03
	25	4.03E−06	1.78E−03	0.0023	2.06E−03
	50	3.51E−06	1.98E−03	0.0018	8.80E−04

enzymes produced by FXII autoactivation vary in response to activator surface energy. Hydrophilic surfaces tend to induce more and higher proportion of procoagulant fragments than hydrophobic ones, which may account for their corresponding catalytic potential in plasma coagulation.

1.4.5 Current understanding on molecular events occurring during FXII contact activation

Explaining FXII autoactivation behaviors by different surface types requires an increased understanding of how FXII responds to solid activator surfaces at the molecular level. Advanced techniques allow us to take a close look at the interactions of FXII and activation surfaces. As early as the 1960s, physical alterations of FXII following activation had been demonstrated [51]. Later, it was reported that Hageman FXII remained in its native size (80–90 KD) after contact activation by kaolin (negatively charged surfaces) implying the conformational change upon binding of FXII to negatively charged surfaces [52,53]. At the same time, proteolytic cleavage of FXII into smaller fragments was observed in the presence of plasma (fluid phase activator) likely due to the interaction of FXII with its natural substrates (proteolytic enzymes) kallikrein, plasmin, and trypsin [18,52]. Conformational changes of FXII following contact activation were initially visualized by circular dichroism (CD) spectroscopy [54]. It was shown that the conformation of inactivated HF was aperiodic, implying its susceptibility to environmental perturbators. Activation of FXII by both ellagic acid and quartz resulted in changes in the CD spectrum corresponding to larger aromatic ellipticities compared with inactivated FXII [54]. Low temperature (<37°C) induced similar conformational changes in FXII, consistent with previous findings on spontaneous onset of the kinin-generating system at low temperatures [55]. However, further understanding of FXII-derived activation products is still hampered by their low physiological concentration, rendering them difficult to separate and isolate for further analysis. Recently, high-resolution electrophoresis was employed to separate FXII-derived proteins by molecular weight. This emerging technique separates small amounts of proteins (as low as 15 μg/mL) through gel-stain-filled microchannels built in a microfluidic chip. Under denaturing conditions, the sample proteins migrate through the separation channels at a rate based on their molecular weight. Golas et al. [45] first used Experion Pro260 chips to examine FXII-derived products in neat buffer by different activators. It found that FXII autoactivation products displayed the same molecular weight as that of intact FXII regardless of incubation time, incubation temperature, FXII solution concentration, activator surface types, and area. The addition of PK and HMWK during FXII contact activation in buffer induced proteolytic cleavage of FXII as shown by multiple protein fragments with molecular weights smaller than that of original FXII. These findings suggest that FXII contact activation in buffer solution does not produce proteolytic fragments, and it is likely that FXII undergoes nonenzymatic conformational changes in response to surface contact. These different types of FXII "conformers" induced by surfaces of varying wettability are hypothesized based on different procoagulant and amidolytic activities.

1.5 Influences of plasma proteins on FXII autoactivation

Contact activation of FXII is moderated by the protein composition of the fluid phase in which FXII is dissolved [56]. Plasma is a complex mixture consisting of a large variety of proteins present at levels spanning 12 orders of magnitude [57]. Comprehensive understanding of FXII/surface interactions cannot be achieved without considering the effects of the plasma proteome. In this section, we review the influences of plasma proteins unrelated and related with the coagulation cascade to FXII contact activation.

1.5.1 Effects on FXII autoactivation by plasma proteins not directly related to intrinsic pathway

Plasma proteins unrelated to active participation in the plasma coagulation moderate both FXII autoactivation and plasma coagulation itself [5,33,56]. Arbitrary protein mixtures prepared in buffer increase procoagulant yield produced by hydrophilic glass-induced FXII autoactivation and reduce yield by hydrophobic activators compared with single protein solutions. In addition, the reduced catalytic potential of hydrophobic activators in plasma compared with neat buffer confirms the moderating effects of plasma proteins. It is proposed that an adsorption-dilution effect accounts for different behaviors of FXII contact activation depending on protein composition in solution. The hypothesis states that competitive adsorption of plasma proteins to hydrophobic surfaces impedes FXII/surface contacts, effectively rendering a lower efficiency of FXII contact activation in plasma than in neat buffer [5]. As is well known, when a material is brought into contact with protein solutions (or plasma), protein adsorption is the first step in the biological response to materials [58]. Rapid adsorption of blood proteins on biomaterial surfaces profoundly influences the sequential interfacial events such as blood coagulation and even the long-term performance of the medical devices [59]. The Vroman effect is well known for its description of competitive adsorption of plasma proteins on biomaterial surfaces, stating that the proteins that generally arrive first are later replaced by less motile proteins that have a higher affinity to the surface [60]. Note that competitive adsorption also affects the adsorption/desorption of activated FXII and thus moderates its ability to propagate down the intrinsic pathway [44]. This could potentially be yet another reason accounting for the differences in FXII contact activation in neat buffer and in plasma.

Both activator surfaces and protein properties exert moderating effects on the efficiency of FXII contact activation. Fig. 1.7 demonstrates the influences on procoagulant and amidolytic yield by three proteins spanning three decades of molecular weight. They are albumin (the most abundant plasma protein, 66 kDa and 1 mg/mL), immunoglobulin G (IgG, 150 kDa and 10 mg/mL), ubiquitin (8.5 kDa and 0.1 mg/mL), and a mixture of the three (11.1 mg/mL). Procoagulant yields of FXII contact activation by hydrophilic glass were significantly increased in the order of BSA > cocktail > IgG > ubiquitin by 3–20 times. Amidolytic yield was enhanced in a similar way as that of procoagulant yield but at a milder level by 1.3–2.9 times. Plasma proteins enhanced the procoagulant yield of OTS by 2–11 times in the order of BSA > cocktail > ubiquitin > IgG, a similar trend

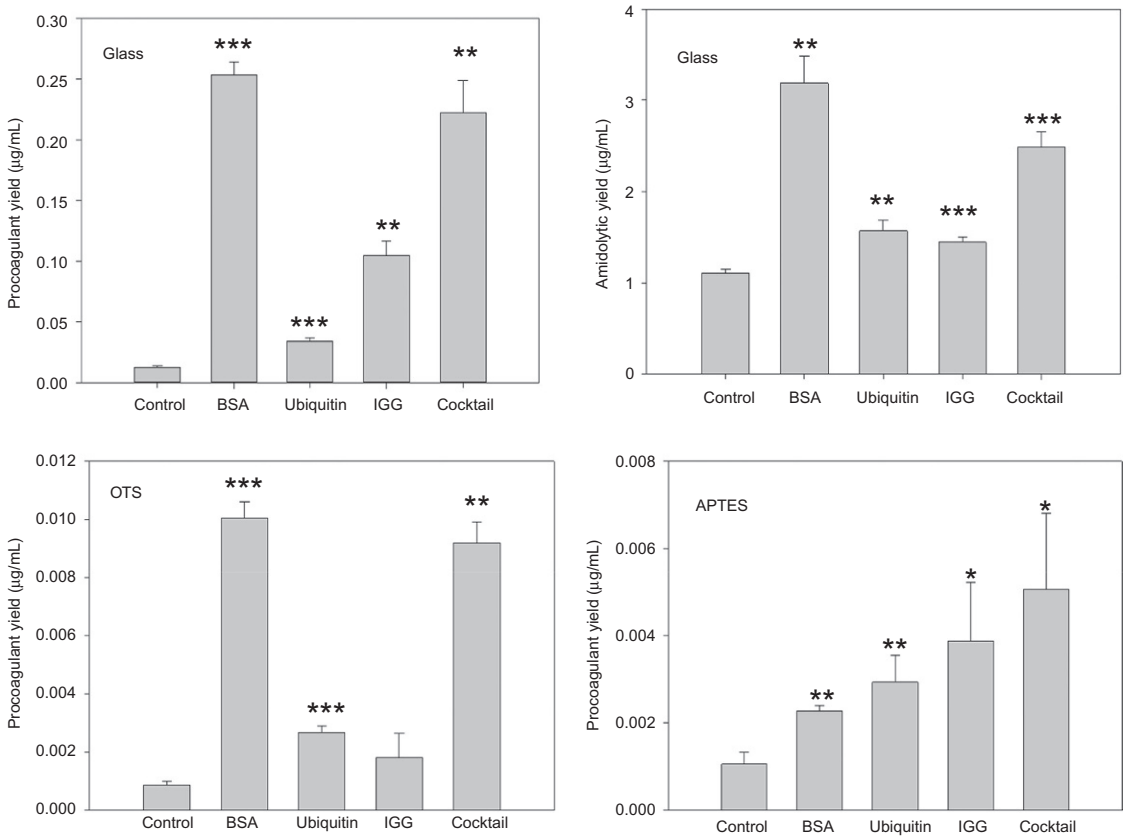


Fig. 1.7 FXII contact activation by different solid activators with or without the presence of plasma proteins. The symbol * represents statistical significance with respect to procoagulant and/or amidolytic yields obtained in neat buffer without plasma proteins. (*: $P<0.05$; **: $P<0.01$; ***: $P<0.001$)

as that seen with hydrophilic glass. The different protein adsorption capacities of hydrophobic OTS, dependent on both the concentration and molecular weight of the proteins, may be contributing to these different influences on FXII activation [61]. Procoagulant yields by APTES were amplified by 2–5 times in the order of cocktail > IgG > ubiquitin > BSA, opposite to the orders of glass and OTS. APTES-modified glass particles bear a combination of functional groups displaying both capacities of hydrogen bonding to water and dispersion-force interactions [62]. Full understanding of the relationships among surface functional group chemistry, contact activation, and influences of protein adsorption remains to be unsolved problems (Fig. 1.8, [15])

There is a clear influence of plasma proteins on FXII activation that is dependent on properties of individual proteins and the activator surfaces. FXII autoactivation with plasma protein(s) represents a significant increase in biochemical complexity over FXII autoactivation in buffer.

1.5.2 Kallikrein-mediated amplification of FXIIa from surface induced activation

FXII-derived products produced by surface activation are amplified by kallikrein-mediated reciprocal activation during propagation down the intrinsic pathway. Kallikrein generated by FXIIa-mediated hydrolysis of PK in turn cleaves FXII to FXIIa. Previous studies found that FXII-Kal reciprocal amplification is the major contributor to FXII activation in blood plasma [15]. Mathematical modeling of PK-deficient platelet-poor plasma (d_{pk}PPP) and PK-reconstituted d_{pk}PPP (R d_{pk}PPP) coagulation showed that the autoactivation process of FXII activation accounts for no more than 25% of the total FXIIa yield by intrinsic pathway (Fig. 1.9). However, kallikrein-mediated FXIIa amplification in neat buffer was even more profound (Fig. 1.10). Adding PK increases the yield of both amidolytic and procoagulant fragments via reciprocal activation. Specifically, procoagulants at clean glass were amplified by 6.5 times in the presence of PK, which in turn strengthens the efficiency of FXII autoactivation by hydrophilic glass more than by OTS and APTES. However, PK appeared to attenuate the differences in amidolytic yield produced by contact activation with activators of varying surface energy. In all, kallikrein-mediated amplification of FXIIa plays a critical role in the generation of FXIIa and thus the potential to induce plasma coagulation.

1.6 Role of platelets in FXII contact activation

Platelets serve a variety of functions in the circulation [63]. The main role of platelets in hemostasis is to preserve the integrity of the vascular wall through formation of a platelet plug [64]. In the conventional scheme of cell-based control of coagulation, platelets become activated when they contact any thrombogenic surface such as injured endothelium, subendothelium, and artificial surfaces and/or they are exposed to soluble activators [65,66]. Activated platelets can secrete and present various molecules, changing their shape and the expression pattern of adhesion molecules. As a

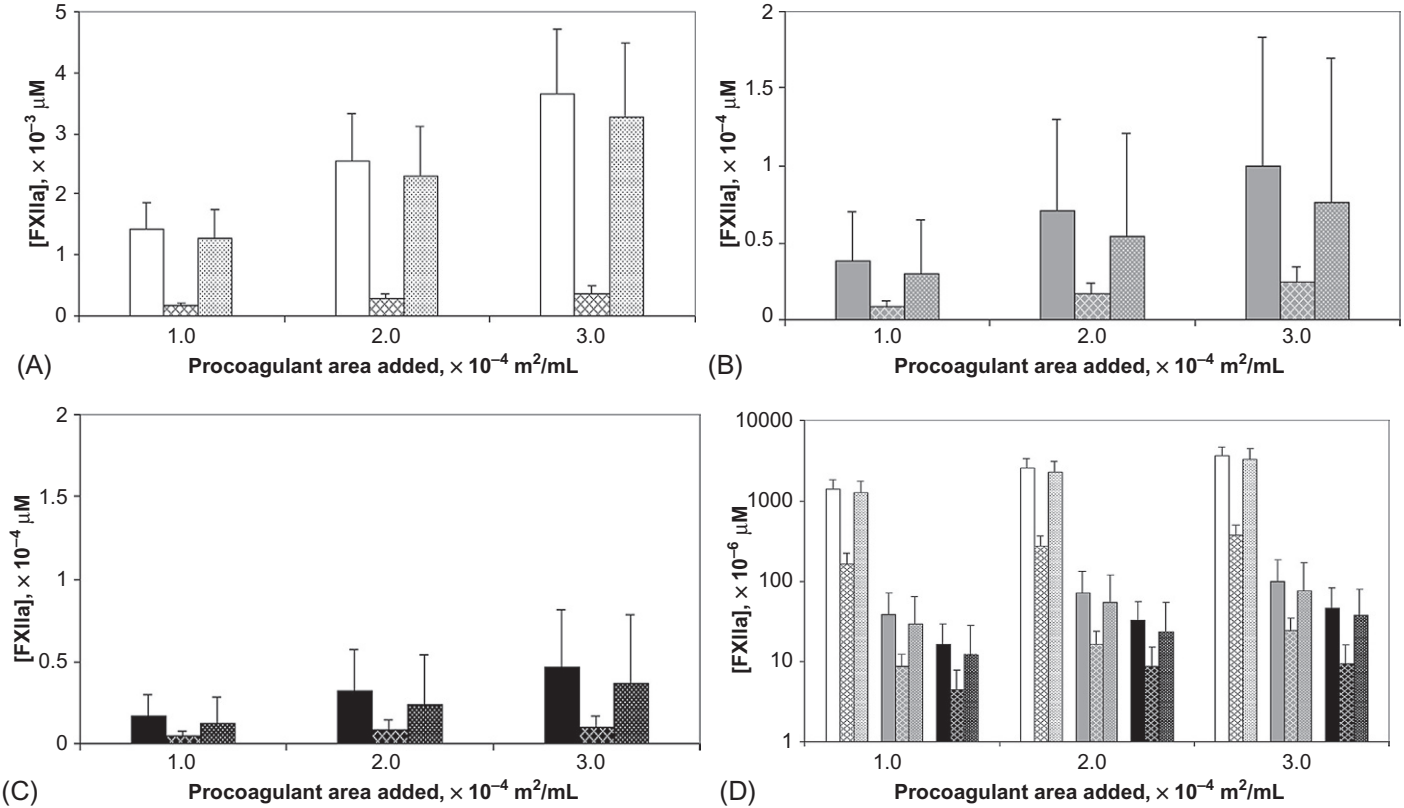


Fig. 1.8 FXIIa produced in total and via the autoactivation and reciprocal activation pathways at three surface area values for each of the three solid test activators (A) glass, (B) APTES, and (C) OTS. (D) A compilation of values from the different surface presented using a semi-log plot for ease of comparison among the procoagulants showing glass (white background), APTES (gray background), and OTS (black background) from left to right at each surface area.
Adapted from K. Chatterjee, Z. Guo, E.A. Vogle, C.A. Siedlecki, Contributions of contact activationpathways of coagulation factor XII in plasma, J. Biomed. Mater. Res. A 90A (2009) 27–34.

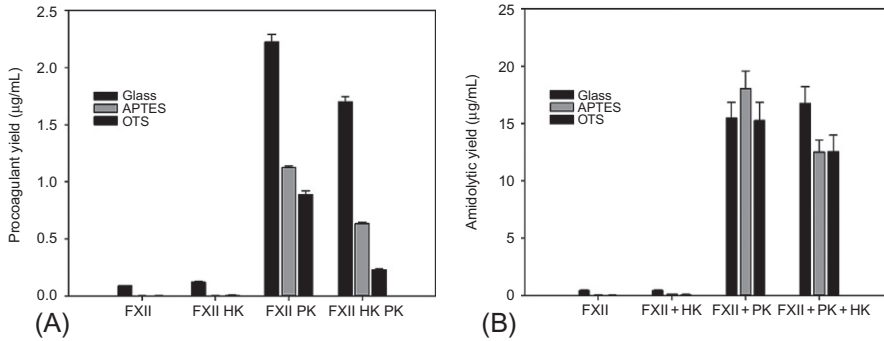


Fig. 1.9 FXII contact activation in buffer by different activators with or without PK and/or HK: (A) procoagulant yield and (B) amidolytic yield.

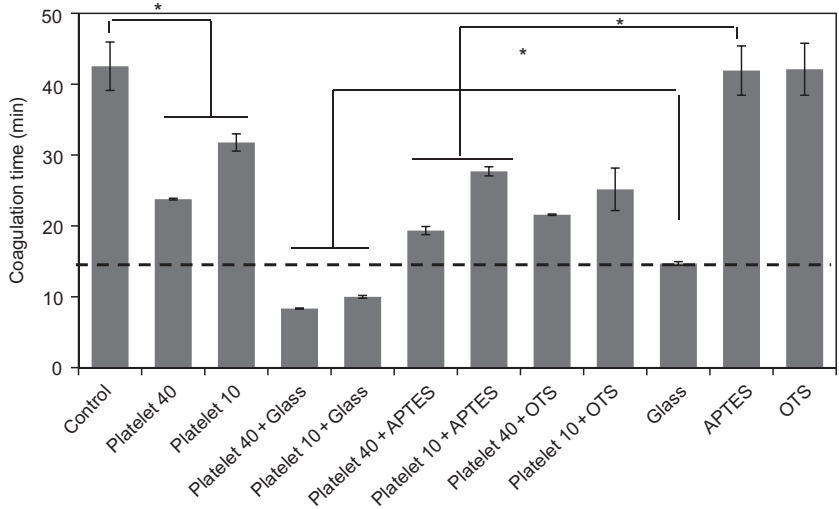


Fig. 1.10 Coagulation time of human plasma in the presence of a variety of procoagulant surfaces. Human platelet-rich plasma (PRP) was separated from healthy donor blood, and platelets were isolated through Sepharose 4B column using PBS effluent. Isolated platelets were incubated with an RGDS peptide to block the binding sits of αIIbβ3 receptor on the platelet membrane for prevention of aggregation and then were activated by ADP. Coagulation assay was performed similarly as previously described [42]. (Platelet 40 = 40×10^3 platelets/mL, platelet 10 = 10×10^3 platelets/mL, APTES = 3-aminopropyltriethoxysilane-coated glass beads, and OTS = octadecyltrichlorosilane-coated glass beads. All glass beads weigh 100 mg, equivalent to 500 mm^2 surface area. The *broken line* indicating coagulation time for bare glass surfaces is shown for comparison (14.7 ± 0.3 min). (*: $P<0.05$).

result, activated platelets promote platelet-platelet contact and multiple adhesion processes, which involve distinct receptors and adhesive ligands, leading to aggregation [67]. Also, aggregated platelets and fibrin form the main constituents of intra-arterial thrombi in thrombosis [68]. Heemskerk et al. reviewed the platelet-based coagulation and summarized that platelet coagulation was surface property-dependent,

which platelets with elevated Ca^{2+} and exposed phosphatidylserine control thrombin and fibrin generation and platelets with activated $\alpha_{IIb}\beta_3$ regulate clot retraction [69]. However, evidence shows that platelets have a role in contact activation of intrinsic coagulation, particularly for the activated platelets [70,71].

Activated platelet surfaces contain the negatively charged lipid phosphatidylserine and play an essential role in propagating and enhancing the coagulation reactions. Similar to the negatively charged artificial surfaces, activated platelets accelerate plasma coagulation. Fig. 1.10 shows that platelets stimulated by adenosine diphosphate (ADP) significantly shortened the coagulation time of human plasma after recalcification compared with coagulation times of plasma without platelets. The further acceleration of plasma coagulation was observed in the presence of dual procoagulant surfaces (activated platelets and negatively charged glass beads). In the case of APTES and OTS—glass beads, the silane-coated glass beads have no significant difference in coagulation time of plasma compared with control; however, the addition of activated platelets with silane-coated beads significantly shortened the coagulation time. It has been suggested that the mechanism by which negatively charged surfaces promote the activation of FXII involves conformational changes in its native structure [72,73]. Results suggest that the activated platelets could provide this surface, similar to the negatively charged artificial surfaces, and render FXII more susceptible to proteolytic activation and promote plasma coagulation.

Activated platelets trigger FXII activation and initiate the intrinsic coagulation pathway. In a series of activation experiments, FXII was incubated and rocked with solid procoagulants or activated platelets in neat PBS buffer. A coagulation time assay for activated FXII (FXIIa) shows that activated platelets with concentration of $100\times10^3/\mu L$ (corresponding $CT = 39.1 \pm 1.4$ min) have similar activation to 500 mm^2 surface area of bare glass beads (corresponding $CT = 38.8 \pm 0.7$ min), while the activation of FXII in higher concentrations of platelets ($200\times10^3/\mu L$) significantly increased as noted by a sharply decreasing plasma coagulation time (33.7 ± 3.3 min) (Fig. 1.11), demonstrating that platelet-induced coagulation of plasma is platelet concentration-dependent. Fig. 1.12 plots the decreasing coagulation time of plasma arising from increasing numbers of activated platelets added to PPP. A good fit ($R^2 = 0.995$) between varying doses of activated platelets and coagulation time was obtained using the model for FXIIa titration that has been described as [42] $CT = \dfrac{a[E]+b}{[E]+c}$, where CT = coagulation time, $[E]$ = concentration of activator, and a, b, and c are the parameters. The three adjustable parameters are $a = 20.2 \pm 0.6$, $b = 436.6 \pm 46.8$, and $c = 10.0 \pm 1.1$ and are comparable with parameters for FXIIa titration dose curves in PPP [74]. Taking all results together, the activated platelets exhibit the ability to trigger FXII activation, serving as an activator of plasma coagulation leading to generation of FXIa and contributing to clotting formation. Activated platelets may thereby constitute an intravascular locus for contact activation [75].

The role of platelets in contact activation appears to be dependent on the mechanism of platelet stimulation. It was shown that ADP-treated platelets could enhance the intrinsic coagulation reactions in the presence of FXII but not in its absence [70], while collagen-treated platelets could accelerate coagulation reactions in the absence

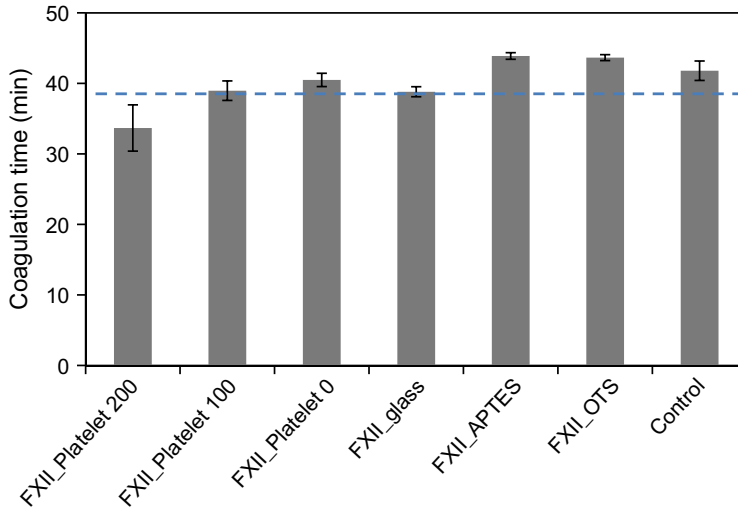


Fig. 1.11 Coagulation time assay of FXII activated by platelets, bare glass, APTES-coated glass, and OTS-coated glass beads in PPP. FXII at concentration of 30 μg/mL was incubated with solid procoagulants or activated platelets for 30 min, and the supernatant in each activation was dosed into plasma, and coagulation time was recorded after recalcification. The number behind the platelet indicates the concentration of activated platelets (platelet 200 = platelet 200×10^3/μL and platelet 100 = platelet 100×10^3/μL) during activation. Control = plasma without any addition. All glass beads weigh 100 mg each.

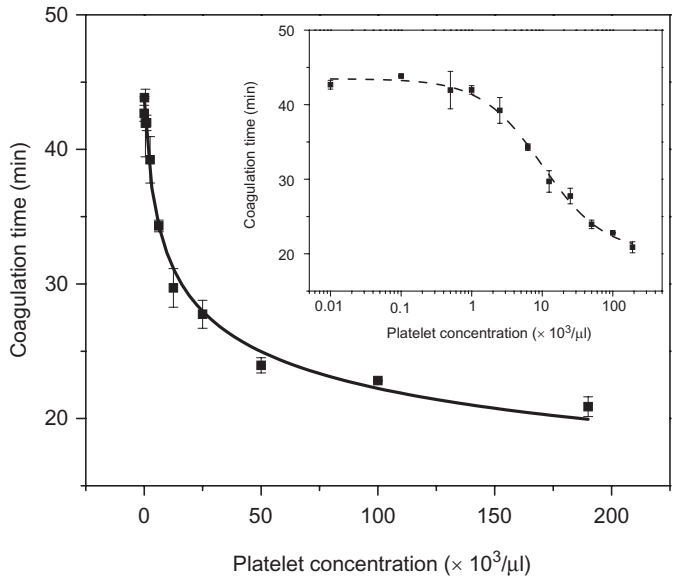


Fig. 1.12 Activated platelet titration in human platelet-poor plasma (PPP) showing experimental coagulation time versus concentration of exogenous activated platelets. The smooth curve was drawn through the data results from least square fitting of mathematical model of FXIIa titration equation [42]. The inset shows the results in log scale for clarity. Data shown as mean ± standard deviation for $n = 3$.

of FXII in the presence of FXI or platelet factor XI-like activity [71]. These distinct observations suggested that the platelets treated with ADP or collagen could stimulate contact activation by two separate and different mechanisms, one of which requires FXII and another is independent of FXII. Further experiments demonstrated that ADP- or collagen-treated platelets could promote the proteolytic activation of FXII in mixtures containing kallikrein and high-molecular-weight kininogen [76]. Collagen was thought not only to stimulate platelet activation but also to bind to FXII and activate FXII to stimulate thrombin generation and potentiate the formation of platelet-fibrin thrombi [12]; however, collagen-treated platelets appear to provide more than simply a surface (e.g., kaolin) that could affect the proteolytic activation of FXI in the absence of FXII. Such proteolytic activation of coagulation zymogens might be due to the secretion or stimulus-specific activation of platelet proteolytic enzymes, which are unknown yet [76]. There is also some evidence that FXII and FXI can bind to glycoprotein Ibalpha to the platelet surface, but the activity of platelet-bound FXIa and cleavage of FIX could not be confirmed [77].

The role of platelets in contact activation of FXII in intrinsic coagulation is still controversial and remains unclear, although the ideas regarding contact activation of FXII on platelet surfaces were raised as early as in the 1960s [78]. Early studies showed that coagulation time of platelet-rich plasma in the presence of foreign surfaces such as kaolin could be shortened, while plasma alone with kaolin resulted in slower coagulation. Platelet activity, termed as platelet factor 3 availability, was found to be responsible for this phenomenon [79–81]. This finding in platelets was confirmed from more thrombasthenic patients. Castaldi et al. found that thrombasthenic platelets having a defect in platelet factor 3 availability resulted in prolonged clotting time, suggesting its importance in FXII activation [82]. However, the exact nature of the defect was still unknown but was associated with poor platelet secretion [83]. Recently, it was demonstrated that platelet-secreted polyphosphates (polyP) [6,7] and platelet-derived MPs [8] trigger in vivo thrombin and fibrin formation via activation of FXII. The findings of polyP with the dense granules of platelets are a breakthrough in hemostasis and understanding the role of platelets in intrinsic coagulation. Platelet polyP is a natural activator of FXII, which links platelet activation, intrinsic coagulation, and inflammation [84,85] although the overall role of platelets and polyP in FXII activation is still not fully understood [86].

PolyP is a linear polymer of inorganic phosphate residues that is widely present in biology. PolyP in platelet dense granules is secreted upon platelet activation. It is a potent hemostatic regulator that modulates the blood coagulation cascade in three steps [6,87,88]: It triggers the contact pathway via activating FXII, it accelerates factor V activation that in turn results in abrogation of the function of the natural anticoagulant protein TF pathway inhibitor, and it enhances fibrin clot structure. PolyP is also found to accelerate FXI activation by thrombin [89]. Müller et al. [7] reported the physiological role of polyP release from platelets in the thrombosis and demonstrated that a polymer of 60–100 phosphate residues directly bound to and activated the plasma protease FXII, and polyP-driven FXII activation triggered release of the inflammatory mediator bradykinin by plasma kallikrein-mediated kininogen processing. Polyphosphate polymers of the size secreted by activated human platelets accelerate factor XI activation by α-thrombin, β-thrombin, and factor XIa [89]. As a result, polyphosphate inhibitors

including cationic proteins, polymers, and small molecules have been proposed to act as novel antithrombotic/antiinflammatory agents [90].

However, the role of platelet and platelet polyP in contact activation is still questioned and debated [86,91,92]. Faxalv et al. [86] found that platelet-derived polyP only weakly activated FXII with an FXIIa-generating activity of 10% compared with an equivalent concentration of kaolin. Such a discrepancy may result from the instability of polyP in blood or plasma due to the presence of phosphatases. In addition, it has been shown that polyP exerts effects on blood clotting that are strongly dependent on polymer size. Smith et al.[93] reported that long polymers (≥500 phosphate residues, most present in microorganisms) were required for optimal activation of the contact pathway, while the shorter polymer (~100 phosphate residues, similar to the polymers released by platelets) was sufficient to accelerate factor V activation and abrogate the anticoagulant function of the TF pathway inhibitor. This would suggest that bacterial infection may activate the clotting cascade via FXII. The latest study also shows that FXII preferentially binds to procoagulant phosphatidylserine-exposing platelets, which promotes FXII activation through their surface, retains bound essential levels of FXIIa, and triggers contact pathway clotting of plasma regardless of the materials secreted outside the platelet [94].

The role of platelets in FXII contact activation and the intrinsic coagulation cascade is complicated, with many outstanding questions. For instance, what is the difference and relative importance for platelets stimulated by ADP, collagen, or thrombin versus the platelet themselves in arterial thrombosis or activated by contact with foreign surfaces? Does the platelet surface directly participate in FXII activation? Are there other products such as MPs released from platelet activation that participate in FXII activation? Clearly, there is more work needed to better understand the role of platelet polyP, platelet surface, and other released materials including MPs in the activation of FXII in vivo [85].

1.7 Summary and future perspectives

The contact activation system of intrinsic pathway of blood plasma coagulation is a plasma protease cascade potentiated by the assembly of activation-complex proteins (FXII, FXI, PK, and high-molecular-weight kininogen) in activating procoagulant surfaces through protein/surface interactions. New findings on the roles of hydrophobic surfaces in contact activation of FXII revised the standard paradigm of the traditional intrinsic pathway, in which anionic hydrophilic surfaces were viewed as a requirement to induce FXII zymogen activation to form proteolytically active FXIIa. The finding of polyphosphates in the dense granules of platelets revealed the potential role of natural activators in contact system of blood plasma coagulation including the activated platelets and the microorganisms, although the role of these natural activators is still controversial and more questions need to be answered.

Despite decades of research, understanding of the contact system is still ongoing. This important system has the ability to activate various vascular and immunological pathways and act as an interface between inflammation, coagulation, and innate

immunity [95]. While the biochemistry of FXII is well defined, the details of how FXII behaves as a zymogen and mechanisms of conformational changes by activators remain poorly understood. The characterization and identification of fragment products of FXII in various contact activation systems remain significant challenges for understanding the intrinsic pathway of coagulation.

References

[1] B.D. Ratner, The catastrophe revisited: blood compatibility in the 21st century, Biomaterials 28 (2007) 5144–5147.
[2] E. Vogler, C. Siedlecki, Contact activation of blood-plasma coagulation, Biomaterials 30 (2009) 1857–1869.
[3] A.L. Kuharsky, A.L. Fogelson, Surface-mediated control of blood coagulation: the role of binding site densities and platelet deposition, Biophys. J. 80 (2001) 1050–1074.
[4] O.D. Ratnoff, J.M. Rosenblum, Role of Hageman factor in the initiation of clotting by glass—evidence that glass frees Hageman factor from inhibition, Am. J. Med. 25 (1958) 160–168.
[5] R. Zhuo, C. Siedlecki, E. Vogler, Autoactivation of blood factor XII at hydrophilic and hydrophobic surfaces, Biomaterials 27 (2006) 4325–4332.
[6] S.A. Smith, N.J. Mutch, D. Baskar, P. Rohloff, R. Docampo, J.H. Morrissey, Polyphosphate modulates blood coagulation and fibrinolysis, Proc. Natl. Acad. Sci. USA 103 (2006) 903–908.
[7] F. Müller, N.J. Mutch, W.A. Schenk, S.A. Smith, L. Esterl, H.M. Spronk, et al., Platelet polyphosphates are proinflammatory and procoagulant mediators in vivo, Cell 139 (2009) 1143–1156.
[8] P.E.J. Van Der Meijden, M. Van Schilfgaarde, R. Van Oerle, T. Renné, H. Ten Cate, H.M.H. Spronk, Platelet- and erythrocyte-derived microparticles trigger thrombin generation via factor XIIa, J. Thromb. Haemost. 10 (2012) 1355–1362.
[9] C. Kannemeier, A. Shibamiya, F. Nakazawa, H. Trusheim, C. Ruppert, P. Markart, et al., Extracellular RNA constitutes a natural procoagulant cofactor in blood coagulation, Proc. Natl. Acad. Sci. USA 104 (2007) 6388–6393.
[10] L. Bergamaschini, C. Donarini, C. Foddi, G. Gobbo, L. Parnetti, A. Agostoni, The region 1-11 of Alzheimer amyloid-beta is critical for activation of contact-kinin system, Neurobiol. Aging 22 (2001) 63–69.
[11] C. Maas, J.W.P. Govers-Riemslag, B. Bouma, B. Schiks, B.P.C. Hazenberg, H.M. Lokhorst, et al., Misfolded proteins activate Factor XII in humans, leading to kallikrein formation without initiating coagulation, J. Clin. Investig. 118 (2008) 3208–3218.
[12] P.E.J. van der Meijden, I.C.A. Munnix, J.M. Auger, J.W.P. Govers-Riemslag, J.M.E.M. Cosemans, M.J.E. Kuijpers, et al., Dual role of collagen in factor XII-dependent thrombus formation, Blood 114 (2009) 881–890.
[13] C.T. Oschatz, C. Maas, J. Bjorkqvist, W. Mueller-Esterl, W.A. Wuillemin, T. Renne, Mast cell-heparin increases vascular permeability in vivo by contact system-driven bradykinin formation, J. Thromb. Haemost. 9 (2011) 739.
[14] C. Sperling, M. Fischer, M.F. Maitz, C. Werner, Blood coagulation on biomaterials requires the combination of distinct activation processes, Biomaterials 30 (2009) 4447–4456.
[15] K. Chatterjee, Z. Guo, E.A. Vogle, C.A. Siedlecki, Contributions of contact activation pathways of coagulation factor XII in plasma, J. Biomed. Mater. Res. A 90A (2009) 27–34.

[16] A. Golas, C. Yeh, C. Siedlecki, E. Vogler, Amidolytic, procoagulant, and activation-suppressing proteins produced by contact activation of blood factor XII in buffer solution, Biomaterials 32 (2011) 9747–9757.
[17] D.E. Cool, R.T.A. Macgillivray, Characterization of the human-blood coagulation factor-XII gene—intron exon gene organization and analysis of the 5'-flanking region, J. Biol. Chem. 262 (1987) 13662–13673.
[18] S.D. Revak, C.G. Cochrane, A.R. Johnston, T.E. Hugli, Structural-changes accompanying enzymatic activation of human Hageman-factor, J. Clin. Investig. 54 (1974) 619–627.
[19] J.T. Dunn, A.P. Kaplan, Formation and structure of human Hageman-factor fragments, J. Clin. Investig. 70 (1982) 627–631.
[20] M.J. Pebusque, F. Coulier, D. Birnbaum, P. Pontarotti, Ancient large-scale genome duplications: phylogenetic and linkage analyses shed light on chordate genome evolution, Mol. Biol. Evol. 15 (1998) 1145–1159.
[21] M. Pathak, P. Wilmann, J. Awford, C. Li, B.K. Hamad, P.M. Fischer, et al., Coagulation factor XII protease domain crystal structure, J. Thromb. Haemost. 13 (2015) 580–591.
[22] F. Citarella, D.M. Ravon, B. Pascucci, A. Felici, A. Fantoni, C.E. Hack, Structure/function analysis of human factor XII using recombinant deletion mutants—evidence for an additional region involved in the binding to negatively charged surfaces, Eur. J. Biochem. 238 (1996) 240–249.
[23] F. Citarella, H. te Velthuis, M. Helmer-Citterich, C.E. Hack, Identification of a putative binding site for negatively charged surfaces in the fibronectin type II domain of human factor XII—an immunochemical and homology modeling approach, Thromb. Haemost. 84 (2000) 1057–1065.
[24] D.X. Beringer, L.M.J. Kroon-Batenburg, The structure of the FnI-EGF-like tandem domain of coagulation factor XII solved using SIRAS, Acta Crystallogr. Sect. F: Struct. Biol. Cryst. Commun. 69 (2013) 94–102.
[25] C. Maas, B. Schiks, R.D. Strangi, T.M. Hackeng, B.N. Bouma, M.F.B.G. Gebbink, et al., Identification of fibronectin type I domains as amyloid-binding modules on tissue-type plasminogen activator and three homologs, Amyloid 15 (2008) 166–180.
[26] J.T. Dunn, M. Silverberg, A.P. Kaplan, The cleavage and formation of activated human Hageman-factor by autodigestion and by kallikrein, J. Biol. Chem. 257 (1982) 1779–1784.
[27] A.P. Kaplan, K.F. Austen, A pre-albumin activator of prekallikrein, J. Immunol. 105 (1970) 802–811.
[28] S.D. Revak, C.G. Cochrane, J.H. Griffin, Binding and cleavage characteristics of human Hageman-factor during contact activation—comparison of normal plasma with plasmas deficient in factor-XI, prekallikrein, or high molecular-weight kininogen, J. Clin. Investig. 59 (1977) 1167–1175.
[29] K. Vanderkamp, W. Vanoeveren, Factor-XII fragment and kallikrein generation in plasma during incubation with biomaterials, J. Biomed. Mater. Res. 28 (1994) 349–352.
[30] S. de Maat, S. van Dooremalen, P.G. de Groot, C. Maas, A nanobody-based method for tracking factor XII activation in plasma, Thromb. Haemost. 110 (2013) 458–468.
[31] S.D. Revak, C.G. Cochrane, B.N. Bouma, J.H. Griffin, Surface and fluid phase activities of 2 forms of activated Hageman-factor produced during contact activation of plasma, J. Exp. Med. 147 (1978) 719–729.
[32] A. Golas, C. Yeh, H. Pitakjakpipop, C. Siedlecki, E. Vogler, A comparison of blood factor XII autoactivation in buffer, protein cocktail, serum, and plasma solutions, Biomaterials 34 (2013) 607–620.
[33] A. Golas, P. Parhi, Z. Dimachkie, C. Siedlecki, E. Vogler, Surface-energy dependent contact activation of blood factor XII, Biomaterials 31 (2010) 1068–1079.

[34] E.A. Vogler, Protein adsorption in three dimensions, Biomaterials 33 (2012) 1201–1237.
[35] N.L. Anderson, N.G. Anderson, The human plasma proteome—history, character, and diagnostic prospects, Mol. Cell. Proteomics 1 (2002) 845–867.
[36] F.W. Putnam, Alpha Beta Gamma Omega the Past Present and Future of Plasma Proteins, Academic Press, New York, 1975.
[37] R. Zhuo, R. Miller, K. Bussard, C. Siedlecki, E. Vogler, Procoagulant stimulus processing by the intrinsic pathway of blood plasma coagulation, Biomaterials 26 (2005) 2965–2973.
[38] E.A. Vogler, J.G. Nadeau, J.C. Graper, Contact activation of the plasma coagulation cascade. III. Biophysical aspects of thrombin-binding anticoagulants, J. Biomed. Mater. Res. 40 (1998) 92–103.
[39] H. Ishitoya, M. Kawamura, J. Linneweber, T. Motomura, S. Ichikawa, I. Nishimura, et al., Titania gel reduces thrombin generation, Artif. Organs 26 (2002) 959–963.
[40] E.A. Vogler, J.C. Graper, G.R. Harper, H.W. Sugg, L.M. Lander, W.J. Brittain, Contact activation of the plasma coagulation cascade. 1. Procoagulant surface-chemistry and energy, J. Biomed. Mater. Res. 29 (1995) 1005–1016.
[41] K.A. Mitropoulos, High affinity binding of factor XIIa to an electronegative surface controls the rates of factor XII and prekallikrein activation in vitro, Thromb. Res. 94 (1999) 117–129.
[42] Z. Guo, K. Bussard, K. Chatterjee, R. Miller, E. Vogler, C. Siedlecki, Mathematical modeling of material-induced blood plasma coagulation, Biomaterials 27 (2006) 796–806.
[43] L. Vroman, What factors determine thrombogenicity, Bull. N. Y. Acad. Med. 48 (1972) 302–310.
[44] C.-H.J. Yeh, Z.O. Dimachkie, A. Golas, A. Cheng, P. Parhi, E.A. Vogler, Contact activation of blood plasma and factor XII by ion-exchange resins, Biomaterials 33 (2012) 9–19.
[45] A. Golas, H. Pitakjakpipop, S.M. Rahn, A.C. Siedlecki, A.E. Vogler, Enzymes produced by autoactivation of blood factor XII in buffer, Biomaterials 37 (2015) 1–12.
[46] E.A. Vogler, Water and the acute biological response to surfaces, J. Biomater. Sci. Polym. Ed. 10 (1999) 1015–1045.
[47] E.A. Vogler, J.C. Graper, H.W. Sugg, L.M. Lander, W.J. Brittain, Contact activation of the plasma coagulation cascade. 2. Protein adsorption to procoagulant surfaces, J. Biomed. Mater. Res. 29 (1995) 1017–1028.
[48] M.A. Griep, K. Fujikawa, G.L. Nelsestuen, Possible basis for the apparent surface selectivity of the contact activation of human-blood coagulation factor-XII, Biochemistry 25 (1986) 6688–6694.
[49] H. Noh, S.T. Yohe, E.A. Vogler, Volumetric interpretation of protein adsorption: ion-exchange adsorbent capacity, protein pI, and interaction energetics, Biomaterials 29 (2008) 2033–2048.
[50] X. Xu, A.M. Lenhoff, A predictive approach to correlating protein adsorption isotherms on ion-exchange media, J. Phys. Chem. B 112 (2008) 1028–1040.
[51] V.H. Donaldso, O.D. Ratnoff, Hageman factor—alterations in physical properties during activation, Science 150 (1965) 754–756.
[52] C.G. Cochrane, S.D. Revak, K.D. Wuepper, Activation of Hageman-factor in solid and fluid phases—critical role of kallikrein, J. Exp. Med. 138 (1973) 1564–1583.
[53] J. Margolis, Interrelationship of coagulation of plasma and release of peptides, Ann. N. Y. Acad. Sci. 104 (1963) 133–145.
[54] C.R. McMillin, H. Saito, O.D. Ratnoff, A.G. Walton, Secondary structure of human Hageman-factor (factor-XII) and its alteration by activating agents, J. Clin. Investig. 54 (1974) 1312–1322.
[55] D. Armstron, Effects of temperature on response of human plasma kinin-forming system to promoting and inhibiting agents, Br. J. Pharmacol. 34 (1968) P670–P671.

[56] R. Zhuo, C. Siedlecki, E. Vogler, Competitive-protein adsorption in contact activation of blood factor XII, Biomaterials 28 (2007) 4355–4369.
[57] M. Rahman, S. Laurent, N. Tawil, L.H. Yahia, M. Mahmoudi, Protein-Nanoparticle Interactions: The Bio-Nano Interface, Springer, Heidelberg, 2013.
[58] A. Krishnan, J. Sturgeon, C. Siedlecki, E. Vogler, Scaled interfacial activity of proteins at the liquid-vapor interface, J. Biomed. Mater. Res. A 68A (2004) 544–557.
[59] A.M. Moulin, S.J. O'Shea, R.A. Badley, P. Doyle, M.E. Welland, Measuring surface-induced conformational changes in proteins, Langmuir 15 (1999) 8776–8779.
[60] L. Vroman, A.L. Adams, G.C. Fischer, P.C. Munoz, Interaction of high molecular-weight kininogen FACTOR-XII, and fibrinogen in plasma at interfaces, Blood 55 (1980) 156–159.
[61] P. Parhi, A. Golas, N. Barnthip, H. Noh, E.A. Vogler, Volumetric interpretation of protein adsorption: capacity scaling with adsorbate molecular weight and adsorbent surface energy, Biomaterials 30 (2009) 6814–6824.
[62] E.A. Vogler, How Water Wets Biomaterials, John Wiley and Sons, New York, NY, 2001.
[63] S.S. Smyth, R.P. McEver, A.S. Weyrich, C.N. Morrell, M.R. Hoffman, G.M. Arepally, et al., Platelet functions beyond hemostasis, J. Thromb. Haemost. 7 (2009) 1759–1766.
[64] M.B. Gorbet, M.V.M.V. Sefton, Biomaterial-associated thrombosis: roles of coagulation factors, complement, platelets and leukocytes, Biomaterials 25 (2004) 5681–5703.
[65] A. Zarbock, R.K. Polanowska-Grabowska, K. Ley, Platelet-neutrophil-interactions: linking hemostasis and inflammation, Blood Rev. 21 (2007) 99–111.
[66] C. Cicala, G. Cirino, Linkage between inflammation and coagulation: an update on the molecular basis of the crosstalk, Life Sci. 62 (1998) 1817–1824.
[67] S.P. Jackson, The growing complexity of platelet aggregation, Blood 109 (2007) 5087–5095.
[68] J.W. Heemskerk, E.M. Bevers, T. Lindhout, Platelet activation and blood coagulation, Thromb. Haemost. 88 (2002) 186–194.
[69] J.W.M. Heemskerk, N.J.A. Mattheij, J.M.E.M. Cosemans, Platelet-based coagulation: different populations, different functions, J. Thromb. Haemost. 11 (2013) 2–16.
[70] P.N. Walsh, The role of platelets in the contact phase of blood coagulation, Br. J. Haematol. 22 (1972) 237–254.
[71] P.N. Walsh, The effects of collagen and kaolin on the intrinsic coagulant activity of platelets. Evidence for an alternative pathway in intrinsic coagulation not requiring factor XII, Br. J. Haematol. 22 (1972) 393–405.
[72] C.R. McMillin, H. Saito, O.D. Ratnoff, A.G. Walton, The secondary structure of human Hageman factor (factor XII) and its alteration by activating agents, J. Clin. Invest. 54 (1974) 1312–1322.
[73] B.D. Fair, H. Saito, O.D. Ratnoff, W.B. Rippon, Detection by fluorescence of structural changes accompanying the activation of Hageman factor (factor XII), Exp. Biol. Med. 155 (1977) 199–202.
[74] K. Chatterjee, E.A. Vogler, C.A. Siedlecki, Procoagulant activity of surface-immobilized Hageman factor, Biomaterials 27 (2006) 5643–5650.
[75] J. Bäck, J. Sanchez, G. Elgue, K.N. Ekdahl, B. Nilsson, Activated human platelets induce factor XIIa-mediated contact activation, Biochem. Biophys. Res. Commun. 391 (2010) 11–17.
[76] P.N. Walsh, J.H. Griffin, Contributions of human platelets to the proteolytic activation of blood coagulation factors XII and XI, Blood 57 (1981) 106–118.
[77] F.A. Baglia, C.N. Shrimpton, J. Emsley, K. Kitagawa, Z.M. Ruggeri, J.A. Lopez, et al., Factor XI interacts with the leucine-rich repeats of glycoprotein Ibalpha on the activated platelet, J. Biol. Chem. 279 (2004) 49323–49329.

[78] P.G. Iatridis, S.G. Iatridis, J.H. Ferguson, Surface factor mechanisms in relation to blood platelets: evidence that activated hageman factor is present on surface of platelets, Thromb. Diath. Haemorrh. 11 (1964) 355–371.
[79] R.M. Hardisty, R.A. Hutton, The kaolin clotting time of platelet-rich plasma: a test of platelet factor- 3 availability, Br. J. Haematol. 11 (1965) 258–268.
[80] R.M. Hardisty, K.M. Dormandy, R.A. Hutton, Thrombasthenia—studies on 3 cases, Br. J. Haematol. 10 (1964) 371–387.
[81] T.H. Spaet, J. Cintron, Studies on platelet factor-3 availability, Br. J. Haematol. 11 (1965) 269–275.
[82] P.A. Castaldi, M.J. Larrieu, J. Caen, Availability of platelet factor 3 and activation of factor XII in thrombasthenia, Nature 207 (1965) 422–424.
[83] J. Caen, Q. Wu, Hageman factor, platelets and polyphosphates: early history and recent connection, J. Thromb. Haemost. 8 (2010) 1670–1674.
[84] P.E. van der Meijden, J.W. Heemskerk, Polyphosphates: a link between platelet activation, intrinsic coagulation and inflammation? Expert. Rev. Hematol. 3 (2010) 269–272.
[85] N. Mackman, A. Gruber, Platelet polyphosphate: an endogenous activator of coagulation factor XII, J. Thromb. Haemost. 8 (2010) 865–867.
[86] L. Faxalv, N. Boknas, J.O. Strom, P. Tengvall, E. Theodorsson, S. Ramstrom, et al., Putting polyphosphates to the test: evidence against platelet-induced activation of factor XII, Blood 122 (2013) 3818–3824.
[87] S.A. Smith, J.H. Morrissey, Polyphosphate as a general procoagulant agent, J. Thromb. Haemost. 6 (2008) 1750–1756.
[88] S.A. Smith, J.H. Morrissey, Polyphosphate enhances fibrin clot structure, Blood 112 (2008) 2810–2816.
[89] S.H. Choi, S.A. Smith, J.H. Morrissey, Polyphosphate is a cofactor for the activation of factor XI by thrombin, Blood 118 (2011) 6963–6970.
[90] S.A. Smith, S.H. Choi, J.N. Collins, R.J. Travers, B.C. Cooley, J.H. Morrissey, Inhibition of polyphosphate as a novel strategy for preventing thrombosis and inflammation, Blood 120 (2012) 5103–5110.
[91] K.F. Nickel, H.M. Spronk, N.J. Mutch, T. Renne, Time-dependent degradation and tissue factor addition mask the ability of platelet polyphosphates in activating factor XII-mediated coagulation, Blood 122 (2013) 3847–3849.
[92] N. Boknäs, L. Faxälv, J.O. Ström, P. Tengvall, E. Theodorsson, S. Ramström, et al., Response: platelets do not generate activated factor XII—how inappropriate experimental models have led to misleading conclusions, Blood 124 (2014) 1692–1694.
[93] S.A. Smith, S.H. Choi, R. Davis-Harrison, J. Huyck, J. Boettcher, C.M. Rienstra, et al., Polyphosphate exerts differential effects on blood clotting, depending on polymer size, Blood 116 (2010) 4353–4359.
[94] N.V. Zakharova, E.O. Artemenko, N.A. Podoplelova, A.N. Sveshnikova, I.A. Demina, F.I. Ataullakhanov, et al., Platelet surface-associated activation and secretion-mediated inhibition of coagulation factor XII, Plos One 10 (2015) e0116665.
[95] A.T. Long, E. Kenne, R. Jung, T.A. Fuchs, T. Renné, Contact system revisited: an interface between inflammation, coagulation, and innate immunity, J. Thromb. Haemost. 14 (2016) 427–437.

Mechanisms of blood coagulation in response to biomaterials: Extrinsic factors

2

M.T. Kalathottukaren, J.N. Kizhakkedathu
University of British Columbia, Vancouver, BC, Canada

2.1 Introduction

Biomaterials made of polymers, proteins, metals, and ceramics are used in various implant and device applications [1]. Examples include cardiovascular stents, grafts, catheters, and vascular assist devices used to treat patients suffering from cardiovascular disorders [2]. Insufficient hemocompatibility of biomaterials can cause adverse foreign body reactions that can lead to the functional failure of biomaterials [3]. The most common adverse event associated with blood-contacting biomaterials is the thrombus formation on its surface leading to occlusion in the blood vessels [4]. Worldwide, thrombosis or pathologic clot formation is a major cause of morbidity and mortality [5].

Upon exposure of a biomaterial to blood, the initial event is the adsorption of multitude blood proteins onto its surface [6]. This includes proteins of the intrinsic (contact) clotting system that can trigger the activation of clotting reaction. Subsequently, blood cells such as platelets, endothelial cells (ECs), and leukocytes are activated to release prothrombotic molecules [7]. Additionally, endothelium loses its nonthrombogenic nature and supports thrombus growth. Even though significant progress has been made to reduce the number of adverse events associated with biomaterials, developing a complete nonthrombogenic biomaterial seems to be challenging. The principal reason for this impediment is the involvement of multiple physiological players in the pathogenesis of thrombosis.

Until recently, coagulation factor (F) XII (FXII) in the coagulation system did not receive much attention as its role in hemostasis remained elusive. Reappraisal of FXII activity exposed its important role in thrombosis [8]. Moreover, recent studies have identified new endogenous prothrombotic molecules such as polyphosphate (PolyP), extracellular nucleic acids (ecNAs), and neutrophil extracellular traps (NETs) [9]. Considering these developments, it is important for biomaterial scientists to understand how blood-contacting materials initiate clotting so that novel strategies can be envisioned to create nonthrombogenic materials or control the thrombogenic nature of blood contacting surfaces. In this chapter, we will first describe the blood clotting cascade and the roles of various pathways/factors followed by the involvement of platelets, endothelium, and complement system in biomaterial-induced thrombosis.

Hemocompatibility of Biomaterials for Clinical Applications. https://doi.org/10.1016/B978-0-08-100497-5.00003-3
© 2018 Elsevier Ltd. All rights reserved.

2.2 The blood coagulation cascade and physiological inhibitors

Hemostasis is a physiological mechanism that seals damaged blood vessels, maintains blood fluidity and degrades blood clots after the restoration of vascular integrity [10]. A cell-based model of coagulation is widely used to describe mechanisms of in vivo blood coagulation. According to this model, coagulation can be divided into three phases: initiation, amplification, and propagation phases [11]. However, traditionally, the coagulation system has been divided into two major pathways: the extrinsic and intrinsic pathway. Both of these pathways culminate in the common pathway, leading to the generation of the hemostatic fibrin clot (the end product of coagulation reactions) [11]. The main goal of this chapter is to discuss the mechanism/s by which blood-contacting biomaterials trigger undesirable blood clotting resulting in thrombosis. So, in the following section, we will briefly explain the blood clotting pathways, discuss plausible role/s of newly identified endogenous prothrombotic molecules on blood clotting, and physiological inhibitors of blood clotting.

2.2.1 The extrinsic clotting pathway

Upon damage to the vascular endothelium, tissue factor (TF) expressed on cell membranes of subendothelial layers of blood vessels gets exposed to FVIIa circulating in blood (Fig. 2.1). The TF interact with FVIIa and forms the TF:FVIIa complex known

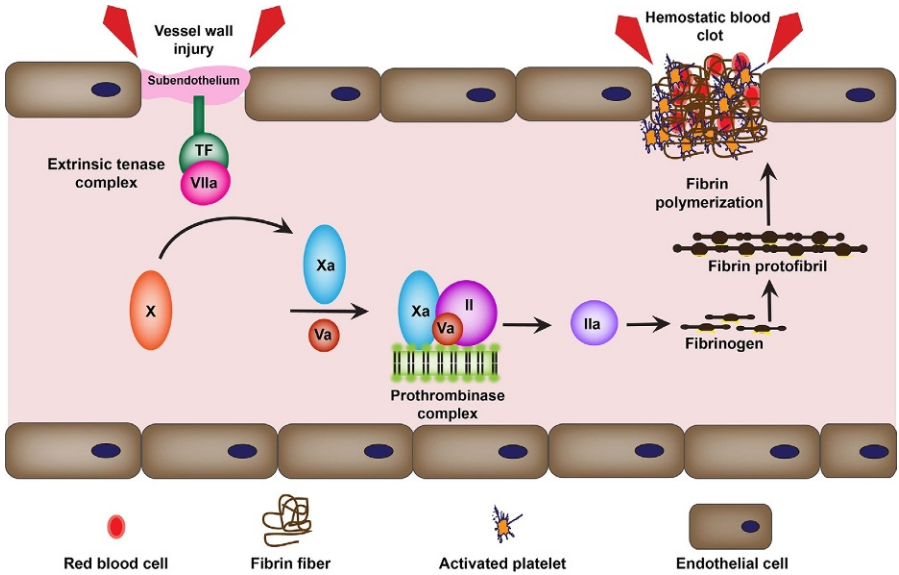


Fig. 2.1 The extrinsic clotting pathway. Upon injury, TF present on the subendothelium is exposed to blood. TF binds to FVIIa and forms the extrinsic tenase complex (TF:FVIIa). The extrinsic tenase complex activates FX into FXa. FXa will then bind to cofactor FVa to form the prothrombinase complex. The prothrombinase complex will convert prothrombin into thrombin. Thrombin polymerizes fibrin to form the stable hemostatic blood clot.

as the extrinsic tenase complex. This complex activates FIX to FIXa, and FX to FXa, respectively [10,11]. FXa then associates with cofactor FVa to form prothrombinase complexes (FVa:FXa) which activate prothrombin (FII) into thrombin (FIIa), a crucial protease of the coagulation system [12]. Thrombin cleaves fibrinogen (340 kDa protein present in the blood at 2–4 mg/mL concentration), into fibrin monomers that subsequently polymerize into stable fibrin clot [12]. Also, thrombin activates FXIII to FXIIIa which cross-links fibrin fibers of blood clots and provides clot strength and stability [13]. This is indispensable for blood clots to stop bleeding from injury sites. In addition, thrombin activates cofactors FV and FVIII [13].

2.2.2 The intrinsic (contact) clotting pathway

In addition to the extrinsic pathway, coagulation can be initiated by contact activation process, also known as the intrinsic clotting pathway. When blood comes into contact with negatively charged molecules or surfaces, FXII undergoes a conformational change and subsequent activation. Once activated, FXII (FXIIa) will then sequentially activate FXI and FIX. In addition, FXIIa proteolytically cleaves plasma kallikrein (PK) into active kallikrein which then produces potent proinflammatory mediator bradykinin (BK), from high molecular weight kininogen (HK) [14–16] (Fig. 2.2).

Activated FIX (FIXa) complexed with cofactor FVIIIa (FIXa:FVIIIa) known as the intrinsic tenase complex, converts FX to FXa, leading to thrombin production [14].

The intrinsic and extrinsic pathway converges at the final common pathway of coagulation which includes the formation of prothrombinase complex and thrombin generation. Even though we can delineate coagulation reactions into three pathways, there is significant overlap between pathways. For instance, thrombin can activate FXI, circumventing the need for FXII activation.

Adequate amount of coagulation factors in plasma is essential for hemostasis. Deficiency of coagulation factors lead to bleeding disorders such as hemophilia. For instance, hemophilia A and B is due to the deficiency of FVIII and FIX, respectively [17]. Interestingly, patients with FXII deficiency do not display bleeding diathesis, suggesting that FXII might not be necessarily involved in the hemostatic process [18]. Recent studies reveal emerging role/s for clotting enzymes of the intrinsic coagulation pathway, especially FXI and FXII [19]. Studies performed in mouse model suggest that FXI and FXII appear to be equally important drivers of thrombosis [20]. However, currently available epidemiological evidence and studies in nonhuman primates suggest, FXI is a dominant player involved in the pathogenesis of thrombosis [21]. So, strategies that target and avert activation of FXI or FXII could be a beneficial antithrombotic therapy with reduced risk of bleeding.

Antithrombotics that target FXI or FXII which are currently under investigation include (i) antisense oligonucleotides (ii) antibodies (iii) small molecule inhibitors, and (iv) aptamers [22–24]. However, inhibiting FXII activation or activity might be safer considering the fact that, patients with severe FXI deficiency experience mild bleeding complications with surgery or trauma [24]. In addition, biomaterials, extracorporeal circuits, and other blood-contacting medical devices trigger blood clotting by the direct activation of FXII. The inhibition of FXII activity could also, attenuate inflammation by abrogating BK generation.

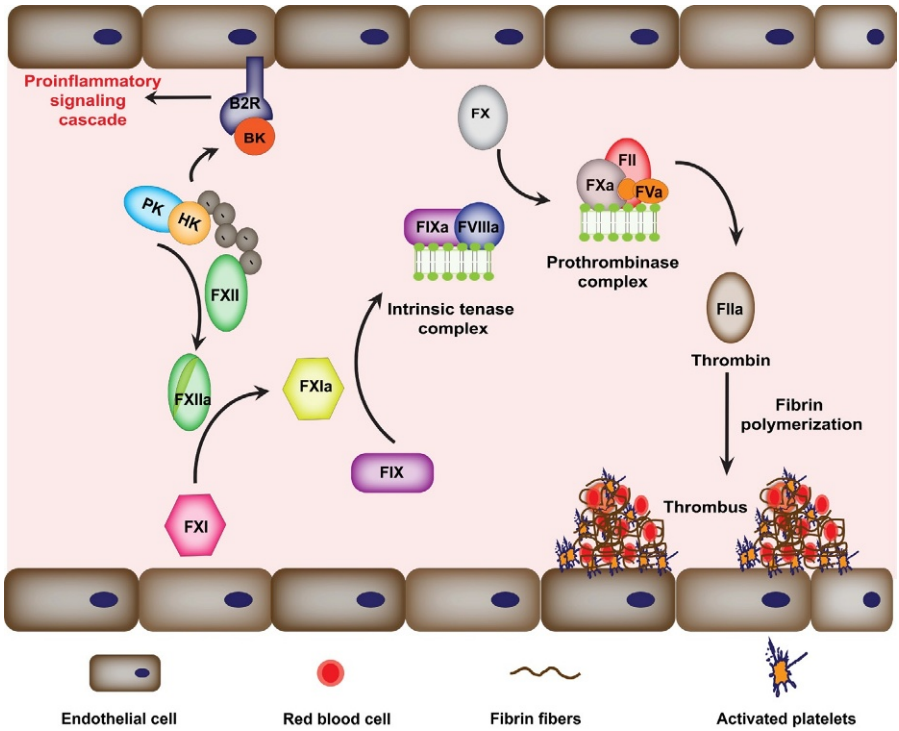


Fig. 2.2 The intrinsic clotting pathway. Intrinsic pathway (contact-clotting pathway) is initiated when artificial surfaces are exposed to blood. Trimolecular assembly of FXII, high molecular weight kininogen (HK) and PK bound to the surface of the foreign material generates FXIIa, and cleaves PK to generate active kallikrein. Active kallikrein produces BK from HK and also activates FXII. Binding of BK to kinin B2 receptor (B2R) activates proinflammatory signaling cascade. FXIIa activates FXI to FXIa, which in turn activates FIX. FIXa:FVIIa complex (intrinsic tenase complex) will generate prothrombinase complex leading to thrombin generation and fibrin clot.

2.2.3 Newly identified prothrombotic biomolecules

Studies provide conclusive evidence that contact activation of blood clotting is not essential for hemostasis; however, may contribute to the pathogenesis of thrombosis. The contact-clotting system is triggered when FXII comes into contact with polyanionic biomolecules or surfaces. Upon binding to these charged surfaces, FXII undergoes conformational change into FXIIa, followed by activation of coagulation factor zymogens such as FIX and FXI leading to fibrin clot formation. Studies have identified that endogenous polyanionic molecules such as polyphosphate (polyP) and extracellular nucleic acids possess such prothrombotic activity [9].

2.2.3.1 Polyphosphate and cell-free nucleic acids

Polyphosphate (polyP) is a highly anionic inorganic polymer composed of phosphate monomers, connected by high-energy phosphoanhydride bonds [25]. PolyP of varying

lengths is ubiquitously found in every prokaryotic and eukaryotic cell. Microorganisms contain long-chain polyP, composed of 100 to 1000 phosphate units in their storage granules (acidocalcisomes). PolyP found in dense granules of human platelets is smaller (60 to 100 phosphate units) and less heterogeneous compared to microbial polyP [26]. Studies show that the potential of polyP to trigger contact clotting by activating FXII depends on its chain length. Long chain microbial polyP is a potent FXII activator (template mechanism) compared to shorter polyP released from platelets [27].

In addition to FXII activation, polyP has multiple acting points in the coagulation cascade that can augment thrombin generation. PolyP accelerates the generation of cofactor FVa and FXIa and inhibits the anticoagulant activity of tissue factor pathway inhibitor (TFPI) [28]. Moreover, polyP incorporates into fibrin clots and produce thicker fibrin fibers that are more resistant to fibrinolysis [29,30] (Fig. 2.3). PolyP also displays

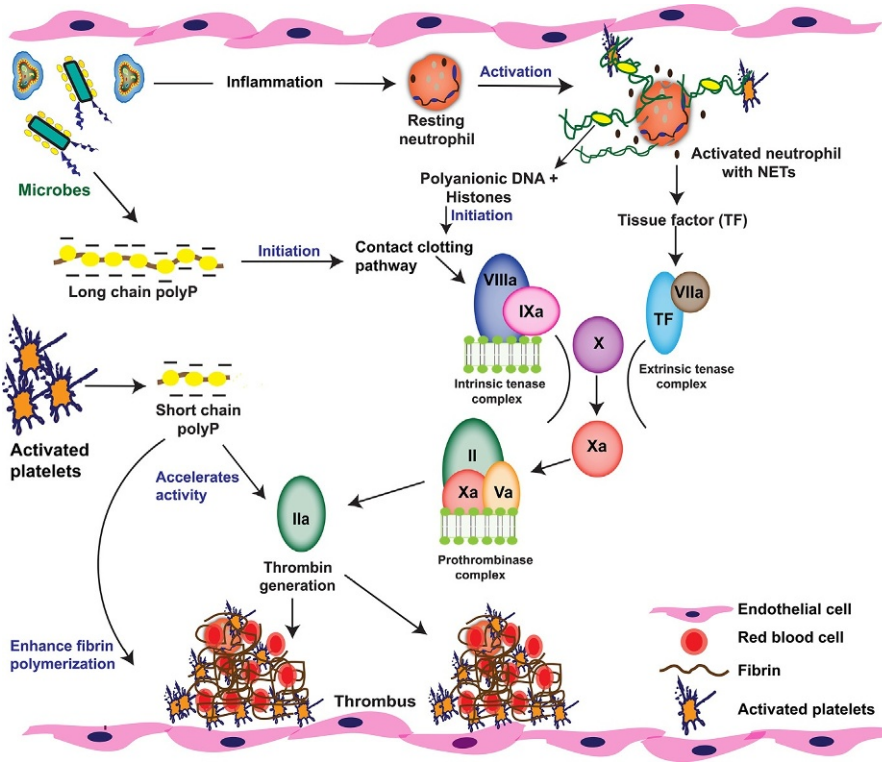


Fig. 2.3 Novel prothrombotic biomolecules. Microbial infections result in inflammation and subsequent activation of neutrophils. Activated neutrophils release web-like structures known as neutrophil extracellular traps (NETs) through a process called NETosis. NETs are mainly composed of DNA –histone complexes. NETs can trigger clotting via the contact-clotting pathway. Polyanionic DNA on NETs can act as a scaffold for contact protein assembly leading to thrombin generation. In addition, NETs possess highly procoagulant TF molecules which can activate the extrinsic clotting pathway. Microorganisms also release long chain polyphosphate (polyP) which can act as a template for FXII activation. Activated human platelets release short-chain polyP which potentiates clotting by enhancing thrombin generation and fibrin polymerization.

proinflammatory effects through numerous mechanisms involving, FXII mediated BK release, binding and potentiating proinflammatory actions of histones etc. [31]. Conversely, the physiological relevance of platelet polyP is evident from the fact that, patients with the Hermansky-Pudlak syndrome (lack of dense granules in platelets) exhibit mild bleeding diathesis due to defective thrombin generation [31]. Hence, detailed studies are needed to uncover the precise role of polyP in hemostasis and thrombosis.

Another endogenous macromolecule that has been implicated in the pathogenesis of thrombosis is cell-free nucleic acids (cfNAs) such as DNA [32]. cfNAs are released by cells undergoing necrotic and/or apoptotic process as well as certain strains of bacteria [32]. In addition, activation of blood cells such as neutrophils, generate web-like structures known as NETs, through a unique process called NETosis [33]. NETs entrap and kill infectious microorganisms and thus assist our immune system in its fight against infections [34]. However, recent studies show that NETs initiate pathologic thrombosis through multiple mechanisms. NET fibers are decorated with scores of prothrombotic molecules such as DNA-histone complexes (DNA acts as a scaffold for FXII activation; histones activate platelets), TF and neutrophil elastase (proteolytically cleaves and abrogates anticoagulant activity of TFPI) [35] (Fig. 2.3). Studies performed in mouse models of thrombosis show that initiation and propagation of thrombosis by NETs can be reduced by administering DNAase or RNAase; enzymes that disintegrate nucleic acid structures [36].

The pathophysiological relevance of NETs is evident from the fact that elevated plasma levels of cfNAs are observed in patients with disease conditions such as sepsis, malignancy, stroke and autoimmune disorders [34]. Furthermore, Riegger et al. report an interesting observation that thrombus from patients with stent thrombosis (ST; a rare, but, serious thrombotic complication after stent implantation) are highly heterogeneous and contain NETs [37]. This study highlights the pathophysiologic role of NETs in stent thrombosis. Based on these findings, it is evident that further studies are necessary to discover role/s of polyP and NETs in biomaterial-induced thrombosis.

2.2.4 Physiological inhibition of blood clotting

Hemostasis is a tightly controlled mechanism that comprises procoagulant and anticoagulant players. Any perturbation to this balance might lead either to thrombosis or hemorrhage. Upon injury to a blood vessel, clotting is triggered to produce fibrin clots that seal the injury site, and halt bleeding from the damaged blood vessel. However, uncontrolled clotting could generate clots that could obstruct the normal blood flow (thrombosis). Natural anticoagulant proteins act as brakes on clotting reactions and restrict clot formation to the specific site of injury. In this section, we will review actions of three major anticoagulant proteins that regulate blood coagulation.

Antithrombin (AT), a serine protease inhibitor (serpin), forms 1:1 stoichiometric complexes with serine coagulation proteases such as FIIa, FIXa, and FXa to inhibit their activity [38] (Fig. 2.4). AT is the most important physiological inhibitor of blood coagulation; inherited or acquired deficiency of AT increases risk of thrombosis [39]. To achieve maximal protease inhibition, AT requires a cofactor. Proteoglycans such as heparan sulfate expressed on the surface of endothelium and in the subendothelial

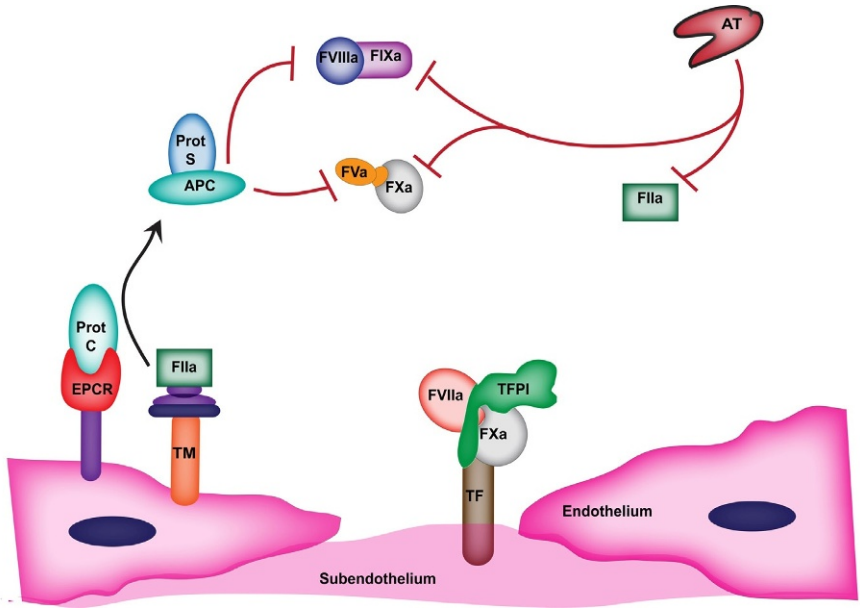


Fig. 2.4 Physiologic inhibitors of blood clotting. To maintain normal blood flow in the vasculature there are inhibitors of the clotting cascade. The most important anticoagulant protein is a serine protease inhibitor, antithrombin (AT). AT inhibits mainly FIXa, FXa, and thrombin. However, AT requires a cofactor for complete inhibitory activity. Proteoglycans such as heparan sulfate expressed on endothelial surface, bind AT and induce conformational change on AT thus acting as an endogenous cofactor of AT. Activated protein C (APC) along with its cofactor protein S inhibits the activity of FVIII and FVa, respectively. Thrombin is the key protease involved in the protein C activation pathway. Thrombin loses its procoagulant activity when it binds thrombomodulin (TM). The thrombin-thrombomodulin complex (T-TM) activates protein C bound to endothelial protein C receptor (EPCR) to APC. TFPI binds TF-FVIIa-FXa complexes and inhibits their procoagulant activity.

matrix binds to AT and induce a conformational change which dramatically increases the coagulation protease inhibitory activity of AT [40]. This is also the mechanism of action for heparin-based drugs known as the indirect anticoagulants as these drugs bind to AT for anticoagulation activity [41]. Heparins are widely used for the prophylaxis and treatment of thrombosis and to avert thromboembolic complication during invasive surgical procedures such as cardiopulmonary bypass [5].

Protein C activation is an important step in the regulation of coagulation (Fig. 2.4). Like most clotting proteins, protein C is synthesized in the liver and is present in plasma at a concentration of 70 nM [42]. Thrombin is the key protease that activates protein C. Thrombin binds thrombomodulin (TM), an integral membrane protein present on the endothelium to form thrombin-thrombomodulin complex (T-TM complex) [43]. TM occupies the crucial exosite I of thrombin, and as a result, thrombin loses its procoagulant activity. The T-TM complex converts protein C into activated protein C (APC) [44]. In addition, the binding of protein C to endothelial protein C receptor

(EPCR) assists generation of APC [44]. APC along with its cofactor protein S, proteolytically cleaves FVa and FVIIIa, respectively. The clinical significance of APC is evident from the fact that a dysfunctional protein C pathway contributes to pathologic conditions such as sepsis [45].

Another important molecule that is synthesized primarily by ECs and megakaryocytes is TFPI. TFPI exists in two major isoforms: TFPIα and TFPIβ [46] (Fig. 2.4). TFPIα is the predominant isoform expressed on platelets and TFPIβ is mainly expressed on ECs. Both isoforms of TFPI binds TF-FVIIa-FXa ternary complex and inhibit TF-FVIIa and FXa through distinct mechanisms. Very recently, it has been shown that TFPIα can also inhibit the activity of prothrombinase complex assembled on platelet surfaces [47].

2.3 Mechanisms by which clinically used biomaterials induce blood clotting (thrombosis)

The interaction of biomaterials with body can initiate foreign body reactions [3]. These host reactions can cause tissue damage, acute inflammation, thrombotic complications and other host of problems [3]. Therefore, testing a biomaterial for plausible adverse reactions is an important phase in the development of biomaterials for medical use. One major adverse biological reaction observed with blood-contacting biomaterial is the activation of clotting pathway and resulting thrombus formation on its surface [48]. This is a significant clinical concern ultimately leading to functional failure of biomaterials, and may lead to vascular occlusion and infarction. Mechanisms that induce blood clotting by biomaterials are multifaceted due to crosstalk between different regulation systems present in our body such as coagulation, vascular and complement [49]. Over the years, substantial progress has been made to understand the cascade of events responsible for thrombotic complications associated with biomaterials, and the strategies to minimize these adverse events. However, the issue has not been fully resolved. In this section, we will review major events that are involved in biomaterial-associated thrombosis.

2.3.1 Role of blood cells and proteins on biomaterial surfaces

Blood is a complex biological fluid made up of plasma, cells and proteins. There are thousands of unique blood proteins and some are present at high concentrations, for instance, albumin (35–50 mg/mL) and fibrinogen (2–4 mg/mL), respectively. In addition to this, blood also contains a multitude of other organic and inorganic molecules including salts, metabolites, and polyanions such as cfNAs [50]. Upon contact with blood, blood proteins breach the blood-biomaterial interface and instantaneously get deposited on the biomaterial surface. This is fundamentally considered as the preliminary step involved in the triggering of clotting activation by biomaterials [51]. The adsorbed protein layer will then mediate adhesion and activation of blood cells such as platelets, which then amplifies the clotting reactions.

2.3.1.1 Impact of protein adsorption

The duration of exposure of biomaterials to biological fluids depends on its clinical application. For example, vascular catheters are exposed to blood for a relatively shorter time frame, whereas kidney dialyzers and tissue implants will be exposed to blood for an extended period of time [52]. Nonetheless, protein adsorption is an unavoidable process that negatively impacts the clinical utility of biomaterials [48,49]. To date, we have only limited success in developing biomaterials that can totally repel protein accumulation [53]. The adsorption of blood proteins onto a material surface is influenced by both physical and chemical properties of materials and proteins. Proteins adsorb more rapidly to hydrophobic surfaces than hydrophilic surfaces [54]. For instance, polydimethylsiloxane and polyurethane (PU) are widely used to manufacture medical devices which readily adsorb blood proteins onto their surface due to hydrophobicity [55]. Once adsorbed, proteins interact with the surface mainly through hydrophobic, dispersion, or electrostatic forces. Adsorbed proteins rapidly form a monolayer or multilayers on the surface. Consequently, the local concentration of certain proteins on a biomaterial surface is expected to be as high as 1000-fold, higher than that found in blood. However, protein adsorption on material surface is a dynamic process, where some of the adsorbed proteins are gradually replaced by other circulating proteins [56].

It is widely recognized that components of contact-clotting system (FXII, HK, and PK) adsorb to biomaterial surface, leading to thrombus generation. The positively charged lysine residues of FXII, bind to anionic hydrophilic surfaces leading to activation of FXII to FXIIa. HK serves as a cofactor and also binds to artificial surfaces and enables FXII activation [57]. However, Zhuo et al. challenge this traditional concept of contact activation by showing that hydrophobic surfaces in buffer conditions also possess the capability to activate FXII. This shows that anionic hydrophilic surface is not a prerequisite for activation of FXII, and FXII is not unique from other coagulation enzymes that readily adsorbs onto hydrophobic surfaces [58]. Nevertheless, Zhuo et al. explain that hydrophobic surfaces in plasma/blood would be less effective FXII activator compared to anionic hydrophilic surfaces, due to an effect called adsorption-dilution effect, where other abundant blood proteins would adsorb rapidly and mask the hydrophobic surface [59]. The importance of inhibition of FXII activity is demonstrated by the fact that conjugating corn trypsin inhibitor (specific FXIIa inhibitor) to PU catheters reduces its prothrombotic activity, in vitro and in vivo, respectively [60]. Hence, further studies are needed to understand how FXII show unique specificity towards artificial surfaces in blood and induce thrombus formation via the contact-clotting pathway.

2.3.1.2 Adhesion and activation of platelets

Platelets are small (1–3 μm) anucleate cells with a characteristic discoid shape. Platelets are produced by megakaryocytes in the bone marrow and released into the blood stream, where they circulate for 7–10 days. Platelets are the second abundant blood cells at an average concentration of $150–400 \times 10^9$ cells/L [61]. The primary function of platelets is to stop bleeding from injury sites. In addition, to the central role in hemostasis, they are also involved in other physiological mechanisms such as wound healing, inflammation, and immunity [62]. Upon endothelial damage, circulating platelets adhere to collagen

or von Willebrand factor (vWF) in the subendothelial matrix, mediated by adhesion receptors on platelet plasma membrane. This binding activates platelets to release bioactive molecules from their secretory granules (alpha and dense granules), leading to platelet aggregation and the generation of hemostatic platelet plug [63].

Conversely, unwanted platelet activation leads to thrombosis. It has been shown that activation of platelets adhered to protein/s on biomaterials contributes significantly towards thrombotic complications. For example, platelets adhere to plasma proteins (predominantly fibrinogen) adsorbed onto hydrophobic surfaces such as poly(2-methoxyethylacrylate), polystyrene, polysilicone, and polysulfone etc., and undergo a shape change and activation [64–67]. Even though, blood contains myriad of proteins, fibrinogen is readily adsorbed onto biomaterial surfaces, for reasons not completely understood. Platelets recognize and adhere to fibrinogen on these surfaces through its most abundant integrin receptor αIIbβ3 (GPIIb-IIIa) [63]. Adhesion leads to activation of platelets, followed by the release of procoagulant biomolecules such as adenosine diphosphate, thrombin (FIIa), polyP etc. from its storage granules which can amplify platelet activation on artificial surfaces. However, αIIbβ3 receptor must be conformationally active via inside-out signalling to bind, fibrinogen. Interestingly, αIIbβ3 even in its quiescent state is capable of mediating the binding of platelets to fibrinogen on the surface. In addition, the density of adsorbed fibrinogen as low as 7 ng cm^{-2} is enough to mediate platelet adhesion and activation [68]. Also, it has been shown that the amount of adsorbed fibrinogen is not the key determinant of platelet adhesion, but that the conformational state of bound fibrinogen dictates the adhesion process [69]. Additionally, platelets can adhere to vWF, fibronectin, and vitronectin on biomaterial surface [70].

Other blood cells that contribute towards thrombus formation on biomaterials include leukocytes, mainly neutrophils and monocytes [49]. Neutrophils play an important role in innate immunity. However, the prothrombotic property of NETs highlights the crucial role of neutrophils in the pathogenesis of thrombosis [34]. In addition, activation and subsequent degranulation of neutrophils release numerous bioactive molecules that can activate cellular components of clotting, inflammation, and vascular system [71]. Studies have shown that neutrophils can adhere to fibrinogen on the biomaterial surface, via the β_2-integrin receptor CD11b/CD18 present on neutrophils [72]. This binding activates neutrophils to undergo degranulation, leading to the release of molecules such as platelet activating factor, tumour necrosis factor (TNF) and interleukins. In addition, activated platelets express P-selectin on their surface. Leukocytes interact with activated platelets through P-selectin glycoprotein ligand −1 expressed on their surface leading to neutrophil activation [73,74].

Monocytes are also known to interact with adsorbed proteins on a biomaterial surface through its integrin receptors [75]. Activated monocytes express TF on its surface. For instance, materials that are made up of extracorporeal circuits used during CPB are known to activate monocytes leading to TF expression [76]. In addition, it has been reported that the procoagulant activity of monocytes, adhered to polyethylene terephthalate vascular grafts and polymethyl methacrylate surfaces, is due to TF expression [77]. Also, activated monocytes release inflammatory cytokines and differentiate into macrophages. Fusion of macrophages can result in the formation of

multinucleated foreign body giant cells which is capable of releasing lysosomal enzymes and peroxides. This is reported to be one of the reasons for biodegradation and failure of PU based cardiovascular implants [78,79].

2.3.1.3 Role of endothelium

The endothelium is a vital organ that acts as an interface between blood and underlying tissues. An intact and healthy endothelium is nonthrombogenic [80]. To maintain the nonthrombogenic nature of endothelium, endothelial cells (ECs) express or release molecules that can modulate coagulation, platelet reactivity and fibrinolysis (degradation of clots). As mentioned in the previous sections, ECs express anticoagulant proteins such as TM and TFPI. In addition, ECs release nitric oxide (NO) and prostacyclin which regulates platelet reactivity and vasoconstriction. Also, EC express proteins such as tissue plasminogen activator (tPA) and urokinase plasminogen activator needed for fibrinolysis [80,81].

Endothelial injury is common during implantation of biomaterial into the vasculature or during cardiovascular surgical procedures [82,83]. TF exposed upon injury, initiates the coagulation reaction via the extrinsic clotting pathway. Alongside, proinflammatory cytokines, TNFα and interleukin (IL)-6, mediates ECs activation which is characterized by upregulation of cell-surface adhesion molecules such vascular cell adhesion molecule (VCAM-1), intercellular adhesion molecule-1 (ICAM-1), and endothelial leukocyte adhesion molecule (ELAM) on ECs. This leads to adhesion of leukocytes on ECs which perpetuate inflammatory responses. Additionally, proinflammatory cytokine-mediated ECs activation inhibit expression of endothelial nitric oxide synthase (eNOS) necessary for NO synthesis. Reduced NO bioavailability diminish the nonthrombogenic nature of endothelium since NO regulate vasoconstriction, platelet aggregation, smooth muscle cell proliferation and leukocyte adhesion [84–87].

Clots formed must undergo degradation to complete the wound healing process without further tissue damage. The dissolution of clots is executed by the fibrinolytic system on the endothelium (Fig. 2.5). tPA, an important component of the fibrinolytic system is synthesized by ECs, and released into the blood. To degrade clots, tPA and plasminogen bind to lysine residues on fibrin clots. This trimolecular assembly activates plasminogen into plasmin which degrades fibrin, exposing more lysine residues. Fibrin enhances its own degradation by localizing tPA and plasminogen on its surface, thereby enhancing plasmin generation. The endothelium regulates fibrinolysis by producing plasminogen activator inhibitor-1 (PAI-1) [88,89]. Generally, it is considered that cytokine-mediated endothelial dysfunction can cause downregulation of tPA expression and upregulation of PAI-1 [90]. Interestingly, studies suggest that plasmin can initiate contact-clotting system by activating FXII, leading to the production of PK [91]. In addition, plasmin mediates complement activation in animal models of thrombosis [92]. This is an important observation considering the use of tPA to coat biomaterial for thrombolytic activity [93–95]. Unfortunately, little is known about the influence of blood-contacting biomaterials on the fibrinolytic system and its contribution to biomaterials-associated thrombosis, if any. Further studies are needed to uncover the role of fibrinolysis and thrombus development on biomaterials.

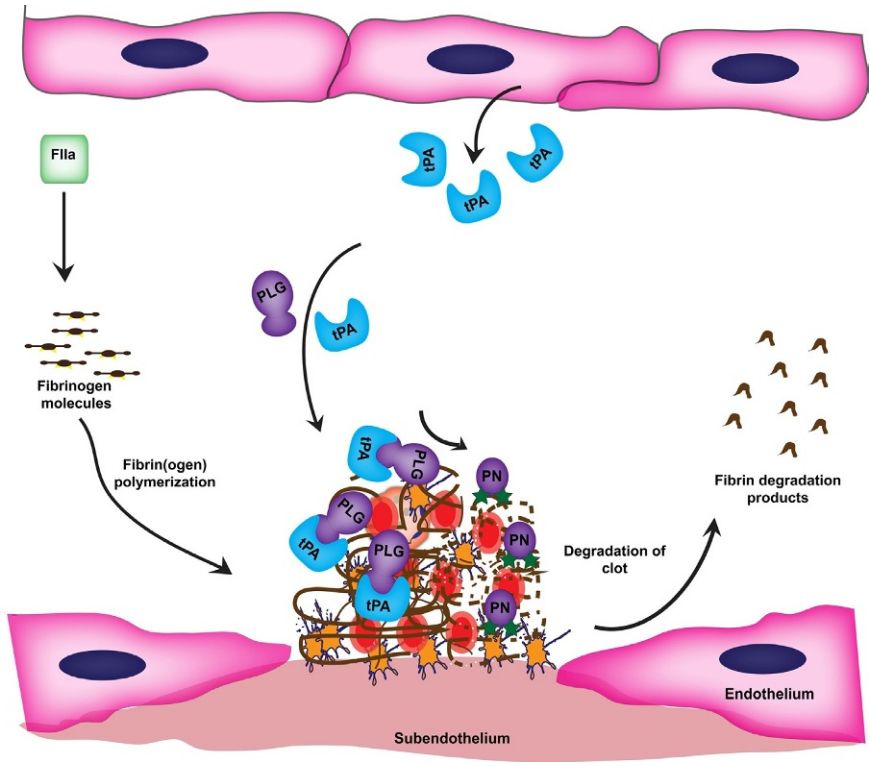


Fig. 2.5 The fibrinolytic system. Clots formed are degraded by the fibrinolytic system. Tissue plasminogen activator is the major protein involved in this pathway. It is synthesized and secreted by endothelial cells. tPA and plasminogen (PLG) bind to lysine residues of fibrin. This converts PLG into plasmin (PN) which degrades fibrin clots.

2.3.2 Activation of the complement system

The complement system, an integral component of the innate immune system helps to clear invading pathogens by their direct lysis or by promoting phagocytosis via leukocytes. The complement system is activated via the classical (CP), lectin (LP) and/or alternative (AP) pathways. CP is activated when C1 complex bind immune complexes (IgG/IgM-pathogen), whereas, LP is activated upon binding of mannose-binding lectin or ficolin to carbohydrate structures of pathogens. Carbohydrates, lipids, and proteins on foreign surfaces trigger activation of AP. Similar to other physiological players discussed in previous sections, undesirable activation of the complement system is detrimental for the host organism. Activation of complement system can occur in fluid phase (in the blood), on cell surfaces (ECs) or on the surface of a biomaterial [96–98]. It is known that complement activation can occur during cardiovascular procedures such as CPB, hemodialysis, and implantation of vascular grafts [99] leading to the production of anaphylatoxins which increases P-selectin expression on platelets, activate neutrophil and

ECs, contributing towards thrombosis [62]. In this section, we will discuss complement activation on biomaterial surfaces and crosstalk with the clotting cascade.

Generally, adsorption of plasma or complement proteins on a surface and subsequent conformational changes is considered as the initial trigger for complement activation. The most abundant complement protein C3 and immunoglobulin G (IgG) adsorb readily onto hydrophobic surfaces. This can initiate the complement activation via the AP or CP, respectively, and lead to the generation of C3a and C5a. For instance, IgG adsorbs onto methylated silicon surface and activate the complement system. Also, materials used for hemodialysis such as polysulfone could trigger complement activation and subsequent generation of C5a [98,100–102]. It has been demonstrated that C5a induce TF expression on leukocytes leading to hemodialysis-associated thrombosis [103–106]. In addition, FXIIa activates PK into kallikrein which can generate C3a and C5a without activation of the complement pathway. Moreover, coagulation proteases such as FIXa, FXa, and thrombin can activate C5 [62]. Another protein that links coagulation and complement is FVII-activating protease (FSAP). It has been shown that negatively charged polymers can activate FSAP which is then capable of cleaving C3 and C5 to generate C3a and C5a, respectively [107,108].

2.4 Summary and concluding remarks

Thrombus formation on blood-contacting implants/devices is a significant drawback as it may lead to treatment failure, device rejection, and medical complications. As discussed in previous sections, the mechanism that triggers undesirable clotting on biomaterial surface is intricate. Adsorption of plasma protein/s of contact-clotting pathway activates the intrinsic clotting pathway to generate thrombin. Proteins adsorbed are recognized by blood cells such as platelets, neutrophils and monocytes/macrophages and undergo receptor mediated-activation leading to the initiation of blood coagulation via the extrinsic and intrinsic pathways. Upon activation, these cells release prothrombotic molecules and inflammatory cytokines which can also contribute to thrombosis. Activation of the complement system and endothelial dysfunction augments the thrombotic potential of a biomaterial surface (Fig. 2.6).

Due to the involvement of multiple factors, it is challenging to develop nonthrombogenic biomaterials. However, several strategies have been adopted to reduce thrombotic events associated with medical devices. Abrogating nonspecific protein adsorption is a widely applied strategy to create nonthrombogenic biomaterials [109]. For instance, biomaterials coated with neutral polymers such as polyethylene glycol, 2-hydroxylethyl methacrylate, poly (*N*,*N*-dimethylacrylamide), or with zwitterionic polymers such as 2-methacryloyloxyethyl phosphorylcholine, poly(sulfobetaine methylacrylate) have shown to reduce protein adsorption, and display nonthrombogenic behavior [110–112]. Also, covalent conjugation of heparin, thrombomodulin, or direct thrombin inhibitors such as argatroban or hirudin onto biomaterial surface has been evaluated; but displayed limited success [113–117].

Enabling activation of fibrinolytic system on biomaterial surfaces is shown to reduce thrombus formation. For this purpose, surfaces conjugated with lysine residues

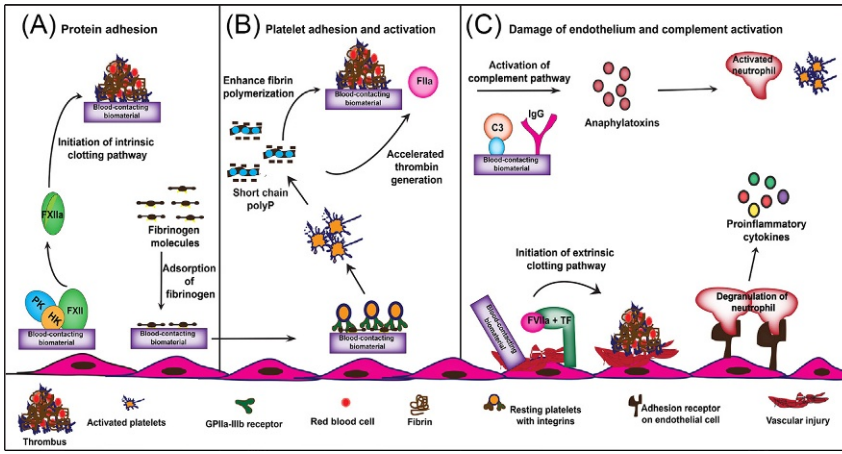


Fig. 2.6 Events leading to biomaterial-associated thrombosis. (A) Proteins of contact-clotting pathway adsorb onto blood-contacting biomaterial. This activates the intrinsic clotting cascade leading to thrombin generation. Also, fibrinogen is readily adsorbed onto the biomaterial surface. (B) Platelets bind to fibrinogen through GPIIa-IIIb receptor and undergo activation. Upon activation, platelets release numerous biomolecules from their secretory granules. For example, short chain polyP, released from dense granule, enhances thrombin generation and fibrin polymerization. (C) The introduction of biomaterials into the vasculature injures the endothelium. Injury exposes the TF expressed on the subendothelium. TF-FVIIa complex drives the extrinsic clotting pathway. In addition, activated endothelium expresses adhesion receptors such as VCAM that attracts circulating leukocytes to adhere onto the endothelium. Adhesion results in activation/degranulation of leukocytes to release potent proinflammatory cytokines such as TNFα, IL-6 etc. In addition, adsorption of protein C3 and IgG activates the complement system to release anaphylatoxins such as C5a which activates platelets and neutrophil leading to the activation of blood coagulation.

(facilitates assembly of plasminogen and tPA) were developed. For example, lysine coated PU and PDMA showed nonthrombogenic behavior by degrading clots [93]. Also, direct conjugation of tPA onto materials has been shown to be effective in degrading thrombus [118]. To emulate nonthrombogenic nature of endothelium, strategies to promote endothelialization of blood-contacting biomaterials such as implants and stents have been tested [119].

To sum up, elimination of thrombotic risk associated with biomaterials is of utmost clinical importance. Despite existing strategies to reduce the thrombogenicity of biomaterial, further studies, particularly taking into account of the role of novel prothrombotic biomolecules such as polyP and NETs are needed to create bioactive biomaterials where the blood interaction with biomaterials can be controlled.

Acknowledgments

M.T.K is supported by a Center for Blood Research graduate student award. J.N·K acknowledges funding from Canadian Institutes of Health Research and the Natural Sciences and

Engineering Council of Canada. J.N·K is a recipient of a Michael Smith Foundation for Health Research Career Scholar Award.

References

[1] N. Huebsch, D.J. Mooney, Inspiration and application in the evolution of biomaterials, Nature 462 (7272) (2009) 426–432.
[2] D.F. Williams, On the nature of biomaterials, Biomaterials 30 (30) (2009) 5897–5909.
[3] J.M. Anderson, A. Rodriguez, D.T. Chang, Foreign body reaction to biomaterials, Semin. Immunol. 20 (2) (2008) 86–100.
[4] L. Tang, W. Hu, Molecular determinants of biocompatibility, Expert Rev. Med. Devices 2 (4) (2005) 493–500.
[5] N. Mackman, Triggers, targets and treatments for thrombosis, Nature 451 (7181) (2008) 914–918.
[6] B.D. Ratner, S.J. Bryant, Biomaterials: where we have been and where we are going, Annu. Rev. Biomed. Eng. 6 (2004) 41–75.
[7] D.F. Williams, On the mechanisms of biocompatibility, Biomaterials 29 (20) (2008) 2941–2953.
[8] J. Bjorkqvist, K.F. Nickel, E. Stavrou, T. Renne, In vivo activation and functions of the protease factor XII, Thromb. Haemost. 112 (5) (2014) 868–875.
[9] J.E. Geddings, N. Mackman, New players in haemostasis and thrombosis, Thromb. Haemost. 111 (4) (2014) 570–574.
[10] H.H. Versteeg, J.W. Heemskerk, M. Levi, P.H. Reitsma, New fundamentals in hemostasis, Physiol. Rev. 93 (1) (2013) 327–358.
[11] D.M. Monroe, M. Hoffman, What does it take to make the perfect clot? Arterioscler. Thromb. Vasc. Biol. 26 (1) (2006) 41–48.
[12] B. Furie, B.C. Furie, Mechanisms of thrombus formation, N. Engl. J. Med. 359 (9) (2008) 938–949.
[13] A. Dorgalaleh, J. Rashidpanah, Blood coagulation factor XIII and factor XIII deficiency, Blood Rev. 30 (6) (2016) 461–475.
[14] D. Gailani, T. Renne, Intrinsic pathway of coagulation and arterial thrombosis, Arterioscler. Thromb. Vasc. Biol. 27 (12) (2007) 2507–2513.
[15] A.T. Long, E. Kenne, R. Jung, T.A. Fuchs, T. Renne, Contact system revisited: an interface between inflammation, coagulation, and innate immunity, J. Thromb. Haemost. 14 (3) (2016) 427–437.
[16] T. Renne, The procoagulant and proinflammatory plasma contact system, Semin. Immunopathol. 34 (1) (2012) 31–41.
[17] P.H. Bolton-Maggs, K.J. Pasi, Haemophilias A and B, Lancet 361 (9371) (2003) 1801–1809.
[18] T. Renne, A.H. Schmaier, K.F. Nickel, M. Blomback, C. Maas, In vivo roles of factor XII, Blood 120 (22) (2012) 4296–4303.
[19] R.S. Woodruff, B. Sullenger, R.C. Becker, The many faces of the contact pathway and their role in thrombosis, J. Thromb. Thrombolysis 32 (1) (2011) 9–20.
[20] A. Matafonov, P.Y. Leung, A.E. Gailani, S.L. Grach, C. Puy, Q. Cheng, et al., Factor XII inhibition reduces thrombus formation in a primate thrombosis model, Blood 123 (11) (2014) 1739–1746.
[21] M. Cushman, E.S. O'Meara, A.R. Folsom, S.R. Heckbert, Coagulation factors IX through XIII and the risk of future venous thrombosis: the longitudinal investigation of thromboembolism etiology, Blood 114 (14) (2009) 2878–2883.

[22] D. Gailani, C.E. Bane, A. Gruber, Factor XI and contact activation as targets for antithrombotic therapy, J. Thromb. Haemost. 13 (8) (2015) 1383–1395.
[23] R.S. Woodruff, Y. Xu, J. Layzer, W. Wu, M.L. Ogletree, B.A. Sullenger, Inhibiting the intrinsic pathway of coagulation with a factor XII-targeting RNA aptamer, J. Thromb. Haemost. 11 (7) (2013) 1364–1373.
[24] Y. Xu, T.Q. Cai, G. Castriota, Y. Zhou, L. Hoos, N. Jochnowitz, et al., Factor XIIa inhibition by infestin-4: in vitro mode of action and in vivo antithrombotic benefit, Thromb. Haemost. 111 (4) (2014) 694–704.
[25] J. Caen, Q. Wu, Hageman factor, platelets and polyphosphates: early history and recent connection, J. Thromb. Haemost. 8 (8) (2010) 1670–1674.
[26] J.H. Morrissey, S.H. Choi, S.A. Smith, Polyphosphate: an ancient molecule that links platelets, coagulation, and inflammation, Blood 119 (25) (2012) 5972–5979.
[27] S.A. Smith, S.H. Choi, R. Davis-Harrison, J. Huyck, J. Boettcher, C.M. Rienstra, et al., Polyphosphate exerts differential effects on blood clotting, depending on polymer size, Blood 116 (20) (2010) 4353–4359.
[28] J.H. Morrissey, Polyphosphate multi-tasks, J. Thromb. Haemost. 10 (11) (2012) 2313–2314.
[29] S.A. Smith, J.H. Morrissey, Polyphosphate enhances fibrin clot structure, Blood 112 (7) (2008) 2810–2816.
[30] N.J. Mutch, R. Engel, S. Uitte de Willige, H. Philippou, R.A. Ariens, Polyphosphate modifies the fibrin network and down-regulates fibrinolysis by attenuating binding of tPA and plasminogen to fibrin, Blood 115 (19) (2010) 3980–3988.
[31] F. Muller, N.J. Mutch, W.A. Schenk, S.A. Smith, L. Esterl, H.M. Spronk, et al., Platelet polyphosphates are proinflammatory and procoagulant mediators in vivo, Cell 139 (6) (2009) 1143–1156.
[32] T.A. Fuchs, A. Brill, D. Duerschmied, D. Schatzberg, M. Monestier, D.D. Myers Jr., et al., Extracellular DNA traps promote thrombosis, Proc. Natl. Acad. Sci. USA 107 (36) (2010) 15880–15885.
[33] M. Demers, D.D. Wagner, NETosis: a new factor in tumor progression and cancer-associated thrombosis, Semin. Thromb. Hemost. 40 (3) (2014) 277–283.
[34] O.E. Sorensen, N. Borregaard, Neutrophil extracellular traps-the dark side of neutrophils, J. Clin. Invest. 126 (5) (2016) 1612–1620.
[35] K. Martinod, D.D. Wagner, Thrombosis: tangled up in NETs, Blood 123 (18) (2014) 2768–2776.
[36] A. Brill, T.A. Fuchs, A.S. Savchenko, G.M. Thomas, K. Martinod, S.F. De Meyer, et al., Neutrophil extracellular traps promote deep vein thrombosis in mice, J. Thromb. Haemost. 10 (1) (2012) 136–144.
[37] J. Riegger, R.A. Byrne, M. Joner, S. Chandraratne, A.H. Gershlick, J.M. Ten Berg, et al., Histopathological evaluation of thrombus in patients presenting with stent thrombosis. A multicenter european study: a report of the prevention of late stent thrombosis by an interdisciplinary global european effort consortium, Eur. Heart J. 37 (19) (2016) 1538–1549.
[38] P.S. Maclean, R.C. Tait, Hereditary and acquired antithrombin deficiency: epidemiology, pathogenesis and treatment options, Drugs 67 (10) (2007) 1429–1440.
[39] M.M. Patnaik, S. Moll, Inherited antithrombin deficiency: a review, Haemophilia 14 (6) (2008) 1229–1239.
[40] J.I. Weitz, Heparan sulfate: antithrombotic or not? J. Clin. Invest. 111 (7) (2003) 952–954.
[41] L. Jin, J.P. Abrahams, R. Skinner, M. Petitou, R.N. Pike, R.W. Carrell, The anticoagulant activation of antithrombin by heparin, Proc. Natl. Acad. Sci. USA 94 (26) (1997) 14683–14688.

[42] J.H. Griffin, B.V. Zlokovic, L.O. Mosnier, Protein C anticoagulant and cytoprotective pathways, Int. J. Hematol. 95 (4) (2012) 333–345.
[43] W.C. Aird, Natural anticoagulant inhibitors: activated protein C, Best Pract. Res. Clin. Haematol. 17 (1) (2004) 161–182.
[44] C.T. Esmon, The protein C pathway, Chest 124 (3 Supplement) (2003) 26S–32S.
[45] S.N. Faust, M. Levin, O.B. Harrison, R.D. Goldin, M.S. Lockhart, S. Kondaveeti, et al., Dysfunction of endothelial protein C activation in severe meningococcal sepsis, N. Engl. J. Med. 345 (6) (2001) 408–416.
[46] J.P. Wood, P.E. Ellery, S.A. Maroney, A.E. Mast, Biology of tissue factor pathway inhibitor, Blood 123 (19) (2014) 2934–2943.
[47] J.P. Wood, M.W. Bunce, S.A. Maroney, P.B. Tracy, R.M. Camire, A.E. Mast, Tissue factor pathway inhibitor-alpha inhibits prothrombinase during the initiation of blood coagulation, Proc. Natl. Acad. Sci. USA 110 (44) (2013) 17838–17843.
[48] I.H. Jaffer, J.C. Fredenburgh, J. Hirsh, J.I. Weitz, Medical device-induced thrombosis: what causes it and how can we prevent it? J. Thromb. Haemost. 13 (Suppl. 1) (2015) S72–S81.
[49] M.B. Gorbet, M.V. Sefton, Biomaterial-associated thrombosis: roles of coagulation factors, complement, platelets and leukocytes, Biomaterials 25 (26) (2004) 5681–5703.
[50] N.L. Anderson, M. Polanski, R. Pieper, T. Gatlin, R.S. Tirumalai, T.P. Conrads, et al., The human plasma proteome: a nonredundant list developed by combination of four separate sources, Mol. Cell. Proteomics 3 (4) (2004) 311–326.
[51] K.C. Dee, D.A. Puleo, R. Bizios, Blood-biomaterial interactions and coagulation, in: An Introduction to Tissue-Biomaterial Interactions, John Wiley & Sons, New York, USA, 2002; 2003, pp. 53–88.
[52] A.S. Hoffmann, Blood—biomaterial interactions: an overview, in: Biomaterials: Interfacial Phenomena and Applications, Advances in Chemistry, American Chemical Society, Washington, DC, 1982, pp. 3–8.
[53] B.D. Ratner, The catastrophe revisited: blood compatibility in the 21st century, Biomaterials 28 (34) (2007) 5144–5147.
[54] M. Rabe, D. Verdes, S. Seeger, Understanding protein adsorption phenomena at solid surfaces, Adv. Colloid Interf. Sci. 162 (1–2) (2011) 87–106.
[55] L. Xu, C.A. Siedlecki, Effects of surface wettability and contact time on protein adhesion to biomaterial surfaces, Biomaterials 28 (22) (2007) 3273–3283.
[56] H. Noh, E.A. Vogler, Volumetric interpretation of protein adsorption: competition from mixtures and the vroman effect, Biomaterials 28 (3) (2007) 405–422.
[57] R. Zhuo, R. Miller, K.M. Bussard, C.A. Siedlecki, E.A. Vogler, Procoagulant stimulus processing by the intrinsic pathway of blood plasma coagulation, Biomaterials 26 (16) (2005) 2965–2973.
[58] E.A. Vogler, C.A. Siedlecki, Contact activation of blood-plasma coagulation, Biomaterials 30 (10) (2009) 1857–1869.
[59] R. Zhuo, C.A. Siedlecki, E.A. Vogler, Autoactivation of blood factor XII at hydrophilic and hydrophobic surfaces, Biomaterials 27 (24) (2006) 4325–4332.
[60] J.W. Yau, A.R. Stafford, P. Liao, J.C. Fredenburgh, R. Roberts, J.L. Brash, et al., Corn trypsin inhibitor coating attenuates the prothrombotic properties of catheters in vitro and in vivo, Acta Biomater. 8 (11) (2012) 4092–4100.
[61] M. Leslie, Cell biology. Beyond clotting: the powers of platelets, Science 328 (5978) (2010) 562–564.
[62] O.A. Hamad, J. Back, P.H. Nilsson, B. Nilsson, K.N. Ekdahl, Platelets, complement, and contact activation: partners in inflammation and thrombosis, Adv. Exp. Med. Biol. 946 (2012) 185–205.

[63] E.M. Golebiewska, A.W. Poole, Platelet secretion: from haemostasis to wound healing and beyond, Blood Rev. 29 (3) (2015) 153–162.
[64] A. Higuchi, K. Sugiyama, B.O. Yoon, M. Sakurai, M. Hara, M. Sumita, et al., Serum protein adsorption and platelet adhesion on pluronic-adsorbed polysulfone membranes, Biomaterials 24 (19) (2003) 3235–3245.
[65] B. Shenkman, N. Savion, R. Dardik, I. Tamarin, D. Varon, Testing of platelet deposition on polystyrene surface under flow conditions by the cone and plate (let) analyzer: role of platelet activation, fibrinogen and von willebrand factor, Thromb. Res. 99 (4) (2000) 353–361.
[66] M. Tanaka, T. Motomura, M. Kawada, T. Anzai, Y. Kasori, T. Shiroya, et al., Blood compatible aspects of poly(2-methoxyethylacrylate) (PMEA)—relationship between protein adsorption and platelet adhesion on PMEA surface, Biomaterials 21 (14) (2000) 1471–1481.
[67] Y. Wu, F.I. Simonovsky, B.D. Ratner, T.A. Horbett, The role of adsorbed fibrinogen in platelet adhesion to polyurethane surfaces: a comparison of surface hydrophobicity, protein adsorption, monoclonal antibody binding, and platelet adhesion, J. Biomed. Mater. Res. A 74 (4) (2005) 722–738.
[68] B. Savage, Z.M. Ruggeri, Selective recognition of adhesive sites in surface-bound fibrinogen by glycoprotein IIb-IIIa on nonactivated platelets, J. Biol. Chem. 266 (17) (1991) 11227–11233.
[69] B. Sivaraman, R.A. Latour, The relationship between platelet adhesion on surfaces and the structure versus the amount of adsorbed fibrinogen, Biomaterials 31 (5) (2010) 832–839.
[70] J.M. Grunkemeier, W.B. Tsai, C.D. McFarland, T.A. Horbett, The effect of adsorbed fibrinogen, fibronectin, von willebrand factor and vitronectin on the procoagulant state of adherent platelets, Biomaterials 21 (22) (2000) 2243–2252.
[71] T.N. Mayadas, X. Cullere, C.A. Lowell, The multifaceted functions of neutrophils, Annu. Rev. Pathol. 9 (2014) 181–218.
[72] J.N. Barbosa, M.A. Barbosa, A.P. Águas, Adhesion of human leukocytes to biomaterials: an in vitro study using alkanethiolate monolayers with different chemically functionalized surfaces, J. Biomed. Mater. Res. A 65A (4) (2003) 429–434.
[73] C. Rubel, G.C. Fernandez, G. Dran, M.B. Bompadre, M.A. Isturiz, M.S. Palermo, Fibrinogen promotes neutrophil activation and delays apoptosis, J. Immunol. 166 (3) (2001) 2002–2010.
[74] F.W. Lam, K.V. Vijayan, R.E. Rumbaut, Platelets and their interactions with other immune cells, Compr Physiol. 5 (2015) 1265–1280.
[75] A.J. García, Get a grip: integrins in cell–biomaterial interactions, Biomaterials 26 (36) (2005) 7525–7529.
[76] M. Ernofsson, S. Thelin, A. Siegbahn, Monocyte tissue factor expression, cell activation, and thrombin formation during cardiopulmonary bypass: a clinical study, J. Thorac. Cardiovasc. Surg. 113 (3) (1997) 576–584.
[77] P.G. Kalman, O.D. Rotstein, J. Niven, M.F.X. Glynn, A.D. Romaschin, Differential stimulation of macrophage procoagulant activity by vascular grafts, J. Vasc. Surg. 17 (3) (1993) 531–536.
[78] M. Shen, I. Garcia, R.V. Maier, T.A. Horbett, Effects of adsorbed proteins and surface chemistry on foreign body giant cell formation, tumor necrosis factor alpha release and procoagulant activity of monocytes, J. Biomed. Mater. Res. A 70 (4) (2004) 533–541.
[79] Q. Zhao, N. Topham, J.M. Anderson, A. Hiltner, G. Lodoen, C.R. Payet, Foreign-body giant cells and polyurethane biostability: in vivo correlation of cell adhesion and surface cracking, J. Biomed. Mater. Res. 25 (2) (1991) 177–183.

[80] A. Lerman, A.M. Zeiher, Endothelial function: cardiac events, Circulation 111 (3) (2005) 363–368.
[81] J.W. Yau, H. Teoh, S. Verma, Endothelial cell control of thrombosis, BMC Cardiovasc. Disord. 15 (2015) 130.
[82] A.P. McGuigan, M.V. Sefton, The influence of biomaterials on endothelial cell thrombogenicity, Biomaterials 28 (16) (2007) 2547–2571.
[83] B. Tesfamariam, Platelet function in intravascular device implant-induced intimal injury, Cardiovasc. Revasc. Med. 9 (2) (2008) 78–87.
[84] M.E. Widlansky, N. Gokce, J.F. Keaney Jr., J.A. Vita, The clinical implications of endothelial dysfunction, J. Am. Coll. Cardiol. 42 (7) (2003) 1149–1160.
[85] H.A. Hadi, C.S. Carr, J. Al Suwaidi, Endothelial dysfunction: cardiovascular risk factors, therapy, and outcome, Vasc. Health Risk Manag. 1 (3) (2005) 183–198.
[86] B.J. Hunt, K.M. Jurd, Endothelial cell activation. A central pathophysiological process, BMJ 316 (7141) (1998) 1328–1329.
[87] Z. Yang, Y. Yang, K. Xiong, X. Li, P. Qi, Q. Tu, et al., Nitric oxide producing coating mimicking endothelium function for multifunctional vascular stents, Biomaterials 63 (2015) 80–92.
[88] J.C. Chapin, K.A. Hajjar, Fibrinolysis and the control of blood coagulation, Blood Rev. 29 (1) (2015) 17–24.
[89] G. Lippi, C. Mattiuzzi, E.J. Favaloro, Novel and emerging therapies: thrombus-targeted fibrinolysis, Semin. Thromb. Hemost. 39 (1) (2013) 48–58.
[90] T. Keller, Infections and endothelial cells, Cardiovasc. Res. 60 (1) (2003) 40–48.
[91] G.A. Ewald, P.R. Eisenberg, Plasmin-mediated activation of contact system in response to pharmacological thrombolysis, Circulation 91 (1) (1995) 28–36.
[92] J.H. Foley, B.L. Walton, M.M. Aleman, A.M. O'Byrne, V. Lei, M. Harrasser, et al., Complement activation in arterial and venous thrombosis is mediated by plasmin, EBioMedicine 5 (2016) 175–182.
[93] D. Li, H. Chen, J.L. Brash, Mimicking the fibrinolytic system on material surfaces, Colloids Surf. B: Biointerfaces 86 (1) (2011) 1–6.
[94] K.A. Woodhouse, J.I. Weitz, J.L. Brash, Lysis of surface-localized fibrin clots by adsorbed plasminogen in the presence of tissue plasminogen activator, Biomaterials 17 (1) (1996) 75–77.
[95] Z. Wu, H. Chen, D. Li, J.L. Brash, Tissue plasminogen activator-containing polyurethane surfaces for fibrinolytic activity, Acta Biomater. 7 (5) (2011) 1993–1998.
[96] D. Ricklin, G. Hajishengallis, K. Yang, J.D. Lambris, Complement: a key system for immune surveillance and homeostasis, Nat. Immunol. 11 (9) (2010) 785–797.
[97] U. Amara, D. Rittirsch, M. Flierl, U. Bruckner, A. Klos, F. Gebhard, et al., Interaction between the coagulation and complement system, Adv. Exp. Med. Biol. 632 (2008) 71–79.
[98] A.E. Engberg, J.P. Rosengren-Holmberg, H. Chen, B. Nilsson, J.D. Lambris, I.A. Nicholls, et al., Blood protein-polymer adsorption: implications for understanding complement-mediated hemoincompatibility, J. Biomed. Mater. Res. A 97 (1) (2011) 74–84.
[99] P. Bruins, H. te Velthuis, A.P. Yazdanbakhsh, P.G. Jansen, F.W. van Hardevelt, E.M. de Beaumont, et al., Activation of the complement system during and after cardiopulmonary bypass surgery: postsurgery activation involves C-reactive protein and is associated with postoperative arrhythmia, Circulation 96 (10) (1997) 3542–3548.
[100] J. Andersson, K.N. Ekdahl, J.D. Lambris, B. Nilsson, Binding of C3 fragments on top of adsorbed plasma proteins during complement activation on a model biomaterial surface, Biomaterials 26 (13) (2005) 1477–1485.

[101] J. Andersson, K.N. Ekdahl, R. Larsson, U.R. Nilsson, B. Nilsson, C3 adsorbed to a polymer surface can form an initiating alternative pathway convertase, J. Immunol. 168 (11) (2002) 5786–5791.
[102] B. Nilsson, K. Nilsson Ekdahl, The tick-over theory revisited: is C3 a contact-activated protein? Immunobiology 217 (11) (2012) 1106–1110.
[103] P. Tengvall, A. Askendal, I.I. Lundstrom, Ellipsometric in vitro studies on the activation of complement by human immunoglobulins M and G after adsorption to methylated silicon, Colloids Surf. B: Biointerfaces 20 (1) (2001) 51–62.
[104] K. Ikeda, K. Nagasawa, T. Horiuchi, T. Tsuru, H. Nishizaka, Y. Niho, C5a induces tissue factor activity on endothelial cells, Thromb. Haemost. 77 (2) (1997) 394–398.
[105] I. Kourtzelis, M.M. Markiewski, M. Doumas, S. Rafail, K. Kambas, I. Mitroulis, et al., Complement anaphylatoxin C5a contributes to hemodialysis-associated thrombosis, Blood 116 (4) (2010) 631–639.
[106] K. Lhotta, R. Wurzner, F. Kronenberg, M. Oppermann, P. Konig, Rapid activation of the complement system by cuprophane depends on complement component C4, Kidney Int. 53 (4) (1998) 1044–1051.
[107] S.M. Kanse, A. Gallenmueller, S. Zeerleder, F. Stephan, O. Rannou, S. Denk, et al., Factor VII-activating protease is activated in multiple trauma patients and generates anaphylatoxin C5a, J. Immunol. 188 (6) (2012) 2858–2865.
[108] L. Muhl, S.P. Galuska, K. Oorni, L. Hernandez-Ruiz, L.C. Andrei-Selmer, R. Geyer, et al., High negative charge-to-size ratio in polyphosphates and heparin regulates factor VII-activating protease, FEBS J. 276 (17) (2009) 4828–4839.
[109] S. Chen, L. Li, C. Zhao, J. Zheng, Surface hydration: principles and applications toward low-fouling/nonfouling biomaterials, Polymer 51 (23) (2010) 5283–5293.
[110] W. Feng, S. Zhu, K. Ishihara, J.L. Brash, Adsorption of fibrinogen and lysozyme on silicon grafted with poly(2-methacryloyloxyethyl phosphorylcholine) via surface-initiated atom transfer radical polymerization, Langmuir 21 (13) (2005) 5980–5987.
[111] P.A. George, B.C. Donose, J.J. Cooper-White, Self-assembling polystyrene-block-poly(ethylene oxide) copolymer surface coatings: resistance to protein and cell adhesion, Biomaterials 30 (13) (2009) 2449–2456.
[112] J.H. Park, Y.H. Bae, Hydrogels based on poly(ethylene oxide) and poly(tetramethylene oxide) or poly(dimethyl siloxane): synthesis, characterization, in vitro protein adsorption and platelet adhesion, Biomaterials 23 (8) (2002) 1797–1808.
[113] K.N. Sask, L.R. Berry, A.K. Chan, J.L. Brash, Modification of polyurethane surface with an antithrombin-heparin complex for blood contact: influence of molecular weight of polyethylene oxide used as a linker/spacer, Langmuir 28 (4) (2012) 2099–2106.
[114] J. Deng, X. Liu, L. Ma, C. Cheng, W. Shi, C. Nie, et al., Heparin-mimicking multilayer coating on polymeric membrane via LbL assembly of cyclodextrin-based supramolecules, ACS Appl. Mater. Interfaces 6 (23) (2014) 21603–21614.
[115] Y. Nakayama, S. Yamaoka, M. Yamanami, M. Fujiwara, M. Uechi, K. Takamizawa, et al., Water-soluble argatroban for antithrombogenic surface coating of tissue-engineered cardiovascular tissues, J. Biomed. Mater. Res. B Appl. Biomater. 99 (2) (2011) 420–430.
[116] M.C. Wyers, M.D. Phaneuf, E.M. Rzucidlo, M.A. Contreras, F.W. LoGerfo, W.C. Quist, In vivo assessment of a novel dacron surface with covalently bound recombinant hirudin, Cardiovasc. Pathol. 8 (3) (1999) 153–159.
[117] H.Y. Yeh, J.C. Lin, Bioactivity and platelet adhesion study of a human thrombomodulin-immobilized nitinol surface, J. Biomater. Sci. Polym. Ed. 20 (5–6) (2009) 807–819.

[118] Y.H. Ma, S.Y. Wu, T. Wu, Y.J. Chang, M.Y. Hua, J.P. Chen, Magnetically targeted thrombolysis with recombinant tissue plasminogen activator bound to polyacrylic acid-coated nanoparticles, Biomaterials 30 (19) (2009) 3343–3351.

[119] T. Liu, S. Liu, K. Zhang, J. Chen, N. Huang, Endothelialization of implanted cardiovascular biomaterial surfaces: the development from in vitro to in vivo, J. Biomed. Mater. Res. A 102 (10) (2014) 3754–3772.

This page intentionally left blank

Developing standards and test protocols for testing the hemocompatibility of biomaterials

3

S. Braune, A. Lendlein, F. Jung
Institute of Biomaterial Science and Berlin-Brandenburg Center for Regenerative Therapies, Teltow, Germany

3.1 Introduction

Morbidity and mortality due to atherosclerotic diseases are still increasing as a consequence of an aging society, a decrease of physical activity, changed diet habits, and the growing incidence of somatic cardiovascular risk factors like diabetes mellitus [1–3]. This in turn, leads also to an increase of revascularization procedures. When veins for autologous arterial by-passes [4] cannot be obtained, the implantation of synthetic vascular grafts in polyethylene terephthalate (Dacron) or expanded polytetrafluoroethylene is the method of choice. Such polymeric grafts are successful in replacing large diameter vessels, but they fail in small diameters (<6 mm) [5–7], most likely due to thrombotic occlusion [8,9]. The current control of thrombus formation in patients with cardiovascular implants generally requires a systemic anticoagulation or dual antiplatelet therapy, which is clearly not ideal, due to associated adverse effects, such as thrombocytopenia, neutropenia, or haemorrhage [10]. Therefore the development of a biomaterial that offers improved—if not perfect—hemocompatibility is still a clinical need.

Key elements of the blood-biomaterial interactions are platelets—specialized fragments of megakaryocytes—that play central roles in the process of thrombus formation [11]. Therefore, the interaction of platelets with the surface of blood contacting biomaterials is the key for understanding the thrombogenicity of a material [12–14]. Thrombogenicity is still not clearly defined, but at least comprises the activation, secretion, adherence and aggregation of further platelets. This process is influenced by several factors: Surface properties such as availability of certain functional groups, domain structure, surface electrical charge, hydrophilicity/hydrophobicity, linker molecules, interfacial adaptability, or surface roughness are considered to determine the adherence and conformation of proteins and platelets [15–18]. Depending on the composition of the adsorbed protein layer, the conformation of the proteins and the shear rate of the local blood flow, passing platelets can adhere (according to the shear rates different plasma proteins mediate the platelet adhesion [19] via different platelet membrane receptors [20]). This initiates abruptly an activation process so that the aggregation of further platelets occurs including also other blood cells and ending up in thrombus growth. In arteries, the bulk of the thrombus often seems

Hemocompatibility of Biomaterials for Clinical Applications. https://doi.org/10.1016/B978-0-08-100497-5.00004-5
© 2018 Elsevier Ltd. All rights reserved.

to be a mass of platelets, the so called white clot [21,22]. Of all possible complications of polymer-blood interactions, thrombus formation is considered to be the earliest and most frequent unwanted result [23]. Thrombi are able to occlude vessels, especially in the vicinity of implants, or detach and form emboli, possibly leading to life-threatening events. Thrombogenicity represents the most common cause of graft failure and of acute or late stent thrombosis [24,25].

While material-induced activation of platelets is a very rapid process (ca. 180 ms), the stable adherence of proteins and platelets on implanted materials is in the order of seconds. The subsequent activation of the coagulation cascade with fibrin polymerization takes at least 30 s and the formation of a stable clot 3 to 5 min [26–29]. Certain materials can also involve the contact activation and the complement system [30,31]. In a very short period of time, platelet activation and the so called "contact activation" occur where high molecular weight kininogen and the activated factor XII interact and generate bradykinin. This will further enhance the activation of the coagulation cascade also implying the activation of the complement system. More or less generalized complement activation can have serious consequences due to the reduced removal of antibody complexes, which generally need complement decoration for their elimination. And there are more mechanisms to burden the immune system besides the lack of complement. For example, degradation products from polymers can become coupled to haptens and lead to immune reactions. This very complex process of different interactions and feedback loops can be defined as hemocompatibility of biomaterials.

In this chapter we discuss how defining common references and test protocol standards enables diagnostically conclusive interstudy/lab comparisons, which may enable an enhanced systematic and knowledge-based approach for finding improved hemocompatible biomaterials for cardiovascular applications.

3.2 Requirements for a reproducible and standardized in vitro testing

To fulfill minimum requirements necessary for a standardized approach, the thrombogenicity/hemocompatibility of biomaterials for cardiovascular devices has to be evaluated conforming the ISO norm 10,993 (Biological evaluation of medical devices) Part 4 (Selection of tests for interactions with blood) and Part 5 (Tests for in vitro cytotoxicity). In the following paragraphs we discuss how the standards depicted by the regulatory agencies can be applied and supplemented in view of: the preparation of material samples (e.g., cleaning and sterilization, reference materials), selection of blood donors, preparation and aging of blood samples, and the standardization of in vitro test protocols.

3.2.1 Preparation of materials for in vitro testing

Synthesis and formation of biomaterials for medical applications require an appropriate preparation, which can be realized, e.g., by working under clean-room conditions with approved endotoxin low/free starting materials [32].

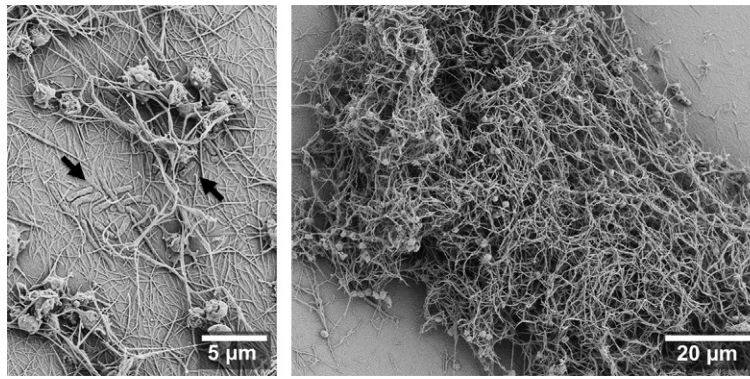


Fig. 3.1 Scanning electron microscopic (SEM) images of platelet adhesion and activation on a bacterial contaminated polymer (left) as well as the resulting 3D-fibrin mesh with single platelets (right). Material surface adherent bacteria are representatively marked by *black arrows*.

Appropriate washing/cleaning after these processes is a further requirement, which is necessary to remove unwanted chemical residues, such as cytotoxic reaction-initiators, unreacted monomers, and intermediate- or by-products of the synthesis or solvents. Sterilization of the materials is mandatory and should be approved, not to influence physical or chemical properties of the bulk or the surface [33]. Prior to any biological evaluation, the load of soluble and adherent endotoxins has to be tested ($< 0.5\,\mathrm{EU}\cdot\mathrm{mL}^{-1}$) in order to exclude that bacterial contaminations cause material-unspecific interactions with blood proteins or blood cells [32,34,35].

The testing of the endotoxin load is of utmost importance because endotoxins can lead to an activation of platelets and other blood cells (Fig. 3.1), which has nothing to do with the material-induced activation which can lead to false negative results [36–40]. Indirect and direct cytotoxicity tests should be performed according to the ISO 10993-5 norm to ensure that the candidate material does not cause a deterioration of the mitochondrial activity, of the integrity of the cell membrane or even necrosis or apoptosis [41].

3.2.2 Reference materials

Though the principles of thrombogenicity/hemocompatibility testing have been established in ISO 10993-4, they are generally considered as minimum requirements, and most groups perform supplementary tests. Moreover, the thrombogenicity or hemocompatibility of a material is not a defined physical quantity with an absolute value. Both characteristics can only be evaluated or classified with reference to known thrombogenic or hemocompatible surfaces. Using such an approach, the materials studied can be categorized between these two extremes [42]. Reference materials may also be useful in identifying test procedures which are most sensitive to describe thrombogenic materials or hemocompatible materials. The National Heart, Lung, and Blood Institute called for more reliable approaches to the study of biomaterials and their interactions

with blood in 1977. Three primary reference materials were selected for immediate testing: low-density polyethylene, silica-free polydimethylsiloxane, and fluorinated ethylene propylene. By 1980, recommendations for standardized methods and materials were published [43,44]. In the early 1990s, the International Union for Pure and Applied Chemistry (IUPAC) started a second inititative "Interactions of Polymers with Living Systems." The main topics were: (1) the interactions of materials with blood; (2) biocompatibility and inflammation; and (3) in vivo studies. Unfortunately, the results of these studies were never published. In 1992, the publication of the book "The reference materials of the European communities: results of hemocompatibility tests" continued a number of publications released by the European Concerted Action "EUROBIOMAT—Hemocompatibility"(Medical Research Program, Project: II.1.2/2, supported from 1988 to 1992) [45]. Despite these valuable efforts, many current research projects do not include reference materials or methods suggested in these earlier consensus initiatives, which also indicates that they may not represent state of the art technology.

3.2.3 Anticoagulation

To avoid uncontrolled coagulation during the collection of blood, its preparation and the in vitro test procedure, anticoagulation of the samples is inevitable. The choice of the appropriate anticoagulant for the study depends on various aspects that comprise:

- The scientific question of the study—basic research on, e.g., new concepts on how to improve certain blood-material interactions or comprehensive evaluation of the hemo- and immunocompatibility of advanced materials for a defined clinical application.
- The aimed application of the tested material and its clinical background—e.g., systemic anticoagulation of the patient or local anticoagulation of an extracorporeal device.
- The tested blood specimen [whole blood, platelet rich plasma (PRP) or platelet poor plasma (PPP)] and the targeted analyte (proteins or cells), which should maintain appropriately functional.

Tri-sodium citrate, heparin, and hirudin represent the most frequently applied anticoagulants in studies utilizing fresh human blood for evaluating the thrombogenicity/hemocompatibility of biomaterials in vitro [14,46]. The determination and standardization of an appropriate anticoagulation, which allows balancing the inhibition of coagulation processes and appropriate function of blood cells/components, is still a matter of concern that is based on the kind of anticoagulant as well as its concentration. Heparin, for instance, is widely used in whole blood test systems, since it is applied in a broad variety of therapeutic treatments with systemic anticoagulation [47–51]. As a consequence, different functional forms (e.g., unfractionated heparin and low molecular weight heparins) as well as markedly varying concentrations (e.g., from 0.5 to 5 IU heparin per mL blood) are applied for in vitro hemocompatibility studies, which hinders interlaboratory and interstudy comparisons [52–57]. Certain limitations have been reported and have to be considered when heparin is applied for in vitro studies: its potential to induce platelet activation and thrombocytopenia (HIT), the impaired inhibition of prothrombinase-bound Factor Xa and fibrin/material bound thrombin [58–61]. While early stages platelet-material interactions are not affected by

this, the suppressed thrombin activity might lead to an inhibited thrombus formation. Standardization is also lacking for hirudin, despite its very recent utilization in whole blood platelet aggregometry (Multiplate Analyzer, Roche, Mannheim, Germany) and principal evaluations on its efficiency for in vitro hemocompatibility tests [62,63]. However, in the last few years, hirudin has been established as appropriate anticoagulant for studying interactions of biomaterial surfaces and the complement system [64–66]. Clear recommendations exist for the use of tri-sodium citrate as anticoagulant (0.105–0.109 and 0.129 M tri-sodium citrate) for a range of clinical routine tests based on PRP and PPP (e.g., platelet function, global, or local tests) [67–69]. These guidelines should be followed when studying the molecular basics of platelet-material interactions and evaluating the material's thrombogenicity. Furthermore, citrate is also recommended as one of the anticoagulants suited for hemolysis testing in whole blood. Ethylene diamine tetra-acetic acid (EDTA) should not be applied in thrombogenicity studies, since it causes conformational changes in the GPIIb/IIIa receptor of platelets and inhibits platelet aggregation as well as material-induced thrombus growth [70,71]. This functionality, however, is utilized for counting single circulating platelets as an indirect marker for the retention of platelets on biomaterial surfaces [72]. Recommendations for dipotassium or tripotassium EDTA concentrations range from 1.5 to 2.2 $g \cdot L^{-1}$ [73–75]. Platelet morphology is strongly time-dependent in EDTA anticoagulated blood, and parameters such as the mean platelet volume (MPV) vary significantly if measurements are not performed at fixed time points. A rather rare phenomenon is the EDTA-dependent in vitro pseudothrombocytopenia. Here, aggregation of platelets and the formation of platelet-leucocytes aggregates can lead to an artificially low platelet count [76]. More recently, EDTA was suggested as anticoagulant for studying the adsorption of various proteins from human blood plasma to polymer particles [65].

Today, international guidelines that determine appropriate anticoagulants and the respective concentrations utilized to test the hemocompatibility of biomaterials are missing. Following the recommendations for routine testing of coagulation and cellular parameters provides one suitable approach. Applying anticoagulant and the respective concentration similarly to the clinical setting might be another. However, these parameters need to be defined clearly in order to enable a valid comparison of materials evaluated in different studies and institutions.

3.2.4 Donor selection and stratification

The application of sources other than freshly drawn human blood should be carefully reviewed and reconsidered for each approach. In platelet concentrates or fresh frozen plasma, for instance, a significant number of analytes undergo changes during the processing (e.g., cooling or freezing) and with increasing storage time. The preparation- and time-dependent functional loss is particularly described for platelets (adhesion and aggregation) as well as for coagulation factors V and VIII [77–81]. Also influences on the activated partial thromboplastin time (APTT) and prothrombin time (PT) have been previously reported [82]. The utilization of blood samples with altered or inhibited analyte function may consequently lead to a false evaluation of the

material's hemocompatibility, such as an underestimated thrombogenicity, if platelets from platelet concentrates are applied that exhibit a reduced ability to adhere and aggregate [83,84].

To enable standardized testing with sufficiently functional blood cells/components, hemocompatibility studies should be conducted with blood from apparently healthy subjects in accordance with the criteria for reference values in laboratory medicine [85]. Prior to the blood withdrawal, donors should be questioned concerning known diseases, medication, nutrition, and physical activity. In order to achieve a sufficient standardization, subjects should be excluded if any of the latter is categorized to influence haemostasis, such as allergies or diabetes, use of platelet function inhibitors (e.g., aspirin) or excessive consumption of spicy food, dark chocolate, garlic, or long distance running [86–92].

To characterize the donor prior to the material testing, pre-analytical tests should be carried out stringently. Analysis should at least include a small haemogram, acute-phase protein (e.g., CRP) determination and, particularly for thrombogenicity studies, spontaneous/induced platelet function testing. An example of an analysis is given in Table 3.1. Because of the high interindividual variability of many analytes (e.g., platelet reactivity), at least $n = 10$ donors should be included for in vitro hemocompatibility studies of biomaterials. At an advanced stage of material or medical device development, tests should also be carried out with blood from the designated patient group [93]. These analyses are crucial for understanding how the disease, associated comorbidities, and also the applied medication may influence the material properties and the blood cells/components-material interactions. The importance of this approach was recently proven in a pilot study which confirmed that the adhesion and activation of platelets from subjects with coronary artery disease was significantly increased compared to apparently healthy individuals on different reference biomaterials such as medical grade PTFE and silicone [94].

3.2.5 Blood collection, preparation, and storage

In order to avoid an undesired activation and clotting during the collection and preparation of blood samples, recommendations stated in the guidelines of the International Society on Thrombosis and Haemostasis and the British Committee for Standards in Haematology can be followed [67,68]. Blood should be taken from a resting donor with minimal venostasis before and during blood withdrawal [95]. Venipuncture—e.g., from the cubital vein—requires the use of needles with a minimum of 21 gauge, in order to avoid high shear stresses in the syringe cannula. Drawn blood should be collected into siliconized glass or polymer tubes (e.g., polypropylene) and immediately mixed with the anticoagulant under continuous mild agitation. This can be realized by using a winged/butterly infusion set with associated tubing, which allows agitation of the collection tube while the needle maintains position during the blood withdrawal. Complete filling of the tube is mandatory for obtaining the correct blood-anticoagulant ratio. Since venipuncture—and the associated lesion of the vessel wall tissue—may result in the activation of coagulation processes in the syringe (e.g., by tissue factor/thromboplastin), current guidelines recommend discarding the

Table 3.1 Data sheet for the preanalytical donor/blood characterization including laboratory specific reference ranges

Parameter	Unit	Data/reference ranges			
Donor data					
Donor number, measurement date					
First name, last name					
Date of birth					
Sex	m/f				
Age	years				
Height, weight, body mass index	cm, kg				
Blood pressure		Low	Elevated slightly	Moderate	Strong
Blood pressure systolic	mmHg	<100	140–159	160–179	>180
Blood pressure diastolic	mmHg	<60	90–99	100–109	>110
Heart rate	1/min				
Hemogram		Woman		Men	
Leukocytes (WBC)	$1 \times 10^3 \cdot \mu L^{-1}$	3.9–10.0		4.2–9.1	
Erythrocytes (RBC)	$1 \times 10^6 \cdot \mu L^{-1}$	3.9–5.2		4.6–6.1	
Hemoglobin (HGB)	$mmol \cdot L^{-1}$	7.5–9.9		8.7–11.2	
Hematocrit (HCT)	%	34.1–44.9		40.1–51.0	
Mean corpuscular volume (MCV)	fL	79.4–94.8		79.0–92.2	
Platelets (PLT)	$1 \times 10^3 \cdot \mu L^{-1}$	182–369		163–337	
Mean platelet volume (MPV)	fL	7–13		7–13	
Unspecific inflammatory markers	$\mu g \cdot mL^{-1}$	≤ 5 = negative, >5 ≤ 10 = suspicious, >10 = positive			
C-reactive protein (CRP)					

Continued

Table 3.1 Continued

Parameter	Unit	Data/reference ranges		
Platelet aggregation				
Maximum induced platelet aggregation (mPA)				
mPA collagen ($10\,\mu g \cdot mL^{-1}$)	%	81–95		
mPA ADP($20\,\mu M$)	%	79–98		
mPA ristocetine $1\,mg \cdot mL^{-1}$)	%	72–105		
Spontaneous aggregation	%	1–10		
Aggregation speed (vPA)				
vPA collagen ($10\,\mu g \cdot mL^{-1}$)	$\% \cdot min^{-1}$	79–183		
vPA ADP ($20\,\mu M$)	$\% \cdot min^{-1}$	97–164		
vPA ristocetin ($1\,mg \cdot mL^{-1}$)	$\% \cdot min^{-1}$	33–138		
Spontaneous aggregation	$\% \cdot min^{-1}$	1–10		
Platelet function analyzer (PFA-100)				
Closure time collagen/ epinephrine	s	84–160		
Closure time collagen/ADP	s	68–121		
Platelet activation				
$CD42a^+/CD62P^+$ platelets	%	≤5		

initial 3–4 mL of blood [96,97]. This procedure however, is under debate [98–100]. Prior to the final test, a resting phase of at least 30 min is mandatory since function of blood cells can be altered due to the above mentioned preparatory steps. Particularly aggregation of platelets was reported to be reduced if measurements were conducted directly after blood taking [101]. Processing of whole blood into PRP or PPP should follow recommendations for platelet- or plasma-based coagulation assays in the international guidelines for thrombosis and haemostasis testing [67,68,99,102,103]. All preparation steps should continuously be performed at room temperature to reduce the activation of cells by temperature gradients, e.g., cooling to 4°C during the centrifugation of whole blood to obtain PRP [104,105]. To allow cells to interact at a normal physiological body temperature, the final test will be performed at 37°C, which is in accordance with test protocols of commercially available routine coagulation test systems [106–110]. It should be noted that recent reports suggest retaining the temperature during all preparational and testing procedures at 37°C to further diminish the influence of temperature gradients on the function of blood cells [111–114]. The final experiment should be finished within 4 h after the blood donation since morphology and functions of cells (e.g., platelet adhesion and aggregation) and the stabilization of plasma proteins (e.g., due to proteolytic digestions) are significantly altered with increasing storage time [50,102,114–119]. A representative workflow for the in vitro thrombogenicity testing of biomaterials is shown in Fig. 3.2.

3.3 Test protocols

The decision for a specific test protocol may be driven by varied considerations, e.g., of the targeted analyte, the development status of the material (e.g., screening or prototype evaluation) and the (patho-) physiological conditions of the final medical device (e.g., vascular implant or extracorporeal system).

Static tests—performed under no or low flow conditions—are widely applied, e.g., for determining protein- or platelet-material interactions after sedimentation and interaction of single cells with the material surface [94,120]. With the advantage of a rapid and sensitive screening system, static setups have been reported to be indicative of data from dynamic systems [48,121]. Microscopic, colorimetric, and ELISA-based techniques can be applied for analyzing, e.g., the density of adherent platelets, the adsorption of blood plasma proteins, or the activation of the coagulation system [120,122,123]. For the evaluation of materials at an advanced stage of development, dynamic setups can be utilized to simulate conditions in the flowing blood [47,124–128]. Currently applied dynamic tests comprise fundamentally varying setups including agitators, centrifugation systems, flow chambers, chandler loops, and closed loop systems [129,130]. However, an ideal dynamic model should—as close as possible—simulate the (patho-) physiological conditions of the device as present in vivo. Here, the following aspects should be considered:

- Onset and duration of the activation processes.
- Duration of the test ($\leq$ 240 min, functionality of the blood cells/components) [14,50,93].

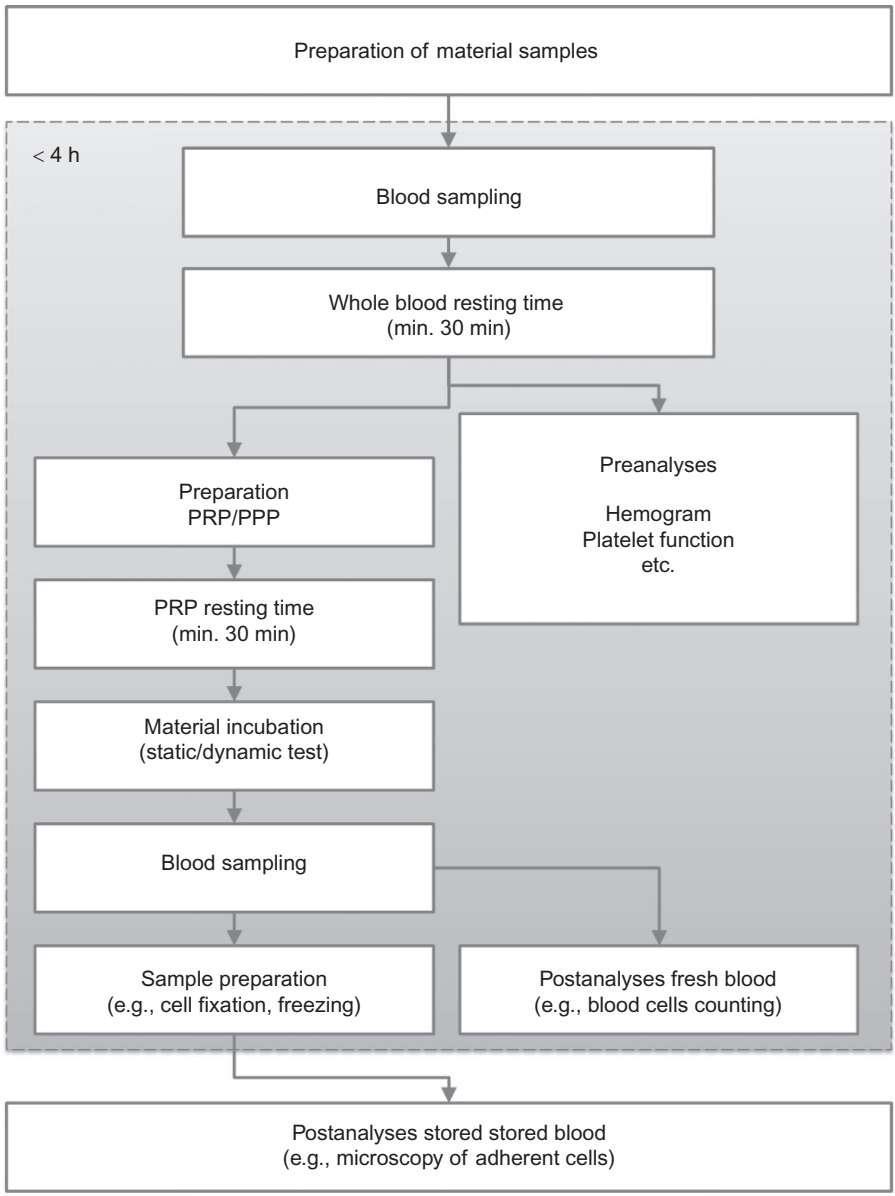


Fig. 3.2 Workflow for the in vitro thrombogenicity testing of biomaterials.

- Shear conditions.
- Temperature of the application.
- Geometry and size of the device (proportional miniaturization).
- Application site of the device (e.g., intravascular or extracorporeal).
- Limitations of the test setups (e.g., thrombogenicity of tubings or time-dependent hemolysis when applying roller pumps).

In many test scenarios, the application of varying flow conditions might be reasonably considered [131,132]. However, elevated shear forces were shown to induce conformational changes in blood plasma proteins in vitro (e.g., von Willebrand factor) and, beyond this, induce the activation of platelets and leukocytes, including platelet-leukocyte aggregation as well as microparticle formation [133–137]. Particularly in dynamic setups, air should thoroughly be removed to avoid air-induced hemolysis as well as the activation, adhesion/aggregation of platelets, leucocytes and the complement system [138,139]. Microscopic air bubbles (nuclei) are described to occur on rough and particularly on porous implant surfaces and have been shown to induce complement activation as well as platelet aggregation [140]. Therefore, evacuation of air nuclei should be carried out prior to any testing.

In the following paragraph we will introduce how static or dynamic in vitro approaches are reasonably applied to evaluate the thrombogenicity and hemocompatibility of biomaterials.

3.3.1 Thrombogenicity

The thrombogenicity of a material surface is described as one of the major reasons for the failure of blood-contacting medical devices [51]. Consequently and as described in the ISO 10993-4 (Selection of Tests for Interactions of Blood), the examination of material-induced thrombosis (thrombogenicity) is one of the key requirements in the evaluation of new biomaterials (Fig. 3.3). A rapid and robust evaluation of biomaterial's thrombogenicity includes in the analysis of platelet adhesion, activation and spreading on biomaterial surfaces (Fig. 3.4 Top), earlier described by Breddin as a diagnostic tool for platelet disorders [141]. Today, automated image-based analysis or colorimetric assays can be utilized to assess the platelet function. Particularly, static test setups are well suited for realizing such screening approaches [46,123,142]. On material samples that are in contact with flowing blood in dynamic test systems, platelet adhesion and thrombus formation can be analyzed qualitatively with microscopic techniques (e.g., scanning electron microscopy) [126,127]. Time-resolved monitoring of thrombus formations on material surfaces can be carried out, e.g., by video microscopy and has been applied particularly in the stagnation point flow chambers [131,132,143]. Indirect quantification of platelet retention on the material surface can be realized by counting still circulating platelets, e.g., in haematology analyzers or by flow cytometry [144]. In case of strongly thrombogenic materials, platelet counts will decrease with time. Flow cytometry also allows analyzing the activation of these circulating platelets, e.g., by determining the percentage of P-Selectin expressing platelets (CD62P-positive platelets), a marker for the activation-induced degranulation of α-granula [145,146]. This activation process can further be studied by measuring the release of soluble agonists from lysosomes, dense- and α-granules with enzyme-linked immunosorbent assays (e.g., platelet factors, serotonin, β-thromboglobulin and sP-Selectin) [147,148]. The formation of thrombin—the key factor/enzyme of the coagulation cascade—should be considered in thrombogenicity studies and can be assessed, e.g., by determining thrombin-antithrombin-complex III levels or from the hydrolysis rate of chromogenic substrates as a measure of thrombin activity [149–151].

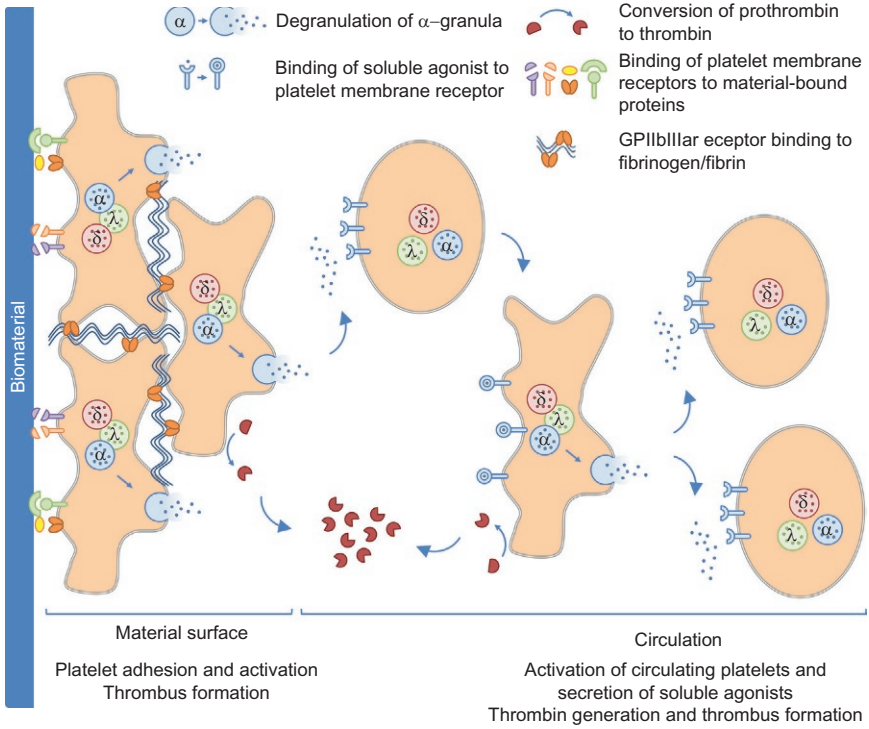


Fig. 3.3 Schematic overview of platelet adhesion, activation and thrombus growth on a body foreign implant surface in the circulation.

3.3.2 Hemocompatibility

In addition to the thrombogenicity testing, further in vitro analyses are required to evaluate the interactions of a material with the contacting human whole blood. These complex interactions are summarized by the term haemocompatibility. Here, the ISO 10993(4) formulates tests in the categories coagulation, thrombosis, haematology, and immunology [50,130]. Across these categories, qualitative microscopic analysis enables a first judgment of the material's blood compatibility, since the formation of thrombi on the material surface can be observed directly (Fig. 3.4 Bottom). To quantitatively assess the blood cell consumption (retention) within material-adherent thrombi or as single adherent platelets, a whole blood cell count (including the differential blood cell count) of the circulating cells can be performed.

Strongly associated with the adsorption of blood plasma proteins is the activation of the contact phase of the coagulation system. This leads to an induction of the intrinsic coagulation and the kinin system and—finally—results in the generation of thrombin and fibrin rich thrombi [152]. Contact activation is often assessed with the classical global tests (a) PTT (activated partial thromboplastin time) and the activated plasma recalcification time. Also, factor XIIa (Hageman Factor) activity can be determined, e.g., in chromogenic or ELISA assay formats [153–155]. Thrombin generation (thrombin antithrombin III),

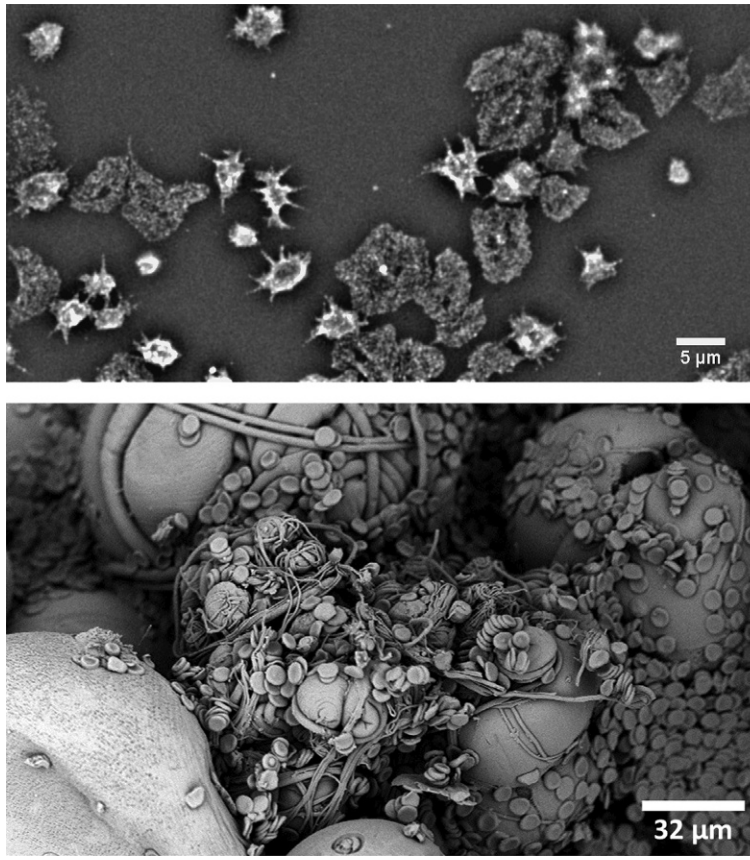


Fig. 3.4 Top: Stimulated emission depletion (STED) microscopy of biomaterial adherent platelets (static test system) in different states of activation (CD42a antibody staining; states of activation: round/discoid: slightly activated → platelets showing pseudopodia formation: medium activated → partially and fully spreaded = strongly activated). Bottom: SEM images of thrombus formation on polymeric microparticles after exposure to human whole blood in a dynamic test system.

fibrinogen-fibrin conversion (e.g., fibrinogen, fibrinogen split products, D-Dimers) and fibrinolysis (reptilase time, thrombin time, D-Dimers) are included in the categories coagulation and thrombosis and can be determined in similar assay formats.

Minimum requirements in the evaluation of material-induced inflammatory response comprise the analyses of complement activation, leukocyte activation and the occurrence of respiratory burst [156]. The latter describes the rapid release of reactive oxygen species (ROS: hypochlorite, hydroxyl anions and superoxide radicals) from, e.g., activated neutrophil granulocytes and monocytes [157,158]. An ongoing production of ROS contributes to oxidative degradation of the material surface and can cause oxidative stress in the surrounding tissue (damage to proteins, lipids, and DNA) [159–161]. Available techniques for studying the generation of ROS in vitro include,

e.g., the spectrophotometrically determination of ferrocytochrome c (total amounts of superoxide released by inflammatory cells) and flow-cytometric assessment of the intracellular conversion of dihydrorhodamine-123 to rhodamin-123 as a measure of ROS producing cells [162,163]. Activation of leukocytes leads to the upregulation of CD11b (Mac-1) due to translocation of the molecule from intracellular granules to the cell membrane [164]. Increasing percentages of CD11b positive leukocytes have therefore been associated with material-induced activation and are classically studied by flow cytometry [165,166]. As a further parameter of immune cell activation, the release of elastase from polymorphonuclear (PMN) granulocytes, particularly neutrophils, has been analyzed [56,167]. Released PMN-elastase complexes with α1-proteinase inhibitor (α1-Pi) can be quantified by ELISA. Alternatively, PMN-elastase activity can be determined as elastase-specific conversion of a nonfluorescent substrate into a fluorescent compound [168].

As part of the human innate immune response, complement activation has become an important parameter in the hemocompatibility testing of biomaterials [51,64,65,169]. Whereas systemic inflammation results in the activation of all three complement pathways and surgical interventions can lead to an activation of the classical pathway, blood-contacting biomaterials are reported to induce activation of the alternative pathway [46,170]. Standards for the determination of complement activation are still under debate [63,171]. Particularly, anticoagulants including their dosage used for the tests is varying between the laboratories, limiting comparisons between different studies [65,161,172]. Most commonly tested parameters include the anaphylatoxins C3a and C5a as well as the terminal lytic C5b-9a complex, which can be analyzed by the ELISA technique. More recent studies pay further attention to the role of complement component C4 and its inhibitor the C4 binding protein [65,173]. Also, visualization of material surface adsorbed complement components can be applied to study complement activation [174]. It should be noted that concentrations determined in vitro have been reported to be approximately 10 times higher, compared to those observed in vivo. This phenomenon is most probably due to the missing in vivo clearance, which results in the accumulation of complement components in the small blood volumes used for in vitro studies [46].

The interaction of erythrocytes (red blood cells, RBC) with biomaterials can result in the damage of the cells and the release of intracellular hemoglobin. This process is termed hemolysis and can be induced by physical forces, such as turbulent flow and high shear rates, but also by substances that leach out of the implant (e.g., monomers), metal ions and electrical forces [175–179]. Furthermore, hemolysis can be induced by activated components of the complement system, such as C5a [169,170,180]. Despite standards for hemolysis testing being formulated in the ISO and ASTM-norm [181], experiments are carried out under varying conditions. This includes static or dynamic test setups, blood from human or animal origin (e.g., rabbit) and the evaluation of bulk materials or eluates of the latter [179]. Increased levels of free plasma hemoglobin are classically determined in PPP by the addition of cyanmethemoglobin, which can be spectro-photometrically detected at 540 nm wavelength. Other available methods, including automated haematology analyzers, pulse cooximeters, and point-of-care photometers are currently under revision [182,183]. Recently, an excellent review concerning the opportunities for standardization in hemolysis testing of biomaterials was reported by van Oeveren and colleagues [179].

3.4 Summary

In this chapter, we have emphasized that the standards given by regulatory institutions, such as the ASTM or the ISO norm committee, describe only minimum requirements for studying the thrombogenicity and hemocompatibility of biomaterials. As a consequence, it is still under debate as to which supplementary assays need to be performed to enhance our understanding of the processes at the blood-material interface and to improve the hemocompatibility of new materials for blood-contacting implants. Prior to any biological analyses, manufacturing and characterization processes of the materials need to be appropriately standardized. This comprises the use of medical-grade starting materials, synthesis and processing under clean-room conditions, cleaning (residues of the synthesis), and the selection of an appropriate sterilization technique that does not affect the desired properties of the final product.

After a profound physico-chemical characterization of the material bulk and surface, endotoxin load should be the first tested parameter within the biological evaluation. Bacterial contamination at any production-stage can lead to false in vitro evaluations, particularly in view of material-induced immune responses and the activation of platelets. Moreover, undetected contaminations of the implant will lead to severe inflammatory reactions in the human body. The decision for a specific anticoagulant and the respective concentration should be carefully reviewed to ensure an appropriate functionality of the targeted blood cell/component. The latter has to be tested in a well standardized preanalytical characterization of the blood. Though reference materials have been proposed in former consensus initiatives, application of the latter has to be carefully reconsidered since they may not reflect the state of the art technology anymore. A reasonable selection may comprise current implant materials of the targeted medical application but should, at least, allow a categorization, e.g., between low and highly thrombogenic controls. Test for the evaluation of thrombogenicity and hemocompatibility should at least be selected according to the categories formulated in the ISO norm: platelet adhesion and activation, coagulation, thrombosis, haematology, and immunology. In an ideal testing scenario, the selection of all above mentioned parameters should enable a comprehensive interstudy and interlaboratory comparison for different tested materials. Formulation of appropriate standards that allow reproducible testing and harmonized categorization of biomaterials should be consequently approached as a common consensus not just of the regulatory but also of the scientific community as it is already realized in the clinical chemistry and haematology.

References

[1] G. Montalescot, U. Sechtem, S. Achenbach, et al., 2013 ESC guidelines on the management of stable coronary artery disease: the task force on the management of stable coronary artery disease of the European Society of Cardiology. Eur heart J 34 (2013) 2949–3003, https://doi.org/10.1093/eurheartj/eht296.

[2] D. Butler, UN targets top killers. Nature 477 (2011) 260–261, https://doi.org/10.1038/477260a.

[3] A. Fontana, S. Spadaro, M. Copetti, et al., Association between resistin levels and all-cause and cardiovascular mortality: a new study and a systematic review and meta-analysis. PLoS One 10 (2015), e0120419, https://doi.org/10.1371/journal.pone.0120419.
[4] B. Perek, A. Malinska, S. Stefaniak, et al., Predictive factors of late venous aortocoronary graft failure: ultrastructural studies. PLoS One 8 (2013), e70628, https://doi.org/10.1371/journal.pone.0070628.
[5] P. Menu, J.F. Stoltz, H. Kerdjoudj, Progress in vascular graft substitute, Clin. Hemorheol. Microcirc. 53 (2013) 117–129, https://doi.org/10.3233/CH-2012-1580.
[6] E. Paternotte, H. Kerdjoudj, T. Kokten, et al., Endothelialized and preconditioned natural umbilical arteries with long term patency open the route for future human uses. Clin. Hemorheol. Microcirc. 54 (2013) 223–234, https://doi.org/10.3233/CH-131728.
[7] M. Rémy, R. Bareille, V. Rerat, et al., Polyethylene terephthalate membrane grafted with peptidomimetics: endothelial cell compatibility and retention under shear stress, J. Biomater. Sci. Polym. Ed. 24 (2013) 269–286, https://doi.org/10.1080/09205063.2012.690275.
[8] W.H. Reinhart, Platelets in vascular disease, Clin. Hemorheol. Microcirc. 53 (2013) 71–79, https://doi.org/10.3233/CH-2012-1577.
[9] A.W. Clowes, A.M. Gown, S.R. Hanson, M.A. Reidy, Mechanisms of arterial graft failure. 1. Role of cellular proliferation in early healing of PTFE prostheses, Am. J. Pathol. 118 (1985) 43–54.
[10] I.B. Riaz, M. Asawaeer, H. Riaz, et al., Optimal anticoagulation duration of unfractionated and low molecular weight heparin in non-ST elevation acute coronary syndrome: a systematic review of the literature. Int. J. Cardiol. 177 (2014) 461–466, https://doi.org/10.1016/j.ijcard.2014.09.105.
[11] K. Jurk, B.E. Kehrel, Platelets: physiology and biochemistry, Semin. Thromb. Hemost. 31 (2005) 381–392, https://doi.org/10.1055/s-2005-916671.
[12] B.D. Ratner, The catastrophe revisited: blood compatibility in the 21st century. Biomaterials 28 (2007) 5144–5147, https://doi.org/10.1016/j.biomaterials.2007.07.035.
[13] B.D. Ratner, A.S. Hoffman, F.J. Schoen, J.E. Lemons, Biomaterials Science—An Introduction to Materials in Medicine, second ed., Elsevier Academic Press, Amsterdam; London, 2004.
[14] F. Jung, S. Braune, A. Lendlein, Haemocompatibility testing of biomaterials using human platelets. Clin. Hemorheol. Microcirc. 53 (2013) 97–115, https://doi.org/10.3233/CH-2012-1579.
[15] J.-P. Cazenave, Blood-Surface Interactions: Biological Principles Underlying Haemocompatibility With Artificial Materials, Elsevier Science Ltd, 1986.
[16] B. Sivaraman, R.A. Latour, Time-dependent conformational changes in adsorbed albumin and its effect on platelet adhesion, Langmuir 28 (2012) 2745–2752, https://doi.org/10.1021/la204777x.
[17] E.W. Salzman, E.W. Merrill, K.C. Kent, Interaction of blood with artificial surfaces, in: R.W. Colman, J. Hirsh, V.J. Marder, E.W. Salzman (Eds.), Hemostasis and Thrombosis: Basic Principles and Clinical Practice, Lippincott Company, Philadelphia, 1999.
[18] S. Braune, M. Grunze, A. Straub, F. Jung, Are there sufficient standards for the in vitro hemocompatibility testing of biomaterials? Biointerphases 8 (2013) 33, https://doi.org/10.1186/1559-4106-8-33.
[19] J.E. Sadler, Biochemistry and genetics of von Willebrand factor, Annu. Rev. Biochem. 67 (1998) 395–424, https://doi.org/10.1146/annurev.biochem.67.1.395.
[20] D. Varga-Szabo, I. Pleines, B. Nieswandt, Cell adhesion mechanisms in platelets, Arterioscler. Thromb. Vasc. Biol. 28 (2008) 403–413, https://doi.org/10.1161/ATVBAHA.107.150474.

[21] B. Savage, J.J. Sixma, Z.M. Ruggeri, Functional self-association of von Willebrand factor during platelet adhesion under flow. Proc. Natl. Acad. Sci. USA 99 (2002) 425–430, https://doi.org/10.1073/pnas.012459599.
[22] A.J. Reininger, H.F.G. Heijnen, H. Schumann, et al., Mechanism of platelet adhesion to von Willebrand factor and microparticle formation under high shear stress, Blood 107 (2006) 3537–3545, https://doi.org/10.1182/blood-2005-02-0618.
[23] M.C. Bélanger, Y. Marois, Hemocompatibility, biocompatibility, inflammatory and in vivo studies of primary reference materials low-density polyethylene and polydimethylsiloxane: a review, J. Biomed. Mater. Res. 58 (2001) 467–477, https://doi.org/10.1002/jbm.1043.
[24] L.P. Brewster, D. Bufallino, A. Ucuzian, H.P. Greisler, Growing a living blood vessel: insights for the second hundred years, Biomaterials 28 (2007) 5028–5032, https://doi.org/10.1016/j.biomaterials.2007.07.048.
[25] M. Joner, A.V. Finn, A. Farb, et al., Pathology of drug-eluting stents in humans: delayed healing and late thrombotic risk, J. Am. Coll. Cardiol. 48 (2006) 193–202, https://doi.org/10.1016/j.jacc.2006.03.042.
[26] G.V.R. Born, P.D. Richardson, Activation time of blood platelets, J. Membr. Biol. 57 (1980) 87–90, https://doi.org/10.1007/BF01868994.
[27] W. Feng, X. Gao, G. McClung, et al., Methacrylate polymer layers bearing poly(ethylene oxide) and phosphorylcholine side chains as non-fouling surfaces: in vitro interactions with plasma proteins and platelets, Acta Biomater. 7 (2011) 3692–3699, https://doi.org/10.1016/j.actbio.2011.06.007.
[28] R.E. Baier, R.C. Dutton, Initial events in interaction sof blood with a foreign surface, J. Biomed. Mater. Res. 3 (1969) 191–206, https://doi.org/10.1002/jbm.820030115.
[29] E. Morgenstern, A. Ruf, H. Patscheke, Ultrastructure of the interaction between human platelets and polymerizing fibrin within the first minutes of clot formation, Blood Coagul. Fibrinolysis 1 (1990) 543–546.
[30] B.M. Matata, S. Wark, S. Sundaram, et al., In vitro contact phase activation with haemodialysis membranes: role of pharmaceutical agents, Biomaterials 16 (1995) 1305–1312, https://doi.org/10.1016/0142-9612(95)91045-z.
[31] J. Janatova, A.K. Cheung, C.J. Parker, Biomedical polymers differ in their capacity to activate complement, Complement Inflamm. 8 (1991) 61–69.
[32] T. Roch, B.F. Pierce, A. Zaupa, et al., Reducing the endotoxin burden of desaminotyrosine- and desaminotyrosyl tyrosine-functionalized gelatin, Macromol. Symp. 309-310 (2011) 182–189, https://doi.org/10.1002/masy.201100048.
[33] D. Rickert, A. Lendlein, A.M. Schmidt, et al., In vitro cytotoxicity testing of AB-polymer networks based on oligo(epsilon-caprolactone) segments after different sterilization techniques, J. Biomed. Mater. Res. B Appl. Biomater. 67 (2003) 722–731, https://doi.org/10.1002/jbm.b.10069.
[34] M.B. Gorbet, M.V. Sefton, Endotoxin: the uninvited guest. Biomaterials 26 (2005) 6811–6817, https://doi.org/10.1016/j.biomaterials.2005.04.063.
[35] T. Roch, J. Cui, K. Kratz, et al., Immuno-compatibility of soft hydrophobic poly (n-butyl acrylate) networks with elastic moduli for regeneration of functional tissues, Clin. Hemorheol. Microcirc. 50 (2012) 131–142, https://doi.org/10.3233/CH-2010-1449.
[36] F. Cognasse, The inflammatory role of platelets via their TLRs and Siglec receptors, Front. Immunol. 6 (2015) 1–15, https://doi.org/10.3389/fimmu.2015.00083.
[37] H. Hamzeh-Cognasse, P. Damien, A. Chabert, et al., Platelets and infections-complex interactions with bacteria, Front. Immunol. 6 (2015) 1–18, https://doi.org/10.3389/fimmu.2015.00082.

[38] O. Garraud, F. Cognasse, Are platelets cells? And if yes, are they immune cells? Front. Immunol. 6 (2015) 1–8, https://doi.org/10.3389/fimmu.2015.00070.
[39] J. Hawiger, A. Hawiger, S. Steckley, et al., Membrane changes in human platelets induced by lipopolysaccharide endotoxin. Br. J. Haematol. 35 (1977) 285–299, https://doi.org/10.1111/j.1365-2141.1977.tb00585.x.
[40] M.C. Morris, E.A. Gilliam, L. Li, Innate immune programing by endotoxin and its pathological consequences, Front. Immunol. 5 (2015) 1–8, https://doi.org/10.3389/fimmu.2014.00680.
[41] B. Hiebl, K. Lützow, M. Lange, et al., Cytocompatibility testing of cell culture modules fabricated from specific candidate biomaterials using injection molding, J. Biotechnol. 148 (2010) 76–82, https://doi.org/10.1016/j.jbiotec.2010.01.006.
[42] F. Jung, C. Wischke, A. Lendlein, Degradable, multifunctional cardiovascular implants: challenges and hurdles. MRS Bull. 35 (2010) 607–613, https://doi.org/10.1557/mrs2010.529.
[43] National Heart and Blood Institute. L, (U.S.) NI of H, Guidelines for Physicochemical Characterization of Biomaterials, US Dept. of Health and Human Services, Public Health Service, National Institutes of Health, Bethesda, MD, 1980.
[44] National Heart and Blood Institute. L, (U.S.) NI of H, Guidelines for Blood-Material Interactions: Report of the National Heart, Lung, and Blood Insitute Working Group, US Dept. of Health and Human Services, Public Health Service, National Institutes of Health, Bethesda, MD, 1985.
[45] W. Lemm, The Reference Materials of the European Communities: Results of Hemocompatibility Tests, Kluwer Academic Publishers, Dordrecht; Boston, MA; London, 1992.
[46] W. van Oeveren, Obstacles in haemocompatibility testing, Scientifica 2013 (2013) 392584, https://doi.org/10.1155/2013/392584.
[47] S. Sinn, T. Scheuermann, S. Deichelbohrer, et al., A novel in vitro model for preclinical testing of the hemocompatibility of intravascular stents according to ISO 10993-4, J. Mater. Sci. Mater. Med. 22 (2011) 1521–1528, https://doi.org/10.1007/s10856-011-4335-2.
[48] U. Streller, C. Sperling, J. Hübner, et al., Design and evaluation of novel blood incubation systems for in vitro hemocompatibility assessment of planar solid surfaces, J. Biomed. Mater. Res. B Appl. Biomater. 66 (2003) 379–390, https://doi.org/10.1002/jbm.b.10016.
[49] A. Thor, L. Rasmusson, A. Wennerberg, et al., The role of whole blood in thrombin generation in contact with various titanium surfaces, Biomaterials 28 (2007) 966–974, https://doi.org/10.1016/j.biomaterials.2006.10.020.
[50] U. Seyfert, In vitro hemocompatibility testing of biomaterials according to the ISO 10993-4, Biomol. Eng. 19 (2002) 91–96, https://doi.org/10.1016/S1389-0344(02)00015-1.
[51] M.B. Gorbet, M.V. Sefton, Biomaterial-associated thrombosis: roles of coagulation factors, complement, platelets and leukocytes, Biomaterials 25 (2004) 5681–5703, https://doi.org/10.1016/j.biomaterials.2004.01.023.
[52] M. Alquwaizani, L. Buckley, C. Adams, J. Fanikos, Anticoagulants: a review of the pharmacology, dosing, and complications, Curr. Emerg. Hosp. Med. Rep. 1 (2013) 83–97, https://doi.org/10.1007/s40138-013-0014-6.
[53] H. Bussey, J.L. Francis, Consensus Group TH, Heparin overview and issues, Pharmacotherapy 24 (2004) 103S–107S, https://doi.org/10.1592/phco.24.12.103S.36109.
[54] X. Chang, M. Gorbet, The effect of shear on in vitro platelet and leukocyte material-induced activation, J. Biomater. Appl. 28 (2013) 407–415, https://doi.org/10.1177/0885328212454689.

[55] C. Sperling, M.F. Maitz, S. Talkenberger, et al., In vitro blood reactivity to hydroxylated and non-hydroxylated polymer surfaces, Biomaterials 28 (2007) 3617–3625, https://doi.org/10.1016/j.biomaterials.2007.04.041.
[56] H.P. Wendel, N. Hauser, F. Briquet, G. Ziemer, Hemocompatibility of medical connectors with biopassive or bioactive surface coatings, J. Biomater. Appl. 17 (2002) 5–17, https://doi.org/10.1177/088532820201700159 6.
[57] A. Waterhouse, Y. Yin, S.G. Wise, et al., The immobilization of recombinant human tropoelastin on metals using a plasma-activated coating to improve the biocompatibility of coronary stents, Biomaterials 31 (2010) 8332–8340, https://doi.org/10.1016/j.biomaterials.2010.07.062.
[58] C.G. Solomon, A. Greinacher, Heparin-induced thrombocytopenia, N. Engl. J. Med. 373 (2015) 252–261, https://doi.org/10.1056/NEJMcp1411910.
[59] J. Hirsh, Guidelines for Antithrombotic Therapy, 5th ed., B.C. Decker Inc., Hamilton, Ontario, CA, 2004.
[60] C. Gao, B. Boylan, J. Fang, et al., Heparin promotes platelet responsiveness by potentiating alphaIIbbeta3-mediated outside-in signaling, Blood 117 (2011) 4946–4952, https://doi.org/10.1182/blood-2010-09-307751.
[61] G.M. Arepally, T.L. Ortel, Heparin-induced thrombocytopenia, Annu. Rev. Med. 61 (2010) 77–90, https://doi.org/10.1146/annurev.med.042808.171814.
[62] O.A. Hamad, P.H. Nilsson, D. Wouters, et al., Complement component C3 binds to activated normal platelets without preceding proteolytic activation and promotes binding to complement receptor 1, J. Immunol. 184 (2010) 2686–2692, https://doi.org/10.4049/jimmunol.0902810.
[63] F. Bexborn, A.E. Engberg, K. Sandholm, et al., Hirudin versus heparin for use in whole blood in vitro biocompatibility models, J. Biomed. Mater. Res. A 89 (2009) 951–959, https://doi.org/10.1002/jbm.a.32034.
[64] B. Nilsson, K.N. Ekdahl, T.E. Mollnes, J.D. Lambris, The role of complement in biomaterial-induced inflammation, Mol. Immunol. 44 (2007) 82–94, https://doi.org/10.1016/j.molimm.2006.06.020.
[65] A.E. Engberg, P.H. Nilsson, S. Huang, et al., Prediction of inflammatory responses induced by biomaterials in contact with human blood using protein fingerprint from plasma, Biomaterials 36 (2015) 55–65, https://doi.org/10.1016/j.biomaterials.2014.09.011.
[66] S. Huang, K. Sandholm, N. Jonsson, et al., Low concentrations of citrate reduce complement and granulocyte activation in vitro in human blood, Clin. Kidney J. 8 (2014) 31–37, https://doi.org/10.1093/ckj/sfu127.
[67] I. Mackie, P. Cooper, A. Lawrie, et al., Guidelines on the laboratory aspects of assays used in haemostasis and thrombosis, Int. J. Lab. Hematol. 35 (2013) 1–13, https://doi.org/10.1111/ijlh.12004.
[68] M. Cattaneo, C. Cerletti, P. Harrison, et al., Recommendations for the standardization of light transmission aggregometry: a consensus of the working party from the platelet physiology subcommittee of SSC/ISTH, J. Thromb. Haemost. 11 (2013) 1183–1189, https://doi.org/10.1111/jth.12231.
[69] G. Lippi, E. Favaloro, M. Plebani, Quality in hemostasis and thrombosis—part IV, Semin. Thromb. Hemost. 41 (2015) 263–266, https://doi.org/10.1055/s-0035-1549093.
[70] J.G. White, G. Escolar, EDTA-induced changes in platelet structure and function: adhesion and spreading, Platelets 11 (2000) 56–61.
[71] J.G. White, EDTA-induced changes in platelet structure and function: clot retraction, Platelets 11 (2000) 49–55.

[72] European Standard, EN ISO 10993-4 Biological Evaluation of Medical Devices Part 4: Selection of Tests for Interactions With Blood, European Committee for Standardization, Geneva, Switzerland, 2009.
[73] NCCLS, Additives to Blood Collection Devices: EDTA. Proposed Standard, NCCLS, Villanova, PA, 1989.
[74] S. Narayanan, The preanalytic phase: an important component of laboratory medicine, Am. J. Clin. Pathol. 113 (2000) 429–452, https://doi.org/10.1309/C0NM-Q7R0-LL2E-B3UY.
[75] G. Banfi, G.L. Salvagno, G. Lippi, The role of ethylenediamine tetraacetic acid (EDTA) as in vitro anticoagulant for diagnostic purposes, Clin. Chem. Lab. Med. 45 (2007) 565–576, https://doi.org/10.1515/CCLM.2007.110.
[76] G. Lippi, M. Plebani, EDTA-dependent pseudothrombocytopenia: further insights and recommendations for prevention of a clinically threatening artifact, Clin. Chem. Lab. Med. 50 (2012) 1281–1285, https://doi.org/10.1515/cclm-2012-0081.
[77] M. Lamboo, D.C.W. Poland, J.C.J. Eikenboom, et al., Coagulation parameters of thawed fresh-frozen plasma during storage at different temperatures, Transfus. Med. 17 (2007) 182–186, https://doi.org/10.1111/j.1365-3148.2007.00729.x.
[78] R. Latza, J. Koscielny, H. Radtke, et al., Platelet function in platelet concentrates during storage: comparison of two blood cell separators, Transfus. Med. Hemother. 27 (2000) 94–100, https://doi.org/10.1159/000025250.
[79] A.-M. Albanyan, M.F. Murphy, P. Harrison, Evaluation of the impact-R for monitoring the platelet storage lesion, Platelets 20 (2009) 1–6, https://doi.org/10.1080/09537100802468653.
[80] D.V. Devine, K. Serrano, The platelet storage lesion, Clin. Lab. Med. 30 (2010) 475–487, https://doi.org/10.1016/j.cll.2010.02.002.
[81] V. Rumjantseva, K.M. Hoffmeister, Novel and unexpected clearance mechanisms for cold platelets, Transfus. Apher. Sci. 42 (2010) 63–70, https://doi.org/10.1016/j.transci.2009.10.008.
[82] M.S. Isaacs, K.D. Scheuermaier, B.L. Levy, et al., In vitro effects of thawing fresh-frozen plasma at various temperatures, Clin. Appl. Thromb. Hemost. 10 (2004) 143–148, https://doi.org/10.1177/107602960401000204.
[83] N. Tynngård, M. Wallstedt, A.L. Södergren, et al., Platelet adhesion changes during storage studied with a novel method using flow cytometry and protein-coated beads. Platelets 26 (2014) 177–185, https://doi.org/10.3109/09537104.2014.891728.
[84] C. Wang, M. Mody, R. Herst, et al., Flow cytometric analysis of platelet function in stored platelet concentrates, Transfus. Sci. 20 (1999) 129–139.
[85] B. Berg, H. Solberg, J. Nilsson, N. Tryding, Practical experience in the selection and preparation of reference individuals: empirical testing of the provisional Scandinavian recommendations, in: H. Solberg, R. Grasbeck, T. Alstrom (Eds.), Reference Values in Laboratory. Medicine, John Wiley & Sons, Chichester, 1981, pp. 55–64.
[86] D. Rein, T.G. Paglieroni, T. Wun, et al., Cocoa inhibits platelet activation and function, Am. J. Clin. Nutr. 72 (1) (2000) 30–35.
[87] D. Prisco, I. Francalanci, M. Filippini, M.I. Hagi, Physical exercise and hemostasis, Int. J. Clin. Lab. Res. 24 (1994) 125–131, https://doi.org/10.1007/BF02592441.
[88] R. Rauramaa, S.B. Väisänen, Interaction of physical activity and diet: implications for haemostatic factors. Public Health Nutr. 2 (1999) 383–390, https://doi.org/10.1017/S136898009900052X.
[89] J.E. Smith, Effects of strenuous exercise on haemostasis, Br. J. Sports Med. 37 (2003) 433–435, https://doi.org/10.1136/bjsm.37.5.433.

[90] H.H. Vorster, J.H. Cummings, F.J. Veldman, Diet and haemostasis: time for nutrition science to get more involved, Br. J. Nutr. 77 (1997) 671–684, https://doi.org/10.1079/BJN19970067.
[91] M. Pieters, M.P.M. de Maat, Diet and haemostasis—a comprehensive overview, Blood Rev. 29 (2015) 231–241, https://doi.org/10.1016/j.blre.2014.12.005.
[92] H. Kiesewetter, F. Jung, G. Pindur, et al., Effect of garlic on thrombocyte aggregation, microcirculation, and other risk factors, Int. J. Clin. Pharmacol. Ther. Toxicol. 29 (1991) 151–155.
[93] J. Vienken, The need for a systems approach in biomaterials testing, Med. Device Technol. 18 (12–4) (2007) 16–17.
[94] S. Braune, M. Groß, M. Walter, et al., Adhesion and activation of platelets from subjects with coronary artery disease and apparently healthy individuals on biomaterials. J. Biomed. Mater. Res. B Appl. Biomater. 104 (2015) 210–217, https://doi.org/10.1002/jbm.b.33366.
[95] G. Lima-Oliveira, G. Lippi, G.L. Salvagno, et al., Venous stasis and whole blood platelet aggregometry. Blood Coagul. Fibrinolysis 26 (2015) 665–668, https://doi.org/10.1097/MBC.0000000000000342.
[96] E. Briët, L. Engesser, E.J. Brommer, Regulation of blood coagulation and thrombosis, Haemostasis 15 (1985) 228–232.
[97] M.T.M. Raijmakers, C.H.F. Menting, H.L. Vader, F. Van Der Graaf, Collection of blood specimens by venipuncture for plasma-based coagulation assays: necessity of a discard tube, Am. J. Clin. Pathol. 133 (2010) 331–335.
[98] K.J. Smock, R.A. Crist, S.J. Hansen, et al., Discard tubes are not necessary when drawing samples for specialized coagulation testing, Blood Coagul. fibrinolysis 21 (2010) 279–282.
[99] G. Lippi, G.L. Salvagno, M. Montagnana, et al., Quality standards for sample collection in coagulation testing, Semin. Thromb. Hemost. 38 (2012) 565–575, https://doi.org/10.1055/s-0032-1315961.
[100] M. Cole, L. Price, A. Parry, et al., A study to determine the minimum volume of blood necessary to be discarded from a central venous catheter before a valid sample is obtained in children with cancer, Pediatr. Blood Cancer 48 (2007) 687–695.
[101] M.L. Kalb, L. Potura, G. Scharbert, S.A. Kozek-Langenecker, The effect of ex vivo anticoagulants on whole blood platelet aggregation, Platelets 20 (2009) 7–11, https://doi.org/10.1080/09537100802364076.
[102] D.M. Adcock, D.M. Hoefner, K. Kottke-Marchant, et al., Collection, Transport, and Processing of Blood Specimens for Testing Plasma-Based Coagulation Assays and Molecular Hemostasis Assays: Approved Guideline, CLSI document H21-A5, fifth ed., Clinical and Laboratory Standards Institute, Wayne, PA, 2008.
[103] E.J. Favaloro, D.M. Funk, G. Lippi, Pre-analytical variables in coagulation testing associated with diagnostic errors in hemostasis, Lab. Med. 43 (2012) 1–10, https://doi.org/10.1309/LM749BQETKYPYPVM.
[104] M. Böhm, S. Täschner, E. Kretzschmar, et al., Cold storage of citrated whole blood induces drastic time-dependent losses in factor VIII and von Willebrand factor: potential for misdiagnosis of haemophilia and von Willebrand disease, Blood Coagul. Fibrinolysis Int. J. Haemost. Thromb. 17 (2006) 39–45, https://doi.org/10.1097/01.mbc.0000198990.16598.85.
[105] E.J. Favaloro, S. Soltani, J. McDonald, Potential laboratory misdiagnosis of hemophilia and von Willebrand disorder owing to cold activation of blood samples for testing, Am. J. Clin. Pathol. 122 (2004) 686–692, https://doi.org/10.1309/E494-7DG4-8TVY-19C2.

[106] K. Breddin, M. Ziemen, O. Bauer, et al., Time and temperature dependent changes of ADP- and collagen-induced and "spontaneous" aggregation, Thromb. Res. 19 (1980) 621–638, https://doi.org/10.1016/0049-3848(80)90034-1.
[107] N. Tynngård, T.L. Lindahl, S. Ramström, Assays of different aspects of haemostasis—what do they measure? Thromb. J. 13 (2015) 1–10, https://doi.org/10.1186/s12959-015-0036-2.
[108] H.J.M. Brinkman, Global assays and the management of oral anticoagulation, Thromb. J. 13 (2015) 1–14, https://doi.org/10.1186/s12959-015-0037-1.
[109] M.D. Lancé, A general review of major global coagulation assays: thrombelastography, thrombin generation test and clot waveform analysis, Thromb. J. 13 (2015) 1, https://doi.org/10.1186/1477-9560-13-1.
[110] E.J. Favaloro, G. Lippi, M. Franchini, Contemporary platelet function testing, Clin. Chem. Lab. Med. 48 (2010) 579–598, https://doi.org/10.1515/CCLM.2010.121.
[111] K.H. Polderman, Hypothermia and coagulation, Crit. Care 16 (2012) A20, https://doi.org/10.1186/cc11278.
[112] A. Straub, M. Breuer, H.P. Wendel, et al., Critical temperature ranges of hypothermia-induced platelet activation: possible implications for cooling patients in cardiac surgery, Thromb. Haemost. 97 (2007) 608–616.
[113] A. Straub, S. Krajewski, J.D. Hohmann, et al., Evidence of platelet activation at medically used hypothermia and mechanistic data indicating ADP as a key mediator and therapeutic target, Arterioscler. Thromb. Vasc. Biol. 31 (2011) 1607–1616, https://doi.org/10.1161/ATVBAHA.111.226373.
[114] L. Feng, Y. Zhao, H. Zhao, Z. Shao, Effects of storage time and temperature on coagulation tests and factors in fresh plasma, Sci. Rep. 4 (2014) 3868, https://doi.org/10.1038/srep03868.
[115] D. Adcock, D. Kressin, R.A. Marlar, The effect of time and temperature variables on routine coagulation tests, Blood Coagul. Fibrinolysis 9 (1998) 463–470.
[116] L.V. Rao, A.O. Okorodudu, J.R. Petersen, M.T. Elghetany, Stability of prothrombin time and activated partial thromboplastin time tests under different storage conditions, Clin. Chim. Acta 300 (2000) 13–21.
[117] H.K. Breddin, Can platelet aggregometry be standardized? Platelets 16 (2005) 151–158, https://doi.org/10.1080/09537100400020161.
[118] S. Braune, M. Walter, F. Schulze, et al., Changes in platelet morphology and function during 24 hours of storage. Clin. Hemorheol. Microcirc. 58 (2014) 159–170, https://doi.org/10.3233/CH-141876.
[119] S. Ayache, M. Panelli, F.M. Marincola, D.F. Stroncek, Effects of storage time and exogenous protease inhibitors on plasma protein levels. Am. J. Clin. Pathol. 126 (2006) 174–184, https://doi.org/10.1309/3WM7-XJ7R-D8BC-LNKX.
[120] A.C. Eriksson, P.A. Whiss, Measurement of adhesion of human platelets in plasma to protein surfaces in microplates. J. Pharmacol. Toxicol. Methods 52 (2005) 356–365, https://doi.org/10.1016/j.vascn.2005.06.002.
[121] L. Muthusubramaniam, R. Lowe, W.H. Fissell, et al., Hemocompatibility of silicon-based substrates for biomedical implant applications, Ann. Biomed. Eng. 39 (2011) 1296–1305, https://doi.org/10.1007/s10439-011-0256-y.
[122] M. Vanícková, J. Suttnar, J.E. Dyr, The adhesion of blood platelets on fibrinogen surface: comparison of two biochemical microplate assays, Platelets 17 (2006) 470–476, https://doi.org/10.1080/09537100600758875.
[123] S. Braune, S. Zhou, B. Groth, F. Jung, Quantification of adherent platelets on polymer-based biomaterials. Comparison of colorimetric and microscopic assessment. Clin. Hemorheol. Microcirc. 61 (2015) 225–236, https://doi.org/10.3233/CH-151995.

[124] H.L. Goldsmith, D.N. Bell, S. Braovac, et al., Physical and chemical effects of red cells in the shear-induced aggregation of human platelets, Biophys. J. 69 (1995) 1584–1595, https://doi.org/10.1016/S0006-3495(95)80031-7.
[125] H.L. Goldsmith, S.S. Yu, J. Marlow, Fluid mechanical stress and the platelet, Thromb. Diath. Haemorrh. 34 (1975) 32–41.
[126] F. Jung, R. Bach, C. Mrowietz, et al., Haemocompatibility of endovascular coronary stents: Wiktor GX, Biomed. Tech. 46 (2001) 200–206.
[127] C. Mrowietz, R.P. Franke, U.T. Seyfert, et al., Haemocompatibility of polymer-coated stainless steel stents as compared to uncoated stents, Clin. Hemorheol. Microcirc. 32 (2005) 89–103.
[128] G. Tepe, J. Schmehl, H.P. Wendel, et al., Reduced thrombogenicity of nitinol stents-in vitro evaluation of different surface modifications and coatings, Biomaterials 27 (2006) 643–650, https://doi.org/10.1016/j.biomaterials.2005.06.004.
[129] W. van Oeveren, I.F. Tielliu, J. de Hart, Comparison of modified chandler, roller pump, and ball valve circulation models for in vitro testing in high blood flow conditions: application in thrombogenicity testing of different materials for vascular applications, Int. J. Biomater. 2012 (2012) 673163, https://doi.org/10.1155/2012/673163.
[130] U.T. Seyfert, F. Jung, Criteria and principles of in vitro hemocompatibility testing according to the ISO 10993(4), Transfus. Med. Hemother. 27 (2000) 317–322, https://doi.org/10.1159/000053546.
[131] T. Kragh, J. Schaller, U. Kertzscher, et al., Platelet adhesion, aggregation, and embolism on artificial surfaces in non-parallel blood flow. Microfluid. Nanofluid. 19 (2015) 155–167, https://doi.org/10.1007/s10404-015-1557-5.
[132] J. Schaller, T. Kragh, A. Reininger, et al., Biocompatibility material test for cardiovascular devices using stagnation point flow, Biomed. Tech. 58 (2013) 29–31, https://doi.org/10.1515/bmt-2013-4366.
[133] R.M.A. Vergauwe, H. Uji-I, K. De Ceunynck, et al., Shear-stress-induced conformational changes of von Willebrand factor in a water-glycerol mixture observed with single molecule microscopy, J. Phys. Chem. B 118 (2014) 5660–5669, https://doi.org/10.1021/jp5022664.
[134] S.W. Schneider, S. Nuschele, A. Wixforth, et al., Shear-induced unfolding triggers adhesion of von Willebrand factor fibers, Proc. Natl. Acad. Sci. USA 104 (2007) 7899–7903, https://doi.org/10.1073/pnas.0608422104.
[135] L. Novák, H. Deckmyn, S. Damjanovich, J. Hársfalvi, Shear-dependent morphology of von Willebrand factor bound to immobilized collagen, Blood 99 (2002) 2070–2076, https://doi.org/10.1182/blood.V99.6.2070.
[136] X. Chang, M. Gorbet, The effect of shear on in vitro platelet and leukocyte material-induced activation. J. Biomater. Appl. 28 (2012) 407–415, https://doi.org/10.1177/0885328212454689.
[137] P.A. Holme, U. Orvim, M.J. Hamers, et al., Shear-induced platelet activation and platelet microparticle formation at blood flow conditions as in arteries with a severe stenosis, Arterioscler. Thromb. Vasc. Biol. 17 (1997) 646–653, https://doi.org/10.1161/01.ATV.17.4.646.
[138] J.R. Pohlmann, J.M. Toomasian, C.E. Hampton, et al., The relationships between air exposure, negative pressure, and hemolysis, ASAIO J. 55 (2009) 469–473, https://doi.org/10.1097/MAT.0b013e3181b28a5a.
[139] A.M. El-Sabbagh, C.J. Toomasian, J.M. Toomasian, et al., Effect of air exposure and suction on blood cell activation and hemolysis in an in vitro cardiotomy suction model, ASAIO J. 59 (2013) 474–479, https://doi.org/10.1097/MAT.0b013e31829f0e6e.

[140] P.G. Kalman, D.A. McCullough, C.A. Ward, Evacuation of microscopic air bubbles from Dacron reduces complement activation and platelet aggregation, J. Vasc. Surg. 11 (1990) 591–598.
[141] K. Breddin, In-vitro-Methoden zur Beurteilung der Plättchenfunktion. Blutalkohol 18 (1968) 84–89, https://doi.org/10.1007/BF01632412.
[142] S. Braune, G. Alagöz, B. Seifert, et al., Automated image-based analysis of adherent thrombocytes on polymer surfaces, Clin. Hemorheol. Microcirc. 52 (2012) 349–355, https://doi.org/10.3233/CH-2012-1610.
[143] K. Affeld, L. Goubergrits, N. Watanabe, U. Kertzscher, Numerical and experimental evaluation of platelet deposition to collagen coated surface at low shear rates, J. Biomech. 46 (2013) 430–436, https://doi.org/10.1016/j.jbiomech.2012.10.030.
[144] A.G. Kidane, G. Burriesci, M. Edirisinghe, et al., A novel nanocomposite polymer for development of synthetic heart valve leaflets, Acta Biomater. 5 (2009) 2409–2417, https://doi.org/10.1016/j.actbio.2009.02.025.
[145] S. Braune, M. von Ruesten-Lange, C. Mrowietz, et al., Dynamic in vitro hemocompatibility testing of poly(ether imide) membranes functionalized with linear, methylated oligoglycerol and oligo(ethylene glycol). Clin. Hemorheol. Microcirc. 54 (2013) 235–248, https://doi.org/10.3233/CH-131729.
[146] P.E. Stenberg, R.P. McEver, M.A. Shuman, et al., A platelet alpha-granule membrane protein (GMP-140) is expressed on the plasma membrane after activation, J. Cell Biol. 101 (1985) 880–886, https://doi.org/10.1083/jcb.101.3.880.
[147] I. Chung, A. Choudhury, J. Patel, G.Y.H. Lip, Soluble, platelet-bound, and total P-selectin as indices of platelet activation in congestive heart failure, Ann. Med. 41 (2009) 45–51, https://doi.org/10.1080/07853890802227089.
[148] C. Sperling, R.B. Schweiss, U. Streller, C. Werner, In vitro hemocompatibility of self-assembled monolayers displaying various functional groups, Biomaterials 26 (2005) 6547–6557, https://doi.org/10.1016/j.biomaterials.2005.04.042.
[149] W. van Oeveren, J. Haan, P. Lagerman, P. Schoen, Comparison of coagulation activity tests in vitro for selected biomaterials, Artif. Organs 26 (2002) 506–511, https://doi.org/10.1046/j.1525-1594.2002.06872.x.
[150] M.F. Gouzy, C. Sperling, K. Salchert, et al., In vitro blood compatibility of polymeric biomaterials through covalent immobilization of an amidine derivative, Biomaterials 25 (2004) 3493–3501, https://doi.org/10.1016/j.biomaterials.2003.10.091.
[151] A. Straub, D. Schiebold, H.P. Wendel, et al., Platelet anaesthesia during extracorporeal circulation: differential effects of GP IIb/IIIa blockers on platelet activation marker P-selectin expression at hypothermia, Thromb. Res. 122 (2008) 383–389, https://doi.org/10.1016/j.thromres.2008.01.001.
[152] E.A. Vogler, C.A. Siedlecki, Contact activation of blood-plasma coagulation, Biomaterials 30 (2009) 1857–1869, https://doi.org/10.1016/j.biomaterials.2008.12.041.
[153] R.K. Kainthan, D.E. Brooks, In vivo biological evaluation of high molecular weight hyperbranched polyglycerols, Biomaterials 28 (2007) 4779–4787, https://doi.org/10.1016/j.biomaterials.2007.07.046.
[154] A. Golas, P. Parhi, Z.O. Dimachkie, et al., Surface-energy dependent contact activation of blood factor XII, Biomaterials 31 (2010) 1068–1079, https://doi.org/10.1016/j.biomaterials.2009.10.039.
[155] K. Chatterjee, Z. Guo, E.A. Vogler, C.A. Siedlecki, Contributions of contact activation pathways of coagulation factor XII in plasma, J. Biomed. Mater. Res. A 90 (2009) 27–34, https://doi.org/10.1002/jbm.a.32076.
[156] R. Franke, F. Jung, Interaction of blood components and blood cells with body foreign surfaces, Ser. Biomech. 27 (2012) 51–58.

[157] D.F. Williams, On the mechanisms of biocompatibility, Biomaterials 29 (2008) 2941–2953, https://doi.org/10.1016/j.biomaterials.2008.04.023.
[158] J.M. Anderson, A. Rodriguez, D.T. Chang, Foreign body reaction to biomaterials, Semin. Immunol. 20 (2008) 86–100, https://doi.org/10.1016/j.smim.2007.11.004.
[159] W.F. Liu, M. Ma, K.M. Bratlie, et al., Real-time in vivo detection of biomaterial-induced reactive oxygen species, Biomaterials 32 (2011) 1796–1801, https://doi.org/10.1016/j.biomaterials.2010.11.029.
[160] K. Sutherland, J.R. Mahoney, A.J. Coury, J.W. Eaton, Degradation of biomaterials by phagocyte-derived oxidants, J. Clin. Invest. 92 (1993) 2360–2367, https://doi.org/10.1172/JCI116841.
[161] T. Roch, N. Ma, K. Kratz, A. Lendlein, Cell-based detection of microbial biomaterial contaminations. Clin. Hemorheol. Microcirc. 60 (2015) 51–63, https://doi.org/10.3233/CH-151939.
[162] W.-W. Jiang, S.-H. Su, R.C. Eberhart, L. Tang, Phagocyte responses to degradable polymers, J. Biomed. Mater. Res. A 82 (2007) 492–497, https://doi.org/10.1002/jbm.a.31175.
[163] T. Roch, C. Schulz, F. Jung, et al., Interaction of poly(ether imide) films with early immune mechanisms, Clin. Hemorheol. Microcirc. 57 (2014) 203–212, https://doi.org/10.3233/CH-141831.
[164] N. Rebuck, A. Finn, Polymorphonuclear granulocyte expression of CD11a/CD18, CD11b/CD18 and L-selectin in normal individuals, FEMS Immunol. Med. Microbiol. 8 (1994) 189–195.
[165] M.R. Barnard, M.D. Linden, A.L. Frelinger, et al., Effects of platelet binding on whole blood flow cytometry assays of monocyte and neutrophil procoagulant activity, J. Thromb. Haemost. 3 (2005) 2563–2570, https://doi.org/10.1111/j.1538-7836.2005.01603.x.
[166] M.K. Rooney, K.A. Woodhouse, Decreased tissue factor expression with increased CD11b upregulation on elastin-based biomaterial coatings, Biomater. Sci. 2 (2014) 1377–1383, https://doi.org/10.1039/c4bm00099d.
[167] F. Chua, Neutrophil elastase: mediator of extracellular matrix destruction and accumulation, Proc. Am. Thorac. Soc. 3 (2006) 424–427, https://doi.org/10.1513/pats.200603-078AW.
[168] S.L. Diamond, Methods for mapping protease specificity, Curr. Opin. Chem. Biol. 11 (2007) 46–51, https://doi.org/10.1016/j.cbpa.2006.11.021.
[169] M.M. Markiewski, B. Nilsson, K.N. Ekdahl, et al., Complement and coagulation: strangers or partners in crime? Trends Immunol. 28 (2007) 184–192, https://doi.org/10.1016/j.it.2007.02.006.
[170] D.H. DeHeer, J.A. Engels, A.S. DeVries, et al., In situ complement activation by polyethylene wear debris, J. Biomed. Mater. Res. 54 (2001) 12–19.
[171] T. Mollnes, P. Garred, G. Bergseth, Temperature and anticoagulants on in vitro complement activation: consequences for collection and preservation of samples to be examined for complement activation, Clin. Exp. Dermatol. 73 (1988) 484–488.
[172] I. Kourtzelis, S. Rafail, R.A. DeAngelis, et al., Inhibition of biomaterial-induced complement activation attenuates the inflammatory host response to implantation, FASEB J. 27 (2013) 2768–2776, https://doi.org/10.1096/fj.12-225888.
[173] A.E. Engberg, K. Sandholm, F. Bexborn, et al., Inhibition of complement activation on a model biomaterial surface by streptococcal M protein-derived peptides, Biomaterials 30 (2009) 2653–2659, https://doi.org/10.1016/j.biomaterials.2009.01.001.
[174] R. Kopp, K. Mottaghy, M. Kirschfink, M.I.K. Irschfink, Mechanism of complement activation during extracorporeal blood-biomaterial interaction: effects of heparin coated and uncoated surfaces, ASAIO J. 48 (2002) 598–605, https://doi.org/10.1097/01.MAT.0000033639.23941.7E.

[175] M. Kameneva, J. Antaki, Mechanical trauma to blood, in: O. Baskurt, M. Hardeman, M. Rampling, H. Meiselman (Eds.), Handb. Hemorheol. Hemodymics, IOS Press, Amsterdam, 2007, pp. 206–227.
[176] P.A. Lang, J. Huober, C. Bachmann, et al., Stimulation of erythrocyte phosphatidylserine exposure by paclitaxel, Cell. Physiol. Biochem. 18 (2006) 151–154, https://doi.org/10.1159/000095190.
[177] O.M. Niemoeller, V. Kiedaisch, P. Dreischer, et al., Stimulation of eryptosis by aluminium ions, Toxicol. Appl. Pharmacol. 217 (2006) 168–175, https://doi.org/10.1016/j.taap.2006.09.001.
[178] M. Föller, M. Sopjani, H. Mahmud, F. Lang, Vanadate-induced suicidal erythrocyte death, Kidney Blood Press. Res. 31 (2008) 87–93, https://doi.org/10.1159/000119704.
[179] S. Henkelman, G. Rakhorst, J. Blanton, W. van Oeveren, Standardization of incubation conditions for hemolysis testing of biomaterials, Mater. Sci. Eng. C 29 (2009) 1650–1654, https://doi.org/10.1016/j.msec.2009.01.002.
[180] I. Kourtzelis, M.M. Markiewski, M. Doumas, et al., Complement anaphylatoxin C5a contributes to hemodialysis-associated thrombosis, Blood 116 (2010) 631–639, https://doi.org/10.1182/blood-2010-01-264051.
[181] American Society for Testing and Materials ASTM F756-13, Standard Practice for Assessment of Hemolytic Properties of Materials, ASTM Int, West Conshohocken, PA, 2013. www.astm.org, https://doi.org/10.1520/F0756.
[182] I. Adam, S. Ahmed, M.H. Mahmoud, M.I. Yassin, Comparison of HemoCue® hemoglobinmeter and automated hematology analyzer in measurement of hemoglobin levels in pregnant women at Khartoum hospital, Sudan, Diagn. Pathol. 7 (2012) 30, https://doi.org/10.1186/1746-1596-7-30.
[183] R. Hiscock, D. Kumar, S.W. Simmons, Systematic review and meta-analysis of method comparison studies of Masimo pulse co-oximeters (radical-7™ or pronto-7™) and HemoCue® absorption spectrometers (B-hemoglobin or 201+) with laboratory haemoglobin estimation, Anaesth. Intensive Care 43 (2015) 341–350.

Test methods for hemocompatibility of biomaterials

4

C. Sperling, M.F. Maitz, C. Werner
Max Bergmann Center of Biomaterials Dresden, Dresden, Germany

4.1 Introduction

Hemocompatibility is not an immanent characteristic of a material alone—hemocompatibility always has to be viewed as the interaction of a material with the surrounding environment, depending on the conditions of blood flow or the endothelium. These have to be considered when designing a system to probe the hemocompatibility. Such systems therefore should reflect the intended use of the medical product as good as possible.

The reason for hemocompatibility testing can be as diverse as materials and incubation methods:

Material manufacturers need to prove safety and reliability of their products complying to the DIN/EN/ISO 10993-4 standard [1]. Industry testing and applied science need to demonstrate the conformity or success of a specific modification strategy according to the standard. Hemocompatibility tests in the field of basic science however, frequently focus on the interaction of materials with blood (components) on a molecular level and only marginally follow the ISO standard [2].

Due to the increasing importance of biomaterials in our society over the past decades, there are numerous new developments of blood contacting materials. A big percentage of the industrialized society owes their (quality of) life to medical products like stents, hemodialyzers, central venous catheters, and artificial heart valves. Meanwhile many traditional biomaterials have been replaced with advanced biomaterials providing biologically inspired design and responsive characteristics.

Therefore testing methods have to encompass routine methods with fast and reliable characterization of basic blood-material interactions as well as special methods that analyze specific interactions.

In vitro determination of blood interaction with materials always has to rely on a certain incubation setting, enabling the contact of blood with materials. Earliest experiments were already performed in the first half of the 19th century. Hewson [3] noticed that stationary blood showed different clotting behavior in a living vein segment compared to an open bowl. Later Virchow [4] showed that in addition to the blood-material interface other factors also have relevance on measurable blood clotting: blood composition and blood flow.

First test systems that shed light on important material characteristics and primary steps of blood activation were open and incubation was conducted under static conditions. This was later substituted by more complex incubation systems that integrate blood flow.

Hemocompatibility of Biomaterials for Clinical Applications. https://doi.org/10.1016/B978-0-08-100497-5.00005-7
© 2018 Elsevier Ltd. All rights reserved.

The basis for modern testing methods were gained in the 1970s and 80s where a series of seminars [5] and consensus conferences [6] paved the way for hemocompatibility testing and the legal regulations that are formulated in the DIN/EN/ISO 10993 part 4 [1].

Apart from the incubation set-up there is variation on the incubated medium and the parameters that are used for hemocompatibility assessment as outlined in this chapter.

This chapter will focus on in vitro test systems only. Relevant information for appropriate animal models complying with DIN/EN/ISO 10993-4 can be found there [1].

4.2 Incubation of whole blood versus blood fractions

Blood fulfills a multitude of functions in the body supported by cells, many proteins, enzyme cascades, and signaling molecules, which are in constant interchange. Concerning hemocompatibility studies, most important are the coagulation cascade and platelets for the thrombogenic reactions and immune cells (granulocytes, monocytes) as well as the complement system for immunologic reactions as stated in Fig. 4.1. Yet none of these pathways acts isolated—there is an intense crosstalk with mutual impact.

The base of all hemocompatibility is the adsorption of plasma proteins, meaning that blood cells only in rare cases have contact to the material itself. Instead proteins adsorb within seconds, and within minutes the composition of the protein corona undergoes dynamic changes. During this time, some of the proteins change conformationally. There has been extensive research on this rather complex topic with Leo Vroman presenting pioneering results on sequential protein adsorption of the contact phase of blood coagulation. Several original articles and reviews give a nice overview on protein adsorption to surfaces [7–10]. In depth understanding of the material-blood

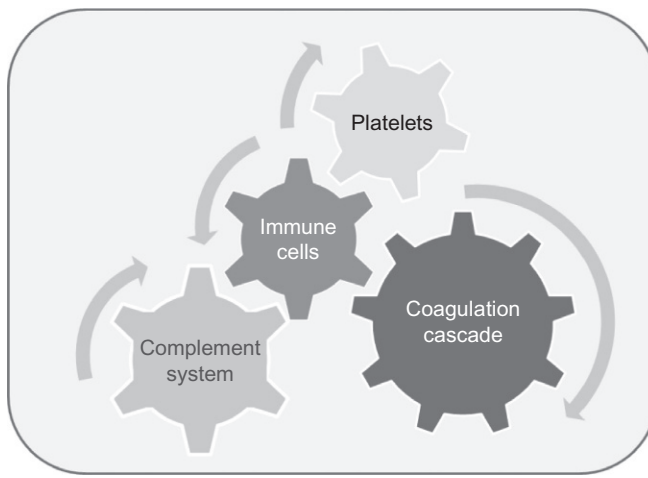


Fig. 4.1 Interaction of defense systems in blood. The contact of blood with materials induces several defense systems simultaneously. They are interconnected and influence each other.

interaction therefore also requires thorough physical-chemical characterization of the material for properties which have an impact on protein adsorption. However, this will not be covered in this chapter. Further, endotoxin contamination is a frequent reason for incompatibility reactions and should be excluded before the specific hemocompatibility assays [11,12].

4.2.1 Use of different blood fractions for testing

Hemocompatibility assays, using the complex organ human whole blood, allow analyzing all activation reactions at the interface blood-material at once. Yet the complexity sometime also hinders the analysis of isolated interactions between single cells and molecules. Therefore the implementation of platelet rich plasma (PRP), plasma (platelet poor plasma, PPP), and serum or isolated platelets or leukocytes can be advisable for some questions (Fig. 4.2 and Table 4.1).

4.2.2 Requirements for valid incubation results with whole blood

Usually, it is advisable to use fresh blood and to use human blood. Blood aging leads to factor preactivation and to a shift in concentration of active players within a few hours. This can only be partly halted through inhibitors and nourishment. It was shown

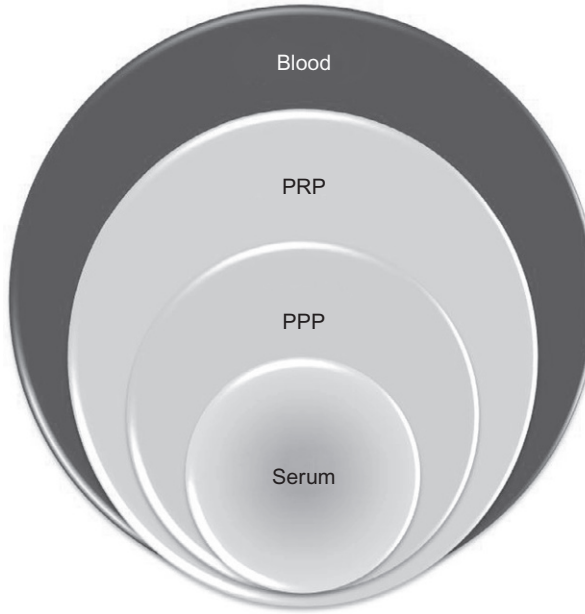


Fig. 4.2 Blood fractions used for in vitro incubation. Apart from whole blood platelet rich or poor plasma (PRP, PPP), serum or isolated cells can be used for the incubation depending on the relevant aspect of blood-material interaction that is analyzed.

Table 4.1 Use of blood fractions for in vitro incubation

Blood fraction	Type of incubation	Parameter
Isolated proteins	Microplate well, reaction tubes	Single factor analysis
Serum	Microplate well, reaction tubes	Activation complement system Adsorption of complement fragments
Plasma (platelet poor plasma, PPP)	Microplate well, reaction tubes	Adsorption of plasma proteins Activation of coagulation enzymes
platelet rich plasma (PRP)	Microplate well, reaction tubes, complex systems	Adhesion of platelets Activation of platelets
Isolated granulocytes/ monocytes	Microplate well, reaction tubes, complex systems	Adhesion of immune cells Activation of immune cells
Whole blood	Microplate well, reaction tubes, complex systems	Activation of various blood activation systems in parallel

that short term (0.5–4 h) storage at RT preserves natural functions better than storage at 37°C, but that processing times below 2 h should be preferred [13]. Animal blood exhibits big differences in amount and activities of proteins, enzymes and cells in dependence of the species [14–16].

Healthy voluntary blood donors are supposed to be nonsmokers, without drug intake for 10 days (especially aspirin and antiphlogistics should be avoided), they should not be pregnant or use oral contraceptives. Also physical stress right before blood donation as well as the donor´s diet was reported to influence scientific results [17]. The control of the C-reactive protein to be below 10 µg/mL is another useful preanalytical parameter to exclude false inflammatory responses.

Blood drawing should be sterile, applying only short or no stasis. The syringe or collection tube should be filled through a thick cannula, without vacuum and directly into the anticoagulant.

4.2.3 Blood anticoagulation

Only few test methods rely on the determination of blood coagulation without blood pretreatment. Usually the influence of the tested material on coagulation time with recalcified blood plasma or dynamics and intensity of thrombin formation in uncoagulated or recalcified blood/plasma is determined. More details on these experiments can be found in Sections 4.3.6 and 4.4.1. Nonanticoagulated blood outside the vascular system in test conditions has the tendency for coagulation within minutes. During this time, differences between weak and strong activating materials can hardly be differentiated. Response processes of granulocytes also occur in longer time scales and could not be determined due to preterm blood clotting. Therefore, for most assays anticoagulation is used to allow longer incubation times.

Table 4.2 Anticoagulation for in vitro blood incubation test systems

Anticoagulant	Mode of action	Chemistry
Sodium citrate	Ca^{2+} chelator, inhibits vitamin K dependent proteins, interferes with Ca^{2+} dependent adhesion reactions	Organic acid
Heparin	Cofactor for antithrombin, inhibits coagulation factors mainly of the intrinsic pathway, inhibits complement, but may activate platelets	Sulfated glycos-aminoglycan
Hirudin	Direct thrombin inhibitor, irreversible, inhibits activated thrombin	65 amino acid peptide
Corn trypsin inhibitor (CTI)	Irreversible FXIIa inhibitor	112 amino acid protein

There are several possibilities for anticoagulation as listed in Table 4.2. Anticoagulation for in vitro assays relies on calcium-chelation (citrate), support of a natural serpin (heparin), or the direct inhibition of a single blood coagulation enzyme [hirudin, corn trypsin inhibitor (CTI)].

The choice of anticoagulation should consider which of the diagnostic parameters are most relevant, as all options have their specific advantages and disadvantages.

Citrate as a Ca^{2+} chelator typically is used for blood collection with 3.2% or 3.8% sodium citrate. It should not be used in whole blood incubation systems, as the Vitamin K dependent enzymes, coagulation complex formation, and platelet activation are impaired. As the contact phase system of the coagulation, kallikrein, FXIIa, and FXIa are not calcium dependent, this system can be well tested with citrate plasma. Although integrin-mediated platelet adhesion should be Ca^{2+} dependent, PRP based assays of platelet adhesion are recommended to be performed in citrate anticoagulated plasma by the British Committee for Standards in Haematology (BCSH) and International Society on Thrombosis and Haemostasis (ISTH) [18–20].

Recalcified citrated plasma often is used to study enzyme activation and for global coagulation assays (see below), yet significant differences in reaction dynamics were seen compared to blood anticoagulated with CTI [21].

Heparin is a cofactor to the serpin antithrombin (ATIII) and enhances its inhibitory effect over 1000 times [22]. Due to the parallel inhibition of several coagulation factors at once, coagulation runs slower and allows for a better discrimination of procoagulant processes. In a low heparin concentration, the formation of fibrin is possible, therefore also fibrinolytic processes can be monitored. A major disadvantage is the pleiotropic effects on coagulation (through the support of ATIII), platelets [23–25], and the complement system [26]. Nevertheless it is often used for hemocompatibility assays because, as a matter of fact, patients frequently also receive heparin anticoagulation

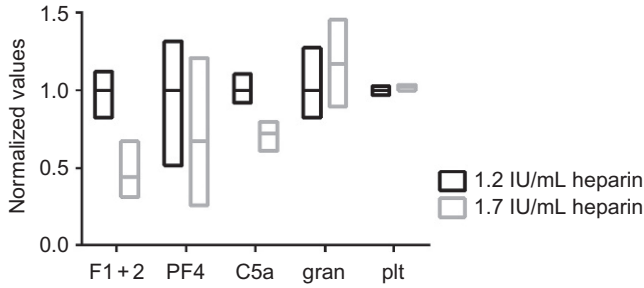


Fig. 4.3 Comparison of the influence of heparin concentration on hemocompatibility parameters. Coagulation activation (F1 + 2), platelet activation (PF4), complement activation (C5a) as well as the number of granulocytes (gran) and platelets (plt) after incubation of fresh whole blood treated with heparin in a higher (1.7 IU/mL) or lower (1.2 IU/mL) concentration. Values ($n = 3$) are normalized to the mean of the values for 1.2 IU/mL. Incubation was performed for 3 h at 37°C in the agitated incubation chamber presented in Section 4.3.5.

during the exposure to the biomaterials, meaning that heparin has a strong relevance in the clinical situation. The use of heparin should be limited to a minimum, depending on the expected activation potential of the samples, the incubation time, and the incubation type. Fig. 4.3 shows, how the absolute values of hemocompatibility parameters are influenced by the heparin-concentration in the assay. As expected, parameters of coagulation and platelet activation are mainly suppressed by a higher amount of heparin, but also complement activation (C5a) decreases while the numbers of granulocytes and platelets is not altered.

Hirudin is a bivalent direct inhibitor of activated thrombin [27,28]. It binds not only to the reactive center of the enzyme, but also to the fibrinogen binding site (exosite I). Therefore fibrin formation is not possible. The initial coagulation cascade, platelets, and complement are not directly influenced by hirudin, but their activity is indirectly decreased due to the lack of amplifying feedback loops of thrombin. Test parameters in hirudin-anticoagulated blood are more sensitive to material characteristics than in the case of heparin-anticoagulation [29]. However, as all of the thrombin mediated activation processes are also inhibited, platelet adhesion seems to be also lower for hirudin anticoagulated blood [30], yet this effect was not confirmed by others [31]. Studies that emphasize complement analysis do profit from hirudin, as no influence of hirudin on the complement system was reported [31].

CTI selectively blocks the contact pathway activation through inhibition of FXIIa. Thus, it can be used to discriminate between contact cascade and tissue factor initiated processes [32,33]

4.3 Incubation settings

The lack of standardized test settings as well as the diversity of biomaterial application sites leads to a variety of incubation techniques. To ensure reliable and reproducible results, the following basic requirements need to be met:

- easy set-up of incubation system to keep processing times short
- good relation of material surface area to incubated blood volume
- small surface area of foreign material to contact the blood
- prevention of blood-air contact
- prevention of blood cell sedimentation
- prevention of cell damage not related to biomaterial contact

In the following, the most frequently applied incubation types are presented. All of these settings make some compromises for one or more of the above mentioned requirements. The design of an appropriate test system therefore includes a careful consideration of the technical possibilities, the material shape, and the intended application. In addition to the technical conditions, the incubation time is a parameter that needs close consideration while the variability of blood as the test medium sparks the requirement of reliable reference materials.

4.3.1 Duration of incubation

The duration of the incubation has to take into account the time course of the biochemical pathways for the formation of the test parameters, half-life of the analytes, and inhibition kinetics but also experimental conditions like material differences and anticoagulation, as sketched in Fig. 4.4. In practice, the duration is chosen between a few

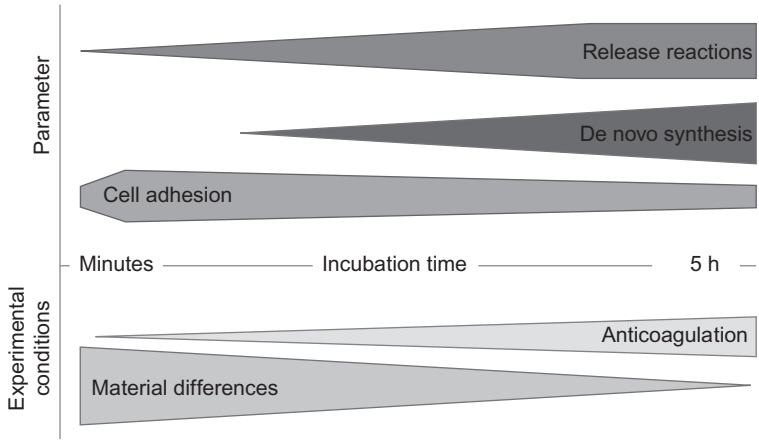


Fig. 4.4 Choice of material incubation time in dependence of chosen parameter and experimental conditions. While discrimination and intensity of cell release reactions generally increase with incubation time, saturation effects might arise for longer incubation times. De novo synthesis reactions usually need some minimum incubation time before being detectable. Cell adhesion on the other hand happens right after incubation initiation and most of the cells do not get released after full adhesion. Yet, especially platelets exhibit a strong shape change depending on material surface properties and incubation time duration, which could interfere with quantitation. A higher anticoagulation regime allows for longer incubation times while materials that provide only small differences might need a longer incubation time for clear comparison.

minutes (e.g., for single pass incubation) to 5 h [34]. Longer incubation times are also reported, yet this can only be relevant for very special questions as the deterioration of blood would interfere with material related reactivity [13]. While some parameters can be detected right at the beginning of the materials contact (initiating reactions like contact activation, initial cell adhesion phenomena), some parameters are only measurable after a certain time due to a lag time in production (gene transcription and protein synthesis in cells, enzymatic cascades). Some cellular parameters are release products from internal vesicles, some require de novo synthesis, sometimes both reactions superimpose each other. Additionally the possibility to differentiate between several materials with similar characteristics is enhanced with a longer incubation time. Therefore the stronger the differences between the materials are, the shorter the incubation time should be chosen and vice versa. On the other hand, differences decrease when the maximum of activation is reached for one of the parameters.

4.3.2 Reference materials

Blood composition and reactivity shows a strong variation between the different donors [35] but also on a day-to-day basis for one single donor. Therefore, results gained with different donors or on different days often vary with regard to the absolute values. This problem can be avoided with the use of reference materials to relate the different experiments to each other. An overview on appropriate materials can be found in this chapter.

4.3.3 Incubation settings—Overview

Incubation settings as listed in Table 4.3 in dependence of blood flow conditions (stagnant, agitated, flowing) and the material geometry (flat, coating, three-dimensional) should always take into account which information is desired. All the proposed

Table 4.3 Overview of incubation settings. Details of the various set-ups are described in the following

Blood flow condition	Incubation/material geometry	Information gained
Stagnant blood	Well plate, customized set up with defined surface/flat materials	Protein adsorption, cell adhesion
Agitated blood	Parallel plate chamber/flat materials on a shaker or overhead rotator	Complex activation profile w/o shear related cell adhesion processes but avoiding pure sedimentation processes
Flowing blood	Chandler loop, parallel plate chamber, cone-plate-system/ coatings, 3 dimensional, nanomaterials (chandler loop) + flat surfaces	Complex activation profile

incubation settings have the limitation of working with a constant blood pool, which accumulates activation products. This can be intended, because detection of stable products increases with time. Nevertheless in in vivo situation usually no accumulation occurs because the blood volume is much larger.

4.3.4 Incubation systems with stagnant blood

The most simple and fast incubation type of blood or blood fragments with materials always is the placement of a small volume of blood/blood fractions on the materials. Alternatively, a certain blood volume is incubated on the material in any container, possibly a well plate, as can be seen in Fig. 4.5A.

This system is easy to assemble, can be performed without specialized equipment and therefore enables the parallel incubation of a high number of samples. Nevertheless only rudimentary results concerning hemocompatibility can be gained because the blood has a big interface with air which acts as an activating surface. The gas exchange might also have implications on the blood pH value. Although cell sedimentation may be limited by shaking, it is not completely avoided. Further, the material surface that contacts blood/blood fragments is relatively low.

With the more advanced system as shown Fig. 4.5B, the material surface area is better defined, the backside of the material will not have blood/plasma contact and provided a low amount of liquid is used, the contact to the container material also can be limited.

4.3.5 Closed, agitated systems for incubation

A more advanced incubation set-up as presented in Fig. 4.6 is sometimes referred to as Bowry chamber. It is a flat incubation chamber completely filled with blood and the top and bottom surfaces are made of the test material [36–38].

Its concept is based on the above mentioned minimal requirement of blood incubation and combines a favorable relation of material surface to blood volume (e.g., 6 cm^2 to 2 mL of blood), a small area of foreign material, and the almost total exclusion of air-contact. The filling process is simple and can be performed directly from the syringe through openings on the side of the container while for sample withdrawal pipettes are used to prevent additional shear stress on the blood cells when sucking the blood from the container. The blood volume and the test surfaces are available for

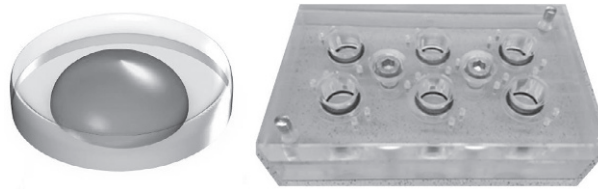


Fig. 4.5 Simple open incubation system with stagnant blood: (A) blood drop on surface and (B) customized set-up with clamped material and well-defined surface area.

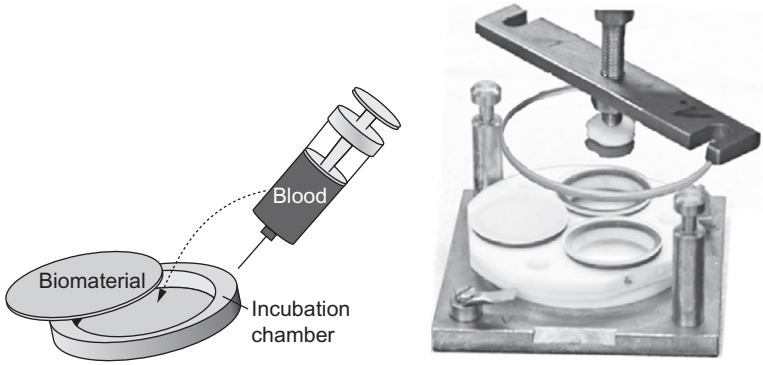


Fig. 4.6 Closed system for incubation of agitated blood [36]. The incubated material makes up the top and the bottom of the individual test chamber. Three individual test chambers are combined in one set-up (right photograph).

further analysis. The containers can be assembled fast and analysis of a high amount of parallel samples is possible.

There is no directed blood flow, yet effective blood mixing occurs as the containers are slowly but constantly turned overhead. This slow blood movement does not enable shear associated cell adhesion, yet a constant interaction of blood cells/proteins with the surface. Coincubation of different materials on top and bottom of the chamber with the blood can be used to probe responsive or modulating effects of one surface in presence of a defined stimulator [39–41].

The intentional exclusion of an interface with air also prevents gas exchange, which is necessary for pH control. As the coagulation cascade and leukocyte activity are highly sensitive to shifts in pH, the blood pH has to be monitored carefully. However, under most conditions, pH during a 2-h incubation time does not drop more than 0.1 pH unit.

The lack of real shear forces may be regarded as a disadvantage, however also physiologically there are only negligible shear forces in the capillary bed, in the venous system behind venous valves (where many catheters are placed) and some zones at the branching or confluence of blood vessels. In clinical settings, on dialysis membranes or the reservoirs of extracorporeal membrane oxygenation devices are examples of blood-biomaterial contact with highly reduced shear forces.

4.3.6 Incubation with streaming blood

The incubation of a surface with flowing blood in many cases appears to be clinically the most relevant way of blood incubation and several systems are proposed here. Flowing blood enables effective mixing and the intense interaction of blood with the surface. Additionally shear induced platelet reactivity can be monitored. It is desirable that shear stress be varied on a range encompassing venous blood flow (100–200 s^{-1}) as well as the conditions of arteries (300–1000 s^{-1}). Yet as a consequence of the increased complexity of these incubation systems artificial blood activation also rises.

Peristaltic blood pumps, which induce the flow easily induce hemolysis and platelet activation [42]. Lysed erythrocytes activate platelets through the release of ADP as well through free hemoglobin [43]. While for a long time no effect of hemolytic blood on coagulation was suspected [44] it was shown recently that the membrane of red blood cells might independently support thrombin formation [45].

For many of the reported incubation settings the ratio of the test specimen surface to the area of the incubation system in contact with blood is not favorable. The sensitivity of the system to detect influences of the test specimen on blood activation processes thus decreases. Some of the suggested flow chambers with two parallel plates are complex to assemble and to fill with blood which prevents the parallel incubation of several samples.

4.3.6.1 Chandler loop

In the chandler loop (see sketch in Fig. 4.7), tubings formed to loops and partly filled with blood are rotated with a speed between 10 and 30 rounds/min. This enables the simulation of flow conditions without the need of an external pump. Temperature control can be obtained through an open water bath or a heated incubator [46]. The use of a CO_2 incubator can be advisable to maintain constant pH values, as the tubing might enable gas transfer. The method, introduced by A.B. Chandler already in 1958, was first used to investigate blood-clotting phenomena [47] under well reproducible flow conditions [48]. The system later was adapted to biomaterials research [49] for coatings directly to the tubing [34,50]. Recently, Chandler loops proved to be suitable also to study the hemocompatibility of vascular stents [51] or nanoparticles [52]. Despite the ease of the set-up, calculation of shear conditions inside the Chandler loop is rather complex [53] and impedes wider application.

Although there is a big contact area between blood and the nonspecific tube material, Chandler loop systems do allow sensitive differentiation of the thrombogenicity of small vascular stents inside the tube [51].

Another drawback of this method is the permanent high interface between blood and air. The empty (air-filled) part of the tube is also constantly covered with a blood film which regularly is exposed to air. This can be avoided using a one-way ball valve integrated into the loop. The loop is placed on a rotary table with semirotating

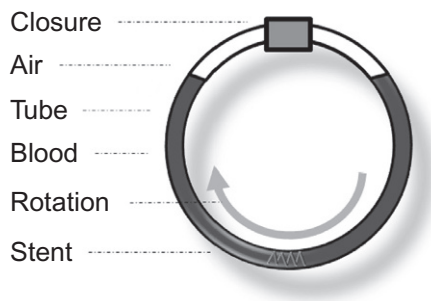


Fig. 4.7 Simplified sketch of Chandler loop for stent testing.

fore- and backward movements to generate a pulsed unidirectional flow inside the tubes [54]. Another possibility to move blood in a fully filled Chandler loop implements a roller pump. The comparison of these three systems showed differences for platelets and hemolysis but coagulation activation was similar [54].

4.3.6.2 Parallel plate flow chambers

Parallel plate chambers are a frequent setting for the incubation of planar materials with flowing blood or isolated blood cells. They are used for blood recirculation or, by far more often, for single pass incubation. They can be adapted to a wide variety of material surface size, blood volume, and shear regime. Several commercially available systems allow to study the influence of surface-adsorbed proteins to blood. Yet there is only a limited potential of material surface modification with commercially available flow chambers restricting them to a narrow application range.

A parallel plate chamber with a roller pump driven recirculation of blood is sketched in Fig. 4.8.

A main advantage of parallel plate chambers is the possibility to calculate and adjust shear stress values in a wide range [55]. This is relevant for studying cell adhesion/activation. Blood flow also was shown to possibly affect complement activation [56].

Blood flow can be achieved through a roller pump [36,57] or with the use of a syringe pump [58,59]. In the latter case usually single pass incubation with a main focus on the analysis of cell adhesion is performed [60]. Usually these systems are connected to a microscope to study platelet or granulocyte adhesion in situ [61–63] but typically in these cases there is no analysis of humoral parameters.

A recent publication features an innovative method to enable incubation without a pump [64]. A tilting platform induces a pulsatile flow and enables shear rates up to $370\,s^{-1}$. At each side, open containers collect the blood before recirculation causing short-term air contact. This well characterized system was used to show that platelet adhesion to four different materials was discriminated well with dynamic incubation while for static incubation no differences were noticeable.

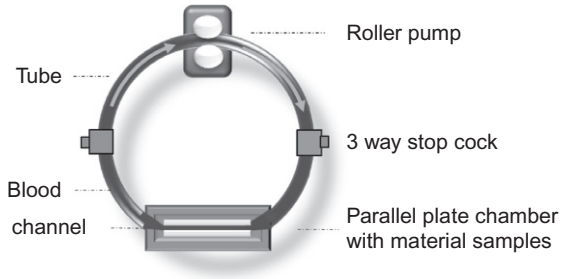


Fig. 4.8 Simplified sketch of parallel plate chamber. A roller pump is used to recirculate the blood. Care has to be taken for air-free filling of the system to avoid foam formation. A reservoir with air trap cannot be applied due to the altered flow conditions in there.

4.3.6.3 Cone-plate-incubation

A few cone plate incubation devices were employed for hemocompatibility research—mainly for the study of cell adhesion [63,65,66]. While this method realizes laminar flow with uniform shear stress over the entire plate surface it must be stressed that the modified surface usually is restricted to the base material while the cone remains unchanged—displaying a large area of foreign material.

4.3.6.4 Model miniature hemodialyzer

If possible the use of the final product for blood incubation is the best choice. Miniaturized models of hemodialyzer hollow fiber modules are an excellent example because they combine several aspects that enable their efficient use for in vitro testing. The incubated material has the appropriate size and the fluid regime can be tuned very well so that final testing of modified materials [67,68] but also the analysis of special biochemical reactions like the amount of contact activation is feasible [69].

4.4 Analytical parameters

An excellent parameter for in vitro hemocompatibility testing should represent an overall estimate of the blood response towards a certain material. Yet due to the complexity of blood reactions at the material interface there is not a single parameter that enables an easy and fast estimation of the materials thrombogenicity [70,71]. While global parameters—like the formation of a blood clot—allow an overall prediction of the materials coagulation response, no detailed analysis of initiating reactions is possible. Therefore the methods to be employed need to be adjusted to the relevant questions:

- Are materials with discrete differences or with only small modifications compared?
- Is information on the whole variety of blood initiated reactions needed, or just the reaction of isolated parameters?
- Are reactions with significance for long-term incubation of interest or is the focus on initial reactivity?
- Is the focus on initiating reactions at the start of enzymatic cascades or is it on the final product?

With the constant improvements in analytical techniques, more sophisticated parameter emerged during the last decade. Changes in protein synthesis can be observed already on a molecular level and allow a deeper understanding of material-induced cellular reactivity.

The use of surrogate markers to forecast the thrombogenicity or inflammatory reactions needs to be considered with scrutiny. These surrogate markers like the measurement of protein adsorption, enzyme activation, or cellular adhesion/activation measured from isolated blood components can give valuable hints about an activating potential of the material. They are frequently used because of their ease of detection. Yet the implication of simple causative mechanisms of action may lead to wrong

conclusions. For instance, it could be demonstrated that typical parameters of hemocompatibility assessment like the analysis of platelet adhesion and the measurement of FXII activation on surfaces cannot directly be translated to a procoagulant potential if regarded separate from other reactions because a strong synergism of these parameters (contact activation and platelet adhesion) was asserted and surfaces with moderate activation of both individual parameters were most thrombogenic [72].

4.4.1 Global parameters

Thrombus formation is a very obvious consequence of surface initiated blood activation and a relatively straightforward parameter to detect.

Several methods are applied to either directly quantify the formed thrombus on the material surface or to test pro-coagulant reactivity after the contact of material and blood.

4.4.1.1 Determination of clotting times of blood plasma

Clinical coagulation tests like (activated) partial thromboplastin time (PTT, aPTT) and prothrombin time after incubation of a biomaterial with citrate-anticoagulated plasma are sometimes used to determine pro- or anticoagulant potential of materials. Results have to be interpreted carefully: Possible adsorption of coagulation factors to the test-surface will lead to decreased concentrations in the plasma. Prolonged coagulation times after the materials contact in this case would not reflect the situation in the body. Activators in the aPTT assay always induce higher contact activation than typical biomaterials, thus it is especially advised against the use of activated partial thromboplastin time and only PTT is allowed in the ISO standard [1].

The recalcification time, the time until clot formation of recalcified blood or plasma directly on the test sample, is a simple and better parameter. However, its value is still limited due to ill-defined surface-volume rations, low mixing, and difficulties in determining an exact clotting time.

4.4.1.2 Thromboelastography

Thromboelastography is a comprehensive assay of the overall clotting process and overcomes the problems of exact clotting time determination. Especially for soluble biomaterials or nanomaterials this test combines blood incubation with a direct parameter evaluation. It provides parallel information on coagulation, fibrinolysis, and platelet function [73,74]. A serious disadvantage is the need for special equipment (2 separate techniques are commercially available) as well as the big area of other materials in contact with blood.

4.4.1.3 Thrombin formation

Thrombin formation time can be measured also directly in a plasma or blood sample using chromogenic [75] or fluorogenic substrates [76]. Situated at the end of the coagulation cascade, thrombin formation has a very similar kinetic to the fibrin formation and the blood clotting. Providing the test material as a coating in a microplate, testing can be done in direct contact with the sample.

4.4.1.4 *Microscopic and gravimetric analysis of blood clot formation*

Microscopic visualization of mural thrombogenesis on materials or a gravimetric analysis of the thrombus sometimes is used to assess the coagulation potential. Yet all of these parameters are strongly dependent on the experimental set-up and not easy to be compared among each other.

4.4.2 *Humoral markers*

Most humoral markers are tested in plasma after centrifugation of the incubated blood. Yet there are also a few parameters that adsorb to the surface and will be measured on the material. Usually additional stabilizers are added right after incubation to reduce further reactions in blood/plasma during processing.

Table 4.4 lists parameters that are determined from plasma. Activation of coagulation, fibrinolysis, and complement but also cell release products can be detected. It is desirable that these parameters are largely stable—either as a result of complex

Table 4.4 Humoral parameter measured in plasma

Category	Parameter	Information on…
Coagulation	Active FXIIa	Contact activation
	Active tissue factor (TF)	"Extrinsic" coagulation activation
	TAT (thrombin-antithrombin-complex)	Thrombin formation, integral parameter
	F1 + 2 (prothrombin fragment 1 + 2, released during thrombin formation)	Thrombin formation, integral parameter
	Free active thrombin	Thrombin formation, punctual parameter
	Fibrinopeptide A (FPA)	Fibrin formation
Fibrinolysis	D-Dimers	Fibrinolysis
Platelet activation	PF4 (platelet factor 4, release product from α-granules)	Platelet degranulation
	β-TG (β-thromboglobulin, release product from α-granules)	Platelet degranulation
Leukocyte activation	Elastase	Granulocyte degranulation
	Reactive oxygen species	Granulocyte respiratory burst metabolism
Hemolysis	Hemoglobin (released from ruptured erythrocytes)	Hemolysis
Complement activation	Bb	Alternative pathway
	C4d	Classical pathway
	C3a, C5a, sC5b-9 (terminal complement complex)	Common pathway

formation with an inhibitor or as a single molecule and can be quantified by ELISA. Usually, because of the missing exchange of blood in the in vitro hemocompatibility assays, accumulation of the markers occurs, that—even though it is not physiologic—often is desired for enhanced detection limits.

Blood coagulation leads to fibrin formation and is started on the extrinsic or intrinsic pathway. As biomaterials are supposed to mainly initiate coagulation through contact activation, several approaches to test this hypothesis were reported. A robust assay to test this is the implementation of a chromogenic substrate for FXIIa/kallikrein after a short-term contact of citrate plasma to the biomaterial [72,77]. The detection of free XIIa or of FXIIaC1-inhibitor complexes from plasma after biomaterial incubation can also be applied to determine the significance of contact activation [49].

Another possible coagulation initiator that was only recently suspected to play a role also for biomaterials is the tissue factor (TF)/FVIIa complex. Tissue factor is exposed by and released from activated leukocytes. Analysis of TF and TF activity is not a method for routine analysis and is therefore not a main tool in biomaterials evaluation [78].

Thrombin, the main enzyme of the coagulation cascade and responsible for fibrin formation, platelet activation, and several feedback reactions, has a half-life of only seconds to minutes and is rapidly inhibited by antithrombin and usually not accessible for direct analysis. Therefore either the inhibitor complex TAT or the prothrombin fragment F1 + 2 are detected—both presenting the integral activation over the whole incubation period. The dynamics of thrombin formation without addition of anticoagulants can be tested using a chromogenic substrate in recalcified plasma with inhibitors to fibrin formation or in fibrinogen poor plasma. Yet these assays depend on a certain fine-tuning of experimental conditions and should only be applied with experience. Recently a test has been developed to detect free active thrombin even in whole blood incubation settings [79,80]. This assay also provides a momentary testimony of the thrombin concentration and allows the analysis of the dynamics of thrombin formation over time.

Fibrin formation as a consequence of thrombin activity can be monitored using an ELISA for the fibrinopeptide A (FPA) [81]. FPA values usually give redundant information to the thrombin formation as well as SEM analysis of fibrin surface deposition (unpublished results), but they may be informative, if different test materials cause different kinetics of thrombin inhibition. Additionally, fibrin deposition on the sample can be detected by immunochemistry. Yet, generally no differentiation between fibrin/fibrinogen adsorption is possible.

For some studies also fibrinolysis during blood-material contact is of interest. This can be achieved by measuring D-Dimer by ELISA. However, D-Dimer formation requires a FXIIIa stabilized fibrin clot first, which usually is just under formation during typical in vitro whole blood incubation times. The interpretation of D-Dimer concentrations therefore also has to consider the amount and dynamic of clot formation besides the fibrinolytic activity.

Platelet activation determination is discussed in more detail in Section 4.4.3.1 of this chapter. Degranulation is one relevant step in this process, and released content of α-granules can be determined in plasma by ELISA: Platelet factor 4 (PF4) and β-thromboglobulin (β-TG) proved to be relevant markers with no other source than

platelets. They usually correlate well with other physiologic responses of the platelets towards biomaterials.

Leukocyte activation on biomaterials is restricted to granulocytes and monocytes, because adaptive, lymphocyte dependent immune reactions do not occur against synthetic biomaterials. Mainly two parameters are determined in plasma with high selectivity for myeloid leukocyte activation: elastase and reactive oxygen species (ROS). Granulocyte elastase is a content of the azurophil granules and released from monocytes and polymorphonuclear neutrophils as a result of the activation process [82,83]. The parameter is stable and was shown to correlate well with upregulation of the activation marker CD11b on the leukocyte membrane (unpublished results). The leukocyte activation goes along with an enhanced oxygen metabolism, the so-called respiratory burst, and the formation of ROS. Detection of ROS thus correlates with leukocyte activation and also has been suggested sometimes in the field of biomaterials testing using luminogenic [84–87] or fluorogenic detector molecules. It is interesting to note, that granulocyte activation also can lead to the ejection of their DNA, the so-called neutrophil extracellular trap (NET) formation, which recently found some attention in hemocompatibility evaluation, as the NETs themselves show procoagulant behavior [88].

Hemolysis measurement is extensively covered in the ISO standard [1]. Hemolysis is seen not only as a direct parameter for erythrocyte rupture but also generally as an indirect parameter for destructive processes. Especially pumping processes during the in vitro incubation could provoke red blood cell lysis independent of the material characteristics. But also the geometry of the biomaterial as well as chemical substances leaching form the material can be responsible for hemolysis. Several techniques to detect hemoglobin in blood as well as in blood plasma using direct measures (optical detection of oxyhemoglobin at 415, 541, or 577 nm) or derivatization leading to cyanmethemoglobin are recommended [89].

Complement activation is an early, surface-mediated, calcium dependent reaction of the innate immune system. It is generally accepted that the adsorption of C3 and C3b to the surface initiates complement activation while surface adsorbed immune complexes initiate the classical cascade. This induces the formation of the C3- and in consequence of the C5-convertase and it supports leukocyte adhesion to the surface [41]. Further on, the anaphylatoxin C5a that activates neutrophilic granulocytes and monocytes, as well as the terminal complement complex C5b-9 are formed. Most of the surface mediated complement activation products can be detected by a variety of antibody based methods [90] such as ELISA, fluorescence- or radiolabeling-techniques, QCM [91], and ellipsometry [92]. As the complement activation needs a surface as template, the C3b molecules and the bigger complement complexes are best determined on the surface using HRP (horse-radish-peroxidase)- or fluorescently labeled antibodies [41,93,94]. The minor fragments C3a and C5a however, are released to the liquid and can be determined in serum or plasma with high sensitivity. Due to the signal amplification effect of the complement cascade, C5a may be the more sensitive parameter however, it can be quenched by adsorption to receptors on the leukocytes. On the other hand C3a was shown to adsorb to surfaces [95], leading to falsely negative results [96]. Therefore the detection of several factors is helpful to avoid misinterpretation. The terminal complement complex also assembles to the plasma S-protein and can be measured as

sC5b-9 complex. In vivo it stays soluble in plasma with a considerable longer $t_{1/2}$ than C3a or C5a [97]. Analysis of the fragments Bb and C4d allow differentiation between alternative and classical pathway activation, respectively. This differentiation can further benefit from the application of specific inhibitors for one of these pathways [compstatin (alternative), MgEGTA (classical pathway)].

4.4.3 Cellular activation

Cells can adhere to biomaterial surfaces, and in consequence show signs of activation including a shift in surface adhesion molecules, shape change, and the release of granular content or the shedding of microparticles. Finally cells can become apoptotic. Depending on the type of activation several techniques as listed in Table 4.5 are usually applied to characterize material induced blood cell activation.

Suspended cells can be characterized through their absolute numbers, conjugate or aggregate formation, microparticle shedding, the release of active substances to plasma (see Section 4.4.2), or via labeling of surface associated markers. These markers also serve as parameter when detecting cell activation on surfaces via fluorescence microscopy. Additionally, shape change and cell numbers and cell association indicate activation processes.

4.4.3.1 Platelets

Activated platelets have abundant markers as sketched in Fig. 4.9 that can be determined (semi)quantitatively or qualitatively.

Table 4.5 Techniques to characterize material-induced blood cell activation

Technique	Parameter	Surface adherent cells	Suspended cells
Scanning electron microscopy	Number of adherent cells	X	
	Shape of adherent cells	X	
Fluorescence microscopy	Shape of adherent cells	X	
	Existence of surface marker		
Blood cell counter	Cell count in blood before and after incubation (indirect measure of adhesion processes)		X
Flow cytometry	Increase/decline in activation markers on cell surface		X
	Aggregate/conjugate formation		X
	Microparticle shedding		X

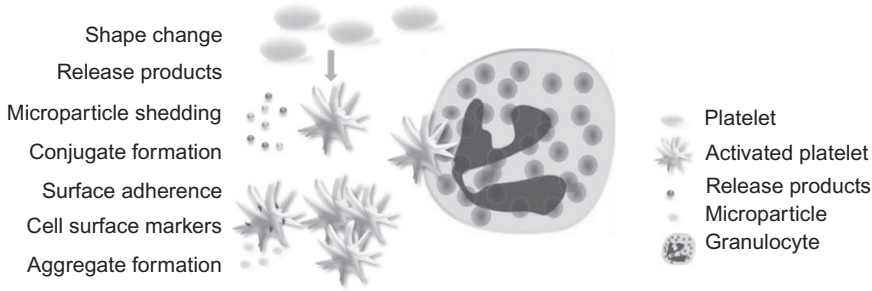


Fig. 4.9 Platelet activation and platelet activation markers.

Platelet activation through biomaterial surfaces is supposed to be primarily triggered through contact with adsorbed proteins. The conformation as well as the amount of adsorbed proteins are influential for this process. The contact of the platelets can be stable or transient. Thrombin is a strong trigger of platelet activation, thus coagulant surfaces can lead to platelet activation even without direct platelet-material contact.

Platelet-leukocyte conjugates, platelet aggregates or microparticle shedding as well as surface markers on the platelet are best measured using flow cytometry [98–100]. This technique also allows the detection of samples with low platelet count or small sample volume [101]. One common parameter for flow cytometric analysis is P-selectin (CD62p) which gets exposed on platelet surfaces [102] but also is released to the surrounding plasma [103]. Platelet P-selectin is a thrombo-inflammatory molecule involved in platelet activation and a receptor for neutrophil related PSGL-1 (P-selectin glycoprotein ligand-1) enabling platelet-neutrophil conjugate formation. This results in a loss of free P-selectin positive platelets. As P-selectin and $GPII_bIII_a$ participate in the formation of leukocyte-platelet-conjugates, these molecules do not serve as reliable activation markers on the free platelets after extended whole blood incubation experiments. More appropriate is the direct detection of conjugates or aggregates in consequence of biomaterial-platelet contact using a pan-leukocyte (usually CD45) and a pan-platelet marker [CD42b (GPIbα), CD42a (GPIX)] [104–106]. The detection of microparticles is not trivial due to their small size. Yet improved flow cytometers showed their applicability for this detection [107].

Frequently, pure quantification of the adherent platelet numbers from PRP is performed as a preliminary test to rate surface thrombogenicity. Lysis of the platelets and determination of the released lactate dehydrogenase has evolved as the standard method for this [108]. However, care has to be taken when interpreting these results for thrombogenicity, as the interplay of platelets and the coagulation cascade is neglected in this assay [72].

Microscopic (scanning electron or fluorescence microscopy) quantification of platelet adhesion and scoring the platelet shape can disclose surface-induced platelet activation [109–112] either after platelet-rich plasma- or after whole blood incubation. Microscopic techniques recently were complemented by real- time measurement of various stages of platelet adhesion and activation, indicating a dynamic process.

(QCM-D measurement of platelet activation in situ [113]; surface plasmon resonance detection of blood coagulation and platelet adhesion [114].)

This surface centered analysis always should take into account that it is just one side of the medal. For instance, many hydrogels were shown to be highly platelet-activating but not platelet-adhesive. Activated platelets shed off in form of aggregates and form microemboli in posterior organs [115].

4.4.3.2 Granulocytes/monocytes

Similar to blood platelets, also the activation of leukocytes can be observed both on the material's surface and at the cells suspended in blood. Monocytes are much less abundant in blood compared to neutrophilic granulocytes, therefore analysis usually puts enhanced focus on the latter cells. Granulocyte adhesion and activation from whole blood is an important parameter for all aspects of hemocompatibility, because there is a strong interrelation between immunologic and thrombogenic reactions.

The adhesion of granulocytes on surfaces was related to complement fragment but also to fibrinogen adsorption [41]. Neutrophil adhesion usually initiates the release of intracellular granules that contain proteolytic enzymes and ROS. Several experiments focus on the analysis of adhesion phenomena from isolated cells, yet mostly the focus of these studies lies on the molecular elucidation of adhesion molecule participation in these processes [59,62]. Surface adherent granulocytes can be analyzed with microscopic techniques to determine cell adhesion quantitatively. Nucleus staining provides an easily automated possibility. Contrary to platelets, the activation state of granulocytes is not classified by morphologic characteristics. Surface staining for release products like the NETs containing granulocyte elastase and citrullinated histones does nevertheless enable a semiquantitative analysis of activation. Recently release and surface expression of TF on granulocytes were shown. As TF strongly supports coagulation this link would be relevant for biomaterial thrombogenicity. A relation between material characteristics, TF cell surface concentration, and TF mRNA formation was shown. Yet under the experimental conditions that were applied, no pro-coagulant effect of the elevated TF formation was shown [78].

Suspended cells can be quantified through a cell counter. Their decrease during incubation enables an indirect measurement of cell adhesion and destruction. Additionally surface CD11b presents a fast responding parameter for detecting granulocyte activation in the suspended cells [41]. During activation, cells respond with upregulation of the CD11b integrin and with its activation. Conformation-specific antibodies of CD11b are available and may provide additional information about the leukocyte activation [116].

4.5 Future trends and open problems

Despite all approaches to design in vitro hemocompatibility testing as close to the physiological conditions as possible, there are still significant limitations [117]. Blood outside the circulation still needs stabilization with anticoagulants to prevent

coagulation, which in vivo are not necessary or in much lower dose. Incubation settings, which can reduce the use of anticoagulants further certainly would be favorable. Most urgently needed are smart incubation settings that enable fast and easy parallel incubation of materials with variable shear stress.

All blood responses in vivo are modulated by the endothelium. The powerful influence of endothelial cells on the reaction of blood to foreign materials was demonstrated recently [39], but the complex co-culture system of endothelial cells, blood and biomaterial still awaits further optimization for routine application as a hemocompatibility test. Such setting might provide an approach also to decrease anticoagulation.

For practical reasons, hemocompatibility tests usually are performed with blood from young and healthy donors without medication, which are not representative of the target population of the test materials. Comparative studies with blood from patients versus blood from volunteers are urgently needed.

Smart materials gain additional functions besides the hemocompatibility, such as drug delivery using nanoparticles or materials with antimicrobial properties. These effects need to be tested in parallel with hemocompatibility, as protein- or cell-deposits on the surface may affect the new functions.

References

[1] ISO/TC194, ISO 10993-4, Biological Evaluation of Medical Devices—Part 4: Selection of Tests for Interactions With Blood (ISO/DIS 10993-4:2015), Beuth Verlag GmbH, Berlin, 2016.
[2] U.T. Seyfert, V. Biehl, J. Schenk, In vitro hemocompatibility testing of biomaterials according to the ISO 10993-4, Biomol. Eng. 19 (2002) 91–96.
[3] G. Gulliver, Works of William Hewson, Sydenham Society, London, 1846.
[4] R. Virchow, Thrombose und Embolie. Gefässentzündung und septische Infektion, in: R. Virchow (Ed.), Gesammelte Abhandlungen zur wissenschaftlichen Medicin, Grote'sche Buchhandlung, Hamm, 1862.
[5] R.E. Baier, M. Kurusz, Understanding blood/material interactions: contributions from the columbia university biomaterials seminar, ASAIO J 58 (2012) 450–454.
[6] H.J. Gurland, A.M. Davison, V. Bonomini, D. Falkenhagen, S. Hansen, T. Kishimoto, M.J. Lysaght, J. Moran, A. Valek, Definition and terminology in biocompatibility, Nephrol. Dial. Transplant. 9 (1994) 4–10.
[7] E.A. Vogler, Protein adsorption in three dimensions, Biomaterials 33 (2012) 1201–1237.
[8] L. Vroman, Finding seconds count after contact with blood (and that is all I did), Colloids Surf. B Biointerfaces 62 (2008) 1–4.
[9] L. Vroman, A.L. Adams, G.C. Fischer, P.C. Munoz, Interaction of high molecular weight kininogen, factor XII, and fibrinogen in plasma at interfaces, Blood 55 (1980) 156–159.
[10] L.C. Xu, J.W. Bauer, C.A. Siedlecki, Proteins, platelets, and blood coagulation at biomaterial interfaces, Colloids Surf. B: Biointerfaces 124 (2014) 49–68.
[11] M.F. Maitz, J. Teichmann, C. Sperling, C. Werner, Surface endotoxin contamination and hemocompatibility evaluation of materials, J. Biomed. Mater. Res. B Appl. Biomater. 90 (2009) 18–25.
[12] F. Mazzotti, J. Beuttler, R. Zeller, U. Fink, S. Schindler, A. Wendel, T. Hartung, S. Von Aulock, In vitro pyrogen test—a new test method for solid medical devices, J. Biomed. Mater. Res. A 80 (2007) 276–282.

[13] S.L.J. Blok, G.E. Engels, W. Van Oeveren, In vitro hemocompatibility testing: the importance of fresh blood, Biointerphases 11 (2016). 029802.
[14] A. Pelagalli, M.A. Belisario, S. Tafuri, P. Lombardi, D. D'Angelo, L. Avallone, N. Staiano, Adhesive properties of platelets from different animal species, J. Comp. Pathol. 128 (2003) 127–131.
[15] A. Pelagalli, P. Lombardi, D. D'angelo, R. Della Morte, L. Avallone, N. Staiano, Species variability in platelet aggregation response to different agonists, J. Comp. Pathol. 127 (2002) 126–132.
[16] J.M. Siller-Matula, R. Plasenzotti, A. Spiel, P. Quehenberger, B. Jilma, Interspecies differences in coagulation profile, Thromb. Haemost. 100 (2008) 397–404.
[17] R. Barbucci, S. Lamponi, A.M. Aloisi, Effect of behavioral stress on platelet reactivity on polymeric surfaces, J. Biomed. Mater. Res. 48 (1999) 9–12.
[18] M. Cattaneo, C. Cerletti, P. Harrison, C.P.M. Hayward, D. Kenny, D. Nugent, P. Nurden, A.K. Rao, A.H. Schmaier, S.P. Watson, F. Lussana, M.T. Pugliano, A.D. Michelson, Recommendations for the standardization of light transmission aggregometry: a consensus of the working party from the platelet physiology subcommittee of SSC/ISTH, J. Thromb. Haemost. 11 (2013) 1183–1189.
[19] M. Cattaneo, C.P.M. Hayward, K.A. Moffat, M.T. Pugliano, Y. Liu, A.D. Michelson, Results of a worldwide survey on the assessment of platelet function by light transmission aggregometry: a report from the platelet physiology subcommittee of the SSC of the ISTH, J. Thromb. Haemost. 7 (2009) 1029.
[20] I. Mackie, P. Cooper, A. Lawrie, S. Kitchen, E. Gray, M. Laffan, British Committee for Standards in Haematology, Guidelines on the laboratory aspects of assays used in haemostasis and thrombosis, Int. J. Lab. Hematol. 35 (2013) 1–13.
[21] K.G. Mann, M.F. Whelihan, S. Butenas, T. Orfeo, Citrate anticoagulation and the dynamics of thrombin generation, J. Thromb. Haemost. 5 (10) (2007) 2055–2061.
[22] I. Bjork, U. Lindahl, Mechanism of the anticoagulant action of heparin, Mol. Cell. Biochem. 48 (1982) 161–182.
[23] M. Broberg, C. Eriksson, H. Nygren, Early reactions between whole blood and hydrophilic or hydrophobic glass surfaces: effects of heparin and hirudin on von Willebrand factor binding and CD62P exposure on platelets, Colloids Surf. B: Biointerfaces 11 (1998) 123–130.
[24] C. Gao, B. Boylan, J. Fang, D.A. Wilcox, D.K. Newman, P.J. Newman, Heparin promotes platelet responsiveness by potentiating alphaIIbbeta3-mediated outside-in signaling, Blood 117 (2011) 4946–4952.
[25] E.W. Salzman, R.D. Rosenberg, M.H. Smith, J.N. Lindon, L. Favreau, Effect of heparin and heparin fractions on platelet aggregation, J. Clin. Invest. 65 (1980) 64–73.
[26] R.E. Edens, R.J. Linhardt, J.M. Weiler, Heparin is not just an anticoagulant anymore: six and one-half decades of studies on the ability of heparin to regulate complement activity, in: J.M. Cruse, R.E. Lewis (Eds.), Complement Today, Karger, Basel, 1993.
[27] M. Di Nisio, S. Middeldorp, H.R. Buller, Direct thrombin inhibitors, N. Engl. J. Med. 353 (2005) 1028–1040.
[28] G. Nowak, K. Schror, Hirudin—the long and stony way from an anticoagulant peptide in the saliva of medicinal leech to a recombinant drug and beyond. A historical piece, Thromb. Haemost. 98 (2007) 116–119.
[29] R. Kopp, R. Bernsberg, A. Kashefi, K. Mottaghy, R. Rossaint, R. Kuhlen, Effect of hirudin versus heparin on hemocompatibility of blood contacting biomaterials: an in vitro study, Int. J. Artif. Organs 28 (2005) 1272–1277.

[30] T.M. Alkhamis, R.L. Beissinger, J.R. Chediak, Effect of hirudin on platelet deposition to an artificial surface during low-stress shear flow of whole blood, Biomaterials 14 (1993) 865–870.
[31] F. Bexborn, A.E. Engberg, K. Sandholm, T.E. Mollnes, J. Hong, K. Nilsson Ekdahl, Hirudin versus heparin for use in whole blood in vitro biocompatibility models, J. Biomed. Mater. Res. A 89A (2009) 951–959.
[32] M.S. Goel, S.L. Diamond, Factor VIIa-mediated tenase function on activated platelets under flow, J. Thromb. Haemost. 2 (2004) 1402–1410.
[33] M.D. Rand, J.B. Lock, C. Van't Veer, D.P. Gaffney, K.G. Mann, Blood clotting in minimally altered whole blood, Blood 88 (1996) 3432–3445.
[34] K.N.J. Stevens, Y.B.J. Aldenhoff, F.H. Van Der Veen, J.G. Maessen, L.H. Koole, Bioengineering of improved biomaterials coatings for extracorporeal circulation requires extended observation of blood-biomaterial interaction under flow, J. Biomed. Biotechnol. 2007 (2007) 29464.
[35] K.E. Brummel-Ziedins, R.L. Pouliot, K.G. Mann, Thrombin generation: phenotypic quantitation, J. Thromb. Haemost. 2 (2004) 281–288.
[36] U. Streller, C. Sperling, J. Hubner, R. Hanke, C. Werner, Design and evaluation of novel blood incubation systems for in vitro hemocompatibility assessment of planar solid surfaces, J. Biomed. Mater. Res. 66B (2003) 379–390.
[37] J. Hong, K.N. Ekdahl, H. Reynolds, R. Larsson, B. Nilsson, A new in vitro model to study interaction between whole blood and biomaterials. Studies of platelet and coagulation activation and the effect of aspirin, Biomaterials 20 (1999) 603–611.
[38] B. Oedekoven, Biocompatibility research on extracorporeal components, in: A. Krian, D. Baykut (Eds.), Current Perspectives of the Extracorporeal Circulation, Springer, Heidelberg, 2000.
[39] M. Herklotz, J. Hanke, S. Hänsel, J. Drichel, M. Marx, M.F. Maitz, C. Werner, Biomaterials trigger endothelial cell activation in co-incubation with human whole blood, Biomaterials 104 (2016) 258–268.
[40] M.F. Maitz, U. Freudenberg, M.V. Tsurkan, M. Fischer, T. Beyrich, C. Werner, Bioresponsive polymer hydrogels homeostatically regulate blood coagulation. Nat. Commun. 4 (2013) 2168, https://doi.org/10.1038/ncomms3168.
[41] C. Sperling, M.F. Maitz, S. Talkenberger, M.-F. Gouzy, T. Groth, C. Werner, In vitro blood reactivity to hydroxylated and non hydroxylated polymer surfaces, Biomaterials 28 (2007) 3617–3625.
[42] P. Borgdorff, R.H. Van Den Berg, M.A. Vis, G.C. Van Den Bos, G.J. Tangelder, Pump-induced platelet aggregation in albumin-coated extracorporeal systems, J. Thorac. Cardiovasc. Surg. 118 (1999) 946–952.
[43] C.C. Helms, M. Marvel, W. Zhao, M. Stahle, R. Vest, G.J. Kato, J.S. Lee, G. Christ, M.T. Gladwin, R.R. Hantgan, D.B. Kim-Shapiro, Mechanisms of hemolysis-associated platelet activation, J. Thromb. Haemost. 11 (2013) 2148–2154.
[44] A.C. Laga, T.A. Cheves, J.D. Sweeney, The effect of specimen hemolysis on coagulation test results, Am. J. Clin. Pathol. 126 (2006) 748–755.
[45] M.F. Whelihan, K.G. Mann, The role of the red cell membrane in thrombin generation, Thromb. Res. 131 (2013) 377–382.
[46] M. Mueller, B. Krolitzki, B. Glasmacher, Dynamic in vitro hemocompatibility testing—improving the signal to noise ratio, Biomed. Tech. 57 (Suppl.1) (2012) 549–552.
[47] A.B. Chandler, In vitro thrombotic coagulation of the blood; a method for producing a thrombus, Lab. Invest. 7 (1958) 110–114.

[48] R.A. Gardner, An examination of the fluid mechanics and thrombus formation time parameters in a Chandler rotating loop system, J. Lab. Clin. Med. 84 (1974) 494–508.
[49] R. Frank, U. Mueller, R. Lanzmich, J. Floege, Factor XII activation markers do not reflect FXII dependence of thrombin generation induced by polyvinylchloride, J. Mater. Sci. Mater. Med. 24 (2013) 2561–2566.
[50] W.G. Mcclung, D.E. Babcock, J.L. Brash, Fibrinolytic properties of lysine-derivatized polyethylene in contact with flowing whole blood (Chandler loop model), J. Biomed. Mater. Res. A 81A (2007) 644–651.
[51] S. Sinn, T. Scheuermann, S. Deichelbohrer, G. Ziemer, H.P. Wendel, A novel in vitro model for preclinical testing of the hemocompatibility of intravascular stents according to ISO 10993-4, J. Mater. Sci. Mater. Med. 22 (2011) 1521–1528.
[52] S. Krajewski, R. Prucek, A. Panacek, M. Avci-Adali, A. Nolte, A. Straub, R. Zboril, H.P. Wendel, L. Kvitek, Hemocompatibility evaluation of different silver nanoparticle concentrations employing a modified Chandler-loop in vitro assay on human blood, Acta Biomater. 9 (2013) 7460–7468.
[53] H. Touma, I. Sahin, T. Gaamangwe, M.B. Gorbet, S.D. Peterson, Numerical investigation of fluid flow in a chandler loop, J. Biomech. Eng. 136 (2014) 071004-1–071004-8.
[54] W. Van Oeveren, I.F. Tielliu, J. De Hart, Comparison of modified chandler, roller pump, and ball valve circulation models for in vitro testing in high blood flow conditions: application in thrombogenicity testing of different materials for vascular applications, Int. J. Biomater. 2012 (2012). 673163.
[55] R.G. Bacabac, T.H. Smit, S.C. Cowin, J.J.W.A. Van Loon, F.T.M. Nieuwstadt, R. Heethaar, J. Klein-Nulend, Dynamic shear stress in parallel-plate flow chambers, J Biomech. 38 (2005) 159–167.
[56] N.M.K. Lamba, J.D.S. Gaylor, J.M. Courtney, G.D.O. Lowe, Complement activation by cellulose: investigation of the effects of time, area, flow rate, shear rate and temperature on C3a generation in vitro, using a parallel plate flow cell, J. Mater. Sci. Mater. Med. 9 (1998) 409–414.
[57] M. Otto, C.L. Klein, H. Kohler, M. Wagner, O. Rohrig, C.J. Kirkpatrick, Dynamic blood cell contact with biomaterials: validation of a flow chamber system according to international standards, J. Mater. Sci. Mater. Med. 8 (1997) 119–129.
[58] N.M.K. Lamba, J.M. Courtney, J.D.S. Gaylor, G.D.O. Lowe, In vitro investigation of the blood response to medical grade PVC and the effect of heparin on the blood response, Biomaterials 21 (2000) 89–96.
[59] M.B. Lawrence, L.V. Mcintire, N.F. Eskin, Effect of flow on polymorphonuclear leukocyte/endothelial cell adhesion, Blood 70 (1987) 1284–1290.
[60] J.A. Hubbell, L.V. Mcintire, Visualization and analysis of mural thrombogenesis on collagen, polyurethane and nylon, Biomaterials 7 (1986) 354–363.
[61] S.M. De Witt, F. Swieringa, R. Cavill, M.M.E. Lamers, R. Van Kruchten, T. Mastenbroek, C. Baaten, S. Coort, N. Pugh, A. Schulz, I. Scharrer, K. Jurk, B. Zieger, K.J. Clemetson, R.W. Farndale, J.W.M. Heemskerk, J.M.E.M. Cosemans, Identification of platelet function defects by multi-parameter assessment of thrombus formation, Nat. Commun. 5 (2014) 4257.
[62] J.A. Di Vietro, M.J. Smith, B.R.E. Smith, L. Petruzzelli, R.S. Larson, M.B. Lawrence, Immobilized IL-8 triggers progressive activation of neutrophils rolling in vitro on p-selectin and intercellular adhesion molecule-1, J. Immunol. 167 (2001) 4017–4025.
[63] J. Sheriff, T.E. Claiborne, P.L. Tran, R. Kothadia, S. George, Y.P. Kato, L. Pinchuk, M.J. Slepian, D. Bluestein, Physical characterization and platelet interactions under shear flows of a novel thermoset polyisobutylene-based co-polymer, ACS Appl. Mater. Interfaces 7 (2015) 22058–22066.

[64] C. Boudot, A. Boccoz, K. Duregger, A. Kuhnla, A novel blood incubation system for the in-vitro assessment of interactions between platelets and biomaterial surfaces under dynamic flow conditions: the Hemocoater, J. Biomed. Mater. Res. A 104 (10) (2016) 2430–2440.
[65] N.P. Rhodes, A.P. Shortland, A. Rattray, D.F. Williams, Platelet reactions to modified surfaces under dynamic conditions, J. Mater. Sci. Mater. Med. 9 (1998) 767–772.
[66] D. Varon, R. Dardik, B. Shenkman, S. Kotev-Emeth, N. Farzame, I. Tamarin, N. Savion, A new method for quantitative analysis of whole blood platelet interaction with extracellular matrix under flow conditions, Thromb. Res. 85 (1997) 283–294.
[67] T. Bosch, B. Schmidt, P.C. Spencer, W. Samtleben, H.J. Gurland, Ex vivo biocompatibility evaluation of a new modified cellulose membrane, Trans. Am. Soc. Artif. Int. Org. 31 (1985) 495–498.
[68] B.M. Matata, H.Q. Yin, J.M. Courtney, J.D.S. Gaylor, N.M.K. Lamba, G.D.O. Lowe, K. Suzuki, H. Kimura, K. Izumi, H. Klinkmann, In vitro blood compatbility evaluation of hollow fibre membrane using a controlled flow system: a comparative study, Int. J. Artif. Organs 19 (1996) 582–589.
[69] R.D. Frank, J. Weber, H. Dresbach, H. Thelen, C. Weiss, J. Floege, Role of contact system activation in hemodialyzer-induced thrombogenicity, Kidney Int. 60 (2001) 1972–1981.
[70] M.B. Gorbet, M.V. Sefton, Biomaterial-associated thrombosis: roles of coagulation factors, complement, platelets and leukocytes, Biomaterials 25 (2004) 5681–5703.
[71] D.A. Lane, S.K. Bowry, The scientific basis for selection of measures of thrombogenicity, Nephrol. Dial. Transplant. 9 (1993) 18–28.
[72] C. Sperling, M. Fischer, M.F. Maitz, C. Werner, Blood coagulation on biomaterials requires the combination of distinct activation processes, Biomaterials 30 (2009) 4447–4456.
[73] H.T. Peng, Thromboelastographic study of biomaterials, J. Biomed. Mater. Res. B Appl. Biomater. 94 (2010) 469–485.
[74] V. Shankarraman, G. Davis-Gorman, J.G. Copeland, M.R. Caplan, P.F. Mcdonagh, Standardized methods to quantify thrombogenicity of blood-contacting materials via thromboelastography, J. Biomed. Mater. Res. B: Appl. Biomater. 100B (2012) 230–238.
[75] T.W. Stief, Specific determination of plasmatic thrombin activity, Clin. Appl. Thromb. Hemost. 12 (2006) 324–329.
[76] E. De Smedt, R. Al Dieri, H.M. Spronk, K. Hamulyak, H. Ten Cate, H.C. Hemker, The technique of measuring thrombin generation with fluorogenic substrates: 1. Necessity of adequate calibration, Thromb. Haemost. 100 (2008) 343–349.
[77] R. Zhuo, E.A. Vogler, Practical application of a chromogenic FXIIa assay, Biomaterials 27 (2006) 4840–4845.
[78] M. Fischer, C. Sperling, P. Tengvall, C. Werner, The ability of surface characteristics of materials to trigger leukocyte tissue factor expression, Biomaterials 31 (2010) 2498–2507.
[79] S. Krajewski, S. Krauss, J. Kurz, B. Neumann, C. Schlensak, H.P. Wendel, Real-time measurement of free thrombin: evaluation of the usability of a new thrombin assay for coagulation monitoring during extracorporeal circulation, Thromb. Res. 133 (2014) 455–463.
[80] J. Müller, T. Becher, J. Braunstein, P. Berdel, S. Gravius, F. Rohrbach, J. Oldenburg, G. Mayer, B. Pötzsch, Profiling of active thrombin in human blood by supramolecular complexes, Angew. Chem. Int. Ed. Engl. 50 (2011) 6075–6078.
[81] C.B. Geer, I.A. Rus, S.T. Lord, M.H. Schoenfisch, Surface-dependent fibrinopeptide A accessibility to thrombin, Acta Biomater. 3 (2007) 663–668.

[82] J.V. Edwards, N. Prevost, Thrombin production and human neutrophil elastase sequestration by modified cellulosic dressings and their electrokinetic analysis, J. Funct. Biomater. 2 (2011) 391–413.
[83] N. Weber, H.P. Wendel, G. Ziemer, Hemocompatibility of heparin-coated surfaces and the role of selective plasma protein adsorption, Biomaterials 23 (2002) 429–439.
[84] A. Arvidsson, P. Malmberg, P. Kjellin, F. Currie, M. Arvidsson, V. Franke Stenport, Early interactions between leukocytes and three different potentially bioactive titanium surface modifications, J. Biomed. Mater. Res. B Appl. Biomater. 97 (2011) 364–372.
[85] B. Descamps-Latscha, B. Goldfarb, A.T. Nguyen, P. Landais, G. London, N. Haeffner-Cavaillon, C. Jacquot, A. Herbelin, M. Kazatchkine, Establishing the relationship between complement activation and stimulation of phagocyte oxidative metabolism in hemodialyzed patients: a randomized prospective study, Nephron 59 (1991) 279–285.
[86] M.F. Maitz, E. Gabriel, R.P. Franke, Einfluß von bioaktiven Gläsern auf den Respiratory Burst Metabolismus von Granulozyten, Biomed. Tech. 44 (1999) 172–175.
[87] H. Nygren, M. Braide, C. Karlsson, Different kinetics of the respiratory burst response in granulocytes, induced by serum from blood coagulated in contact with polymer materials, Biomaterials 21 (2000) 173–182.
[88] C. Sperling, M. Fischer, M.F. Maitz, C. Werner, Biomaterial induced NET formation on hydrophobic surfaces supports blood coagulation, in: World Biomaterials Conference, Montreal, 2016.
[89] A. Zwart, O.W. Van Assendelft, B.S. Bull, J.M. England, S.M. Lewis, W.G. Zijlstra, Recommendations for reference method for haemoglobinometry in human blood (ICSH standard 1995) and specifications for international haemiglobinocyanide standard (4th edition), J. Clin. Pathol. 49 (1996) 271–274.
[90] T.E. Mollnes, T.S. Jokiranta, L. Truedsson, B. Nilsson, S. Rodriguez De Cordoba, M. Kirschfink, Complement analysis in the 21st century, Mol. Immunol. 44 (2007) 3838–3849.
[91] M. Andersson, J. Andersson, A. Sellborn, M. Berglin, B. Nilsson, H. Elwing, Quartz crystal microbalance-with dissipation monitoring (QCM-D) for real time measurements of blood coagulation density and immune complement activation on artificial surfaces, Biosens. Bioelectron. 21 (2005) 79–86.
[92] P. Tengvall, A. Askendal, I.I. Lundstrom, Ellipsometric in vitro studies on the activation of complement by human immunoglobulins M and G after adsorption to methylated silicon, Colloids Surf. B: Biointerfaces 20 (2001) 51–62.
[93] J. Andersson, K.N. Ekdahl, J.D. Lambris, B. Nilsson, Binding of C3 fragments on top of adsorbed plasma proteins during complement activation on a model biomaterial surface, Biomaterials 26 (2005) 1477–1485.
[94] M. Harboe, E.B. Thorgersen, T.E. Mollnes, Advances in assay of complement function and activation, Adv. Drug Deliv. Rev. 63 (2011) 976–987.
[95] A. Kandus, R. Ponikvar, J. Drinovec, S. Kladnik, P. Ivanovich, Anaphylatoxins C3a and C5a adsorption on acrylonitrile membrane of hollow-fiber and plate dialyzer—an in vivo study, Int. J. Artif. Organs 13 (1990) 176–180.
[96] A.K. Cheung, C.J. Parker, L.A. Wilcox, J. Janatova, Activation of complement by hemodialysis membranes: polyacrylonitrile binds more C3a than cuprophan, Kidney Int. 37 (1990) 1055–1059.
[97] G. Bergseth, J.K. Ludviksen, M. Kirschfink, P.C. Giclas, B. Nilsson, T.E. Mollnes, An international serum standard for application in assays to detect human complement activation products, Mol. Immunol 56 (2013) 232–239.

[98] V. Schmidt, T. Hilberg, ThromboFix TM platelet stabilizer: advances in clinical platelet analyses by flow cytometry? Platelets 17 (2006) 266–273.
[99] G. Schmitz, G. Rothe, A. Ruf, S. Barlage, D. Tschöpe, K.J. Clemetson, A.H. Goodall, A.D. Michelson, A.T. Nurden, T.V. Shankey, European working group on clinical cell analysis: consensus protocol for the flow cytometric characterisation of platelet function, Thromb. Haemost. 79 (1998) 885–896.
[100] J.F. Van Velzen, B.A.P. Laros-Van Gorkom, G.A.M. Pop, W.L. Van Heerde, Multicolor flow cytometry for evaluation of platelet surface antigens and activation markers, Thromb. Res. 130 (2012) 92–98.
[101] I.M. De Cuyper, M. Meinders, E. Van De Vijver, D. De Korte, L. Porcelijn, M. De Haas, J.A. Eble, K. Seeger, S. Rutella, D. Pagliara, T.W. Kuijpers, A.J. Verhoeven, T.K. Van Den Berg, L. Gutiarrez, A novel flow cytometry-based platelet aggregation assay, Blood 121 (2013) e70–e80.
[102] J.-F. Theoret, D. Yacoub, A. Hachem, M.-A. Gillis, Y. Merhi, P-selectin ligation induces platelet activation and enhances microaggregate and thrombus formation, Thromb. Res. 128 (2011) 243–250.
[103] K. Kawabata, Y. Nagake, K. Shikata, S. Fukuda, H. Nakazono, M. Takahashi, H. Ichikawa, H. Makino, Soluble P-Selectin is released from activated platelets in vivo during hemodialysis, Nephron 78 (1998) 148–155.
[104] A.H. Goodall, J. Appleby, Flow-cytometric analysis of platelet-membrane glycoprotein expression and platelet activation, in: J.M. Gibbins, M.P. Mahaut-Smitz (Eds.), Platelets and Megakaryocytes, Vol.1: Functional Assays, Humana Press, Totowa, NJ, 2004.
[105] R.P. Mcever, P-selectin, in: M.C. Berndt (Ed.), Platelets, Thrombosis and the Vessel Wall, Harwood Academic Publishers, Amsterdam, 2000.
[106] D. Pidard, M. Si-Tahar, M. Chignard, Neutrophil-platelet interactions, in: M.C. Berndt (Ed.), Platelets, Thrombosis and the Vessel Wall, Harwood Academic Publishers, Amsterdam, 2000.
[107] S. Robert, R. Lacroix, P. Poncelet, K. Harhouri, T. Bouriche, C. Judicone, J. Wischhusen, L. Arnaud, F. Dignat-George, High-sensitivity flow cytometry provides access to standardized measurement of small-size microparticles—brief report, Arterioscler. Thromb. Vasc. Biol. 32 (2012) 1054–1058.
[108] J.M. Grunkemeier, W.B. Tsai, T.A. Horbett, Hemocompatibility of treated polystyrene substrates: contact activation, platelet adhesion, and procoagulant activity of adherent platelets, J. Biomed. Mater. Res. 41 (1998) 657–670.
[109] R.D. Allen, L.R. Zacharski, S.T. Widirstky, R. Rosenstein, L.M. Zaitlin, D.R. Burgess, Transformation and motility of human platelets: details of the shape change and release reaction observed by optical and electron microscopy, J. Cell Biol. 83 (1979) 126–142.
[110] S. Braune, G.M. Frohlich, A. Lendlein, F. Jung, Effect of temperature on platelet adherence, Clin. Hemorheol. Microcirc. 61 (2016) 681–688.
[111] S.L. Goodman, T.G. Grasel, S.L. Cooper, R.M. Albrecht, Platelet shape change and cytoskeletal reorganization on polyurethaneureas, J. Biomed. Mater. Res. 23 (1989) 105–123.
[112] K. Park, F.W. Mao, H. Park, Morphological characterization of surface-induced platelet activation, Biomaterials 11 (1990) 24–31.
[113] J. Fatisson, S. Mansouri, D. Yacoub, Y. Merhi, M. Tabrizian, Determination of surface-induced platelet activation by applying time-dependency dissipation factor versus frequency using quartz crystal microbalance with dissipation, J. R. Soc. Interface 8 (2011) 988–997.

[114] K.M. Hansson, K. Johansen, J. Wettero, G. Klenkar, J. Benesch, I. Lundstrom, T.L. Lindahl, P. Tengvall, Surface plasmon resonance detection of blood coagulation and platelet adhesion under venous and arterial shear conditions, Biosens. Bioelectron. 23 (2007) 261–268.
[115] S.R. Hanson, L.A. Harker, B.D. Ratner, A.S. Hoffman, Factors influencing platelet consumption by polyacrylamide hydrogels, Ann. Biomed. Eng. 7 (1979) 357–367.
[116] Y.-M. Xiong, J. Chen, L. Zhang, Modulation of CD11b/CD18 adhesive activity by its extracellular, membrane-proximal regions, J. Immunol. 171 (2003) 1042–1050.
[117] I. Reviakine, F. Jung, S. Braune, J.L. Brash, R. Latour, M. Gorbet, W. Van Oeveren, Stirred, shaken, or stagnant: what goes on at the blood-biomaterial interface, Blood Rev. 31 (2016) 11–21.

Part Two

Improving the hemocompatibility of biomaterial surfaces

This page intentionally left blank

Analyzing biomaterial surfaces and blood-surface interactions

5

M. Nezafati
Emory University, Atlanta, GA, United States

Implantable materials must be compatible with blood. To emphasize the importance of hemocompatibility, just in the brain alone, there are 500 mi of blood vessels [1], so when a prosthetic device is implanted in brain tissue, interaction with a vascular vessel is not only probable but also inevitable.

The brain vasculature system is illustrated in Fig. 5.1. It can be seen that the network of blood vessels is packed densely so any foreign object that is implanted in a patient's head must not cause any thrombosis when it contacts a blood vessel [2,3]. As a part of the premedical evaluation of implantable biomaterials and devices, performing a test that can determine the blood compatibility (i.e., hemocompatibility) is necessary. Embolic problems with catheters, failure of biosensors due to thrombus accumulation, and platelet activation on long-term implants are just a few examples of the problems that may occur if an implantable biomaterial is not hemocompatible [4].

In the literature, which has been focused on the topic of blood compatibility, researchers try to answer the following questions:

- How can blood compatibility be measured?
- What materials can be called "hemocompatible"?
- What is the biological basis of the reaction of materials with blood [4]?

Based on these questions, in this chapter, the focus is on both hemocompatibility methodology and material evaluation. The minimum requirements for hemocompatibility measurements are mentioned in section 4 of ISO 10993. Based on ISO 10993-4, we describe an experiment that we designed to evaluate the blood compatibility of the materials in both the static and dynamic state.

The first step was to understand the thrombosis model, then to develop the experimental methods, and finally to select the experimental controls based on the current information present in the ISO. Statistical data (mean value, standard deviation, and 95% confidence interval) must be the experimental outcome of any hemocompatibility assessment. Tests have to be performed with a minimum delay of usually 2 h since some properties of blood change rapidly following collection. Various conditions (depending on the wall shear rate) were simulated within the circulation system (i.e., dynamic testing). The qualities and aspects of hemocompatibility that can be analyzed are platelet activation, oxidative burst, hemolysis, fibrinolysis, fibrin formation, generation of thrombin, contact activation, and complement activation [5]. In this chapter, the major focus is on platelet activation in the dynamic state. The results were entered nondimensionally into a nondimensional score system, where 0 points stand for the

Hemocompatibility of Biomaterials for Clinical Applications. https://doi.org/10.1016/B978-0-08-100497-5.00014-8
© 2018 Elsevier Ltd. All rights reserved.



Fig. 5.1 Human brain and neck blood vessel network (i.e., brain vasculature) [1] showing how dense is the brain vasculature. Clearly, any neural implant will subtend a blood vessel, thus making the hemocompatibility of biomaterials an important property of implantable devices.
Reproduced with permission from to-BBB and presented in Appendix A.

best and 100 points for the worst experimental outcome. The goal was to find a good correlation between the total platelet activation score in the high-shear-stress system. Before explanation about the circuit design, some basic flow dynamics phenomena about human physiology must be explained [6,7].

5.1 Flow dynamics

The blood flow in veins, arteries, and capillaries can be considered as a laminar flow that is consisted of parallel streamlines in the rigid tubes. Since the blood flow is considered as a laminar flow, the thin blood layer that is in contact with the blood vessel can be considered as a steady layer without any velocity. The velocity in the center of the blood vessel has the highest value. Fig. 5.2 shows the flow gradient within a blood vessel. A flow that has a velocity lower than the critical velocity is called the laminar flow, and if the velocity is equal or higher than the critical value, it is called the turbulent flow. The turbulent flow normally generates sound; on the other hand, the laminar flow is silent; the sound created by the turbulent flow is called a bruit and is so useful in medical sciences.

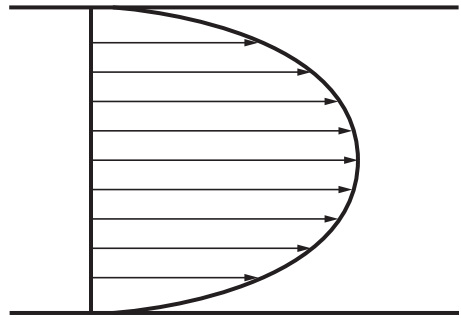


Fig. 5.2 Velocity vector distribution of a laminar flow pattern in tube geometry. Zero velocity occurs on the blood vessel walls, and a maximum flow occurs in the blood vessel center, as shown.

There are two parameters that affect the probability of turbulence flow occurrence: First is the radius of the tube, and second is the viscosity of the blood. The mathematical relation of the inertial ratio to viscous forces is a unitless number called Reynolds number that can specify the probability of having a turbulence flow [8,9]. The magnitude of the Reynolds number has a direct relation with the probability of turbulence; the increase in value of the number will result in the increase of value of probability.

In humans, by the time of constriction in the artery and when the maximum systolic ejection occurs, the blood flow becomes a turbulence flow, and the velocity value is more than critical velocity value [10,11]. In the patient with anemia due to lower blood viscosity, the Reynolds number increases, so the probability of the turbulence flow increases, and they will have systolic murmurs [10].

At the time of study, the flow dynamics recognizes the difference between the velocity that is defined as displacement in unit time (e.g., m/s) and the flow that can be defined as moved volume per unit time (e.g., cm^3/s). The value of volumetric flow rate (Q) is equal to velocity (V) multiplied by cross-sectional area of the tube (A); the following equation is showing the value:

$$V = Q / A \tag{5.1}$$

In the tube network such as human vascular system, the total cross-sectional area of the blood vessels has an inverse effect on the average blood velocity at that specific point. For example, the average blood velocity in the aorta is higher than the capillaries that have the slowest velocity due to a larger total cross-sectional area. It must be kept in mind that the diameter of an individual capillary is smaller than the aorta but the total cross section of the capillaries is 1000 times larger than the value for the aorta, and in blood flow, the total cross section is considered not the individual cross section. When the blood enters the veins, the velocity increases, but it is not as fast as the aorta.

The average velocity of blood is 40 cm/s in the aorta; also the maximum velocity occurs in systolic state that is 120 cm/s, and the same value but with opposite direction happens in diastolic state.

5.2 Chandler's loop

A useful test configuration was developed by Chandler in 1958 to measure blood-clotting times [7]. Chandler's loop system consisted of a tube that was filled 70% of its capacity with blood and connected with a silastic collar to close the loop; the circuit was tilted at 45 degrees. The tube was rotating till the blood clot in the tube; the time that requires to form a blood layer on the surface and form the blood clot was the goal of his initial study [12].

In recent years, the Chandler loop system has been modified for anticoagulated blood to measure biomaterial-induced platelet activation [8]. The most noticeable modification in the chandler's loop is the increase of surface-area-to-blood-volume ratio that will result in the reduction of background noise. Even with the modifications in the Chandler's loop, the presence of air bubbles that causes blood-air interface is a major drawback in this method of evaluating the hemocompatibility of the materials. The presence of blood-air interface could result in protein aggregation that will result in platelet activation. In the empirical experiments, the presence of even microscopic air nuclei resulted in increase of platelet adhesion and activation of them afterward [13].

5.3 Current design

These experiments were designed to use a modified Chandler's loop. The loop consists of a peristaltic pump, 0.2 in (5.08 mm) diameter S-50-HL PVC Medical Surgical Tubing, Clear (Tygon) tubing (the surgical grade PVC provided by Tygon is different from the fuel PVC tubes that contain organotin and used as positive control), sample holder, polymeric gasket, and vacuum system as shown in Fig. 5.3. The circuit was placed inside a 1 m^3 polyethylene chamber including an electric heater that maintains the temperature at 37 ± 1°C. The system is housed in the pathology and cell biology laboratory of Dr. K. Muffly, USF Morsani College of Medicine.

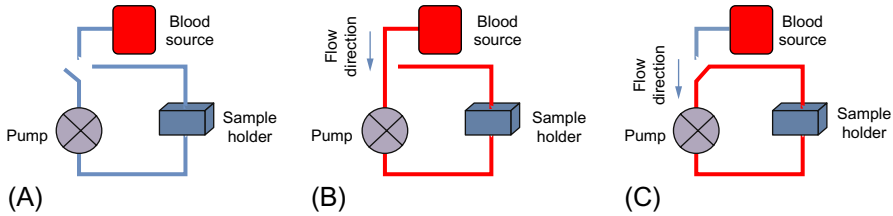


Fig. 5.3 The schematic of the modified Chandler's circuit design in (A) stage 0, where the circuit is open and the tubes were rinsed with PBS; (B) stage 1, where the circuit is still open but the blood source is connected; and (C) stage 2, where the circuit is closed and the tubes are completely filled with PRP.

The sample size was originally 50×75 mm. A new sample holder was designed using solid works and printed using the USF SiC Group 3D printer (using nylon). The sample size from the new design is 10×30 mm, which was done to conserve area and reduce material cost, especially for the SiC samples. Once the new system passed the leaching test, it replaced the old one. Fig. 5.3 (right) shows the initial sample holder.

Fig. 5.4 shows the new sample holder design. The left figure shows the 3D-printed sample holder, the center figure is the solid works design, and the right one is the sample holder that was machined out of Teflon. Due to surface roughness issues, which disturbed the fluid flow during prototype testing, it was decided to machine a block of Teflon instead of using the 3D-printed nylon cell. The Teflon cell will be used for all subsequent experiments presented in this chapter (Fig. 5.5).

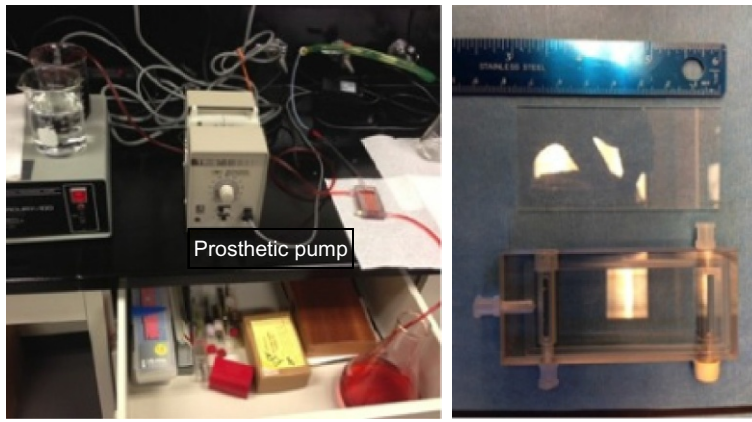


Fig. 5.4 The current dynamic hemocompatibility test set up in Dr. Muffly's lab in the USF College of Medicine (left). The original sample holder, which can accommodate large 50×75 mm samples (right).

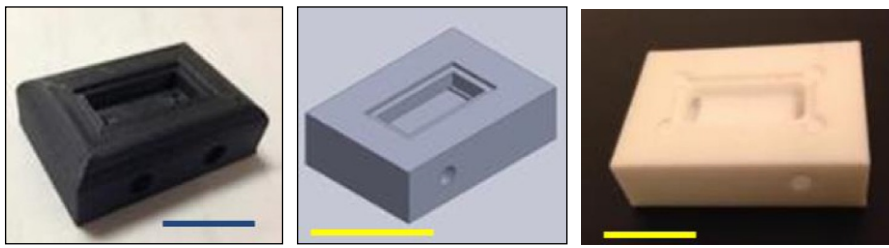


Fig. 5.5 Design and fabrication of a new, more cost-effective sample holder. USF SiC Group 3D-printed nylon cell (left), solid-works schematic (center), and sample holder machined out of Teflon by the USF engineering machine shop (right). The scale bars have the length of 2 cm in all the images.

5.4 Method and materials

The test materials were Si (100) from University Wafers lot 567434, 3C-SiC grown in the University of South Florida SiC group hot-wall CVD reactor MF2 (sample ID USF2-14-28), *a*-SiC deposited via PECVD on Si in the USF NREC, polyethylene (as negative control), and PVC (Tygon) (as positive control).

5.4.1 Platelet rich plasma preparation

Farm pig blood was provided by the University of South Florida's Center for Advanced Medical Learning and Simulation (USF-CAMLS) labs under Institutional Animal Care and Use Committee (IACUC) certification (protocol ID, T IS00000216). The blood was collected postmortem by the CAMLS lab technician in blood bags including acid citrate dextrose (ACD) as an anticoagulant (1:9 ACD, blood volume ratio). The blood bags were stored in a portable refrigerator at 4°C and transported to the IDRB 313 lab using a portable refrigerator at 4°C. Next, 50 mL ACCUSPIN centrifuge tubes were filled with 45 mL of whole blood. The tubes were centrifuged at 4°C for 10 min at 1000 *g*. As shown in Fig. 5.6A, the blood consists of three phases after centrifuge: 55% of total blood is the plasma that will be above the other layers due to its lower density; the buffy coat that includes leukocytes and platelets forms 1% of whole blood and is located between the plasma and erythrocyte layers; the erythrocyte layer has the highest density and will be under the two other layers after centrifuge. In Fig. 5.6B, the whole blood sample after centrifuge is shown. Due to the presence of the membrane in the ACCUSPIN, the plasma, leukocytes, and platelet phases were not mixed with the erythrocytes and form a type of media that had a high concentration

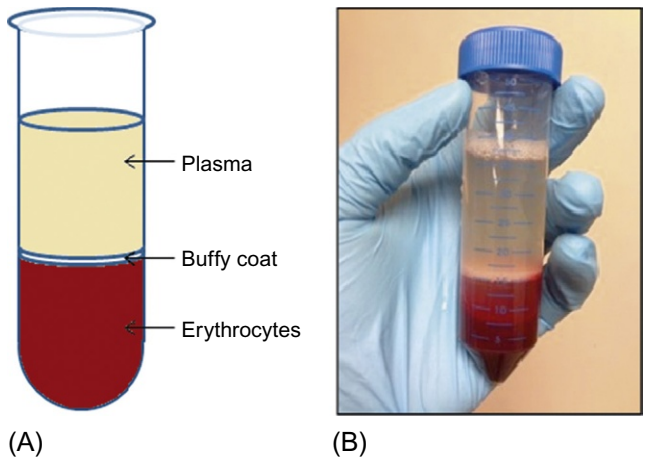


Fig. 5.6 Formulation of PRP for hemocompatibility testing: (A) schematic that shows the three phases of the blood after centrifuge and (B) the 50 mL ACCUSPIN centrifuge tube including the separated PRP and erythrocyte phases. The PRP is the nearly clear liquid layer on top of the two red layers below.

of the platelets. The platelet rich plasma (PRP) was collected in the 50 mL conical centrifuge tubes and stored in the refrigerator at 4°C. The concentration of platelets in the PRP was measured using a hemocytometer, and it was found to be ~150,000 platelets per 1 μL.

The PRP was then transported to the pathology and cell biology laboratory of Dr. K. Muffly, USF Morsani College of Medicine (transit time ~20 min) where it was used to test the platelet interaction with various materials as outlined above.

We can determine the PRP velocity directly from Eq. (5.1) (i.e., $V = Q/A$). By measuring the flow Q and knowing the cross-sectional area, the velocity V can be determined. Based on the velocity, we can control the flow to be laminar or turbulent.

The flow rate was measured right before and after the sample holder. The tube area is 0.2 cm^2, so the flow must be less than 8 cm^3/s. So we have adjusted the pump in a way that the flow that enters the sample holder is equal to the flow that exits the sample holder and is less than 8 cm^3/s. When we did this measurement, the PRP was replaced with 100 mL of fresh PRP, the flow cell tubing was filled, and the flow was initiated with a syringe by hand. When the tube was filled and air bubbles were minimized, the two ends of the tube were connected to have a closed-loop flow system (Fig. 5.3B). The pump ran for 15 min, and the sample under test was retrieved for platelet fixing and subsequent microscope analysis.

Platelet activation was evaluated by using fluorescence microscopy as described by N. Schettini of the USF SiC group during her static hemocompatibility tests of SiC materials [6]. Her sample preparation involved 1 μL/mL Rothamin solution in 1X PBS that was used as the fluorescent dye, and the micrographs were analyzed using imageJ analysis software. Surface changes were evaluated using SEM and AFM analyses after platelet removal and sample cleaning. In that work, it was demonstrated that 3C-SiC had superior hemocompatibility to 4H- and 6H-SiC, as well as Si, via the observation of significantly lower platelet adhesion and activation [6]. Indeed, the work reported by Schettini was the basis for the dynamic work reported here, as a more realistic model of the physiological environment is a more reliable measure of a material compatibility with blood.

5.5 Static hemocompatibility experiment

The hemocompatibility of semiconductor materials and specifically silicon carbide in the static state was studied by Schettini in 2009 [6], and 3C-SiC showed a promising result in those experiments. So in this set of experiments, the hemocompatibility of Si (100), 3C-SiC, SiO_2, and *a*-SiC was evaluated when the flow rate was equal to 0 cm^3/s to achieve two goals: first to study the platelet adhesion to the surface when the shear forces are not present and second to have a comparable result with the previous studies.

As shown in Fig. 5.7A, the 3C-SiC fluorescence micrograph shows little platelet activation. By comparing this result with the *a*-SiC micrograph in Fig. 5.7B and Si (100) in Fig. 5.7D, it can be concluded that 3C-SiC showed an acceptable hemocompatibility in comparison with the other two silicon-based materials that are already

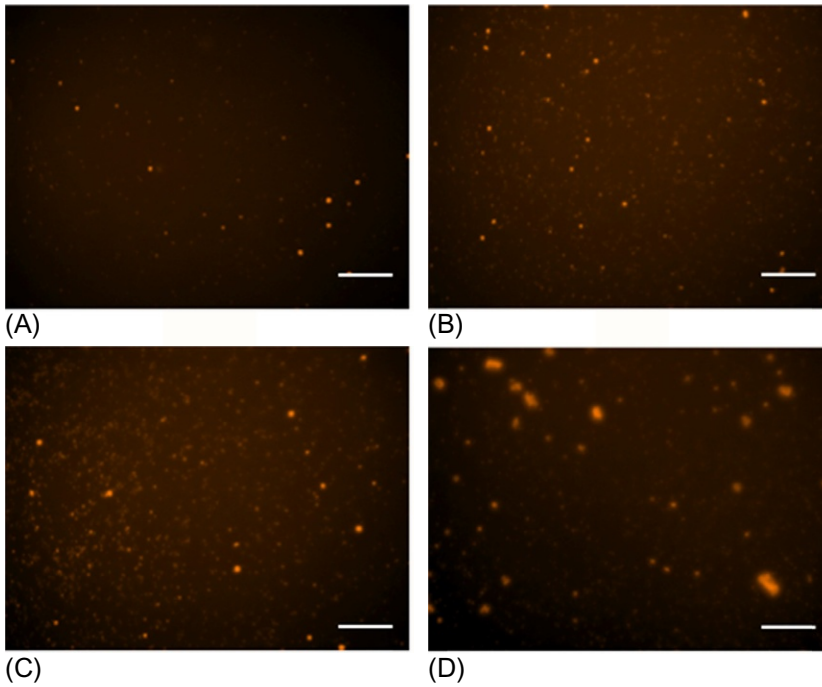


Fig. 5.7 Static hemocompatibility test fluorescence micrographs using Rothamin as a fluorescence tag at 50 times of magnification: (A) 3C-SiC, (B) *a*-SiC, (C) SiO_2, and (D) Si (100). Scale bar is equal to 100 μm.

used in prosthetic devices. Also SiO_2 was tested as positive control to show that the test is working. As it can be seen in Fig. 5.7C, the platelets were completely activated on the surface of SiO_2 that verifies the role of glass as a positive control for blood compatibility.

The statistical analysis was performed on the results of hemocompatibility test. The ANOVA analysis showed the value of 4.1 for "F" that is higher than the 3.4 value for Fc. This means that the samples behaved significantly differently. Also by doing the paired t-test on the results, we can conclude that 3C-SiC showed the lowest platelet activation, *a*-SiC had more platelet activation than 3C-SiC, and Si (100) showed higher values in comparison with the first two samples. The SiO_2 showed the highest value of platelet activation among the tested materials.

5.6 Dynamic hemocompatibllity experiments

The hemocompatibility of the biomaterials was tested in a dynamic state to simulate the real conditions of the in vivo environment. Tests in a static state showed a promising result, but to verify the performance of a device for biomedical applications, it must be tested in more realistic environment. Applied shear forces to the blood proteins could

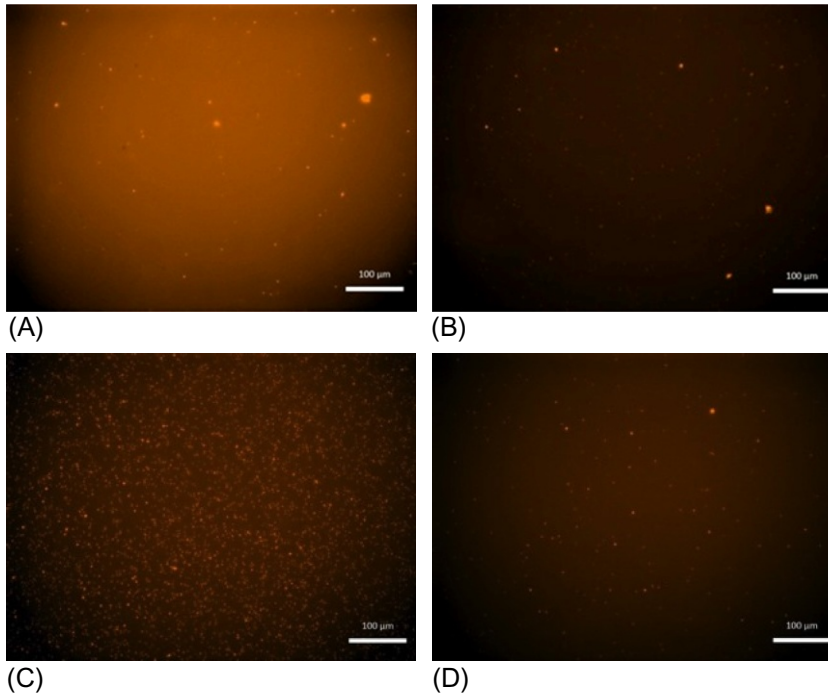


Fig. 5.8 Dynamic hemocompatibility test fluorescence micrographs using Rothamin as a fluorescence tag at 50 times of magnification: (A) 3C-SiC, (B) *a*-SiC, (C) SiO_2, and (D) Si (100). Scale bar is equal to 100 µm.

alter the platelet adhesion to the surface of implanted samples. Therefore, a study of the effect of various flow rates and exposure time on platelet binding and activation is very important. The samples for the dynamic experiment were 3C-SiC, *a*-SiC, Si (100), and SiO_2 thin film.

Fig. 5.8A shows the fluorescence micrograph of 3C-SiC after dynamic hemocompatibility testing with the rate of less than 8 cm^3/s for 15 min. As can be seen in the figure, the 3C-SiC samples showed the lowest platelet activation. The platelet activation was higher on *a*-SiC in comparison with 3C-SiC and also Si (100) (Fig. 5.8D) that showed higher platelet activation in comparison with the first two types of materials.

The qualitative data of Fig. 5.8 can be more meaningful when statistical analysis was performed on the obtained data. Fig. 5.9 shows a histogram including the data standard deviation as error bars. Two important points can be understood from the statistical analysis of dynamic test. First, the platelet activation decreased when a shear force was applied to the cells in the flow even for the laminar flow conditions of the test. The activation of the platelets decreased by a factor of 9% when the materials were tested under laminar flow. Second point that can be understood from Fig. 5.9 is the performance of the materials. The materials behaved the same way in the dynamic test as they behaved under a static state.

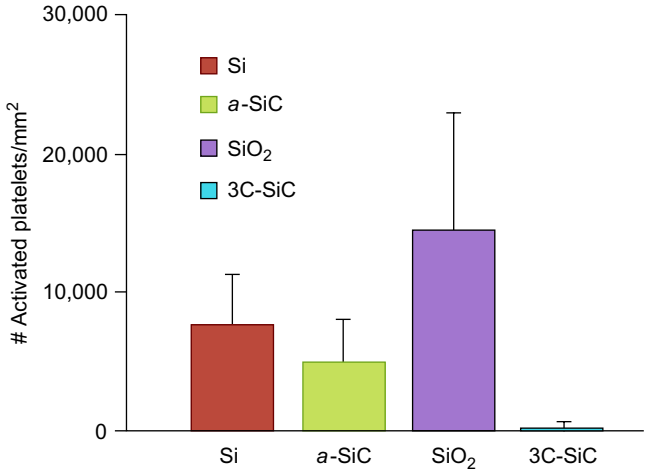


Fig. 5.9 Dynamic hemocompatibility histogram of platelet activation of the Si, *a*-SiC, SiO_2, and 3C-SiC using standard deviation as the error bar. Activated platelets per square millimeter used to evaluate the hemocompatibility of the materials.

5.7 Summary

In the last two chapters, the stability and cytotoxicity of biomaterials were studied. In this chapter, the blood compatibility of biomaterials under the static state and under laminar flow using PRP was studied. A modified Chandler's loop was used as the blood circuit. The platelet activation as measure of hemocompatibility was studied using fluorescence microscopy. The data obtained from the static test verified the previous work reported using the same method by Schettini in 2009 [6]. That is, 3C-SiC showed lower platelet attachment and activation in comparison with conventional implant materials such as Si (100), *a*-SiC, and SiO_2. The obtained result from dynamic testing under laminar flow had the same performance as the samples in static state, but 9% lower platelet attachment, on average, for almost all samples tested. While these preliminary dynamic flow data are encouraging, we need to study the performance of the materials in various flow rates and time frames to fully understand the hemocompatibility of a particular material.

References

[1] M. Scudellari, Penetrating the Brain, Available from: http://www.the-scientist.com/?articles.view/articleNo/37957/title/Penetrating-the-Brain/, 2013.

[2] K. Kottkemarchant, et al., Effect of albumin coating on the in vitro blood compatibility of Dacron arterial prostheses, Biomaterials 10 (3) (1989) 147–155.

[3] K. Kottkemarchant, J.M. Anderson, A. Rabinovitch, The platelet reactivity of vascular graft prostheses: an in vitro model to test the effect of preclotting, Biomaterials 7 (6) (1986) 441–448.

[4] B.D. Ratner, Blood compatibility—a perspective, J. Biomater. Sci. Polym. Ed. 11 (11) (2000) 1107–1119.
[5] R.K. Roy, et al., Hemocompatibility of surface-modified, silicon-incorporated, diamond-like carbon films, Acta Biomater. 5 (1) (2009) 249–256.
[6] N. Schettini, Hemocompatibility Assessment of 3C-SiC for Cardiovascular Applications, in Electrical Engineering, University of South Florida, Tampa, FL, 2009.
[7] U.T. Seyfert, V. Biehl, J. Schenk, In vitro hemocompatibility testing of biomaterials according to the ISO 10993-4, Biomol. Eng. 19 (2–6) (2002) 91–96.
[8] A. Bolz, M. Schaldach, Hemocompatibility optimization of implants by hybrid structuring, Med. Biol. Eng. Comput. 31 (1993) S123–S130.
[9] B.A. Weisenberg, D.L. Mooradian, Hemocompatibility of materials used in microelectromechanical systems: platelet adhesion and morphology in vitro, J. Biomed. Mater. Res. 60 (2002) 8.
[10] L. Muthusubramaniam, et al., Hemocompatibility of silicon-based substrates for biomedical implant applications, Ann. Biomed. Eng. 39 (4) (2011) 1296–1305.
[11] K. Ishihara, et al., Hemocompatibility of human whole-blood on polymers with a phospholipid polar group and its mechanism, J. Biomed. Mater. Res. 26 (12) (1992) 1543–1552.
[12] A. Chandler, In vitro thrombotic coagulation of the blood; a method for producing a thrombus, Lab. Invest. 7 (2) (1958) 110.
[13] C.L. Haycox, B.D. Haycox, Ratner, in vitro platelet interactions in whole human blood exposed to biomaterial surfaces: insights on blood compatibility, J. Biomed. Mater. Res. 27 (9) (1993) 1181–1193.

This page intentionally left blank

Surface analysis technique for assessing hemocompatibility of biomaterials

6

V. Kumar[*], *P. Gopinath*[*], *V.-K. Lakshmanan*[†], *K. Navaneetha Pandiyaraj*[‡]
[*]Indian Institute of Technology Roorkee, Roorkee, India, [†]Chonnam National University Medical School, Gwangju, South Korea, [‡]Sri Shakthi Institute of Engineering and Technology, Coimbatore, India

6.1 Introduction

In living organism, blood is a complex biochemical system that contains various blood components that play important roles in various life functions, like oxygen transporter, destruction of harmful pathogens, and repair of damaged tissues. So, these various functions of blood are very crucial for any medical devices because these devices are interacted with the blood components when they are implanted inside the body, and these devices must be hemocompatible in nature. If these medical devices are not compatible with blood components, then there will be an immune reaction taking place to reject that graft or implant. For example, disruption of red blood cells called hemolysis takes place that is mediated by the biomaterials. Due to damage of the RBCs, it directly diminishes the ability of the circulatory system to carry oxygen to body tissues [1].

The main constituents of the blood are plasma and red blood cells (RBCs), the composition of blood plasma containing isotonic electrolyte solution that is having 0.9% sodium chloride and high amount of protein content ~(40–60 g/L). In blood, the concentration of albumin protein is more than half of the total plasma proteins present in the human blood. Apart from proteins, there are other low-level constituents present in blood that is really helpful for many functions of a whole organism; these constituents are various clotting factors, various antiproteases enzymes, transporter proteins, and immunoglobulins. Blood contains the platelet that is very essential for vascular homeostasis. It means that platelets can easily adhere on the wall and activate. During activation, there will be high chances of exposed components from the blood vessel walls and granting protection for vascular bed integrity. Thrombosis is also one of the major obstacles when we use the biomaterials contacted with blood. When the biomaterial is contacted with blood components, then at the site of vascular injury, there will be thrombosis that starts to cause adhesion of platelets on the biomaterial that further activate the blood-clotting cascade and start the formation of fibrin clot. The major morphotic component of the thrombus is activated platelets and other cells like erythrocytes and leukocytes; these cells are also accumulating at the site of fibrin deposition. Like activated platelets, activated leukocytes also easily adhere to the surface of

Hemocompatibility of Biomaterials for Clinical Applications. https://doi.org/10.1016/B978-0-08-100497-5.00006-9
© 2018 Elsevier Ltd. All rights reserved.

endothelial cells and migrate out of bloodstream into surrounding tissues. So with the adherence of the leukocytes and platelets eon, the material is also important for testing of hemocompatibility; after contacting with the surface, these cells can activate alongside the platelets and adhere to the vascular wall promoting thrombosis [2].

Major roles of biomedical devices that are made up of biomaterials are to fulfill the shortage of organs and treat damaged organs caused by the accidents and injuries. These biomedical devices are the artificial heart, lungs, and kidneys. There are some interventional devices also present like cardiovascular stents and catheters. When these devices are placed inside the body, there will be some human immune reactions taking place against to repair and heal the damaged organs rapidly. Water and protein adsorption takes place on the surface of the blood vessel walls. Then, there is immune reaction that starts in that region where biomaterial is implanted; in this reaction, leucocytes and platelets are interacted with the biomaterial surfaces and are activated. After adherence on the surface of the biomaterials, these adhered platelets are activated due to stimulation by cytokines and growth factors. So due to adherence of more platelets on the biomaterial surface causing clotting of blood that confirms that the biomaterial is not hemocompatible in nature, there is a significant factor present to confirm hemocompatibility of biomaterials is the response of platelets present inside the body when it interact with surface of the material [3].

Hemocompatibility property of the biomaterial surface is improved by the less adsorption of proteins on the surface of the biomaterials; due to less adherence of proteins, there will be less number of platelets adhered on the surface of the biomaterial. Nowadays, vascular-related diseases are major diseases worldwide. For treating vascular-related diseases, only transplantation of vessels (vasotransplantation) is present. Currently, statistics shows that the more than 1.4 million bypass surgery is performed in the United States alone, and about three times this number are performed worldwide [4]. The ideal bypass grafts are autologous vessels that are harvested from patient's saphenous vein or internal mammary artery. Harvesting vessels from patients who suffer from vascular diseases with sufficient length for effective bypass without causing additional morbidity can be difficult to achieve in many patients, due to previous surgery or injury [5]. For solving these major problems, researchers made artificial vascular grafts using different forms of biomaterials that are therefore widely used to replace or bypass diseased arteries. At the macrovascular level, these synthetic grafts are made up of ePTFE and PET materials. There are some biological challenges with these synthetic grafts causing blood clots as soon as its being implanted because of the low-flow, high-resistance condition [6]. So, bioactive compounds are used as a coated material or grafted onto the luminal walls of PET vascular grafts to improve their hemocompatibility.

6.2 Biomaterials

Biomaterials are the materials made up from natural, inorganic, and organic substances that show high biocompatibility and low level of toxicity. Biomaterials are used for making a 3-D scaffold that mimics as an artificial support to the cells on

which the isolated are seeded on 3-D scaffold. On this scaffold, they start adhering and proliferating and make an artificial ECM for growing into a whole tissue; then, this tissue mimics as a living tissue used for repairing damaged tissue [7]. Biomaterials are provided with a suitable combination of chemical, mechanical, physical, and biological properties. Currently, biomaterials are frequently used in various biomedical applications like synthetic skin, drug delivery systems, tissue cultures, hybrid organs, synthetic blood vessels, artificial hearts, cardiac pacemakers, screws, plates, wires and pins for bone treatments, total artificial joint implants, skull reconstruction, and dental and maxillofacial applications.

On the basis of the application of biomaterials, it is divided into three types:

- Metals
- Ceramics
- Polymer

Metals are the most important biomaterials for biomedical applications due to its diversified structural, physical, chemical, and mechanical properties that show excellent properties when it goes inside the body. Metals are attractive biomaterials having high mechanical properties like strength, elasticity coefficient, and fatigue and having load-bearing capacity [8]. These materials are degraded by a process called corrosion. During degradation using corrosion process, they released some by-products that mainly affect the biological reaction when they interact with the biological material.

Ceramics are highly useful biomaterials for bone-related problems. These biomaterials can be converted into a bone implant during bone injury problems. For bone-related problems, hydroxyapatite (HAP) is used as a ceramic that shows very effective properties like biocompatible, antibacterial, and biodegradable in nature.

Polymers are important and durable biomaterials for various biomedical applications due to their attractive and effective properties that are biocompatible in nature, biodegradable and high mechanical strength, and many more. There are two types of polymers present: one is natural, and other is synthetic polymers. These polymers are mainly used in various biomedical applications like cardiovascular diseases and formation of new tissues as 3-D scaffold, and they are also used as a source of a carrier for drug delivery application and tissue engineering applications [9].

Cardiovascular disease is the leading cause of death worldwide killing 17.3 million people a year. Current treatments for cardiovascular diseases include transplantation of organs and surgery, metabolic products, and mechanical/synthetic implants [10]. Of these, mechanical and synthetic implants have shown great promise in recent years. Metals, natural polymers, and synthetic polymers have been used in these mechanical and synthetic cardiovascular implants. However, synthetic polymers have been recognized as better candidates for cardiovascular repair due to the thrombogenic nature of metals and limit in process ability of natural polymers. In particular, synthetic polymers such as polyurethane, poly-L-lactic acid, polyglycolic acid, and polycaprolactone (PCL) have proved to be of tremendous use due to their biocompatibility and controlled mechanical properties. These polymers have been used to develop cardiovascular devices such as vascular grafts, artificial hearts, and

heart valves, all of which have been widely used in recent years. These implants have the potential to replace the damaged components of the cardiovascular system while maintaining the normal tissue function. Integration of tissue is an important property when inducing transplant as a long-term allograft survival in the absence of continuous immunosuppressive treatment. For the successful implant, the hemocompatibility of the implantable biomaterials played an important role in order to induce long-term vitality of implants in the absence of immunosuppressive therapy to understand the interaction behavior of the different components of blood on the surface of the biomaterials [11].

Hemocompatibility is an essential property of biomaterials and can be measured by the interaction between the material and the various blood components, such as blood plasma proteins, erythrocytes, platelets, and leukocytes. The lack of hemocompatibility can lead to either rejection or the loss of function initially through the activation of the blood coagulation cascade followed by initiation of immune responses. Blood reactions occur as a result of the physical and chemical properties of implant surface; therefore, tolerance can potentially be achieved by altering the biomaterial surface properties.

Biomaterials are implanted inside the body; then, the blood proteins are adsorbed on the material surface followed by platelet adhesion and activation, eventually leading to the formation of thrombus. Previous work has investigated various surface modifications strategies to alter the hemocompatibility of biomaterial surfaces. Inorganic and organic coatings, polymer surface chemical modification, and chemically patterned surfaces have been used to alter hemocompatibility. These surfaces have proved to produce favorable hemocompatible response through inertness, chemical and mechanical stability, and low protein adsorption. Unfortunately, these surfaces are not stable when exposed to the shear stresses of blood flow [12]; thus, it is important to have a robust surface that can withstand physiological forces. The hierarchy of the natural tissue extracellular matrix (ECM), from nano- to macroscale, has inspired fabrication of surfaces with different topographies.

In recent years, nanostructured surfaces have emerged as a potential solution to improve material integration with the tissue. Studies have shown that surfaces that mimic the ECM nanotopography can promote tissue integration and regeneration. Thus, polymers with tunable properties have been extensively researched. Polymeric nanostructured surfaces have shown to affect cellular growth and functionality. In particular, these surfaces have demonstrated improved fibroblast cell adhesion, neuronal cell differentiation, and osteoblast phenotypic activity. An understanding of blood/nanomaterial interaction is essential to understand how transplant tolerance is induced using nanostructured surfaces.

In this chapter, we discussed the hemocompatibility of various different biocompatible nanostructured surfaces like nanoparticles (NPs), nanotubes (NTs), nanowires (NWs), nanofibers (NFs), and nanofilms (NFs). Initially, two nanotopographies were chosen; they are nanowires and nanofibers because they have similar sized features that are aligned differently. NWs are aligned perpendicular to the surface, while NFs are aligned parallel to the surface. It is hypothesized that this alteration in the alignment of nanostructures on the surface will result in a very different response to blood

components, thus altering the hemocompatibility. PCL was chosen as the material since it is bioresorbable polyester with exceptional mechanical strength, and low degradation rate PCL scaffolds have been used extensively in many tissue engineering applications, specifically for vascular tissue, bone and cartilage, nerve, dental, and skin. The low degradation rate of PCL is favorable for long-term implants. Further, degradation products of PCL in the body can be removed naturally by the metabolic pathways eliminating the possibility of foreign body reactions. PCL can also be processed into unique nanostructured surfaces such as NWs, thin-film NWs, nanofibrous networks [13], and NFs. These nanostructured features are capable of being tuned. For example, electrospinning has shown promising results with its ability to fabricate surfaces that mimic the ECM hierarchy. By changing electrospinning parameters such as voltage, working distance, and polymer concentration, the surface properties can be easily tuned to match the natural ECM hierarchy. To evaluate interactions at the blood-nanomaterial interface, it is necessary to understand the events that occur during the introduction of a foreign object inside the body. Driven by a need for understanding potential biomedical and clinical uses of PCL nanostructured surfaces, the in vitro adsorption of human blood serum proteins, adherence of platelets, and coagulation of whole blood show the earliest stages of blood-material interactions. In this study, blood serum protein adsorption on nanostructured surfaces was investigated using a colorimetric assay and x-ray photoelectron spectroscopy (XPS). Fluorescence microscopy and scanning electron microscope (SEM) were used to determine the adhesion and activation of platelets. A simple hemolysis assay was used to investigate the whole blood-clotting kinetics. It was found that surfaces fabricated from the same material PCL with altered nanotopography orientation induce different hemocompatible responses.

6.3 Nano-biomaterials

The fastest developing and most promising area of nanotechnology is the interaction between the biology and the inorganic materials that mimics as a biomaterial or nanobiomaterial for various biomedical applications. Various nanomaterials show different properties or different biological effects when any biological entity is contacted with the nanomaterial because these properties depend on the chemical composition of the materials. So for analyzing the chemical and structural properties of nanomaterials, there are the various physicochemical characterization techniques present for nanomaterials. For analyzing the interaction of the nanomaterials, the biological entity comprises the dynamic physicochemical interaction and kinetics between them. Further, there are several nanotechnology-based approaches that are being investigated for various biomedical applications like tissue engineering, bioimaging, drug delivery, and biosensors. There are huge amount of researchers that employ these approaches for nanoscale materials or bio-/nanomaterials to develop the unique functionalities required by the biomedical systems. For this nanobiomaterial area, we must understand the dynamic forces and molecular components that shape these interactions [14].

6.3.1 Hemocompatibility or blood compatibility

When blood components are interacted with the foreign body, it initiates a cascade that contains the following steps:

- Protein adsorption at the surface
- Adhesion of platelets to the foreign body surface via adherent proteins
- Activation of further neighbored platelets
- The stabilization of the thrombi by fibrin in a local network structure

6.3.2 Protein adsorption

Adsorption of blood plasma protein occurs when the human blood plasma proteins instantly interact with the surface of the subendothelium or on surface of the foreign body. There is necessary time required to adhere on the surface of the foreign body that depends on the chemical structure of proteins and surface properties of the foreign materials. These are the following very useful proteins present in the process: fibrinogen, vitronectin, fibronectin, immunoglobulins, vWF, HMW-kininogen, prekallikrein, factor XI, and factor XII [15].

Fibrinogen is one of the most important adsorbed protein of human blood that induces the adhesion of platelets especially when these platelets experience shear stress. These adsorbed proteins might be mediated by the GPIIb/IIIa receptor binding to RGD like motifs in the adsorbed protein. The group of Latour could show recently that platelet adhesion response did not correlate to the amount of the fibrinogen adsorbed. The adsorption-induced conformational changes of the fibrinogen molecules apparently led to the exposure of platelet-binding motifs that are otherwise not accessible to platelet receptors in the native state of the circulating protein [16] (the main reason why in the streaming blood under physiological conditions no interaction with nonactivated platelets occur and no clots are formed). A similar conformational change of the natively globular von Willebrand molecule during adhesion was shown recently as well. These studies show that not only the amount of adhered proteins but also far more the structure and the type of adherent proteins determine the subsequent platelet reaction.

The main constituent of the plasma protein is albumin with 40 mg/ml concentration that is useful for nonadherence of platelets; it means that the surface of the foreign body lacks platelet-binding motifs (amino acid sequence) for binding platelets. The absence of motifs on the biomaterial surface improves the hemocompatibility of the biomaterials [17]. When platelet adhesion occurred on albumin-coated surfaces, it has been discussed (i) as the interaction between platelets and surface areas, at which albumin detached, and not as an interaction with albumin itself or (ii) due to the replacement of precoated albumin by other proteins. For albumin, unfolding did not influence platelet adhesion significantly up to a level of 34% helix loss, supporting the understanding of albumin as a passivating blood plasma protein in the context of platelet adhesion. But above this level, conformational changes resulted in the exposure of cryptic platelet receptor recognition domains, which were then able to induce platelet adhesion. These studies demonstrated that not only the amount of adhering proteins but also the conformation of the proteins plays an important role for the interaction

with platelets. Only when certain cryptic epitopes—binding sites that are hidden as long as the proteins circulate—become accessible for neighbored platelets, an interaction between immobilized proteins and platelets can occur.

The adsorption of proteins is not necessarily a stable process in time; depending on the type of the protein, they can desorb after minutes and can be replaced by other proteins [18]. An example is fibrinogen adsorbed on polyethylene, which is replaced step by step by other proteins with time. In this process, called Vroman effect [19], the highest mobility proteins arrive first and replaced by proteins that have a highest affinity for the surface of the biomaterials. A prediction how this replacement process takes place is not possible in detail. Detached fibrinogen can be replaced by HMW-kininogen or FXII. Both would initiate a sequence of enzymatic reactions initializing the contact activation of the plasmatic coagulation, the fibrinolytic system, the kininogen, and the complement system. Hence, already in the phase of protein adsorption, the hemocompatibility of a biomaterial is influenced decisively. There are certain materials that are able to adsorb complement factor C3b and may cause less activation of the plasmatic coagulation by complement activation. Other specific materials are able to adsorb factor XII in its nonactivated state and may cause less activation of the plasmatic coagulation by contact activation. Up to now, the basic mechanisms underlying the interaction between proteins and foreign body surfaces and especially whether platelet adhesion, activation, and secretion and thrombus formation follow protein adhesion are understood to some extent, but the basic biology still remains an active area of research.

6.3.3 Platelet activation and adhesion

Nonactivated platelets have small nuclear cell fragments of 1–2 m in length, 1 m in thickness, and weighing ~10 pg. They are produced by megakaryocytes (up to 8000 platelets from one megakaryocyte) inside the bone marrow by the extension of dynamic protrusions into microvessels, which seem to be sheared from their transendothelial stems by the flowing blood [20]. Under physiological conditions, they circulate in a quiescent state for approximately 10 days before they are cleared by macrophages in the spleen and liver. During their lifetime, most platelets never undergo firm adhesion. The initial steps in primary hemostasis are that the platelets are adhered on the subendothelial matrix or foreign body surfaces. When platelets are adhered on the surface of the foreign body, they interact with the less and highly specific adhesive proteins called adhesive glycoproteins (Gp). When the platelets bind to the surface of the foreign body, they release the biochemical agonist to their receptors, cross-linking, transduced from the membrane into the cytoplasm resulting in activation of platelets. After adhesion of platelets on the surface, they start spreading, activating, secreting, and lastly aggregating with more platelets [21].

After the adherence of platelets on the surface of the foreign body, it will get activated in milliseconds (~180 ms). Due to this rapid activation of platelets, nearby passing platelets can be activated and then adhere. A change in the assembly of cytoskeleton proteins of activated platelets results in a change in shape with extended pseudopodia initiating from plasma membrane. After adherence of the platelets on the

surface, the materials initiate spreading that takes 1–3 min requiring for nonactivated functional platelets with basic and simple energy metabolism (anaerobic glycolysis) that is assisted by the release of substances, which act as vasoconstrictors (thromboxane, platelet-derived growth factor (PDGF), and serotonin) and promote adhesion of nearby platelets in the surrounding plasma (fibronectin and von Willebrand factor) and mediate the aggregation of neighbored platelets (fibrinogen, von Willebrand factor, thrombospondin, adenosine diphosphate (ADP), and platelet-activating factor (PAF)) and growth of cells (PDGF, transforming growth factor (TGF), fibroblast growth factor (FGF), and platelet-activating factor (PAF)). Platelets attach to foreign body surfaces by a complex series of events [22].

Blood is flowing in the center of the blood vessels with higher velocity than near the wall, because in the center platelets experience a shear force between adjacent layers of the fluid that become maximum near the blood vessel wall. In such regions of high shear stress, platelets can also become activated only by shear forces (greater than 50 N/m^2). Since they circulate near the vessel wall in the so-called cell-free plasma layer, such activated platelets are able to adhere to foreign body surfaces or injured or denuded vessel walls. The activation of platelets is associated with a cytoskeletal rearrangement (mediated by actin, actin-binding protein, actinin, and myosin) a shape change, the generation of thromboxane A2 and thrombin and the release of the contents of stored granules. This whole process is complex and very dynamic.

In bloodstream, the shear stress or shear rate was determined, to which proteins the platelets adhere via these different receptors. At very low or zero shear stress, platelets adhere to fibronectin, vitronectin, and/or fibrinogen. At middle shear rates, mainly fibrinogen mediates the adhesion process, and at high shear rates, the vWF is favored [23]. There are recent investigations to explain mainly the situation at high shear rates—such as is found in small arteries and arterioles—where preferentially the vWF is involved. At low shear rates (10–1000 L/s), vWF is circulating in blood (plasmatic concentration of around 10 g/mL) in a spheroid-like shape with molecule diameters of about 2 m. With increasing shear rate, the molecule is stretching, and finally, at shear rates of more than 5000 L/s, it is a linear chain of about 100 m to 1 mm in length. In this configuration, the molecule has now a 50× higher likeliness to adhere to the surface of a foreign body or injured endothelia, and hence, at high shear stress, platelets adhere mainly to vWF. In addition, the platelets are able to adhere shear-resistant also in a nonactivated state. This process is arbitrate by GPIb-V-IX, which is highly generous receptor complex (~25,000 copies per platelet) exclusively expressed in platelets (and megakaryocytes).

6.3.4 Hemocompatibility test for various nano-biomaterials

6.3.4.1 Hemocompatibility test for nanoparticles

In this study, they described the interaction between nanoparticles and RBC membrane for that they synthesized two different types of MSN nanoparticles (MCM-41 and SBA-15). Then, they investigated the interaction behavior of the two nanoparticles with RBC membranes using various characterization techniques like fluorescence studies and electron microscopies and molecular cell biology technique. They also studied the

effect of the different sizes of nanoparticles and its surface area on hemolytic behavior of MSNs, and they investigated the interaction behavior of RBCs with the surface functionalized. So in this research, they finally investigated the effect of MSN nanoparticles interacted with the RBCs and the membrane deformability by using the nucleopore filtration technique [24].

These are the following three important criteria used to assess the hemocompatibility nature of the synthesized nanoparticles:

(1) RBC lyses potential
(2) Change in shape of the RBCs or deformation of RBC
(3) Propensity to debilitate RBC deformability

By investigating these criteria, it will enhance a more accurate measurement of the hemocompatibility of various types of nanomaterials (i.e., nanoparticles).

The effect of the nanoparticle size has been already discussed; in this, the effect of the MCM-41-type MSNs having larger size particles shows lower hemolysis of RBCs, but they try to investigate the hemocompatibility of larger size SBA-15-type MSN nanoparticles. They found other important issue that how various different sizes and surface areas of MSN nanoparticles interact with the RBCs and with other biological studies suggested [25]. To overcome or investigate this problem, they synthesize the two types of MSN nanoparticles; these are MCM-41 and SBA-15. The morphology or size of the synthesized nanoparticles is visualized by using scanning electron microscopy (SEM) and transmission electron microscopy (TEM) images that showed particle sizes in the range of 100–200 nm for the MCM-41-type MSNs (referred to as s-MSN as shown in Fig. 6.1A–D). According to the dynamic light scattering (DLS),

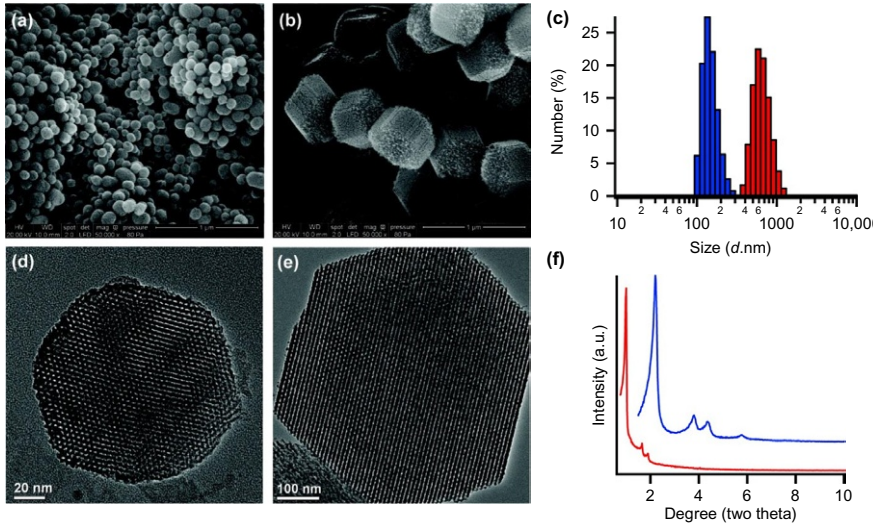


Fig. 6.1 SEM image (top) and TEM (bottom) images of (A and D) s-MSN and (B and E) l-MSN. (C) Hydrodynamic size distributions of s-MSN *(blue)* and l-MSN *(red)* suspended in PBS (100 μg mL^{-1}) measured by dynamic light scattering. (F) XRD patterns of s-MSN *(blue)* and l-MSN *(red)*. Copyright 2011, American Chemical Society.

the hydrodynamic particle size giving average sizes of 122 nm for s-MSN and 531 nm for l-MSN is shown in Fig. 6.1C. XRD patterns showed that both s-MSNs and l-MSNs exhibit 2-D hexagonal pore arrangements as shown in Fig. 6.1F.

For evaluating the hemocompatibility of synthesize nanoparticles, hemolysis assay was used to identify the behaviors of synthesized nanoparticles like s-MSN and l-MSN on RBCs (lysis and change in shape). Initially, they isolate the RBCs from fresh human blood using centrifugation (1300 rpm for 10 min) and washed five times with phosphate-buffered saline (PBS), and then, these isolated 5% RBCs diluted with PBS before incubation with MSN nanoparticles suspensions of different concentrations. After that, they prepared the different controls like negative (PBS) and positive control (without water) according to the previous method for preparation of RBCs instead of the nanoparticles suspensions. Hemoglobin released from the hemolyzed RBCs was detected and spun down after 2 h incubation. The lysis of RBCs depends on the different sizes of the s-MSN nanoparticles. They found that larger particle size of MSN shows a higher lysis of red blood cells (hemolytic activity) than the small size particles of MSN [26]. They also observed that the hemolytic activity of l-MSNs at 50 $\mu g\,mL^{-1}$ with 5% hemolysis was detected as shown in Fig. 6.2A–C. s-MSN nanoparticles show less disruption of red blood cells that means good hemocompatibility (<2% hemolysis) at higher concentration (100 $\mu g\,mL^{-1}$) of s-MSN as shown

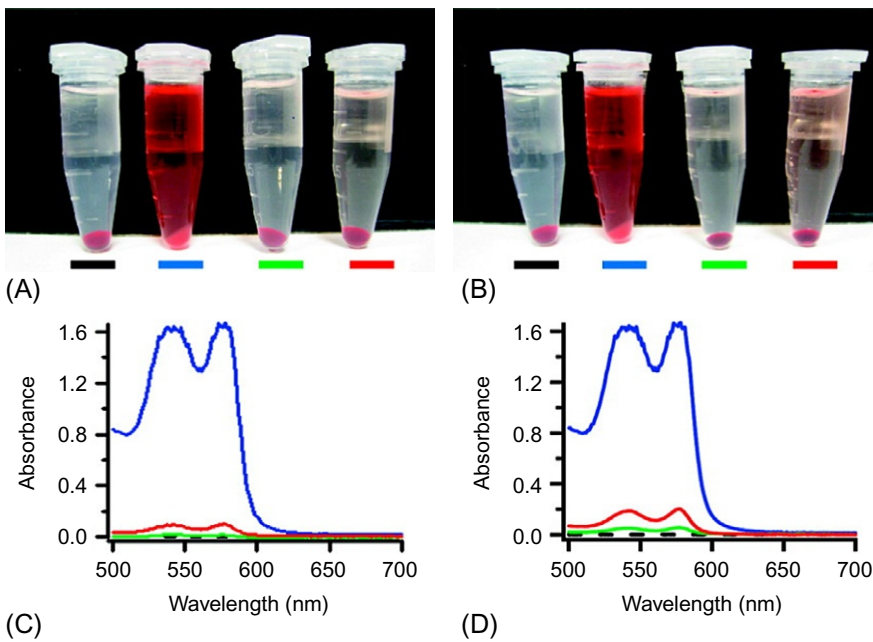


Fig. 6.2 Hemolysis assay for s-MSN *(green lines)* and l-MSN *(red lines)*, using water as a positive control *(blue lines)* and PBS as a negative control *(dashed black lines)*. The materials were suspended at 50 (A and C) and 100 $\mu g\,mL^{-1}$ (B and D). Copyright 2011, American Chemical Society.

in Fig. 6.2B–D. The large size nanoparticles (225 nm) are highly hemocompatible nanoparticles, but if the size of nanoparticles are increased above 225 nm, it will not improve the hemocompatibility.

SEM and TEM are used as a characterization techniques to observed and understand the mechanism behind the lysis of red blood cells (RBC) and the effect of different sizes of the nanoparticles on the lysis of RBC(hemolysis) that is shown in Figs. 6.3 and 6.4. They found that the small amount of the s-MSNs is adsorbed on the surface of the red blood cells. There is no change in shape of red blood cell membrane observed after binding or adsorption of the nanoparticles on the cells surface. After treatment with s-MSNs to the RBC, they maintained their shape that is in the form of the biconcave and are compared with the without treatment RBCs. In contrast, they found a deformation in a cell membrane when the large amount of the s-MSNs is attached to the surface of the red blood cells; they induce the membrane disruption resulted in encapsulation of nanoparticles by RBC [27].

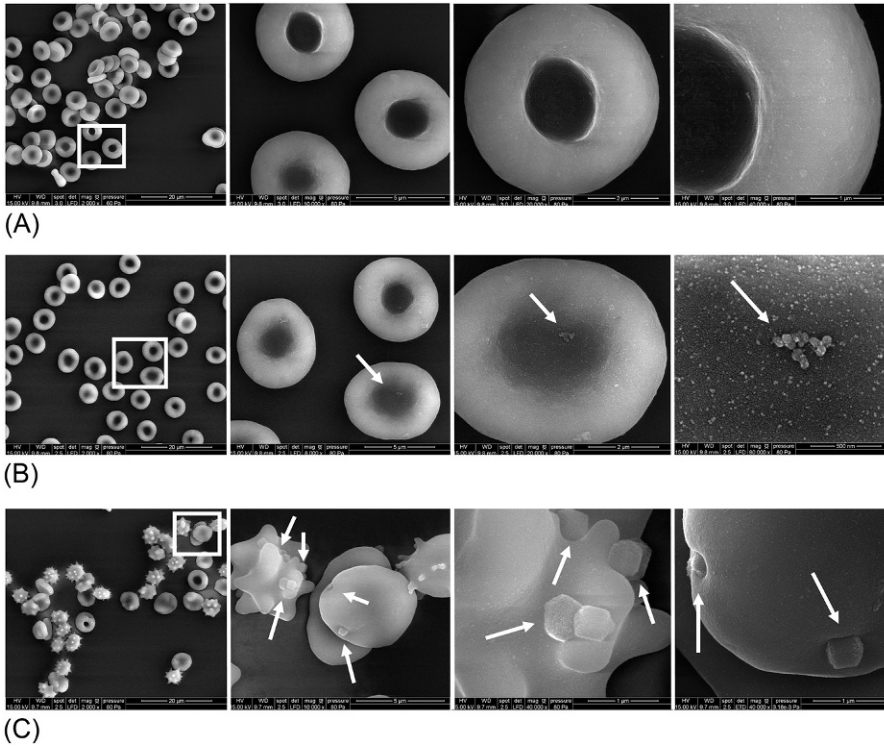


Fig. 6.3 SEM images of RBCs (5% hematocrit) incubated for 2 h at room temperature with (A) PBS as control, (B) 100 μg mL^{-1} of s-MSN, and (C) 100 μg mL^{-1} of l-MSN. Copyright 2011, American Chemical Society.

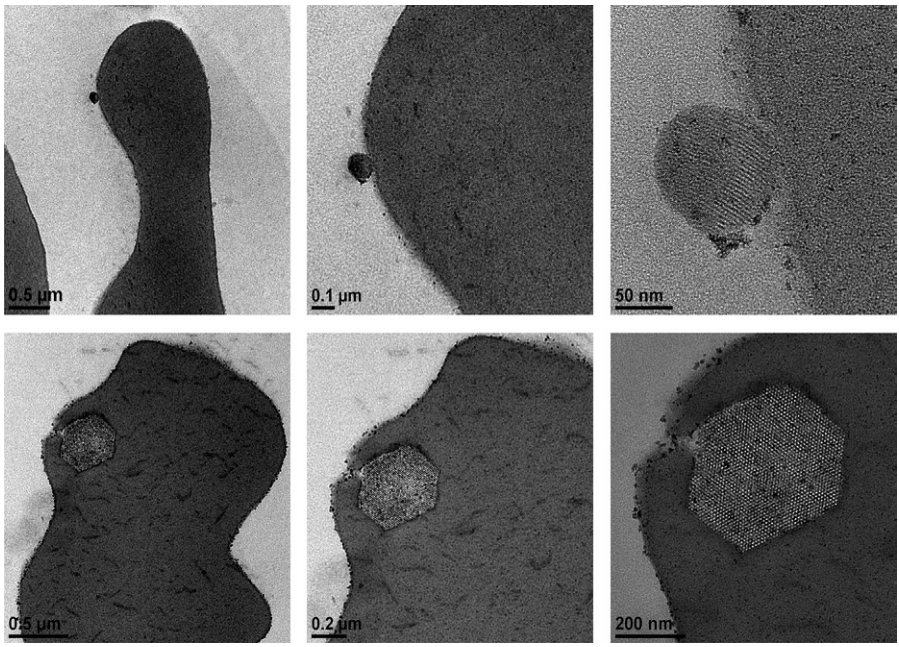


Fig. 6.4 TEM images of RBCs (5% hematocrit) incubated for 2 h at room temperature with 100 μg mL^{-1} s-MSN (top) and l-MSN (bottom). Copyright 2011, American Chemical Society.

6.3.4.2 Hemocompatibility of nanofibers

The fabrication of core-shell electrospun nanofibrous scaffolds by using electrospinning method containing two natural polymer solutions such as gelatin and PVA. In core-shell nanofibers, gelatin is present in the shell, and poly(vinyl alcohol) (PVA) is present inside the core that is applicable for a potential vascular material. The surface roughness analysis of core-shell electrospun nanofibrous scaffold was done by using AFM technique. Human platelet deposition and activation on the coaxial nanofibrous scaffold are varying according to the surface roughness of the scaffold.

The result of the surface roughness for different polymeric scaffolds was observed, and they got the highest surface roughness (Ra = 65.5 ± 6.8 nm) of PVA scaffold that shows less deposition of platelets on the surface of the PVA nanofibrous scaffold (34.2 ± 5.8) as compared with the gelatin nanofibrous scaffold having surface roughness (Ra = 36.8 ± 3.0 nm) that shows more number of platelets are adhered on the gelatin nanofibrous scaffold. For core-shell nanofibers, having different ratios of PVA and gelatin ((1:1) and (3:1)) shows different surface roughness (Ra = 24.0 ± 1.5 nm and Ra = 37.1 ± 2.8 nm) and platelet adhesion (150.2 ± 17.4 and 167.8 ± 15.4). Therefore, the deposition of the platelets depends on the chemical structure of the gelatin and PVA nanofibrous scaffold and surface roughness of these electrospun nanofibrous scaffolds. Highest rate of platelet activation and thrombin formation is depending on the stiffness of the gelatin and PVA nanofibrous scaffold [28].

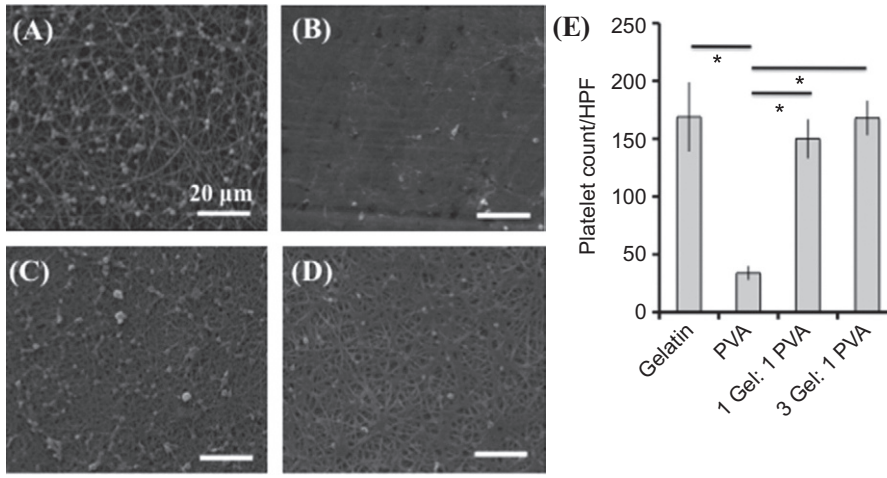


Fig. 6.5 Platelet deposition under static conditions on electrospun scaffolds (A) gelatin, (B) PVA, (C) 1 Gel/1 PVA coaxial, and (D) 3 Gel/1 PVA coaxial. Platelet deposition per HPF (high-powered field 3000× magnification, approximately 8400 µm^2) for each of the electrospun scaffolds is depicted (E). Scale bar is 20 µm. Asterisk (*) indicates significance with $p < 0.001$. Copyright 2015, American Chemical Society.

Platelet deposition after incubation was calculated using SEM images (3000× magnification, approximately 8400 µm^2) and the National Institute of Health's ImageJ software as shown in Fig. 6.5A–D. The gelatin scaffolds (169 ± 30 platelets) and the coaxial scaffolds (1 Gel/1 PVA coaxial, 150 ± 17 platelets; 3 Gel/1 PVA coaxial scaffold, 168 ± 15 platelets) possessed similar platelet deposition and significantly more platelets than the PVA scaffolds (34 ± 6 platelets). Despite the PVA fibers having the highest surface roughness, these fibers had the lowest platelet deposition out of all of the scaffolds [29]. Gelatin, rich in cellular attachment sites, has higher platelet deposition than the PVA fibers with significantly higher surface roughness and lacking cellular attachment sites. Therefore, surface roughness was not a dominating factor in platelet deposition. The chemical signals present on the biocompatible gelatin fibers were a dominant factor in platelet deposition in comparison with the synthetic polymer PVA, lacking these cellular recognition sites as shown in graph 5(E).

They also determined platelet deposition on the nanofiber surface that was preactivated through different mechanisms (i.e., mechanical or chemical activation). They first evaluated the deposition of platelets that were mechanically activated prior to incubating on the scaffolds Fig. 6.6A–D. The platelets were mechanically activated using a hemodynamic shear device (HSD) that exposes the platelets to dynamic shear stresses similar to the mechanical forces experienced in vivo. Additionally, the HSD provides uniform and repeatable stress to the platelet samples [30]. In this study, the 3 Gel/1 PVA coaxial scaffold had the highest mechanically activated platelet deposition when compared with the gelatin scaffolds, PVA scaffolds, and 1 Gel/1 PVA coaxial scaffold ($p < 0.03$) shown in Fig. 6.6I. This high platelet deposition correlated with the stiffness of the underlying substrate as discussed previously with the 3 Gel/1 PVA coaxial scaffold having

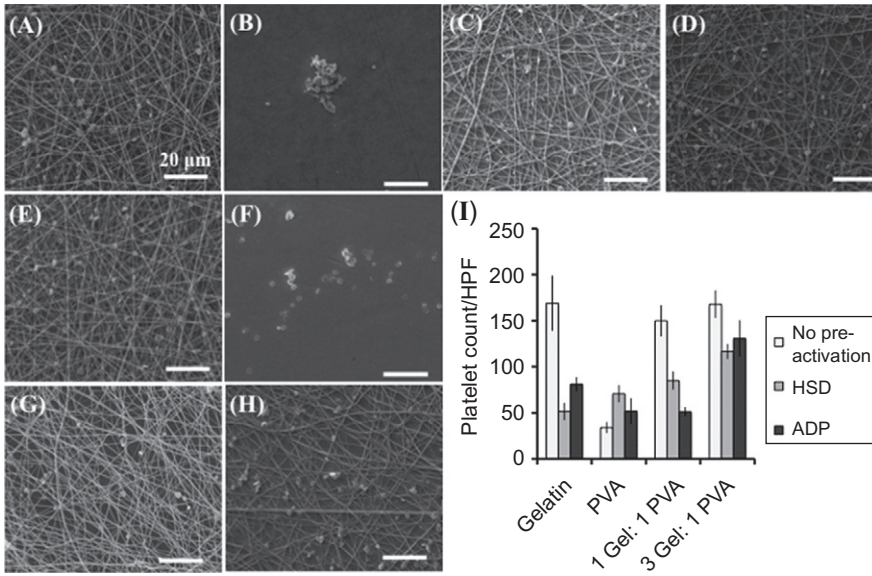


Fig. 6.6 Deposition of platelets preactivated (A–D) mechanically (HSD) or (E–H) chemically (ADP) on defined surfaces: gelatin scaffolds (A and E), PVA scaffolds (B and F), 1 Gel/1 PVA coaxial scaffolds (C and G), and 3 Gel/1 PVA coaxial scaffolds (D and H). Platelet deposition is determined per high-powered field (HPF) (3000× magnification, approximately 8400 μm^2). Deposition is compared with platelets that were not preactivated through mechanical (hemodynamic shearing device, HSD) or chemical (adenosine diphosphate, ADP) means (I). Scale bar equals 20 μm. Copyright 2015, American Chemical Society.

the highest stiffness and subsequent highest platelet deposition. Then, platelets were chemically activated using adenosine diphosphate (ADP), a known platelet activator. 4-ADP activates platelets through a GTP-binding proteins or G proteins. This ADP-platelet interaction causes a platelet shape change and a decline in cyclic adenosine monophosphate (cAMP) formation, leading to platelet activation. Therefore, ADP is an important chemical factor at locations of vascular injury for the propagation of platelet activation. In this study, the deposition of chemically activated platelets deposited per high-powered field (HPF) on each scaffold was calculated Fig. 6.6E–H. Similar to the mechanically activated platelets, the 3 Gel/1 PVA coaxial scaffolds had the highest chemically activated platelet deposition when compared with the gelatin scaffolds, PVA scaffolds, and 1 Gel/1 PVA coaxial scaffolds ($p < 0.03$) in Fig. 6.6I. This high platelet deposition correlated with the high stiffness of the 3 Gel/1 PVA coaxial scaffolds [31].

In this study, the preactivated platelets (both chemical and mechanical preactivation) had lower deposition on the scaffolds (gelatin, 1 Gel/1 PVA coaxial, and 3 Gel/1 PVA coaxial) than platelets that had no preactivation (Fig. 6.6I). Platelets preactivated either mechanically or chemically undergo numerous changes, including physical shape change, exposure/activation of surface receptors, and secretion of chemical agonists. Exposure and activation surface receptors play a role in platelet aggregation. These preactivated platelets via chemical or mechanical means had less deposition on

the scaffold surface (gelatin, 1 Gel/1 PVA coaxial, and 3 Gel/1 PVA coaxial) than the platelets that were not preactivated prior to incubation. They postulated that the preactivation through chemical or mechanical means is causing platelet aggregation of the platelets in solution over the incubation period leading to less platelet deposition on the fiber surface for a given/fixed concentration of platelets.

To determine platelet deposition on the nanofiber surfaces when they are covered with a monolayer of smooth muscle cells or endothelial cells, first, electrospun scaffolds were preseeded with smooth muscle cells (SMC) for 72 h to ensure a confluent monolayer of cells on the scaffold surface [32]. Once the confluent monolayer of SMC was attained, platelets were incubated for 4 h on the scaffold surfaces prior to fixation and determination of platelet deposition as shown in Fig. 6.7A–D. The PVA had similar platelet deposition as the gelatin scaffold ($p=0.38$) and 1 Gel/1 PVA coaxial scaffold ($p=0.16$) and significantly more platelets than the 3 Gel/1 PVA coaxial scaffold ($p=0.02$). Gelatin scaffolds had similar platelet deposition to the 1 Gel/1 PVA coaxial scaffold ($p=0.22$) and 3 Gel/1 PVA coaxial scaffold ($p=0.39$).

These studies showed the antithrombogenic properties of the native endothelium such as the release of nitric oxide (NO) and prostacyclin to decrease platelet activation and adhesion. Therefore, the scaffolds (i.e., gelatin, 1 Gel/1 PVA coaxial, and 3 Gel/1 PVA coaxial) that had a confluent monolayer of endothelial cells similar to the native vasculature displayed a decline in platelet deposition compared with the scaffolds with no

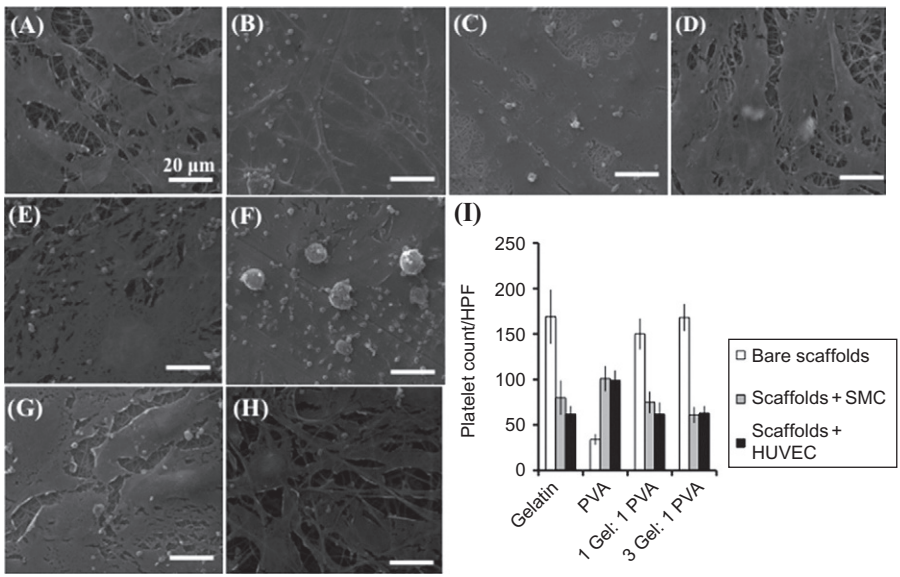


Fig. 6.7 Platelet deposition on surfaces preseeded with smooth muscle cells (SMC) (A–D) or human umbilical vein endothelial cells (HUVEC) (E–H) on gelatin scaffolds (A and E), PVA scaffolds (B and F), 1 Gel/1 PVA coaxial scaffolds (C and G), and 3 Gel/1 PVA coaxial scaffolds (D and H). Platelet deposition is determined per high-powered field (3000×) and compared with scaffolds that were not preseeded with SMC or HUVEC (I). Scale bar equals 20 µm. Copyright 2015, American Chemical Society.

endothelial preseeding. Interestingly, scaffolds that were preseeded with smooth muscle cells also showed a decline in platelet deposition. After vascular injury, various mitogenic and chemotactic factors are released from the wound area and from aggregated platelets that are on the damaged intimal surface [33]. These factors will initiate the neointimal response. They hypothesized that in the absence of vascular injury, cell preseeding would reduce platelet deposition for gelatin and gelatin-coated fibers, as was observed for both endothelial cells and smooth muscle cells respectively in this experiment.

In a study conducted by Badimon et al., a deendothelialized vessel wall showed an increase in platelet deposition with an increase in exposure time and shear. Taking only flow rate into consideration, the increase in shear will activate platelets mechanically, leading to an increase in platelet deposition. Herein, we also observed the latter published results, where platelet deposition increased when the shear was increased from 1 to 3 dyn/cm^2 for the 3 Gel/1 PVA coaxial scaffolds ($p < 0.001$) with less significance seen in the 1 Gel/1 PVA coaxial scaffolds ($p < 0.07$) and gelatin scaffolds ($p < 0.09$). They postulate that the mechanical shear stress not only induced platelet activation but also mobilized them toward the scaffolds, such that an increase in platelet deposition was observed with an increase in shear stress. Overall, platelet deposition under shear conditions was still much less than static condition [34]. For instance, PVA had the least platelet deposition of all the scaffolds for the static conditions (Fig. 6.7I, bare scaffold) and the shear conditions (Fig. 6.8I, 1 or 3 dyn/cm^2). This low platelet deposition for the

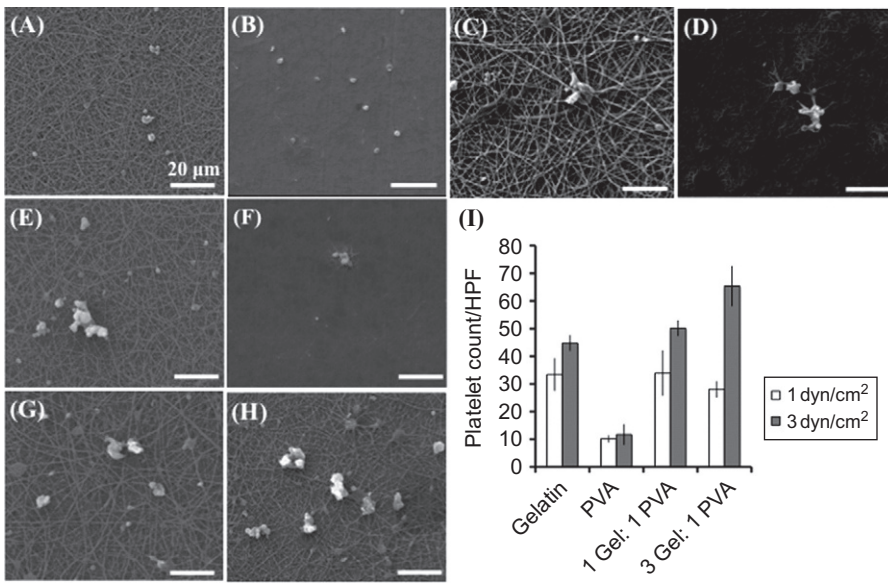


Fig. 6.8 Platelet deposition on electrospun scaffolds under shear, 1 dyn/cm^2 (A–D) and 3 dyn/cm^2 (E–H). Platelet deposition was calculated on the following scaffolds per high-powered field (3000×): gelatin scaffolds (A and E), PVA scaffolds (B and F), 1 Gel/1 PVA coaxial scaffolds (C and G), and 3 Gel/1 PVA coaxial scaffolds (D and H). Platelet deposition on gelatin, PVA, 1 Gel/1 PVA coaxial, or 3 Gel/1 PVA coaxial scaffolds under shear (1 or 3 dyn/cm^2) is presented in this bar graph per high-powered field (3000×) (I). Scale bar 20 µm. Copyright 2015, American Chemical Society.

static and shear conditions was attributed to the hydrophilic nature of PVA and poor cellular attachment and proliferative nature of the PVA scaffolds. Ikada et al. showed that there was less platelet deposition and fibrin formation using PRP than on nongrafted and acrylic acid-grafted polyethylene. Overall, the platelet deposition was significantly decreased under shear than in static conditions, suggesting that the scaffolds perform better under dynamic flow than in a static environment.

6.3.4.3 Hemocompatibility of nanotubes

In this work, they proposed a new surface modification to titanium with three features inspired by the endothelial glycocalyx. First, titanium surfaces are anodized to produce titania nanotubes with high surface area. Second, the nanostructured surfaces are coated with heparin-chitosan polyelectrolyte multilayers to provide glycosaminoglycan functionalization. Third, chitosan is modified with a nitric oxide-donor chemistry to provide an important antithrombotic small-molecule signal. They showed that these surfaces are nontoxic with respect to platelets and leukocytes. The combination of glycocalyx-inspired features results in a dramatic reduction of platelet and leukocyte adhesion and platelet activation as shown in Fig. 6.9 [35].

The endothelial glycocalyx lining the inside surfaces of blood vessels has multiple features that prevent inflammation, blood clot formation, and infection. This surface represents the highest standard in blood compatibility for long-term contact with blood under physiological flow rates. Engineering materials used in blood-contacting biomedical devices, including metals and polymers, have undesirable interactions with blood that lead to failure modes associated with inflammation, blood clotting, and infection. Platelet adhesion and activation are key events governing these undesirable interactions.

Scanning electron micrographs of TiO_2 nanotubes (left), PEM-modified nanotubes (center), and nitrosated PEM-modified nanotubes (right) at two different magnifications. Hereafter, these are identified as TiO_2NT, TiO_2NT + PEM, and TiO_2NT + PEM + NO, respectively. The 10-bilayer PEM modification conformally

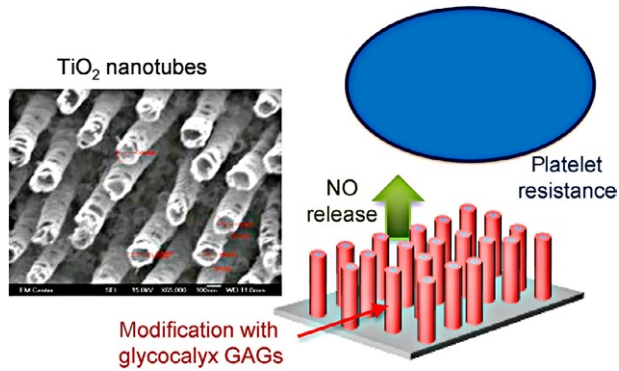


Fig. 6.9 Graphic representation of ritanium surface modified with glycocalyx GAGs. Copyright 2017, American Chemical Society.

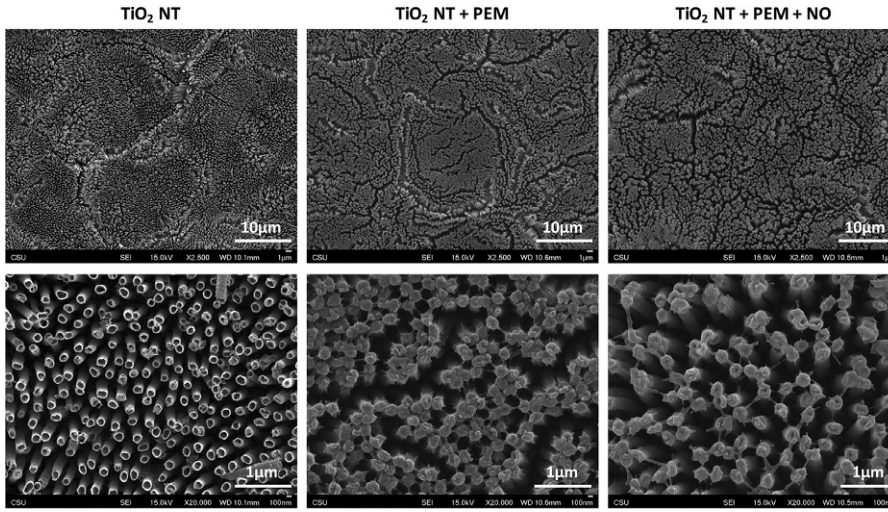


Fig. 6.10 Scanning electron micrographs of different surface modifications. Copyright 2017, American Chemical Society.

coats the nanotubes and blocks the individual nanotube pores [36]. However, the nanotubes remain distinct, with space between the nanotubes remaining. Subsequent nitrosation does not physically alter the PEM structure at a length scale observable by SEM as shown in Fig. 6.10.

Fluorescence Microscopy: The cells were stained with a cell-permeate dye calcein-AM that labels viable cells by converting the nonfluorescent calcein-AM into a green fluorescent calcein as shown in Fig. 6.11. The fluorescence micrograph experimental surfaces, the noncytotoxic PS control, and the HEPES (no cells) control were significantly less cytotoxic than the cytotoxic control (Triton X) [37].

Adhesion and Activation of Platelets: Platelet adhesion and activation were characterized qualitatively by scanning electron microscopy. During activation, platelets undergo cytoskeletal-dependent membranous shape changes. This commences with the disassembly of the microtubule ring followed by actin polymerization to form dendritic extensions that are thought to release chemoattractants and summon additional platelets to form aggregates and commence the production of the platelet plug [38]. Five morphological groups of dendritic expressions on implant surfaces have been identified corresponding with four levels of activation: round (unactivated), disc shaped with no pseudopodia present; dendritic (partially activated), early pseudopodia, i.e., short reversible dendritic extensions; spread-dendritic (moderately activated), irreversible long-dendritic extensions with some spreading and some pseudopodal flattening; spreading (fully activated), pseudopodia almost fully flattened, hyaloplasmic spreading; and fully spread (fully activated), no pseudopodia present and full hyaloplasmic spreading [39,40]. Ti surfaces exhibit moderate activation of platelets with mostly short dendritic extensions. TiO_2NT surfaces exhibit a large amount of platelet aggregation; however, there are no visible dendritic extensions as shown in Fig. 6.12.

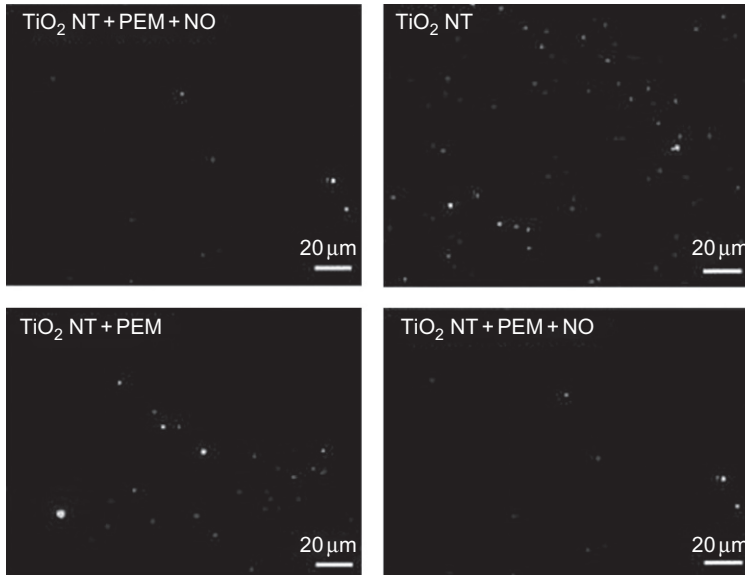


Fig. 6.11 Representative (median from at least five samples for each experimental group) fluorescence micrographs of adhered cells stained with calcein-AM on Ti, TiO_2NT, TiO_2NT + PEM, and TiO_2NT + PEM + NO surfaces. Copyright 2017, American Chemical Society.

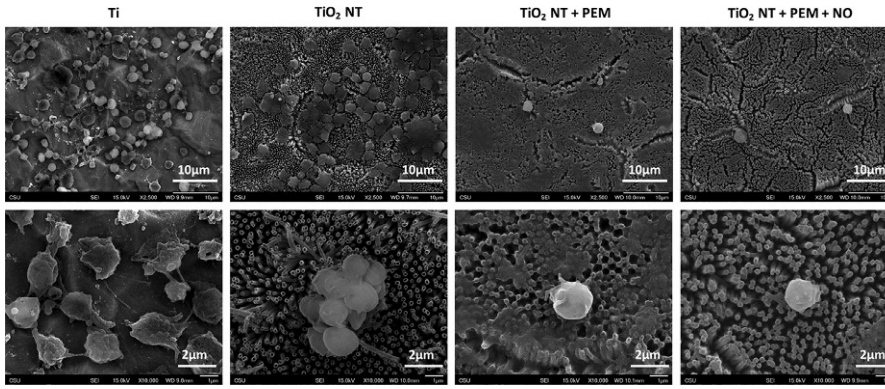


Fig. 6.12 Representative SEM images of adhered cells on Ti, TiO_2NT, TiO_2NT + PEM, and TiO_2NT + PEM + NO surfaces. Copyright 2017, American Chemical Society.

6.3.4.4 Hemocompatibility of nanofilms

In this study, they fabricated layer-by-layer 3-D porous multilayer films using self-assembly method on polymeric substrate with enhanced blood compatibility that is coated with multifunctional and heparin-mimicking star-shaped supramolecules. This star-shaped heparin supramolecules coated on a surface mimicking as

polyanions and polycations were fabricated by using a method called atom transfer radical polymerization from β-cyclodextrin-based cores. After the fabrication of star-shaped heparin polyanions and polycations, deposition of the 3-D porous multilayers on the polymeric film surface is introduced by the method called alternating deposition of synthesized polyanions and polycations using electrostatic interaction as shown in Fig. 6.13A–B. Finally, they evaluated the blood compatibility properties like blood activation, thrombotic potential of the fabricated nanofilms coated with polyanions and polycations. And further, they characterized its surface morphology and composition, wettability, and cell viability of the nanofilms coated with star-shaped heparin supramolecules [41,42].

The successful deposition of the star-shaped heparin supramolecules on the surface of the nanofilms for biomedical application was verified by using physical characterization techniques like ATR-FTIR spectra and XPS. The 3-D porous surface morphology of the modified substrate was visualized by electron microscopy like scanning electron microscopy (SEM) and atomic force microscopy (AFM); these surface morphology observations interpret that the 3-D porous surface of modified substrate has a great biological influence like adhesion and spreading of the cells on the biointerface. The in vitro assessment of the blood-material interaction of the nanofilms coated with star-shaped heparin supramolecules on the surface having 3-D porous surface morphology was done by using following test: blood protein (fibrinogen, albumin, and immunoglobulin) adsorption, platelet adhesion test, APTT, TT, TAT, and blood-related complement. These blood-material interaction test confirmed that the heparin-mimicking multilayer-coated membranes show less number of blood component activations and excellent hemocompatibility [43].

Typical SEM observations for the pristine membrane surface and star-shaped supramolecule-deposited 3-D porous thin-film surfaces are shown in Fig. 6.14A, B-6.1, B-2, B-3, C-1, C-2, and C-3. It was noticed that the pristine membrane had an even surface morphology, while obviously, the star-shaped supramolecule-assembled substrates exhibited 3-D porous surface structures, especially the M-SA membranes. An interesting phenomenon was observed that there was a large difference in the surface morphology between the M-SA and the M-SE. The M-SA membranes were much rougher than the membranes of M-SE. Furthermore, with the increase of the bilayers from 5 to 25, the surface roughness of M-SE increased gradually and the M-SE membranes showed more homogeneous surface 3-D structures than M-SA [44,45]. The star-shaped supramolecule-assembled PVDF and PSf membrane surfaces with 15 bilayers were also examined by SEM images shown in Fig. 6.14; the coating surface also exhibited 3-D porous morphologies as PES membrane surface, which indicated that this proposed strategy could also be applied in the surface coating of many other polymeric membrane substrates.

AFM (with a tapping mode at a scan rate of 0.8 Hz over an area of $10 \times 10\,\mu m^2$) was further used to evaluate the surface morphology and roughness of the star-shaped supramolecule-deposited multilayer surfaces. As shown in Fig. 6.14 (a, b-1, b-2, b-3, c-1, c-2, and c-3), the surface of the pristine membrane was clearly verified to be a characteristic 2-D flat surface, while after assembly of the star-shaped

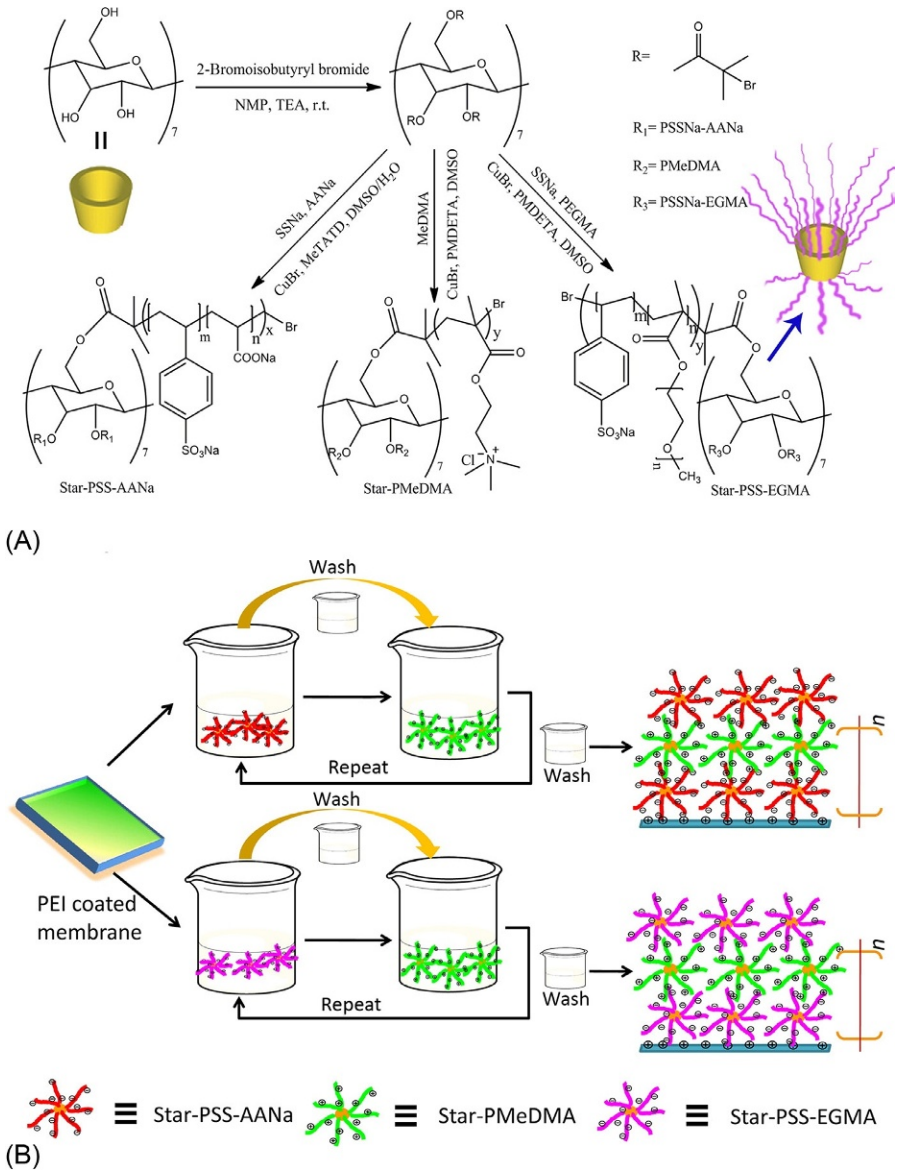


Fig. 6.13 Synthesis route of CD-based macroinitiator and polymerization of star-shaped supramolecules via ATRP (A); procedures for preparation of LbL assembly of 3-D porous multilayer thin films on membrane substrates ($n = 4$, 14, and 24) (B). Copyright 2014, American Chemical Society.

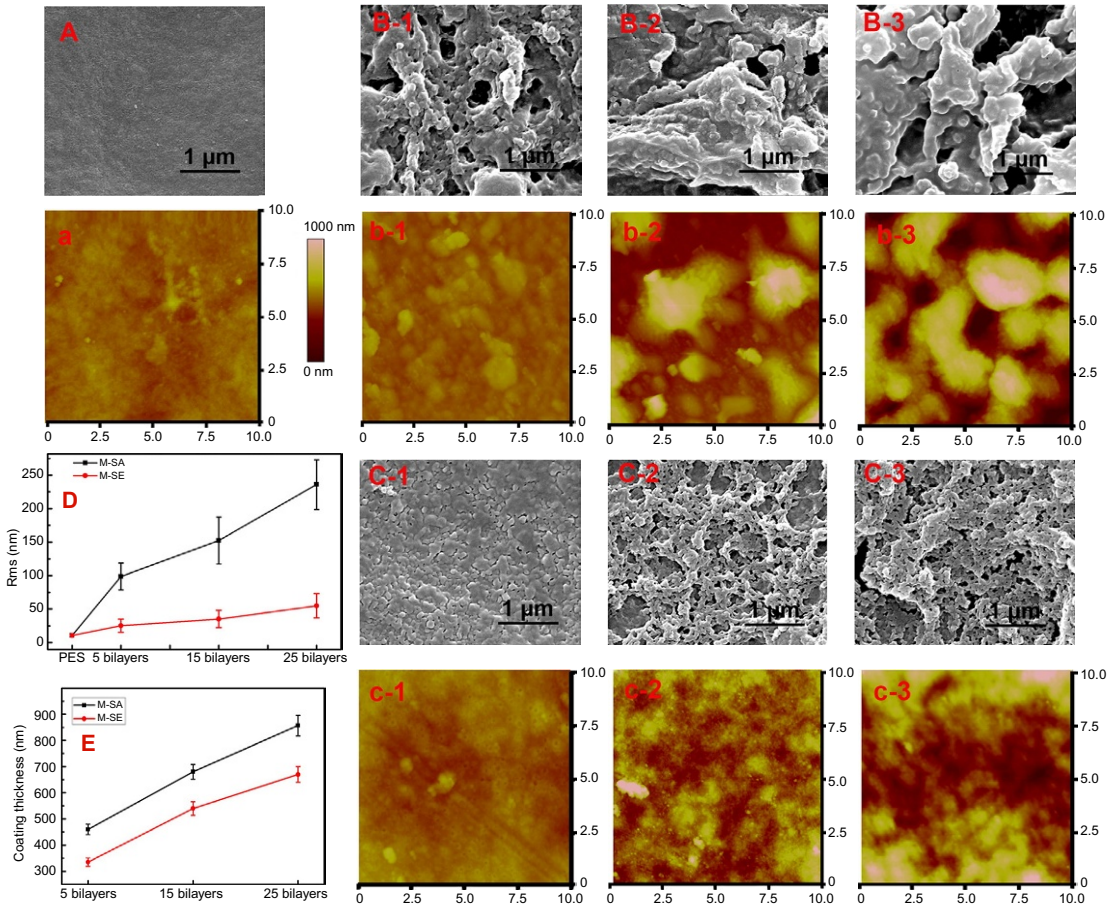


Fig. 6.14 Typical scanning electron micrograph of the surface morphologies for pristine PES membrane (A), M-SA (B-1, M-SA-5; B-2, M-SA-15; and B-3, M-SA-25) and M-SE (C-1, M-SE-5; C-2, M-SE-25; and C-3, M-SE-25). AFM images of the membranes for pristine PES membrane (a), M-SA (b-1, M-SA-5; b-2, M-SA-15; and b-3, M-SA-25) and M-SE (c-1, M-SE-5; c-2, M-SE-25; and c-3, M-SE-25). Surface roughness calculated from 5 AFM images (D). Coating thickness measured from 5 cross-sectional SEM observation (E), cross section. Copyright 2014, American Chemical Society.

supramolecules, 3-D porous structures were observed on the membrane surfaces, which showed an identical result to the SEM observation. As shown in Fig. 6.14D, Rms was used to evaluate the average surface roughness of these membranes. It was observed that the surfaces of the M-SA membranes were much rougher than those of the M-SE membranes; the surface roughness of the M-SA membranes increased dramatically with the increase of the coating bilayers from 5 to 25. However, the M-SE membranes showed slightly increased surface roughness with the increase of the bilayers from 5 to 25. Though it was hard to detect the detailed assembly mechanism between these two star-shaped supramolecules, the different surface-assembled morphologies should be greatly influenced by the AA and EGMA segments. During assembly, the EGMA fragments might twine around each other [46]. In addition, introduction of EGMA fragments decreased the negative charge of the Star-PSS-EGMA; thus, the repulsion between the Star-PSS-EGMA molecules was lower than that for Star-PSS-AANa, which might also lead to the lower roughness of M-SE. In general, after LbL coating of the star-shaped supramolecules, both of the membranes showed 3-D surface architectures compared with the pristine membrane.

For blood-contacting materials, platelet adhesion is the key event during thrombus formation. Many kinds of coagulation factors can be further activated by the activated platelets followed by acceleration of thrombosis and coagulations. In this study, platelet adhesion measurement was evaluated. As shown in Fig. 6.15, both the spreading and formation of pseudopodium for the platelets were dramatically suppressed, indicating lowered platelet activation and improved blood compatibility by the star-shaped supramolecule-deposited heparin-mimicking 3-D porous multilayer thin-film surfaces [47,48].

Fig. 6.16A shows the clotting times for the pristine, M-SA, and M-SE membranes. It could be observed that the APTTs for the modified membranes had a maximum increase by 39 s compared with the pristine membrane, while the TT increased with a maximum of 8.7 s. The results indicated that the modified biomedical membranes had an effect on the endogenous pathway of coagulation, which might be ascribed to the combination or reaction between the coagulation factors (V and X) in plasma and the hydrophilic surfaces of the modified biomedical membranes. By using TAT concentration, the generation of thrombin was evaluated since the thrombin would be immediately neutralized by antithrombin III, resulting in TAT complex formation [49].

Fig. 6.16B describe the level TAT in plasma after the interaction of blood and membranes, as observed in TAT level in Fig. 6.16B; the concentrations of TAT for the samples decreased compared with those of blood and pristine polymeric membrane. Furthermore, with the increase of the coated bilayers for the M-SA and M-SE membranes, the generated TAT values decreased gradually. The results confirmed that the TAT generation was successfully suppressed by the star-shaped supramolecule-deposited heparin-mimicking multilayers; thus, combined with the platelet adhesion and activation results, it might be concluded that the surface-modified polymeric membranes showed excellent blood compatibility [50–52].

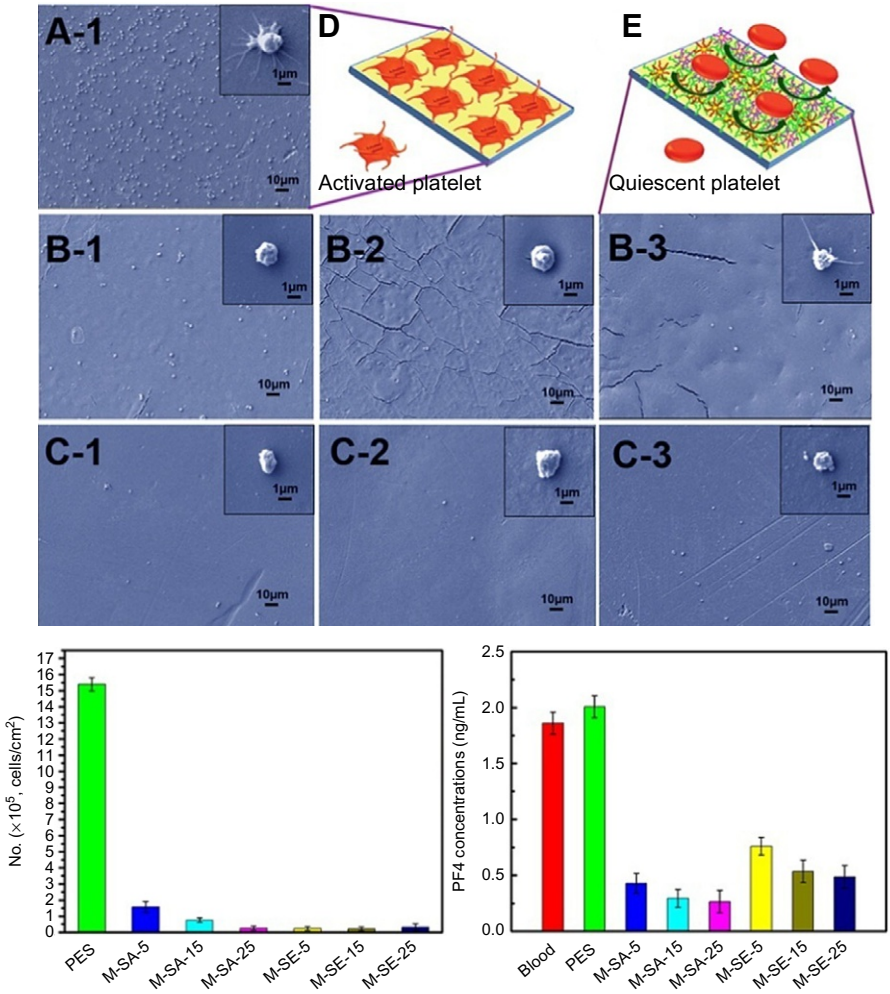


Fig. 6.15 Typical scanning electron micrograph of adhered platelets on the PES (A-1), M-SA-5 (B-1), M-SA-15 (B-2), M-SA-25 (B-3), M-SE-5 (C-1), M-SE-15 (C-2), and M-SE-25 (C-3). (D) Activated platelets on PES membrane surface. (E) Antiplatelet adhesion and platelets remaining in quiescent after exposing with polymeric membrane. (F) Average numbers of the adhered platelets onto the membranes from PRP estimated via SEM images. (G) Generated concentrations of PF4 of these samples with whole blood, which can act as an index for platelet activation; values are expressed as means ± SD and $n = 3$. Copyright 2014, American Chemical Society.

6.4 Surface characterization of biomaterials

Biomaterials are designed to be biocompatible or biologically acceptable; they are to cause no harm to the host, and the material itself is not to be rendered nonfunctional by the host. In addition to this minimal requirement, the surfaces of implantable medical devices are modified to improve the functionality of the materials such as promote

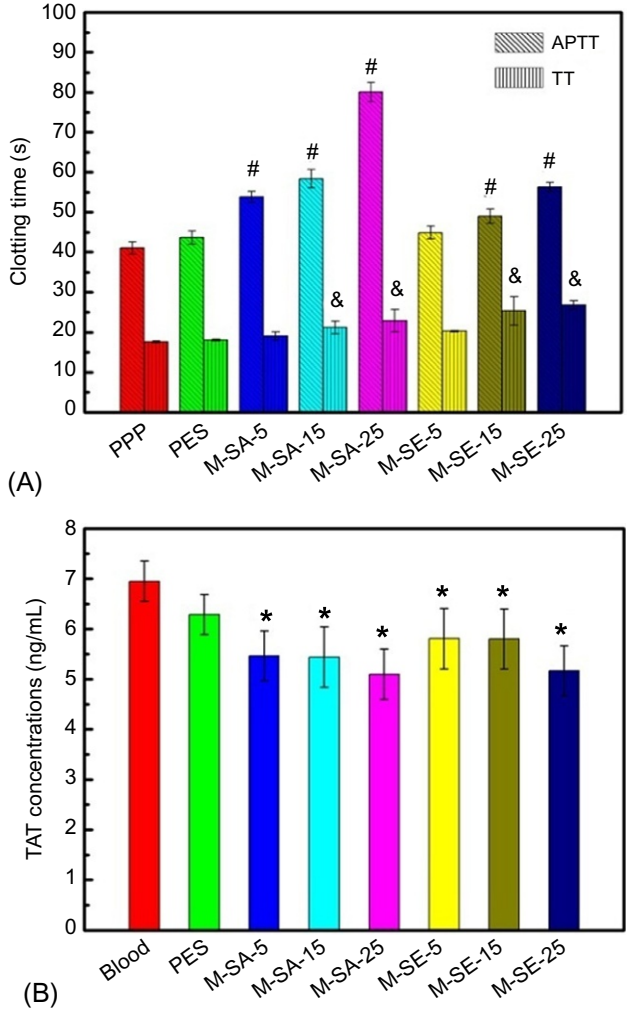


Fig. 6.16 APTT and TT assays of the pristine membrane and star-shaped supramolecules assembled membranes; values were expressed as means ± SD, $n = 3$ (A), &P, and #$P < 0.05$ compared with the value of PES. TAT generation of all membranes with blood flowing for 2 h; values were expressed as means ± SD, $n = 3$, and *$P < 0.05$ (B) compared with the value of PES. Copyright 2014, American Chemical Society.

osteointegration of orthopedic implants and prevent unfavorable physiological reactions such as thrombosis formation. Biological response of the surface coatings is determined by their structure, chemical composition, and functionalities. Changing the surface characteristics is the most obvious way to control cell attachment, proliferation, and differentiation. Thin-film coatings could be in the form of a layer deposited on the substrate (e.g., chemical vapor deposition and Langmuir-Blodgett film) or may be in the form as the biomolecules adsorbed onto the surface of an implanted device. In addition to these physical means, the surface film can be formed chemically by

chemisorption, plasma, or ozone treatments and by radiation such as γ, electron beam or ion beam. The performance of these surface layers is highly dependent on their interaction with the host, which is initiated and mediated by host proteins adsorbing on the thin-film surface immediately upon implantation [53]. For example, hemocompatibility and thrombogenicity of thin-film coatings on medical devices are largely dependent on the proteins adsorbed at the blood-thin-film interface [54].

The tissue response is determined by a sequence of events that occur at several different time and length scales. After the hydration of the implanted surface that occurs on microsecond timescale, small molecules migrate toward the surface in milliseconds and protein over a timescale of minutes. The subsequent cell attachment that occurs over the adsorbed protein layers determines the long tissue response of the implanted material. Each of these processes needs to be characterized and understood in designing the surface to elicit the required tissue response. Some of the features of the surface layer that are typically monitored include macroscopic characteristics such as the thickness and the surface energy of the layer, the hydration state of the surface layer, the structure and the conformation of the molecules in the surface layer, their chemical composition, and the nature of the biological interactions between the surface layer and the surrounding biological environment. The techniques described in this chapter will span the timescale on the scale of protein and cell attachment, but not the water or the ions interacting with the substrate.

There are following areas where such measurements are useful: tissue scaffolds, regenerative medicine, drug discovery, biosensors, and biofouling. For the most part, the study of the adsorption of proteins is amenable to detailed investigation and is often used as a proxy to predict cell response to substrates. In vitro measurements do not always correlate with the in vivo results. Nevertheless, understanding the fundamental biophysical chemistry of the protein adsorption can provide useful insight to the tissue response. These measurements are useful in applications such as in drug discovery, food science, and, in general, any material development effort.

The techniques are used to characterize the biomaterials that are divided into three sections, physical characterization, chemical analysis, and characterization of biointerfacial events. The emphasis is on the methods to quantitate and characterize protein adsorption on biomaterials like coated thin films that precede; host biological responses are also described.

6.4.1 Surface characterization techniques

Characteristics of the surface coatings that influence the performance of a biomedical device include the thickness of the coating, the adhesivity of the coating, surface topography, mechanical characteristics, and phase compositions or inhomogeneity of the surface layers. The thickness of surface layers, a primary consideration in studying the adsorption of cells and proteins onto substrates, can be studied by one of the four main techniques: ellipsometry (ELM), surface plasmon resonance (SPR), quartz crystal microbalance (QCM), and x-ray reflectivity (XRR). In some instance, x-ray photoelectron spectroscopy (XPS) and time-of-flight mass spectrometry (ToF-MS) are used to obtain the film thickness. X-ray scattering provides additional information

about the structural features of the adsorbed layers. These measurements can be used to understand the mechanism and the strength of the interactions between host molecules that interact and the substrate and how much is it adsorbed and how fast does they get adsorbed.

6.4.2 Ellipsometry

This is an optical method used to analyze the thickness and surface roughness of ultrathin films in semiconductor industry. It measures the changes in polarization of a beam light reflected from a surface. This can be related to the characteristics of the surface layer, such as an adsorbed protein layer or a layer of cells attached onto a surface [53,55]. When a linearly polarized light is incident onto a surface, the surface will alter the intensity of the E-field perpendicular and parallel to the surface. As a result, the characteristics of the polarization perpendicular and parallel to the surface will change, and this is measured by the relative attenuation of the *p*- and *s*-polarized light, r_p and r_s, respectively. This is expressed and written in equation in terms of ratio of the magnitude (tan ψ) and phase shift (Δ), as

$$\frac{r_p}{r_s} = \tan(\Psi)e^{i\Delta}$$

This change in the polarization state of the reflected light can be graphically expressed as elliptical polarization. The parameters Ψ and Δ correspond to the tilt angle and the ellipticity of the ellipse, respectively; ellipsometry is an indirect method in that in most cases, an iterative procedure is used to calculate the optical constants and the thickness of the films to fit the observed tan Ψ and Δ values at various wavelengths.

A beam of laser light falls directly onto the sample surface, and the reflected light is captured by a detector. Data are collected at more than one angle of incidence, the data obtained from mussel adhesive protein [56], which is a glue-type protein used to anchor on a solid surface, such as the hull of a ship. It is made of repeating units of decapeptide that has an open flexible conformation in solution. Sodium periodate is used for cross-linking, which can change this conformation and the mechanical properties of the protein. The data show that as the proteins are attached to the surface, there is an increase in mass. Upon rinsing and cross-linking, there is no change perhaps a small decrease in mass. On QCM-D, this mass is the dry mass of the protein and does not contain any information about the coupled water.

The advantages of ellipsometry are that it is a simple technique sensitive to small changes in mass, thickness, and surface roughness [57–59] and can be used in real time and in situ. Because a ratio of two attenuations, r_p and r_s, are measured, it is a very precise measurement independent of the source fluctuations. As a contact-free, nondestructive method, ellipsometry also allows for real-time data collection for studying kinetics of protein binding.

Disadvantages are that the technique requires thick samples with flat and reflective surfaces. Therefore, most polymers with low refractive indexes cannot be tested in this modality, though one could overcome this hurdle by spin coating the polymer onto a suitable surface [60]. Since the details of the material characteristics that can

be derived depend on the optical model used to interpret the data, the choice of the appropriate models and the parameters for protein adsorption measurement, such as the refractive indexes and extinction coefficients of proteins and buffers [61–63], becomes critical. Although samples are label-free, sample preparation can be tedious and need to be done with special care.

The dry thickness of the layers was measured using an OMT ellipsometer and VisuEl software version 3.4.1 (Optische Messtechnik GmbH) at the angle of incidence of 70° and a spectral method with wavelength range from 460 to 870 nm. The swelling study was performed with an RC2 spectroscopic ellipsometer from J.A. Woollam Co., Inc. using a quartz in situ cell. The modeling of the measurement was done with CompleteEASE software version 5.07. The analysis was conducted in a wavelength range 193–1000 nm using spectra of a high-resolution (800 wavelengths per spectrum). For the swelling experiments, the cell window offsets and the influence of the ambient liquid on the signal were taken into account.

6.4.3 Characterization of the swelling behavior using in situ ellipsometry

The swelling behavior of chitosan and chitosan functionalized with polymer brushes was measured in PBS buffer at room temperature with in situ spectroscopic ellipsometry. For this, we determined Ψ and Δ in the dry state and after equilibration with the buffer. The study of the swelling of ultrathin films combined with precise optical modeling of the film gave us access for the first time to the hierarchical structure of the swollen multilayer films. The optical properties of pure components, necessary for the subsequent precise modeling of the swollen multilayer films, were determined on spin-coated chitosan and poly(HEMA) and poly(MeOEGMA) directly grown from silicon wafers modified with 11-(2 bromoisobutyryl)undecyltrichlorosilane. Ψ and Δ were recorded at broad spectral (192–1000 nm) and angular (AOI, 55–80° every 1°) ranges followed by B-spline-based fit of both real and imaginary parts (complex refractive index, $N = n + i \cdot k$) of the dielectric function. In the B-spline fit, first, a Cauchy layer is used to fit the approximate layer thickness and the real part of the complex refractive index in the visible range (where the sample can be considered transparent). Then, the layer is converted to B-spline, and the model is extended to include the ultraviolet part of the spectrum, thus determining the imaginary part of the complex refractive index (associated with light absorption). The obtained refractive indexes at $\lambda = 632.8$ nm were 1.501 for poly(MeOEGMA), 1.515 for poly(HEMA), and 1.533 for chitosan. The rather similar refractive indexes of the three materials result in poor optical contrast in the visible range making it difficult to model a stack of chitosan and brushes. To enhance the contrast and to differentiate between brushes and chitosan, we utilized the UV absorption of chitosan at $\lambda \sim 300$ nm, which is not present in the polymer brushes. For the determination of the thickness in the dry state of the brushes on chitosan, the films were approximated with a two-layer optical model utilizing the UV absorption of chitosan to discriminate it from the brushes. The total thicknesses were

41.6 nm for poly(HEMA) on chitosan and 48.7 nm for poly(MeOEGMA) on chitosan. The thicknesses of each individual layer were determined to be 18.0 nm poly(HEMA) on 23.6 nm chitosan and 35.5 nm poly(MeOEGMA) on 13.2 nm chitosan. While the total thicknesses can be considered of very high accuracy, the values of the thicknesses of individual layers heavily rely on the assumption of a sharp optical interface between the two layers [64,65].

The modeled chitosan thickness in the poly(MEOEGMA) sample is close to its value before brush growth (16.6 nm), suggesting that poly(MeOEGMA) brushes predominantly grew from the interface. On the other hand, the thickness of the chitosan layer underneath poly(HEMA) is considerably higher than the thickness of the same chitosan layer measured before the grafting of the brushes (16.3 nm), suggesting that the poly(HEMA) simultaneously grew from interface and inside the chitosan layer, thus modifying and smearing out the position of the optical interface. The smaller monomer size of HEMA probably allows for the growth deeper within the chitosan layer. When the brush-functionalized samples were equilibrated in PBS, a large difference in the overall swelling factor (SF = h h swollen dry) of both samples could be seen. For the poly(MeOEGMA) grown from chitosan, the total swollen thickness was much larger, approximately 171 nm giving an overall SF = 3.5. For this sample, a two-layer model was found to be numerically valid and unique. The swollen thicknesses of the chitosan layer and the poly(MeOEGMA) layers were found to be 71 and 100 nm, respectively. Using the previously ellipsometry-derived dry chitosan thickness (13.2 nm), the SF of the chitosan layer alone equals to 5.4, which is much larger than for a nonfunctionalized chitosan, SF = 1.55. This pronounced increase in the SF could be ascribed to the forces exerted by the brushes onto the chitosan film caused by the osmotic pressure and entropic effects arising from the stretched polymer chain conformation. The SF for poly(MeOEGMA) layer on chitosan is found to be 2.8, which is larger than that of the same brushes directly grown from silicon (SF = 1.9), suggesting that the grafting density of brushes on chitosan might be lower than that of brushes directly grown from a sharp rigid interface. Since poly(HEMA) grew from inside and from the interface of chitosan, a two-layer model was deemed not valid, and instead, a graded optical model was utilized. A graded optical model assumes a continuous variation of the sample refractive index orthogonal to the substrate. The choice of the graded model was substantiated by a large reduction of the fit error parameter (mean square error, MSE) going from a uniform single-layer model to graded single-layer model (from MSEuniform = 17 to MSEgraded = 9). The resulting total swollen thickness was 74 nm and SF = 1.8. The latter is considerably lower than for the more hydrophilic poly(MeOEGMA)-functionalized chitosan [66]. After recalculation using the effective medium approximation 61 and a typical refractive index for the system, it was found that the bottom of the sample possessed a slightly higher water volume fraction than the top (approximately 60% vs 40%). This may suggest a larger degree of swelling within the underlying chitosan structure than within the poly(HEMA) brush residing on the top.

6.4.4 Surface plasmon resonance

Oscillations of the electron cloud in a lattice of positive charges that occurs in some metals are called plasma oscillations. Collective oscillations of this electron cloud gives rise to a plasma wave, which when quantized is referred to as a plasmon. Surface plasmons occur at the interfaces between a metal and a dielectric such as water/a buffer/air. Since the surface as a whole is neutral, the electron oscillation gives rise to compensating collection of positive charges at the surface. The periodicities of these oscillations are on the order of wavelength of 1000–5000 Å and therefore can absorb visible light. Consider a beam of light is incident on a glass surface, usually bottom of a prism at such an angle so that light undergoes total internal reflection. Not all the other energy is reflected at the surface, and a wave (evanescent wave) of decreasing intensity propagates into the metal layer. If the wavelength of this light is equal to that of the plasma waves at the interface, there is a resonance, between the evanescent wave and the plasmon. As a result, at this particular angle, the intensity of the light wave is reduced. In SPR, a resonance enhancement is achieved by evaporating a thin metal (gold or silver) layer at the base of the prism.

In SPR, the incident light has to be p-polarized, i.e., the E-vector has to be in the incident plane. In practice, a flow cell is used on the under surface of the prism. At the metal liquid interface, there is a change in the refractive index (n) that changes the intensity and the angle of the reflected light. These two changes are monitored using a photodiode array. When the receptor or an antigen is deposited onto the surface at time t_1, there is a resonance at one angle. As the antibody binds to the antigen, the resulting change in n causes SPR to occur at a different angle. This shift in the angle corresponds to the change in the n or the change in the thickness [67].

The binding of blood proteins, albumin, Fg, and IgG, onto the substrate is compared. When the evanescent field is altered by adding a liquid or a protein layer, then the angle at which the SPR shift is to be larger. The rate of change of the SPR angle is shown here. An SPR spectrum is a record of the reflected light intensity versus the angle of incidence. In case of plasmon resonance, a dip in the reflected spectrum is observed. By calibrating the magnitude of the change with some other technique, the shift in the position of the peak that occurs with increase in thickness of the film can be used to monitor the deposition. SPR signal also depends on the distance, so that it can be used as a microscope. It is also possible to simulate the shapes of these curves and obtain the thickness by comparing the simulated data with the observed data.

Many of the comments made with respect of ELM apply to SPR as well. One additional advantage of SPR is that because a cell membrane has different components with different n, kinetics of cell membrane formation in the form of a thin film can be studied.

6.4.5 Quartz crystal microbalance

QCM is essentially an extremely sensitive balance that can measure changes in mass of micrograms of films deposited on a substrate with nanogram sensitivity [68–70]. The mass change can be followed in real time, for example, as the protein is being

adsorbed onto the substrate over which the medium is flown. Adsorptions at sub-μg levels, binding kinetics, and the rigidity of the protein layer can be monitored, and by monitoring the dissipation, viscous properties can be determined.

The quartz crystal that is used is cut in such a way that it undergoes shear deformation when external electric voltage is applied. The resonant frequency of this deformation, typically 5 MHz, depends on the mass of the crystal. The change in the frequency (Δf) due to a change in mass of the crystal (Δm) is given by the Sauerbrey equation:

$$\Delta f = -C \cdot \Delta m$$

where C is the mass sensitivity of the crystal ($C = 17.7\,\text{ng/cm}^2\,\text{s}$). This equation assumes that the adsorbed layer is rigid. If the adsorbed mass is not rigid, then the decay in the oscillations that occurs once the excitation is turned off is used to calculate a dissipation factor, D; D is the ratio of the energy lost per oscillation to the energy stored in the system that can be related to the viscosity (η) and the shear modulus (μ) of the adsorbed layer. Thus, QCM can measure both the areal mass density $\Delta m/A$ of the adsorbed and the viscoelastic properties of the film deposited onto the crystal if $\Delta D > 10\%\ \Delta f$.

In a typical experiment, the decay characteristics of several overtones are measured, usually up to 13. The instruments ping sequentially at fundamental, third, fifth, and so on up to 13th harmonics, and the output frequency shift and the dissipation at each harmonics as a function of time. All the 13 measurements are repeated in about ~0.2 s. Only the odd harmonics are observed because when the crystal oscillates, the node at the center and antinodes are at the surface.

The change in the frequency at various stages of absorption of proteins and cells on the surface of the material [71]. These frequency shifts can be converted into areal mass using Sauerbrey equation and, if the density of the deposited layer is known, then into thicknesses. The results show that formation of a thin layer and the BSA that follows Fn covers the area not covered by Fn. BSA serves to block the adsorption of additional protein that is present in the culture medium that is used deposit cells on to the surface. The eventual goal of this experiment was to follow the formation of the layer of MC3T3 cells on fibronectin-coated substrate.

To fully interpret these data, it is necessary to model the frequency and dissipation plots using an appropriate model; Voigt model is generally used. In this model, elastic component of the coating is represented by a spring and the viscous component by a dashpot. The modeling consists of calculating the frequency and dissipation curves for at least two overtones and refining the parameters until the results are meaningful and reproduce the observed data. Other alternate models are also being investigated [72].

QCM is extremely sensitive and accurate. Data can be collected in real time and thus follow the kinetics of adsorption, reaction, and film growth. In addition to measuring the mass, the instrument can also measure the mechanical properties, e.g., changes in the stiffness and viscosity of the material, in real time. These viscoelastic effects can, however, complicate the interpretation of the data. Attachment of cells and formation of biofilms can also be monitored. The drawbacks are that the measurement can be time. Automation using robots may be necessary to increase the otherwise low throughput.

6.4.6 Comparison of the different techniques

The SPR and QCM data of the adsorption of the protein onto a hydrophobic surface and subsequent cross-linking using sodium periodate was discussed in Section 6.4.2. In the QCM data, the large decrease in the frequency upon attaching the polymer onto the substrate is due to the expected increase in mass that occurs during this step. However, the frequency increases upon cross-linking suggesting a large decrease in mass compared with a small change seen in ELM. This discrepancy between QCM and ELM results can be interpreted as follows. The film that forms when the protein is adsorbed onto the surface contains significant amount of water. When the film is cross-linked, some of this water is expelled from the film; thereby, the total mass and the thickness decrease. $NaIO_4$ does not significantly bind to the protein film. Calculations show that 91% of the coupled mass before cross-linking and 82% after cross-linking are due to water. Cross-linking radically increases the shear modulus and shear viscosity. The film becomes rigid, and the dissipation decreases. These effects on the mechanical properties are not captured by ellipsometry or by SPR. The three steps correspond to the adsorption of proteins, cleaning with a detergent (SDS) and then rinsing with PBS. As in the case of ELM, there are differences between QCM and SPR data. In particular, notice that upon washing with the detergent and PBS, all proteins show an increase in mass, relative to the starting mass, in QCM. But SPR shows a decrease in mass, which is least in Fg and is most in IgG. This decrease in SPR reflects the different percentages of the proteins that are removed with SDS. The increase in QCM seen in detergent-treated proteins is due to water; this water content depends on the protein.

This difference in QCM and the other two techniques is because ELM and SPR measure the changes in dry mass whereas and QCM measures the changes in mass and viscoelastic properties. Specifically, ELM and SPR do not measure the coupled water because the changes in n due to coupled and free water are not that much different. But it affects the viscoelastic properties of the surface and thus the QCM signal.

The advantage of ELM, SPR and QCM, and the x-ray reflectivity technique to be described in Section 6.4.5, over other techniques such as XPS and fluorescence microscopy, is that it does not require any labeling and is real-time measurement. In all these instances, pre-prepared surface can be used to immobilize different types of molecules. In all these techniques, with the exception of QCM and rigid surface layers, some modeling is required to simulate the observed data before parameters such as sample thickness can be obtained.

X-ray photoelectron spectroscopy (*XPS*): XPS, also known as electron microscopy for chemical analysis (ESCA), is a powerful tool for elemental detection, chemical state identification, and quantification of various atomic species at the surface [73]. XPS utilizes the photoelectrons that are emitted following the absorption of x-rays. In XPS, samples are irradiated with a monochromatic beam of x-rays with a known energy (usually Mg Kα (1253.5 eV) or Al Kα (1486.6 eV)) that penetrates deep into the sample, the depth varying from μm to mm, resulting in the emission of electrons. Because electrons are readily absorbed, only the electrons emitted from the few top atomic layers escape the material and are detected. Consequently, the information

depth of XPS is less than 10 nm, depending upon the nature of the material under evaluation and the kinetic energy (E_k) of the emitted electrons. Kinetic energy of the emitted electrons will be

$$E_k = h\nu - E_B - \phi_{spec}$$

where $h\nu$ is the energy of interacting photon, E_B is the binding energy of electron in the atomic orbital from which it originates, and ϕ_{spec} is the work function of the spectrometer. Binding energy can be interpreted as the ionization energy of a particular atom, and hence, it is a characteristic of the atom in a particular orbital with a specific bonding environment. This results in a distinctive energy distribution, peak position, and intensity that is characteristic for a particular atom (except hydrogen and helium), enabling its identification and quantification with a sensitivity of up to 0.1 at. %.

Typically, low-resolution survey scans are used to identify the surface elemental composition and high-resolution scans to evaluate the chemical environment of a particular atomic species. In the high-resolution scans, the core level peaks show characteristic shift in binding energies (ranges from 0.2 eV or more) depending on the specific environment of the functional groups associated with the emitting element and thereby enabling identification of various functional moieties [74]. Even though the XPS is generally considered as a nondestructive analytic technique, overexposure to x-rays can result in altered surface chemistry. Coexistence of certain functional groups can make it difficult to directly identify and quantify them during the normal XPS analysis. For example, identification and estimation of amine on an aminated surface are often tedious while present with other nitrogen-containing functional groups with very similar binding energies [71]. In such cases, specific identification and quantification of the functional groups can be achieved by using chemical derivatization XPS (CD-XPS) [75].

In addition to its capability for quantitatively analyzing both elemental and chemical state information, XPS can also be used to obtain additional film features such as thickness, growth mechanism, and interface properties with relative simplicity from a single analysis. Assuming the overlayer thin film is homogenous in nature, the thickness (t) of the film can be calculated from the peak intensity of a particular peak from the thin film (I_f) and the substrate (I_s^0), usually from a high-resolution scan, using standard uniform overlayer model [76,77], which is given by the equation

$$I_f = I_s^0 \exp\left(-\frac{t}{E_L}\right)$$

where E_L is electron attenuation length of the peak under evaluation. In general, E_L of a particular peak is a characteristic of its electron energy [78], and this overlayer model provides greater accuracy in determining film thickness in nanometer ranges, provided the film thickness is less than nearly three times the mean escape depth (λ, MED). Alternatively, the film thickness can also be expressed as a function of λ and electron takeoff angle (θ) as given by the equation [79]

$$t = 3\lambda \sin\theta$$

The overlayer model has been successfully used to quantify the thickness of various surface films including those made from silica, nickel [80], poly(ethylene glycol) [81], and DNA [82]. XPS intensities can be used to determine the film thickness irrespective of the geometry of the surface such as arbitrarily shaped rough and curved substrates and small particles such as catalysts.

In many cases, the thin-film measurements using XPS at a single-electron takeoff angle can result in significant errors caused by geometry of the instrument, nature of the overlayer, and its thickness. This can be overcome by using angle-resolved x-ray photoelectron spectroscopy (AR-XPS) in which photoemission spectra is measured as a function of θ [78,83,84]. The distance traveled by the photoelectron through the material increases at low θ. Consequently, at lower θ, the sensitivity of the measurement will be higher because of the increased inelastic photoelectron scattering. Additionally, AR-XPS provides a useful tool for constructing concentration-depth profiles for various thin films [85,86] and allows nondestructive depth profiling on buried interfaces without sputtering the sample surfaces.

Time-of-flight secondary ion mass spectrometry (*ToF-SIMS*). ToF-SIMS is a versatile surface analytic technique that provides detailed molecular composition and imaging of surface monolayers with high sensitivity and resolution. In a typical secondary-ion mass spectroscopy (SIMS), sample surfaces are exposed to a beam of energetic primary ions or atoms (5–25 keV), which results in the emission of secondary ions including quasi-molecular ions, atoms, and molecule [83]. The secondary ions formed as a result of this sputtering process are analyzed as a function of the mass over charge ratio (m/z) using any conventional mass spectrometric technique. In static SIMS (S-SIMS), very low primary ion fluxes are used to achieve small sputtering rate so that less than 10% of the surface atoms erode away from the sample surface. Consequently, S-SIMS causes minimal damages to the sample surfaces, and the secondary ions produced during this process have very close resemblances to the surface structures. This technique has been used to characterize surface thin films made from chromium oxide and various amino acids including alanine, phenylalanine, cysteine, and arginine by Benninghoven et al. as early as in the early 1970s.

In contrast to S-SIMS, in dynamic SIMS (D-SIMS), a high-flux continuous etching of the surface is used for determining the surface composition as a function of depth. The development of highly sensitive ToF-SIMS analyzer significantly improved the capabilities of this surface characterization technique with exceptional mass resolution, range, transmission, and sensitivity and molecular imaging capabilities.

In ToF-SIMS analysis, the secondary ions generated during the analysis have to enter the flight path simultaneously or within the shortest possible time interval to allow the simultaneous extraction of the secondary ions by the analyzer. This simultaneous extraction of the secondary ions is achieved by bombarding the area of the surface to be analyzed with primary ions having very short pulse durations (Δtp). The secondary ions generated from one single pulse are then accelerated by a constant accelerating voltage (V_{ac}, ~3 keV) over a short distance before entering the flight path of length L with a constant kinetic energy, E_{kin}, given by the following equation:

$$E_{kin} = zV_{ac} = \frac{mv^2}{2}$$

where z is the secondary-ion charge, m is the mass, and v is its velocity. Because of the differences in velocities, which can be attributed to the variations in their mass, mass separation will occur as a function of the flight time t and enables to calculate the mass to charge ratio (m/z):

$$t = \frac{L}{v} = L\sqrt{\frac{m}{2zV_{ac}}}$$

$$\frac{m}{z} = \frac{2V_{ac}\,t^2}{L^2}$$

In general, ToF-SIMS can operate in four different modes, namely, large-area surface analysis, surface imaging and micro-area analysis, depth profiling, and trace analysis. Large-area surface analysis can provide information about wide range of surface characteristics including chemical and physical surface modifications, molecular layer structures surface defect [87], and adhesion properties. High-resolution surface imaging capabilities of SIMS are extensively utilized in various microelectronics and micromechanics, nanotechnology, and biomolecular surface imaging applications [88,89]. Beyond complementing other depth profiling techniques such as XPS, ToF-SIMS offers superior spatial and depth resolutions, high molecular specificity, and better mass resolution. Consequently, this technique is widely used for depth profiling applications in many areas, ranging from materials to biological sciences [90–92]. The capability of SIMS to detect and identify even minute quantities of unknown substances from the surface monolayers, particularly for those materials that cannot be vaporized, makes this technique extremely useful for trace analysis applications. In brief, ToF-SIMS, in any of the abovementioned four modes or in combination, is routinely used for characterizing thin films.

IR-Spectroscopy: Even though the optical spectroscopic techniques are less sensitive than the abovementioned electron-based spectrometric methods, these techniques are extensively employed for thin-film characterization because of the very specific and characteristic vibrational spectrum presented by various functional groups and molecules present in the film. Most commonly used vibrational spectroscopic techniques are infrared (IR) and Raman spectroscopies. Because of the interference caused by absorption of IR by the underlying substrate, infrared reflection-adsorption spectroscopy (IRRAS) and its polarization modulation (PM) analog, PM-IRRAS (which utilizes the polarization selectivity of the surface adsorption) is typically employed for characterizing thin films [93]. In IRRAS spectroscopic analysis of thin films, a well-defined either p- or s-polarized light is directed onto the sample surface at a grazing angle. The vibrations of molecules from the surface layers of the films (that are adsorbed on IR nontransparent planar surfaces, particularly metal surfaces characterized with high reflectivity) are recorded in reflection mode at an angle equal to the angle of incidence. Theoretical interpretation of the spectra is based on measuring the wavelength dependence of the reflectance R, which can be defined as [94]

$$R = \frac{I_{reflected}}{I_{incident}}$$

where $I_{reflected}$ and $I_{incident}$ are the intensity of the reflected and the corresponding incident light beams on the sample surface at a grazing angle. Because of the absorption of light by the thin film, a change in reflection will occur as given by the equation

$$\frac{\Delta R}{R_0} = \frac{R_0 - R}{R_0} = \frac{4n_1^3 \sin^2 \psi_0}{n_2^3 \operatorname{Cos} \psi_0} at$$

where R and R_0 are the reflectance with and without the thin film, n_1 and n_2 are the refractive indexes of the ambient medium and the film, ψ_0 is the incident angle, a is the absorption coefficient, and t is the film thickness. Consequently, measuring the change in reflection in IRRAS analysis will enable direct measurements of thin-film thickness.

IRRAS spectroscopy has been used for characterizing chain conformational changes in Langmuir monolayer and lipid films since the late 1980s [95,96]. This technique allowed extensive and detailed characterization and structural analysis of monolayers and thin films on various surfaces and interfaces over the last decade. However, sensitivity of the IRRAS technique is often limited by weak signals for the thin-layer sample and noise in the spectra due to the background adsorptions caused by atmospheric water vapor and CO_2. Utilizing the advantage of the polarization selectivity of surface absorption, polarization modulation IRRAS (PM-IRRAS) offers a convenient option to reduce these background noises and provides a surface selective and sensitive method for characterizing very thin surface films In a PM-IRRAS experiment, an IR beam is directed to the sample surface, after passing through a polarizer and a photoelastic modulator (PEM). The reflected beam from the sample is collected with an IR lens (BaF_2) into a detector. The entire instrumentation can be evacuated to avoid any background atmospheric adsorptions.

PM-IRRAS technique measures the intensity differences between the s- and p-polarized lights by using the PEM, and the sum of their intensities is used as reference, and hence, there is no requirement for additional reference substances:

$$I_{(t)} = \left[I_P + I_S + \left(I_P - I_S \right) \cos\left(\frac{V_m}{\lambda} \cos\left(\gamma t \right) \right) \right] / 2$$

where $I_{(t)}$ is the intensity of the output light at time t; I_P and I_S are the intensities of p- and s-polarized lights, respectively; γ is the modulation frequency; V_m is the modulation voltage; and λ is the wavelength of the IR light.

PM-IRRAS spectroscopy has been used extensively for characterizing SAMs on various reflective metal substrates, particularly on gold surfaces [97,98]. For example, Vanderah et al. used PM-IRRAS spectroscopy to investigate the conformation, organization, and phase of isostructural SAMs of a series of octadecyl 1-thiaoligo(ethylene oxide) disulfide adsorbed on a gold surface. Using the PM-IRRAS spectral data, the researchers were able to evaluate the detailed conformational behavior of 1-thiaoligo(ethylene oxide), poly(ethylene oxide) (PEO), and hydrocarbon segments present in the SAMs of these long-chain alkanethiols. PM-IRRAS spectroscopy has been employed routinely for following surface monolayer reaction, including carbodiimide-mediated amine conjugation [99] and electrochemical reactions commonly used for protein and polypeptide immobilizations. Using this tool, Brand et al.

successfully evaluated the structural features of the *d*-alkane and the oligoethylene glycol (OEG) parts of perdeuterated hexaethylene glycol-terminated alkanethiol, $HS(CD_2)_{12}(O\text{-}CH_2\text{-}CH_2)_6OCH_3$, (D-OEG) SAMs on gold. Progress of OEG SAM oxidation by bromine was monitored by PM-IRRAS spectra after exposing the SAMs to a Br_2 solution A galvanic cell Au|D-OEG SAM| 25 μM Br_2 + 0.1 M Na_2SO_4|| 50 μM KBr + 0.1 M Na_2SO_4|Au. Reaction with Br_2 resulted in reduced surface coverage of OEG and consequently reduced the intensities of IR bands over a period of time. However, in the galvanic cell, the oxidant is scavenged by a heterogeneous electron transfer reaction and results in slower removal of the OEG chains. Moreover, the initial increase in the integrated intensities of γ_s (OCH_2) at 2880 cm^{-1}, γ_s (COC) at 1110 cm^{-1}, and CH_2 wagging mode at 1357 cm^{-1} confirms an increase in disorder in the SAM followed by a gradual inclination of the OEG chains.

Surface-enhanced Raman scattering (*SERS*) is another important vibrational spectroscopic technique commonly employed for thin-layer characterizations. This technique provides enhanced Raman signals, with an enhancement factor as high as 10^{14}–10^{15}, for Raman-active surface thin layers adsorbed onto certain specially prepared metal surfaces [100]. The importance of SERS technique is that the method provides both surface sensitivity and selectivity extending the utility of Raman scattering (RS) to wide varieties of interfacial surface characterizations, whereas the RS is not surface sensitive. This enhancement process has a twofold origin, namely, electromagnetic and chemical enhancements, with the electromagnetic enhancement being the dominant mechanism. Since the primary enhancement in the SERS technique is due to an electromagnetic process, the technique is distance-dependent, and the theoretical SERS surface enhancement factor, *G*, can be defined as

$$G \approx \left[\frac{r}{(r+d)}\right]^{12}$$

where *r* is the radius of the spherical metal roughness feature and *d* is the distance of the analyte to that feature [101]. This equation clearly indicates the decay of the enhancement factor over the distance, and the experimental values suggest a 10-fold decrease at a distance of 20–30 Å or a monolayer or two. The SERS technique is commonly employed for characterizing thin layers adsorbed onto coinage (Au, Ag, or Cu) or alkali (Li, Na, or K) metal surfaces using an excitation wavelength near the visible region.

The technique is used for determining the adenine concentration as low as 10 nM on SERS-active silver(Ag)-deposited silica magnetic particles (Fe_3O_4/SiO_2@Ag) and for measuring the film thickness add (RhBITC-PAH) film on a glass slide by doping with the same magnetic particles [102]. A series of SERS spectra of adenine in various concentrations ranging from 10^{-4} to 10^{-8} M were recorded, and the intensity of the characteristic adenine peak at 734 cm^{-1} was used for plotting the intensity-concentration standard curve for determining the unknown concentration Similarly, this technique has been routinely used for characterizing various surface thin films including those made from synthetic [103] and of natural origin (additionally, SERS studies provided detailed structural and stability features of various SAMs and Langmuir-Blodgett (LB) films).

6.5 Conclusion

For analyzing the surface properties of biomaterials to assess its hemocompatibility studies, these techniques, ELM and SPR, provide us the dry mass; QCM provides information about the coupled water. Thus, a combination of the technique can reveal much about the interaction of protein with the substrates and the surrounding medium. XRR provides another dimension by providing the structural detail in the form of electron density distribution normal to the surface. Further information about the surface can be obtained by using GID. Thus, each of the methods described here provides details of particular aspects of the thin-film coatings and more importantly of the adsorption process that leads to the formation of a surface layer. Most of these methods can be used in real time so that the kinetics of the formation of thin films can be observed. In all these techniques, the interpretation of the data using a proper model is critical. The results obtained using inadequate models would lead to erroneous conclusion that may continue to be cited in the literature. Advances in understanding the mechanism of adsorption and the formation of thin layers will lead to better experimental protocols and robust methods of analyzing the data. The significance of such advances will be reliable coatings and consistent performances, which will lead to further advances in thin-film coatings. For the relatively nascent field of characterizing biological interactions on thin films interfacing material/device and host, much development is still needed to efficiently investigate the suitability of thin films for specific applications. Various analytic tools are already available to study the events taking place at the interface; the difficulties lie in the inherent complexities that come with biology (e.g., the same type of thin film could face vastly different responses from the host upon implantation depending on its implantation site). Hence, for assessing the hemocompatibility properties of biomaterials whose surface properties are analyzed by the techniques such as ellipsometry, SEM, TEM, fluorescence microscopy, spectroscopy, and other important techniques described in this chapter.

Acknowledgment

PG and VK give sincere thanks to the Department of Biotechnology and Centre of Nanotechnology, Indian Institute of Technology (IIT), Roorkee, UK, India, for providing necessary infrastructure to carry out this research. VK is especially thankful to the Ministry of Human Resource Development, India, for the fellowship.

References

[1] J. Matthew Buchanan, P.J. Upman, R.F. Wallin, A practical guide to ISO 10993-4: hemocompatibility, Med. Device Diagn. Ind. 20 (1998) 79–80.

[2] M. Sanak, B. Jakieła, W. Węgrzyn, Assessment of hemocompatibility of materials with arterial blood flow by platelet functional tests, Bull. Acad. Pol. Sci. 58 (2) (2010) 317–322.

[3] J.M. Lackner, et al., Hemocompatibility of inorganic physical vapor deposition (PVD) coatings on thermoplastic polyurethane polymers, J. Funct. Biomater. 3 (2) (2012) 283–297.
[4] F.M. Elahi, G. Guan, L. Wang, Hemocompatibility of surface modified silk fibroin materials: a review, Rev. Adv. Mater. Sci. 38 (2) (2014) 148–159.
[5] A.C. Thomas, G.R. Campbell, J.H. Campbell, Advances in vascular tissue engineering, Cardiovasc. Pathol. 12 (5) (2003) 271–276.
[6] G.W. Bos, et al., Small-diameter vascular graft prostheses: current status, Arch. Physiol. Biochem. 106 (2) (1998) 100–115.
[7] J.W. Boretos, M. Eden, Contemporary biomaterials: material and host response, clinical applications, new technology and legal aspects, J. Membr. Sci. 21 (2) (1984) 209.
[8] D.F. Williams, Tissue-biomaterial interactions, J. Mater. Sci. 22 (10) (1987) 3421–3445.
[9] M. Niinomi, Recent metallic materials for biomedical applications, Metall. Mater. Trans. A 33 (3) (2002) 477–486.
[10] H.M. Nugent, E.R. Edelman, Tissue engineering therapy for cardiovascular disease, Circ. Res. 92 (10) (2003) 1068–1078.
[11] L. Muthusubramaniam, et al., Hemocompatibility of silicon-based substrates for biomedical implant applications, Ann. Biomed. Eng. 39 (4) (2011) 1296–1305.
[12] M. Faria, P. Brogueira, M.N. de Pinho, Sub-micron tailoring of bi-soft segment asymmetric polyurethane membrane surfaces with enhanced hemocompatibility properties, Colloids Surf. B: Biointerfaces 86 (1) (2011) 21–27. E. Sachlos, J.T. Czernuszka, Making tissue engineering scaffolds work. Review: the application of solid freeform fabrication technology to the production of tissue engineering scaffolds, Eur. Cell. Mater. 5 (29) (2003) 39–40.
[13] B. Seifert, B. Hiebl, F. Jung, Interaction of platelets with body foreign surfaces, Ser. Biomech. 25 (2010) 140–146.
[14] G. Anupam, et al., Bio–nanomaterials: understanding key biophysics and their applications, In: Nanotechnology, Vol. 11: Biomaterials, Studum Press LLC, India, 2013.
[15] R.P. Zahedi, et al., Phosphoproteome of resting human platelets, J. Proteome Res. 7 (2) (2007) 526–534.
[16] B. Sivaraman, R.A. Latour, The relationship between platelet adhesion on surfaces and the structure versus the amount of adsorbed fibrinogen, Biomaterials 31 (5) (2010) 832–839.
[17] W.-B. Tsai, J.M. Grunkemeier, T.A. Horbett, Variations in the ability of adsorbed fibrinogen to mediate platelet adhesion to polystyrene-based materials: a multivariate statistical analysis of antibody binding to the platelet binding sites of fibrinogen, J. Biomed. Mater. Res. A 67 (4) (2003) 1255–1268.
[18] S.M. Slack, J.L. Bohnert, T.A. Horbett, The effects of surface chemistry and coagulation factors on fibrinogen adsorption from plasma, Ann. N. Y. Acad. Sci. 516 (1) (1987) 223–243.
[19] L. Vroman, et al., Interaction of high molecular weight kininogen, factor XII, and fibrinogen in plasma at interfaces, Blood 55 (1) (1980) 156–159.
[20] T.J. Marder, Consumptive thrombohemorrhagic disorders, in: Hemostasis and Thrombosis: Basic Principles and Clinical Practice, Lippincott Williams & Wilkins, Philadelphia, PA, 1994.
[21] J.J. Sixma, P.G. Groot, Regulation of platelet adhesion to the vessel wall, Ann. N. Y. Acad. Sci. 714 (1) (1994) 190–199.
[22] L. Tang, P. Thevenot, H. Wenjing, Surface chemistry influences implant biocompatibility, Curr. Top. Med. Chem. 8 (4) (2008) 270–280.
[23] Y. Zhao, et al., Interaction of mesoporous silica nanoparticles with human red blood cell membranes: size and surface effects, ACS Nano 5 (2) (2011) 1366–1375.

[24] E. Chambers, S. Mitragotri, Prolonged circulation of large polymeric nanoparticles by non-covalent adsorption on erythrocytes, J. Control. Release 100 (1) (2004) 111–119.
[25] H.L. Reid, et al., A simple method for measuring erythrocyte deformability, J. Clin. Pathol. 29 (9) (1976) 855.
[26] Y.-S. Lin, C.L. Haynes, Impacts of mesoporous silica nanoparticle size, pore ordering, and pore integrity on hemolytic activity, J. Am. Chem. Soc. 132 (13) (2010) 4834–4842.
[27] I.I. Slowing, et al., Mesoporous silica nanoparticles for reducing hemolytic activity towards mammalian red blood cells, Small 5 (1) (2009) 57–62.
[28] C. Steinem, Cell Membrane. The Red Blood Cell as A Model. By Yoshihito Yawata, Wiley-VCH, Weinheim, Germany, 2003, pp. 5541–5542.
[29] Y. Roiter, et al., Interaction of nanoparticles with lipid membrane, Nano Lett. 8 (3) (2008) 941–944.
[30] R. Lipowsky, H.-G. Döbereiner, Vesicles in contact with nanoparticles and colloids, Europhys. Lett. 43 (2) (1998) 219.
[31] M. Deserno, W.M. Gelbart, Adhesion and wrapping in colloid – vesicle complexes, J. Phys. Chem. B 106 (21) (2002) 5543–5552.
[32] C.C. Fleck, R.R. Netz, Electrostatic colloid-membrane binding, Europhys. Lett. 67 (2) (2004) 314.
[33] B.J. Reynwar, et al., Aggregation and vesiculation of membrane proteins by curvature-mediated interactions, Nature 447 (7143) (2007) 461–464.
[34] V.M. Merkle, et al., Hemocompatibility of poly (vinyl alcohol)–gelatin core–shell electrospun nanofibers: a scaffold for modulating platelet deposition and activation, ACS Appl. Mater. Interfaces 7 (15) (2015) 8302–8312.
[35] M. Nobili, et al., Platelet activation due to hemodynamic shear stresses: damage accumulation model and comparison to in vitro measurements, ASAIO J. 54 (1) (2008) 64.
[36] J. Sheriff, et al., High-shear stress sensitizes platelets to subsequent low-shear conditions, Ann. Biomed. Eng. 38 (4) (2010) 1442–1450.
[37] V. Merkle, et al., Gelatin shells strengthen polyvinyl alcohol core–shell nanofibers, Polymer 54 (21) (2013) 6003–6007.
[38] D.J. Angiolillo, M. Ueno, S. Goto, Basic principles of platelet biology and clinical implications, Circ. J. 74 (4) (2010) 597–607.
[39] L.K. Jennings, Mechanisms of platelet activation: need for new strategies to protect against platelet-mediated atherothrombosis, Thromb. Haemost. 102 (2) (2009) 248–257.
[40] V.M. Merkle, et al., Core-shell nanofibers: integrating the bioactivity of gelatin and the mechanical property of polyvinyl alcohol, Biopolymers 101 (4) (2014) 336–346.
[41] K.L. Gregg, A Mathematical Model of Blood Coagulation and Platelet Deposition Under Flow (Ph.D. Thesis), The University of Utah, 2010.
[42] U. Landmesser, H. Burkhard, H. Drexler, Vascular effects of statins, Circulation 109 (2004) II-27.
[43] J. Loscalzo, Nitric oxide insufficiency, platelet activation, and arterial thrombosis, Circ. Res. 88 (8) (2001) 756–762.
[44] J.J. Zwaginga, et al., Thrombogenicity of vascular cells. Comparison between endothelial cells isolated from different sources and smooth muscle cells and fibroblasts, Arterioscler. Thromb. Vasc. Biol. 10 (3) (1990) 437–448.
[45] H. Samady, et al., Coronary artery wall shear stress is associated with progression and transformation of atherosclerotic plaque and arterial remodeling in patients with coronary artery disease, Circulation 124 (2011) 779–788.
[46] L. Badimon, et al., Influence of arterial damage and wall shear rate on platelet deposition. Ex vivo study in a swine model, Arterioscler. Thromb. Vasc. Biol. 6 (3) (1986) 312–320.

[47] Y. Ikada, et al., Blood compatibility of hydrophilic polymers, J. Biomed. Mater. Res. A 15 (5) (1981) 697–718.
[48] R. Simon-Walker, et al., Glycocalyx-inspired nitric oxide-releasing surfaces reduce platelet adhesion and activation on titanium, ACS Biomater. Sci. Eng. 3 (1) (2016) 68–77.
[49] B.Z.S. Paul, J.L. Daniel, S.P. Kunapuli, Platelet shape change is mediated by both calcium-dependent and-independent signaling pathways role of p160 Rho-associated coiled-coil-containing protein kinase in platelet shape change, J. Biol. Chem. 274 (40) (1999) 28293–28300.
[50] S.L. Goodman, et al., Platelet shape change and cytoskeletal reorganization on polyurethaneureas, J. Biomed. Mater. Res. A 23 (1) (1989) 105–123.
[51] T.-M. Ko, S.L. Cooper, Surface properties and platelet adhesion characteristics of acrylic acid and allylamine plasma-treated polyethylene, J. Appl. Polym. Sci. 47 (9) (1993) 1601–1619.
[52] J. Deng, et al., Heparin-mimicking multilayer coating on polymeric membrane via LbL assembly of cyclodextrin-based supramolecules, ACS Appl. Mater. Interfaces 6 (23) (2014) 21603–21614.
[53] M.B. Gorbet, M.V. Sefton, Biomaterial-associated thrombosis: roles of coagulation factors, complement, platelets and leukocytes, Biomaterials 25 (26) (2004) 5681–5703.
[54] J.M. Anderson, Biological responses to materials, Annu. Rev. Mater. Res. 31 (1) (2001) 81–110.
[55] J.B. Theeten, D.E. Aspnes, Ellipsometry in thin film analysis, Annu. Rev. Mater. Sci. 11 (1) (1981) 97–122.
[56] H. Elwing, Protein absorption and ellipsometry in biomaterial research, Biomaterials 19 (4–5) (1998) 397–406.
[57] C.-G. Gölander, E. Kiss, Protein adsorption on functionalized and ESCA-characterized polymer films studied by ellipsometry, J. Colloid Interface Sci. 121 (1) (1988) 240–253.
[58] M.F. Mora, et al., Investigating protein adsorption via spectroscopic ellipsometry, in: Biological Interactions on Materials Surfaces, Springer, New York, 2009, pp. 19–41.
[59] L.D. Unsworth, H. Sheardown, J.L. Brash, Polyethylene oxide surfaces of variable chain density by chemisorption of PEO-thiol on gold: adsorption of proteins from plasma studied by radiolabelling and immunoblotting, Biomaterials 26 (30) (2005) 5927–5933.
[60] U. Nilsson, B. Nilsson, Analogous antigenic alterations elicited in C3 by physiologic binding and by denaturation in the presence of sodium dodecyl sulfate, J. Immunol. 129 (1982) 2594–2597.
[61] J.M. Brockman, B.P. Nelson, R.M. Corn, Surface plasmon resonance imaging measurements of ultrathin organic films, Annu. Rev. Phys. Chem. 51 (1) (2000) 41–63.
[62] G. Anand, F. Zhang, R.J. Linhardt, G. Belfort, Protein-associated water and secondary structure effect removal of blood proteins from metallic substrates, Langmuir 27 (2010) 1830–1836.
[63] K.A. Marx, Quartz crystal microbalance: a useful tool for studying thin polymer films and complex biomolecular systems at the solution-surface interface, Biomacromolecules 4 (2003) 1099–1120.
[64] M. Rodahl, et al., Quartz crystal microbalance setup for frequency and Q-factor measurements in gaseous and liquid environments, Rev. Sci. Instrum. 66 (7) (1995) 3924–3930.
[65] I. Reviakine, D. Johannsmann, R.P. Richter, Hearing what you cannot see and visualizing what you hear: interpreting quartz crystal microbalance data from solvated interfaces, Anal. Chem. 83 (2011) 8838–8848.

[66] H.P. Felgueiras, S.D. Sommerfeld, N.S. Murthy, J. Kohn, V. Migonney, Poly (NaSS) functionalization modulates the conformation of fibronectin and collagen type I to enhance osteoblastic cell attachment onto Ti6Al4V, Langmuir 30 (2014) 9477–9483.
[67] M.V. Voinova, M. Rodahl, M. Jonson, B. Kasemo, Viscoelastic acoustic response of layered polymer films at fluid-solid interfaces: continuum mechanics approach, Phys. Scr. 59 (1999) 391.
[68] N.B. Eisele, et al., Viscoelasticity of thin biomolecular films: a case study on nucleoporin phenylalanine-glycine repeats grafted to a histidine-tag capturing QCM-D sensor, Biomacromolecules 13 (8) (2012) 2322–2332.
[69] M. Birkholz, Thin Film Analysis by X-Ray Scattering, John Wiley & Sons, Weinheim, Germany, 2006.
[70] S. Kubowicz, et al., Gold nanoparticles at the liquid – liquid interface: X-ray study and monte Carlo simulation, Langmuir 25 (2) (2008) 952–958.
[71] W. Wang, et al., Structure of biodegradable films at aqueous surfaces: X-ray diffraction and spectroscopy studies of polylactides and tyrosine-derived polycarbonates, Langmuir 29 (36) (2013) 11420–11430.
[72] S.V. Dorozhkin, Calcium orthophosphate coatings, films and layers, Prog. Biomater. 1 (2012) 1–40.
[73] A.L. Paschoal, et al., Metallic biomaterials TiN-coated: corrosion analysis and biocompatibility, Artif. Organs 27 (5) (2003) 461–464.
[74] F. Izumi, in: R.A. Young (Ed.), Rietveld Method, Oxford University Press, Oxford, UK, 1993.
[75] R. Williams (Ed.), Surface Modification of Biomaterials: Methods Analysis and Applications, Elsevier, Cambridge, UK, 2010.
[76] J.E. Devries, Surface characterization methods—XPS, TOF-SIMS, and SAM a complimentary ensemble of tools, J. Mater. Eng. Perform. 7 (3) (1998) 303–311.
[77] B.D. Ratner, D.G. Castner, Electron spectroscopy for chemical analysis, Surface Analysis: The Principal Techniques, second ed., 200947–112.
[78] V.B. Damodaran, et al., Conformational studies of covalently grafted poly (ethylene glycol) on modified solid matrices using X-ray photoelectron spectroscopy, Langmuir 26 (10) (2010) 7299–7306.
[79] U. Oran, et al., Surface analysis of plasma deposited polymer films, 7, Plasma Process. Polym. 3 (3) (2006) 288–298.
[80] P.-L. Girard-Lauriault, et al., Chemical characterisation of nitrogen-rich plasma-polymer films deposited in dielectric barrier discharges at atmospheric pressure, Plasma Process. Polym. 5 (7) (2008) 631–644.
[81] C.D. Batich, Chemical derivatization and surface analysis, Appl. Surf. Sci. 32 (1–2) (1988) 57–73.
[82] A.J. Hartmann, R.N. Lamb, X-ray photoemission spectroscopy of thin films, Curr. Opinion Solid State Mater. Sci. 2 (5) (1997) 511–516.
[83] D.Y. Petrovykh, et al., Quantitative characterization of DNA films by X-ray photoelectron spectroscopy, Langmuir 20 (2) (2004) 429–440.
[84] P.J. Cumpson, M.P. Seah, Elastic scattering corrections in AES and XPS. II. Estimating attenuation lengths and conditions required for their valid use in overlayer/substrate experiments, Surf. Interface Anal. 25 (6) (1997) 430–446.
[85] S. Bhaskar, D. Allgeyer, J.A. Smythe III, Depth profiling of dielectric Sr Ti O 3 thin films by angle-resolved x-ray photoelectron spectroscopy, Appl. Phys. Lett. 89 (25) (2006) 254103.
[86] K.J. Kim, K.T. Park, J.W. Lee, Thickness measurement of SiO 2 films thinner than 1 nm by X-ray photoelectron spectroscopy, Thin Solid Films 500 (1) (2006) 356–359.

[87] R.L. Opila, J.E. Jr, Thin films and interfaces in microelectronics: composition and chemistry as function of depth, Prog. Surf. Sci. 69 (4) (2002) 125–163.
[88] S. Oswald, et al., Angle-resolved XPS: a critical evaluation for various applications, Surf. Interface Anal. 38 (4) (2006) 590–594.
[89] R. Champaneria, et al., Non-destructive analysis of ultrathin dielectric films, Surf. Interface Anal. 35 (13) (2003) 1028–1033.
[90] A. Benninghoven, Chemical analysis of inorganic and organic surfaces and thin films by static time-of-flight secondary ion mass spectrometry (TOF-SIMS), Angew. Chem. Int. Ed. 33 (10) (1994) 1023–1043.
[91] D. Leonard, et al., Part 1. N-(m-(3-(trifluoromethyl) diazirine-3-yl) phenyl)-4-maleimido-butyramide (MAD) on silicon, silicon nitride and diamond, Surf. Interface Anal. 26 (11) (1998) 783–792.
[92] K. Idla, et al., XPS and SIMS study: adhesion of polypyrrole film on titanium, Surf. Interface Anal. 30 (1) (2000) 557–560.
[93] J. Brison, et al., ToF-SIMS imaging and depth profiling of HeLa cells treated with bromodeoxyuridine, Surf. Interface Anal. 43 (1–2) (2011) 354–357.
[94] J. Brison, S. Muramoto, D.G. Castner, ToF-SIMS depth profiling of organic films: a comparison between single-beam and dual-beam analysis, J. Phys. Chem. C 114 (12) (2010) 5565–5573.
[95] W. Schnabel, Polymers and Electromagnetic Radiation: Fundamentals and Practical Applications, John Wiley & Sons, Weinheim, Germany, 2014.
[96] M. Richard, G. Mao, C.R. Flach, Infrared reflection–absorption spectroscopy: principles and applications to lipid–protein interaction in Langmuir films, Biochim. Biophys. Acta 1798 (4) (2010) 788–800.
[97] M.A. Ramin, et al., PM-IRRAS investigation of self-assembled monolayers grafted onto SiO2/Au substrates, Langmuir 27 (10) (2011) 6076–6084.
[98] F. Meiners, et al., Local control of protein binding and cell adhesion by patterned organic thin films, Anal. Bioanal. Chem. 405 (11) (2013) 3673–3691.
[99] E.E. Bedford, et al., Effect of SAM chain length and binding functions on protein adsorption: β-lactoglobulin and apo-transferrin on gold, Colloids Surf. B: Biointerfaces 116 (2014) 489–496.
[100] M. Moskovits, Surface-enhanced Raman spectroscopy: a brief retrospective, J. Raman Spectrosc. 36 (6–7) (2005) 485–496.
[101] K. Kneipp, et al., Surface-enhanced Raman scattering and biophysics, J. Phys. Condens. Matter 14 (18) (2002) R597.
[102] J.-Y. Choi, K. Kim, K.S. Shin, Surface-enhanced Raman scattering inducible by recyclable Ag-coated magnetic particles, Vib. Spectrosc. 53 (1) (2010) 117–120.
[103] E. Hariprasad, T.P. Radhakrishnan, In situ fabricated polymer–silver nanocomposite thin film as an inexpensive and efficient substrate for surface-enhanced raman scattering, Langmuir 29 (42) (2013) 13050–13057.

Further reading

[1] U.T. Seyfert, F. Jung, Criteria and principles of in vitro hemocompatibility testing according to the ISO 10993 (4), Transfus. Med. Hemother. 27 (6) (2000) 317–322.
[2] S. Nie, et al., Biologically inspired membrane design with a heparin-like interface: prolonged blood coagulation, inhibited complement activation, and bio-artificial liver related cell proliferation, Biomater. Sci. 2 (1) (2014) 98–109.

This page intentionally left blank

Coatings for biomaterials to improve hemocompatibility

7

M. Fischer, M.F. Maitz, C. Werner
Leibniz Institute of Polymer Research Dresden, Dresden, Germany

Abbreviations

ADP	adenosin diphosphate
AT	antithrombin
ATH	antithrombin-heparin complex
cAMP	cycylic adenosin monophosphate
CBAS	Carmeda bioactive surface
DLC	diamond-like carbon
EC	endothelial cell
EPC	endothelial progenitor cell
ePTFE	expanded polytetrafluoroethylene
GPIIb/IIIa	glycoprotein IIb/IIIa
PDMS	polydimethylsiloxane
PE	polyethylene
PEG	polyethylene glycol
PEO	polyethylene oxide
PET	polyethylene terephthalate
PGE2	prostaglandin E2
pHEMA	poly (2-hydroxyethyl methacrylate)
PLL-PEG	poly-lysine polyethylene glycol
PP	polypropylene
PPACK	D-Phe-Pro-Arg-chloromethylketone
PS	polystyrene
PTFE	polytetrafluoroethylene
PU	polyurethane
PVC	polyvinyl chloride
ROS	radical oxygen species
SMC	smooth muscle cell
t-PA	tissue-type plasminogen activator
TXA2	thromboxane A2
u-PA	urokinase

7.1 Introduction

Undesired interactions at the blood-material interface are still a critical issue of blood-contacting devices such as vascular stents, catheters, artificial heart valves, and biosensors. The medical device and implant technology evolved over the second

Hemocompatibility of Biomaterials for Clinical Applications. https://doi.org/10.1016/B978-0-08-100497-5.00007-0
© 2018 Elsevier Ltd. All rights reserved.

Table 7.1 Clinically applied materials for cardiovascular interventions

Material category	Material	Medical device
Metals and alloys	Stainless steel	Stents
	CoCrMo alloys	Carotid stents
	NiTi alloy	Artificial heart valves
	Ti alloys	
Ceramics	SiC, DLC	Artificial heart valves
	TiOx, TiN, TiNOx	Artificial heart valves, stents
Polymers	PTFE, PET	Vascular grafts, catheters
	PU	Vascular grafts, artificial heart valves
	PE, PVC	Catheters
	Polysiloxane, PP	Oxgenator membrane

half of the 20th century bringing along rapid advances in cardiovascular technology. However, none of the cardiovascular materials in clinical use (see Table 7.1) can fulfill all the requirements of blood compatibility.

Despite large efforts in developing low-activating device coatings, the humoral host responses and subsequent cellular adhesion lead to incompatibility reactions and often limit the device performance [1], as summarized in Fig. 7.1. Most medical products

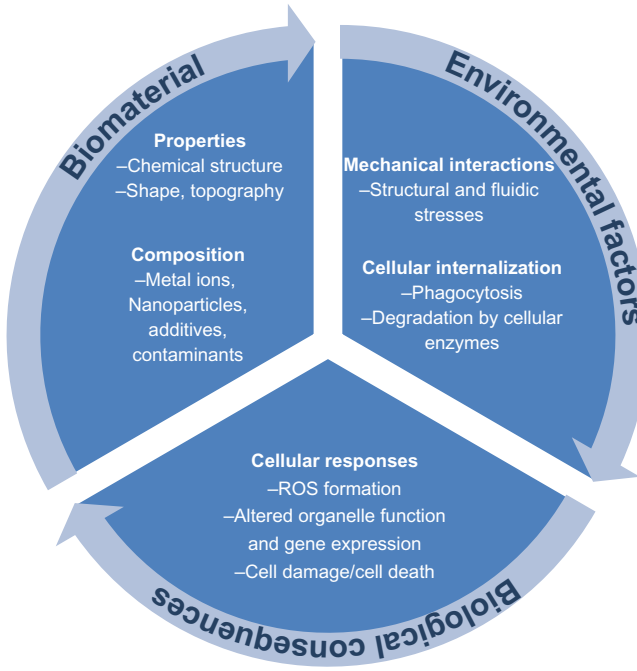


Fig. 7.1 Interplay of factors that influence biocompatibility.

possess acceptable but suboptimal hemocompatibility entailing the need for continuous anticoagulation of the patient, causing a labile balance between bleeding and thrombosis. Material-related blood activation processes result from the material itself or from bioactive substances incorporated to, e.g., achieve antiseptic protection [2]. The appropriate design of nonthrombogenic materials is of great concern and combines advantageous effects of reduced blood activation and low biofilm formation through minor fibrin deposition.

To overcome unfavorable material-related biological responses, surface modification strategies enable the combination of material's bulk properties with desired biological attributes and this dominates the content of numerous related publications [1,3,4]. Surface-initiated incompatibility reactions can be reduced by selection of surfaces with low activation potential or by active pharmacologic targeting of the biological response reactions and by the combination thereof. During the recent 20 years, different strategies have been developed that can be divided into four main categories: (1) bioinert or biopassive also in combination with adjusted microstructure and topography, (2) endothelial cells (ECs) as biological surface coatings, (3) bioactive (immobilization and release of bioactives), and (4) biomimetic modification techniques.

7.2 Main

7.2.1 Physicochemical properties

The design of hemocompatible coatings depends on consolidated knowledge of material-blood interactions. For this, a simplified summary of general factors that influence hemocompatibility reactions facilitates the choice of appropriate materials. Notwithstanding the extensive interactions within the complex system of whole blood, general factors of hemocompatibility were defined like surface energy, charge, and topography.

7.2.1.1 Wettability

Hydrophilicity is mostly associated with low surface interactions with blood components. On the other hand, hydrophobic surfaces were found to adsorb more proteins upon surface blood plasma exposure with increased degree of protein's conformational change [5]. This in turn may alter function and activity of the proteins, additionally it can promote cell adhesion and inflammatory reactions. Protein adsorption to hydrophobic surfaces was described as protein expellence from aqueous solution to increase hydrogen bonding among water molecules. This occurs at the expense of less-favorable interactions between H_2O and proteins [6].

Studies applying self-assembled monolayers of graded hydrophilicity revealed significantly increased fibrinogen adsorption at the hydrophobic 100% $-CH_3$ surface compared to hydrophilic 100% −COOH, with the same tendency for platelet adhesion [7]. However, exceptions were reported for strongly hydrophobic surfaces with contact angles above 120 degrees that possess high blood compatibility as seen for ePTFE [8–11] and ultrahydrophobic gas membranes for heart-lung machines [12].

7.2.1.2 Specific surface functional groups

Negatively charged surfaces revealed reduced conversion of adsorbed fibrinogen to fibrin, but the coagulation activation through the contact system was elevated [5]. The latter activation pathway is triggered by factor XII auto-activation upon contact with a surface. On positively charged surfaces, increased platelet activation and an influence of coagulation factor FVIII were reported [13]. More recent data elucidate the influence of FVII in procoagulant processes on positively charged surfaces [14]. Hydroxyl groups were found to activate the alternative pathway of the complement system, being also correlated to increased leukocyte adhesion that is mediated by C3b adsorption to the hydroxylated surfaces [15]. Complement activation on surfaces that display amino groups is controversially discussed [16].

7.2.1.3 Roughness/topography

Surface patterning in micro- and nanoscale influences protein adsorption [17] and cell behavior such as adhesion of bacteria [18,19], platelets [20,21], leukocytes [22,23], and ECs [24,25] to a higher degree than most chemical surface modifications. Surface topography impacts the amount, conformation, and spatial distribution of adherent proteins. It remains difficult to scrutinize general trends in protein adsorption to patterned surfaces. However, several studies emphasize on the importance of specific structural dimensions with low protein adsorption to nanoscaled surfaces while increased adsorption was found on micrometer-sized substrates [17,26]. Nanoscaled roughness impacts protein adsorption due to similar dimensions of proteins and substrate structure. In submicrometer range, the achieved increase in surface area plays a more relevant role in material-related adsorption of proteins and cell adhesion. Similar correlations of pattern dimensions and platelet adhesion were recently observed in a study applying carbonanotubes of varying topographic properties ranging from 120 nm to 1400 nm interspacing. Decreased cell adhesion was reported for surfaces with an aspect ratio of pillar height to width of >3:1 and lower interspacing (<200 µm). By this, the surface area given by the pillar tips for platelet adhesion is reduced [26].

The influence of flow conditions on protein adsorption is rarely considered and might give a distinct picture on interfacial phenomena. In a recent study using buffered albumin solution, nanostructured surfaces of different dimensions were incubated under flow revealing nearly complete protein desorption from hydrophobic nanoscaled surfaces with 10 nm pore sizes compared to controls of static incubation [17].

7.2.1.4 Other factors (air bubbles)

The interfaces between water and air are known for its high interface energy that results in strong conformational changes of proteins. The presence of air bubbles in blood incubation systems may lead to complement activation [27–29]. On the other hand, a decreased protein adsorption to nanostructured hydrophobic ePTFE surfaces was shown to occur through interstitially trapped air that prevents protein-surface interactions [8].

7.2.2 Inorganic passive coatings

Inorganic coatings include inorganic carbon-based materials and bioinert metal-oxide and metal-nitride films.

7.2.2.1 Carbon-based inorganic coatings

It dates back to 1960 when low-temperature isotropic pyrolytic carbon (LTIC) coatings were used for mechanical heart valves but these coatings were soon replaced by diamond-like carbon (DLC) films with improved thromboresistance that is related to specific sp^2/sp^3 ratios. DLC layers show high smoothness with low friction coefficients, high hardness and are chemically inert. DLCs are applied on artificial heart valves and vascular stents [30]. However, stability problems through carbide formation in the presence of iron were observed and preferential platelet adhesion triggered by the material's hydrophobicity. The hemocompatibility of DLCs can be tuned by incorporation of different elements (Si, F, P, N) and combinations thereof. Alternatively, the use of boron-carbon-nitrogen coatings [31] or tetrahedral amorphous carbon (ta-C) [32] was described with improved hemocompatibility, which was attributed to a reduced electron transfer from plasmatic fibrinogen to ta-C in the latter case. The prevention of fibrinogen oxidation by the surface also prevents the formation of fibrin monomers on LTIC.

7.2.2.2 Metal-oxides, metal-nitrides

Titanium oxide and titanium nitride are intensively studied inorganic coatings applied to improve the hemocompatibility of metallic devices [33,34]. Chemical inertness, corrosion resistance, and biocompatibility are partly attributed to surface oxide layers [35]. Surface energy and semiconductor properties affect the material's hemocompatibility that was found to depend on the thickness of the titanium oxide films with advantages seen for thicker oxide films compared to the naturally grown counterparts [36,37]. The *n*-type semiconductor properties of titanium reportedly resulted in beneficial effect on hemocompatibility with low platelet adhesion and activation [36,38–40].

Applications of titanium are restricted to dental and orthopedic surgery, the use of Ti-O and Ti-N coatings and Ti-based ultrathin films however, opens wider opportunities for use in artificial heart valves and stents [41]. Photocatalytic effects of TiO_2 were discussed to improve the material's hemocompatibility [42].

7.2.3 Organic passive coatings

This group includes polymer-modified substrates that act passively, meaning to induce minimal interactions with coagulation and other cascade reactions.

Surface passivation intends to minimize protein-surface interactions, since cells interact with preadsorbed proteins and not with the bare surface. Material-induced cellular responses depend on the protein quantity in the adsorbed monolayer and the configuration of the protein layer including package density and adsorption orientation.

Strategies to minimize interfacial activation processes either include the preparation of protein-resistant surfaces or surfaces that specifically dictate the adsorption of passivating proteins (albumin). Protein resistant surfaces are defined by the adsorption of only a few ng/cm^2 [43]. Ostuni et al. proposed hydrophilicity, incorporated hydrogen bond acceptors and electrical neutrality as basic criteria for protein resistance [44]. In general there are lower adsorption quantities associated with smaller proteins and side-on orientations. Simplifications of the complex protein adsorption phenomena are often required to understand fundamental concepts. The risk of oversimplification, however remains leaving difficulties to discern fundamental principles to explain or predict protein resistance. Despite extensive research in that field, basic questions on proteins in the adsorbed state concerning its structural details, activation levels, and the effect of crowding by other proteins are still difficult to answer.

7.2.3.1 Hydrophilic coatings/polymer brushes

Brush-forming polymers applied for coatings encompass polyethylene glycol (PEG) [45], poly (ethylene) oxide (PEO) [46], and polyhydroxyethyl methacrylate (HEMA) [47]. Immobilization of brush-forming polymers is achieved by covalent bonding or through integration as block segments. By this, surface hydrophilicity can be increased. Protein resistance depends on the graft molecular weight and density with lowest protein adsorption for graft molecular weights of a few thousand and for brush-like structures. Brush polymer coatings find applications in cell microencapsulation [48], coating for stents and dialysis membranes [49], and as drug release systems [50].

Surface conjugation with uncharged PEG molecules provides broad solubility in both aqueous and nonaqueous media. PEG molecules can be grafted to substrates like metals, glass, and polymers through physical adsorption, self-assembly, chemical coupling, or graft polymerization. The high density of grafted molecules enables high steric hindrance and an increased hydration capacity. This in combination with the high PEG chain length equips the surface with protein repellent properties [45,51].

PEG spacers are frequently used for immobilization of bioactives, as they provide sufficient flexibility for the molecule to enter a binding pocket and they shield the bioactive molecule from properties of the substrate. PEG-derived reactive hydroxyl end groups facilitate grafting or covalent attachment to substrates, either directly or via intermediate layers [52]. PEG molecules act as spacers to provide a protective distance between the underlying substrate and the biological surroundings. Surface PEGylation using polycationic poly(llysine)-PEG revealed good hemocompatibility through protein resistance against small biomolecules, fibrinogen, and blood cells [45]. Hansson et al. observed decreased protein adsorption to surfaces modified with PEG that resulted in prolonged coagulation time and reduced platelet activation compared to the bare titanium oxide substrate. However, the clinical use of PEG-modified materials remains limited, because protein resistance in vivo is not as good as expected from in vitro observations [53], and the OH termini activate the complement system. The decomposition of PEG in the presence of oxygen or transition metal ions further restricts its application spectrum [54].

Alternatively to PEG, also PEO was used to coat surfaces with its nonfouling properties relying on hydration via hydrogen bonding. Its good solubility in water,

its favorable chain conformation, and high chain mobility in aqueous media rank among the main benefits that enable low protein adsorption and cellular adhesion. Taking advantage of the simple chemical structure, PEO can be immobilized to surfaces via quantitative end-group coupling [55]. However, protein resistance observed for fibrinogen solution was not found in plasma and blood. Metal-ion catalyzed oxidation of chain-derived oxygen atoms was observed to result in polymer decomposition [56].

7.2.3.2 Zwitterionic materials

Materials of this category contain both positive and negative charged groups while the overall net charge remains neutral. Through ionic solvation zwitterionic materials are strongly hydrated that enables nonspecific protein resistance which can be modulated by changing the type of charged groups and the distance in between. Phosphorylcholine based coatings are used to mimic biomembranes. The compatibility of phosphorylcholine coatings is achieved through minimal disturbance of water molecules that remain highly mobile within the polymer layer, capable of flexible exchange with bulk water. Phosphorylcholine methacrylate (MPC) coatings on a siloxane bonding layer on glass or silicone have been shown to exhibit strong protein resistance [57]. MPCs are clinically applied as nonthrombogenic surfaces for cardiovascular devices in dialysis, heart pumps, and ventricular assist devices [58]. Intermediate layers of MPCs further serve covalent immobilization of bioactives (growth factors, antibiotics, and other drugs) [59].

Further modification strategies to produce antifouling surfaces include functionalization with carboxybetaines and sulfobetaines. This class of compounds possesses a high hydration capacity and electroneutrality with a high level of protein resistance. By providing multiple functional groups, betaine surfaces serve as a platform for versatile immobilization of biomolecules. Reduced thrombosis and infection was recently reported for poly-sulfobetaine coatings on polyurethane catheters tested in canine models [60]. The low stability observed for betain surfaces however, restricts its use to short-term applications.

7.2.3.3 Passivating proteins

All above described physical and chemical surface treatments produce hemocompatible coatings based on substances foreign to the host. To reduce the risk of foreign body responses, autologous proteins or small molecules are used to generate bioinert surfaces. Surface coating with albumin as a passivation strategy was intensively studied since 1986 and revealed decreased platelet reactivity [61–63]. Albumin readily adsorbs to hydrophobic surfaces and lacks peptide sequences for the interaction with platelets, leukocytes, and enzymes of the coagulation cascades [64]. However, immobilized albumin in biological environments is likely to undergo denaturation and displacement by other proteins [65]. To avoid albumin denaturation, surfaces were reversibly immobilized with albumin by incorporation of sulfonic acid [66] or C18 alkyl chains [67]. In the latter case, pHEMA hydrogel films were modified with aliphatic C18 chains making use of the function of albumin as carrier for fatty acids, and affinity

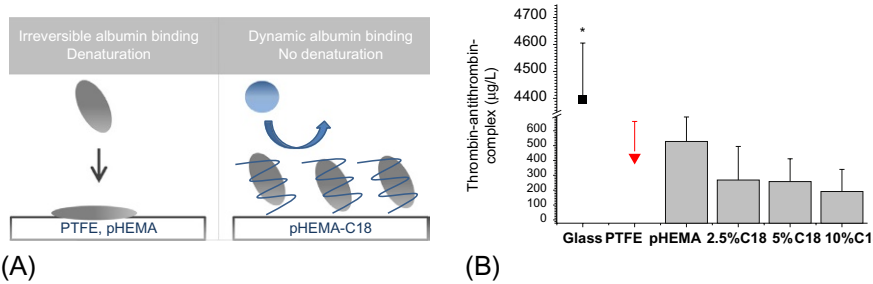


Fig. 7.2 (A) Schematic mode of action of pHEMA hydrogels modified with C18 alkyl chains for reversible albumin binding. (B) Thrombin-antithrombin-complex levels in plasma after surface incubation with whole blood for 2 h at 37°C [67].

for alkyl chains. C18 alkyl chain grafted surfaces adsorbed albumin in a reversible way at physiological conformation that enabled combination of advantageous low platelet activation with a reduced complement activation, leukocyte adhesion, and coagulation activation (Fig. 7.2).

7.2.4 Bioactive coatings

To prevent undesired material-related blood responses, bioactive coatings are designed to regulate blood coagulation enzymes. This group of coatings includes proteins, peptides, siRNA, and drugs of natural or synthetic nature that are introduced into the surfaces of biomaterials. Selected components are listed in Table 7.2. Bioactive surface modifications are used to equip the surfaces with specific loading and release capacities whilst preserving the material's bulk properties. Incorporated bioactives modulate hemocompatibility, inflammation, endothelialization, and smooth muscle cell (SMC) proliferation.

7.2.4.1 Anticoagulants

Indirect thrombin inhibitors: Heparin

The glycosaminoglycan heparin is an indirect thrombin inhibitor catalyzing the activity of the serpin AT.

Heparin coatings are successfully applied active surface modifications on vascular grafts [96,97], stents [98–102], heart valves [103], extracorporeal circulation systems [104], and dialysis membranes [105]. Heparinization of biomaterials dates back to 1963 [106] and its commercial use is summarized in Table 7.3 with end-point immobilized heparin (CBAS, Carmeda bioactive surface) having a long history in clinical use.

Physical adsorption of heparin to the surface or covalent linkage rank among possible immobilization strategies of heparin and determine the anticoagulant activity of the immobilized molecule [107]. Regarding the low stability of physical immobilization where heparin is easily displaced by ion exchange, numerous examples of covalent heparin grafting appeared since 1974 [68]. However, covalently bound heparin may be inactivated by structural changes due to immobilization reactions [108]. Diverse strategies to preserve the biological activity of heparin were successfully implemented.

Table 7.2 Selected bioactive component used for surface modification of hemocompatible devices

Bioactive component	Properties and action	References
Coagulation inhibitors		
Heparin	Negatively charged sulfated polysaccharide Catalyzes the inhibitory activity of antithrombin III against thrombin and FXa	[68,69]
Hirudin	Polypeptide from *Hirudo medicinalis* Direct thrombin inhibitor	[70,71]
Argatroban	Direct thrombin inhibitor	[72]
Benzamidine	Direct inhibitor of thrombin and other coagulation factors	[73,74]
Thrombomodulin	Membrane protein of endothelial cells Changes substrate specificity of thrombin for activation of anticoagulant protein C	[75,76]
Platelet inhibitors		
Dipyridamole	Vasodilator Platelet inhibitor that blocks ADP receptor	[77,78]
Prostacyclin	Platelet aggregation inhibitor with specific receptor	[79]
Apyrase	Decreases platelet activation and adhesion through ADP degradation	[80]
Abciximab, Tirofiban	Platelet inhibitor, GPIIb/IIIa receptor blocker	[81]
Other inhibitors		
Paclitaxel Rapamycin (Sirolimus)	Antiproliferative agents	[82,83]
Diazeniumdiolate (Nitric oxide release)	Cellular signaling molecule Inhibitor of smooth muscle cells and platelet activation	[84–89]
Plasmin/tPA	Fibrinolytic blood enzyme Binds Lys-residues exposed during fibrin degradation	[90–93]
DNA	Plasmids and viruses used as vectors Targets: antithrombotic and antiproliferative genes, genes for reendothelialization	[94,95]

End-point immobilized heparin via its aldehyde group to enable coupling to a primary amino group of the foreign surface was presented and used for stents [109] and vascular grafts. The use of hydrophilic spacers like PEG [110] and PEO [111] rendered the molecule more accessible for interactions with AT and reduced steric hindrance of the heparin molecule.

The invention of cross-linked multilayers of heparin combined with a second bioactive component like fibronectin [112–114], phosphorylcholine [115], chitosan [116,117], alginate [118], collagen [119], and dexamethasone [120] by electrostatic adsorption in layer-by-layer technique and subsequent cross-linking were described.

Table 7.3 Heparin coating techniques approved for clinical purpose

Product	Product description	Application	Year
Carmeda Bioactive surface (Gore)	Covalent attachment End-point attached heparin	Vascular graft, stents, oxygenators	1983
Duraflo II (Baxter Corp)	Heparin-surfactant complex being coated from solution	Aortocoronary bypass products	1988
BioLine coating (Jostra)	Covalent and ionically immobilized heparin to polypeptide priming layer	Cardiopulmonary bypass products	1992
AOThel (AOT)	Covalently bound LMWH-conjugate to polyamine priming layer	Oxygenation systems	1997
Corline (Corline systems AB)	Heparin-polymer conjugate immobilization to polyamine priming layer	Extra corporeal circulation, vascular grafts, catheters, stents	1997
BIBA-HEPCOAT/ Trillium (Biointeractions Ltd)	Heparin-PEO immobilization to priming layer	Cardiopulmonary bypass products	1998

Besides its anticoagulant action, heparin also has unfavorable side effects, such as hemorrhagic complications and heparin-induced thrombocytopenia [69]. This together with the low incidence of the active pentasaccharide unit per heparin molecule and the inability of heparin to inhibit enzymatically active and fibrin-bound thrombin motivated for the design of alternative heparin analogs. Further attempts thus focused on the development of heparin with increased pentasaccharide content per molecule and higher anticoagulant activity through additional inhibition of surface-bound coagulation factors [121–123]. Covalent linkage of heparin to AT resulted in prolonged lifetime of the heparin molecule. Immobilization of the covalent antithrombin-heparin complex (ATH) onto polyurethane catheters to enhance the adsorption of plasmatic AT and achieved increased anti-FXa activities compared to heparinized coatings [124]. ATH complexes were attached to gold [125], polyurethane [126], and polydimethylsiloxane (PDMS) [127] via PEO spacers and achieved improved antithrombotic activities.

Heparin-based hydrogels are widely applied as anticoagulant coatings [128], carriers for growth factors [129], and scaffolds for tissue regeneration. Hydrogels retain large amounts of water without dissolving and exhibit low interactions with proteins and cells [130]. Applied 3D meshworks combining poly(ethylene glycol) (PEG) and heparin have been developed and used in biological applications. The cross-linking of amino end-functionalized four-armed PEG with the carboxylic groups of heparin using carbodiimide chemistry enables the formation of hydrogels with low immunogenicity, low protein absorption, and low cell adhesion [131]. The degree of cross-linking between the components can be modulated with effects on gel stiffness, permeability, and swelling, whilst keeping the biomolecular composition constant.

In cell transplantation settings, these bioinert properties can be modified by binding growth factors and incorporating ligands for cell adhesion molecules and enzyme-sensitive peptide sequences to allow the cells of interest to attach, proliferate, and function [129]. Through integration of thrombin-responsive peptide linkers into the hydrogel network, feedback-controlled delivery system were produced [132]. The authors presented degradable hydrogels that underwent degradation in the presence of thrombin enabling situation-adjusted heparin release and targeted coagulation inhibition (Fig. 7.3). This recent development showed superior thromboprotective properties, even outperforming the clinical reference (CBAS; heparin grafted ePTFE surface) in repeated incubation with nonanticoagulated human whole blood (Fig. 7.3B).

Direct thrombin inhibitors

Direct thrombin inhibitors block the active site of thrombin. They can inhibit thrombin in solution and—unlike heparin—can inhibit fibrin-associated thrombin.

Hirudin and its derivatives

Hirudin is the anticoagulant component of the saliva of medicinal leech and inhibits thrombin by formation of irreversible complexes through binding of its active site. Hirudin was covalently immobilized to various substrates, amongst them polyester [70,133], polyurethane [134,135], polyethylene [136], PTFE [137], and nitinol [138], partly through the use of intermediate coupling layers. Despite promising results in hemocompatibility parameters, the use is limited though saturation effects due to its irreversible binding behavior.

Alternative hirudin analogs include bivalirudin and boophilin being direct thrombin inhibitors with the advantage to inhibit thrombin reversibly enabling substrate regeneration. Boopholin and Bivalirudin are synthetic peptides with the latter one being in clinical use. Immobilization of bivalirudin and boophilin was tried onto 316L stainless steel [139] and gold [140], respectively. However, no clinically applied hirudin-based cardiovascular devices are reported by now.

Small synthetic inhibitors

Besides the above described natural inhibitors of blood coagulation factors, also synthetic inhibitors of trypsin-like serine proteases were immobilized to polymeric materials to address coagulation enzymes. Benzamidine-derivatives as amidine-based active site inhibitors of thrombin were used to generate anticoagulant coatings [73]. Whole blood incubation of immobilized amidine-based inhibitors grafted to maleic anhydride copolymer films achieved thrombin inhibition and enhanced short-term blood compatibility. Further attempts include immobilization of arginine derivatives, like PPACK to PEGylated polymer thin films [141–143].

Thrombomodulin

Thrombomodulin is a glycoprotein of the EC surface that promotes protein C activation and inactivates cofactors FVa and FVIIIa. Thrombomodulin received approval for clinical application however, is impeded through rapid degradation in vivo, loss of

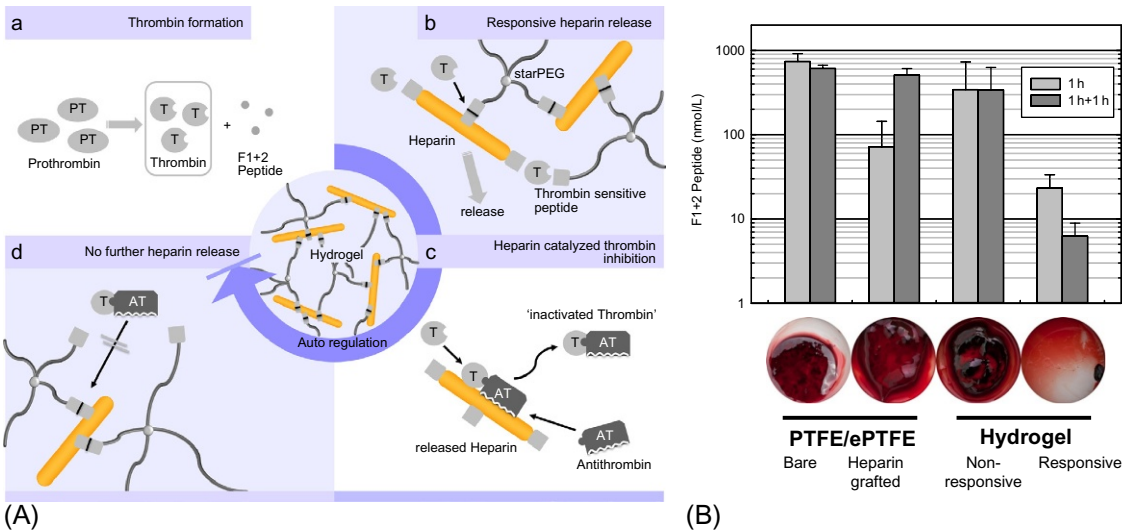


Fig. 7.3 (A) Thrombin responsive hydrogel system for feed-back-controlled heparin release [132]. (B) Plasmatic levels of coagulation marker F1 + 2 measured upon surface whole blood incubation after 1 h and after subsequent exchange with fresh whole blood (1 + 1 h) using nonanticoagulated human whole blood.

activity during sterilization and storage, and due to high costs. Despite efforts in covalent surface immobilization of thrombomodulin alone [144] or in combination with heparin [76] and endothelial protein C receptor [145], there is no clinical application of surface grafted thrombomodulin so far.

7.2.4.2 Other pharmaceutics

Antiplatelet agents

Recent developments in the immobilization of antiplatelet agents address different stages of platelet metabolism by targeting platelet enzymes (cyclo-oxygenase) or receptors (ADP and GPIIb/IIIa receptors).

Dipyridamole inhibits platelets through cyclic phosphodiesterase inhibition. By this, cycylic adenosin monophosphate (cAMP) degradation is reduced leading to increased cAMP levels at the expense of ADP. It irreversibly inhibits the synthesis of thromboxane A_2 (TXA2) leading to inhibited platelet aggregation. Aldenhoff et al. presented data on dipyridamol modified polyurethane surfaces through covalent attachment [77,78].

Pharmaceutic agents like ticlopidine that address platelet activation and aggregation through inhibition of ADP receptors have been used for surface modification of stents [146].

By immobilization of prostaglandin PGE1 onto PTFE and PET grafts, platelet adhesion was reduced in an in vitro assay [79]. PGE1 acts through increasing cAMP levels via adenylate cyclase activation resulting in platelet inhibition. Another approach is given by functionalization of PS with apyrase, an enzyme that degrades ADP [80].

Nitric oxide

This signaling molecule of ECs acts as a versatile regulatory agent with thromboprotective functions on the vascular system through the inhibition of SMCs, platelets, and leukocyte chemotaxis. Restoration of local NO production through NO-releasing devices inhibits thrombosis and promotes vascular integrity. Immobilization approaches focused on immobilization of NO donor substrates like diazeniumdiolates [147–149], whose application, however, is restricted through limited amount of NO released from the prosthetic material. Diazeniumthiolate polymer matrices additionally release carcinogenic nitrosamines [150]. In light of these limitations, the alternative use of catalytic agents capable of synthesizing NO using physiologic sources were described. For this, cysteine-modified polymers achieved NO generation through transnitrosation of endogenous S-nitrosinols in blood (S-nitrosoglutathione, S-nitrosoalbumin) [151,152]. Advancements in this field include doping of surfaces with Cu^{+} [153], lipophilic Cu^{2+} [154], and Cu^{2+}-cyclen [155,156] to achieve endogenous and unlimited NO generation. Promising applications include indwelling cardiovascular devices but await clinical validation [157,158].

Antiproliferative agents

Paclitaxel and sirolimus have antiproliferative activities and are widely used as immunsupressiva, in cancer therapeutics and for drug eluting stents [159,160].

Although effectively inhibiting cell cycle and growth of SMCs, drug-eluting stents based on these agents were found to provoke late thrombotic events through delayed reendothelialization [82].

Fibrinolytic agents

Fibrinolysis describes the process of thrombus degradation triggered through tissue-type plasminogen activator (t-PA) that converts plasminogen to plasmin. The latter enzyme acts by degrading insoluble fibrin clots to generate soluble fibrin fragments. Thrombolytic therapies are based on administration of plasminogen activators (t-PA, u-PA) or recombinant compounds like alteplase, reteplase, or teneceplase. Surface modifications based on plasminogen activators need to act fast enough to prevent the growth of a thrombus, otherwise the risk of releasing the complete thrombus as an embolus to the blood flow remains. Strategies include: (1) mimicking the activation of fibrinolytic mechanisms and (2) release of immobilized t-PA [161].

The use of fibrinolytic surfaces for medical devices enable lysis of preformed clots, being promising for catheter applications. To induce fibrinolysis, lysine-functionalized surfaces are used, which capture plasmatic t-PA [162]. Substrates for this type of functionalization include PE [92,163], PU [164], PDMS and immobilization onto PU via PEG spacers [165] and via HEMA intermediate layers [90].

Alternative concepts based on surface-mediated t-PA release were described for fibro-collagen tubes [166], PEG hydrogels [167], and PU [93]. Plasminogen activators in these cases are electrostatically bound by substrate immersion in enzyme solution. t-PA immobilization to biodegradable substrates as carriers for drug release was further developed based on PEG either combined with poly lactic acid [168] or gelatin [169] being magnetically guided and providing ultrasound-driven plasminogen-activator release respectively. The transfer of fibrinolysis-stimulating medical device coatings into clinical fields awaits realization.

7.2.4.3 Gene elution

Surface modifications using gene vectors on stents and catheters for vascular gene therapy was reported during the last 25 years [170,171]. Initial studies provided important insights in plasmid transfectability and transducibility, and uncovered molecular targets to prevent therapeutic complications such as restenosis [172]. Gene eluting therapies are composed of a therapeutic gene product, a suitable delivery system, and an appropriate vector. The latter embrace plasmids [95], retroviruses, adenoviruses [94], or adeno-associated viruses. Sustained delivery of genes is used to address restenosis in late stent thrombosis by accelerating the regenerative capacity of reendothelialization. The modulation of genes with plasmid DNA or RNA interference has been used to modulate local concentrations of specific signaling molecules that promote reendothelialization while inhibiting SMCs in order to achieve vessel healing. Targets include antithrombotic (hirudin) and antiproliferative genes (thymidine kinase, cytosine deaminase, cyclin B and p53), genes for reendothelialization (VEGF), and genes of mixed mechanisms (eNOS, iNOS) [173]. Alternatively the use of nonviral vectors based on copolymers of ethylenimine, aspartic acid, and lysine were described for

gene delivery [174]. Advantages of gene therapy include its capacity for long lasting therapeutic substrate modifications, selective inhibition of SMC proliferation/migration while maintaining endothelial regrowth, and a modulation of the biological activity through systemically administered compounds [175].

7.2.5 Coatings to promote endothelialization

The endothelium represents in all respects an intrinsically nonthrombogenic lining of the vessel wall with significant impact in mediating thrombosis. Through the expression of bioactive substances, like heparan sulfate, NO, thrombomodulin, and t-PA, ECs influence thrombotic, fibrinolytic, and inflammatory pathways.

Since accelerated reendothelialization of vascular stents and rapid restoration of endothelium integrity is the best strategy for preventing the recurrence of blood vessel occlusion (restenosis), the endothelialization of biomaterials has become an attractive approach including in vivo and in vitro endothelialization techniques. Pioneer work for in vitro endothelialization to achieve multifunctional cell layers date back to 1980, where ECs were seeded onto polymer scaffolds [176–178]. Problems arose from insufficient cell coverage, cell detachment (especially under flow conditions), and lacking recovery of cell morphology and function upon seeding. Approaches to overcome these drawbacks include the implementation of positive charges in the substrate surface to speed up the adhesion process [179], the introduction of cell recognition sites to enhance receptor-ligand mediated cell attachment [180], and the employment of ECM-derived proteins and peptides [181,182]. The use of endothelial mitogens (VEGF) to promote reendothelialization was described through VEGF coating on stents [183] or through VEGF-transfection of ECs prior to stent seeding [184]. Complete EC monolayer formation and improved supply of seeded cells was achieved through preseeding with ECs [185]. Preferred sources are cells from the umbilical cord vein or the use of autologous endothelial progenitor cells (EPCs) circulating in peripheral blood that avoid immune rejections. Consequently, core problems derive from restricted EC yield due to their weak proliferation capacities, poor adhesion, shedding phenomena, and cell damage caused by isolation. Recent attempts, therefore, focused on in vivo endothelialization being either based on substrate-mediated EC migration from adjacent tissue to generate a natural endothelium or on capture of EPCs from patient's own blood to promote differentiation into functional EPCs.

Substrate design to encourage EC migration was tried for vascular grafts but was found to fail in human models [186], despite successful animal studies [187]. The underlying insufficient coverage of bigger graft sizes used in humans was discussed, bringing along trans-mural endothelialization approaches as possible alternatives [188]. Further attempts include substrate-induced homing of EPCs—cells that possess a high proliferative capacity and play a pivotal role in vascular remodeling and reendothelialization of injured sites. Implantation of animal blood derived-EPC seeded stents in porcine and sheep models showed promising results with regard to implant integration and cellular phenotype and function [189,190]. Endogenous EPS capture is mediated through specific surface-coupled molecules including monoclonal antibodies (CD34 [191] and VEGFR-2 [192]), aptamers (CD31 binding aptamer [193]) and

supramagnetic labeling of the stent surface and EPCs [194]. EPC capture stents like Genous Stent that is coated with anti-CD34 antibodies emerged showing beneficial properties according to acute/subacute stent thrombosis. However, CD34-capturing was not specific enough for addressing EPCs only and CD34-posisitve cells were associated with increased thrombosis through in-stent restenosis and late stent thrombosis caused by cell differentiation into inflammatory cells and SMCs [195]. Improved EPC capture was achieved through aptamer immobilization [193] and supramagnetic cell labeling [193]. The use of EPCs transfected with human tissue kallikrein containing plasmids was further reported to improve cell therapeutic effects [196].

7.3 Future trends

Current strategies for improved hemocompatibility either passivate the material surfaces for reduced biointeraction or they regulate blood activation processes through the presentation and release of bioactive substances. Future hemocompatible surfaces will target much more specifically the intended biological responses and suppress undesired cellular and molecular reactions.

The most promising trend for advanced future modification technologies with bioactive substances is seen in a situation adjusted response behavior to maintain the homeostasis of dedicated parameters, by the release of the bioactive substances under tight control of the conditions in the local environment. As a first model, coatings with coagulation adjusted release of the anticoagulant heparin have been developed successfully. The next challenge for further developments is to address specifically blood platelets or immune responses through development of immuno-responsive and immuno-modulating surfaces. Another benchmark is given by stimulated adsorption of anticoagulant or pro-fibrinolytic plasma proteins on the surface or by supported endothelialization through stimulated adhesion of blood-derived ECs, progenitor cells, and stem cells to the material surface.

Besides improvement of the materials, safety, and economic considerations will gain increasing attention at the future developments.

7.4 Conclusion

Medical devices in contact with streaming blood always have to compete against the activation of physiological hemostatic and inflammatory mechanisms. The adverse reactions can have local but also systemic effects as embolism or by circulating activated immune components. The specific requirements for various applications are different, therefore promising targeted approaches based on biopassivation and bioactive surface modification have been developed in the recent decades, but problems with material-related inflammation persist and still a systemic anticoagulation is required in many applications. The development of improved and safe blood-contacting materials aims to omit or largely reduce the need of hazardous systemic anticoagulation for patients being treated with medical devices in contact with streaming blood.

Future strategies to improve the hemocompatibility require in depth understanding of the physiological activation pathways and its intercorrelations. Feedback controlled strategies and stimulated recovery of the physiological properties are identified as the most promising trend for future developments.

Acknowledgment

We acknowledge the help of Dr. Claudia Sperling inthis text with useful discussion and scientific advices.

References

[1] D.F. Williams, There is no such thing as a biocompatible material, Biomaterials 35 (2014) 10009–10014.
[2] M. Fischer, M. Vahdatzadeh, R. Konradi, J. Friedrichs, M.F. Maitz, U. Freudenberg, C. Werner, Multilayer hydrogel coatings to combine hemocompatibility and antimicrobial activity, Biomaterials 56 (2015) 198–205.
[3] I.H. Jaffer, J.C. Fredenburgh, J. Hirsh, J.I. Weitz, Medical device-induced thrombosis: what causes it and how can we prevent it? J. Thromb. Haemost. 13 (2015) S72–S81.
[4] B.D. Ratner, The catastrophe revisited: blood compatibility in the 21st century, Biomaterials 28 (2007) 5144–5147.
[5] K.M. Evans-Nguyen, M.H. Schoenfisch, Fibrin proliferation at model surfaces: influence of surface properties, Langmuir 21 (2005) 1691–1694.
[6] A. Krishnan, P. Cha, Y.H. Liu, D. Allara, E.A. Vogler, Interfacial energetics of blood plasma and serum adsorption to a hydrophobic self-assembled monolayer surface, Biomaterials 27 (2006/6) 3187–3194.
[7] M. Fischer, C. Sperling, C. Werner, Synergistic effect of hydrophobic and anionic surface groups triggers blood coagulation in vitro, J. Mater. Sci. Mater. Med. 21 (2010) 931–937.
[8] E.S. Leibner, N. Barnthip, W. Chen, C.R. Baumrucker, J.V. Badding, M. Pishko, E.A. Vogler, Superhydrophobic effect on the adsorption of human serum albumin, Acta Biomater. 5 (2009) 1389–1398.
[9] T.M. Massa, M.L. Yang, J.Y. Ho, J.L. Brash, J.P. Santerre, Fibrinogen surface distribution correlates to platelet adhesion pattern on fluorinated surface-modified polyetherurethane, Biomaterials 26 (2005/12) 7367–7376.
[10] T.L. Sun, H. Tan, D. Han, Q. Fu, L. Jiang, No platelet can adhere—largely improved blood compatibility on nanostructured superhydrophobic surfaces, Small 1 (2005) 959–963.
[11] Y. Wu, F.I. Simonovsky, B.D. Ratner, T.A. Horbett, The role of adsorbed fibrinogen in platelet adhesion to polyurethane surfaces: a comparison of surface hydrophobicity, protein adsorption, monoclonal antibody binding, and platelet adhesion, J. Biomed. Mater. Res. A 74 (2005) 722–738.
[12] M. Paven, P. Papadopoulos, S. Schottler, X. Deng, V. Mailander, D. Vollmer, H.J. Butt, Super liquid-repellent gas membranes for carbon dioxide capture and heart-lung machines, Nat. Commun. 4 (2013) 2512.

[13] S. Liebe, Effect of ampholines on blood coagulation: 1. Activation of factor VIII (antihemophilic globulin A), Folia Haematol. Int. Mag. Klin. Morphol. Blutforsch. 102 (1975) 454–461.
[14] S. Yamamichi, M. Nishitani, N. Nishimura, Y. Matsushita, K. Hasumi, Polyamine-promoted autoactivation of plasma hyaluronan-binding protein, J. Thromb. Haemost. 8 (2010) 559–566.
[15] C. Sperling, M.F. Maitz, S. Talkenberger, M.F. Gouzy, T. Groth, C. Werner, In vitro blood reactivity to hydroxylated and non-hydroxylated polymer surfaces, Biomaterials 28 (2007) 3617–3625.
[16] M. Toda, T. Kitazawa, I. Hirata, Y. Hirano, H. Iwata, Complement activation on surfaces carrying amino groups, Biomaterials 29 (2008) 407–417.
[17] Y. Koc, A.J. De Mello, G. Mchale, M.I. Newton, P. Roach, N.J. Shirtcliffe, Nano-scale superhydrophobicity: suppression of protein adsorption and promotion of flow-induced detachment, Lab Chip 8 (2008) 582–586.
[18] L.C. Hsu, J. Fang, D.A. Borca-Tasciuc, R.W. Worobo, C.I. Moraru, Effect of micro- and nanoscale topography on the adhesion of bacterial cells to solid surfaces, Appl. Environ. Microbiol. 79 (2013) 2703–2712.
[19] C.M. Magin, S.P. Cooper, A.B. Brennan, Non-toxic antifouling strategies, Mater. Today 13 (2010) 36–44.
[20] K.R. Milner, C.A. Siedlecki, A.J. Snyder, Development of novel submicron textured polyether(urethane urea) for decreasing platelet adhesion, ASAIO J. 51 (2005) 578–584.
[21] K.R. Milner, A.J. Snyder, C.A. Siedlecki, Sub-micron texturing for reducing platelet adhesion to polyurethane biomaterials, J. Biomed. Mater. Res. A 76A (2006) 561–570.
[22] H. Sahlin, R. Contreras, D.F. Gaskill, L.M. Bjursten, J.A. Frangos, Anti-inflammatory properties of micropatterned titanium coatings, J. Biomed. Mater. Res. A 77 (2006) 43–49.
[23] J. Tan, H. Shen, K.L. Carter, W.M. Saltzman, Controlling human polymorphonuclear leukocytes motility using microfabrication technology, J. Biomed. Mater. Res. 51 (2000) 694–702.
[24] J. Lu, M.P. Rao, N.C. Macdonald, D. Khang, T.J. Webster, Improved endothelial cell adhesion and proliferation on patterned titanium surfaces with rationally designed, micrometer to nanometer features, Acta Biomater. 4 (2008) 192–201.
[25] A. Ranjan, T.J. Webster, Increased endothelial cell adhesion and elongation on micron-patterned nano-rough poly(dimethylsiloxane) films, Nanotechnology 20 (2009) 305102.
[26] L.B. Koh, I. Rodriguez, S.S. Venkatraman, The effect of topography of polymer surfaces on platelet adhesion, Biomaterials 31 (2010) 1533–1545.
[27] P.G. Kalman, D.A. Mccullough, C.A. Ward, Evacuation of microscopic air bubbles from Dacron reduces complement activation and platelet aggregation, J. Vasc. Surg. 11 (1990) 591–598.
[28] P.G. Kalman, C.A. Ward, N.B. Mckeown, D. Mccullough, A.D. Romaschin, Improved biocompatibility of silicone rubber by removal of surface entrapped air nuclei, J. Biomed. Mater. Res. 25 (1991) 199–211.
[29] C.A. Ward, A. Koheil, W.R. Johnson, P.N. Madras, Reduction in complement activation from biomaterials by removal of air nuclei from the surface roughness, J. Biomed. Mater. Res. 18 (1984) 255–269.
[30] M. Fedel, A. Motta, D. Maniglio, C. Migliaresi, Surface properties and blood compatibility of commercially available diamond-like carbon coatings for cardiovascular devices, J. Biomed. Mater. Res. B Appl. Biomater. 90 (2009) 338–349.

[31] M.F. Maitz, R. Gago, B. Abendroth, M. Camero, I. Caretti, U. Kreissig, Hemocompatibility of low-friction boron-carbon-nitrogen containing coatings, J. Biomed. Mater. Res. B Appl. Biomater. 77B (2006) 179–187.
[32] L.J. Yu, X. Wang, X.H. Wang, X.H. Liu, Haemocompatibility of tetrahedral amorphous carbon films, Surf. Coat. Technol. 128 (2000) 484–488.
[33] M.F. Maitz, M.T. Pham, E. Wieser, I. Tsyganov, Blood compatibility of titanium oxides with various crystal structure and element doping, J. Biomater. Appl. 17 (2003) 303–319.
[34] S. Windecker, I. Mayer, G. De Pasquale, W. Maier, O. Dirsch, P. De Groot, Y.P. Wu, G. Noll, B. Leskosek, B. Meier, O.M. Hess, Working Group on Novel Surface Coating of Biomedical Devices, Stent coating with titanium-nitride-oxide for reduction of neointimal hyperplasia, Circulation 104 (2001) 928–933.
[35] X. Liu, P.K. Chu, C. Ding, Surface modification of titanium, titanium alloys, and related materials for biomedical applications, Mater. Sci. Eng. R. Rep. 47 (2004) 49–121.
[36] T.C. Huang, D.A. Graham, L.D. Nelson, B.R. Alevriadou, Fibrinolytic agents inhibit platelet adhesion onto collagen type I-coated surfaces at high blood flow conditions, Blood Coagul. Fibrinolysis 9 (1998) 213–226.
[37] H. Nygren, C. Eriksson, J. Lausmaa, Adhesion and activation of platelets and polymorphonuclear granulocyte cells at TiO2 surfaces, J. Lab. Clin. Med. 129 (1997) 35–46.
[38] J.Y. Chen, Y.X. Leng, X.B. Tian, L.P. Wang, N. Huang, P.K. Chu, P. Yang, Antithrombogenic investigation of surface energy and optical bandgap and hemocompatibility mechanism of Ti(Ta(+5))O2 thin films, Biomaterials 23 (2002) 2545–2552.
[39] M.F. Maitz, R.W. Poon, X.Y. Liu, M.T. Pham, P.K. Chu, Bioactivity of titanium following sodium plasma immersion ion implantation and deposition, Biomaterials 26 (2005) 5465–5473.
[40] C.C. Shih, C.M. Shih, Y.Y. Su, R.A. Gerhardt, S.J. Lin, The interaction of selected semiconducting biomaterials with platelet-rich plasma and whole blood, J. Biomed. Mater. Res. A 74 (2005) 325–337.
[41] S. Windecker, R. Simon, M. Lins, V. Klauss, F.R. Eberli, M. Roffi, G. Pedrazzini, T. Moccetti, P. Wenaweser, M. Togni, D. Tuller, R. Zbinden, C. Seiler, J. Mehilli, A. Kastrati, B. Meier, O.M. Hess, Randomized comparison of a titanium-nitride-oxide-coated stent with a stainless steel stent for coronary revascularization: the TiNOX trial, Circulation 111 (2005) 2617–2622.
[42] P. Linderback, N. Harmankaya, A. Askendal, S. Areva, J. Lausmaa, P. Tengvall, The effect of heat- or ultra violet ozone-treatment of titanium on complement deposition from human blood plasma, Biomaterials 31 (2010) 4795–4801.
[43] X.L. Liu, L. Yuan, D. Li, Z.C. Tang, Y.W. Wang, G.J. Chen, H. Chen, J.L. Brash, Blood compatible materials: state of the art, J. Mater. Chem. B 2 (2014) 5718–5738.
[44] E. Ostuni, R.G. Chapman, R.E. Holmlin, S. Takayama, G.M. Whitesides, A survey of structure-property relationships of surfaces that resist the adsorption of protein, Langmuir 17 (2001) 5605–5620.
[45] K.M. Hansson, S. Tosatti, J. Isaksson, J. Wettero, M. Textor, T.L. Lindahl, P. Tengvall, Whole blood coagulation on protein adsorption-resistant PEG and peptide functionalised PEG-coated titanium surfaces, Biomaterials 26 (2005) 861–872.
[46] J.H. Lee, Y.M. Ju, D.M. Kim, Platelet adhesion onto segmented polyurethane film surfaces modified by addition and crosslinking of PEO-containing block copolymers, Biomaterials 21 (2000) 683–691.
[47] S. Abraham, S. Brahim, K. Ishihara, A. Guiseppi-Elie, Molecularly engineered p(HEMA)-based hydrogels for implant biochip biocompatibility, Biomaterials 26 (2005) 4767–4778.

[48] L.M. Weber, J. He, B. Bradley, K. Haskins, K.S. Anseth, PEG-based hydrogels as an in vitro encapsulation platform for testing controlled β-cell microenvironments, Acta Biomater. 2 (2006) 1–8.
[49] M. Billinger, F. Buddeberg, J.A. Hubbell, D.L. Elbert, T. Schaffner, D. Mettler, S. Windecker, B. Meier, O.M. Hess, Polymer stent coating for prevention of neointimal hyperplasia, J. Invasive Cardiol. 18 (2006) 423–426. discussion 427.
[50] N. Akkilic, W.M. De Vos, Responsive polymer brushes for biomedical applications, in: Z. Zhang (Ed.), Switchable and Responsive Surfaces and Materials for Biomedical Applications, Woodhead Publishing, Oxford, 2015 (Chapter 5).
[51] N.A. Alcantar, E.S. Aydil, J.N. Israelachvili, Polyethylene glycol-coated biocompatible surfaces, J. Biomed. Mater. Res. 51 (2000) 343–351.
[52] N.A. Alcantar, E.S. Aydil, J. Israelachvili, Effect of water plasma on silica surfaces: synthesis, characterization and applications, in: J. Blitz, C. Little (Eds.), Fundamental and Applied Aspects of Chemically Modified Surfaces, Woodhead Publishing, 1999, pp. 212–222.
[53] C. Wischke, A. Lendlein, Designing multifunctional polymers for cardiovascular implants, Clin. Hemorheol. Microcirc. 49 (2011) 347–355.
[54] B. Wieland, J.P. Lancaster, C.S. Hoaglund, P. Holota, W.J. Tornquist, Electrochemical and infrared spectroscopic quantitative determination of the platinum-catalyzed ethylene glycol oxidation mechanism at CO adsorption potentials, Langmuir 12 (1996) 2594–2601.
[55] J.M. Harris, Poly(Ethylene Glycol) Chemistry: Biotechnical and Biomediacal Application, Plenum Press, New York, NY, 1992.
[56] U. Gröllmann, W. Schnabel, On the kinetics of polymer degradation in solution, 9. Pulse radiolysis of poly(ethylene oxide), Die Makromolekulare Chemie 181 (1980) 1215–1226.
[57] L. Ferez, T. Thami, E. Akpalo, V. Flaud, L. Tauk, J.M. Janot, P. Dejardin, Interface of covalently bonded phospholipids with a phosphorylcholine head: characterization, protein nonadsorption, and further functionalization, Langmuir 27 (2011) 11536–11544.
[58] M. Yamamoto, Y. Sakakibara, K. Nishimura, M. Komeda, Y. Tabata, Improved therapeutic efficacy in cardiomyocyte transplantation for myocardial infarction with release system of basic fibroblast growth factor, Artif. Organs 27 (2003) 181–184.
[59] A.L. Lewis, T.A. Vick, A.C. Collias, L.G. Hughes, R.R. Palmer, S.W. Leppard, J.D. Furze, A.S. Taylor, P.W. Stratford, Phosphorylcholine-based polymer coatings for stent drug delivery, J. Mater. Sci. Mater. Med. 12 (2001) 865–870.
[60] R.S. Smith, Z. Zhang, M. Bouchard, J. Li, H.S. Lapp, G.R. Brotske, D.L. Lucchino, D. Weaver, L.A. Roth, A. Coury, J. Biggerstaff, S. Sukavaneshvar, R. Langer, C. Loose, Vascular catheters with a nonleaching poly-sulfobetaine surface modification reduce thrombus formation and microbial attachment, Sci. Transl. Med. 4 (2012) 153ra132.
[61] A. Golas, P. Parhi, Z.O. Dimachkie, C.A. Siedlecki, E.A. Vogler, Surface-energy dependent contact activation of blood factor XII, Biomaterials 31 (2010) 1068–1079.
[62] Y. Ishikawa, S. Sasakawa, M. Takase, Y. Osada, Effect of albumin immobilization by plasma polymerization on platelet reactivity, Thromb. Res. 35 (1984) 193–202.
[63] H. Noh, E.A. Vogler, Volumetric interpretation of protein adsorption: mass and energy balance for albumin adsorption to particulate adsorbents with incrementally increasing hydrophilicity, Biomaterials 27 (2006) 5801–5812.
[64] M.V. Sefton, C.H. Gemmel, Nonthrombogenic treatments and strategies, in: B.D. Ratner, A.S. Hoffman (Eds.), Biomaterials Science, second ed., Elsevier Academic Press, Amsterdam, 2004.
[65] D.E. Graham, M.C. Phillips, Proteins at liquid interfaces: I. Kinetics of adsorption and surface denaturation, J. Colloid Interface Sci. 70 (1979) 403–414.

[66] J.Z. Zhu, X.W. Xiong, R. Du, Y.J. Jing, Y. Ying, X.M. Fan, T.Q. Zhu, R.Y. Zhang, Hemocompatibility of drug-eluting coronary stents coated with sulfonated poly (styrene-block-isobutylene-block-styrene), Biomaterials 33 (2012) 8204–8212.
[67] M. Fischer, C.P. Baptista, I.C. Goncalves, B.D. Ratner, C. Sperling, C. Werner, C.L. Martins, M.A. Barbosa, The effect of octadecyl chain immobilization on the hemocompatibility of poly (2-hydroxyethyl methacrylate), Biomaterials 33 (2012) 7677–7685.
[68] A.G. Kidane, H. Salacinski, A. Tiwari, K.R. Bruckdorfer, A.M. Seifalian, Anticoagulant and antiplatelet agents: their clinical and device application(s) together with usages to engineer surfaces, Biomacromolecules 5 (2004) 798–813.
[69] R. Lever, C.R. Page, Novel drug development opportunities for heparin, Nat. Rev. Drug Discov. 1 (2002) 140–148.
[70] D.M. Phaneuf, S.A. Berceli, M.J. Bide, W.C. Quist, F.W. Logerfo, Covalent linkage of recombinant hirudin to poly(ethylene terephthalate) (Dacron): creation of a novel antithrombin surface, Biomaterials 18 (1997) 755–765.
[71] M.D. Phaneuf, M. Szycher, S.A. Berceli, D.J. Dempsey, W.C. Quist, F.W. Logerfo, Covalent linkage of recombinant hirudin to a novel ionic poly(carbonate) urethane polymer with protein binding sites: determination of surface antithrombin activity, Artif. Organs 22 (1998) 657–665.
[72] T. Richey, H. Iwata, H. Oowaki, E. Uchida, S. Matsuda, Y. Ikada, Surface modification of polyethylene balloon catheters for local drug delivery, Biomaterials 21 (2000) 1057–1065.
[73] M.F. Gouzy, C. Sperling, K. Salchert, T. Pompe, C. Rauwolf, C. Werner, Benzamidine-based coatings: implication of inhibitor structure on the inhibition of coagulation enzymes in solution and in vitro hemocompatibility assessment, Biointerphases 1 (2006) 146–155.
[74] M.F. Gouzy, C. Sperling, K. Salchert, T. Pompe, U. Streller, P. Uhlmann, C. Rauwolf, F. Simon, F. Bohme, B. Voit, C. Werner, In vitro blood compatibility of polymeric biomaterials through covalent immobilization of an amidine derivative, Biomaterials 25 (2004) 3493–3501.
[75] C. Sperling, U. Konig, G. Hermel, C. Werner, M. Muller, F. Simon, K. Grundke, H.J. Jacobasch, V.N. Vasilets, Y. Ikada, Immobilization of human thrombomodulin onto PTFE, J. Mater. Sci. Mater. Med. 8 (1997/12) 789–791.
[76] P.Y. Tseng, S.S. Rele, X.L. Sun, E.L. Chaikof, Membrane-mimetic films containing thrombomodulin and heparin inhibit tissue factor-induced thrombin generation in a flow model, Biomaterials 27 (2006) 2637–2650.
[77] Y.B.J. Aldenhoff, R. Blezer, T. Lindhout, L.H. Koole, Photo-immobilization of dipyridamole (Persantin) at the surface of polyurethane biomaterials: reduction of in vitro thrombogenicity, Biomaterials 18 (1997) 167–172.
[78] Y.B.J. Aldenhoff, F.H. Van Der Veen, W. Ter, J. Habets, L.A. Poole-Warren, L.H. Koole, Performance of a polyurethane vascular prosthesis carrying a dipyridamole (Persantin) coating on its lumenal surface, J. Biomed. Mater. Res. 54 (2001) 224–233.
[79] T. Chandy, G.S. Das, R.F. Wilson, G.H.R. Rao, Use of plasma glow for surface-engineering biomolecules to enhance bloodcompatibility of Dacron and PTFE vascular prosthesis, Biomaterials 21 (2000) 699–712.
[80] P.H. Nilsson, A.E. Engberg, J. Back, L. Faxalv, T.L. Lindahl, B. Nilsson, K.N. Ekdahl, The creation of an antithrombotic surface by apyrase immobilization, Biomaterials 31 (2010) 4484–4491.
[81] A.B. Fontaine, J.J. Borsa, S.D. Passos, E.K. Hoffer, R.D. Bloch, F. Starr, C. So, Evaluation of local abciximab delivery from the surface of a polymer-coated covered stent: in vivo canine studies, J. Vasc. Interv. Radiol. 12 (2001) 487–492.

[82] J. Daemen, P.H. Van Twisk, R.T. Van Domburg, N. Kukreja, Y.N. Onuma, H. Boersma, P.W.J.C. Serruys, The long-term safety of bare-metal, sirolimus- or paclitaxel-eluting stents for on-versus off-label indications, Eur. Heart J. 29 (2008) 516.
[83] N. Kukreja, Y. Onuma, J. Daemen, P.W. Serruys, The future of drug-eluting stents, Pharmacol. Res. 57 (2008) 171–180.
[84] H. Handa, E.J. Brisbois, T.C. Major, L. Refahiyat, K.A. Amoako, G.M. Annich, R.H. Bartlett, M.E. Meyerhoff, In vitro and in vivo study of sustained nitric oxide release coating using diazeniumdiolate-doped poly(vinyl chloride) matrix with poly(lactide-co-glycolide) additive, J. Mater. Chem. B 1 (2013) 3578–3587.
[85] M.C. Jen, M.C. Serrano, R. Van Lith, G.A. Ameer, Polymer-based nitric oxide therapies: recent insights for biomedical applications, Adv. Funct. Mater. 22 (2012) 239–260.
[86] N. Naghavi, A. De Mel, O.S. Alavijeh, B.G. Cousins, A.M. Seifalian, Nitric oxide donors for cardiovascular implant applications, Small 9 (2013) 22–35.
[87] D.A. Riccio, P.N. Coneski, S.P. Nichols, A.D. Broadnax, M.H. Schoenfisch, Photoinitiated nitric oxide-releasing tertiary S-nitrosothiol-modified xerogels, ACS Appl. Mater. Interfaces 4 (2012) 796–804.
[88] A.B. Seabra, D. Martins, M.M.S.G. Simões, R. Da Silva, M. Brocchi, M.G. De Oliveira, Antibacterial nitric oxide-releasing polyester for the coating of blood-contacting artificial materials, Artif. Organs 34 (2010) E204–E214.
[89] Y.J. Weng, Q.A. Song, Y.J. Zhou, L.P. Zhang, J. Wang, J.Y. Chen, Y.X. Leng, S.Y. Li, N. Huang, Immobilization of selenocystamine on TiO2 surfaces for in situ catalytic generation of nitric oxide and potential application in intravascular stents, Biomaterials 32 (2011) 1253–1263.
[90] D. Li, H. Chen, S.S. Wang, Z.Q. Wu, J.L. Brash, Lysine-poly(2-hydroxyethyl methacrylate) modified polyurethane surface with high lysine density and fibrinolytic activity, Acta Biomater. 7 (2011) 954–958.
[91] D. Li, S.S. Wang, Z.Q. Wu, H. Chen, J.L. Brash, A new t-PA releasing concept based on protein-protein displacement, Soft Matter 9 (2013) 2321–2328.
[92] N.A. Samojlova, M.A. Krayukhina, I.A. Yamskov, Use of the affinity chromatography principle in creating new thromboresistant materials, J. Chromatogr. B Analyt. Technol. Biomed. Life Sci. 800 (2004) 263–269.
[93] Z.Q. Wu, H. Chen, D. Li, J.L. Brash, Tissue plasminogen activator-containing polyurethane surfaces for fibrinolytic activity, Acta Biomater. 7 (2011) 1993–1998.
[94] F. Sharif, S.O. Hynes, J. Crowley, K. Daly, T. O'Brien, Accelerated re-endothelilization in eNOS transduced iliac artery following gene delivery from an adenoviral eluting stent, Mol. Ther. 13 (2006) S334–S335.
[95] J. Yang, Y. Zeng, C. Zhang, Y.X. Chen, Z.Y. Yang, Y.J. Li, X.G. Leng, D.L. Kong, X.Q. Wei, H.F. Sun, C.X. Song, The prevention of restenosis in vivo with a VEGF gene and paclitaxel co-eluting stent, Biomaterials 34 (2013) 1635–1643.
[96] M. Bosiers, K. Deloose, J. Verbist, H. Schroe, G. Lauwers, W. Lansink, P. Peeters, Heparin-bonded expanded polytetrafluoroethylene vascular graft for femoropopliteal and femorocrural bypass grafting: 1-year results, J. Vasc. Surg. 43 (2006) 313–318.
[97] R.A. Hoshi, R. Van Lith, M.C. Jen, J.B. Allen, K.A. Lapidos, G. Ameer, The blood and vascular cell compatibility of heparin-modified ePTFE vascular grafts, Biomaterials 34 (2013) 30–41.
[98] C. Bickel, H.J. Rupprecht, H. Darius, C. Binz, B. Hauroder, F. Krummenauer, J. Meyer, Substantial reduction of platelet adhesion by heparin-coated stents, J. Interv. Cardiol. 14 (2001) 407–413.

[99] P.A. Hardhammar, H.M.M. Vanbeusekom, H.U. Emanuelsson, S.H. Hofma, P.A. Albertsson, P.D. Verdouw, E. Boersma, P.W. Serruys, W.J. Vandergiessen, Reduction in thrombotic events with heparin-coated Palmaz-Schatz stents in normal porcine coronary arteries, Circulation 93 (1996) 423–430.
[100] M. Haude, T.F.M. Konorza, U. Kalnins, A. Erglis, K. Saunamaki, H.D. Glogar, E. Grube, R. GIL, A. Serra, H.G. Richardt, P. Sick, R. Erbel, C.T. Invest, Heparin-coated stent placement for the treatment of stenoses in small coronary arteries of symptomatic patients, Circulation 107 (2003) 1265–1270.
[101] Z. Yang, J. Wang, R. Luo, M.F. Maitz, F. Jing, H. Sun, N. Huang, The covalent immobilization of heparin to pulsed-plasma polymeric allylamine films on 316L stainless steel and the resulting effects on hemocompatibility, Biomaterials 31 (2010) 2072–2083.
[102] Z.L. Yang, Q.F. Tu, J. Wang, N. Huang, The role of heparin binding surfaces in the direction of endothelial and smooth muscle cell fate and re-endothelialization, Biomaterials 33 (2012) 6615–6625.
[103] P. Jansen, W. Van Oeveren, A. Capel, A. Carpentier, In vitro haemocompatibility of a novel bioprosthetic total artificial heart, Eur. J. Cardiothorac. Surg. 41 (2012) e166–e172.
[104] G.I. Tagarakis, N.B. Tsilimingas, Heparin-coated extracorporeal circulation systems in heart surgery, Recent Pat. Cardiocasc. Drug Discov. 4 (2009) 177–179.
[105] J. Chanard, S. Lavaud, H. Maheut, I. Kazes, F. Vitry, P. Rieu, The clinical evaluation of low-dose heparin in haemodialysis: a prospective study using the heparin-coated AN69 ST membrane, Nephrol. Dial. Transplant. 23 (2008) 2003–2009.
[106] V.L. Gott, J.D. Whiffen, R.C. Dutton, Heparin bonding on colloidal graphite surfaces, Science 142 (1963) 1297–1298.
[107] S. Murugesan, J. Xie, R.J. Linhardt, Immobilization of heparin: approaches and applications, Curr. Top. Med. Chem. 8 (2008) 80–100.
[108] H. Chen, L. Yuan, W. Song, Z.K. Wu, D. Li, Biocompatible polymer materials: role of protein-surface interactions, Prog. Polym. Sci. 33 (2008) 1059–1087.
[109] W.J. Vandergiessen, P.A. Hardhammar, H.M.M. Vanbeusekom, H.U. Emanuelsson, P.A. Albertsson, P.D. Verdouw, P.W. Serruys, Reduction of thrombotic events using heparin-coated Palmaz-Schatz stents, Circulation 88 (1993) 661.
[110] T.W. Chuang, D.T. Lin, F.H. Lin, Immobilization of NaIO4-treated heparin on PEG-modified 316L SS surface for high anti-thrombin-III binding, J. Biomed. Mater. Res. A 86A (2008) 648–661.
[111] Y. Byun, H.A. Jacobs, S.W. Kim, Heparin surface immobilization through hydrophilic spacers—thrombin and antithrombin-III binding-kinetics, J. Biomater. Sci. Polym. Ed. 6 (1994) 1–13.
[112] G. Li, P. Yang, W. Qin, M.F. Maitz, S. Zhou, N. Huang, The effect of coimmobilizing heparin and fibronectin on titanium on hemocompatibility and endothelialization, Biomaterials 32 (2011) 4691–4703.
[113] G.C. Li, F.M. Zhang, Y.Z. Liao, P. Yang, N. Huang, Coimmobilization of heparin/fibronectin mixture on titanium surfaces and their blood compatibility, Colloids Surf. B Biointerfaces 81 (2010) 255–262.
[114] C. Sperling, M. Houska, E. Brynda, U. Streller, C. Werner, In vitro hemocompatibility of albumin-heparin multilayer coatings on polyethersulfone prepared by the layer-by-layer technique, J. Biomed. Mater. Res. A 76 (2006) 681–689.
[115] M.Q. Tan, Y.K. Feng, H.Y. Wang, L. Zhang, M. Khan, J.T. Guo, Q.L. Chen, J.S. Liu, Immobilized bioactive agents onto polyurethane surface with heparin and phosphorylcholine group, Macromol. Res. 21 (2013) 541–549.

[116] J.H. Fu, J. Ji, W.Y. Yuan, J.C. Shen, Construction of anti-adhesive and antibacterial multilayer films via layer-by-layer assembly of heparin and chitosan, Biomaterials 26 (2005) 6684–6692.
[117] S. Meng, Z.J. Liu, L. Shen, Z. Guo, L.S.L. Chou, W. Zhong, Q.G. Du, J. Ge, The effect of a layer-by-layer chitosan-heparin coating on the endothelialization and coagulation properties of a coronary stent system, Biomaterials 30 (2009) 2276–2283.
[118] M. Liu, X.L. Yue, Z.F. Dai, L. Xing, F. Ma, N.Q. Ren, Stabilized hemocompatible coating of nitinol devices based on photo-cross-linked alginate/heparin multilayer, Langmuir 23 (2007) 9378–9385.
[119] J.L. Chen, C. Chen, Z.Y. Chen, J.Y. Chen, Q.L. Li, N. Huang, Collagen/heparin coating on titanium surface improves the biocompatibility of titanium applied as a blood-contacting biomaterial, J. Biomed. Mater. Res. A 95A (2010) 341–349.
[120] Q.K. Guo, Z.Q. Lu, J.Y. Wang, T. Li, In vivo evaluation of a novel dexamethasone-heparin-double-coated stent for inhibition of artery restenosis and thrombosis, J. Mater. Sci. Mater. Med. 22 (2011) 1615–1623.
[121] L. Berry, A. Stafford, J. Fredenburgh, H. O'Brodovich, L. Mitchell, J. Weitz, M. Andrew, A.K. Chan, Investigation of the anticoagulant mechanisms of a covalent antithrombin-heparin complex, J. Biol. Chem. 273 (1998) 34730–34736.
[122] A. Chan, L. Berry, H. O'Brodovich, P. Klement, L. Mitchell, B. Baranowski, P. Monagle, M. Andrew, Covalent antithrombin-heparin complexes with high anticoagulant activity. Intravenous, subcutaneous, and intratracheal administration, J. Biol. Chem. 272 (1997) 22111–22117.
[123] S. Patel, L.R. Berry, A.K. Chan, Covalent antithrombin-heparin complexes, Thromb. Res. 120 (2007) 151–160.
[124] Y.J. Du, J.L. Brash, G. Mcclung, L.R. Berry, P. Klement, A.K. Chan, Protein adsorption on polyurethane catheters modified with a novel antithrombin-heparin covalent complex, J. Biomed. Mater. Res. A 80 (2007) 216–225.
[125] K.N. Sask, W.G. Mcclung, L.R. Berry, A.K.C. Chan, J.L. Brash, Immobilization of an antithrombin-heparin complex on gold: anticoagulant properties and platelet interactions, Acta Biomater. 7 (2011) 2029–2034.
[126] K.N. Sask, L.R. Berry, A.K.C. Chan, J.L. Brash, Modification of polyurethane surface with an antithrombin-heparin complex for blood contact: influence of molecular weight of polyethylene oxide used as a linker/spacer, Langmuir 28 (2012) 2099–2106.
[127] J.M. Leung, L.R. Berry, A.K.C. Chan, J.L. Brash, Surface modification of polydimethylsiloxane with a covalent antithrombin-heparin complex to prevent thrombosis, J. Biomater. Sci. Polym. Ed. 25 (2014) 786–801.
[128] Y.K. Liang, K.L. Kiick, Heparin-functionalized polymeric biomaterials in tissue engineering and drug delivery applications, Acta Biomater. 10 (2014) 1588–1600.
[129] A. Zieris, S. Prokoph, K.R. Levental, P.B. Welzel, M. Grimmer, U. Freudenberg, C. Werner, FGF-2 and VEGF functionalization of starPEG-heparin hydrogels to modulate biomolecular and physical cues of angiogenesis, Biomaterials 31 (2010) 7985–7994.
[130] A.S. Hoffman, Hydrogels for biomedical applications, Adv. Drug Deliv. Rev. 54 (2002) 3–12.
[131] U. Freudenberg, A. Hermann, P.B. Welzel, K. Stirl, S.C. Schwarz, M. Grimmer, A. Zieris, W. Panyanuwat, S. Zschoche, D. Meinhold, A. Storch, C. Werner, A star-PEG-heparin hydrogel platform to aid cell replacement therapies for neurodegenerative diseases, Biomaterials 30 (2009) 5049–5060.
[132] M.F. Maitz, U. Freudenberg, M.V. Tsurkan, M. Fischer, T. Beyrich, C. Werner, Bioresponsive polymer hydrogels homeostatically regulate blood coagulation, Nat. Commun. 4 (2013) 2168.

[133] M.C. Wyers, M.D. Phaneuf, E.M. Rzucidlo, M.A. Contreras, F.W. Logerfo, W.C. Quist, In vivo assessment of a novel Dacron surface with covalently bound recombinant hirudin, Cardiovasc. Pathol. 8 (1999) 153–159.
[134] D.D. Kim, M.M. Takeno, B.D. Ratner, T.A. Horbett, Glow discharge plasma deposition (GDPD) technique for the local controlled delivery of hirudin from biomaterials, Pharm. Res. 15 (1998) 783–786.
[135] M.D. Phaneuf, D.J. Dempsey, M.J. Bide, M. Szycher, W.C. Quist, F.W. Logerfo, Bioengineering of a novel small diameter polyurethane vascular graft with covalently bound recombinant hirudin, ASAIO J. 44 (1998) M653–M658.
[136] C. Lin, M. Tseng, Surface characterization and platelet adhesion studies on polyethylene surface with hirudin immobilization, J. Mater. Sci. Mater. Med. 12 (2001) 827–832.
[137] S. Onder, K. Kazmanli, F.N. Kok, Alteration of PTFE surface to increase its blood compatibility, J. Biomater. Sci. Polym. Ed. 22 (2011) 1443–1457.
[138] J. Lahann, D. Klee, W. Pluester, H. Hoecker, Bioactive immobilization of r-hirudin on CVD-coated metallic implant devices, Biomaterials 22 (2001) 817–826.
[139] L. Lu, Q.L. Li, M.F. Maitz, J.L. Chen, N. Huang, Immobilization of the direct thrombin inhibitor-bivalirudin on 316L stainless steel via polydopamine and the resulting effects on hemocompatibility in vitro, J. Biomed. Mater. Res. A 100 (2012) 2421–2430.
[140] S.C. Freitas, T.B. Cereija, A.C. Figueiredo, H. Osorio, P.J.B. Pereira, M.A. Barbosa, M.C.L. Martins, Bioengineered surfaces to improve the blood compatibility of biomaterials through direct thrombin inactivation, Acta Biomater. 8 (2012) 4101–4110.
[141] C. Kettner, L. Mersinger, R. Knabb, The selective inhibition of thrombin by peptides of boroarginine, J. Biol. Chem. 265 (1990) 18289–18297.
[142] M.F. Maitz, C. Sperling, C. Werner, Immobilization of the irreversible thrombin inhibitor D-Phe-Pro-Arg-chloromethylketone: a concept for hemocompatible surfaces? J. Biomed. Mater. Res. A 94 (2010) 905–912.
[143] C. Salvagnini, S. Gharbi, T. Boxus, J. Marchand-Brynaert, Synthesis and evaluation of a small library of graftable thrombin inhibitors derived from (L)-arginine, Eur. J. Med. Chem. 42 (2007) 37–53.
[144] C. Sperling, K. Salchert, U. Streller, C. Werner, Covalently immobilized thrombomodulin inhibits coagulation and complement activation of artificial surfaces in vitro, Biomaterials 25 (2004) 5101–5113.
[145] K.E. Kador, T.G. Mamedov, M. Schneider, A. Subramanian, Sequential co-immobilization of thrombomodulin and endothelial protein C receptor on polyurethane: activation of protein C, Acta Biomater. 7 (2011) 2508–2517.
[146] M.A. Brockmann, K. Gutensohn, J. Bau, P. Kuehnl, T. Meinertz, C. Nienaber, C. Beythien, Influence of heparin coating of coronary stents and ex vivo efficacy of different doses of acetylsalicylic acid and ticlopidine in a pulsed floating model of recirculating human plasma, Platelets 13 (2002) 443–449.
[147] G.M. Annich, J.P. Meinhardt, K.A. Mowery, B.A. Ashton, S.I. Merz, R.B. Hirschl, M.E. Meyerhoff, R.H. Bartlett, Reduced platelet activation and thrombosis in extracorporeal circuits coated with nitric oxide release polymers, Crit. Care Med. 28 (2000) 915–920.
[148] P.G. Parzuchowski, M.C. Frost, M.E. Meyerhoff, Synthesis and characterization of polymethacrylate-based nitric oxide donors, J. Am. Chem. Soc. 124 (2002) 12182–12191.
[149] M.H. Schoenfisch, K.A. Mowery, M.V. Rader, N. Baliga, J.A. Wahr, M.E. Meyerhoff, Improving the thromboresistivity of chemical sensors via nitric oxide release: fabrication and in vivo evaluation of NO-releasing oxygen-sensing catheters, Anal. Chem. 72 (2000) 1119–1126.

[150] K.A. Mowery, M.H. Schoenfisch, J.E. Saavedra, L.K. Keefer, M.E. Meyerhoff, Preparation and characterization of hydrophobic polymeric films that are thromboresistant via nitric oxide release, Biomaterials 21 (2000) 9–21.
[151] X. Duan, R.S. Lewis, Improved haemocompatibility of cysteine-modified polymers via endogenous nitric oxide, Biomaterials 23 (2002) 1197–1203.
[152] H. Gappa-Fahlenkamp, R.S. Lewis, Improved hemocompatibility of poly(ethylene terephthalate) modified with various thiol-containing groups, Biomaterials 26 (2005) 3479–3485.
[153] B.K. Oh, M.E. Meyerhoff, Catalytic generation of nitric oxide from nitrite at the interface of polymeric films doped with lipophilic CuII-complex: a potential route to the preparation of thromboresistant coatings, Biomaterials 25 (2004) 283–293.
[154] B.K. Oh, M.E. Meyerhoff, Spontaneous catalytic generation of nitric oxide from S-nitrosothiols at the surface of polymer films doped with lipophilic copperII complex, J. Am. Chem. Soc. 125 (2003) 9552–9553.
[155] S. Hwang, W. Cha, M.E. Meyerhoff, Polymethacrylates with a covalently linked CuII-cyclen complex for the in situ generation of nitric oxide from nitrosothiols in blood, Angew. Chem. Int. Ed. Engl. 45 (2006) 2745–2748.
[156] S. Hwang, M.E. Meyerhoff, Polyurethane with tethered copper(II)-cyclen complex: preparation, characterization and catalytic generation of nitric oxide from S-nitrosothiols, Biomaterials 29 (2008) 2443–2452.
[157] P. Qi, X. Li, Y. Yang, R. Shen, J. Wang, Z. Yang, Q. Tu, N. Huang, Constructing biomimic catalytic coating with controlled nitric oxide release properties by immobilizing 3,3-diselenodipropionic acid on plasma polymerized allylamine film, Plasma Process. Polym. 11 (2014) 952–960.
[158] Z. Yang, Y. Yang, K. Xiong, X. Li, P. Qi, Q. Tu, F. Jing, Y. Weng, J. Wang, N. Huang, Nitric oxide producing coating mimicking endothelium function for multifunctional vascular stents, Biomaterials 63 (2015) 80–92.
[159] M. Chorny, I. Fishbein, B.B. Yellen, I.S. Alferiev, M. Bakay, S. Ganta, R. Adamo, M. Amiji, G. Friedman, R.J. Levy, Targeting stents with local delivery of paclitaxel-loaded magnetic nanoparticles using uniform fields, Proc. Natl. Acad. Sci. USA 107 (2010) 8346–8351.
[160] M.K. Hong, G.S. Mintz, C.W. Lee, J.M. Song, K.H. Han, D.H. Kang, J.K. Song, J.J. Kim, N.J. Weissman, N.E. Fearnot, S.W. Park, S.J. Park, Paclitaxel coating reduces in-stent intimal hyperplasia in human coronary arteries: a serial volumetric intravascular ultrasound analysis from the Asian Paclitaxel-Eluting Stent Clinical Trial (ASPECT), Circulation 107 (2003) 517–520.
[161] D. Li, H. Chen, J.L. Brash, Mimicking the fibrinolytic system on material surfaces, Colloids Surf. B: Biointerfaces 86 (2011) 1–6.
[162] W.G. Mcclung, D.L. Clapper, A.B. Anderson, D.E. Babcock, J.L. Brash, Interactions of fibrinolytic system proteins with lysine-containing surfaces, J. Biomed. Mater. Res. A 66 (2003) 795–801.
[163] W.G. Mcclung, D.E. Babcock, J.L. Brash, Fibrinolytic properties of lysine-derivatized polyethylene in contact with flowing whole blood (Chandler loop model), J. Biomed. Mater. Res. A 81 (2007) 644–651.
[164] Z. Tang, X. Liu, Y. Luan, W. Liu, Z. Wu, D. Li, H. Chen, Regulation of fibrinolytic protein adsorption on polyurethane surfaces by modification with lysine-containing copolymers, Polym. Chem. 4 (2013) 5597–5602.
[165] H. Chen, Y. Zhang, D. Li, X. Hu, L. Wang, W.G. Mcclung, J.L. Brash, Surfaces having dual fibrinolytic and protein resistant properties by immobilization of lysine on polyurethane through a PEG spacer, J. Biomed. Mater. Res. A 90 (2009) 940–946.

[166] F. Senatore, F. Bernath, K. Meisner, Clinical study of urokinase-bound fibrocollagenous tubes, J. Biomed. Mater. Res. 20 (1986) 177–188.
[167] Y. Park, J. Liang, Z. Yang, V.C. Yang, Controlled release of clot-dissolving tissue-type plasminogen activator from a poly(L-glutamic acid) semi-interpenetrating polymer network hydrogel, J. Control. Release 75 (2001) 37–44.
[168] X. Liu, M.D. Kaminski, H. Chen, M. Torno, L. Taylor, A.J. Rosengart, Synthesis and characterization of highly-magnetic biodegradable poly(d, l-lactide-co-glycolide) nanospheres, J. Control. Release 119 (2007) 52–58.
[169] Y. Uesugi, H. Kawata, J. Jo, Y. Saito, Y. Tabata, An ultrasound-responsive nano delivery system of tissue-type plasminogen activator for thrombolytic therapy, J. Control. Release 147 (2010) 269–277.
[170] E.G. Nabel, G. Plautz, F.M. Boyce, J.C. Stanley, G.J. Nabel, Recombinant gene expression in vivo within endothelial cells of the arterial wall, Science 244 (1989) 1342–1344.
[171] F. Sharif, K. Daly, J. Crowley, T. O'Brien, Current status of catheter- and stent-based gene therapy, Cardiovasc. Res. 64 (2004) 208–216.
[172] C.E. Appleby, P.A. Kingston, Gene therapy for restenosis—what now, what next? Curr. Gene. Ther. 4 (2004) 153–182.
[173] R.X. Yin, D.Z. Yang, J.Z. Wu, Nanoparticle drug- and gene-eluting stents for the prevention and treatment of coronary restenosis, Theranostics 4 (2014) 175–200.
[174] G.P. Tang, Z. Yang, J. Zhou, Poly (ethylenimine)-grafted-poly [(aspartic acid)-co-lysine], a potential non-viral vector for DNA delivery, J. Biomater. Sci. Polym. Ed. 17 (2006) 461–480.
[175] S.B. King 3rd, Applying drug-eluting stents in clinical practice, Am. J. Cardiol. 100 (2007) 25k–31k.
[176] K.L. Boyd, S.P. Schmidt, T.R. Pippert, W.V. Sharp, Endothelial cell seeding of ULTI carbon-coated small-diameter PTFE vascular grafts, ASAIO Trans. 33 (1987) 631–635.
[177] M. Herring, S. Baughman, J. Glover, K. Kesler, J. Jesseph, J. Campbell, R. Dilley, A. Evan, A. Gardner, Endothelial seeding of Dacron and polytetrafluoroethylene grafts: the cellular events of healing, Surgery 96 (1984) 745–755.
[178] G.B. Koveker, W.E. Burkel, L.M. Graham, T.W. Wakefield, J.C. Stanley, Endothelial cell seeding of expanded polytetrafluoroethylene vena cava conduits: effects on luminal production of prostacyclin, platelet adherence, and fibrinogen accumulation, J. Vasc. Surg. 7 (1988) 600–605.
[179] W. He, Z. Ma, T. Yong, W.E. Teo, S. Ramakrishna, Fabrication of collagen-coated biodegradable polymer nanofiber mesh and its potential for endothelial cells growth, Biomaterials 26 (2005) 7606–7615.
[180] K.J. Pawlowski, S.E. Rittgers, S.P. Schmidt, G.L. Bowlin, Endothelial cell seeding of polymeric vascular grafts, Front. Biosci. 9 (2004) 1412–1421.
[181] H.W. Jun, J.L. West, Endothelialization of microporous YIGSR/PEG-modified polyurethaneurea, Tissue Eng. 11 (2005) 1133–1140.
[182] Y. Zhu, C. Gao, Y. Liu, J. Shen, Endothelial cell functions in vitro cultured on poly(L-lactic acid) membranes modified with different methods, J. Biomed. Mater. Res. A 69 (2004) 436–443.
[183] N. Swanson, K. Hogrefe, Q. Javed, N. Malik, A.H. Gershlick, Vascular endothelial growth factor (VEGF)-eluting stents: in vivo effects on thrombosis, endothelialization and intimal hyperplasia, J. Invasive Cardiol. 15 (2003) 688–692.
[184] D.H. Walter, M. Cejna, L. Diaz-Sandoval, S. Willis, L. Kirkwood, P.W. Stratford, A.B. Tietz, R. Kirchmair, M. Silver, C. Curry, A. Wecker, Y.S. Yoon, R. Heidenreich,

A. Hanley, M. Kearney, F.O. Tio, P. Kuenzler, J.M. Isner, D.W. Losordo, Local gene transfer of phVEGF-2 plasmid by gene-eluting stents: an alternative strategy for inhibition of restenosis, Circulation 110 (2004) 36–45.

[185] K.O. Cardinal, G.T. Bonnema, H. Hofer, J.K. Barton, S.K. Williams, Tissue-engineered vascular grafts as in vitro blood vessel mimics for the evaluation of endothelialization of intravascular devices, Tissue Eng. 12 (2006) 3431–3438.

[186] K. Berger, L.R. Sauvage, A.M. Rao, S.J. Wood, Healing of arterial prostheses in man: its incompleteness, Ann. Surg. 175 (1972) 118–127.

[187] A.W. Clowes, A.M. Gown, S.R. Hanson, M.A. Reidy, Mechanisms of arterial graft failure. 1. Role of cellular proliferation in early healing of PTFE prostheses, Am. J. Pathol. 118 (1985) 43–54.

[188] P. Zilla, D. Bezuidenhout, P. Human, Prosthetic vascular grafts: wrong models, wrong questions and no healing, Biomaterials 28 (2007) 5009–5027.

[189] J. Allen, S. Khan, M.C. Serrano, G. Ameer, Characterization of porcine circulating progenitor cells: toward a functional endothelium, Tissue Eng. Part A 14 (2008) 183–194.

[190] K. Mendelson, E. Aikawa, B.A. Mettler, V. Sales, D. Martin, J.E. Mayer, F.J. Schoen, Healing and remodeling of bioengineered pulmonary artery patches implanted in sheep, Cardiovasc. Pathol. 16 (2007) 277–282.

[191] J. Aoki, P.W. Serruys, H. Van Beusekom, A.T. Ong, E.P. Mcfadden, G. Sianos, W.J. Van Der Giessen, E. Regar, P.J. De Feyter, H.R. Davis, S. Rowland, M.J. Kutryk, Endothelial progenitor cell capture by stents coated with antibody against CD34: the HEALING-FIM (healthy endothelial accelerated lining inhibits neointimal growth-first in man) registry, J. Am. Coll. Cardiol. 45 (2005) 1574–1579.

[192] B.D. Markway, O.J. Mccarty, U.M. Marzec, D.W. Courtman, S.R. Hanson, M.T. Hinds, Capture of flowing endothelial cells using surface-immobilized anti-kinase insert domain receptor antibody, Tissue Eng. Part C Methods 14 (2008) 97–105.

[193] J. Hoffmann, A. Paul, M. Harwardt, J. Groll, T. Reeswinkel, D. Klee, M. Moeller, H. Fischer, T. Walker, T. Greiner, G. Ziemer, H.P. Wendel, Immobilized DNA aptamers used as potent attractors for porcine endothelial precursor cells, J. Biomed. Mater. Res. A 84 (2008) 614–621.

[194] S.V. Pislaru, A. Harbuzariu, G. Agarwal, T. Witt, R. Gulati, N.P. Sandhu, C. Mueske, M. Kalra, R.D. Simari, G.S. Sandhu, Magnetic forces enable rapid endothelialization of synthetic vascular grafts, Circulation 114 (2006) I314–I318.

[195] M. Klomp, M.A.M. Beijk, R.J. De Winter, Genous (TM) endothelial progenitor cell-capturing stent system: a novel stent technology, Expert Rev. Med. Devices 6 (2009) 365–375.

[196] C.X. Liu, D.Q. Li, Y. Zhang, H. Jiang, R. Wang, X.P. Wang, Culture of endothelial progenitor cells from rabbit peripheral blood and HTK gene modification, Basic Clin. Med. 11 (2007) 1241–1245.

Techniques for modifying biomaterials to improve hemocompatibility

8

N. Kasoju[*], *L.T.B. Nguyen*[†], *A.R. Padalhin*[‡], *J.F. Dye*[†], *Z. Cui*[†], *H. Ye*[†]
[*]Sree Chitra Tirunal Institute for Medical Sciences and Technology (SCTIMST), Thiruvananthapuram, India, [†]University of Oxford, Oxford, United Kingdom, [‡]Soonchunhyang University, Asan, South Korea

Abbreviations

APTT	activated partial thromboplastin time
CD	cluster of differentiation
EDC	1-ethyl-3-(dimethylaminopropyl) carbodiimide hydrochloride
EOCs	endothelial outgrowth cells
EPCs	endothelial progenitor cells
ePTFE	expanded poly(tetrafluoroethylene)
HUVECs	human umbilical vein endothelial cells
NHS	*N*-Hydroxysuccinimide
PCL	poly(caprolactone)
PEO	poly(ethylene oxide)
PES	poly(ethersulfone)
PET	poly(ethylene terephthalate)
PLA	poly(lactide)
PLGA	poly(lactide-*co*-glycolide)
SEM	scanning electron microscopy
TiO_2	titanium dioxide
VEGF	vascular endothelial growth factor

8.1 Introduction

The human body is fortified with an efficient reparative mechanism to tackle certain defects caused by diseases or accidents. Yet, when it comes to dealing with large or complicated defects, the native healing machinery fails due to congenital limitations [1]. However, materials available in nature, either in pure or in processed form, have been explored to repair those defects [2,3]. For instance, silk threads (natural polymer) were used as sutures to close wounds, gold plates (metal) were used to repair cranial fractures, and seashells (ceramic) were used to make artificial teeth. Subsequently, some accidental inventions or discoveries also led to the production of novel materials. For example, after discovering that shattered pieces of cockpit windshield were well-tolerated in the eyes of a pilot, the windshield material,

Hemocompatibility of Biomaterials for Clinical Applications. https://doi.org/10.1016/B978-0-08-100497-5.00015-X
© 2018 Elsevier Ltd. All rights reserved.

i.e., poly(methyl methacrylate) (a synthetic polymer) was used to make artificial intraocular lenses. Consequently, metals, polymers, and ceramics were explored in various combinations to prepare new materials (composites) for a range of medical applications. Lately, these *materials intended to interface with biological systems* are termed as "biomedical materials" or simply "biomaterials" [4]. So far, while there are several noted eureka moments in biomaterials research, we believe there are innumerable moments of distress. This is because, irrespective of our good intentions, the native healing machinery reminds us of the limitations in its own way, i.e., by rejecting some under given circumstances [5]. Whereas there is no way to make a universal "biocompatible material," there are ways in which we can modify them in order to realize a "biocompatible system" [6]. While much of the latest biomaterials research has focused on achieving a fascinating tissue response, one should not ignore the fundamental fact that these biomaterials invariably interact with blood or blood components in the first place and therefore, it is of foremost importance to ensure that they are accepted by blood or in other words to achieve an acceptable blood-biomaterials interactions [7,8].

In this chapter, we begin with a brief biological account of blood-biomaterials interactions to give an insight into the considerations while modifying the biomaterials (Section 8.2); this is followed by a description of various approaches to enhance blood compatibility (Section 8.3). We then conclude with a summary and notes on future prospects (Section 8.4). In particular, this chapter highlights, under Section 8.3, the state-of-the-art biomaterials modification methods, which we broadly categorize into four classes (Fig. 8.1). The first class (Section 8.3.1) includes physical methods which aim to modify the surface by altering hydrophobicity, surface charge, etc. Here we cover plasma treatment approaches as they are simple and one-step. The second class (Section 8.3.2) describes the chemical methods but, as these are widely explored and there is a vast amount of literature in the field, this section is subdivided into three groups. Section (8.3.2.1) covers methods that aim to introduce functional groups such as $-NH_2$ by simple one-step reactions such as aminolysis. Section (8.3.2.2) highlights methods that focus on immobilizing the hemocompatible molecules such as heparin, by means of simple physical adsorption or blending. Section (8.3.2.3) describes the methods that involve the covalent crosslinking of blood compatible molecules, such as heparin, either by chemical, photo, or enzymatic conjugation approaches. The third class (Section 8.3.3) discusses cellular methods which include preseeding of the biomaterials with cells, usually endothelial cells. The fourth and final class (Section 8.3.4) elaborates on other techniques that are not covered in any of the above classes. To the best of our knowledge, we cover the most popular, if not all, methods reported in the literature across various indexing platforms. The methods described herein are suitable for metallic, polymeric (both natural and synthetic), ceramics, and composite biomaterials that are made in the form of sheets, porous foams, membranes, etc., and are explored in clinical applications including, but not limited to, extracorporeal medical devices such as hemo-oxygenators, intracorporeal medical devices such as stents, and tissue engineered devices such as vascular grafts (Fig. 8.1). The chapter, therefore, is up-to-date and comprehensive in its scope.

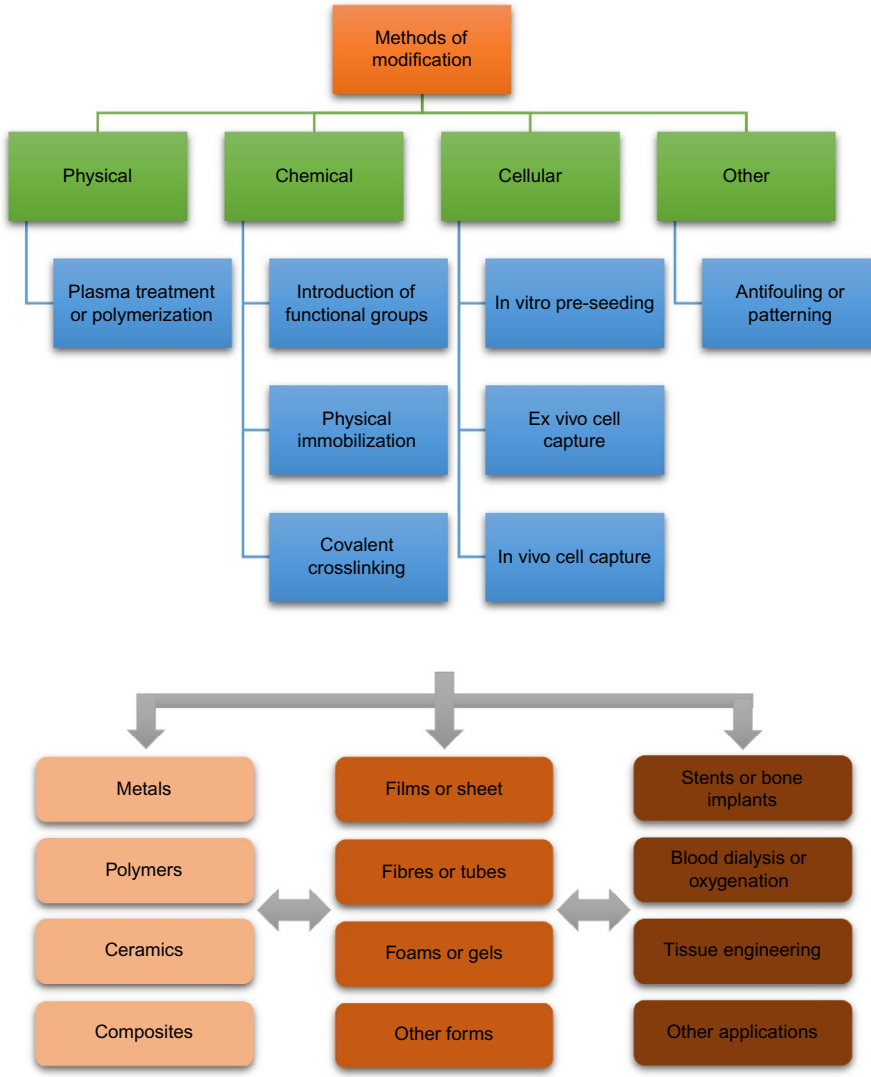


Fig. 8.1 A summary of various classes of biomaterial modification methods that are covered in this chapter, including their suitability for material types, product forms, and intended applications.

8.2 Blood and its interactions with interfaces

Blood is anatomically classified as a connective tissue and considered as a physiological transport fluid carrying not just gases, nutrients, and waste but also a multitude of cellular and extracellular factors that control its interactions with either a native or a foreign interface. In the native state, blood is maintained within a closed system

that is separated from the tissues it perfuses by a cellular barrier, the endothelium. This monolayer lining not only restricts the extracellular diffusion of molecules from plasma through paracelllar clefts and tight junctions but also possess both general and specialized mechanisms for regulating the interface with the blood components [9,10]. The external phospholipid is phosphatidyl choline, a zwitterionic lipid which is overall neutral at neutral pH. However, the membrane potential and zwitterionic properties will result in electric field and counter ion gradients. Endothelial cells also have a luminal glycocalyx, formed by integral membrane proteoglycans such as syndecan, extrinsic membrane proteoglycans such as glypicans and sequestered heparin [11]. Both these components are negatively charged and contribute substantively to the net endothelial surface charge [12]. The glycoclyx is also thought to sequester a boundary layer of proteins such as albumin; this has a major physiological function in maintaining the colloid osmotic pressure within the vasculature. [13]. Overall, the electrical, chemical, and mechanical structure of the endothelial surface is the quiescent interface between blood and tissue which acts as a natural reference point for any synthetic material.

The potential for interaction of materials with blood spans a range of complexity from the molecular level to the cellular, involving concerted biological responses (Fig. 8.2 and Table 8.1) [14–16]. One type of mediator in this process are humoral factors such as those in blood plasma. This cell-free fraction of blood consists of a large number of proteins that typically have globular nature thus presenting a hydrophilic and ionic surface to blood. Exposure to a foreign surface can alter protein conformation, perhaps due to change in entropy on binding, and may result in denaturation. These processes are likely to be irreversible and may potentially result in activating coagulation, complement, and innate or acquired immune responses. Among the diverse array of plasma proteins there are a number of which regulate significant physiological interactions with the vessel wall and with extracellular matrix [16,17]. This diverse set of proteins have varying propensities for binding to foreign bodies and foreign surfaces, opsonization, and therefore are important for blood-biomaterial interactions. In addition, consideration of specific cascades of coagulation and complement are highly relevant. An important proximal initiating event in coagulation is the surface expression of phosophatidylserine which is normally maintained on the internal bilayer membrane leaflet. Exposure to a foreign interface may switch this phospholipid to the exterior surface, by an enzymatic activity, and act as a binding site for factors that activate complement and coagulation cascades [18]. Therefore, a biomaterial surface that either directly provides sites for activating clotting factors or otherwise influences neighboring cells to provide sites for such factors is potentially hazardous as a blood-contacting implant.

Equally, the cellular components of blood play critical roles in blood-biomaterial interactions (Fig. 8.2 and Table 8.1) [16,19]. The most abundant cells in blood are erythrocytes, but adhesive activation of platelets (thrombocytes) is pivotal in thrombosis, by activating thrombin (factor II) in response to contact with a damaged tissue or a foreign body [20]. They have integrin receptors which bind to collagen, fibronectin, vitronectin, fibrin, von Willebrand factor, and VCAM. Such specific adhesion

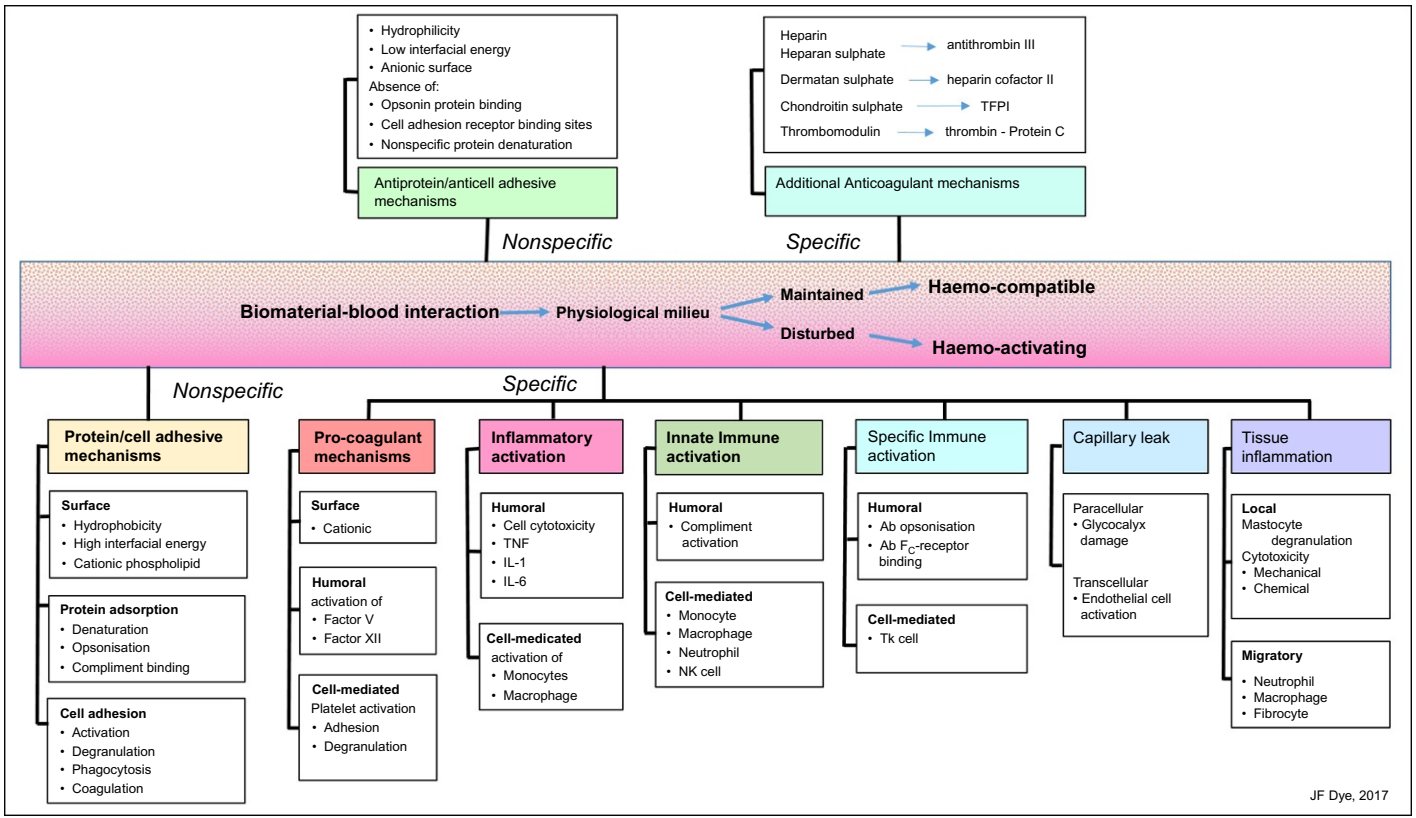


Fig. 8.2 Mechanisms of blood-biomaterial interactions leading to hemocompatibility or hemoactivation: hemocompatibility may be achieved by exploiting specific or nonspecific mechanisms which stabilize circulating blood. A number of pathways leading to activation of coagulation complement, inflammatory, or immune responses may also be triggered by specific or nonspecific interactions.

Table 8.1 Acellular and cellular components of blood relevant to biomaterial interactions

Anticoagulant mechanisms

Factor	Binding function(s)	Potential response
Antithrombin III	Heparin and heparan sulfate	Inhibits thrombin and factors XIa and Xa
Thrombomodulin CD141	Thrombin	Activates protein C
Heparin cofactor II	Dermatan sulfate	Inhibits thrombin
Tissue factor pathway inhibitor	Chondroitin sulfate	Inhibits VIIa and Xa

Acellular components

Factor	Binding function(s)	Potential response
Fibronectin	Integrin α4β1 and αVβ3, fibrin, heparan sulfate	Platelet adhesion, opsonization cell migration
Vitronectin	Integrin αVβ3 and platelet GpIb	Fibrinolysis (PAI-1 binding) and hemostasis
Von Willebrand factor (vWF)	Heparin, factor VIII	Hemostasis and platelet adhesion (a11bB3)
Ficollins (FNC1, FNC2, FNC3)	Ficol-recognition lectins	Lectin pathway of complement activation
Collectins (mannose binding protein)	N-Acetylglucosamine	Lectin pathway of complement activation
C-reactive protein	Phosphatidylcholine	Complement activation
Complement proteins (C3 and C4)	ECM proteins	Killer cell activation, complement activation
Immunoglobulins (IgM, IgG, IgA, and IgD)	Specific antigen binding	Cell mediated immune responses (phagocytosis or cytotoxicity)

Cellular components

Cell type	Factor(s) released	Potential response
Platelets	Thrombin, vWF, PDGF, VEGF, prostacyclin	Coagulation, degranulation
Neutrophils	Elastase, $HClO_4$, IL8	Phagocytosis, oxidative burst
Monocytes	TNFα and IL1β	Capillary adhesion, diapedesis, and activation
Macrophages (MI and M II response)	TNFα, IL1β, IL6, IL12, IL17 IL4, IL10, VEGF	Adhesion, phagocytosis, diapedesis, and activation
Mastocytes	Histamine, heparin, tryptase, bFGF VEGF	Immune activated degranulation
Fibrocytes, mesenchymal stem cells, endothelial progenitor cells	TGFβ, VEGF, CCN3	Adhesion, diapedesis, differentiation, proliferation
NK cells	Cathepsins, defensins	Cell-mediated cytotoxicity, adhesion, and diapedesis

events result in activation, degranulation, and coagulation. Other critical cell types are monocytes, which bind to exposed ECM and activated endothelial cells, and migrate through capillary walls into tissue stroma [21]. Similarly, macrophages (histiocytes) are critical in implant-host interactions as they produce inflammatory mediators which can orchestrate either type MI or MII inflammatory profiles [21]. The MI response is the production of pro-inflammatory cytokines, which results in a broad activation of immune responses, with local and systemic activation. The MII response is a relatively suppressed chronic inflammatory response profile. Mastocytes (mast cells) are lymphocyte-derived tissue resident cells which when activated result in potent localized inflammation and vascular leakage, and are thus relevant to consideration of blood material interactions for certain implants and loci [22]. More minor but very significant cell types are fibrocytes, endothelial progenitors, and mesenchymal stem cells which contribute to wound granulation [23]. In summary, in considering potential material interactions with blood components, it is important to have an overview of the range of interaction phenomena, both cellular—involving systemic physiological responses, and molecular—involving a variety of specific proteins in some cases exquisitely adapted to maintaining the homeostatic milieu.

8.3 Biomaterials modification techniques

8.3.1 Physical methods

Plasma treatment has long been recognized as an efficient method to modify the surface properties of biomaterials (Fig. 8.3). Plasma is regarded as the fourth state of matter and is a blend of diverse active species such as atoms, molecules, ions, electrons, radicals, photons etc. [24,25]. These species interact with a biomaterial and alters its physical and chemical structure, which in turn influences its topography, surface energy, and wettability [26,27]. It is not only popular for not involving any toxic chemicals but also for the fact that all the modifications occur at the top few nanometers of the interfacial region leaving the bulk properties unaffected. Depending on the material's chemistry, a variety of gases, such as oxygen, argon, ammonia, nitrogen, and sulfur, may be used to generate active plasmas [28]. For instance, Modic et al. treated a poly(ethylene terephthalate) (PET) film with weakly ionized highly nonequilibrium oxygen plasma and observed introduction of functional groups such as hydroxyl and carbonyl groups and increase in surface roughness; while there were 240 platelets per $100\,\mu m^2$ on the untreated sample, there were only about 60 platelets per $100\,\mu m^2$ on the treated sample [29]. Plasma treatment was also used to modify the surface in order to enhance its interactions with endothelial cells. To this end, Solouk et al. prepared a polyhedral oligomeric silsesquioxane and poly(carbonate-urea) urethane based polymer sheet and subjected it to oxygen plasma. A significant decrease in wettability, as evident from a change in water contact angle from 89 to 8 degrees, and significant increase in oxygen containing species on the surface as observed by Fourier transform infrared spectroscopy and energy dispersive X-ray spectroscopy, were noted.

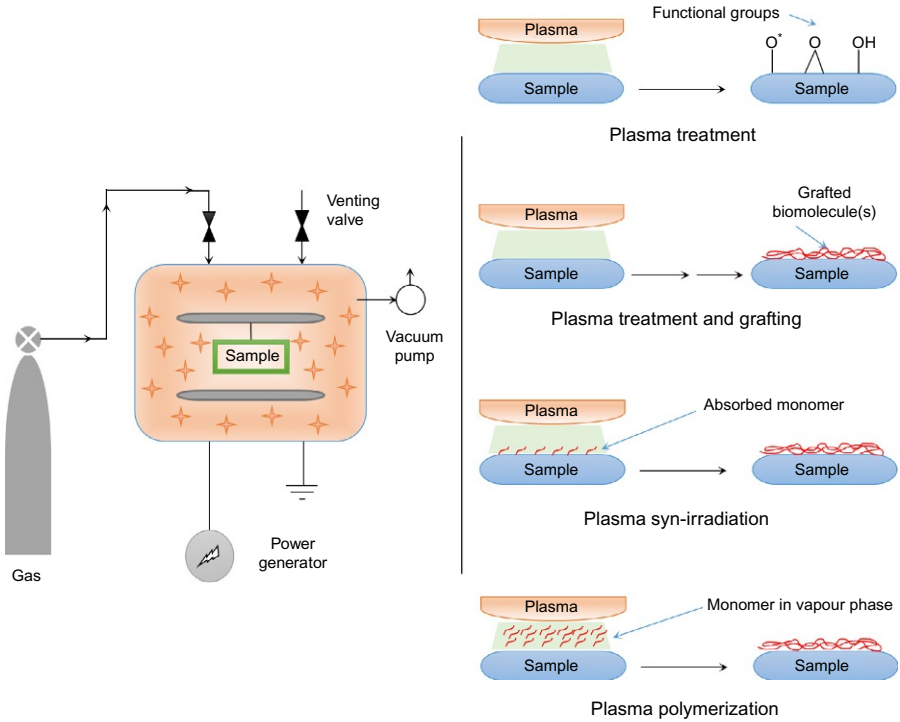


Fig. 8.3 Schematic of a typical plasma treatment reactor and different approaches thereof to alter the biomaterial's surface properties.

More importantly, human umbilical vein endothelial cells (HUVECs) cultured on plasma-treated films showed a significant increase in cell number in comparison to those on untreated films [30].

Plasma treatment is not limited to flat biomaterials, rather it can be used for biomaterials of any shape and size. For instance, Huang et al. used commercially available poly (4-methyl-1-pentene) based hollow fiber membranes that were popular for their use as membrane oxygenators, otherwise known as artificial lung or gas exchange devices. After O_2 plasma treatment and subsequent treatment with $NaBH_4$, the surface chemistry was modified to contain hydroxyl groups. Such changes led to a significant reduction in protein adsorption from ~35 to ~5 μg/cm^2 and in platelet adhesion from ~4×10^7 to ~1×10^7/cm^2 [31]. Similarly, plasma modification is not restricted to polymers, but can be used for other biomaterials as well. Lin et al. reported the preparation of plasma-nitrided austenitic stainless steel using a microwave system, and described that the treated samples showed significantly reduced platelet adhesion and activation and prolonged clotting time (Fig. 8.4) [32]. Conventionally, plasma treatment was majorly explored to modify the hydrophilicity of the material's surface, however lately, the functional groups that have been generated from plasma treatment were explored for further processing steps to incorporate additional biomolecules. For

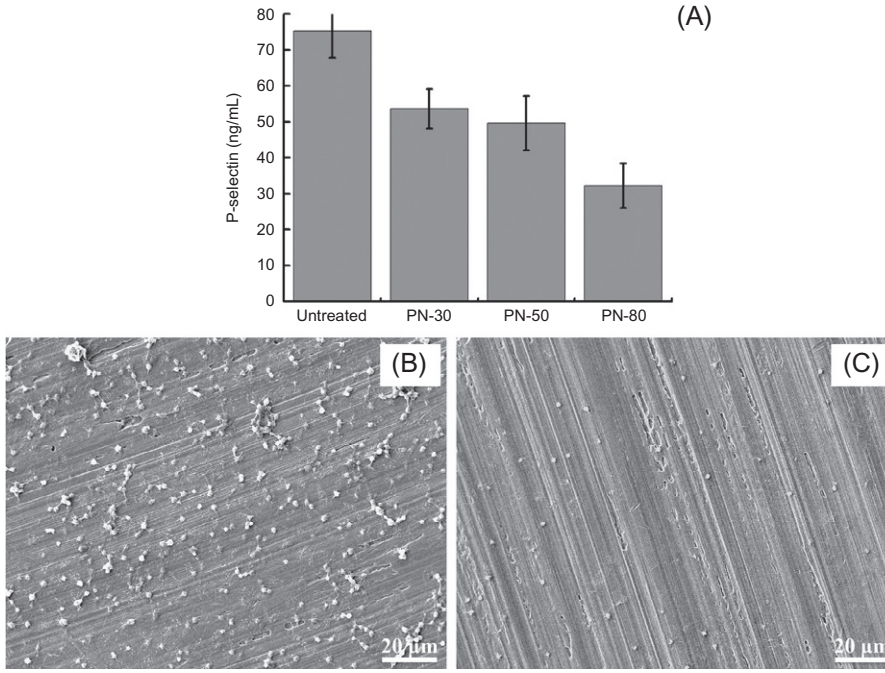


Fig. 8.4 Plasma treatment led to a significant reduction in platelet adhesion and activation on plasma-nitrided (PN) austenitic stainless steel surfaces: (A) platelet activation as indicated by P-selectin release as a function of plasma treatment time, and (B,C) SEM images of adherent platelets on untreated and treated specimens, respectively.
Reproduced with permission from Y.-H. Lin, W.-C. Lan, K.-L. Ou, C.-M. Liu, P.-W. Peng, Hemocompatibility evaluation of plasma-nitrided austenitic stainless steels at low temperature, Surf. Coat. Technol. 206 (2012) 4785–4790. Copyright 2012 Elsevier.

example, Huang et al. modified the hydroxylated-poly (4-methyl-1-pentene) substrates with N_2 plasma to create reactive oxygen species on the surface which were subsequently used for immobilization of heparin [31]. Alternatively, others have explored the plasma treatment in an innovative way such as plasma polymerization and plasma syn-irradiation where a monomer is subjected to react with the substrate and another monomer in a chain reaction to make polymers on the surface [25,33]. Examples include the surface modification of segmented poly(ether urethane) by graft copolymerization with *N*,*N*′-dimethyl-*N*-methacryloyloxyethyl-*N*-(3-sulfopropyl) ammonium in the presence of O_2 plasma, described by Yuan et al. [34].

8.3.2 Chemical methods

8.3.2.1 Methods that introduce functional groups

Alternatively, the surface chemistry of the biomaterials may be modified by simple chemical reactions such as sulfation and aminolysis. For example, the aminolysis

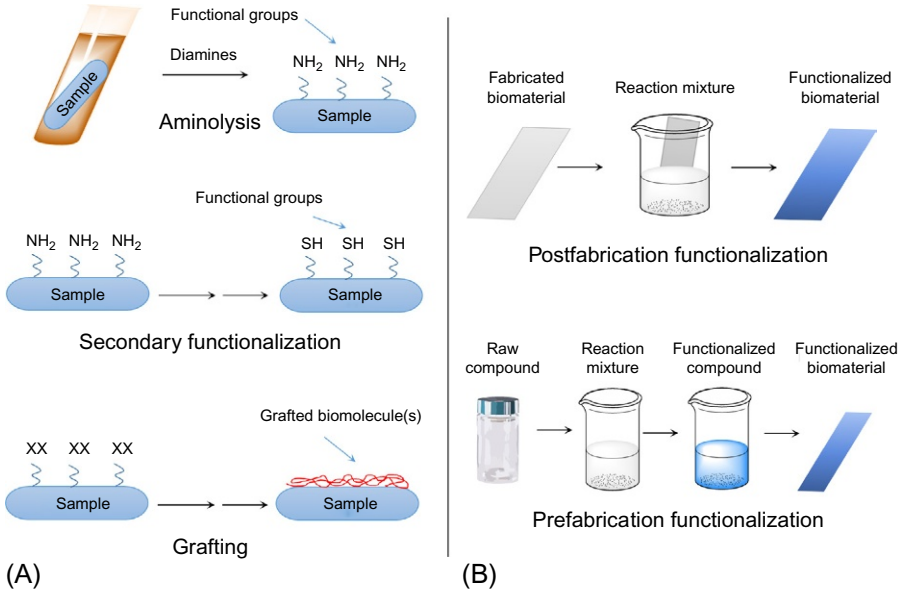


Fig. 8.5 A schematic showing the introduction of amine groups by aminolysis and subsequent secondary functionalization approaches (A); and the possibility of exploring such methods either at post- or at prefabrication levels (B) (xx can be any functional group).

involves cleavage of the ester backbone of polyesters, and subsequent introduction of NH_2 groups (Fig. 8.5). The reaction involves treatment of the biomaterial of interest in a solution of diamine such as 1,6-hexanediamine. Zhu et al. demonstrated that the type and concentration of diamine, type of solvent, reaction temperature, and time may be altered in order to achieve the desired amount of functional groups on the biomaterials surface [35]. The resultant $-NH_2$ and $-OH$ groups may further be explored in secondary reactions to incorporate other functional groups such as $-SH$, $-COOH$ or $-CH=CH_2$ [31,36,37]. The reaction is possible with all polyester materials irrespective of the material shape and form; Zhu et al. described the aminolysis of solvent cast poly(caprolactone) (PCL) membranes [35], and Bech et al. reported the aminolysis of PET fibers [38]. Although the use of diamines was popular, the aminolysis reaction may also be possible by other means; Chen et al., unlike the conventional postfabrication modification step, combined the scaffold fabrication step with the modification step and produced surface modified porous poly(lactide) (PLA) foams [39], and Haddad et al. described the aminolysis of electrospun PLA membranes by treating with polyallylamine or polyvinylamine that contains high amounts of amine groups instead of typical diamines [40]. In any case, while aminolysis can on its own, enhance heamocompatibility by significantly reducing the hydrophobicity of the biomaterial, the functional groups generated by the aminolysis reaction can be explored to develop additional molecules that enhance the blood compatibility to the next level [41,42].

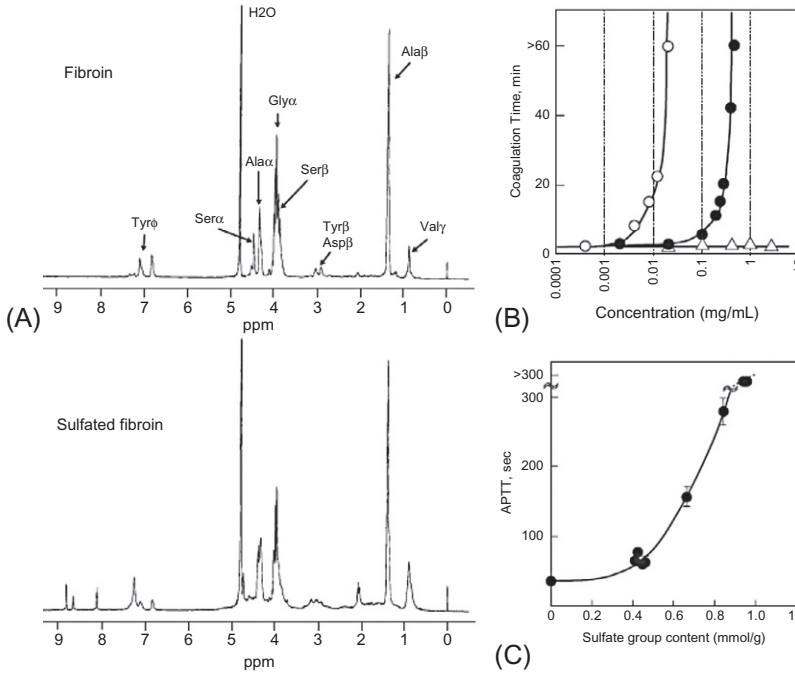


Fig. 8.6 Blood compatibility of sulfated silk fibroin: (A) ^{1}H NMR spectra of pristine and sulfated fibroin, (B) coagulation time of pristine fibroin (*triangles*), sulfated fibroin (*black circles*), and heparin (*white circles*), and (C) APTT of sulfated fibroin with varying amounts of sulfate moieties.
Reproduced with permission fromY. Tamada, Sulfation of silk fibroin by chlorosulfonic acid and the anticoagulant activity, Biomaterials 25 (2004) 377–383. Copyright 2004 Elsevier.

Recognizing the importance of sulfate moieties of heparin in its anticoagulant activity, many researchers came up with the idea of introducing sulfate groups on the biomaterial's surface. For instance, silk fibroin was sulfated by treating with chlorosulfonic acid. The concentration of acid, reaction temperature, and time may be altered in order to achieve the desired amount of sulfate groups on the biomaterial's surface. The reaction is possible irrespective of the material shape and form. For example, Tamada prepared sulfated silk fibroin and found that it prolonged whole blood coagulation time similar to heparin, while pristine fibroin failed to stop coagulation (Fig. 8.6) [43]. Similarly, Kasoju and Bora subjected a micro-nano fibrous silk fibroin scaffold to sulfation and found that the platelet adhesion was reduced by 60% when compared to a pristine scaffold [44]. Sulfation is not just limited to silk or any protein-based polymers. Magnani et al. and Barbucci et al. synthesized hyaluronic acid derivatives with a varying degree of sulfation (HyalSx where x can be 1–4), and showed that $HyalS_{2.5}$ up to $HyalS_4$ significantly prolonged the whole blood clotting time and that $HyalS_4$ resisted thrombin stimulation to a similar extent as heparin [45,46]. Muzzarelli et al. prepared sulfated chitosan by treating *N*-(carboxymethyl)chitosan with sulfuric acid and found that sulfated chitosan in association with antithrombin inhibited thrombin

and factor Xa in human blood [47]. Lately, Huang et al. described the synthesis of polyurea-based synthetic glycopolymers containing sulfated carbohydrates, such as glucose, mannose, glucosamine, or lactose, as pendant groups and found that the mannose and lactose-based biomaterials had the highest anticoagulant activities in terms of activated partial thromboplastin time (APTT), partial thromboplastin time, and thrombin time [48]. In any case, the sulfated biomaterials may be used on their own or may be used to make composite biomaterials [49].

8.3.2.2 *Methods that uses hemocompatible molecules: Physical immobilization approaches*

While plasma or chemical functionalization based approaches may well be able to modify the surface properties, they may not be effective in preventing the thrombosis altogether. Alternatively, functionalization of biomaterials with heparin and heparin-like hemocompatible molecules was proven to be relatively superior in achieving enhanced hemocompatibility (Fig. 8.7) [50,51]. Following direct adsorption approach, Niimi et al. demonstrated that heparin coating of the polypropylene based hemo-oxygenator fibers significantly reduced platelet adhesion on the surface [52]. Similarly,

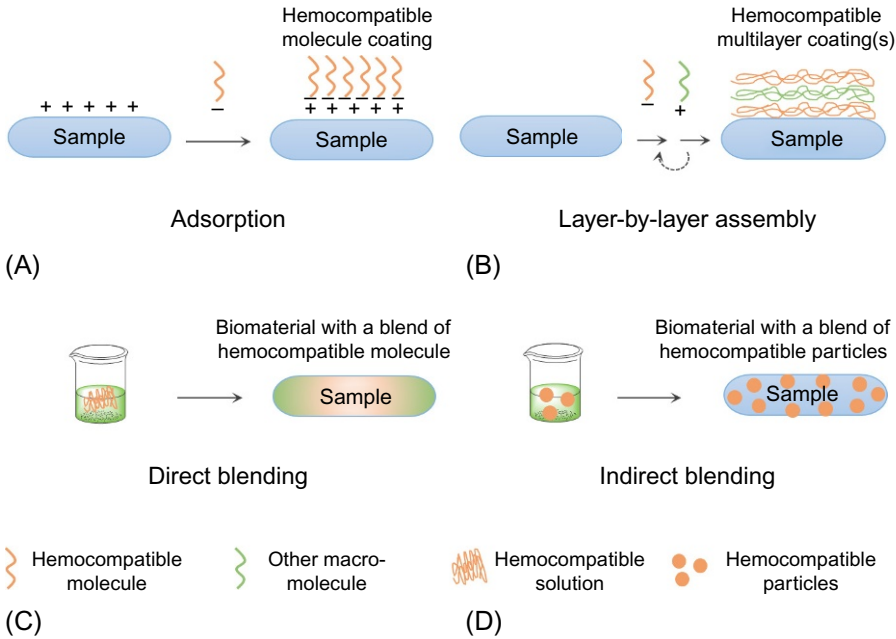


Fig. 8.7 Schematic of various physical immobilization approaches: (A) direct adsorption of hemocompatible molecule based on charge or affinity, (B) layer-by-layer assembly of oppositely charged molecules, of which negatively charged molecules is typically heparin or heparin-like molecules, (C) direct blending of hemocompatible molecule with that of a polymer solution prior to fabrication, and (D) blending of particles loaded with hemocompatible molecule with a polymer solution prior to fabrication.

recombinant human thrombomodulin coated polysulfone-polyvinylpyrrolidone based dialyzer membranes inhibited blood clot formation for over 4 h; but unlike heparin, thrombomodulin did not influence activated clotting time [53]. Some other examples include dip-coating of heparin onto hydrogel-coated angioplasty balloon catheters [54], and onto cardiopulmonary bypass circuits [55]. To strengthen heparin immobilization, interest in using mussel-inspired adhesion molecule polydopamine has increased, mainly because of its strong binding capability to different substrates and secondary reactivity [56]. This was explored by Yang et al. to load heparin unto 316 L stainless steel plates to improve its hemocompatibility both in vitro and in vivo [57]. In another example, electrodeposition technique was used for coating titanium substrates with nanostructured bioactive heparin-hydroxyapatite composite [58].

In recent times, alternative approaches such as layer-by-layer deposition of heparin onto a variety of biomaterials have been examined, mainly to increase loading efficiency and attain sustained release. Following the concept introduced by Decher et al. [59], Li et al. demonstrated the deposition of alternative layers of oppositely charged heparin and fibronectin onto titanium implants [60]. Similarly, Su et al. developed a dual drug-eluting stent, using Duraflo heparin and sirolimus multilayer coating on Multi-Link PIXEL stent, which showed prolonged resistance to thrombosis (Fig. 8.8) [61]. Such layer-by-layer approach was successfully demonstrated on a number of substrates, including glass [62], polymer membrane [63], and layered double hydroxide [64]. When the use of oppositely charged macromolecules is not feasible, or to further enhance the sustainability of the hemocompatible molecules, other indirect surface immobilization approaches may be explored. For instance, Kim et al. prepared a drug-eluting cobalt-chromium metal stent by first ultrasonically spraying a layer of sirolimus-loaded poly(lactide-*co*-glycolide) (PLGA) and then by coating a layer of heparin-loaded calcium alginate; the platelet adhesion was reduced from 1029 to about 84 cells/mm^2 [65]. In another example, Wei et al. prepared heparin loaded mesoporous silica particles and then coated these particles onto surface of various substrates such as silicon wafer, glass, and polyvinylchloride [66].

In contrast to postfabrication surface level immobilization, heparin and heparin-like hemocompatible molecules may be blended with biomaterials while fabrication process. Such bulk loading was achieved by direct mixing or blending of heparin with polymer solutions to fabricate films [67], small diameter venous grafts [68], or electrospun mats [69]. Similarly, heparin-like hemocompatible molecules such as sulfated-chitosan was also blended with polymers like poly(ethersulfone) (PES) to make membranes which showed reduced platelet adhesion and activation as compared to those made of PES and pristine chitosan [49]. However, heparin solubility and miscibility of blend solvents make this approach not attractive in many cases. Alternatively, high heparin amounts may be achieved by other indirect blending approaches. For instance, Moon et al. demonstrated a novel formulation for sustained release of heparin-deoxycholic acid conjugate dispersed as nanoparticles in polyurethane film [70]. Since the release of loaded molecules depend on the degree of erosion or degradation of biomaterial, such bulk loading approaches may further prolong the hemocompatibility efficiency of the resultant product. However, unlike surface level coatings, such bulk loading methods may influence the overall material properties [69].

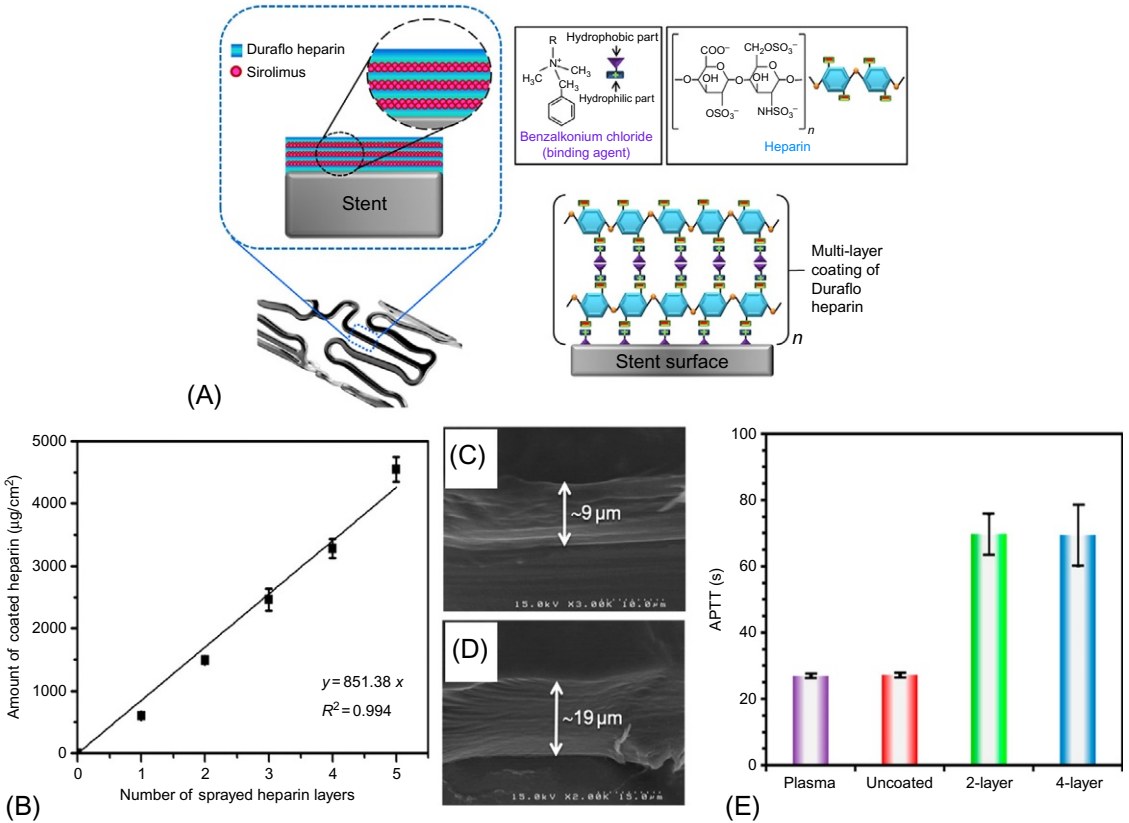


Fig. 8.8 Drug-eluting stent prepared by physical immobilization of multilayer coatings of Duraflo heparin and sirolimus: (A) schematic illustration of the stent composition, (B) a plot showing the amount of loaded heparin as a function of number of layers, (C) and (D) SEM images of a stent coated with 2 and 4 layers, respectively, and (E) changes in APTT of coated vs uncoated stents.
Reproduced with permission from L.-C. Su, Y.-H. Chen, M.-C. Chen, Dual drug-eluting stents coated with multilayers of hydrophobic heparin and sirolimus, ACS Appl. Mater. Interfaces 5 (2013) 12944–12953. Copyright 2013 American Chemical Society.

8.3.2.3 *Methods that use hemocompatible molecules: Covalent crosslinking approaches*

Covalent immobilization of hemocompatible molecules on the biomaterial surfaces is perhaps a desirable approach to achieve stronger immobilization, unlike physical adsorption, but without affecting bulk properties, unlike blending strategy (Fig. 8.9) [71]. Chemical crosslinking is a predominant approach mainly because of the availability of an array of intercalating and nonintercalating crosslinkers that can react with a variety of functional groups of biomaterials. One of the most widely used intercalating crosslinking agent is glutaraldehyde (GA). With its two terminal −COH groups, it can react with −OH or $-NH_2$ groups of various polymers. Recently in an attempt to achieve a biomimetic interface, Haungfu et al. immobilized phosphorylcholine (PC) onto a chitosan (CS) film using GA as a crosslinker, the resultant CS-GA-PC films showed about 70% less protein adsorption and nearly 90% reduced platelet adhesion compared to CS-GA films [72]. The GA-based crosslinking improves the bulk properties of biomaterials such as stiffness but, due to associated cytotoxicity, it should be used at a concentration lower than 8% [71]. Another example of such intercalating crosslinking agent is genipin [73,74]. Using such agents, Kim et al. and few others have demonstrated the immobilization of hemocompatible molecules on various biomaterials [33,75–78].

Due to toxicity of intercalating crosslinkers, methods involving the use of nonintercalating agents have been developed. Amongst these, a combination of EDC and *N*-hydroxysuccinimide (NHS) is the most widely explored. Several antithrombogenic agents such as heparin and hirudin were successfully immobilized on to a number

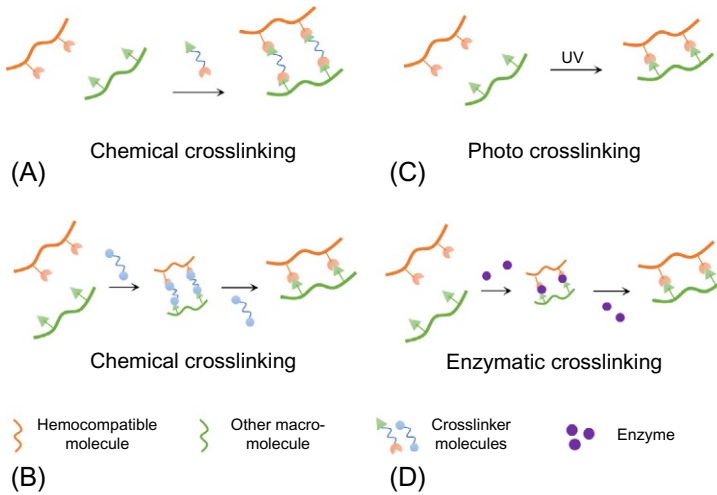


Fig. 8.9 Schematic of various covalent immobilization approaches: (A) chemical crosslinking where a crosslinker being incorporated into the bond, (B) chemical crosslinking where a crosslinker exits the reaction after bonding, (C) photo crosslinking where a UV or a laser energy source is used as a catalyser, and (D) enzymatic crosslinking where an enzyme acts as a catalyser.

of biomaterial surfaces following such carbodiimide coupling chemistry [79–81]. In a typical reaction, EDC reacts with −COOH groups of a hemocompatible molecule to form an activated but unstable complex, which then reacts with NHS to form another intermediate complex; this finally reacts with $-NH_2$ groups of another (or same) macromolecule to form a stable conjugate [78]. Following this principle, heparin was immobilized onto aminolyzed PLA films [82], collageno-elastic grafts [83], and various other biomaterials [84–86]. One example of clinical relevance includes the work of Hoshi et al, who described the immobilization of heparin onto aminated poly(1,8-octanediol-*co*-citrate) (POC) coated expanded poly(tetrafluoroethylene) (ePTFE) vascular grafts and showed that the whole blood clot formation was reduced from 70% to 15% (Fig. 8.10) [87]. EDC/NHS crosslinking chemistry may be explored in alternative ways to improve hemocompatibility. For example, Li et al. immobilized anti-CD34 antibody, following EDC/NHS chemistry, onto a PLA-based polymer coated stent to achieve endothelialization [88]. However, the concentration of EDC/NHS and time of crosslinking needs careful consideration [36,89].

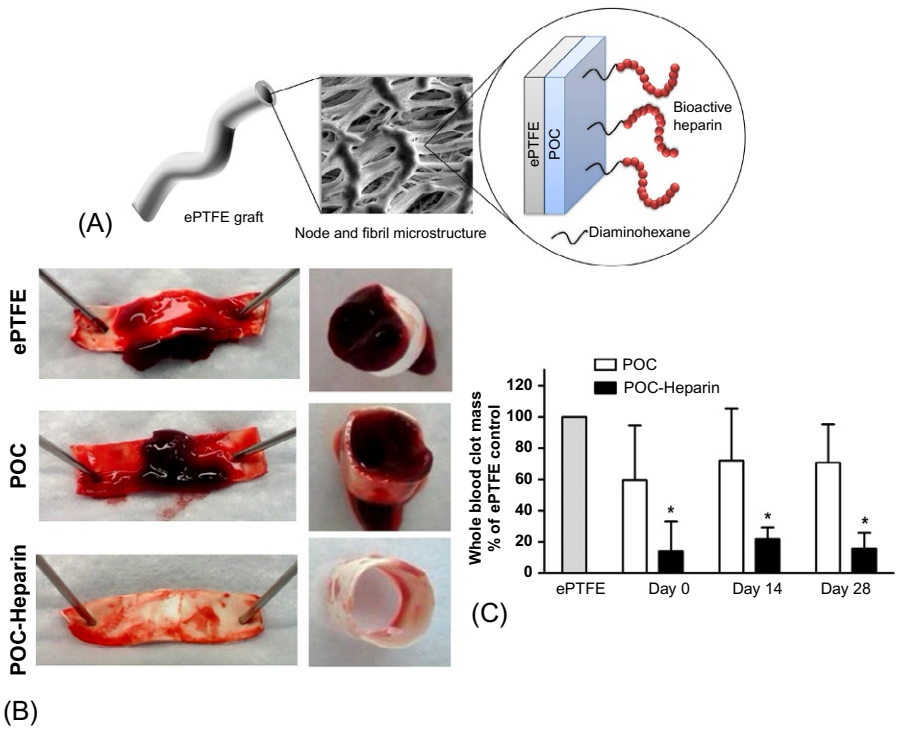


Fig. 8.10 Schematic of a heparinized POC-ePTFE vascular graft (A), and qualitative (B) and quantitative (C) data on whole blood clot formation on test (POC-Heparin) and control (POC and ePTFE) grafts; $*p < 0.05$, significantly less than ePTFE and POC.
Reproduced with permission from R.A. Hoshi, R. van Lith, M.C. Jen, J.B. Allen, K.A. Lapidos, G. Ameer, The blood and vascular cell compatibility of heparin-modified ePTFE vascular grafts, Biomaterials 34 (2013) 30–41. Copyright 2013 Elsevier.

Alternatively, UV or other irradiation based photo crosslinking strategies may be employed to avoid the undesirable effects of chemical crosslinkers or their by-products [71,90]. Following this approach, alginate/heparin based layer-by-layer assembly was coated onto Nitinol—a metal alloy of nickel and titanium. As a result, as evident from a change in APTT of 30–100 s, the clotting time was significantly enhanced [91]. Recently, Xuemin Yu et al. improved the hemocompatibility of PLA membrane by photo crosslinking-based PEGylation, where poly(ethylene glycol)diacrylate (PEGDA) with two active terminal groups was cross linked via UV-generated free radicals which induced polymerization of PEGDA to form self-cross linking networks by persistent immobilization on PLA membrane [92]. Another way of achieving covalent immobilization of hemocompatible molecules onto biomaterials surface is by using enzymes, such as transglutaminase which catalyzes an acyl-transfer reaction between the ε-amino group of lysine residue and the γ-carboximide group of glutamine residue to form an isopeptide bond [71,93]. Some of the successful examples include, a recombinant human elastin-like polypeptide based vascular tissue engineering scaffold that showed excellent compatibility with HUVECs [93], and a 3D patterned PCL-based bioartificial blood vessel construct [94].

8.3.3 Cellular methods

The best way to achieve a positive blood-biomaterials interaction, is by recapitulating a biomimetic, cellular interface by capturing endothelial cells onto the biomaterials surface (Fig. 8.11) [95]. To this end, Bos et al. demonstrated that a conventional polystyrene petri dish seeded with HUVECs (at a rate of 10,000 cells/cm^2 and cultured in vitro for 4 h), upon incubation with platelet cell suspension (1 mL, with 1×10^5 platelets/uL) for 1 h, showed a remarkable 10-fold decrease in the platelet adhesion count when compared to a nonseeded surface. It was also interesting to note that preseeding the surfaces was significantly more effective than using surfaces modified with heparin, albumin, or fibronectin [96]. However, one may have to modify the material's surface in order to enhance the endothelial cell adhesion. Cornelissen et al. showed that the sheets of polypropylene, polyoxymethylpentene, and polydimethylsiloxane, materials usually considered for oxygenator gas exchange membranes, need coating with cell-adhesion promoting molecules such as collagen, fibrinogen, gelatin, or fibronectin in order to enhance the endothelialization [97]. The endothelialization approach may also be adapted to functionalize biomaterials made of metals such as titanium; but even in this case, initial modification with laminin or heparin may be necessary to improve endothelial cell adhesion [98]. Yet, to promote endothelialization, such primary surface modification may not be necessary for biological scaffolds, such as decellularized materials, since they already possess the native extracellular matrix components. For example, Schopka et al. prepared a decellularized and glutaraldehyde-fixed bovine pericardium and without any further chemical modification, preseeded the pericardium with human vascular fibroblasts and endothelial cells from saphenous veins in vitro. The results showed that the recellularized biomaterials did attract less platelets and inflammatory cells; thus confirming that a biologically derived material needs endothelialization to enhance

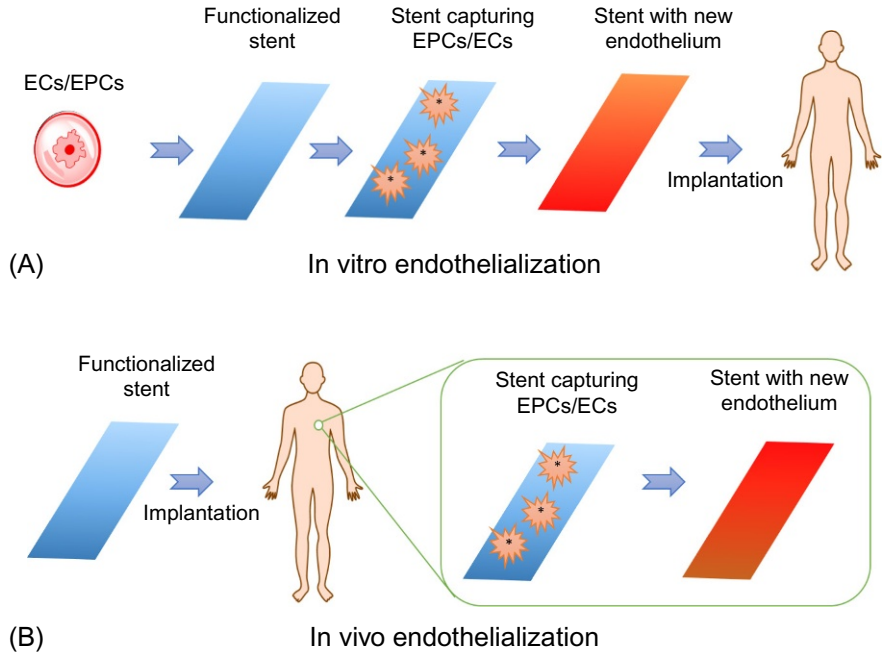


Fig. 8.11 A schematic of the endothelialization process for recapitulating a cellular interface on a biomaterial surface functionalized with cell capturing moieties. In vitro approach includes isolation and expansion of autologous EPCs or ECs, seeding onto the material, culturing until confluence is reached, followed by implantation (A). In vivo approach includes implantation of functionalized biomaterial into the patient where the circulating EPCs or ECs are captured to create an endothelium (B).

blood compatibility, but there is no need for chemical functionalization to encourage endothelial cell adhesion [99].

However, due to lack of sufficient donor endothelial cells, complexities in endothelial cell isolation and potential allogenic reactions, attempts were made to find alternative approaches by modifying the biomaterials in a manner that enables the capture of endothelial cells in vivo. Antibodies are now explored in several translational multidisciplinary projects involving cell sorting and capture in view of their high specificity and affinity towards antigens. Endothelial progenitor cells (EPCs) and endothelial cells express specific cell surface markers such as CD34, CD144, vascular endothelial growth factor (VEGF), and CD133. The biomaterials of interest, for example a stent material, may be functionalized with antibodies against such markers in order to capture those cells. To this end, an anti-CD34 antibody coated EPC capture stent was developed and commercialized as Genous stent (Fig. 8.12) (OrbusNeich, Fort Lauderdale, Florida) [100,101]. Lately, Li et al. demonstrated that anti-CD144 antibody coated stents were superior to Genous stents [102]. Alternatively, developments in materials engineering led to the development of magnetic and nanomaterials. Uthamaraj et al. explored such materials along with autologous endothelial cells

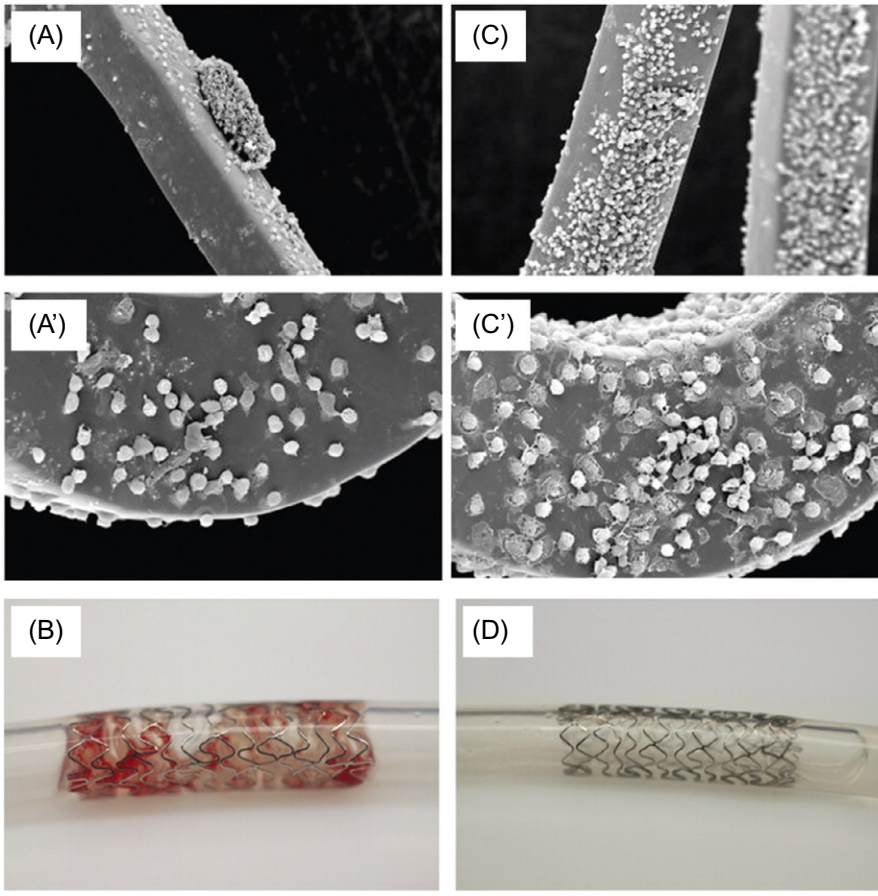


Fig. 8.12 Human arteriovenous shunt model revealed that a EPCs capturing stent showed a marked increase in cell adhesion with a flattened polygonal morphology (A, low and A', high magnification SEM images) and no or low thrombi (B), as compared to a bare-metal stent (C, low and C', high magnification SEM images, and D, image showing thrombi).
Reproduced from K. Larsen, C. Cheng, D. Tempel, S. Parker, S. Yazdani, W.K. den Dekker, J. H. Houtgraaf, R. de Jong, S. Swager-Ten Hoor, E. Ligtenberg, S.R. Hanson, S. Rowland, F. Kolodgie, P.W. Serruys, R. Virmani, H.J. Duckers, Capture of circulatory endothelial progenitor cells and accelerated re-endothelialization of a bio-engineered stent in human ex vivo shunt and rabbit denudation model, Eur. Heart J. 33 (2012) 120–128. Copyright 2011 Larsen et al.

[103–105]. The method included (a) collection of blood from the host animal, isolation of endothelial outgrowth cells (EOCs) and labeling with superparamagnetic iron oxide nanoparticles (SPION), (b) preparation of a weakly ferromagnetic stent from 2205 duplex stainless steel, and by (c) implantation of the stent along with EOCs using a custom made device by occluding the blood flow at the site of implantation for a definite time. This method successfully showed that magnetic stents can attract

and retain SPION labeled autologous EOCs in vivo. In view of concerns associated with nanotoxicity, perhaps the antibody based affinity based cell may be a safer approach. Besides magnetism and antibodies, recent innovations in chemical biology led to the rise of another class of molecules called aptamers for cell capture [106–109]. Aptamers are oligonucleotides or oligopeptides synthesized by following systematic evolution of ligands by exponential enrichment (SELEX) [110]. They have the same selectivity and specificity as conventional antibodies. In an in vivo study, Sim et al. established that EPCs-specific aptamers-coated cobalt-chromium stents successfully led to rapid reendothelization and reduced stent thrombosis compared to bare and drug-eluting stents [111].

8.3.4 Other methods

In contrast to the modifications that aim to modify the surfaces with a directly acting hemocompatible molecules such as heparin, there are alternative surface modification approaches that involve the incorporation of indirectly acting hemocompatible molecules such as antifouling or nonfouling polymers or polymer brushes that act by repelling the blood serum protein adsorption. For example, Jeon et al. demonstrated that surfaces modified with poly(ethylene oxide) (PEO) exhibits low protein adsorption. Though weak hydrophobic interactions between PEO and serum proteins were thought to be an underlying principle, many argue that it is the PEO chain-length dependant steric repulsions that contribute to poor fouling [112,113]. While initial studies rely on PEO, recent developments in polymer chemistry led to the synthesis of many such antifouling polymer brushes by atom transfer radical polymerization (ATRP). In this regard, de los Santos Pereira et al. synthesized poly(2-hydroxyethyl methacrylate) (PolyHEMA), poly(oligo(ethylene glycol) methyl ether methacrylate) (PolyMeOEGMA), poly(carboxybetaine acrylamide) (PolyCBAA), and poly(*N*-(2-hydroxypropyl)methacrylamide) (PolyHPMA) brushes on polycarbonate surfaces and demonstrated that all the polymer brushes under study exhibited a pronounced resistance to protein adsorption and marked reduction in thrombogenicity in relation to control substrate (Fig. 8.13) [114]. This is however not restricted to modeling two dimensional culture substrates, but rather adaptable to three dimensional biomaterial systems. For example, in order to prevent protein fouling of the electrospun PCL nanofibrous scaffolds, Kostina et al. modified the surface by using polymer brushes prepared according to the earlier study. Although the overall morphology of the scaffolds was preserved, there were changes in fiber diameter, but nevertheless, the polymer brush introduction reduced the amount of protein adsorbed from 1150 to a mere 3 pg/mm^2 [115].

Last but not the least, one may avoid all of the above described surface modification techniques and instead simply prepare the material with a surface hemocompatible topography. Koh et al. hypothesized that a precise topographic control may be a powerful approach to modulate platelet responses to a surface. Solvent casting using a master template was employed to fabricate PLGA films with various topographic features at the submicron meter level. The study demonstrated that the increased pillar height and aspect ratio reduces platelet adhesion, while increasing pillar width and

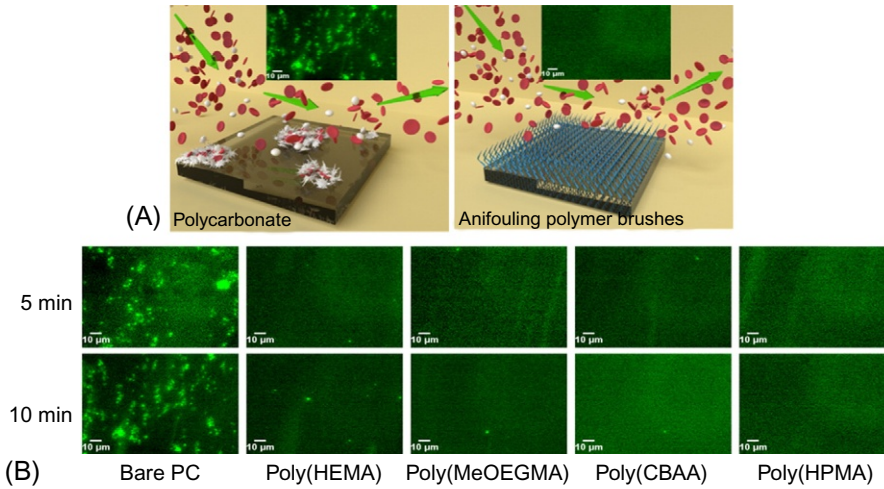


Fig. 8.13 A schematic showing the repelling property of antifouling polymer brush coatings on a polycarbonate substrate (A), and fluorescence microscopy images of polymer-brush-modified and bare substrates, after 5 and 10 min of contact with DiOC6-labeled blood (B). Reproduced with permission from A. de Los Santos Pereira, S. Sheikh, C. Blaszykowski, O. Pop-Georgievski, K. Fedorov, M. Thompson, C. Rodriguez-Emmenegger, Antifouling polymer brushes displaying antithrombogenic surface properties. Biomacromolecules 17 (2016) 1179–1185. Copyright 2016 American Chemical Society.

interspacing to >200 nm increases platelet adhesion/activation. The study suggests that a pillar height of 300–800 nm, width of 100–200 nm, and interspacing of <200 nm were optimal for reduced platelet activity [116]. In a similar study, Liu et al., demonstrated that a reduced level of platelet activity was achieved with a pillar height of 10–12 µm, width of 4–6 µm, and interspacing of 6–8 µm. Both these studies showed significant changes in platelet activity when the surface chemistry was changed with constant pillar features. It is therefore clear that there are no universal units and one needs to optimize depending on the material and its surface chemistry [117]. If for some reason the preparation of materials with such topographical features is not possible due to inability to cast or other reasons, one may simply create a composite structure by incorporating a topographically featured surface material onto the material of interest. For instance, Zhou et al. described a method to fabricate TiO_2 micromesh structures on a silicon substrate and successfully demonstrated its ability to reduce the amount of platelet adhesion (Fig. 8.14) [118].

8.4 Summary and future prospects

Biomaterials offer immense potential to expand the horizons of current clinical practice in many aspects. However, since the immune system is equipped to fight against any intruding foreign object(s), the development of biomaterials requires careful

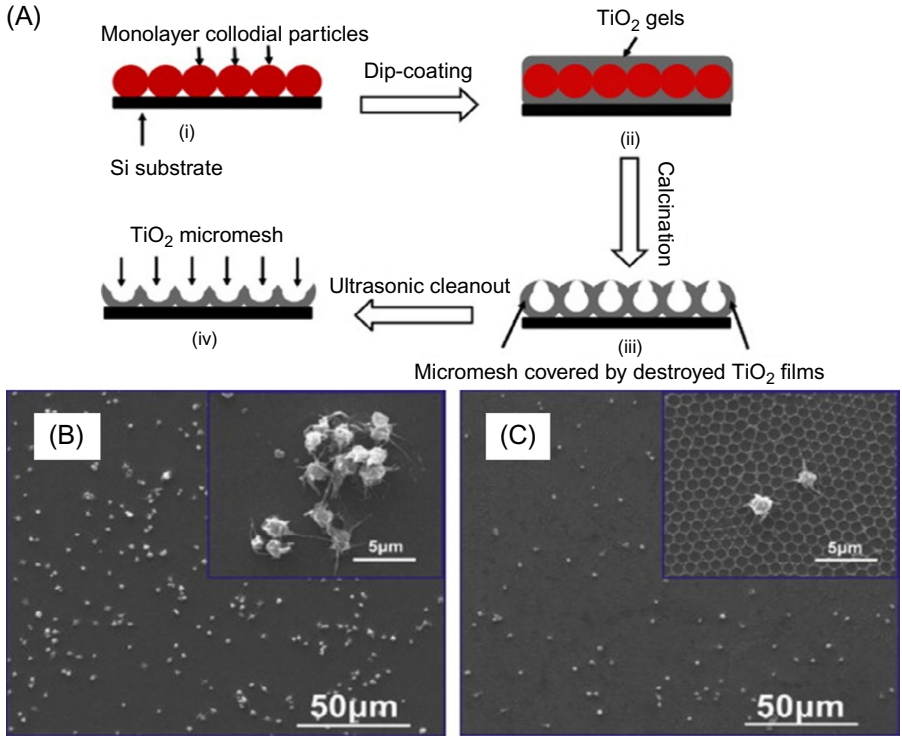


Fig. 8.14 A schematic of the preparation of TiO_2 micromesh by solution-dipping template strategy (A): (i) large area monolayer colloidal particles (template), (ii) the monolayer colloidal particles covered by TiO_2 gels, (iii) micromesh covered by destroyed TiO_2 films, and (iv) TiO_2 micromesh. SEM images of adherent platelets on (B) flat and (C) micromesh covered TiO_2 samples (insets, magnified images).
Reproduced with permission from Z. Zhou, J. Chen, L.-J. Xiang, Y. Xu, P. Yang, J.-A. Li, J.-J. Wu, N. Huang, Fabrication of 3D TiO_2 micromesh on silicon surface and its effects on platelet adhesion, Mater. Lett. 132 (2014) 149–152. Copyright 2014 Elsevier.

considerations with regard to managing its interactions with the body tissues, especially blood. To this end, several methods have been developed to achieve a considerable improvement in the blood compatibility. Physical methods such as plasma treatment have been the most widely used approach for a wide range of material types and forms. This method alters the wettability, charge and to some extent roughness at the surface level. Chemical methods such as amination and sulfation are equally simple and effective in modulating surface hydrophobicity and charge but without significant effects on roughness. Blood-biomaterial interactions may further be enhanced by coating the surface with heparin and heparin-like molecules by means of physical immobilization or covalent crosslinking. Alternatively, biomaterials may be functionalized to capture endothelial cells or EPCs in order to develop a biomimetic endothelial layer on the surface. Lately, innovative approaches such as the use of antifouling coatings were developed to repel the blood components and thereby avoid coagulation.

While some of these methods were explored in clinical applications, others are still in research and development stage. Some successful examples include drug eluting or cell capturing stent materials. We believe many more surface functionalized devices are perhaps under development. Yet, the field of biomaterials modification from the perspective of improving the blood compatibility is still evolving. For example, nitric oxide releasing polymers and an amino acid derivative functionalized polymer are being developed as an alternative to heparin or heparin-like polymers [119,120]. Biomaterials with a unique slippery liquid-infused porous surface (SLIPS) are under development to avoid fouling [121]. Since, one single biomaterial may not be universally acceptable similarly, one modification approach may not fit all. Therefore, we envisage a greater scope for the development of more innovative and alternative methods. However, based on the literature cited in this chapter and our understanding, we believe that the cellular based strategies (i.e., developing a biomimetic endothelial interface) may be worth considering for vascular grafts, stents, heart valves, or any other intracorporeal devices, whereas, the acellular modification strategies, especially those based on antifouling surfaces, may be considered for blood oxygenator, dialyzer, or any other extracorporeal devices.

Acknowledgments

Authors acknowledge China Regenerative Medicine International Limited, Hong Kong (http://www.crmi.hk) for funding, and Dr. Michelle Kümin (CRMI Technology Centre, University of Oxford, United Kingdom) for critical reading.

References

[1] H.L. Huiling Liu, C. Aaron, Y. Huilin, Y. Lei, New frontiers in biomaterials research for tissue repair and regeneration, Transl. Neurosci. Clin. 2 (2016) 120–137.
[2] E. Gentleman, M.D. Ball, M.M. Stevens, Biomaterials, in: B.P. Mansourian, A. Wojtczak, B.M. Sayers (Eds.), Medical Sciences, Eolss Publishers Co. Ltd., Oxford, 2009.
[3] V. Migonney, History of Biomaterials. in: V. Migonney (Ed.), Biomaterials, John Wiley & Sons, Hoboken, NJ, USA, 2014, https://doi.org/10.1002/9781119043553.ch1.
[4] D.F. Williams, On the nature of biomaterials, Biomaterials 30 (2009) 5897–5909.
[5] H. Uludağ, Grand challenges in biomaterials, Front. Bioeng. Biotechnol. 2 (2014) 43.
[6] D.F. Williams, There is no such thing as a biocompatible material, Biomaterials 35 (2014) 10009–10014.
[7] F. Jung, S. Braune, Thrombogenicity and hemocompatibility of biomaterials, Biointerphases 11 (2016). 029601.
[8] D.F. Williams, On the mechanisms of biocompatibility, Biomaterials 29 (2008) 2941–2953.
[9] M. Bundgaard, The paracellular pathway in capillary endothelia, in: S. Chien (Ed.), Vascular Endothelium in Health and Disease, Springer, Boston, MA, 1988.
[10] J.A. Firth, Endothelial barriers: from hypothetical pores to membrane proteins, J. Anat. 200 (2002) 541–548.
[11] S. Weinbaum, J.M. Tarbell, E.R. Damiano, The structure and function of the endothelial glycocalyx layer, Annu. Rev. Biomed. Eng. 9 (2007) 121–167.

[12] F.F. Vargas, M.H. Osorio, U.S. Ryan, M.D. Jesus, Surface charge of endothelial cells estimated from electrophoretic mobility, Membr. Biochem. 8 (1989) 221–227.
[13] A.R. Pries, T.W. Secomb, P. Gaehtgens, The endothelial surface layer, Pflugers Arch. 440 (2000) 653–666.
[14] A. Golas, C.-H. Josh Yeh, H. Pitakjakpipop, C.A. Siedlecki, E.A. Vogler, A comparison of blood factor XII autoactivation in buffer, protein cocktail, serum, and plasma solutions, Biomaterials 34 (2013) 607–620.
[15] C. Sperling, M. Fischer, M.F. Maitz, C. Werner, Blood coagulation on biomaterials requires the combination of distinct activation processes, Biomaterials 30 (2009) 4447–4456.
[16] L.-C. Xu, J.W. Bauer, C.A. Siedlecki, Proteins, platelets, and blood coagulation at biomaterial interfaces, Colloids Surf. B: Biointerfaces 124 (2014) 49–68.
[17] M.B. Gorbet, M.V. Sefton, Biomaterial-associated thrombosis: roles of coagulation factors, complement, platelets and leukocytes, Biomaterials 25 (2004) 5681–5703.
[18] B.R. Lentz, Exposure of platelet membrane phosphatidylserine regulates blood coagulation, Prog. Lipid Res. 42 (2003) 423–438.
[19] J.M. Anderson, A. Rodriguez, D.T. Chang, Foreign body reaction to biomaterials, Semin. Immunol. 20 (2008) 86–100.
[20] G.H.R. Rao, T. Chandy, Role of platelets in blood-biomaterial interactions, Bull. Mater. Sci. 22 (1999) 633–639.
[21] M.E. Ogle, C.E. Segar, S. Sridhar, E.A. Botchwey, Monocytes and macrophages in tissue repair: implications for immunoregenerative biomaterial design, Exp. Biol. Med. 241 (2016) 1084–1097.
[22] L. Tang, T.A. Jennings, J.W. Eaton, Mast cells mediate acute inflammatory responses to implanted biomaterials, Proc. Natl. Acad. Sci. USA 95 (1998) 8841–8846.
[23] R. Abe, S.C. Donnelly, T. Peng, R. Bucala, C.N. Metz, Peripheral blood fibrocytes: differentiation pathway and migration to wound sites, J. Immunol. 166 (2001) 7556.
[24] A. Bogaerts, E. Neyts, R. Gijbels, J. van der Mullen, Gas discharge plasmas and their applications, Spectrochim. Acta B At. Spectrosc. 57 (2002) 609–658.
[25] T. Jacobs, R. Morent, N. de Geyter, P. Dubruel, C. Leys, Plasma surface modification of biomedical polymers: influence on cell-material interaction, Plasma Chem. Plasma Process. 32 (2012) 1039–1073.
[26] N. Dumitrascu, C. Borcia, G. Borcia, Control of the blood–polymer interface by plasma treatment, J. Biomed. Mater. Res. B Appl. Biomater. 87B (2008) 364–373.
[27] E.J. Szili, R.D. Short, D.A. Steele, J.W. Bradley, 1—Surface modification of biomaterials by plasma polymerization, in: R. Williams (Ed.), Surface Modification of Biomaterials, Woodhead Publishing, Cambridge, UK, 2011.
[28] A. Vesel, R. Zaplotnik, M. Modic, M. Mozetic, Hemocompatibility properties of a polymer surface treated in plasma containing sulfur, Surf. Interface Anal. 48 (2016) 601–605.
[29] M. Modic, I. Junkar, K. Stana-Kleinschek, R. Kostanjšek, M. Mozetič, Morphology transformations of platelets on plasma activated surfaces, Plasma Process. Polym. 11 (2014) 596–605.
[30] A. Solouk, B.G. Cousins, H. Mirzadeh, M. Solati-Hashtjin, S. Najarian, A.M. Seifalian, Surface modification of POSS-nanocomposite biomaterials using reactive oxygen plasma treatment for cardiovascular surgical implant applications, Biotechnol. Appl. Biochem. 58 (2011) 147–161.
[31] X. Huang, W. Wang, Z. Zheng, W. Fan, C. Mao, J. Shi, L. Li, Surface monofunctionalized polymethyl pentene hollow fiber membranes by plasma treatment and hemocompatibility modification for membrane oxygenators, Appl. Surf. Sci. 362 (2016) 355–363.

[32] Y.-H. Lin, W.-C. Lan, K.-L. Ou, C.-M. Liu, P.-W. Peng, Hemocompatibility evaluation of plasma-nitrided austenitic stainless steels at low temperature, Surf. Coat. Technol. 206 (2012) 4785–4790.
[33] I. Adipurnama, M.-C. Yang, T. Ciach, B. Butruk-Raszeja, Surface modification and endothelialization of polyurethane for vascular tissue engineering applications: a review, Biomater. Sci. 5 (2017) 22–37.
[34] Y. Yuan, J. Zhang, F. Ai, J. Yuan, J. Zhou, J. Shen, S. Lin, Surface modification of SPEU films by ozone induced graft copolymerization to improve hemocompatibility, Colloids Surf. B: Biointerfaces 29 (2003) 247–256.
[35] Y. Zhu, Z. Mao, H. Shi, C. Gao, In-depth study on aminolysis of poly(ε-caprolactone): back to the fundamentals, Sci. China: Chem. 55 (2012) 2419–2427.
[36] M. Kumorek, O. Janoušková, A. Höcherl, M. Houska, E. Mázl-Chánová, N. Kasoju, L. Cuchalová, R. Matějka, D. Kubies, Effect of crosslinking chemistry of albumin/heparin multilayers on FGF-2 adsorption and endothelial cell behavior, Appl. Surf. Sci. 411 (2017) 240–250.
[37] N. Monteiro, A. Martins, R. Pires, S. Faria, N.A. Fonseca, J.N. Moreira, R.L. Reis, N.M. Neves, Immobilization of bioactive factor-loaded liposomes on the surface of electrospun nanofibers targeting tissue engineering, Biomater. Sci. 2 (2014) 1195–1209.
[38] L. Bech, T. Meylheuc, B. Lepoittevin, P. Roger, Chemical surface modification of poly(ethylene terephthalate) fibers by aminolysis and grafting of carbohydrates, J. Polym. Sci. A Polym. Chem. 45 (2007) 2172–2183.
[39] S. Chen, Z. He, G. Xu, X. Xiao, Fabrication and characterization of modified nanofibrous poly(L-lactic acid) scaffolds by thermally induced phase separation technique and aminolysis for promoting cyctocompatibility, J. Biomater. Sci. Polym. Ed. 27 (2016) 1058–1068.
[40] T. Haddad, S. Noel, B. Liberelle, R. El Ayoubi, A. Ajji, G. de Crescenzo, Fabrication and surface modification of poly lactic acid (PLA) scaffolds with epidermal growth factor for neural tissue engineering, Biomatter 6 (2016). e1231276.
[41] L. Wang, Y. Cai, Y. Jing, B. Zhu, L. Zhu, Y. Xu, Route to hemocompatible polyethersulfone membranes via surface aminolysis and heparinization, J. Colloid Interface Sci. 422 (2014) 38–44.
[42] L. Zhu, F. Liu, X. Yu, L. Xue, Poly(lactic acid) hemodialysis membranes with poly(lactic acid)-block-poly(2-hydroxyethyl methacrylate) copolymer as additive: preparation, characterization, and performance, ACS Appl. Mater. Interfaces 7 (2015) 17748–17755.
[43] Y. Tamada, Sulfation of silk fibroin by chlorosulfonic acid and the anticoagulant activity, Biomaterials 25 (2004) 377–383.
[44] N. Kasoju, U. Bora, Antheraea assama silk fibroin-based functional scaffold with enhanced blood compatibility for tissue engineering applications, Adv. Eng. Mater. 12 (2010) B139–B147.
[45] R. Barbucci, S. Lamponi, A. Magnani, L.F. Poletti, N.P. Rhodes, M. Sobel, D.F. Williams, Influence of sulfation on platelet aggregation and activation with differentially sulfated hyaluronic acids, J. Thromb. Thrombolysis 6 (1998) 109–115.
[46] A. Magnani, A. Albanese, S. Lamponi, R. Barbucci, Blood-interaction performance of differently sulphated hyaluronic acids, Thromb. Res. 81 (1996) 383–395.
[47] R.A.A. Muzzarelli, F. Tanfani, M. Emanuelli, D.P. Pace, E. Chiurazzi, M. Piani, Sulfated N-(carboxymethyl)chitosans: novel blood anticoagulants, Carbohydr. Res. 126 (1984) 225–231.
[48] Y. Huang, M.A. Shaw, E.S. Mullins, T.L. Kirley, N. Ayres, Synthesis and anticoagulant activity of polyureas containing sulfated carbohydrates, Biomacromolecules 15 (2014) 4455–4466.

[49] J. Xue, W. Zhao, S. Nie, S. Sun, C. Zhao, Blood compatibility of polyethersulfone membrane by blending a sulfated derivative of chitosan, Carbohydr. Polym. 95 (2013) 64–71.
[50] C. Cheng, S. Sun, C. Zhao, Progress in heparin and heparin-like/mimicking polymer-functionalized biomedical membranes, J. Mater. Chem. B 2 (2014) 7649–7672.
[51] S. Murugesan, J. Xie, R.J. Linhardt, Immobilization of heparin: approaches and applications, Curr. Top. Med. Chem. 8 (2008) 80–100.
[52] Y. Niimi, F. Ichinose, Y. Ishiguro, K. Terui, S. Uezono, S. Morita, S. Yamane, The effects of heparin coating of oxygenator fibers on platelet adhesion and protein adsorption, Anesth. Analg. 89 (1999) 573.
[53] M. Omichi, M. Matsusaki, S. Kato, I. Maruyama, M. Akashi, Enhancement of the blood compatibility of dialyzer membranes by the physical adsorption of human thrombomodulin (ART-123), J. Biomed. Mater. Res. B Appl. Biomater. 95B (2010) 291–297.
[54] G.L. Nunes, C.N. Thomas, S.R. Hanson, J.J. Barry, S.B. King, N.A. Scott, Inhibition of platelet-dependent thrombosis by local delivery of heparin with a hydrogel-coated balloon, Circulation 92 (1995) 1697.
[55] G. Wimmer-Greinecker, G. Matheis, S. Martens, G. Oremek, U. Abdel-Rahman, A. Moritz, Synthetic protein treated versus heparin coated cardiopulmonary bypass surfaces: similar clinical results and minor biochemical differences, Eur. J. Cardiothorac. Surg. 16 (1999) 211–217.
[56] H. Lee, S.M. Dellatore, W.M. Miller, P.B. Messersmith, Mussel-inspired surface chemistry for multifunctional coatings, Science 318 (2007) 426–430.
[57] Y. Yang, P. Qi, F. Wen, X. Li, Q. Xia, M.F. Maitz, Z. Yang, R. Shen, Q. Tu, N. Huang, Mussel-inspired one-step adherent coating rich in amine groups for covalent immobilization of heparin: hemocompatibility, growth behaviors of vascular cells, and tissue response, ACS Appl. Mater. Interfaces 6 (2014) 14608–14620.
[58] B. Bozzini, A. Barca, F. Bogani, M. Boniardi, P. Carlino, C. Mele, T. Verri, A. Romano, Electrodeposition of nanostructured bioactive hydroxyapatite-heparin composite coatings on titanium for dental implant applications, J. Mater. Sci. Mater. Med. 25 (2014) 1425–1434.
[59] G. Decher, J.D. Hong, J. Schmitt, Buildup of ultrathin multilayer films by a self-assembly process: III. Consecutively alternating adsorption of anionic and cationic polyelectrolytes on charged surfaces, Thin Solid Films 210 (1992) 831–835.
[60] G. Li, P. Yang, N. Huang, Layer-by-layer construction of the heparin/fibronectin coatings on titanium surface: stability and functionality, Phys. Procedia 18 (2011) 112–121.
[61] L.-C. Su, Y.-H. Chen, M.-C. Chen, Dual drug-eluting stents coated with multilayers of hydrophobic heparin and sirolimus, ACS Appl. Mater. Interfaces 5 (2013) 12944–12953.
[62] T. Taniguchi, K.-H. Kyung, S. Shiratori, Layer-by-layer self-assembled thin films of chitin fibers and heparin with anti-thrombus characteristics, RSC Adv. 5 (2015) 107488–107496.
[63] L. Liu, S. Guo, J. Chang, C. Ning, C. Dong, D. Yan, Surface modification of polycaprolactone membrane via layer-by-layer deposition for promoting blood compatibility, J. Biomed. Mater. Res. B Appl. Biomater. 87B (2008) 244–250.
[64] Y. Shu, P. Yin, B. Liang, S. Wang, L. Gao, H. Wang, L. Guo, Layer by layer assembly of heparin/layered double hydroxide completely renewable ultrathin films with enhanced strength and blood compatibility, J. Mater. Chem. 22 (2012) 21667–21672.
[65] J.H. Kim, N.R. Ko, B.-Y. Jung, I.K. Kwon, Development of a novel dual PLGA and alginate coated drug-eluting stent for enhanced blood compatibility, Macromol. Res. 24 (2016) 931–939.
[66] H. Wei, L. Han, J. Ren, L. Jia, Anticoagulant surface coating using composite polysaccharides with embedded heparin-releasing mesoporous silica, ACS Appl. Mater. Interfaces 5 (2013) 12571–12578.

[67] Q. Lv, C. Cao, H. Zhu, A novel solvent system for blending of polyurethane and heparin, Biomaterials 24 (2003) 3915–3919.
[68] Y. Yan, X.H. Wang, D. Yin, R. Zhang, A new polyurethane/heparin vascular graft for small-caliber vein repair, J. Bioact. Compat. Polym. 22 (2007) 323–341.
[69] E. Luong-Van, L. Grøndahl, K.N. Chua, K.W. Leong, V. Nurcombe, S.M. Cool, Controlled release of heparin from poly(ε-caprolactone) electrospun fibers, Biomaterials 27 (2006) 2042–2050.
[70] H.T. Moon, Y.K. Lee, J.K. Han, Y. Byun, A novel formulation for controlled release of heparin-DOCA conjugate dispersed as nanoparticles in polyurethane film, Biomaterials 22 (2001) 281–289.
[71] N. Reddy, R. Reddy, Q. Jiang, Crosslinking biopolymers for biomedical applications, Trends Biotechnol. 33 (2015) 362–369.
[72] P.-B. Huangfu, M. Gong, C. Zhang, S. Yang, J. Zhao, Y.-K. Gong, Cell outer membrane mimetic modification of a cross-linked chitosan surface to improve its hemocompatibility, Colloids Surf. B: Biointerfaces 71 (2009) 268–274.
[73] C.-C. Tsai, Y. Chang, H.-W. Sung, J.-C. Hsu, C.-N. Chen, Effects of heparin immobilization on the surface characteristics of a biological tissue fixed with a naturally occurring crosslinking agent (genipin): an in vitro study, Biomaterials 22 (2001) 523–533.
[74] Y. Xi-Xun, L. Fei, X. Yuan-Ting, W. Chang-Xiu, In vitro study in the endothelial cell compatibility and endothelialization of genipin-crosslinked biological tissues for tissue-engineered vascular scaffolds, J. Mater. Sci. Mater. Med. 21 (2010) 777–785.
[75] S.S. Kim, H.W. Kim, S.H. Yuk, S.Y. Oh, P.K. Pak, H.B. Lee, Blood and cell compatibility of gelatin-carrageenan mixtures cross-linked by glutaraldehyde, Biomaterials 17 (1996) 813–821.
[76] K. Kottke-Marchant, J.M. Anderson, Y. Umemura, R.E. Marchant, Effect of albumin coating on the in vitro blood compatibility of Dacron® arterial prostheses, Biomaterials 10 (1989) 147–155.
[77] Q. Lin, X. Ding, F. Qiu, X. Song, G. Fu, J. Ji, In situ endothelialization of intravascular stents coated with an anti-CD34 antibody functionalized heparin–collagen multilayer, Biomaterials 31 (2010) 4017–4025.
[78] J.L. Robert, M. Saravanababu, X. Jin, Immobilization of heparin: approaches and applications, Curr. Top. Med. Chem. 8 (2008) 80–100.
[79] M.F. Elahi, G. Guan, L. Wang, M.W. King, Influence of layer-by-layer polyelectrolyte deposition and EDC/NHS activated heparin immobilization onto silk fibroin fabric, Materials 7 (2014) 2956–2977.
[80] L. Fang, W. Jin, S. Hong, H. Nan, Surface characterization and in vitro blood compatibility of poly (ethylene terephthalate) immobilized with hirudin, Plasma Sci. Technol. 12 (2010) 235.
[81] G. Steffens, C. Yao, P. Prevel, M. Markowicz, P. Schenck, E. Noah, N. Pallua, Modulation of angiogenic potential of collagen matrices by covalent incorporation of heparin and loading with vascular endothelial growth factor, Tissue Eng. 10 (2004) 1502–1509.
[82] T. Sharkawi, V. Darcos, M. Vert, Poly(DL-lactic acid) film surface modification with heparin for improving hemocompatibility of blood-contacting bioresorbable devices, J. Biomed. Mater. Res. A 98A (2011) 80–87.
[83] F. Senatore, H. Shankar, J.-H. Chen, S. Avantsa, M. Feola, R. Posteraro, E. Blackwell, In vitro and in vivo studies of heparinized-collageno-elastic tubes, J. Biomed. Mater. Res. 24 (1990) 939–957.
[84] T. Jiang, G. Wang, J. Qiu, L. Luo, G. Zhang, Heparinized poly (vinyl alcohol)–small intestinal submucosa composite membrane for coronary covered stents, Biomed. Mater. 4 (2009). 025012.

[85] P. Klement, Y.J. Du, L. Berry, M. Andrew, A.K.C. Chan, Blood-compatible biomaterials by surface coating with a novel antithrombin–heparin covalent complex, Biomaterials 23 (2002) 527–535.
[86] S. Krajewski, B. Neumann, J. Kurz, N. Perle, M. Avci-Adali, G. Cattaneo, H.P. Wendel, Preclinical evaluation of the thrombogenicity and endothelialization of bare metal and surface-coated neurovascular stents, Am. J. Neuroradiol. 36 (2015) 133.
[87] R.A. Hoshi, R. van Lith, M.C. Jen, J.B. Allen, K.A. Lapidos, G. Ameer, The blood and vascular cell compatibility of heparin-modified ePTFE vascular grafts, Biomaterials 34 (2013) 30–41.
[88] J. Li, D. Li, F. Gong, S. Jiang, H. Yu, Y. An, Anti-CD133 antibody immobilized on the surface of stents enhances endothelialization, Biomed. Res. Int. 2014 (2014) 9.
[89] M.J.B. Wissink, R. Beernink, J.S. Pieper, A.A. Poot, G.H.M. Engbers, T. Beugeling, W.G. Van Aken, J. Feijen, Immobilization of heparin to EDC/NHS-crosslinked collagen. Characterization and in vitro evaluation, Biomaterials 22 (2001) 151–163.
[90] Y. Jin, D. Yang, Y. Zhou, G. Ma, J. Nie, Photocrosslinked electrospun chitosan-based biocompatible nanofibers, J. Appl. Polym. Sci. 109 (2008) 3337–3343.
[91] M. Liu, X. Yue, Z. Dai, L. Xing, F. Ma, N. Ren, Stabilized hemocompatible coating of nitinol devices based on photo-cross-linked alginate/heparin multilayer, Langmuir 23 (2007) 9378–9385.
[92] X. Yu, Z. Xiong, J. Li, Z. Wu, Y. Wang, F. Liu, Surface PEGylation on PLA membranes via micro-swelling and crosslinking for improved biocompatibility/hemocompatibility, RSC Adv. 5 (2015) 107949–107956.
[93] S. Bozzini, L. Giuliano, L. Altomare, P. Petrini, A. Bandiera, M.T. Conconi, S. Farè, M.C. Tanzi, Enzymatic cross-linking of human recombinant elastin (HELP) as biomimetic approach in vascular tissue engineering, J. Mater. Sci. Mater. Med. 22 (2011) 2641–2650.
[94] X. Zhao, S.A. Irvine, A. Agrawal, Y. Cao, P.Q. Lim, S.Y. Tan, S.S. Venkatraman, 3D patterned substrates for bioartificial blood vessels—the effect of hydrogels on aligned cells on a biomaterial surface, Acta Biomater. 26 (2015) 159–168.
[95] M. Avci-Adali, N. Perle, G. Ziemer, H.P. Wendel, Current concepts and new developments for autologous in vivo endothelialisation of biomaterials for intravascular applications, Eur. Cell. Mater. 21 (2011) 157–176.
[96] G.W. Bos, N.M. Scharenborg, A.A. Poot, G.H.M. Engbers, T. Beugeling, W.G. van Aken, J. Feijen, Blood compatibility of surfaces with immobilized albumin–heparin conjugate and effect of endothelial cell seeding on platelet adhesion, J. Biomed. Mater. Res. 47 (1999) 279–291.
[97] C.G. Cornelissen, M. Dietrich, K. Gromann, J. Frese, S. Krueger, J.S. Sachweh, S. Jockenhoevel, Fibronectin coating of oxygenator membranes enhances endothelial cell attachment, Biomed. Eng. 12 (2013) 7.
[98] J. Wang, Y. Chen, T. Liu, X. Wang, Y. Liu, Y. Wang, J. Chen, N. Huang, Covalent co-immobilization of heparin/laminin complex that with different concentration ratio on titanium surface for selectively direction of platelets and vascular cells behavior, Appl. Surf. Sci. 317 (2014) 776–786.
[99] S. Schopka, F.-X. Schmid, S. Hirt, D.E. Birnbaum, C. Schmid, K. Lehle, Recellularization of biological heart valves with human vascular cells: in vitro hemocompatibility assessment, J. Biomed. Mater. Res. B Appl. Biomater. 88B (2009) 130–138.
[100] M. Klomp, M.A.M. Beijk, R.J. de Winter, Genous™ endothelial progenitor cell-capturing stent system: a novel stent technology, Expert Rev. Med. Devices 6 (2009) 365–375.
[101] K. Larsen, C. Cheng, D. Tempel, S. Parker, S. Yazdani, W.K. den Dekker, J.H. Houtgraaf, R. de Jong, S. Swager-Ten Hoor, E. Ligtenberg, S.R. Hanson, S. Rowland, F. Kolodgie,

P.W. Serruys, R. Virmani, H.J. Duckers, Capture of circulatory endothelial progenitor cells and accelerated re-endothelialization of a bio-engineered stent in human ex vivo shunt and rabbit denudation model, Eur. Heart J. 33 (2012) 120–128.
[102] J.M. Lee, W. Choe, B.-K. Kim, W.-W. Seo, W.-H. Lim, C.-K. Kang, S. Kyeong, K.D. Eom, H.-J. Cho, Y.-C. Kim, J. Hur, H.-M. Yang, H.-J. Cho, Y.-S. Lee, H.-S. Kim, Comparison of endothelialization and neointimal formation with stents coated with antibodies against CD34 and vascular endothelial-cadherin, Biomaterials 33 (2012) 8917–8927.
[103] B.J. Tefft, S. Uthamaraj, J.J. Harburn, O. Hlinomaz, A. Lerman, D. Dragomir-Daescu, G.S. Sandhu, Magnetizable stent-grafts enable endothelial cell capture, J. Magn. Magn. Mater. 427 (2017) 100–104.
[104] S. Uthamaraj, B.J. Tefft, O. Hlinomaz, G.S. Sandhu, D. Dragomir-Daescu, Ferromagnetic bare metal stent for endothelial cell capture and retention, J. Vis. Exp. 18 (2015). e53100.
[105] S. Uthamaraj, B.J. Tefft, M. Klabusay, O. Hlinomaz, G.S. Sandhu, D. Dragomir-Daescu, Design and validation of a novel ferromagnetic bare metal stent capable of capturing and retaining endothelial cells, Ann. Biomed. Eng. 42 (2014) 2416–2424.
[106] Z. Chen, Q. Li, J. Chen, R. Luo, M.F. Maitz, N. Huang, Immobilization of serum albumin and peptide aptamer for EPC on polydopamine coated titanium surface for enhanced in-situ self-endothelialization, Mater. Sci. Eng. C 60 (2016) 219–229.
[107] J. Hoffmann, A. Paul, M. Harwardt, J. Groll, T. Reeswinkel, D. Klee, M. Moeller, H. Fischer, T. Walker, T. Greiner, G. Ziemer, H.P. Wendel, Immobilized DNA aptamers used as potent attractors for porcine endothelial precursor cells, J. Biomed. Mater. Res. A 84A (2008) 614–621.
[108] S.D. Jayasena, Aptamers: an emerging class of molecules that rival antibodies in diagnostics, Clin. Chem. 45 (1999) 1628.
[109] X. Li, J. Deng, S. Yuan, J. Wang, R. Luo, S. Chen, J. Wang, N. Huang, Fabrication of endothelial progenitor cell capture surface via DNA aptamer modifying dopamine/polyethyleneimine copolymer film, Appl. Surf. Sci. 386 (2016) 138–150.
[110] C. Tuerk, L. Gold, Systematic evolution of ligands by exponential enrichment: RNA ligands to bacteriophage T4 DNA polymerase, Science 249 (1990) 505.
[111] D.S. Sim, J.S. Kwon, Y.S. Kim, H.C. Chung, Y.J. Hong, H.W. Park, J.H. Kim, M.H. Jeong, J.G. Cho, J.C. Park, J.C. Kang, B.S. Han, S. Lothar, Y.K. Ahn, Experience with endothelial progenitor cell capturing aptamers for coating of intracoronary stents in a porcine model, J. Tissue Eng. Regen. Med. 6 (2009) 555–561.
[112] S.I. Jeon, J.D. Andrade, Protein-surface interactions in the presence of polyethylene oxide, J. Colloid Interface Sci. 142 (1991) 159–166.
[113] S.I. Jeon, J.H. Lee, J.D. Andrade, P.G. de Gennes, Protein-surface interactions in the presence of polyethylene oxide, J. Colloid Interface Sci. 142 (1991) 149–158.
[114] A. de Los Santos Pereira, S. Sheikh, C. Blaszykowski, O. Pop-Georgievski, K. Fedorov, M. Thompson, C. Rodriguez-Emmenegger, Antifouling polymer brushes displaying antithrombogenic surface properties, Biomacromolecules 17 (2016) 1179–1185.
[115] N.Y. Kostina, O. Pop-Georgievski, M. Bachmann, N. Neykova, M. Bruns, J. Michálek, M. Bastmeyer, C. Rodriguez-Emmenegger, Non-fouling biodegradable poly(ϵ-caprolactone) nanofibers for tissue engineering, Macromol. Biosci. 16 (2016) 83–94.
[116] L.B. Koh, I. Rodriguez, S.S. Venkatraman, The effect of topography of polymer surfaces on platelet adhesion, Biomaterials 31 (2010) 1533–1545.
[117] Y. Liu, X. Zhang, P. Hao, The effect of topography and wettability of biomaterials on platelet adhesion, J. Adhes. Sci. Technol. 30 (2016) 878–893.

[118] Z. Zhou, J. Chen, L.-J. Xiang, Y. Xu, P. Yang, J.-A. Li, J.-J. Wu, N. Huang, Fabrication of 3D TiO_2 micromesh on silicon surface and its effects on platelet adhesion, Mater. Lett. 132 (2014) 149–152.

[119] W. Everett, D.J. Scurr, A. Rammou, A. Darbyshire, G. Hamilton, A. de Mel, A material conferring hemocompatibility, Sci. Rep. 6 (2016) 26848.

[120] T.C. Major, H. Handa, G.M. Annich, R.H. Bartlett, Development and hemocompatibility testing of nitric oxide releasing polymers using a rabbit model of thrombogenicity, J. Biomater. Appl. 29 (2014) 479–501.

[121] A.B. Tesler, P. Kim, S. Kolle, C. Howell, O. Ahanotu, J. Aizenberg, Extremely durable biofouling-resistant metallic surfaces based on electrodeposited nanoporous tungstite films on steel, Nat. Commun. 6 (2015) 8649.

Part Three

Improving the hemocompatibility of types of biomaterial

This page intentionally left blank

Improving the hemocompatibility of biomedical polymers

9

K. Amoako, R. Gbyli
University of New Haven, West Haven, CT, United States

9.1 Prelude

Biomedical polymers have and still continue to play an important role in how we support and treat patients with various diseases through their use in tissue and blood interacting medical devices and drug delivery systems. Today, a wide variety of blood-contacting devices provide the means for the diagnosis, treatment, and support of life until organ transplantation. Their usage warrants their interaction with cells, bacteria, blood, tissue, and sometimes a combination of these complex living systems and the fates of such interactions are critical for applications including biomimetic surfaces, regenerative medicine, immunomodulation, smart biomaterials for drug delivery, and many more. For blood-contacting devices, their surface interactions with blood mostly lead to blood coagulation, inflammation, device failure, and patient complications (Fig. 9.1). Their lifetimes are thus limited to hours and days due to clot formation. Use on the order of months is however needed for many of these devices including vascular grafts, catheters, artificial lungs, extracorporeal circulation circuits, and dialysis membranes, which rely on the free flow of blood over their surfaces. Clots, however halts this flow and causes the devices to fail. This chapter describes prominent challenges and new directions of hemocompatibility and specifically anticlotting biomaterials research.

9.2 Usage of blood-contacting devices

Large quantities of blood-contacting medical devices with procoagulant surfaces are used annually worldwide [1,2]. It is estimated that >200 million of these devices are utilized in patients in the US alone [3]. They range from devices with small surface areas like catheters, vascular grafts, heart valves, cannulas, glucose, lactate sensors, and stents to those with moderate surface areas like pacemakers, artificial kidneys, and left ventricular assist devices. Then there are those with relatively larger surface areas like the artificial lungs, artificial hearts, and extracorporeal membrane oxygenation circuits. The surfaces of these devices are made up of artificial materials that are different from endothelial cell (EC) surfaces, which interface with flowing blood [4–6]. Among other features, these cells express enzymes and secrete nitric oxide that maintain blood tone [7–10]. For example, nitric oxide inhibits clot formation while thrombolytic enzymes break down formed clots. For artificial materials, these

Hemocompatibility of Biomaterials for Clinical Applications. https://doi.org/10.1016/B978-0-08-100497-5.00016-1
© 2018 Elsevier Ltd. All rights reserved.

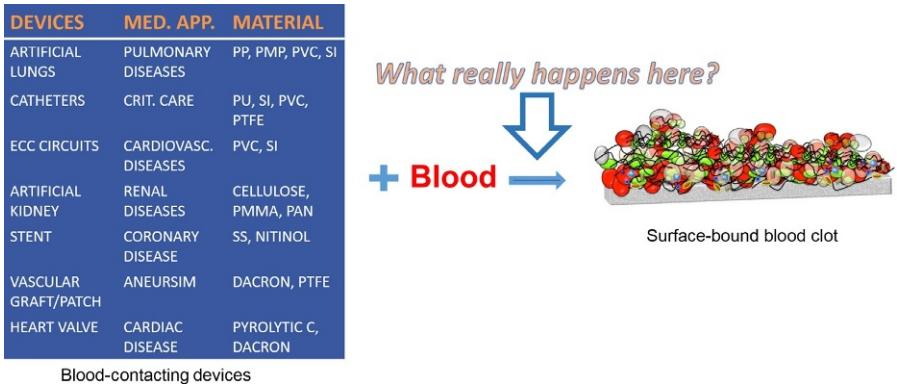


Fig. 9.1 Blood coagulation on polymeric surfaces of devices, an outcome of blood-polymer interaction.

properties are absent and rapidly activate blood into clots upon contact [11,12]. For blood-contacting devices, clot formation can cause cessation of blood flow and lead to device failure [13–15]. Moreover, devices that do not fail may release clots into systemic circulation and cause embolic complications [14,16–18]. In life support devices these clots can result in morbidity and mortality. For instance, a small bore vascular graft serving as a coronary artery may occlude from clot formation and cause myocardial infarction (heart attack). With artificial lungs, clotting is especially problematic as they have relatively large surface areas (1.3–2 m^2) and a period of usage lasting from several weeks to months. Other clot-related problems with artificial lungs include increased device resistance to blood flow and reduced mass transport across their gas exchange membranes and they will typically fail after 7–14 days with accompanying hemorrhagic complications [13–15,18]. As a result their usage is limited with no solution in place for permanent lung replacement. Catheters without soluble heparin locking, on the other hand, have limited lifespan and do not reliably allow repeated sampling of blood or continuous pressure monitoring in patients as their small lumen diameters make them more prone to failure by clots [19–22].

This review will look at some of the major anticoagulation approaches in clinical and experimental use over the last two decades. It will also focus on some of the remaining important and practical aspects of blood/biomaterial compatibility and problems with compatibility testing as well as keys to improve the blood-contacting artificial surface so that systemic anticoagulant drugs do not play a major role. Overall local anticoagulation on blood contacting devices is achievable and may be realized in the near future with robust multifunctional artificial surfaces. These next generation surfaces will be rendered nonfouling/anticlotting and remain so either through a single modification method that is stable to hemodynamic and hemochemical interactions or, more realistically, through multimechanistic techniques. The latter approach will interrupt clot formation at both the contact and propagation phases of the coagulation cascade.

9.3 Biomaterial surface and blood interaction

Under normal physiological conditions, a delicate balance between thrombus formation and destruction is sustained by a complex series of mechanisms and interactions among platelets, the vascular endothelium, the coagulation cascade, and the fibrinolytic system [23]. Blood remains, under healthy hemostasis, in contact only with the normally antithrombogenic endothelium that are lined with cells that prevent adhesion, aggregation, and activation of platelets, preclude the activation of the coagulation cascade, and modulate hemostasis through the expression and secretion of a spectrum of molecules [24]. Among these factors are prostaglandin, nitric oxide, thrombomodulin, heparan sulfate, tissue plasminogen activator (t-PA), urokinase plasminogen activator (u-PA), and plasminogen activator inhibitors [11]. Thrombomodulin combines with thrombin and the resulting complex activates protein C which acts, upon its binding with protein S, as a brake on the coagulation cascade by inactivating FVa and FVIIIa. Also, heparan sulfate inhibits blood coagulation by binding and activating antithrombin, which is the main inhibitor of thrombin and FXa. Moreover, the tissue factor pathway inhibitor (TFPI) inhibits the TF-FVIIa complex by forming a quaternary complex TFPI-TF-FVIIa-FXa [25]. While the aforementioned factors inhibit blood clotting, t-PA, u-PA, and plasminogen activator inhibitors modulate fibrinolysis [26]. ECs also have a low surface energy that keeps blood proteins from changing conformation [25]. However, when the continuity of the healthy endothelium is disrupted, for instance upon an endothelial injury, this nonthrombogenic surface is transformed into a thrombogenic one [24], and a thrombotic reaction starts on the cells' subendothelium matrix and on the connective tissues which get exposed [27]. Circulating platelets then adhere to these structures and start the hemostatic process [27].

In contrast to the healthy endothelium, artificial surfaces lack such endothelial properties, and thus implants, whether intended for short-term use (stents, catheters, heart valves) or long-term applications (extracorporeal circulation), face a challenge, when in contact with blood, to oppose the natural coagulation process that becomes activated. Thrombus formation is a common cause of failure of blood contacting medical devices since artificial biomaterials promote clotting through a complex series of interconnected processes that include protein adsorption, adhesion of platelets, leukocytes, red blood cells, thrombin generation, and complement activation [24].

Coagulation on biomaterials is initiated by the contact system through the activity of three main zymogens produced by the liver. These zymogens, namely Factor XII (hageman factor), Factor XI, and high molecular weight kininogen (HK) all exist in plasma, and upon contacting with artificial surfaces, they go through the adsorption, initiation, and activation phases [11] illustrated in Fig. 9.2.

In the activation phase, zymogen Factor XII first adsorbs to negatively charged surfaces and activates to FXIIa by autoactivation. This process cleaves a single disulfide bridge of FXII allowing its heavy chain to bind to the surface while revealing its active site. At this point FXIIa becomes a cofactor for prekallikrein (PK) and FXI which exist in plasma as noncovalent complexes with HK (PK-HK and XI-HK). The PK-HK complex binds to FXIIa to activate prekallikrein into kallikrein. The FXI-HK complex also binds to FXIIa to activate factor FXI into FXIa to complete the activation phase

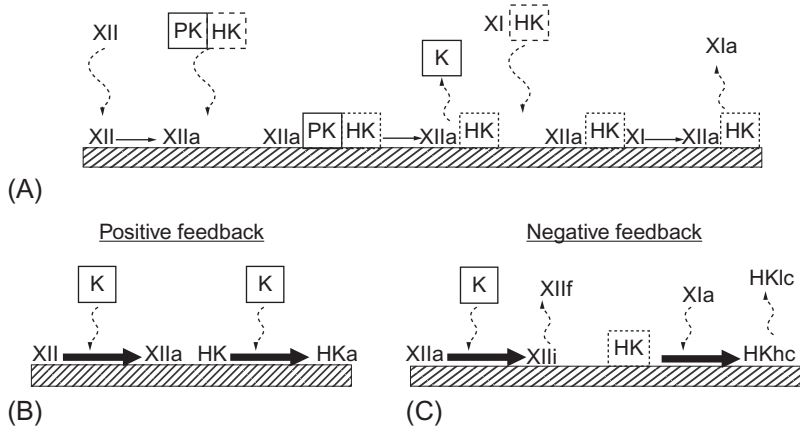


Fig. 9.2 The activation phase of the contact system (A) starts with adsorption and autoactivation of FXII. Activated FXII help activate prekallikrein (PK) which exists as a complex with high molecular weight kininogen (HK). A similar reaction occurs with FXI-HK complex resulting in the activation of FXI. The system also uses a positive feedback mechanism (B) where FXII is rapidly activated by the activated form of PK, kallikrein (K). The activation of HK is also potentiated by K. To balance the positive feedback control, the contact system also uses a negative feedback mechanism (C) to halt the activity of XIIa and HK. It fragments XIIa into soluble/low activity XIIf and inactive XIIi using K and fragments HK into surfacebound inactive heavy chain HK (HKhc) and soluble light chain HK (HKlc) using XIa. Modified from biomaterial science text 2nd edition.

of the contact system. Zymogens XII, XI, and PK at this point have been activated into XIIa, XIa, and K enzymes [11].

Once activated, the contact system uses a positive feedback mechanism potentiated by kallikrein. Kallikrein acts on FXII and HK substrates to speed up their conversion into FXIIa and HKa. For example, HKa binds 10-fold faster than HK to PK and FXI thereby accelerating the association of PK and FXI. This feedback mechanism serves as the initial driver of all amplification reactions in blood coagulation starting from the contact system down to a formed clot. In addition to the positive feedback mechanism, the contact system also has a negative feedback arm to modulate itself. During negative feedback control, Kallikrein cleaves off a fragment of adsorbed FXIIa, (FXIIf), into plasma leaving behind inactivated FXIIi. Although FXIIf is still active, its participation in blood coagulation is decreased as it loses its affinity for surfaces. It therefore exhibits low activity for prekallikrein to kallikrein conversion. FXIa is also a player for the suppression of contact activation. It cleaves off the light chain of adsorbed HK, HKlc, which contains the active site of HK leaving behind the heavy chain portion (HKhc). This reaction terminates the cofactor activity of HK and thus allows FXIa to desorb from the artificial surface [11].

The effect of the negative feedback mechanism has however, not inhibited the contact system adequately to prevent downstream activation of pro-coagulant factors in the intrinsic and extrinsic pathways of the coagulation system that lead to clot formation in blood-contacting devices.

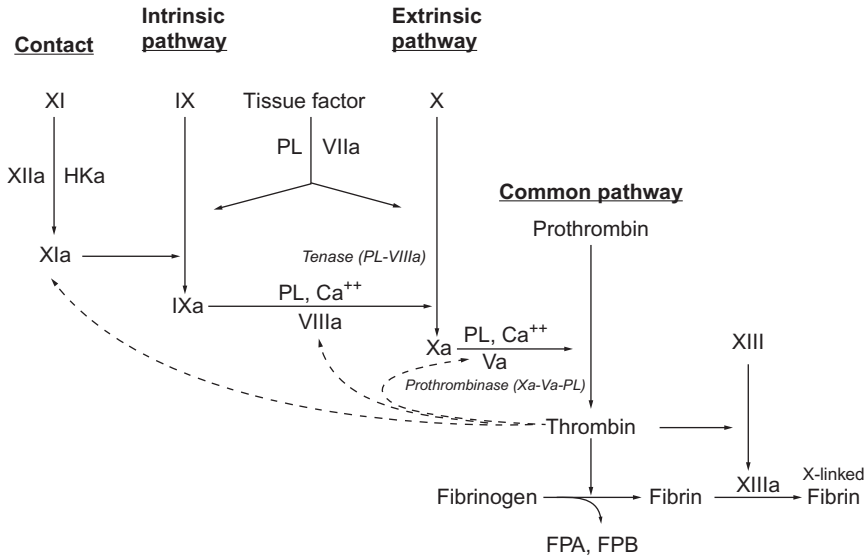


Fig. 9.3 The contact system involves the adsorption and activation of zymogens FXII, FXI, and HK. FXIa from the contact system activates FIX of the intrinsic pathway. A tenase complex consisting of FIXa and a PL surface in the presence of VIIIa and Ca^{2+} activates the FX. FX activation marks the beginning of the extrinsic pathway and can occur independent of TF (VIIa). However TF in the presence of a PL can influence both pathways. With the production of Xa, a prothrombinase complex is formed between FXa and FVa in the presence of a PL surface (e.g., platelet's membrane) to initiate the common pathway. Prothrombin is converted into thrombin inside the platelet. After secretion from platelets, thrombin potentiates the activation of XI, VIII, and V to amplify blood coagulation. Thrombin cleaves fibrinogen into fibrinopeptides A and B so the peptides can polymerize into fibrin resulting in more fibrinogen-GP IIb/IIIa interaction for a stable clot. Finally thrombin, activates FXIII to cross-link fibrin for a solid clot to form.
Modified from biomaterial science text 2nd edition.

Post contact-system blood coagulation has been traditionally viewed in two separate pathways; the intrinsic and extrinsic pathways. Such views have essentially faded as it is now more accepted that the pathways interact in vivo as shown in Fig. 9.3. The contact system is viewed as part of the intrinsic pathway because it initiates that branch of blood coagulation. The intrinsic pathway is associated with artificial surfaces and consists of reactions involving only vascular elements that can occur independent of factor VIIa whereas the extrinsic branch consists of blood in addition to vascular elements. The main difference between the branches lies in the way they activate FIX. The intrinsic system uses FXIa in the presence of Ca^{2+} whereas the extrinsic system requires tissue factor (TF) usually embedded in cell membrane lipid bilayer in addition to calcium.

The intrinsic pathway is initiated by the activation of IX to IXa by Factor XIa which is activated in the contact system. FIX can also be activated by TF in the presence of a phospholipid (PL) surface and cofactor VIIa. For the next reaction to occur, calcium,

FIXa together with the tenase complex (PL surface-cofactor VIIIa) must work together to activate FX. This marks the end of the intrinsic pathway [11,26].

Activation of the extrinsic pathway is achieved again by TF in the presence of PL and VIIa, the same coagulant elements association utilized in the intrinsic pathway.

As TF is present in endothelial tissue, activation of the intrinsic pathway is usually associated with tissue damage. However, biomaterial-induced platelet activation and inflammation can also activate the intrinsic branch, as TF is also present in platelets and leukocytes. When TF associates with a PL and cofactor VIIa, FX is activated into FXa marking the end of the extrinsic pathway and the beginning of the common pathway of blood coagulation [11,26].

The common pathway is activated by the promthrombinase complex consisting of FXa, cofactor Va on platelets' membrane, and a PL surface in the presence of calcium. With FVa serving as the platelet membrane receptor for FXa, the activated platelet produces and secretes prothrombin. The complexing of these four elements to form prothrombinase increases prothrombin activity by 300,000-fold compared to that achieved by FXa and prothrombin alone. Adsorbed and activated platelets on the artificial surface, at this point, are connected by fibrinogen-glycoprotein IIb/IIIa platelet membrane receptor bridges following cleavage of fibrinopeptide A and B from fibrinogen. Platelet aggregation achieved by interconnecting-platelet- secreted fibrinogen bridges is still a premature clot until thrombin cross-links the platelet aggregate by converting fibrinogen into longer fibrin strands that bind to activated platelets multiple times. Finally, a solid clot is formed when thrombin activates FXIII to FXIIIa to cross-link the interconnecting fibrin. This creates an insoluble fibrin network which is the end point of both coagulation pathways. Thrombin has a dual role in hemostasis, as in addition to facilitating the fibrin network formation, it also functions as an activator of two distinct platelet receptors, namely the protease activated receptors (PARs) 1 and 4. It also potentiates the clotting process by activating FV, FVIII, and FXI. It is therefore viewed as the most potent clotting factor in blood coagulation [28].

9.3.1 Platelet activation

Circulating platelets are activated either after damage to healthy endothelium or after blood exposure to an artificial surface. After damage to the endothelium for whatever reason, the endothelium loses its integrity and has to remedy its environment in order to restore its vascular tone. To achieve normal hemostasis, ruptured ECs secrete a "sticky" protein called von Willebrand factor (vWF) to bind to collagen in the exposed subendothelial layer so that circulating platelets can bind to the opposite ends of vWF to form a seal at the damaged area [11,26]. Glycoprotein Ib/IX receptor on platelets membrane allows binding of vWF to activate platelets. On artificial surfaces, the contact system activation leads to generation of FXa. This, in turn, binds to FVa on platelet membrane to activate platelets. After the initial phase where few platelets are activated, a second and massive platelet activation phase ensues. The release of clotting factors from platelets' granules during the first wave of activations acts to systemically activate a substantially large amounts of circulating platelets to potentiate coagulation. For instance, activated platelets will secrete abundant adenosine diphosphate (ADP)

Table 9.1 Agonists secreted from platelets' dense and alpha* granules including other potent agonists and their platelet membrane receptors**

Agonist	Receptor
**Adenosine diphosphate (ADP)	P2Y12 receptor
**Serotonin	5-HT2A receptor (serotonin receptor)
*Platelet activating factor (PAF)	PAF receptor
*vonWillebrand factor (vWF)	Glycoprotein Ib/IX
*Platelet factor 4 (PF4)	PF4 receptor
*Thromboxane A2 (TxA2)	TxA2 receptor
*Thrombin	Protease-activated receptor-1 (human)
Collagen	Glycoprotein IV
Fibrinogen	Glycoprotein IIb/IIIa

and adenosine triphosphate (ATP) from their dense granule that in turn can activate neighboring platelets via ADP and ATP sensitive receptors. ADP is a ligand to the receptors P2Y1 and P2Y12, located on the platelet surface [29,30]. Among the granule content released, those of greatest physiological importance and their platelet membrane receptors, for example are listed in Table 9.1.

During blood flow in blood-contacting devices, flow-induced shear stresses can also lyse platelets to expel their pro-coagulant factors or just activate them. Platelets can thus be activated by such mechanical force in addition to the chemical induction explained above.

9.3.2 Complement activation

Several polymer surfaces were reported to have a strong influence on contact activation and in consequence also on the activation of coagulation and complement systems. Much research has shown that upon exposure to blood, the artificial surface becomes rapidly covered by a protein layer from different cascades and the deposition of this layer triggers the activation of the contact, coagulation, and complement pathways. For instance, the adsorbed fXII and fibrinogen constituents of this layer trigger the activation of the complement, and one of its component, C3 is prone to undergo conformational changes upon binding to that layer leading eventually to the activation of the complement alternative pathway. It has also been shown that activation products of the contact activation system (Factor XIIa [FXIIa] and kallikrein), as well as thrombin and plasmin, are able to cleave purified complement component or fragments thereof in vitro [31–35]. Recently, these early observations have been confirmed and extended, and more factors have been added to the list of proteases that are potentially able to bypass convertases and directly generate complement protein anophylatoxins C3a and C5a, respectively, leading eventually to the activation of the complement alternative pathway. Whereas the incubation of C3 or C5 with FIXa, FXa, FXIa thrombin, and plasmin resulted in the release of C3a and C5a, respectively, the coagulation factor XIIa is able to activate the complement complex C1 initiating the classical pathway.

Thus, there is a crosstalk between the components of the coagulation and complement cascades, and the activation of the complement on top of the adsorbed protein layer leads to the generation of the c3a and c5a that recruit and activate polymorphonuclear leukocytes and monocytes [32–35].

9.4 Biomaterial surface properties and their influence on coagulation

Immediately following the contact of blood with synthetic materials, spontaneous adsorption of proteins, a phenomenon termed "fouling" occurs leading to an advanced adverse biological response afterwards [36]. In general, antifouling surfaces are based on minimizing the intermolecular forces of interactions between extracellular biomolecules and the synthetic surface so that cells do not adhere or an adhered cell is easily released under low shear stresses. A truly antifouling surface, also referred to as a "stealth surface," remains undetected by cells in a biological milieu, and is therefore not prone to biofouling [37]. The interfacial energy between a surface and water is expected to play an important role in conferring antifouling characteristics to the surface. To better understand fouling phenomena theoretically, Baier related fouling with surface energy [38]. A surface is referred to as a theta surface if when glycoproteinaceous macromolecules encounter such surface, they have least probability of getting denatured [38]. Theoretically, minimal bioadhesion occurs at a critical surface tension in the range [39] of 20–30 mN/m preferably between 22 and 24 mN/m which is approximately equal to the dispersive component for water [40]. In a pioneering study on structure-property relationship of surfaces in resisting protein adsorption by Whitesides [41], it was reported that to resist adsorption of proteins a surface needs to exhibit four molecular-level characteristics: hydrophilicity, hydrogen-bond acceptors, do not include hydrogen-bond donors, and charge neutral overall. There are very few exceptions such as mannitol groups, which resist protein adsorption although they are hydrogen-bond donors [42]. Hydrophilic surfaces such as poly(2-hydroxyethyl methacrylate) (PEGMA) have interfacial energy below 5 mJ/m^2 [43]. Although the mechanism of action for polyethylene glycol (PEG) nonfouling is not fully understood [44], it is generally accepted that PEG's effectiveness is due to the steric repulsion effect with loss in entropy exhibited by a PEG-coated surface when proteins attempt to adsorb [45,46]. In contrast, nonpolar hydrophobic surfaces exhibit high interfacial energy with water. When such surfaces are in contact with biological media, amphiphilic biomolecules such as proteins show significant adsorption to minimize the interfacial energy of such surfaces [43]. For example, when zoospores of Ulva are exposed to alternatively patterned hydrophilic and hydrophobic arrangement of self-assembled monolayers (SAM), zoospores preferred to settle on hydrophobic patterns [47]. For effective nonfouling, in terms of surface complexity [43] a surface can be homogeneously hydrophilic (nonfouling), hydrophobic (foul and release if elastic), or amphiphilic (to "confuse" bioorganisms) [48,49]. In addition, surface texturing can also provide useful nonfouling properties as in the case of biomimicking shark-skin inspired polydimethylsiloxane (PDMS) coating using the Sharklet AF

microtopography [50]. Surface modification is arguably the most convenient and effective method of imparting nonfouling properties to material. As per the criteria established by Whitesides [41,51,52] PEG is the prominent candidate for nonfouling applications [41,52,53]. However PEG polymers are prone to oxidation and may have issues with long-term applications especially in water [54]. Among several possible polymers zwitterionic polymers recently emerged as prominent candidate [55]. Due to their strong binding with water, zwitterionic polymers are very effective nonfouling materials [55,56]. These hydrophilic polymers can be attached to a surface to impart nonfouling behavior, and they can be attached to surfaces by various methods [57]; "graft from" in which an initiator is attached to a surface from which the polymer is grown, "graft to" in which a functional chain-end polymer can be grafted, and adsorption of block copolymers. A variety of methods need to be attempted for a given polymer as the nonfouling behavior of the modified surface depends on the graft density and thickness of the given polymer [37]. Atom transfer radical polymerization (ATRP) is one the most widely used method for both "graft from" [58,59] and "graft to" techniques for zwitterionic polymers [60,61] and PEG modification [62–64]. Irrespective of the method used the polymer brushes need to have high density coverage on the surface to be effective at nonfouling. Or if the graft density is lower the polymers then need to be longer [37]. Protein resistance of these surface give an indication about their nonfouling behavior for real world biofouling applications. It is necessary that long-term studies of different polymers in blood contacting applications be performed to select materials for demanding applications [65].

9.5 Surface anticoagulation approaches

Modification approaches developed to combat clot formation on blood-contacting artificial surface have focused on usage of single-mechanistic anticlotting processes through a variety of hydrophilic coatings to prevent nonspecific protein adsorption by biomaterial surface hydration, nitric oxide release from polymers to inhibit platelet activation, and most recently via dual-mechanistic experimental means (Table 9.2).

9.5.1 Limitations of approaches

Several limitations associated with anticlotting surface modification approaches discussed in Table 9.2 still challenge the field and these problems need to be solved in order to design truly hemocompatible surfaces. Such limitations must be addressed using all plausible alternatives including methodical incremental approaches. In the following section, limitations of commonly used coatings are further reviewed.

In heparin coatings, the challenge is that each heparin polymer must first attach to an antithrombin III (ATIII) serine protease inhibitor to work. The formed heparin-ATIII complex must then bind to procoagulant thrombin to deactivate it from propagating coagulation. Realistically, this scenario does not always occur due to the surface-immobilized state of heparin. Another limitation of the heparin arises from

Table 9.2 Surface modification methods for anticoagulation on blood-contacting biomaterials

Coating	Mechanism	Limitations	Comments
Heparin [31,66–69]	Heparin binds to ATIII and to form complex. Thrombin then attaches to complex and loses its function	Limited functionality due to reduced mobility and interaction with ATIII	Insignificant in infants or patients with ATIII deficiency
Hydrophilic coatings (e.g., Sorin, phosphorylcholine, trillium, poly(2-methoxyethlacryalte) [31,67]	Increase hydrophilicity and lower the surface energy of biomaterials; limits protein adsorption	Prone to leach and loses water retention during flow	
(Self-assembled monolayers) SAM coatings [69]	Serves as model surfaces where alkyl groups are attached to metals (usually gold) to allow attachment of polymer of interest	Difficulty in forming ordered monolayer. Largely limited to gold model surface	Important screening tool for new polymers
Biologically active coatings (e.g., nitric oxide) [31,67]	Antibacterial and antiplatelet agent	Toxicity; instability (storage and delivery complications)	Long-term biomaterial self-release has not been achieved; no known effect on protein adsorption
Poly(ethylene oxide) [31,67,70]	Structure repeat unit (CH_2–CH_2–O) is able to form a "liquid like" surface with active molecular chains that have no systematic molecular order	In vitro testing has been successful; however, in vivo testing has been inconsistent	PEO and PEG are basically the same polymer, they are just derived from different monomer/polymerization methods
Polyethylene glycol (PEG) [31,67,70]	Very simple structure (structure repeat unit, CH_2–CH_2–O) that forms a hydrophilic surface	Coating is easily influenced by environmental factors	Hydrophilic and nontoxic

Albumin-coated surfaces [31,67]	Coverage of procoagulant surface. Plasma protein either covalently grafted to the surface or adsorbed onto pretethered long aliphatic chains (C8–C18) or PEO-tether warfarin	Similar antifouling activity in coated and uncoated grafts	Compared with plasma proteins such as fibrinogen and c-globulin, albumin induces less platelet adhesion This finding prompted its use as an inert thromboresistant coating
Pyrolytic carbon-coated surfaces [31,67]	Chemical vapor deposition in which hydrocarbon is heated and graphite layer is crystallized and renders surfaces hydrophilic	Surface irregularities. Reduced platelet adhesion, yet did not affect overall patency rate of grafts	No information found on leaching/other disadvantages/ toxicity. Preclinical studies showed no clear benefit
Phosphorylcholine surfaces [31,67]	Zwitterionic behavior allows it to be electrically neutral at physiologic pH. Is known to limit protein and cell adhesion	Unstable coating; no clear benefit of coating confirmed	
Elastin-inspired coating [31,67]	Limits platelet adhesion and aggregation	Difficult to isolate and purify	
Antiinflammatory coatings [31,71]	• Passive strategy to present a nonfouling surface • Active strategy by the active delivery of antiinflammatory agents.	• Passive strategies coatings lack stability as some proteins can displace preadsorbed proteins • The active strategies and other novel approaches (micro and nanoparticles of biodegradable polymers) still require rigorous testing in in vivo models	Active strategies offer many advantages over the passive one. E.g., control over reaction kinetics, highly controlled presentation of immunomodulatory agents, versatility through hybrid systems
Coatings with endothelial cells attachment [24,68,72]	Endothelial cell receptor modified surface for attachment of cell to create an inert interface	Larger than ideal scaffold surface microscale topography cell attachment	Increased interest in stem-cell directed endothelialization

(Continued)

Table 9.2 Continued

Coating	Mechanism	Limitations	Comments
Biodegradable polymers (e.g., poly(1,8-octanediol citrate) (POC)) [24,73]	Increased hydrophilicity	Biodegradable polymers can influence mechanical properties of devices such as vascular grafts and patches. Porosity may increase with increased degradation rate, increased permeability, and can decrease mechanical stiffness in a nonlinear manner	No effect on graft compliance. Delayed thrombosis in vitro
Hydrogel and ionic liquid based coatings [67,71]	Highly resistant to protein adsorption	Inconsistent results of their effect on reducing in vivo acute and chronic inflammatory responses	Offer many advantages over traditional strategies, including viscoelasticity, tunable material characteristics, incorporation of multiple chemical functionalities, nanoscale dimensions with complex architectures, and the ability to deposit onto a variety of material substrates
Fluoro-containing coatings [70]	Minimization of surface energy and surface tension, to resist fouling		

its degradation due to stresses imposed by its biological surrounding, and it gradually loses its availability to complex with ATIII [31,66,67].

Hydrophilic coatings ranging from Sorin to Trillium increase the hydrophilicity of surfaces and also lower surface energy. Although these mechanisms lead to minimal protein adsorption, the coatings are prone to leaching due to environmental factors which lead to loss of water retention. Similarly, hydrogel and ionic liquid based coatings shown to be highly resistant to protein adsorption and even blood, progressively lose their bioactivity. Despite notable advantages of these coatings, their acute and chronic inflammatory responses in vivo have been inconsistent. Fluoro-containing coatings on the other hand minimize surface energy and lower surface tension [70], and has been shown to inhibit fouling from whole blood in in vitro and acute in in vivo studies [74]. In vitro testing result also showed that liquid perfluorocarbons (PFCs) can be displaced from the surface under hydrodynamic sheer stress [74]. Poly (ethylene oxide) (PEO), otherwise known as PEG is a hydrophilic polyether used as coatings on blood contacting medical devices. It is made up of a structured repeat unit (CH_2–CH_2–O) that drive surface hydration and lowers protein adsorption on devices. Positive results have been shown in in vitro testing although the data has been largely inconsistent [67]. PEG's function can be compromised by their environmental factors, which may explain why in vivo testings have not been consistent.

Antiinflammatory material can be applied as nonfouling surface while others are delivered as antiinflammatory agents. The latter technique allows proteins to passively displace preadsorbed antiinflammatory proteins [71]. Both approaches are influenced by coating stability and more in vivo research is needed.

Biologically active surfaces such as nitric oxide releasing polymers are a relatively new approach for improving blood/biomaterial compatibility. Nitric oxide is an antibacterial and antiplatelet agent that is endogenously released into flowing blood at low flux levels ($0.5–4 \times 10^{-10}$ mol/cm^2/min) [75] by healthy endothelium and can be incorporated into polymers, like PDMS via chemical conjugation reactions. The goal of this anticlotting material modification method is to attain flux levels comparable to what is produced by the endothelium and at nontoxic levels. The ability to control the delivery of nitric oxide and its duration of release continue to be under investigation, as long-term release has also not been achieved yet.

A much different antifouling surface modification approach which involve EC attachment to artificial surfaces is achieved by first adding EC receptors to the preferred nonbiodegradable substrate followed by EC attachment Adequate and appropriate distribution of receptors as well as surface morphology of the substrate are aimed at mimicking the extracellular matrix to promote interaction between the ECs and EC cell receptors. Many of the difficulties associated with conjugating EC receptors to substrates remain unsolved so alternative approaches using stem cells to induce endothelialization are under investigation [24]. Biodegradable polymers such as poly(1,8-octanediol citrate) (POC)) are also being used as substrates to promote endothelialization. The application of POC onto grafts (POC-ePTFE) has been shown to maintain EC adhesion and proliferation of porcine cells similar to that of the native tissues, and within 10 days the EC was confluent, while only random patches were evident on ePTFE controls [24]. For such substrates it is important to maintain an

optimum balance between polymer degradation and cells growth and replication rates, as these factors including porosity influence the polymer's performance and endothelialization. The use of SAM to study antifouling materials are a unique approach as they provide a controlled protocol for evaluating and screening for resistance nonspecific protein fouling. The typical substrate for SAMs is however gold, which is not a medical relevant surface such polyurethane, PDMS, or 316 stainless steel.

Surfaces coated with albumin have demonstrated increased resistance to platelet adhesion especially when compared to other proteins found in human blood. The protein can be covalently attached to the surfaces or selectively adsorbed onto surfaces modified with PEO-tethered warfarin which increases the surface's affinity for endogenous albumin [67]. Hemocompatibility studies of albumin-coated surfaces have generally not shown success. A clinical study examining prosthesis in aortic position [76], recorded that the coating's performance was similar to noncoated vascular prosthesis.

On the other hand, elastin-inspired coatings which are materials containing elastin, a protein found in connective tissue has been shown to limit platelet adhesion and aggregation. However, due to its insolubility, it is difficult to isolate and purify elastin [67]. Another coating inspired by proteins is the phosphorylcholine (PC) which mimicks phosphatidylcholine found in animal cell membranes. While surfaces with PC coating limit protein and cell adhesion in vitro, their electrically neutral property at physiologic pH [67] makes them unstable. PC-coated surfaces have exhibited reduced platelet adhesion in vitro and in some animal studies showed no benefit [31].

Pyrolytic-carbon coating takes the concept of early carbon-coated surfaces and applies it with a modern approach. The process occurs through chemical vapor deposition in which hydrocarbon is heated and a graphite layer is crystallized as a “highly ordered layer of carbon atoms” [67]. Although pyrolytic-carbon coated surfaces were found to reduce platelet adhesion on vascular graft, they did not affect their overall patency rate.

Needless to say that many limitations exist among these antifouling coatings, and by addressing these challenges and evaluating sound alternative approaches, while limiting the risk of bleeding associated with systemic anticoagulant usage, further improvements in blood/biomaterial compatibility can be achieved.

9.6 Current state of systemic anticoagulation usage

Largely due to surface modification limitations discussed earlier, blood coagulation on medical devices remains a challenge yet to be solved through surface/material modification alone. Systemic anticoagulation drugs, especially heparin, are still required as adjunctive therapies with the most commonly used systemic anticoagulant being heparin although other agents such as clopidogrel, aspirin, and warfarin are also used. Heparin's role in inhibiting clots formation is multifaceted acting by inhibiting factor Xa from activating prothrombin into thrombin. When it binds the plasma protein antithrombin III, it directly inhibits thrombin from binding to platelets, and the heparin-AT complex inactivate several coagulation enzymes including thrombin, factors IXa, XIa, and XIIa [26,77]. Heparin slows the process of thromboplastin synthesis, decelerates

the conversion of prothrombin to thrombin, and inhibits the effects of thrombin on fibrinogen, blocking its conversion to fibrin. It also causes an increase in the number of negatively charged ions in the vascular wall, which helps prevent the formation of intravascular clots. In addition, heparin can act through other serine protease inhibitors such as heparin cofactor II, protein C inhibitor, and TF plasminogen inhibitor. The antithrombotic action of heparin in vivo is complex, and interactions with different plasma proteins and cells play significant roles in the living vasculature.

Warfarin, a coumarin derivative, is considered among the most common vitamin K antagonists (VKA) in which it generates its anticoagulation effects by affecting six vitamin K-dependent protein factors involved in the coagulation cascade (factors II, VII, IX and X and proteins C and S) [78,79]. Warfarin and heparin work in slightly different ways, but both block the production of certain cofactors in the liver that work together to promote blood to clot. The points of action of both these anticoagulants are downstream of the onset of blood coagulation and have no effect on protein adsorption. Furthermore, these anticoagulants may compromise hemostasis and cause hemorrhage as they act systemically [80,81].

While Warfarin inhibits Factors II and VII of the extrinsic coagulation pathway, and Factors IX, X, and prothrombin of the intrinsic pathway, heparin exerts its major effect via antithrombin, converting antithrombin to a more efficient inhibitor of circulating thrombin (factor IIa), factor Xa, factor IXa, factor XIIa, and kallikrein. However, due to the multiple anticoagulant mechanisms of heparin, differential molecular weight-based clearance, heparin resistance, and patient-specific characteristics (age, weight, gender, and tobacco), attaining therapeutic anticoagulation is complicated. Moreover, the resultant under- or over-therapeutic anticoagulation is associated with increased risks of ischemic and bleeding complications. Therefore, it is important to maintain heparin anticoagulation within a relatively narrow therapeutic range [82]. Also Heparin-induced thrombocytopenia (HIT), a condition which decreases platelet count during or shortly following exposure to heparin [83], is considered the most frequent drug-induced type of thrombocytopenia and can lead to significant morbidity and mortality if unrecognized. Heparin's interaction with circulating platelets lead to their activation followed by the release of their pro-thrombotic platelet-derived micro- particles, which causes platelet sequestration and consumption, and eventually thrombocytopenia [83,84].

In surgical procedures requiring cardiopulmonary bypass or other blood contacting devices, heparin is used to elevate the activated clotting time (ACT) increasing the activity of the antithrombin. Since some patients are AT deficient and thus have a diminished heparin response, and accordingly fail to reach therapeutic ACT, majority of them may require AT replacement often with antithrombin III (ATryn, recombinant antithrombin III [rhAT], rEVO Biologics) [85,86].

In the same way, although Warfarin inhibits the activation of the vitamin K-dependent clotting factors (Factors II, VII, IX, and X) and regulatory proteins (proteins C, S, and Z), it is one of the leading drugs implicated in emergency room visits for adverse drug reactions. The potential bleeding risk associated with its therapy has led to its limited use especially in the elderly population. Currently, there exists no optimal dose [87] as it is difficult to administer warfarin at the correct dose because

of its narrow therapeutic index, its tendency to cause bleeding, and the individual variability in patient response. Therefore, achieving safe and effective doses of warfarin therapy is both an urgent and important concern. Recent research has focused on pharmacogenomics accounting for individual variation in anticoagulant activity of VKA [88]. Attention has focused on single-nucleotide polymorphisms of genes that encode two proteins: the cytochrome P450 2C9 enzyme and vitamin K epoxide reductase complex (VKORC1) [89]. Studies suggest that CYP 2C9 influences warfarin metabolism and affect warfarin half-life, whereas VKORC1 plays a role in the pharmacodynamic response in expression of the enzymatic target of warfarin. For instance, patients who carry CYP 2C9*2 and CYP 2C9*3 alleles tend to require lower warfarin maintenance doses because of their slowed metabolism compared with patients who carry the "wild-type" allele [88,89].

Aspirin and clopidogrel are also among the commonly used systemic drugs to inhibit platelet activation. Asprin irreversibly inhibits the synthesis of platelet- dependent thromboxane A2 formation and prostaglandins inside platelets and clopidogrel binds to platelets ADP receptor and P2Y12, to block ADP from activating platelets. They inhibit the clotting cascade at the biomaterial's surface and inside platelets in an irreversibly manner and increase the risk of bleeding [15,80]. Many other studies report significantly higher postoperative bleeding complications among patients with continued antiplatelet therapy with clopidogrel [90].

Aspirin is the "gold standard" antiplatelet agent for the prevention of arterial thromboses. The optimum dose of aspirin as an antithrombotic drug can differ in different organ circulations. While 100 mg/day is sufficient for prevention of thrombus formation in the coronary circulation, higher doses may be required for the prevention of vascular events in the cerebral and peripheral circulation.

However, any effective antiplatelet dose of aspirin is associated with an increased risk of bleeding and therefore, the individual benefit/risk ratio determines the administration of the compound [91].

The response to these systemic drugs differ from patient to patient. In fact, many patients are resistant to the effects of a single oral anticoagulation drug, so a therapy that embodies multiple drugs having different mechanisms of action is often used. One example of this is the use of a multitargeted antithrombotic approach, involving anticoagulation (bivalirudin and warfarin) and antiplatelet therapy (dipyridamole and aspirin), in order to mitigate the pro-coagulative effects of mechanical circulatory assist devices, particularly those that are associated with the CardioWest [92] temporary total artificial heart [93,94]. Still, the problem with this approach is that although the mechanisms of action for current antiplatelet agents are known, their combined effect may induce anticoagulation at magnitudes too large to allow restoration to normal hemostasis. The administration of these agents concomitantly can increase risk of bleeding and lead to other unforeseen complications [95]. Careful monitoring of this variant multisystem approach using tools such as efficacy tests, safety tests, and warfarin genomics is therefore important for maximizing the therapeutic actions and minimizing the bleeding risks that are associated with the technique. Ultimately, systemic drugs increase the risk of bleeding complications because of their prolonged half-lives. Bleeding complications become even more devastating in patients with renal insufficiency who cannot efficiently clear

these long lasting drugs. The effects of systemic anticoagulation swing from bleeding in cases where it overwhelms hemostasis to device clotting when inadequate concentrations are used. In devices with large surface area, both effects (bleeding and depletion of systemic clotting factors and platelets) can occur.

Bleeding complications from systemic heparinization are the most common and life-threatening. For example, the Michigan ECMO experience with neonatal mortality is one that can still be improved if bleeding complications due to systemic anticoagulation are reduced. According to the most recent report on the impact of ECMO on neonatal mortality [96], bleeding is the most frequent cause of death in newborns managed with extracorporeal life support. In this population, intracranial hemorrhage occurred in approximately 13% of neonates, 5% of pediatric patients, and 4% of cardiac patients. Clotting complications are also common, occurring in about 26% of patients [97].

Conventional anticoagulants have somehow proven efficacy. However, due to narrow therapeutic window, necessary need for regular monitoring, and other complications, over the last decade or several decades, new oral anticoagulants (NOACs) have been launched and developed [98]. These NOACs range from Factor Xa inhibitors, such as apixaban and rivaroxaban, which selectively and directly bind to the active site of factor Xa, thereby inhibiting both free and clot associated factor Xa, to direct thrombin inhibitors (DTIs). DTIs inhibit the intrinsic activity of the thrombin. Unlike heparin, which also inhibits thrombin, the DTIs do not require a factor, and can inhibit thrombin directly. These drugs, such as bivalirudin, are used for prophylaxis and treatment of venous thromboembolism and acute coronary syndrome, and for prophylaxis of thrombus formation in nonvalvular atrial fibrillation [99,100]. They are also used as anticoagulation alternatives in the setting of HIT.

These NOACs show advantages compared with conventional anticoagulants in the prevention and treatment of patients with thromboembolic events, especially because of lower rates of hemorrhagic outcomes [98–101], the rapid onset and offset, short half-life, predictable therapeutic effect, and wider therapeutic window in addition to the need for no lab monitoring. Nonetheless, there are some conditions for which parental anticoagulants remain the drug of choice. Despite the aforementioned advantages of NOACs, these drugs are not ideal because their use is limited or contraindicated under some circumstances. For example, none of the direct NOACs are approved-to-use drugs during pregnancy or in babies and children [98,101]. Additionally, NOACs have not yet been applied in patients with mechanical mitral valve issues (with increased rates of thromboembolic and bleeding complications) [93,98], patients with malignant disease, and those with antiphospholipid syndrome, which is associated with a greater risk of thrombophilic states [98,101]. More studies are still required to evaluate and further assess the efficacy of NOACs.

9.7 Keys to achieving totally local surface anticoagulation

To advance the current status of surface anticoagulation, it is critical that: novel surface modification approaches are actively pursued, in-clinical-use and promising

experimental techniques are critically reviewed, limitations of the primary mechanisms of action of those modification methods are clearly established, the potential for improving on those limitations through reasonable optimization processes is assessed, and synergy benefits from colocalization of two or more anticoagulation properties on surfaces, an approach arguably of most promise and which logically transitions from proven single mechanistic methods, are evaluated. These are essential factors that need to be addressed in order to advance surface anticoagulation research.

As discussed in preceding sections, there are several ways of organizing surfaces which interact with blood and many are actively being researched. These surfaces have been designed to remain passive and hydrophilic, active and hydrophilic, or active and antithrombogenic. On such designer substrates, we either rely on surface hydration to keep procoagulant blood factors away from settling on the surface or on coupling of soluble proteins (e.g., nondominant form of antithrombin III, beta-antithrombin III) [94] and enzymes to surface-bound active agents such as heparin to inhibit activation of key procoagulant elements like thrombin and factor X. There are also catalyzing surfaces such as copper (II) doped polymers which catalyze the dissociation of nitric oxide from endogenous organic compounds such as *S*-nitrosothiols [102–104] (NO donors). In addition to these designer surfaces, tailored polymeric matrix composites that secrete anticlotting agents such as nitric oxide to limit the activation of key procoagulant platelets have been extensively studied [12,105–109].

Due to the limited and generally short-lived benefits of surface modification approaches, as deducible from the literature, an easier argument to make is that in-clinical-use approaches are either not multiinhibitory/adequate enough to keep blood-contacting surfaces free of clot formation driven by redundantly complex set of reactions, or not robust enough to prevent loss of effectiveness during weeks-long (>2 weeks) exposure to blood flow. Nonetheless it is difficult to confidently conclude whether it is the case of adequacy or loss of function because of the lack of proper scientific data. Some experimental methods on the other hand continue to show exceptional resistance to nonspecific protein adsorption from whole plasma [110–113] and in some cases to whole blood coagulation [74] although only in in vitro and in vivo preclinical settings. For these surface modification techniques, their limitation is that they have been limited to acute in vivo studies at best [74,108,114].

Generally speaking, the optimization approaches to ensure long-term function of in-clinical-use and experimental approaches can be grouped into fortification processes that impart stability to designer surfaces and controlled release of anticlotting agents from matrix composites. Optimized density grafting, covalent attachment strength between graft and substrate materials, and reliable and appropriate measurement techniques to ensure ultralow fouling graft coverage, and stability against typical hemodynamic shear stresses presented to implantable medical devices are needed in the fortification process of designer surfaces. Microenvironment control of matrix composites for tunable release of anticlotting agents will also play a major role in the optimization processes needed to overcome current limitations of blood-contacting surfaces.

Until then, it is reasonable to question whether single-mechanistic modification methods can be fully optimized. And after fortification and micro-control of release

agents, can each method alone lead to totally local surface anticoagulation? As research leads us to making such determination in the future, the potential of drawing synergy from multiple anticlotting agents must not be overlooked. The argument can be made for pushing the boundary of surface anticoagulation research beyond the norm of single-mechanistic anticlotting surface modifications because of millions of years of evolution which have led to equipping the luminal surface of healthy blood vasculature with several anticoagulation functions all working in concert to maintain blood tone.

The significance of this approach is that there is already a wealth of knowledge about many single-mechanistic surface modification approaches and their synergy can lead to increased hemocompatibility of blood-contacting surfaces. Even a minor improvement in the hemocompatibility could result in large upgrades in the patient-care environment.

Synergy benefits that may be extracted from the combination of bioinspired blood-friendly mechanisms including platelet acquiescing nitric oxide release or generation, thrombin inactivating heparin coating, and surface hydration hydrophilic coatings could be those shown in Fig. 9.4. Here three examples of plausible hemocompatibility synergy benefits from surfaces with (A) nitric oxide release combined with zwitterionic coating, (B) nitric oxide release with heparin and zwitterionic coatings, and (C) nitric oxide release with heparin coating are discussed.

Further details on the potential benefits of colocalizing multiple anticlotting mechanisms on biomedical polymers are presented in Table 9.3. Here, the mechanisms of action of a subset of the modification approaches discussed earlier are assessed in pairs and triplets to draw otherwise not obvious conclusions about their potential synergies toward developing a super anticlotting material. For brevity, only a few highly promising and in-clinical-use methods were included in our analyses in Table 9.3. The anticoagulant functions of nitric oxide, zwitterionic coatings, PEG, and heparin coatings are paired and tripled and the resulting multimechanistic action against clot formation are presented. NO's presence on any of the combinations adds the property of inhibiting platelet adsorption and activation. For example, NO release function added to either zwitterionic [102] or PMEA [103] grafted surfaces reduce the adsorption of key

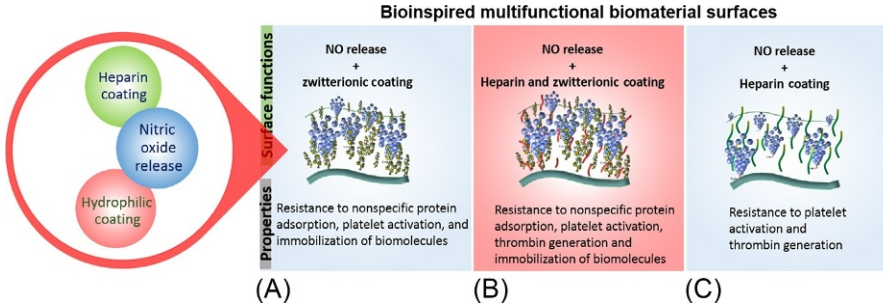
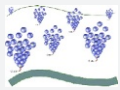
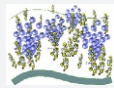
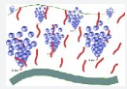
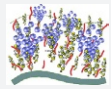
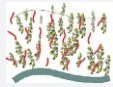
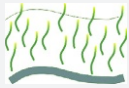
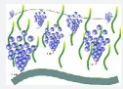
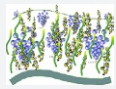
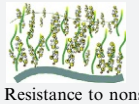
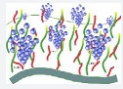
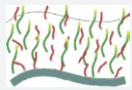
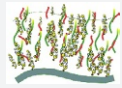


Fig. 9.4 Multimodal biomaterial surface-focused anticoagulation for blood-contacting implantable and extracorporeal medical devices. Examples of synergy benefits from the combination of bioinspired anticlotting mechanisms are depicted.

Table 9.3 Highlighted surface modification approaches and their inferred multimechanistic anticoagulation action when they are colocalized on a surface

Modification with	*Paired Mechanism of Action (MoA)*	*Triple MoA*
Nitric oxide (NO) release 	NO + Zwitterionic  Resistance to nonspecific protein and platelet adsorption and activation/immobilization of	
Zwitterionic materials 		
Polyethylene glycol (PEG) 	NO + PEG  Resistance to nonspecific protein and platelet adsorption and activation	NO + Zwitterionic + PEG  Resistance to nonspecific protein adsorption via strong electrostatic and nonelectrostatic hydration and antiplatelet/immobilization of biomolecules
	Zwitterionic + PEG  Resistance to nonspecific protein adsorption via strong electrostatic and nonelectrostatic hydration and immobiliza-	
Heparin 	NO + Heparin  Resistance to platelet adsorption and activation and antithrombogenic	NO + Zwitterionic + Heparin  Resistance to nonspecific protein adsorption and antithrombogenic/
	Zwitterionic + Heparin  Resistance to nonspecific protein and platelet adsorption and activation/immobilization of biomolecules	NO + PEG + Heparin  Resistance to nonspecific protein and platelet adsorption and activation, antithrombogenic
	PEG + Heparin  Resistance to nonspecific protein and platelet adsorption and activation, antithrombo-	Zwitterionic + PEG + Heparin  Resistance to nonspecific protein adsorption via strong electrostatic and nonelectrostatic hydration and antiplatelet/immobilization of biomolecules/an-

clotting elements (fibrinogen and platelets) at a significantly higher level than surfaces modified with either NO release or coating alone. Zwitterionic polycarboxybetaine coated surfaces not only resist nonspecific protein adsorption much like PEG but also provide immobilization sites for biomolecules [113]. Heparin's action on the other hand is unique as it indirectly inhibits the procoagulant function of soluble thrombin. In theory the ideal surface should effectively inhibit thrombin generation, platelet activation, and fibrinogen adsorption. This is achievable also in theory, by blocking all contact system proteins and thus preventing the activation of the blood coagulation cascade. This method of nonspecific protein resistance is an active and well-funded approach which has resulted in reduced blood activation although surface-induced clot formation is still a clinical challenge. Effective inhibition of thrombin generation, platelet activation, and fibrinogen adsorption could also be achieved by designer surfaces that target each of those procoagulant elements. Such a surface could present heparin and some hydrophilic coating and NO release to blood flow.

9.8 Standardization of in vitro and in vivo test protocols

Hemocompatibility of artificial surfaces has been traditionally evaluated by analyzing the surface (protein fouling, platelet adsorption, and clotting factor deposition), accessing the material property and function based on its intended application (e.g., gas exchange efficiency, detection specificity, and accuracy), and last but not the least the state of the interacting biological media (complement activation, platelet function, and white cell counts) perhaps where more work is needed. As the hemocompatibility of an artificial surface is a function of blood and the interacting surface, variations in these independent variables can influence hemocompatibility outcomes and thus must be included in experiment planning in order to obtain a complete picture of how a surface will perform in clinical trials. The flow chart in Fig. 9.5 is our attempt to guide the decision making for hemocompatibility testing and perhaps add to the preclinical standardization platform greatly desired by the field. Bulk and molecular variables of blood such as shear stress, flow regime and stagnation, blood deficiencies, fouling, platelet function, and inflammation play important roles in surfaces that interact only with blood (e.g., gas exchange membranes), as well as in surfaces that contact both blood and tissue (vascular graft, stents, and heart valves). In the latter surface group however, cell viability, proliferation, cytotoxicity, and fibrous capsule formation are additional cellular factors to be considered. Variables as a result of bulk and molecular level properties of the material or device should also be scrutinized, and they include surface geometry, surface area to volume ratio, porosity, wettability, material-tissue compliance matching, biodegradation rate if degradable, toxicity, irritability, sensitivity, and carcinogenicity.

Accordingly, medical devices and biomaterials must undergo rigorous testing, and testing models, whether in vitro or in vivo, that is as similar as possible to the clinical application environment. Although animal models are considered expensive and time consuming, they are needed to bridge the gap between the lab and the clinic. Animal selection for in vivo studies should be based on the advantages and disadvantages

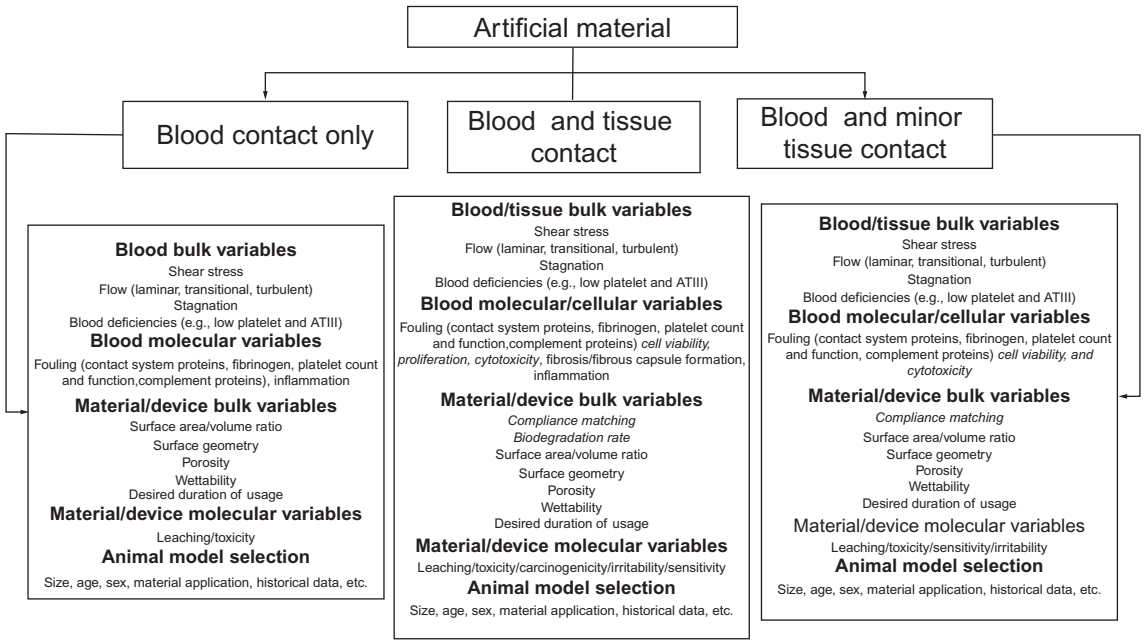


Fig. 9.5 Decision making guideline for preclinical hemocompatibility testing of biomaterials.

for human clinical application. Importantly, it has been shown that the composition of blood differs considerably between various species, which leads to over- or under estimation of human blood reactions to biomaterials [115–118].

Advantages and disadvantages of various in vivo models commonly used in the assessment of biomaterial strategies depend on the chosen model (animal species) and the intended application. For example, adult size artificial lungs would be appropriately tested in adult animals as those will provide the right cardiac output. On the other hand prosthetic heart valves are tested in sheep as they calcify in calves [119]. Caution must be however exercised with animal models as their outcomes sometimes don't translate into clinical studies as seen with small diameter vascular grafts that were successfully endothelialized in all animal models but failed to do so in humans [119]. Therefore, using human blood in a proper in vitro circulation model is recommended.

Overall, due to the complexity of blood-biomaterial surfaces interactions and to the variability in results interpretation among different individuals and species, the clinical relevance of many studies is still a matter of debate and pose difficulties in standardization. As the number of publications in the biomedical field increases, the concern for quality assurance of their results also increase. Since standardization of materials and devices testing is crucial and urgent, the International Organization for Standardization (ISO) provides standards for "Biological evaluation of medical devices" (ISO 10993) although test settings still vary. It is a 20-part series for evaluating the biocompatibility of medical devices prior to clinical testing. Evaluation of the biocompatibility and bio-functionality of materials is conducted by methods based on the assessment of cytotoxicity, mutagenesis/carcinogenesis, and cell biofunction. Blood-contacting medical devices and biomaterials have to be tested according to part 4 of the ISO 10993 standard [120].

The ISO 10993-Part 4 standard is applicable to external communicating devices, either with an indirect blood path (e.g., blood collection devices, storage systems) or in direct contact with circulating blood (e.g., catheters, extracorporeal circulation systems), and implant devices (stents, heart valves, grafts). Testing, according to this standard, should be performed for five categories, based on primary processes: thrombosis, coagulation, platelets/platelet function, haematology, and complement. For each contact category, primary (Level 1) and optional (Level 2) tests are recommended. Since testing should simulate clinical conditions as much as possible, most devices should be tested with heparinized blood under circulating conditions [120].

Regarding hemolysis testing, for devices having direct contact with circulating blood, it is recommended that both direct and indirect (extract) methods for material/surface-mediated hemolysis be conducted per ASTM F756 "Standard Practice for Assessment of Hemolytic Properties of Materials," or an equivalent method. For hemolysis testing of devices having indirect contact with circulating blood, it is recommended that only an indirect (extract) method be conducted per ASTM F756, or an equivalent method. However, for devices or device components that do not have direct or indirect contact with circulating blood, this testing is generally not needed. For some devices where high shear stress due to blood flow may be an issue, dynamic hemolysis assessment under clinical use conditions may also be important. While ISO

10993-4 is the Hemolysis standard, it can be assessed by any of several validated methods to assay hemoglobin in plasma to obtain a hemolytic index assessed by measuring hemoglobin at 1, 2, and 4 h by spectrophotometric analysis. The hemolysis over this period is expressed as a percentage of positive control [120].

Complement activation is the most relevant immunology test for devices exposed to circulating blood. An increase in a downstream complement component over baseline levels indicates activation of the complement cascade. Acceptable complement activation limits have not been established, but comparative data are valuable. For in vitro complement activation testing, the assessment of C3a, C5a, TCC, Bb, iC3b, C4d, SC5b-9 fragments activation using an established ELISA test method is recommended. Complement activation testing whether, in vivo animal models, in vitro "static" methods such as ASTM F1984 "Standard Practice for Testing for Whole Complement Activation in Serum by Solid Materials," or in vitro dynamic testing using simulated clinical flow conditions can be used if accompanied by appropriate validation information.

A device's effects on blood coagulation may be measured in vitro by determining the rate of clot formation or the partial thromboplastin time (PTT) of plasma exposed to the biomaterial or device during an incubation period. Flow conditions, controls that are being used, time of exposure, and the type and concentration of anticoagulation used for in vitro testing, may depend on the test system and the clinical indication of the device [120].

Thrombosis may be addressed by performing either an in vivo or ex vivo test. The Lee White clotting-time test is also sometimes used to satisfy the requirement for a test in this category. If only a portion of the device is being utilized for thrombogenicity testing, it must be representative of all materials and important geometrical/surface features that would have direct contact with the blood. Thrombin-antithrombin complex, PTT are also used as a pseudo substitute for in vivo thrombogenicity testing. Some of in vitro assessment of thrombogenicity (e.g., the effect of extractables and leachables on platelets and the coagulation system) may also be needed for devices with indirect contact with blood.

However, a major problem regarding use of the ISO 10993/4 standard is the lack of acceptance criteria and reference materials. There is no totally satisfactory biological test that can evaluate standard polymers. There are enormous variations between in vivo and in vitro effects, and these vary too, in different animal species. Although the ISO and the World Health Organization has published some trials and standards, it is not universally applied although significant improvements to this standard is underway and being overseen by the ISO committee.

Overall, because of the complex nature of blood compatibility, a standardized in vitro hemocompatibility test panel is needed and should enable the detection and elimination of undesired and excessive material-induced thrombosis and inflammatory events at an early stage of biomaterial development. Also, since the approval by the currently recommended panel of tests does not guarantee clinical device/biomaterial hemocompatibility, there is a major need for improved in vivo and predictive in vitro test setups. Unsolved concerns also include the lack of standards for anticoagulation or reference materials.

9.9 Highlights of promising anticoagulation works

A few surface modification approaches that impart multimechanistic anticoagulation property have shown highly promising findings. Platelet and fibrinogen adsorption on NO transferring polymethylethylacrylate coated PU [102], as well as NO transferring PDMS grafted with polycarboxybetaine [61] have been quantified and shown to highly limit fouling. Similar anticlotting activity has been demonstrated with NO-heparin conjugates [121,122]. The NO-PMEA and NO-pCB work were conducted on PU and PDMS respectively using flowing NO gas. In both cases the PU and PDMS polymers simply transferred NO from a gas supply while either PU, PVC, or silicone rubber-PU copolymer were used to study the effect of NO-heparin conjugate on clotting studies. None of the heparin-NO conjugate studies have used medical grade PDMS as substrate while PMEA-NO and pCB-NO work have only transferred NO gas through PDMS. With the pervasive use of PDMS in many blood-contacting devices due to its biocompatibility and manufacturability [74,123], there are still no studies that have examined the antifouling properties of NO release with hydrophilic coatings on this material. Such materials are easily applied via dip coating to surfaces of many blood-contacting devices including artificial lungs, stents, dialysis membrane, and heart valves.

Antifouling studies using PFC coatings [74] have shown to exhibit nonfouling properties when exposed to blood. PFC is an FDA-approved Teflon-like material widely used in medical applications including liquid ventilation for infants and blood substitution. A recent in vivo antithrombogenecity study of PFC-coated surfaces reported that the presence of PFC prevented clot formation in pigs for 8 h under high blood flow rates [74] and without soluble heparin. Another approach geared towards fast screening for highly protein resistant coatings uses standard poly(ether sulfone) substrates onto which test polymers are conjugated through photo-induced graft polymerization using a library of monomers [114]. Such screening tools are needed to slingshot the discovery of thromboresistant surfaces. Devising a practical method for easy attachment of fouling resistant coatings on medically relevant materials including metals is one of the holy grails in antifouling surface research. Therefore the use of a catecholic initiator, for example dopamine which was inspired by mussel adhesive proteins, for surface-initiated polymerization from metallic surfaces to create antifouling polymer coatings was received with enthusiasm. This approach continues to impact surface modification research as the catecholic anchor has been used in many surface grafting methods [124].

9.10 Conclusion

Interest in surface modification for improved blood-biomaterial interaction is higher now than a decade ago, with more federal funding being poured into this effort. This has in part led to the highly promising antifouling or antithrombogenic surface developments although these newer interfaces alone have not yet eliminated the need for systemic anticoagulation. Thus the risk of life-threatening bleeding complications is still a challenge.

These newer surfaces have focused on single-mechanistic anticlotting processes using hydrophilic coatings to resist nonspecific protein adsorption, nitric oxide release from polymers to inhibit platelet activation, and most recently via dual-mechanistic experimental means. Dual and multipronged approaches draw not only on the anticlotting property of each mechanism but also on potential synergies among the approaches for developing a super anticlotting material. More work is obviously needed in this area to understand how the interactions between two or more anticlotting mechanism would affect blood coagulation.

Clear and comprehensive standards are also needed for a consistent evaluation of these surface modification approaches during their development and after their application to devices for easier assessments and to study comparison at both preclinical and clinical phases of testing. Factors that will drive the nature and rigor of preclinical testing should focus on the types of interaction between host's biological media and surface, duration of contact in the clinical setting; so an appropriate animal model is selected for testing.

So the question of whether totally local anticoagulation on blood-contacting surfaces is achievable is one that we can definitely address by evaluating all potential solutions.

Acknowledgments

A. K. conceived the content and structure of the chapter, and supervised the writing of the manuscript. My research assistants helped with literature review, data collection, organization, writing, reviewing, and editing. I thank my family, the National Institute of Health's National Heart Lung and Blood Institute, the Connecticut NASA Space grant consortium for funding support, and the Tagliatella College of Engineering for the various forms of support provided towards the completion of this chapter.

References

[1] B.D. Ratner, J. Biomed. Mater. Res. 27 (3) (1993) 283.
[2] A.S. Hoffman, F.J. Schoen, J.E. Lemons, Biomaterials Science: An Introduction to Materials in Medicine, Academic Press, San Diego, CA, 2004.
[3] B.D. Ratner, Biomaterials 28 (34) (2007).
[4] D.J. Stuehr, N.S. Kwon, C.F. Nathan, O.W. Griffith, P.L. Feldman, J.N. Wiseman, J. Biol. Chem. 226 (10) (1991).
[5] M.A. Marletta, Trends Biochem. Sci. 14 (12) (1989).
[6] M. Kushwaha, J.M. Anderson, C.A. Bosworth, et al., Biomaterials 31 (7) (2010).
[7] L.J. Ignarro, Annu. Rev. Pharmacol. Toxicol. 30 (1) (1990).
[8] R.M. Rapoport, M.B. Draznin, F. Murad, Nature 306 (5939) (1983).
[9] R.M.J. Palmer, A.G. Ferrige, S. Moncada, Nature 327 (6122) (1987).
[10] W.M. Xu, L.Z. Liu, Cell Res. 8 (4) (1998).
[11] R.W. Colman, J. Hirsh, V.J. Marder, A.W. Clowes, N.J. George, Hemostasis and Thrombosis: Basic Principles & Clinical Practice, fourth ed., Lippincott Williams & Wilkins, Philadelphia, PA, 2001.

[12] T.C. Major, D.O. Brant, C.P. Burney, K.A. Amoako, G.M. Annich, M.E. Meyerhoff, H. Handa, R.H. Bartlett, Biomaterials 32 (26) (2011).
[13] K.E. Cook, C.E. Perlman, R. Seipelt, C.L. Backer, C. Mavroudis, L.F. Mockrost, ASAIO J. 51 (2005) 4.
[14] R.H. Bartlett, ASAIO J. 43 (1) (1997).
[15] H. Sato, G.W. Griffith, C.M. Hall, J.M. Toomasian, R.B. Hirschl, R.H. Bartlett, K.E. Cook, Ann. Thorac. Surg. 84 (3) (2007).
[16] K.A. Amoako, K.E. Cook, ASAIO J. 57 (6) (2011).
[17] J.A. Murphy, C.M. Savage, S.K. Alpard, D.J. Deyo, J.B. Jayroe, J.B. Zwischenberger, Perfusion 16 (6) (2001).
[18] Z. Zhang, M. Zhang, S. Chen, T.A. Horbett, B.D. Ratner, S. Jiang, Biomaterials 29 (32) (2008).
[19] J. Bass, J. Halton, Y. Drouet, A. Ni, N. Barrowman, J.M. Halton, J. Pediatr. Surg. 46 (5) (2011).
[20] P.A. Dillon, R.P. Foglia, J. Pediatr. Surg. 41 (9) (2006).
[21] C. Male, P. Chait, M. Andrew, K. Hanna, J. Julian, L. Mitchell, Blood 101 (11) (2003).
[22] J.M. Journeycake, G.R. Buchanan, J. Clin. Oncol. Off. J. Am. Soc. Clin. Oncol. 24 (28) (2006).
[23] K. Harter, M. Levine, S.O. Henderson, West. J. Emerg. Med. 16 (1) (2015).
[24] A.d. Mel, B.G. Cousins, A.M. Seifalian, Int. J. Biomat. 2012 (2012) 707863.
[25] M. Félétou, The Endothelium. The Endothelium: Part 1: Multiple Functions of the Endothelial Cells—Focus on Endothelium-Derived Vasoactive Mediators, Morgan & Claypool Publishers, Williston, VT, 2011.
[26] S. Palta, R. Saroa, A. Palta, Indian J. Anaesth. 58 (5) (2014).
[27] J.J. Zwaginga, H.C. de Boer, M.J. Jsseldijk, A. Kerkhof, G. Muller-Berghaus, J. Gruhlichhenn, P.G. de Groot, Arteriosclerosis 10 (3) (1990).
[28] J.P. Cazenave, C. Klein-Soyer, A. Beretz, Nouv. Rev. Fr. Hematol. 24 (3) (1982).
[29] J.A. Hayward, D. Chapman, Biomaterials 5 (3) (1984).
[30] B.L. Mejak, A. Stammers, E. Rauch, S. Vang, T. Viessman, Perfusion 15 (1) (2000).
[31] I.H. Jaffer, J.C. Fredenburgh, J. Hirsh, J.I. Weitz, J. Thromb. Haemost. 13 (2015).
[32] K. Oikonomopoulou, D. Ricklin, P.A. Ward, J.D. Lambris, Semin. Immunopathol. 34 (1) (2012).
[33] K.N. Ekdahl, J.D. Lambris, H. Elwing, D. Ricklin, P.H. Nilsson, Y. Teramura, B. Nilsson, Adv. Drug Deliv. Rev. 63 (12) (2011).
[34] J. Andersson, K.N. Ekdahl, R. Larsson, U.R. Nilsson, B. Nilsson, J. Immunol. 168 (11) (2002).
[35] U. Amara, D. Rittirsch, M. Flierl, U. Bruckner, A. Klos, F. Gebhard, M. Huber-Lang, Adv. Exp. Med. Biol. 632 (2008).
[36] J.M. Anderson, Annu. Rev. Mater. Res. 31 (81) (2001).
[37] I. Banerjee, R.C. Pangule, R.S. Kane, Adv. Mater. 23 (6) (2011).
[38] R.E. Baier, J. Mater. Sci. Mater. Med. 17 (2006).
[39] R.E. Baier, Adhesion in Biological Systems, Academic Press, Cambridge, MA, 1970.
[40] R.E. Baier, A.E. Meyer, J.R. Natiella, R.R. Natiella, J.M. Carter, J. Biomed. Mater. Res. 18 (4) (1984).
[41] E. Ostuni, R.G. Chapman, R.E. Holmlin, S. Takayama, G.M. Whitesides, Langmuir 17 (2001).
[42] Y.-Y. Luk, M. Kato, M. Mrksich, Langmuir 16 (24) (2000).
[43] S. Krishnan, C.J. Weinman, C.K. Ober, L.D. Chambers, K.R. Stokes, F.C. Walsh, K.J. Wynne, J. Mater. Chem. 18 (2) (2008).

[44] S. Lowe, N.M. O'Brien-Simpson, L.A. Connal, Polym. Chem. 6 (2) (2015).
[45] S.I. Jeon, J.H. Lee, J.D. Andrade, P.G. de Gennes, J. Colloid Interface Sci. 142 (1991).
[46] S.I. Jeon, J.D. Andrade, J. Colloid Interface Sci. 142 (1991).
[47] J.A. Finlay, S. Krishnan, M.E. Callow, J.A. Callow, R. Dong, N. Asgill, C.K. Ober, Langmuir 24 (2) (2008).
[48] S. Krishnan, R. Ayothi, A. Hexemer, J.A. Finlay, K.E. Sohn, R. Perry, D.A. Fischer, Langmuir 22 (11) (2006).
[49] H.S. Sundaram, Y. Cho, M.D. Dimitriou, C.J. Weinman, J.A. Finlay, G. Cone, C.K. Ober, Biofouling 27 (6) (2011).
[50] J.F. Schumacher, M.L. Carman, T.G. Estes, A.W. Feinberg, L.H. Wilson, M.E. Callow, A.B. Brennan, Biofouling 23 (1–2) (2007).
[51] R.G. Chapman, E. Ostuni, S. Takayama, R.E. Holmlin, L. Yan, G.M. Whitesides, Am. Chem. Soc. 122 (2000).
[52] K.L. Prime, G.M. Whitesides, Science 252 (5009) (1991).
[53] S. Zalipsky, J.M. Harris, Introduction to Chemistry and Biological Applications of Poly(ethylene glycol), ACS Publications, 1997, pp. 1–13.
[54] S. Chen, S. Jiang, Adv. Mater. 20 (2) (2008).
[55] A.L. Lewis, Colloids Surf. B: Biointerfaces 18 (3) (2000).
[56] K. Ishihara, K. Fukumoto, Y. Iwasaki, N. Nakabayashi, Biomaterials 20 (17) (1999).
[57] B. Zhao, W.J. Brittain, Prog. Polym. Sci. 25 (2000).
[58] G. Cheng, G. Li, H. Xue, S. Chen, J.D. Bryers, S. Jiang, Biomaterials 30 (28) (2009).
[59] H. Ma, J. Hyun, P. Stiller, A. Chilkoti, Adv. Mater. 16 (4) (2004).
[60] C. Gao, G. Li, H. Xue, W. Yang, F. Zhang, S. Jiang, Biomaterials 31 (7) (2010).
[61] K.A. Amoako, H.S. Sundaram, A.B. Suhaib, S. Jiang, K.E. Cook, Adv. Mater. Interfaces 3 (6) (2016).
[62] H. Lee, S.M. Dellatore, W.M. Miller, P.B. Messersmith, Science 318 (5849) (2007).
[63] T.S. Sileika, H.D. Kim, P. Maniak, P.B. Messersmith, ACS Appl. Mater. Interfaces 3 (12) (2011).
[64] J.L. Dalsin, B.H. Hu, B.P. Lee, P.B. Messersmith, J. Am. Chem. Soc. 125 (14) (2003).
[65] D.L.S. Pereira, S. Sheikh, C. Blaszykowski, O. Pop-Georgievski, K. Fedorov, M. Thompson, C. Rodriguez-Emmenegger, Biomacromolecules 17 (3) (2016).
[66] K.A. Amoako, Nitric Oxide Therapies for Local Inhibition of Platelets' Activitation on Blood-Contacting Surfaces, Proquest Dissertation Publishing, Baltimore, MD, 2011.
[67] S.W. Jordan, E.L. Chaikof, J. Vasc. Surg. 45 (A104) (2007).
[68] B. Mitton, A. Steineck, Acquired causes of antithrombin deficiency, http://emedicine.medscape.com/article/198573-overview#a8 (accessed October 2015).
[69] A. Ulman, Chem. Rev. 96 (4) (1996).
[70] H. Zhang, M. Chiao, Med. Biol. Eng. 35 (2) (2015).
[71] A.W. Bridges, A.J. García, J. Diabetes Sci. Technol. 2 (6) (2008).
[72] S.R. Meyers, M.W. Grinstaff, Chem. Rev. 112 (3) (2012).
[73] C.G. Jeong, S.J. Hollister, J. Biomed. Mater. Res. B Appl. Biomater. 93 (1) (2010).
[74] D.C. Leslie, A. Waterhouse, et al., Nat. Biotechnol. 32 (2014).
[75] C.N. Hall, J. Garthwaite, Nitric Oxide 21 (2) (2009).
[76] H. Al-Khaffaf, D. Charlesworth, J. Vasc. Surg. 23 (4) (1996).
[77] E. Gray, J. Hogwood, B. Mulloy, Handb. Exp. Pharmacol. 207 (2012).
[78] M. Kuruvilla, C. Gurk-Turner, Proceedings 14 (3) (2001).
[79] P. Weiss, G.A. Soff, H. Halkin, U. Seligsohn, Thromb. Res. 45 (6) (1987).
[80] S.I. Rapaport, L.V. Rao, Arterioscler. Thromb. Vasc. Biol. 12 (10) (1992).
[81] L.Y. Lee, W. DeBois, et al., Perfusion 17 (1) (2002).

[82] A. Krishnaswamy, A.M. Lincoff, C.P. Cannon, Crit. Pathw. Cardiol. 9 (1) (2010).
[83] M. Franchini, Thromb. J. 3 (14) (2005).
[84] T. Dutt, M. Schulz, Clin. Kidney J. 6 (6) (2013).
[85] G.J. Lavandosky, Clin. Case Rep. 3 (8) (2015).
[86] A. Chryssos, S.J. Stroup, et al., J. Extra Corpor. Technol. 47 (1) (2015).
[87] R.S. Kazmi, B.A. Lwaleed, Br. J. Clin. Pharmacol. 72 (4) (2011).
[88] J. Li, S. Wang, J. Barone, B.P. Malone, J. Formul. Manag. 34 (8) (2009).
[89] G. D'Andrea, R.L. D'Ambrosio, et al., Blood 105 (2) (2005).
[90] W. Eichhorn, M. Haase, Biomed. Res. Int. (2015).
[91] K. Schrör, Semin. Thromb. Hemost. 23 (4) (1997).
[92] C.R. Ensor, W.D. Cahoon, M.A. Crouch, et al., Tex. Heart Inst. J. 37 (2) (2010).
[93] J.W. Eikelboom, S.J. Connolly, M. Brueckmann, C.B. Granger, A.P. Kappetein, M.J. Mack, et al., N. Engl. J. Med. 369 (13) (2013).
[94] I. Bjork, S.T. Olson, Adv. Exp. Med. Biol. (425) (1997).
[95] M.M. LaBan, C.E. Whitmore, R.S. Taylor, Am. J. Phys. Med. Rehabil. 82 (5) (2003).
[96] B.T. Campbell, T.M. Braun, R.E. Schumacherb, R.H. Bartlett, R.B. Hirschl, J. Pediatr. Surg. 38 (3) (2003).
[97] R.H. Bartlett, D.W. Roloff, J.R. Custer, J.G. Younger, R.B. Hirschl, JAMA 283 (7) (2000).
[98] A. Mekaj, Y. Mekaj, S. Duci, E. Miftari, Ther. Clin. Risk Manag. (11) (2015).
[99] S.A. Wayangankar, M.S. Abu-Fadel, H.D. Aronow, et al., Circ. Cardiovasc. Interv. 6 (2) (2013).
[100] E.W. Holy, H.J. Beer, J. Cardiovasc. Med. 16 (4) (2013).
[101] R. Hoffman, B. Brenner, Best Pract. Res. Clin. Haematol. 25 (3) (2012).
[102] S. Gupta, K.A. Amoako, A. Suhaib, K.E. Cook, Adv. Mater. Interfaces 1 (8) (2014).
[103] K.A. Amoako, H.S. Sundaram, A.B. Suhaib, S. Jiang, K.E. Cook, Adv. Mater. Interfaces 3 (6) (2006).
[104] K.A. Amoako, P.J. Montoya, T.C. Major, A.B. Suhaib, H. Handa, D.O. Brant, K.E. Cook, J. Biomed. Mater. Res. 101 (12) (2013).
[105] K.A. Mowery, M.H. Schoenfisch, J.E. Saavedra, L.K. Keefer, M.E. Meyerhoff, Biomaterials 21 (1) (2000).
[106] A. Pegalajar-Jurado, J.M. Joslin, M.J. Hawker, M.M. Reynolds, E.R. Fisher, ACS Appl. Mater. Interfaces 6 (15) (2014).
[107] K.A. Amoako, K.E. Cook, ASAIO J. 57 (539) (2011).
[108] K.A. Amoako, C. Archangeli, H. Handa, T.C. Major, M.E. Meyerhoff, G.M. Annich, R.H. Bartlett, ASAIO J. 58 (3) (2012).
[109] C.J. Backlund, B.V. Worley, M.H. Schoenfisch, Acta Biomater. 29 (1) (2016).
[110] A.J. Keefe, S. Jiang, Nat. Chem. 4 (1) (2012).
[111] H.S. Sundaram, X. Han, A.K. Nowinski, N.D. Brault, Y. Li, J.R. Ella-Menye, et al., Adv. Mater. Interfaces 1 (6) (2014).
[112] Z. Cao, L. Zhang, S. Jiang, Langmuir 28 (31) (2012).
[113] Z. Cao, S. Jiang, Nano Today 7 (5) (2012).
[114] N. Peppas, R. Langer, Science 263 (5154) (1994).
[115] B. Bloch, Ann. R. Coll. Surg. Engl. 66 (5) (1984).
[116] Y. Onuki, U. Bhardwaj, F. Papadimitrakopoulos, D.J. Burgess, J. Diabetes Sci. Technol. 2 (6) (2008).
[117] W. van Oeveren, Scientifica (2013). 392584.
[118] F. Jung, S. Braune, A. Lendlein, Clin. Hemorheol. Microcirc. 53 (1–2) (2013).
[119] J.M. Anderson, Annu. Rev. Mater. 31 (61) (2001).

[120] International Standards Organization, Biological evaluation of medical devices—part 4: selection of tests for interactions with blood. ISO 10993-4:2002, 2002, www.iso.org (accessed October 2016).
[121] Z. Zhou, M.E. Meyerhoff, Biomaterials 33 (2005).
[122] B. Wu, B. Gerlitz, B.W. Grinnell, M.E. Meyerhoff, Biomaterials 28 (2007).
[123] Z. Zhang, et al., Lab Chip 13 (3609) (2013).
[124] F. Xiaowu, L. Lijun, L.D. Jeffrey, P.B. Messersmith, J. Am. Chem. Soc. 127 (45) (2005).

Strategies to improve the hemocompatibility of biodegradable biomaterials

10

P. Mulinti[*], *J.E. Brooks*[†], *B. Lervick*[*], *J.E. Pullan*[*], *A.E. Brooks*[*]
[*]North Dakota State University, Fargo, ND, United States, [†]Southern Utah University, Cedar City, UT, United States

10.1 Introduction

Hemocompatibility is a measure of the thrombotic response induced by a material or device in contact with blood that will lead to the activation of the blood coagulation cascade, including platelet response, complement activation, and coagulation cascade initiation. The importance of the interfacial biomaterial surface cannot be overestimated in the evaluation of hemocompatibility as it not only acts as an intermediary for the hemocompatibility of a biomedical device but also more broadly dictates the nature of the foreign body response (FBR). Historically, strategies to improve hemocompatibility have focused, with limited success, on preventing protein adhesion to the material surface; however, a limited number of new approaches are attempting to control and direct adhesion to manipulate the blood-contacting surface. Several bulk material and surface characteristics are significant to blood-contacting devices: (1) biocompatibility as determined by inflammation and cytotoxicity, (2) protein and cellular adhesion leading to stenosis and/or thrombus formation, and (3) degradation. Inflammation and cytotoxicity are often intimately tied to material degradation. Upon material degradation, particles, which act as haptens, are produced, and the surface chemistry and topography of the material change [1,2]. These hapten-like particles subsequently bind to endogenous proteins to create a hapten-protein complex, which is often responsible for triggering an immune response. In addition to degradation complexes provoking an immune response, which may include thrombosis, biomaterial blood interactions are mediated by an ubiquitous host protein coating, the composition of which determines the adherence of cells and the progress of the FBR and can change based on degradation, potentially leading to late-stage thrombosis or restenosis. Immediately after implantation, circulating endogenous proteins adhere to the material and initiate a cell-signaling cascade that may lead to the accumulation and adhesion of platelets and leukocytes. The immunomodulating cells are triggered to induce the adherence and aggregation of further platelets, culminating in the formation and development of thrombi. Other mediators secreted by platelets and leukocytes prompt coagulation and elicit immunological responses. Ultimately, thrombus formation is considered as the earliest of all the complications of the polymer-blood interactions.

Hemocompatibility of Biomaterials for Clinical Applications. https://doi.org/10.1016/B978-0-08-100497-5.00017-3
© 2018 Elsevier Ltd. All rights reserved.

10.2 Biomaterial hemocompatibility

Despite numerous commercially available biomaterials [3], many challenges remain for novel biodegradable polymers, including the optimal biocompatibility, thrombogenicity, and degradation rate of the polymer. Two major problems provide context for the hemocompatibility of biodegradable and hybrid biodegradable materials: (1) the immune response, including toxicity, to the material degradation particles and (2) the ability to continue to function (e.g., load bearing or structural support) during degradation. While the immune response may be modulated by moieties such as magnesium, under physiological conditions, many such ions are degraded quite rapidly by chlorides [4] necessitating an alloy or hybrid molecule to improve biocompatibility. Such a hybrid material may also improve the mechanical integrity of the material under dynamic conditions, such as those encountered at the blood-material interface. Many current hemodialysis catheter materials and designs are plagued by an increased bulk not only to provide proper mechanical function and consequently lack the proper balance of strength and flexibility necessary during catheter insertion and placement [5] but also to maintain proper blood flow according to ISO 10993-4 recommendations under the extreme pressures and flow rates necessary during multiple hemodialysis sessions (high flow in the range of >400 mL/min reliably [6]) [7]. Recently, modification of the hemocompatibility of bulk materials via physical blending [8,9], chemical grafting [10,11], or copolymerization [12] with a hemocompatible component has been reported. Many such materials may be composited to act as both the bulk and surface material. Although much of the hemocompatibility of a material may derive from the underlying bulk material properties, the impact of surface interactions cannot be overstated (Fig. 10.1). Specifically, biopolymers (chitosan [8,13,14], collagen [15–20], silk [21–27], hyaluronic acid [12,15,16,28,29], phosphorylcholine [10,30,31], etc.) or hybrid biomaterials are being explored for both their surface and bulk properties as an exciting new alternative.

10.3 Biodegradable polymeric materials

Although assessing the tissue compatibility of biomedical polymers has been frequently addressed both in scientific and commercial sectors, studies assessing hemocompatibility, particularly over time, are noticeably lacking in the literature [1]. Regardless of their specific hemocompatibility, the material used for biodegradable blood-contacting devices generally falls in two categories: (1) natural biopolymers (e.g., polysaccharides, proteins, and biofibers) and (2) synthetic biodegradable polymers (e.g., polylactic acid (PLA), polyglycolic acid (PGA), poly lactic-*co*-glycolic acid (PLGA) copolymers, and polycaprolactone (PCL)).

10.3.1 Natural polymers

In contrast to many traditional, nonnatural biomedical materials, many natural biopolymers have physiological degradation pathways, hydrophilicity, and chemically

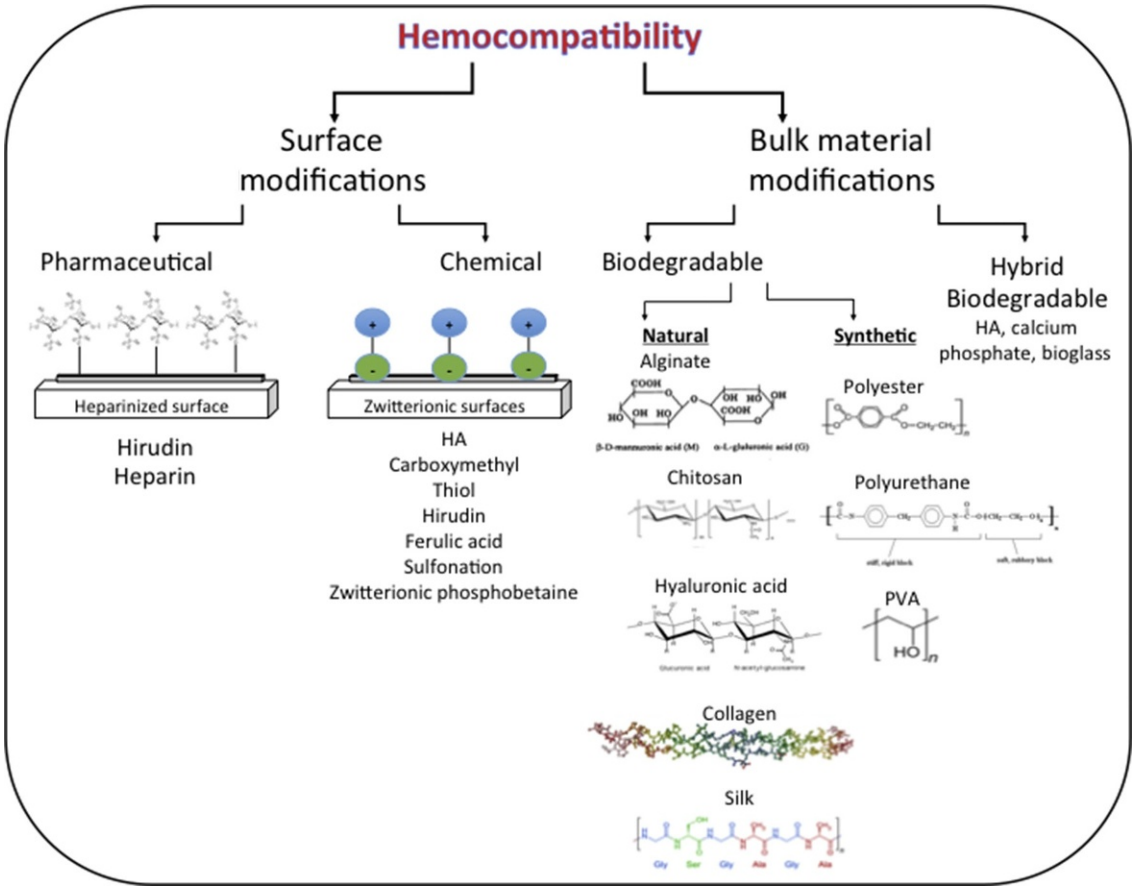


Fig. 10.1 Overview of blood-contacting materials.

reactive groups that allow them to remodel to facilitate cell attachment and infiltration while preventing the adverse FBR often associated with synthetic materials [32]. Additionally, viscoelasticity, often necessitated by the specific application, can be imparted via biological polymers to provide a measure of shape memory-based expansion, overcoming the rigidity that afflicts many synthetic polymers; unfortunately, this same property introduces a new potential complication as mechanical performance may change under cyclic loading flow conditions. The hemocompatibility of several biological polymers has been evaluated, allowing the identification of several candidate biopolymers for use in blood-contacting medical devices (Table 10.1).

10.3.1.1 Alginate

Due to its ability to cross-link with divalent cations like calcium and the reactivity of its carboxylate side groups, alginate, commonly obtained from the cell wall of brown algae, has been widely used in various biomedical applications including drug delivery, wound healing dressings, and tissue engineering scaffolds [33]. Alginate is a polysaccharide copolymer composed of (1–4) linked β-D-mannuronic acid and α-L-guluronic acid monomers along the polymer backbone. While some pure alginate hydrogel-based drug delivery devices have been used as delivery systems, alginate is typically not appropriate as a bulk material. However, recently, the degradation products of alginate were assessed for their in vitro hemocompatibility, revealing that the degradation of higher-molecular-weight alginate shortened blood clotting time and slightly decreased the rate of hemolysis [34]. Despite modest improvements in hemocompatibility when used as a surface coating [35], alginate's effects on biocompatibility are often a result of its inclusion in a composite with other biodegradable, hemocompatible components [36]. Although alginate has abundant properties that make it an attractive biomaterial for biomedical applications, it has two major drawbacks as biomaterial, in vivo degradation and poor cellular adhesion. Compositing alginate with chitosan may overcome some of these pitfalls, although this composition with interpenetrating polyethylene glycol still produced a hydrogel matrix and not a solid bulk material [13].

10.3.1.2 Chitosan

Despite its use as a candidate material for a variety of biomedical applications due to its reported innocuous and biocompatible properties, chitosan, a linear polysaccharide consisting of (1–4) linked D-glucosamine and *N*-acetyl-D-glucosamine residues derived from deacetylation of chitin, may induce thrombosis attributed to its cationic nature [8]. The majority of studies that have considered the hemocompatibility of chitosan have concluded that the interaction of the free amino groups of chitosan with plasma proteins and blood cells could induce coagulation via both complement activation [37] and the extrinsic coagulation pathway [8]. Furthermore, the positive charge of chitosan can induce fibrinogen adsorption and trigger the adhesion of platelets and leukocytes with the degree of chitosan deacetylation being associated with increased fibrinogen adsorption [38]. Historically, it has been reported that in vitro the addition of chitosan to blood has reduced clotting time by 40% [39]. Interestingly, in spite of being regarded as naturally unsuitable as a blood-contacting material, chitosan has

Table 10.1 **The characteristics of a variety of natural polymers are summarized**

Type of biopolymer	Structure	Modification attempts	Hemocompatibility	
			Advantages	Disadvantages
Alginate	Polysaccharide copolymer (1–4) linked β-D-mannuronic acid and α-L-guluronic acid monomers	• Alginate and chitosan • Interpenetrating polyethylene glycol	• Reduced blood clotting time • Slightly decreased rate of hemolysis	• In vivo degradation • Poor cellular adhesion
Chitosan	Linear polysaccharide consisting of (1–4) linked D-glucosamine and *N*-acetyl-D-glucosamine residues derived from deacetylation of chitin	• N-acetylation of chitosan • Sulfated chitosan • Carboxymethyl chitosan • O-substitution of chitosan	• Wound healing • Antibacterial and hemostatic properties	• Induce thrombosis • Complement activation • Extrinsic coagulation pathway activation
Hyaluronic acid	Linear anionic polysaccharide consisting of alternating units of *N*-acetyl-D-glucosamine and glucuronic acid	• Micropatterned HA and collagen type IV HA composite on titanium • Composite HA collagen and nanobioactive glass • Thiolated hydrophobic molecule modification • Polyurethane coated with thiolated HA	• Naturally degraded by hyaluronidase enzyme • Can act as a scaffold	Weak mechanical properties Structural fluidity without ethyl or benzyl ester cross-linkages
Silk	Protein with several amino acid motifs to give a multiple secondary structures	• Sulfonation • Zwitterionic phosphobetaine • Ferulic acid • Heparin grafting • Hirudin • Chitosan, gelatin, and polycaprolactone	• Biocompatible • Low immunogenicity • Slow degradation • Versatility • Mechanical properties • Support stem cell adhesion, proliferation, and differentiation in vitro • Resist pathological adhesion in vivo	• Poor hemocompatibility when pure
Collagen	Triple helix protein	• PCL nanowire • Collagen IV/HA coating on titanium	• Did increase platelet adhesion	• Didn't fully promote platelet activation • Impact seems to be type-dependent

been extensively studied as wound healing material due to its innate antibacterial properties and hemostatic nature and several FDA-approved products exist [40–42]. Importantly, development of a single material that can address the connection between thrombosis and infection remains an important and unresolved challenged [43,44]. Unfortunately, the modification of chitosan to improve its thrombogenicity remains an obstacle to true translatability and broad biomedical utility. Nevertheless, strategies to enhance the hemocompatibility of chitosan, which fall into one of two categories, (1) chemically modified chitosan or (2) composite chitosan with a polymer that has complimentary activity, are progressing. One of the most effective chemical modifications is the N-acetylation of chitosan. Alternatively, sulfated chitosan as well as carboxymethyl chitosan has also demonstrated good hemocompatibility due to its abundant negative charge, which allows for electrostatic repulsion ultimately preventing coagulation while retaining the other benefits of chitosan [45]. Additional modifications, which increase the negative charge density, seem to enhance the anticoagulation effect [46,47]. O-substitution of chitosan has also proved an effective strategy for improve its hemocompatibility [14,48,49]. A complete review of all of chitosan's modifications is beyond the scope of this chapter, but the reader is referred to a recent extensive review by Balan and Verestiuc in 2014 [8]. Chitosan has almost limitless potential as a biomaterial for biomedical applications; however, it is clear that its use as a hemocompatible material will require further development.

10.3.1.3 Hyaluronic acid

Hyaluronic acid (HA) is one of the commonly used biomaterial for tissue engineering and scaffold material. It is a linear anionic polysaccharide consisting of alternating units of *N*-acetyl-D-glucosamine and glucuronic acid with unique viscoelastic properties and biological properties that may assist in tissue repair [28]. Furthermore, Li et al. recently reported increased hemocompatibility when coating a titanium surface with either micropatterned HA [50] or collagen type IV HA composite [15]. This result was confirmed by Yan et al. in 2016 when they observed good anticoagulation using a composite of HA collagen and nanobioactive glass [16]. In addition to improved hemocompatibility, as a biomaterial, HA is capable of being naturally degraded by the mammalian enzyme hyaluronidase. Due to its weak mechanical properties and structural fluidity, HA is often cross-linked with ethyl esters or benzyl esters to act as a scaffold although its hemocompatibility as a bulk material with a thiolated hydrophobic molecule modification in a cross-linkable hydrogel was recently investigated, revealing a biocompatible material [29]. Furthermore, when polyurethane (PU) was coated with a thiolated HA, protein biofouling, which is linked to coagulation, was reduced [51]. Based on these and other studies, the potential of HA as a biodegradable, anticoagulation material should be exploited.

10.3.1.4 Silk

Silk fibroin has been increasingly considered for biomedical applications due to its biocompatibility, low immunogenicity, slow degradation, versatility, and remarkable mechanical properties [52–54]. Silk fibroin can provide enhanced ability to remodel

in response to the biological environment, leading to better integration and perhaps reduced material-associated thrombosis [21]. This presents an attractive opportunity to exploit modified silk motifs as the basis for biomaterials with tailored properties. Specific amino acid motifs, historically correlated with functional properties [3], can be chemically and/or genetically modified while retaining critical secondary structural features, producing recombinant silk polymers that control (1) polymer size, (2) chemical reactivity, and (3) bulk material properties [55]. Unfortunately, pure silkworm silk fibroin poor hemocompatibility [22,23]. Nevertheless, silk fibroin can be rendered anticoagulant via sulfonation, not surprising considering the chemical structure of the natural anticoagulant heparin [24]. Recently, silk fibroin has been modified to improve hemocompatibility via addition of zwitterionic phosphobetaine, which demonstrated good nonthrombogenicity in the platelet adhesion assay. Additionally, ferulic acid silk fibroin, sulfonation, and heparin grafting showed that APTT (activated partial thromboplastin time), PT (prothrombin time), TT (thrombin time), and WBCT (whole-blood clotting time) were prolonged, indicating that modified silk may be an efficient anticoagulant [23]. Modification of silk fibroin with hirudin also improved hemocompatibility as indicated by limited platelet adhesion and aggregation by enhancing anticoagulation properties found in unmodified silk fibroin materials [25]. Defined silk amino acid motifs and periodicity also impart a level of control not possible with many traditional scaffold materials expanding their utility into a range of biomaterial and tissue engineering applications. Silk fibroin in various formats (films, fibers, nets, etc.) has been shown to support stem cell adhesion, proliferation, and differentiation in vitro and promote tissue repair and resist pathological adhesion in vivo [56–59]. Although the majority of previous work has been completed using silkworm silk, spider silks have superior mechanical properties, stemming from an expanded repertoire of specialized fibers and amino acid blocks allowing their sequences to be manipulated and genetically tailored with functional specificity. In 2014, Zhao et al. created a spider silk protein-based bilayer small-diameter vascular scaffold by compositing recombinant silk with chitosan, gelatin, and PCL. Based on the material's recalcification coagulation time, the recombinant silk provided improved biocompatibility and hemocompatibility to the scaffold [26,27].

10.3.1.5 Collagen

Collagen I is ubiquitous in mammalian systems and is a major component of the extracellular matrix prevalent in blood vessels. Thus, it stands to reason that collagen may prove an important surface modifier to modify the body's coagulation response to blood-contacting materials. Recently, PCL nanowires were modified with collagen, and their hemocompatibility was evaluated, leading to the suggestion that collagen modification did not fully promote platelet activation but did increase platelet adhesion when compared with the nanowires [60]. Alternatively, a collagen surface coating has recently been explored as a drug-eluting reservoir by several groups; however, collagen's naturally thrombogenic character may limit the utility of this application [61]. Interestingly, a collagen IV/HA coating on titanium increased the hemocompatibility [15]. Multilayer surfaces with synthetic polymers such as PCL and poly(L-lactic acid) (PLLA) have also been shown to improve the hemocompatibility of titanium and other

substrate materials [17,19]. Thus, the controversy in the literature seems to indicate that the impact of collagen on hemocompatibility is type-dependent.

10.3.2 Synthetic biodegradable polymers

Synthetic polymers not only are perhaps the largest group of biodegradable polymers but also are the default biomedical polymers for blood-contacting devices as they offer several advantages over natural biodegradable polymers, including control over chemical and physical properties to direct a biological response and commercial scale-up [62]. Importantly, the chemical composition, processing and surface morphology of such synthetic polymers seems to directly affect their thrombogenicity [63] with fibers showing short coagulation times and platelet activation similar to highly thrombogenic forms of collagen. The most common synthetic polymers used in biomedical applications include the linear polyesters (e.g., PLA, PGA, PLGA, and PCL, PU, and poly(vinyl alcohol) (PVA)) (Table 10.2).

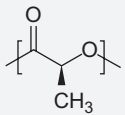
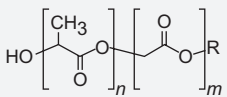
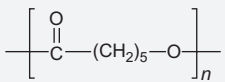
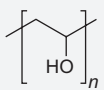
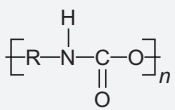
10.3.2.1 Polyesters

Polyesters, including PLA, PLGA, and PCL, are most often utilized for 3D scaffolds in tissue engineering.

Polylactic acid

PLA exists in three forms: L-PLA (PLLA), D-PLA (PDLA), and a racemic mixture of D,L-PLA (PDLLA). Of these, PLLA and PDLLA have shown promise in bioengineering and have been extensively studied [64].Hydrolytic degradation of PLA occurs in the body by de-esterification to form lactic acid, which is normally present in the body and is excreted by tricarboxylic acid cycle. Degradation kinetics are influenced by factors such as structural configuration, copolymer ratio, crystallinity, molecular weight, morphology or porosity, and amount of residual monomer. In spite of the various advantages of PLA as a biomaterial, some disadvantages have raised concerns about the biocompatibility of this polymer. First, PLA and PLGA undergo a bulk erosion process, which may compromise the integrity of the scaffold causing it to fail prematurely and release acidic degradation products that can elicit inflammatory response. In fact, high-molecular-weight PLLA alone has shown to take more than 5 years to be completely resorbed in the body, which may limit its biomedical application [64]. However, more importantly, PLA, a weak polyelectrolyte, has poor hydrophilicity, which can lead to serious protein biofouling, platelet adhesion, and activation of coagulation pathways [65].Nevertheless, although PLLA and PLGA are known to activate the coagulation pathway, this activation falls within the normal reference range as prescribed for biomedical materials [66]. Both chemical modifications and blending with other degradable polymers have been shown to reduce the degradation time. Grafting of a zwitterion (both positive and negative charge moieties) allows formation of a hydration layer, thereby leading to improved biocompatibility and biocompatibility. The zwitterionic molecule, poly(sulfobetaine methacrylate) (PSBMA), was attached to PLA via a polydopamine intermediate layer to change the hydrophilicity

Table 10.2 **Summary of common synthetic polymers used for biomedical applications**

Type of polymer	Structure	Modification attempts	Hemocompatibility	
			Advantages	Disadvantages
Polylactic acid (PLA)		• Heparin • Hirudin • Zwitterion PSBMA	• Degradable • Bioresorbable • Physiological metabolite	• High sensitivity to hydrolytic degradation • High levels provoke undesired inflammatory response • Bulk degradation • Weak electro
Poly(lactic-*co*-glycolide) (PLGA)		• PEG/PLGA copolymer • Processing techniques	• Wide range of degradation rates • Abundant cell adhesion and proliferation properties • Stimuli sensitive	• Rapidly accumulate in the liver, spleen, and bone marrow • Abundant cell adhesion and proliferation properties
Polycaprolactone (PCL)		• Copolymerization mPEG, PLLA, PLGA • Chitosan-montmorillonite • Chitosan-heparin • PMPC • P(DMAPS)	• Low melting temp • Low in vivo degradation rate • High drug permeability	• Long degradation time • Limited biocompatibility for tissue integration
Poly(vinyl alcohol)		• Alginate composite • Polyanionic chains (PSSS, (P(AA-*co*-SSS)), PAA) • Citric acid cross-linking	• Water soluble • Biodegradable • Easy to copolymerize	• Limited mechanical strength • Slow degradation
Polyurethane		• D-PHI • Blended with PLA • Heparin • SO_3H and/or COOH • PEO • Albumin	• Resist platelet adhesion • Degradable and nondegradable	• Activation of complement • Protein adhesion

and negativity polymer and alleviate biofouling, including platelet adhesion and coagulation [65]. Heparin has also been tethered via a polydopamine adhesive layer to improve blood compatibility [67,68]. In 2016, Xiong et al. directly bonded the anticoagulant heparin to PLA via a glycidyl ether reaction to provide a significant improvement in PLA hemocompatibility [69]. Similar results were observed when hirudin, a natural biomolecular inhibitor that can form a hirudin-thrombin complex to prevent blood coagulation, was immobilized on a PLA membrane via hydrogen bonding through PVP [70].

Poly lactic-*co*-glycolide

PLGA, which has been used in a variety of biomedical applications (e.g., sutures, drug delivery devices, and tissue engineering scaffolds), is a block copolymer of PLA and PGA. The block nature of the polymer allows for easy modification to tailor the degradation rate, which is influenced by both the hydrophobic/hydrophilic balance and crystallinity of the composite. Although its copolymer character allows its degradation rate to be designed for specific applications, as with most other polyesters, PLGA experiences bulk degradation. Furthermore, while both PLA and PGA are bioresorbable via the citric acid cycle, high levels of glycolic acid have been shown to provoke an undesired inflammatory response. Additionally, lactic acid, a by-product of PLGA degradation, is a known platelet agonist [1,71]. In fact in a recent study, even undegraded PLGA allowed fourfold higher platelet adhesion when compared with albumin control [1]. Nevertheless, PLGA's touted biocompatibility is largely attributed to its ability to degrade into nontoxic, or at least metabolizable, by-products. To address these problems, the surface of many PLGA-based devices has been surface modified (e.g., blended dexamethasone [72], grafted with the amino groups of mucin [73], and conjugation of PLGA nanoparticles with alendronate [74]) or copolymerized with other polyesters (e.g., polyethylene glycol (PEG), diblock (PLGA-PEG) or triblock molecules with both ABA (PLGA-PEG-PLGA) and BAB (PEG-PLGA-PEG), PCL, chitosan, and PU). For a more complete review of PLGA engineered for hemocompatibility, the reader is referred to the recent book chapter by Thasneem and Sharma [75]. PLGA also demonstrates abundant cell adhesion and proliferation properties making it an excellent candidate for application in tissue engineering.

Polycaprolactone

PCL is a semicrystalline polymer that has found utility in several biomedical applications due to its easy processing, long in vivo degradation rate, and molecular weight-dependent drug release. Furthermore, because of PCL's mechanical properties, it is often copolymerized with other lactones (e.g., valerolactone) [76] or polyesters to provide additional rigidity and altered hydrolysis and degradation. Copolymers of ε-caprolactone with D,L-lactide [76] and chitosan-modified montmorillonite [77] have also been synthesized to yield materials with more rapid degradation and bioresorption rates. Due to PCL's history of use as a biomedical polymer, its thrombogenic potential has been relatively well characterized and may in some measure be associated with its processing. When electrospun into fibers, PCL was found to induce a small measure of hemolysis, depending once again on it molecular weight [63,78]. However,

when processed into a three-layered tubular nanofibrous scaffold with collagen and PLLA (inner, intermediate, and outer layers, respectively), the scaffold exhibited reduced platelet adhesion, hemolysis ratio, and inflammatory response but a similar blood clotting profile when compared with an expanded polytetrafluoroethylene graft [19]. Importantly, coagulation and platelet adhesion have found to be slightly higher for hydrophobic polymers such as PCL and PCL/PLGA blends [78]. However, this is not always the case; an amphiphilic block copolymer of methoxy polyethyleneglycol-polycaprolactone (mPEG-PCL), noted for its water solubility and biodegradation, was recently evaluated for its use in biomedical blood-contacting applications and demonstrated alleviated blood clotting and reduced hemolysis [79]. Furthermore, at high concentration, the copolymer displayed impaired platelet aggregation [79]. Alternatively, small-diameter vascular graft fabricated from a PCL/chitosan blended with heparin ionically bound to the chitosan component demonstrated reduced platelet adhesion and prolonged coagulation time [32]. PCL has also been modified with poly(2-methacryloyloxyethyl phosphorylcholine) (PMPC) [80] and zwitterionic poly(3-dimethyl(methacryloyloxyethyl) ammonium propane sulfonate) (P(DMAPS)) brushes [81] to improve its hemocompatibility. For a review of aminolysis-based surface modifications on polyesters, the reader is referred to Zhu et al. [82].

10.3.2.2 Polyurethane

Although PUs may not traditionally be classified as biodegradable, the chemical versatility of segmented PU (SPU) has earned them a spot in this chapter. SPUs can be made biodegradable by synthesis with either a soft biodegradable segment such as a polyester or a biodegradable hard segment. Interestingly, biodegradable SPUs exhibit properties similar to nondegradable SPUs and Tecoflex medical-grade PU, specifically in their ability to resist platelet adhesion [83]. Alternatively, degradable, polar, hydrophobic, ionic polyurethane (D-PHI) was initially shown to have acceptable blood compatibility and displayed increased intrinsic coagulation cascade time but decreased extrinsic pathway activation when compared with PLGA (either degraded or naive) [1]. Notably while PLGA degradation occurs in bulk, D-PHI degradation occurred via surface erosion, leading to decrease surface topography. In fact, many of the disadvantages of PU in bulk can be overcome by changing the surface topography, leaving the bulk intact [84]. Dey et al. also reported the development of biodegradable, cross-linked, urethane-doped, polyesters with improved hemocompatibility [85]. SPUs have also been electrospun as a blend with PLLA and subsequently surface modified with heparin to improve hemocompatibility [86], while other nondegradable PUs have been endowed with heparin-like qualities by addition of SO_3H and/or COOH functional groups and subsequently blending the modified PU with polyethersulfone [87]. Poly(ethylene oxide) was also used to modify the surface of medical-grade PU and significantly improved the hemocompatibility of raw PU [88]. Coating the polymer with albumin has also been reported to improve the biocompatibility of PU [89,90]. Regardless of their degradation status, the chemical versatility of PUs makes this a versatile class of materials for biomedical applications whose hemocompatibility should be evaluated and in certain cases improved.

10.3.2.3 Poly (vinyl alcohol)

PVA is a biodegradable, water-soluble synthetic polymer with a hydrocarbon backbone [91] used for a variety of applications; however, its ability to swell in water may compromise the strength and stability of PVA [92] for biomedical applications. Nevertheless, recent modifications and composites with PVA have been explored for use in biomedical applications [93]. To improve the mechanical stiffness of PVA and maintain its hemocompatibility, citric acid was recently used as a cross-linker with bacterial cellulose nanowhisker reinforcement as a nanofiller [92]. When evaluated, PVA showed a statistically insignificant different in clotting times (APTT, PT, and TT) in platelet-poor plasma as samples without PVA; however, much of the coagulation cascade relies on the presence of platelets; thus, using PPP may not provide the most accurate evaluation. Specifically, branching of PVA has not only improved the mechanical strength of PVA in a swollen state but also appeared to improve its hemocompatibility although specific tests assessing clotting times were not directly addressed [94]. Alternatively, polyanionic chains (poly(sodium styrenesulfonate) (PSSS), poly(acrylic acid-*co*-sodium styrenesulfonate) (P(AA-*co*-SSS)), and poly(acrylic acid) (PAA)), previously shown to have heparin-like activity, were grafted onto PVA for additional stability and showed excellent anticoagulant activity via intervening in the intrinsic, extrinsic, and common pathways and were nonhemolytic [61]. Furthermore, grafted PSSS chains provided more prolonged APTT and PT when compared with grafts PAA chains; this may be a product of the sulfonate group on PSSS, which is more electronegative when compared with the carboxyl group of the other grafted species [61].The hemocompatibility of PVA was also improved via coupling PVA to alginate via esterification with the degree of hemolysis increasing with an increasing ratio of alginic acid to vinyl alcohol [36].

10.4 Hybrid biodegradable biomaterials

Although there are numerous biodegradable polymers that have been explored for biomedical application, each material suffers from several shortcomings often lacking (1) the mechanical compliance necessary for long-term patency, (2) biodegradability and bioresorption of degradation by-products, and/or (3) desired activity at the material/biology interface. For example, many polymers (e.g., PLGA) release acidic by-products during degradation that can negatively impact surrounding tissue; however, compositing these polymers with calcium phosphate or bioactive glass (BG), which produce more basic degradation by-products, may buffer and protect the tissue [62]. The advent of hybrid biodegradable compositions in the context of rationale materials design may prove the answer to these concerns. Several such composites are explored here.

10.4.1 Substrate materials

10.4.1.1 Bioceramics

Bioceramics have been investigated for over five decades as an alternative to metallic implants to overcome their limited biocompatibility [95]. This is particularly evident

in orthopedics where bioceramics can now be found in almost every area of the skeletal system [95]. Unfortunately, the high stiffness of a bioceramic may restrict its use in soft tissue applications. Therefore, hybrid biomaterials have been developed with the combination of bioceramics with the polymers to produce a composite scaffold that has the advantages of both the materials. Historically, the popularity of bioceramics is tied to their biological and chemical stability and wear resistance. However, more recently, the next generation of bioceramics is being touted for their bioactivity. These second-generation bioceramics include hydroxyapatite, calcium phosphate-based cements, and silica-based BG. Additionally, many of these new bioceramics not only can be degraded over a period of time as the host tissue grows into and replaces the ceramic "template" but also can be endowed with pharmaceutical activity as a drug delivery vehicle [95]. Unfortunately, as is the nature of a ceramic, many if not most bioceramics are brittle, leading to potential issues with catastrophic early failures [62]. Creating hybrid or composite materials based on an underlying bioceramic substrate may be able to circumvent this pitfall.

Calcium phosphates

Calcium phosphates are among the most widely used bioceramics with excellent bioresorption and compatibility specific to enhance bone repair. In 2016, Zou et al. reported using a zinc calcium phosphate coating on a new class of magnesium biodegradable and biocompatible metal alloys to improve the surface cyto- and hemocompatibility, producing lower levels of hemolysis below 5% and having very little influence on blood cells [96]. In contrast to this application and those for most other indwelling materials, which strive to circumvent the coagulation pathway, for bone, controlled clotting may promote hemostasis and tissue bonding. A clinical composite of hydroxyapatite and β-tricalcium phosphate (biphasic calcium phosphate) was preadsorbed with fibrinogen, cleavable by thrombin to yield fibrin, which readily self-associates to create a resorbable fibrin clot. This composition provided rapid coagulation at the defect site and promoted enhanced bone formation [97]. This is not surprising due to the importance of Ca^{+2} on the coagulation cascade and its ability to promote the polymerization of fibrin monomer. In fact, hydroxyapatite, one of the most widely used calcium phosphates, has been employed for its hemostatic activity, as shown when hydroxyapatite was grafted onto poly(D,L-lactide) and lead to an accelerated clotting time [98].

Bioactive glass

BG comes in a couple of different forms (i.e., silica, borate, and phosphate) with a variety of sizes and porosity; however, typically, BG is degradable, silicate-based materials that can trigger a range of biological responses such as tissue regeneration in bone or angiogenesis. In the presence of physiological fluids, BG can tightly bind with living tissue minimizing the interfacial space. This may prove a significant benefit in blood-contacting applications. Upon exposure to physiological fluid, the BG surface forms a layer of hydroxyapatite, which provides a bonding interface with many tissues, particularly bone, while Si, Na, and Ca phosphate ions are leached. The presence of calcium phosphate ions may interact in the coagulation cascade leading to favorable hemocompatibility. Bioglass has also been mixed with degradable polymers (e.g., PVA) and exhibited better degradation and cytocompatibility [55].

10.4.2 Inorganic/organic (I/O) hybrid materials

Due to their unique mixture of form and function, inorganic/organic (I/O) hybrid biomaterials are growing in popularity. These I/O hybrids are a single-phase, homogenous mixture between inorganic and organic components with emergent properties arising from the interface of the components [62] (Fig. 10.2). Importantly, one of the components typically has dimensions ranging from Å to nanometers. Moreover, inorganic materials are traditionally processed under high temperatures, which exclude the inclusion of many organic compounds. Thus, many I/O hybrids are produced via low-temperature sol-gel processing, leaving an interconnected porous framework suitable for tissue engineering [99]. Ultimately, the two parts of I/O hybrids mimic a biologically relevant composition. For example, inorganic carbonated hydroxyapatite mimics the mineral composition of the bone, while the synthetic or organic polymer matrix mimics the functional properties of a collagen-rich extracellular matrix. Alternatively, blood-contacting, I/O hybrid biomaterials use a combination of inorganic (e.g., a biodegradable metal alloy) and organic (e.g., PVA) materials to provide better mechanical properties [100] and hemocompatibility. Hemocompatibility may be limited by small, inorganic particle degradation by-products [101]. These mimicked structures lead to increased mechanical properties and bioactivity and make I/O increasingly relevant as biodegradable, biocompatible scaffolds.

A necessary prerequisite for the successful bench to bedside translation of many if not all blood-contacting or indwelling biomedical devices is hemocompatibility. Importantly, inadequate hemocompatibility can disrupt Virchow's triad, leading to pathological thrombus formation and in certain cases predispose the device to infectious complications [101,102]. I/O hybrid biomaterials may interrupt the device's inherently poor hemocompatibility by replacing the bulk device material either as a degradable alloy or as a biocompatible, hydrogel surface coating. Due to the water swelling of a hydrogel, which contains covalent, cross-linked polymeric structures, hemocompatibility is often positively impacted. Recently, a hydrogel was stabilized with a titanium carbonitride buffer and layered on a PU surface to provide enhanced

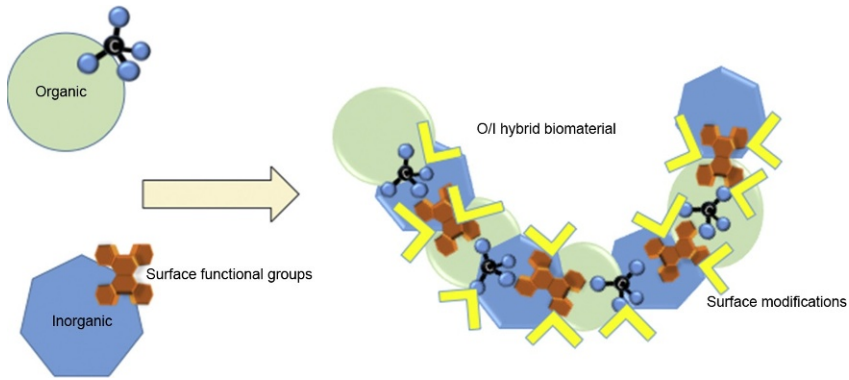


Fig. 10.2 Covalent interaction between organic and inorganic phases, forming a homogenous mixture. Surface modifications can be added to form noncovalent interactions with the solvent.

hemocompatibility under arterial flow mimicking conditions [103]. Degradable alloys are slightly different than hydrogels as they (1) form the bulk of the biomedical device or implant and (2) contain a metal scaffolding material to provide rigidity. Degradable magnesium-based I/O hybrids are useful due to their biodegradability and structural support. Recently, the biodegradable AZ31 alloy was investigated as an I/O hybrid with heparinization of the plasma electrolytic oxidation (PEO)/PLLA coating as a potential stent to (1) inhibit restenosis, (2) improve corrosion resistance, and (3) enhance the device hemocompatibility. As a result of the biodegradability, it is much simpler to replace a stent if required. I/O hybrids combine two areas of chemistry that have remained separate for many years but when combined have the potential to lead to many great scientific discoveries.

10.4.2.1 Nanocomposite materials

Not only does surface topography impact the blood-material interface, but also scale of the inorganic and the molecular weight of the polymer may also have an impact. As reviewed in 2009 by Mayer et al., nanoparticles have unique properties, particularly when in contact with blood. Positively charged and/or smaller particles inducing clot formation [104–106]. Not only does the size and charge of the particle impact hemocompatibility, but also the shape of the particle (e.g., particles, rods, and wires) can also be altered with significant implications for tissue engineering. In fact, several methods have been developed to control and manipulate each of these important properties as part of a biodegradable nanocomposite. Nanosized HA particles amalgamated with synthetic biodegradable polymers have processed into particles, rods, and wires for bone regeneration [99]. A variety of processing techniques include thermally induced phase separation (highly porous PLLA/hydroxyapatite or CP nanocomposite scaffolds) [99], a combination salt leaching/phase inversion (porous nanocomposites with PCL and hydroxyapatite) [99], grafting of the organic onto the inorganic phase (PLLA or PCL grafted to nanosized hydroxyapatite), and solution casting (polylactic acid employing organophilic silica and microcrystalline cellulose) [99]. The processing method may also affect the porosity and ultimately the cellular integration of the composite as well. Nevertheless, the hemocompatibility of nanomaterials maybe altered and improved not only by the size scale and geometric form of the material but also by compositing it. Such an effect was demonstrated by anchoring a phenylalanine-modified PGA (amphiphilic) to reduced graphene oxide. Chemically tethering amphiphilic PGA to reduce graphene oxide prevented interaction of the material with blood cells, whereas reduced graphene alone or mixed with PGA formed aggregates with blood cells [107]. Beyond using a nanomaterial as the bulk biomedical implant or drug delivery system, nanocomposite materials can be prepared by doping a biodegradable polymer matrix with inorganic nanoparticles or nanofibers to increase the strength and stiffness of the polymer matrix [108,109]. Once again, the particle size and morphology have a large influence on the overall impact of nanoparticle incorporation into a degradable polymer matrix with smaller diameters and larger aspect ratios influencing the properties of the bulk to the greatest extent. This effect is particularly evident when considering the incorporation of hydroxyapatite particles

in a PU/PCL polymer matrix. At higher hydroxyapatite loading (weight fraction), the hydroxyapatite particles aggregated, and protein adsorption was increased. Overall, the HA/PU/PCL composite showed a weak angiogenic response and favorable biocompatibility [62]. Similarly, integration of BG nanoparticles and/or nanofibers into a biodegradable polymer matrix is benefiting from the rigidity, osteoconductivity, and osteoinductivity of BG and the ductility and toughness of the polymer matrix in a completely biodegradable composition, which holds great promise for bone tissue engineering [62]. Regardless if they are I/O, O/O, or other polymer hybrids, the promise of nanocomposite materials is just beginning to be realized and should continue to be explored, particularly for implants and devices that have to function at the interface of hard and soft tissues.

10.4.3 Polymer hybrids

Implantable sensors, including glucose sensors, play a significant role in current medical practice; however, their indwelling lifetime is often limited by protein adsorption, which progresses to a chronic FBR. Although several groups have tried coating these sensors with a variety of synthetic polymers such as PU, poly(2-methoxyethyl acrylate), and PVA [110], their durability is still limited. A material that is compatible with blood while still allowing signal molecule (e.g., glucose) transport is needed. Recently, a polyester fabric was coated with a biodegradable PGA sheet and implanted in a rat model. As the PGA degraded, cells deposited their extracellular matrix, much of which is collagen, on the polyester fabric. This hybrid fabric was decellularized, and its mechanical compliance and hemocompatibility were evaluated, revealing a material that resisted platelet adhesion and thrombus formation [111].

10.5 Hemocompatible surface coatings and modifications

The thrombogenicity of a material is either influenced by or a by-product of (1) available surface functional groups, (2) the charge on the molecule and the interfacial adaptability, and (3) physical surface roughness. These characteristics change over the time course of the device as influenced by material degradation. The presence of a fibrin sheath provides an irregular surface with thrombogenic properties that often promotes platelet adhesion to virtually any foreign substance introduced into the vascular system, initiating a chain of coagulation responses. Thus, surface characteristics are key design foci for many blood-contacting device developments.

10.5.1 Pharmaceutically active materials to improve hemocompatibility

Tailored surface coatings have been used for over five decades to improve material performance in blood, tissue, or biological milieu. Historically, several approaches—either actively or passively pharmaceutical—have been exploited specifically to combat thrombosis [112,113]. Two broad approaches (1) altering the surface properties or (2) drug elution

[114,115], specifically systemic anticoagulation with warfarin, low-molecular-weight heparins (LMWH), and unfractionated heparin, have been used. Polymer coatings deliver a pharmaceutical agent at 10 times the local concentration achievable by systemic delivery [116]. However, recent advances and relative success of chemically defined polymer surface coatings in providing a versatile cassette for pharmaceutical immobilization are a driving force behind using biological-based biomimetic therapeutics or synthetic polymer materials as surface coatings.

10.5.1.1 Heparin and heparin-like molecules

Heparin is a naturally produced (average of $19.4 \pm 20.4\,\mu g/mL$ in adult plasma [117]), negatively charged polysaccharide (i.e., sulfated glycosaminoglycan) with potent inhibitory effects on coagulation as it binds to wide range of host proteins [118,119] with nanomolar (nM) affinity. Thus, heparin acts as a clinically powerful anticoagulant by binding to the plasma protein antithrombin-III to neutralize thrombin and activated factor X (X_a). Heparin also prevents platelet adhesion to surfaces, inhibits activated coagulation enzymes, and enhances biocompatibility [120] by serving as a cell-signaling molecule [121].

Heparin's use as a surface-immobilized prophylactic agent has been reported in many forms to improve hemocompatibility [122] in vitro and in vivo on numerous commercial medical devices [123]. Recently, a heparinized, silk-based composite vascular scaffold provided extended antithrombotic properties [124]. Alternatively, a LMWH, tinzaparin, was used to minimize the risk of heparin-induced thrombocytopenia. Additionally, due to its ability to bind multiple human growth factors, tinzaparin also served as a delivery vehicle by carrying vascular endothelial growth factor (VEGF). Binding tinzaparin to silk was able to enhance the hemocompatibility of the underlying silk material. Importantly, there was an initial inflammatory response to the modified silk, but it was well within a normal initial reaction and did not cause the endothelium to switch phenotype to procoagulant [125].

Heparinized surfaces have long been used to modify the coagulation response to synthetic catheter surfaces. Although heparin is hydrophilic and cannot attach directly to many commercial hydrophobic device surfaces without modifications, covalent end-point surface heparinization produced a highly stable, thrombus-resistant coating in vitro and in vivo [123]. The Carmeda bioactive surface (CBAS) method from Carmeda Inc. (San Antonio, Texas) uses a primer layer and end-point attachment of heparin molecules theorizing that presenting a “free” end to the bloodstream maximizes heparin interactions with blood components. Alternately, BioInteractions Biba-Hepcoat technology (Tyco Healthcare) licensed by Medtronic for cardiopulmonary bypass products and marketed under the name of Trillium biopassive surface uses multilayers of sulfonate groups, which have anticoagulation properties with hydrophilic cationic polyethyleneimine chains and surface activation to immobilize heparin. One synthetic water-soluble polymer layer is strongly bonded to the catheter surface, and the second is covalently bonded to the initial layer. The blood-contact layer is strongly hydrophilic, and its negatively charged surface may minimize the adsorption of protein and cell adhesion in addition to the anticoagulant effect that heparin exerts. Novel methods such as plasma deposition [126] to bind bioactive molecules such as

heparin may or may not produce lasting efficacy depending upon (1) surface density, (2) mechanism of action, and (3) intended in vivo application. Unfortunately, once lost, the surface properties desired for heparinized materials are clinically substandard.

10.5.1.2 Heparin binding peptides

Analysis of protein's heparin-binding regions in a variety of growth factors (e.g., VEGF) and key regulators in the coagulation cascade reveals a structural prerequisite and consensus amino acid sequence, XBBBXXBX, where B is a basic residue (e.g., arginine) and X represents a hydrophobic or uncharged amino acid (e.g., alanine) [127,128]. Segregation of discrete hydrophobic and cationic amino acid sectors in this consensus sequence is analogous to many identified antimicrobial peptides and thought to be fundamental to their bactericidal function allowing permeation of the bacterial membrane. Twenty-six different heparin-binding peptides were surveyed for bactericidal activity not only confirming the antimicrobial action of the majority of these peptides but also revealing that bactericidal potential and heparin affinity varied in a length-dependent manner [128] reaching a plateau at ~ 30 amino acids. Heparin-binding peptides have proved efficacious in both soluble and immobilized forms [127,129] being able to selectivity bind heparin from solutions when surface-immobilized using common *N*,*N*′-carbonyldiimidazole conjugation chemistry [130].

10.5.1.3 Nitric oxide

Releasing nitric oxide (NO) from a material surface also holds a great deal of promise for enhancing the hemocompatibility of a variety of biodegradable material surfaces. NO, a biosignaling molecule released from healthy endothelium, can naturally prevent platelet activation and aggregation as well as proliferation of smooth muscle cells [131]. Thus, NO is grafted to a variety of polyester polymers to improve the hemocompatibility of the underlying bulk polymer [132]. In one instance, selenocystamine was covalently immobilized on a modified PU surface to catalyze the release of NO from *S*-nitrosothiols (endogenous NO donors in blood) [131]. The vinyl-functionalized PU surface was also protected against biofouling by graft copolymerization with oligo(ethylene glycol) methyl ether methacrylate (protein resistance) and a lysine-containing methacrylic monomer (LysMA) (clot lysing) [131]. Release of NO has also been explored in conjunction with a zwitterionic-modified polydimethylsiloxane (PDMS) surface [133] and other surfaces. For additional information on the use of NO for biomedical applications, the reader is referred to a 2017 book from Seabra [134].

10.6 Conclusion

The hemocompatibility of polymers for blood-contacting biomedical applications is a key concern that must be assessed. Several surface modifications have evaluated, affirming the importance of surface topography and charge to protein material

interactions, which are often the basis for a pathological coagulation response. Despite the success of many heparin and other pharmaceutical coatings, most coatings are silenced by biofouling; thus, a hybrid of natural and synthetic polymers with inorganic substrate may provide an antifouling; antithrombotic properties may provide the easiest and most environmentally friendly solution for such applications.

Acknowledgment

We would like to thank Zach Storey and Kishore Chittimalli for their input in the preparation of this manuscript. This manuscript was funded in part by the Department of Pharmaceutical Sciences at North Dakota State University.

References

[1] K.S. Brockman, B.F.L. Lai, J.N. Kizhakkedathu, J.P. Santerre, Hemocompatibility of degrading polymeric biomaterials: degradable polar hydrophobic ionic polyurethane versus poly(lactic-co-glycolic) acid. Biomacromolecules 18 (8) (2017) 2296–2305, https://doi.org/10.1021/acs.biomac.7b00456.

[2] D. Li, Q. Zheng, Y. Wang, H. Chen, Combining surface topography with polymer chemistry: exploring new interfacial biological phenomena, Polym. Chem. 5 (1) (2013) 14–24.

[3] W.L. Stoppel, C.E. Ghezzi, S.L. McNamara, L.D.B. Iii, D.L. Kaplan, Clinical applications of naturally derived biopolymer-based scaffolds for regenerative medicine, Ann. Biomed. Eng. 43 (3) (2015) 657–680.

[4] J.-H. Ji, I.-S. Park, Y.-K. Kim, S.-J. Lee, T.-S. Bae, M.-H. Lee, Influence of heat treatment on biocorrosion and hemocompatibility of biodegradable Mg-35Zn-3Ca alloy, Adv. Mater. Sci. Eng. (2015)Available from: https://www.hindawi.com/journals/amse/2015/318696/, .

[5] R.C. Eberhart, et al., Review: bioresorbable polymeric stents: current status and future promise, J. Biomater. Sci. Polym. Ed. 14 (4) (2003) 299–312.

[6] S.O. Trerotola, Hemodialysis catheter placement and management 1, Radiology 215 (3) (2000) 651–658.

[7] S.F. Mohammad, Enhanced risk of infection with device-associated thrombi, ASAIO J. 46 (6) (2000) S63–S68. Available from: http://journals.lww.com/asaiojournal/Fulltext/2000/11000/Enhanced_Risk_of_Infection_with_Device_Associated.39.aspx [Accessed: 11-Feb-2013].

[8] V. Balan, L. Verestiuc, Strategies to improve chitosan hemocompatibility: a review, Eur. Polym. J. 53 (April) (2014) 171–188.

[9] N. Duraiswamy, T.D. Choksi, L. Pinchuk, R.T. Schoephoerster, A phospholipid-modified polystyrene—polyisobutylene—polystyrene (SIBS) triblock polymer for enhanced hemocompatibility and potential use in artificial heart valves, J. Biomater. Appl. 23 (4) (2009) 367–379.

[10] J.-H. Seo, R. Matsuno, T. Konno, M. Takai, K. Ishihara, Surface tethering of phosphorylcholine groups onto poly(dimethylsiloxane) through swelling–deswelling methods with phospholipids moiety containing ABA-type block copolymers, Biomaterials 29 (10) (2008) 1367–1376.

[11] J. Yang, et al., Preparation, characterization and anticoagulant activity in vitro of heparin-like 6-carboxylchitin derivative, Int. J. Biol. Macromol. 50 (4) (2012) 1158–1164.
[12] F. Xu, J.C. Nacker, W.C. Crone, K.S. Masters, The haemocompatibility of polyurethane–hyaluronic acid copolymers, Biomaterials 29 (2) (2008) 150–160.
[13] A. Radhakrishnan, G.M. Jose, M. Kurup, PEG-penetrated chitosan–alginate co-polysaccharide-based partially and fully cross-linked hydrogels as ECM mimic for tissue engineering applications, Prog. Biomater. 4 (2–4) (2015) 101–112.
[14] Q. Zeng, et al., Preparation and hemocompatibility of electrospun O-carboxymethyl chitosan/PVA nanofibers, J. Appl. Polym. Sci. 133 (26) (2016) 43565–43572.
[15] J. Li, et al., Investigation of enhanced hemocompatibility and tissue compatibility associated with multi-functional coating based on hyaluronic acid and type IV collagen, Regen. Biomater. 3 (3) (2016) 149–157.
[16] H. Yan, et al., Assessment of biological properties of collagen/hyaluronic acid composite scaffolds containing nanobioactive glass, Mater. Technol. 31 (3) (2016) 128–133.
[17] C.-C. Chou, S.-W. Hsin, H.-C. Lin, C.-H. Yeh, R. Wu, W.-J. Cherng, Oxidized dopamine as the interlayer between heparin/collagen polyelectrolyte multilayers and titanium substrate: an investigation of the coating's adhesion and hemocompatibility, Surf. Coat. Technol. 303 (October) (2016) 277–282.
[18] M.-C. Chen, H.-F. Liang, Y.-L. Chiu, Y. Chang, H.-J. Wei, H.-W. Sung, A novel drug-eluting stent spray-coated with multi-layers of collagen and sirolimus, J. Control. Release 108 (1) (2005) 178–189.
[19] S. Haghjooy Javanmard, J. Anari, A. Zargar Kharazi, E. Vatankhah, In vitro hemocompatibility and cytocompatibility of a three-layered vascular scaffold fabricated by sequential electrospinning of PCL, collagen, and PLLA nanofibers, J. Biomater. Appl. 31 (3) (2016) 438–449.
[20] F. Boccafoschi, J. Habermehl, S. Vesentini, D. Mantovani, Biological performances of collagen-based scaffolds for vascular tissue engineering, Biomaterials 26 (35) (2005) 7410–7417.
[21] A.E. Thurber, F.G. Omenetto, D.L. Kaplan, In vivo bioresponses to silk proteins, Biomaterials 71 (December) (2015) 145–157.
[22] Y. Tamada, Sulfation of silk fibroin by sulfuric acid and anticoagulant activity, J. Appl. Polym. Sci. 87 (14) (2003) 2377–2382.
[23] M.F. Elahi, G. Guan, L. Wang, X. Zhao, F. Wang, M.W. King, Surface modification of silk fibroin fabric using layer-by-layer polyelectrolyte deposition and heparin immobilization for small-diameter vascular prostheses, Langmuir 31 (8) (2015) 2517–2526.
[24] J. Zhang, et al., In vivo biocompatibility and hemocompatibility of a polytetrafluoroethylene small diameter vascular graft modified with sulfonated silk fibroin, Am. J. Surg. 213 (1) (2017) 87–93.
[25] D. Sun, Y. Hao, G. Yang, J. Wang, Hemocompatibility and cytocompatibility of the hirudin-modified silk fibroin, J. Biomed. Mater. Res. B Appl. Biomater. 103 (3) (2015) 556–562.
[26] L. Zhao, M. He, Y. Xu, M. Li, Study on biological safety of spider silk protein bilayer vascular scaffold, Compos. Interface. 22 (2015) 1–14.
[27] L. Zhao, Y. Xu, M. He, W. Zhang, M. Li, Preparation of spider silk protein bilayer small-diameter vascular scaffold and its biocompatibility and mechanism research, Compos. Interface. 21 (9) (2014) 869–884.
[28] M. Hemshekhar, R.M. Thushara, S. Chandranayaka, L.S. Sherman, K. Kemparaju, K.S. Girish, Emerging roles of hyaluronic acid bioscaffolds in tissue engineering and regenerative medicine, Int. J. Biol. Macromol. 86 (May) (2016) 917–928.

[29] S.S. Pedrosa, P. Pereira, A. Correia, S. Moreira, H. Rocha, F.M. Gama, Biocompatibility of a self-assembled crosslinkable hyaluronic acid nanogel, Macromol. Biosci. 16 (11) (2016) 1610–1620.
[30] N. Hao, Y.-B. Wang, S.-P. Zhang, S.-Q. Shi, K. Nakashima, Y.-K. Gong, Surface reconstruction and hemocompatibility improvement of a phosphorylcholine end-capped poly(butylene succinate) coating, J. Biomed. Mater. Res. A 102 (9) (2014) 2972–2981.
[31] A.L. Lewis, P.W. Stratford, Phosphorylcholine-coated stents, J. Long-Term Eff. Med. Implants 12 (4) (2002) 231–250.
[32] Y. Yao, et al., Effect of sustained heparin release from PCL/chitosan hybrid small-diameter vascular grafts on anti-thrombogenic property and endothelialization, Acta Biomater. 10 (6) (2014) 2739–2749.
[33] M. Fischer, et al., Microbial alginate dressings show improved binding capacity for pathophysiological factors in chronic wounds compared to commercial alginate dressings of marine origin, J. Biomater. Appl. 31 (9) (2017) 1267–1276.
[34] M. Xu, et al., In vitro heterogeneous degradation of alginate and its validation of different molecular weight on blood bio-compatibility, J. Biomater. Sci. Polym. Ed. 28 (4) (2017) 380–393.
[35] W. Gao, T. Lin, T. Li, M. Yu, X. Hu, D. Duan, Sodium alginate/heparin composites on PVC surfaces inhibit the thrombosis and platelet adhesion: applications in cardiac surgery, Int. J. Clin. Exp. Med. 6 (4) (2013) 259–268.
[36] C. Amri, M. Mudasir, D. Siswanta, R. Roto, In vitro hemocompatibility of PVA-alginate ester as a candidate for hemodialysis membrane, Int. J. Biol. Macromol. 82 (January) (2016) 48–53.
[37] Y. Suzuki, K. Miyatake, Y. Okamoto, E. Muraki, S. Minami, Influence of the chain length of chitosan on complement activation, Carbohydr. Polym. 54 (4) (2003) 465–469.
[38] J. Benesch, P. Tengvall, Blood protein adsorption onto chitosan, Biomaterials 23 (12) (2002) 2561–2568.
[39] S.B. Rao, C.P. Sharma, Use of chitosan as a biomaterial: studies on its safety and hemostatic potential, J. Biomed. Mater. Res. 34 (1) (1997) 21–28.
[40] J.J. Devlin, S. Kircher, B.G. Kozen, L.F. Littlejohn, A.S. Johnson, Comparison of ChitoFlex®, CELOX™, and QuikClot® in control of hemorrhage. J. Emerg. Med. 41 (3) (2009) 237–245, https://doi.org/10.1016/j.jemermed.2009.02.017. Epub 2009 April 2.
[41] M. Pozza, R.W.J. Millner, Celox (chitosan) for haemostasis in massive traumatic bleeding: experience in Afghanistan, Eur. J. Emerg. Med. 18 (1) (2011) 31–33.
[42] H.S. Whang, W. Kirsch, Y.H. Zhu, C.Z. Yang, S.M. Hudson, Hemostatic agents derived from chitin and chitosan, J. Macromol. Sci. C Polym. Rev. J. 45 (4) (2005) 309–323.
[43] C.J. van Rooden, et al., Infectious complications of central venous catheters increase the risk of catheter-related thrombosis in hematology patients: a prospective study, J. Clin. Oncol. 23 (12) (2005) 2655–2660.
[44] J.-J. Parienti, et al., Intravascular complications of central venous catheterization by insertion site, N. Engl. J. Med. 373 (13) (2015) 1220–1229.
[45] X. Huang, et al., Heparin-like chitosan hydrogels with tunable swelling behavior, prolonged clotting times, and prevented contact activation and complement activation, Biomacromolecules 17 (12) (2016) 4011–4020.
[46] R. Huang, Y. Du, J. Yang, L. Fan, Influence of functional groups on the in vitro anticoagulant activity of chitosan sulfate, Carbohydr. Res. 338 (6) (2003) 483–489.
[47] R. Shelma, C.P. Sharma, Development of lauroyl sulfated chitosan for enhancing hemocompatibility of chitosan, Colloids Surf. B: Biointerfaces 84 (2) (2011) 561–570.

[48] A.-P. Zhu, N. Fang, Adhesion dynamics, morphology, and organization of 3T3 fibroblast on chitosan and its derivative: the effect of *O*-carboxymethylation, Biomacromolecules 6 (5) (2005) 2607–2614.
[49] A. Zhu, M.B. Chan-Park, S. Dai, L. Li, The aggregation behavior of O-carboxymethylchitosan in dilute aqueous solution, Colloids Surf. B: Biointerfaces 43 (3–4) (2005) 143–149.
[50] J. Li, et al., Tailoring of the titanium surface by preparing cardiovascular endothelial extracellular matrix layer on the hyaluronic acid micro-pattern for improving biocompatibility, Colloids Surf. B: Biointerfaces 128 (April) (2015) 201–210.
[51] H.P. Felgueiras, et al., Octadecyl chains immobilized onto hyaluronic acid coatings by thiol–ene 'click chemistry' increase the surface antimicrobial properties and prevent platelet adhesion and activation to polyurethane, ACS Appl. Mater. Interfaces 9 (9) (2017) 7979–7989.
[52] B. Kundu, R. Rajkhowa, S.C. Kundu, X. Wang, Silk fibroin biomaterials for tissue regenerations, Adv. Drug Deliv. Rev. 65 (4) (2013) 457–470.
[53] P.H. Zeplin, et al., Spider silk coatings as a bioshield to reduce periprosthetic fibrous capsule formation, Adv. Funct. Mater. 24 (18) (2014) 2658–2666.
[54] M.J. Rodriguez, J. Brown, J. Giordano, S.J. Lin, F.G. Omenetto, D.L. Kaplan, Silk based bioinks for soft tissue reconstruction using 3-dimensional (3D) printing with in vitro and in vivo assessments, Biomaterials 117 (February) (2017) 105–115.
[55] N. Shankhwar, M. Kumar, B.B. Mandal, A. Srinivasan, Novel polyvinyl alcohol-bioglass 45S5 based composite nanofibrous membranes as bone scaffolds, Mater. Sci. Eng. C 69 (December) (2016) 1167–1174.
[56] M. Floren, W. Bonani, A. Dharmarajan, A. Motta, C. Migliaresi, W. Tan, Human mesenchymal stem cells cultured on silk hydrogels with variable stiffness and growth factor differentiate into mature smooth muscle cell phenotype, Acta Biomater. 31 (February) (2016) 156–166.
[57] W. Sun, et al., Co-culture of outgrowth endothelial cells with human mesenchymal stem cells in silk fibroin hydrogels promotes angiogenesis, Biomed. Mater. 11 (3) (2016) 035009.
[58] J. Melke, S. Midha, S. Ghosh, K. Ito, S. Hofmann, Silk fibroin as biomaterial for bone tissue engineering, Acta Biomater. 31 (February) (2016) 1–16.
[59] A. Motta, et al., Silk fibroin processing and thrombogenic responses, J. Biomater. Sci. Polym. Ed. 20 (13) (2009) 1875–1897.
[60] V. Leszczak, K.C. Popat, Improved in vitro blood compatibility of polycaprolactone nanowire surfaces, ACS Appl. Mater. Interfaces 6 (18) (2014) 15913–15924.
[61] R. Li, G. Wu, X. Cai, Y. Ye, In vitro anticoagulant activity of polyanionic graft chains modified poly(vinyl alcohol) particles, Radiat. Phys. Chem. 134 (May) (2017) 27–32.
[62] B.A. Allo, D.O. Costa, S.J. Dixon, K. Mequanint, A.S. Rizkalla, Bioactive and biodegradable nanocomposites and hybrid biomaterials for bone regeneration, J. Funct. Biomater. 3 (4) (2012) 432–463.
[63] H. Jana, et al., Comprehensive assessment of electrospun scaffolds hemocompatibility, Mater. Sci. Eng. C (May) (2017). https://doi.org/10.1016/j.msec.2017.05.011.
[64] B.D. Ulery, L.S. Nair, C.T. Laurencin, Biomedical applications of biodegradable polymers, J. Polym. Sci. B Polym. Phys. 49 (12) (2011) 832–864.
[65] L.-J. Zhu, F. Liu, X.-M. Yu, A.-L. Gao, L.-X. Xue, Surface zwitterionization of hemocompatible poly(lactic acid) membranes for hemodiafiltration, J. Membr. Sci. 475 (February) (2015) 469–479.
[66] Y. Ramot, M. Haim-Zada, A.J. Domb, A. Nyska, Biocompatibility and safety of PLA and its copolymers, Adv. Drug Deliv. Rev. 107 (December) (2016) 153–162.

[67] A. Gao, F. Liu, L. Xue, Preparation and evaluation of heparin-immobilized poly (lactic acid) (PLA) membrane for hemodialysis, J. Membr. Sci. 452 (February) (2014) 390–399.
[68] T. Sharkawi, V. Darcos, M. Vert, Poly(DL-lactic acid) film surface modification with heparin for improving hemocompatibility of blood-contacting bioresorbable devices, J. Biomed. Mater. Res. A 98A (1) (2011) 80–87.
[69] Z. Xiong, F. Liu, H. Lin, J. Li, Y. Wang, Covalent bonding of heparin on the crystallized poly(lactic acid) (PLA) membrane to improve hemocompability via surface cross-linking and glycidyl ether reaction, ACS Biomater Sci. Eng. 2 (12) (2016) 2207–2216.
[70] J. Li, et al., A novel natural hirudin facilitated anti-clotting polylactide membrane via hydrogen bonding interaction, J. Membr. Sci. 523 (February) (2017) 505–514.
[71] H. Kilkson, S. Holme, S. Murphy, Platelet metabolism during storage of platelet concentrates at 22 degrees C, Blood 64 (2) (1984) 406–414.
[72] J. Zhang, et al., In vitro hemocompatibility and cytocompatibility of dexamethasone-eluting PLGA stent coatings, Appl. Surf. Sci. 328 (February) (2015) 154–162.
[73] Y.M. Thasneem, M.R. Rekha, S. Sajeesh, C.P. Sharma, Biomimetic mucin modified PLGA nanoparticles for enhanced blood compatibility, J. Colloid Interface Sci. 409 (November) (2013) 237–244.
[74] E. Cenni, et al., Biocompatibility of poly(d, l-lactide-co-glycolide) nanoparticles conjugated with alendronate, Biomaterials 29 (10) (2008) 1400–1411.
[75] Y. Thasneem, C.P. Sharma, Engineered PLGA nanosystems for enhanced blood compatibility, in: M.N.V. Ravi Kumar (Ed.), Handbook of Polyester Drug Delivery Systems, Pan Stanford, 2016, pp. 213–242. Print ISBN: 978-981-4669-65-8; eBook ISBN: 978-981-4669-66-5, https://doi.org/10.1201/b20045-9.
[76] P.A. Gunatillake, R. Adhikari, Biodegradable synthetic polymers for tissue engineering, Eur. Cell. Mater. 5 (May) (2003) 1–16.
[77] V. Mkhabela, S.S. Ray, Biodegradation and bioresorption of poly(ε-caprolactone) nanocomposite scaffolds, Int. J. Biol. Macromol. 79 (August) (2015) 186–192.
[78] A.R. Padalhin, N.T.B. Linh, Y.K. Min, B.-T. Lee, Evaluation of the cytocompatibility hemocompatibility in vivo bone tissue regenerating capability of different PCL blends, J. Biomater. Sci. Polym. Ed. 25 (5) (2014) 487–503.
[79] Q. Hu, et al., Hemocompatibility evaluation in vitro of methoxy polyethyleneglycol–polycaprolactone copolymer solutions, J. Biomed. Mater. Res. A 104 (3) (2016) 802–812.
[80] L. He, L. Huang, S. Zhang, Y. Chen, X. Luo, Poly(ε-caprolactone) modification via surface initiated atom transfer radical polymerization with bio-inspired phosphorylcholine, Mater. Sci. Eng. C 77 (August) (2017) 45–51.
[81] H. Jiang, et al., Improvement of hemocompatibility of polycaprolactone film surfaces with zwitterionic polymer brushes, Langmuir 27 (18) (2011) 11575–11581.
[82] Y. Zhu, Z. Mao, C. Gao, Aminolysis-based surface modification of polyesters for biomedical applications, RSC Adv. 3 (8) (2013) 2509–2519.
[83] L. Chan-Chan, et al., Platelet adhesion and human umbilical vein endothelial cell cytocompatibility of biodegradable segmented polyurethanes prepared with 4,4′-methylene bis(cyclohexyl isocyanate), poly(caprolactone) diol and butanediol or dithioerythritol as chain extenders, J. Biomater. Appl. 28 (2) (2013) 270–277.
[84] S.L. Cooper, J. Guan, Advances in Polyurethane Biomaterials, Woodhead Publishing, Sawston, Cambridge, 2016.
[85] J. Dey, et al., Development of biodegradable crosslinked urethane-doped polyester elastomers, Biomaterials 29 (35) (2008) 4637–4649.

[86] P.C. Caracciolo, M.I. Rial-Hermida, F. Montini-Ballarin, G.A. Abraham, A. Concheiro, C. Alvarez-Lorenzo, Surface-modified bioresorbable electrospun scaffolds for improving hemocompatibility of vascular grafts, Mater. Sci. Eng. C 75 (June) (2017) 1115–1127.
[87] C. Wang, et al., A facile way to prepare anti-fouling and blood-compatible polyethersulfone membrane via blending with heparin-mimicking polyurethanes, Mater. Sci. Eng. C 78 (September) (2017) 1035–1045.
[88] X. Zhou, T. Zhang, D. Guo, N. Gu, A facile preparation of poly(ethylene oxide)-modified medical polyurethane to improve hemocompatibility, Colloids Surf. A Physicochem. Eng. Asp. 441 (January) (2014) 34–42.
[89] D. Hasper, M. Hummel, R. Hetzer, H.D. Volk, Blood contact with artificial surfaces during BVAD support, Int. J. Artif. Organs 19 (10) (1996) 590–596.
[90] Y. Marois, R. Guidoin, Biocompatibility of Polyurethanes, Landes Bioscience, Austin, TX, 2013.
[91] E. Chiellini, A. Corti, S. D'Antone, R. Solaro, Biodegradation of poly(vinyl alcohol) based materials, Prog. Polym. Sci. 28 (6) (2003) 963–1014.
[92] A.K. Sonker, A.K. Teotia, A. Kumar, R.K. Nagarale, V. Verma, Development of polyvinyl alcohol based high strength biocompatible composite films, Macromol. Chem. Phys. 218 (May) (2017) 1700130.
[93] M.I. Baker, S.P. Walsh, Z. Schwartz, B.D. Boyan, A review of polyvinyl alcohol and its uses in cartilage and orthopedic applications, J. Biomed. Mater. Res. B Appl. Biomater. 100B (5) (2012) 1451–1457.
[94] M.V. Semenova, S.V. Osadchenko, Y.O. Mezhuev, M.I. Shtil'man, I.N. Semenova, Synthesis of hemocompatible materials based on branched polyvinyl alcohol, Russ. J. Appl. Chem. 89 (8) (2016) 1286–1291.
[95] D. Arcos, M. Vallet-Regí, Bioceramics for drug delivery, Acta Mater. 61 (3) (2013) 890–911.
[96] Y.-H. Zou, et al., Blood compatibility of zinc–calcium phosphate conversion coating on Mg–1.33Li–0.6Ca alloy, Front. Mater. Sci. 10 (3) (2016) 281–289.
[97] B.-S. Kim, J. Lee, Enhanced bone healing by improved fibrin-clot formation via fibrinogen adsorption on biphasic calcium phosphate granules, Clin. Oral Implants Res. 26 (10) (2015) 1203–1210.
[98] J. Bramhill, S. Ross, G. Ross, Bioactive nanocomposites for tissue repair and regeneration: a review, Int. J. Environ. Res. Public Health 14 (1) (2017) 66.
[99] B.A. Allo, D.O. Costa, S.J. Dixon, K. Mequanint, A.S. Rizkalla, Bioactive and biodegradable nanocomposites and hybrid biomaterials for bone regeneration, J. Funct. Biomater. 3 (2) (2012) 432–463.
[100] A. Li, et al., Bioactive organic/inorganic hybrids with improved mechanical performance, J. Mater. Chem. B 3 (7) (2015) 1379–1390.
[101] A.M. Gatti, S. Montanari, E. Monari, A. Gambarelli, F. Capitani, B. Parisini, Detection of micro- and nano-sized biocompatible particles in the blood, J. Mater. Sci. Mater. Med. 15 (4) (2004) 469–472.
[102] M.A. Jamiolkowski, D.D. Pedersen, W.-T. Wu, J.F. Antaki, W.R. Wagner, Visualization and analysis of biomaterial-centered thrombus formation within a defined crevice under flow, Biomaterials 96 (July) (2016) 72–83.
[103] R. Major, K. Trembecka-Wójciga, M. Kot, J.M. Lackner, P. Wilczek, B. Major, In vitro hemocompatibility on thin ceramic and hydrogel films deposited on polymer substrate performed in arterial flow conditions, Mater. Sci. Eng. C 61 (April) (2016) 15–22.

[104] A. Mayer, M. Vadon, B. Rinner, A. Novak, R. Wintersteiger, E. Fröhlich, The role of nanoparticle size in hemocompatibility, Toxicology 258 (2–3) (2009) 139–147.
[105] C.F. Jones, et al., Cationic PAMAM dendrimers aggressively initiate blood clot formation, ACS Nano 6 (11) (2012) 9900–9910.
[106] E. Fröhlich, Action of nanoparticles on platelet activation and plasmatic coagulation, Curr. Med. Chem. 23 (5) (2016) 408–430.
[107] G. Shim, D. Kim, J. Kim, M.S. Suh, Y.K. Kim, Y.-K. Oh, Bacteriomimetic poly-γ-glutamic acid surface coating for hemocompatibility and safety of nanomaterials, Nanotoxicology 26 (July) (2017) 1–19.
[108] L.L. Hench, J.M. Polak, Third-generation biomedical materials, Science 295 (5557) (2002) 1014–1017.
[109] K. Rezwan, Q.Z. Chen, J.J. Blaker, A.R. Boccaccini, Biodegradable and bioactive porous polymer/inorganic composite scaffolds for bone tissue engineering, Biomaterials 27 (18) (2006) 3413–3431.
[110] M. Tanaka, A. Mochizuki, N. Ishii, T. Motomura, T. Hatakeyama, Study of blood compatibility with poly(2-methoxyethyl acrylate). Relationship between water structure and platelet compatibility in poly(2-methoxyethylacrylate-co-2-hydroxyethylmethacrylate), Biomacromolecules 3 (1) (2002) 36–41.
[111] Y. Inoue, et al., Antithrombotic protein filter composed of hybrid tissue-fabric material has a long lifetime, Ann. Biomed. Eng. 45 (5) (2017) 1352–1364.
[112] J. Gunn, D. Cumberland, Stent coatings and local drug delivery, Eur. Heart J. 20 (1999) 1693–1700.
[113] D. Chen, N. Jepson, Coronary stent technology: a narrative review, Med. J. Aust. 205 (6) (2016) 277–281.
[114] K. Zhang, T. Liu, J.-A. Li, J.-Y. Chen, J. Wang, N. Huang, Surface modification of implanted cardiovascular metal stents: from antithrombosis and antirestenosis to endothelialization: surface modification of implanted cardiovascular metal stents, J. Biomed. Mater. Res. A 102 (2) (2014) 588–609.
[115] J.R. Costa, A. Caixeta, A.A.C. Abizaid, et al., Novel drug-eluting stent systems, in: Interventional Cardiology, John Wiley & Sons, Chichester, 2016, pp. 368–376.
[116] T. Peng, Role of polymers in improving the results of stenting in coronary arteries, Biomaterials 17 (7) (1996) 685–694.
[117] H. Xiao, S.J. Miller, N.U. Bang, W.P. Faulk, Protein-bound heparin/heparan sulfates in human adult and umbilical cord plasma, Pathophysiol. Haemost. Thromb. 29 (4) (1999) 237–246.
[118] H.E. Conrad, Heparin-Binding Proteins, Academic Press, San Diego, CA, 1997.
[119] Y. Monneau, F. Arenzana-Seisdedos, H. Lortat-Jacob, The sweet spot: how GAGs help chemokines guide migrating cells, J. Leukoc. Biol. 99 (6) (2016) 935–953.
[120] S. Tabasum, A. Noreen, A. Kanwal, M. Zuber, M.N. Anjum, K.M. Zia, Glycoproteins functionalized natural and synthetic polymers for prospective biomedical applications: a review, Int. J. Biol. Macromol. 98 (May) (2017) 748–776.
[121] J.J. Castellot, Heparin selectively inhibits a protein kinase C-dependent mechanism of cell cycle progression in calf aortic smooth muscle cells, J. Cell Biol. 109 (6) (1989) 3147–3155 (Published erratum appears in J. Cell. Biol 110 (3) (1990) 863).
[122] S. Gore, J. Andersson, R. Biran, C. Underwood, J. Riesenfeld, Heparin surfaces: impact of immobilization chemistry on hemocompatibility and protein adsorption: heparin surfaces: impact of immobilization chemistry, J. Biomed. Mater. Res. B Appl. Biomater. 102 (8) (2014) 1817–1824.

[123] R. Biran, D. Pond, Heparin coatings for improving blood compatibility of medical devices, Adv. Drug Deliv. Rev. 112 (March) (2017) 12–23.
[124] M. Zamani, M. Khafaji, M. Naji, M. Vossoughi, I. Alemzadeh, N. Haghighipour, A biomimetic heparinized composite silk-based vascular scaffold with sustained antithrombogenicity, Sci. Rep. 7 (June) (2017) 4455.
[125] F.P. Seib, M. Herklotz, K.A. Burke, M.F. Maitz, C. Werner, D.L. Kaplan, Multifunctional silk–heparin biomaterials for vascular tissue engineering applications, Biomaterials 35 (1) (2014) 83–91.
[126] T.I. Valdes, W. Ciridon, B.D. Ratner, J.D. Bryers, Surface modification of a perfluorinated ionomer using a glow discharge deposition method to control protein adsorption, Biomaterials 29 (10) (2008) 1356–1366.
[127] A. Verrecchio, M.W. Germann, B.P. Schick, B. Kung, T. Twardowski, J.D. San Antonio, Design of peptides with high affinities for heparin and endothelial cell proteoglycans, J. Biol. Chem. 275 (11) (2000) 7701–7707.
[128] E. Andersson, V. Rydeng ard, A. Sonesson, M. Mörgelin, L. Björck, A. Schmidtchen, Antimicrobial activities of heparin-binding peptides, Eur. J. Biochem. 271 (6) (2004) 1219–1226.
[129] J.-Y. Lee, et al., Characterization of the surface immobilized synthetic heparin binding domain derived from human fibroblast growth factor-2 and its effect on osteoblast differentiation, J. Biomed. Mater. Res. A 83 (4) (2007) 970–979.
[130] M.C.L. Martins, S.A. Curtin, S.C. Freitas, P. Salgueiro, B.D. Ratner, M.A. Barbosa, Molecularly designed surfaces for blood deheparinization using an immobilized heparin-binding peptide, J. Biomed. Mater. Res. A 88 (1) (2009) 162–173.
[131] H. Gu, et al., A hemocompatible polyurethane surface having dual fibrinolytic and nitric oxide generating functions, J. Mater. Chem. B 5 (5) (2017) 980–987.
[132] M.V. Vellayappan, S.K. Jaganathan, I.I. Muhamad, Unravelling the potential of nitric acid as a surface modifier for improving the hemocompatibility of metallocene polyethylene for blood contacting devices, PeerJ 4 (January) (2016) e1388.
[133] K.A. Amoako, H.S. Sundaram, A. Suhaib, S. Jiang, K.E. Cook, Multimodal, biomaterial-focused anticoagulation via superlow fouling zwitterionic functional groups coupled with anti-platelet nitric oxide release. Adv. Mater. Interfaces 3 (6) (2016) 1500646, https://doi.org/10.1002/admi.201500646.
[134] A. Seabra, Nitric oxide Donors: Novel Biomedical Applications and Perspectives, Academic Press, London, UK, 2017.

Surface treatment of metallic biomaterials in contact with blood to enhance hemocompatibility

11

J.P. Allain[*], *M. Echeverry-Rendón*[†]
[*]University of Illinois at Urbana-Champaign, Champaign, IL, United States, [†]University of Groningen, Groningen, Netherlands

11.1 Multiscale interaction of blood and metals

11.1.1 Metallic materials used in biomedical devices

A variety of material classes are used in biomedical applications: metals, ceramics, polymers, and composite (combination of some or all materials mentioned above). Those materials also can be founded in nature (natural materials) or can be chemically produced (synthetic materials). The criteria for selection from these classes will depend on the specific biomedical application, the characteristics of the native tissue to repair or replace, and the desired overall device function. In this chapter, a general approach about metals and their surface modification, its use as biomaterial and its interaction with body fluids and more specifically with blood will be discussed. We will end with an introduction to recent work on composite metal/polymer biomaterials used for tissue reconstruction and their hemodynamic properties. The chapter is written from a material-centric vantage point in a biomedical device and blood-material interactions context.

According with its mechanical properties, metals are used to replace, treat, or improve the function of some tissues. These materials are particularly used in applications that involve hard tissues such as bone [1,2]. Some of the biomedical areas with the highest demand for metallic implant components are in the orthopedic and orthodontic fields [3–5]. However, these materials can be often used in other applications such as coronary, vascular, and biliary stents [6,7]. In principle, metals can be used in their pure form or combined with other elements (metal alloys). This last group of materials is more often used in the case where an improvement in mechanical or biological properties is necessary. The formation of new composition, structures, phases, and inclusive the processing can have a direct impact in the final product at the moment implant integration. The importance of the biological response of the metal with the tissue or organ treated will depend on different characteristics such as surface-tissue interaction, time of permanency of implant (permanent or temporal), and corrosion resistance [8,9]. Metals are also used in the manufacturing of other elements such as surgical instruments, equipment, and needles (Fig. 11.1). One of the most important advantages is the possibility to sterilize by different methods without affecting the stability of the material. Table 11.1 summarizes some applications of metals that could be in direct contact with blood.

Hemocompatibility of Biomaterials for Clinical Applications. https://doi.org/10.1016/B978-0-08-100497-5.00008-2
© 2018 Elsevier Ltd. All rights reserved.

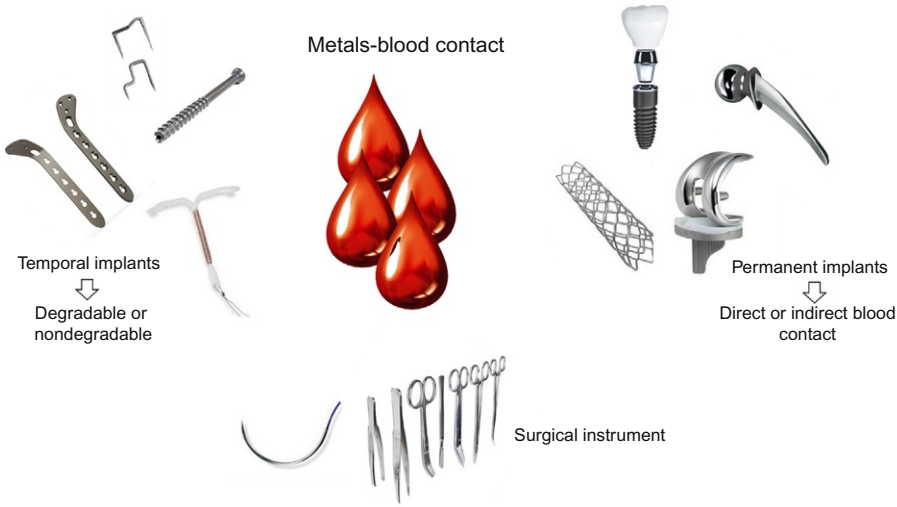


Fig. 11.1 Metallic biomaterials that can be potentially exposed to blood.

Table 11.1 Metals used in biomedical applications

	Application	Material	Reasons
Orthopedic	Hip prosthesis Join substitutes Plates for bone fixation Screws Pins and wires	Stainless steel, Co-based alloys (Cr-Co), Ti-based alloys, Mg-based alloys	Mechanical resistance, biocompatible
Orthodontic	Dental implants Orthodontic archwires	Titanium and Ti-based alloys (NiTi and Ti6Al4V), stainless steel, Cr-Co	Shape memory, resilience, stiffness, and ductility
Cardiovascular	Stents Aneurysm clip Metal coils	Nitinol, (NiTi), magnesium-based alloys	Shape memory Nonthrombogenic effect
Instrumental and supplies	Needles Equipment Scissors Scalpels Tweezers Forceps Clamps	Stainless steel	Inert Reuse (autoclaved)

In the past, metals such as gold, silver, and iron were used in their primitive stage. Over time, other elements were explored, and currently, materials such as stainless steel, titanium and titanium alloys, nitinol, chrome cobalt alloys, and magnesium and magnesium alloys are the most common in biomedical applications [10]. Also, materials science has shown a big progress in the obtaining and processing of the materials.

Most metals are considered bioinert, which means that when implanted and in contact with physiological fluids, it has a minimal biological response that is the opposite of what happens with bioactive materials that can trigger or actively stimulate the growth or the biological activity of the surrounding tissue, such is the case of bioglass and some ceramics such as hydroxyapatite [11]. After implantation, intra- and extracellular interactions occur along the implant and many of those are determined by the composition and multiscale structure of the material and the characteristics of the surface. The absorption of proteins, growth factors, and other chemoattractant agents are a few of the first events after implant placement in the body followed by processes such as cell adhesion, cell proliferation, enzymatic activation, and extracellular matrix production in order to repair tissue function. Although as mentioned above, metallic implants are inert, one of the most common failure pathways for implants are issues associated with corrosion that can affect their biocompatibility. Additionally, in cases such as bone implants, some failures reported are due to weak fixation between bone tissue and the implant surface associated with an intermediate fibrous tissue affecting the osseointegration process ultimately resulting in physical instabilities [12,13].

In orthopedics, spine and orthodontic interventions and metallic implant materials of choice include Ti, Ti alloys, CoCr alloys, and stainless steel. In vascular implants such as stents, shape-memory alloys are used. Nitinol is one of the most common materials used for this applications, and new formulations based on magnesium have been studied during the last few years [6,14]. Magnesium is used due its biodegradable properties and in combination with other elements (magnesium alloys) such as calcium, manganese, zinc, aluminum, and rare earths [15–17]. However, although this material demonstrates improvement on the mechanical and corrosion properties, in some cases, the concentration of those elements can cause cytotoxic effects. Therefore, alternate biodegradable alloys such as Mg-based or Mn-based alloys or Fe-based alloys are currently considered as viable metallic biomaterial options [18].

11.1.2 Immune response and metals

At the moment of implantation of a biomaterial, a chain of events is present in the body that first involves the process of reorganization by the immune system, deposition of proteins in the surface, and attraction of specific cell groups in order to integrate the new element to the system or to reject it. Initially, in order to perform the surgical procedure of implant introduction to the host location, an injury of tissue is required. At this point, blood plays an important role in recognition of the material due to the immune cells present and proteins that will initiate the tissue regeneration process. Initially, this process begins with triggering the inflammatory response in which proteins from blood plasma are deposited on the surface of the material and a provisional extracellular matrix is formed where the basic components are thrombin and fibrin [19]. The consequent interaction between metal and immune cells, basically granulocyte and activated monocytes, will be determined by the composition of the material and the characteristic of the surface. However, for the case of metals, the inflammatory response can also be induced as a consequence of corrosion of the material and liberation of metal ions in high concentration, by the release of material

particulates, the presence of bacteria, among others [19]. The activation of the complementary system and coagulation cascade are the next steps of the process. During these steps, surface energy can have an important effect on protein binding according to the hydrophobic or hydrophilic properties of the implant surface [19,20]. The activation of the complement activation can take place by three pathways: the classical, the alternative, and the lectin. Each of these pathways involves specific cytokines and can affect actor cells in specific ways.

Another important actor for the inflammatory response are anaphylatoxins that complement peptides and play an important role on the inflammatory response due to their direct effect on monocytes (cells that will subsequently differentiate into macrophages), granulocytes, and its induction of reactive oxygen species.

Diverse populations of macrophages with different characteristics in terms of function, markers, and production of cytokine and chemokine can be obtained during the differentiation process of monocytes into macrophages. This depends on the environment and the stimuli received by monocytes. Macrophages can be activated by the classical pathway becoming the pro-inflammatory M1 phenotype or by the alternative pathway calling also the antiinflammatory M2 phenotype. This characteristic of macrophages known as plasticity has recently been the subject of correlations between the immune response and leading factors expressed during the foreign body response process [21]. The M1 phenotype is activated by interferon gamma (IFN-ϒ) IL-1β, TNFα, and LPS, and as result of this, M1 phenotype activated macrophages are able to produce iNOS, CD11c, CCR7, PHD3, and activin A that are a typical profile for chronic inflammation. On the other hand, M2-activated macrophages are stimulated by IL-4, IL-13, IL-10, and TGFβ and can produce ARG1, CD206, Ym1, Fizz1, HO1, DC-sign, FRβ, and CD163 inducing a regenerative effect by the stimulation of cell proliferation and production of antiinflammatory agents [22]. In conclusion, the site of the implant, the surgical conditions and the properties of the material implanted can promote the process of inflammation or the healing of the tissue.

11.1.3 Biocorrosion

An implant needs to be able to replace, treat, or improve the function of an organ or tissue avoiding side effects. However, in the case of metals, one of the most relevant problems associated with complications or rejection of the implant is related with the corrosion process [23,24]. Biocorrosion is defined as the process of material degradation by electrochemical attack. In this process, the differences in the electrochemical potentials in the environment and the liberation of ions from the material can be conducted by its interaction with body fluids, mainly blood, and its organic and inorganic components including proteins, amino acid, plasma, sodium, chloride, fluoride, and water. In some cases, the process of degradation can be controlled by the body, if the concentration does not affect the hemostasis; however, if the limits are exceeded, the inflammation process and necrosis of the tissue may affect the stability of the implant inducing the rejection of the implant [25].

In general, the corrosion in metals consists of different types including uniform or localized, galvanic, intergranular, pitting, or fatigue corrosion [9,14]. Some materials such as titanium and magnesium have in common that they are able to form a stable

oxide protective layer that is linked to the corrosion resistance. However, if some failures are present in this layer, an accelerated corrosion process by pitting, localized or anodic corrosion can be initiated [26,27].

When a process of corrosion is started in the material, anodic and cathodic points are formed with the risk to accelerate the process of degradation of the material. The organic components of the blood, such as proteins in plasma, can interact on the surface of the material in a protective way by creating a layer that decrease the diffusion of oxygen from the material preventing its oxidation. These components also may bind to the free metal ions, and they can be transported away from the surface of the implant. According to Videla [28], a corrosion rate of 2.5×10^{-4} mm/year or 0.01 mils/year for metal implants is tolerable for the human body. On the other hand, issues related with blood-metal interactions is the thrombogenesis or clotting formation promoted by the implant. Although, clotting is a natural process that supports healing of an injured blood vessel, the presence of a foreign body material can complicate the balance that exists intrinsically of active biological factors in during healing. This problem is more critical in cardiovascular applications were the contact between blood and implant is direct. Nitinol, Cr-Co alloys, and Mg alloys are the most common metals used for cardiovascular stents [29,30]. In the first generation of stents, these materials were used as bare metals; however, to prevent clotting problems and restenosis, a new generation emerged where anticoagulant drugs were immobilized in the surfaces of those devices [7]. Thrombogenic properties of materials can be associated with long-term exposure. There are some materials that can cause this problem in some applications but not in others. Other problems associated with metallic materials are related with metallosis, which refers to the allergenic reactions, inflammation, and local anaphylaxis as a consequence of the release of metal ions from an implant [31,32].

As was mentioned before, for the case of temporal and degradable metals, the process of biocorrosion is crucial. In this group, magnesium and its alloys stand out. For those materials, it is important to know the rate and mechanism degradation and the distribution and concentration of elements released with time, factors that can affect the biocompatibility of the implant and cause side effects in the patient [33]. Rejection by corrosion problems is also often in metal-on-metal implants; for example, hip or knee prosthesis is one of the most reported cases where problems associated with corrosion are present due to the release of metal ions as a product of direct contact of both inorganic materials. Also, the detachment of particles that could enter to the bloodstream is considered high risk. Galvanic corrosion is more often present in those cases and in alloys materials due to the presence of different phases or in the use of different metals in the same device [34].

11.2 Evaluation of hemocompatibility of metallic systems

11.2.1 Hemo and biocompatibility evaluation of metallic systems

It is important to validate the materials in contact with blood cells, platelets, and cells from blood vessels. Variability between donors is other important factor to consider and also considers if those material should be evaluated in patients with

special requirements with diseases or damage at vascular level such as endothelial cells. Clotting and inflammation process can happen. Safety evaluation can be performed by the measurement of biological process such as cell proliferation, apoptosis, and necrosis test as also autophagy; the identification of cell-surface activation markers; the evaluation of the stage of the cell cycle, and measurement of some intracellular electrolytes such calcium or potassium. These factors can be correlated with the risk to induce prothrombotic or pro-inflammatory responses. Different techniques can be used to achieve this purpose compromising, simple cytotoxicity text (mitochondrial activity), fluorescent staining, and molecular test to identify the regulation of some genes and the protein activity such as western blot or PCR, flow cytometry, and other immunodetection in general [35]. Also, thrombogeneration and platelet activation assays can be performed. In order to detect levels of metal ions at systemic level, metal ion testing is required. All the implants have specific characteristics according with the anatomic location and the necessities of the patients, and this can involve features in terms of composition, surface, material, size/dimensions, and design.

11.2.2 Regulation and safety aspects in metallic nanomaterials as biomaterials

The evaluation and validation of a material for a biomedical application is a careful and meticulous process that implies several criteria and standards that should be tested in order to guarantee the safety of the patients. Different worldwide organizations have guidelines and standards in order to regulate the products in the biomedical market; in the United States, the agency in charge is the Food and Drug Administration (FDA); its equivalent in Europe is the European Medicines Agency (EMA) and in the United Kingdom the Medicines and Healthcare products Regulatory Agency (MHRA). Most of these standards are supported according with the guidelines determined by the International Organization for Standardization (ISO), and from the side of the materials, there are some standards endorsed by the ASTM International.

According to the FDA, a medical implant is defined as “devices or tissues that are placed inside or on the surface of the body. Many implants are prosthetics, intended to replace missing body parts. Other implants deliver medication, monitor body functions, or provide support to organs and tissues” [36]. As was mentioned previously, surgical instruments are also consider as a medical devices although these will not remain permanently in the body.

Initially, all devices need to meet the requirements of biocompatibility, the ISO 10993 meets a series of standards around this topic. Posteriorly, other evaluation should be performed according with the specifications of the implant and the function in the body. For instance, the evaluation can differ according with the type of material, permanency in the body, composition, among others. The purpose with this normative is to improve the quality of the life of the patients without expose them to future complications. In the Table 11.2, a group of standards related with metals and blood interaction are summarized.

Table 11.2 Standards for testing metals biomaterials

Agency and code	Standard
ISO 10993-4 (2013)	Biological evaluation of medical devices—Part 4: Selection of tests for interactions with blood
ISO 5840-3 (2015)	Cardiac valve prostheses—Part 3: Heart valve substitutes implanted by transcatheter techniques
ISO 14708-5 (2010)	Implants for surgery—active implantable medical devices—Part 5: Circulatory support devices
ISO 10993-1	ISO 10993-1:2009 biological evaluation of medical devices—Part 1: Evaluation and testing in the risk management process
ISO 10993-5:2009	Biological evaluation of medical devices—Part 5: Tests for in vitro cytotoxicity
ISO 10993-6:2016	Biological evaluation of medical devices—Part 6: Tests for local effects after implantation
ISO 10993-8:2001	Biological evaluation of medical devices—Part 8: Selection of reference materials (withdrawn)
ISO 10993-9:1999	Biological evaluation of medical devices—Part 9: Framework for identification and quantification of potential degradation products
ISO 10993-11:2006	Biological evaluation of medical devices—Part 11: Tests for systemic toxicity
ISO 10993-15:2000	Biological evaluation of medical devices—Part 15: Identification and quantification of degradation products from metals and alloys
ISO 10993-16:1997	Biological evaluation of medical devices—Part 16: Toxicokinetic study design for degradation products and leachables
ISO 10993-18:2005	Biological evaluation of medical devices—Part 18: Chemical characterization of materials
ISO/TS 10993-19:2006	Biological evaluation of medical devices—Part 19: Physicochemical, morphological, and topographical characterization of materials
ISO/TS 10993-20:2006	Biological evaluation of medical devices—Part 20: Principles and methods for immunotoxicology testing of medical devices
ASTM G 61-86	Standard test method for conducting cyclic potentiodynamic polarization measurements for localized corrosion susceptibility of iron-, nickel-, or cobalt-based alloys
ASTM G 5-94	Standard reference test method for making potentiodynamic anodic polarization measurements
ASTM G71-81	Standard guide for conducting and evaluating galvanic corrosion tests in electrolytes
ASTM F746-87	Standard test method for pitting or crevice corrosion of metallic surgical implant materials
ASTM F2129-01	Standard test method for conducting cyclic potentiodynamic polarization measurements to determine the corrosion susceptibility of small implant devices
ASTM F756-13	Practice for assessment of hemolytic properties of materials

11.3 Irradiation-driven synthesis and modification to improve the hemo-compatibility behavior of metallic systems

The metallic surface is a critical interface between the foreign body material and tissue system in the body. In vascular tissue, occlusion derived from thrombosis is a critical problem correlated to artificial vascular grafts due to a lack of conforming endothelial cell layer [37]. Understanding this interface and how to manipulate and control platelet adhesion from blood plasma protein interactions that contribute to hemostasis is one goal of surface modification of vascular biomaterials.

The blood-material interface is influenced by numerous multiscale interactions from the molecular-level protein-surface adhesion mechanisms to the cell-level to tissue-level development in response to the foreign material. These interactions dictate the hemocompatibility behavior of metallic systems. Their surfaces can be correspondingly modified with numerous surface modification techniques. In this section, we summarize the key properties at the interface between blood and metallic systems, techniques to modify these materials, and other approaches such as the use of coatings to functionalize and improve the blood-material interaction. The blood-material interface is a multiscale phenomenon as illustrated in Fig. 11.2 where multispatial mechanisms dictate how from nanoscale to the macroscale the hemodynamic behavior is influenced by the material surface.

One of the growing concerns with blood-material interactions is the role of antibacterial properties and the use of antibiotics for in situ treatment of infection when foreign materials are introduced in the body. Blood contact is driven by surface properties uniquely dependent on material surface properties that must be managed when assessing hemocompatibility of metallic systems. Consequently, endothelial cell adhesion must also be managed and therefore presents a significant challenge for biointerfaces that must address two seemingly conflicting design goals: enhancing adherence of endothelial cells and promoting their growth while providing for an antibacterial interface. Understanding the role surface properties play on both cell and platelet adhesion and affecting other metabolic and physiological properties is one of the central goals of current blood-contact biomaterial research.

11.3.1 Surface properties to improve behavior between blood and metals

Surface properties of biomaterials used for treatments of neurovascular and cardiovascular traumas and pathologies are determinant for the success of those treatments. Depending on the contacting tissue with the material, there is a growing need to improve the blood compatibility and the tissue growth and regeneration related with surface properties. Thrombus formation is one of the key challenges for blood-contact complications in vascular applications that seek reconstruction or healing of the vessel wall. Given that conventional biomaterials surfaces do not have the stimuli for tissue growth, these are becoming less attractive for vascular reconstruction intervention. In

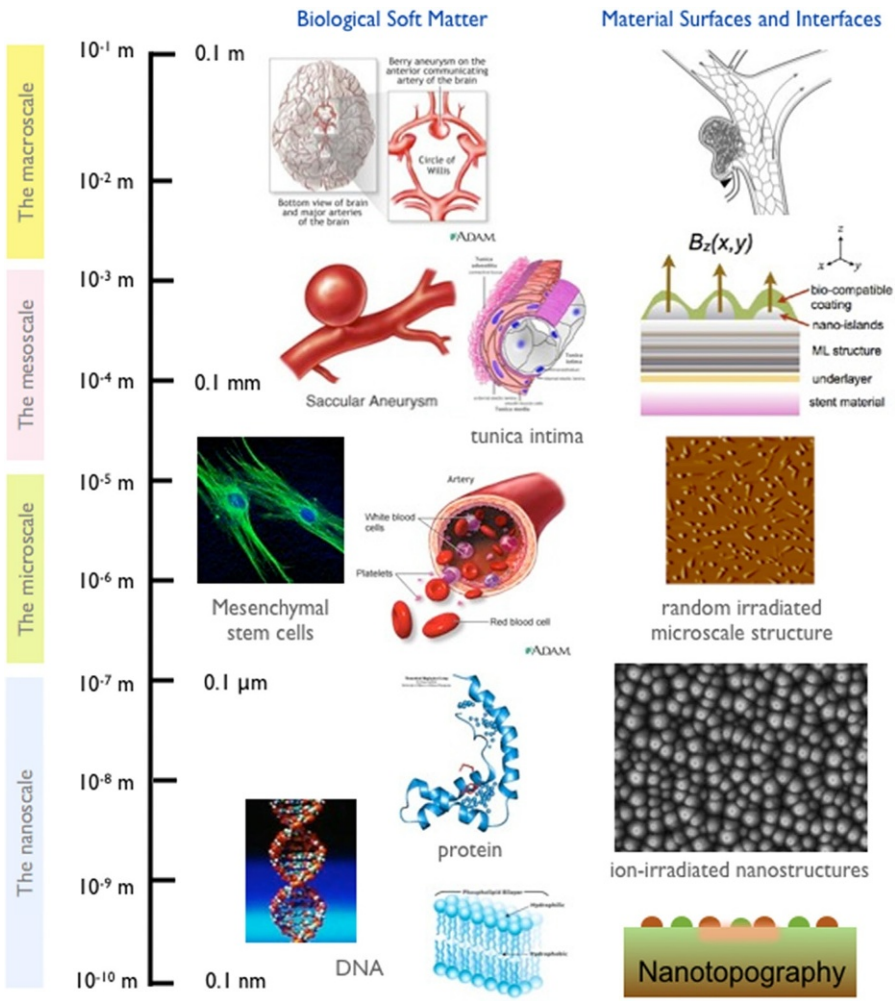


Fig. 11.2 Illustration of the multiscale nature of blood-material interactions. The nanoscale interface of protein-material surface adhesion can influence cell-level interactions that in turn drive tissue growth and development. The example here consists of arterial wall reconstruction.
Copyright Taylor & Francis 2014.

complex stent devices, differing needs for the luminal versus abluminal regions of the stent material surface demands tailored surface treatments.

Advanced tailored tools using low-energy ion irradiation result in novel micro- and nanomorphological and chemical modifications, which can solve coagulation problems associated with blood-contact surfaces of biomedical devices and implants. Furthermore, synthesis by irradiation can help stimulate tissue growth and regeneration in specific surface regions (e.g., luminal side of conventional stent materials

surfaces) where it is necessary depending of the trauma and pathology. Ion irradiation can give tremendous advantages for surface design ensuring blood compatibility and hemostasis of stent devices, and some of those tools can also create surfaces, which will stimulate tissue (blood vessel walls) adhesion to luminal side of the same stent. In the same sense, ion irradiation also can favorably modify scaffolds and grafts in order to stimulate growth tissue from a tissue engineering and cell therapy point of view.

Besides applications of thin-film deposition on substrates [38], ion implantation is another way in which surface properties can be modified toward a specific desired characteristic [39–41]. In this context, the chemical nature of the ions used, as well as the energy of the ion beam, the charge and energy are all parameters that have significant influence on the outcome of the ion-irradiation procedure. Among these, however, the dominant parameter is the energy of ion irradiation. At low ion energies, for example, below 100 eV, desorption and/or adsorption are phenomena that are dominant, as well as migration leading to material island formation. Ion irradiation has been used for surface engineering to induce characteristics such as cleaning, smoothing, film growth, or etching [42–44].

One particular surface property influenced by ion irradiation is a material's surface nanotopography, which can induce changes to the material's wettability [45,46]. More importantly, for the purpose of surface property control and bioactivity enhancement in biomaterials, the wettability can be either enhanced or reduced by manipulating the characteristics of the ion beam. The advantages that this brings for improving the biocompatibility of medical devices, especially vascular stents are obvious; by manipulating the ion beam composition, energy, or flux, one can potentially be able to set up [47] criteria for optimum surface wettability in vascular grafts with consequences in refining our capacity to control thrombogenicity and tissue integration of these implants in synergy with establishing endothelial layer growth. However, surface wettability (or the lack thereof) is not necessarily the only surface mechanism or parameter that can influence or control platelet adhesion and/or bacterial adhesion [37,48]. There are other surface properties that can play a role: surface chemistry, surface charge density, nano- to microscale crystallographic orientation, OH^- ligand distribution, and nitrous oxide (NO) vessel dynamic response, among others. Understanding these correlations to both thrombotic behavior and ultimate vessel failure is one of the most challenging aspects of blood-contact material design and performance to date.

The biomaterial interface is a complex interchange between inorganic, organic, and bioactive systems coupled via complex molecular and chemical interactions. The interface between living cells and materials, for example, relies on interdependent signaling between proteins on surfaces/interfaces in the extracellular matrix (ECM) or inorganic material and cell-adhering receptors or molecules (e.g., integrins and proteins). A hierarchy of surface properties shown in Fig. 11.3 illustrates the underlying mechanisms involved in the interaction between cells and biomaterials. The interactions can be generally described by the following four main mechanisms in order of hierarchy: (1) the surface energy can influence the hydrophilicity and/or hydrophobicity of a biointerface and is correlated by (2) the electric charge distribution, which is dependent on (3) the surface chemistry and crystallographic orientation, which are codependent with the (4) surface topography.

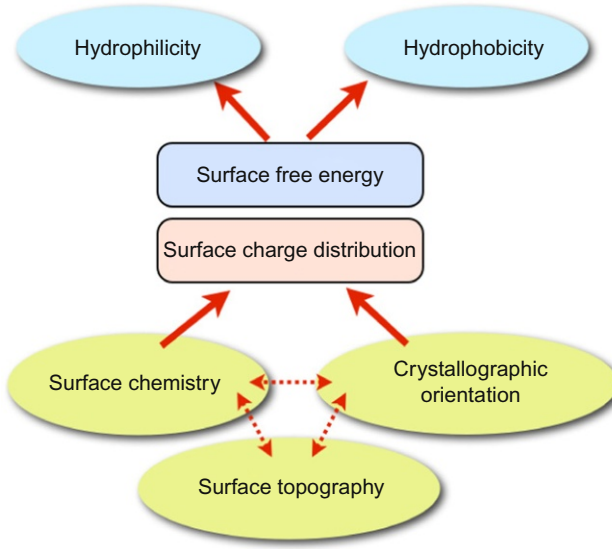


Fig. 11.3 Schematic illustrating the properties responsible for ultimately controlling the hydrophobicity or hydrophilicity of a material biointerface. Blood-contacting material surface properties will depend on a combination of material surface properties. The hydrophilic and hydrophobic property of a material will depend on surface free energy driven by surface charge distribution that can have a complex dependence on surface chemistry, surface topography, and crystallographic orientation.
Copyright from Taylor & Francis, 2014.

11.3.1.1 Cell-surface interactions

Biomedical applications frequently require the use of biomaterials in the fabrication of stent devices and implants in order to improve the behavior of an organ or tissue, or at times for its replacement. Consequently, it is important to have multiple alternatives in terms of design and function of the biomaterial to guarantee an appropriate interaction with the host tissue and the blood-material interaction. There are a variety of biomaterials according to their characteristic nature and class of material (e.g., metals, polymers ceramics or combination thereof), which also depend on the application and expected function. Likewise, the surface of the material requires detailed studies since it is in intimate contact with the tissue and defined as the biointerface where the most important reactions are carried out. The biointerface mechanisms responsible for cell-surface interactions consist of two primary effects: (1) protein adsorption (which can regulate platelet adhesion and blood coagulation cascade (BCC)) and (2) cell response. Proteins in the appropriate conformation and orientation can stimulate a constructive cell response that could include favoring wound repair and tissue reconstruction. The cell response depends on specific proteins for achieving anchorage and receiving extracellular instructions that can guide its differentiation and/or proliferation [49]. In blood-contact material interactions, blood plasma proteins can vary greatly, and with approximately 300 distinct types so far documented, understanding their interaction to materials surfaces can be quite complex.

When a biomaterial is implanted or introduced (e.g., stent scaffold) in the body, a chain of reactions are activated, and this interaction is magnified at the surface of the material. Factors at the interface of the biomaterial such as physical, chemical, physicochemical, and mechanical properties can dictate the biological response defined by biocompatibility and adhesion, cell differentiation, and proliferation. Therefore, one can determinate the localized or the general response of the implant by the body in terms of integration, function, and stability [50]. On the other hand, the stability of a material can be influenced by key aspects at the biointerface. For example, in metals, corrosion resistance plays an important role in achieving a high grade of biocompatibility. Typically, the most external interfaces that cover a metal are oxides that act as a protection barrier between the bulk and tissue preventing chemical reactions between the material surface and the environment [51].

In terms of physical properties, the surface topography is considered one of the most crucial parameters in the biological response after introduction of a biomaterial. Several studies in which different morphology configurations at micro- and nanolevels demonstrated that the roughness profile and surface distribution have a strong and direct influence over cellular behavior, in which is possible to appreciate that cells prefer texturized surfaces in comparison with smooth ones [52]. Similarly, isotropic and aligned fibers can guide cells to grow in the same direction and orientation following the pattern. Moreover, texturized surfaces with pores, canals, or tunnels can promote interaction between different kinds of molecules and even cells, due to an increase in surface area and facilitating the deposition of proteins [53]. The role of surface topography has been extensively studied in the last few decades due to the well-known fact that modifications at the nano- and microlevel can affect cellular activity [54]. This effect has been used as a strategy to improve biomechanical fixation to guarantee stability of the implant. In other cases, surface roughness has been used to immobilize proteins or peptides that can promote cellular adhesion and proliferation [55]. Antimicrobial activity through deposition of antibiotics or antimitotic has been used to control the growth of bacterial and fungus in implants [56]. In other circumstances, the surface topography has also been demonstrated to influence antibacterial properties [48].

The surface of an implant or a medical stent can be modified to transform the bulk material or modified to support a surface coating. The material for the latter case can be metal, ceramic or polymer, or organic compound, depending on the functionality desired that differs from that of the substrate material. Surface coatings can also be used to prevent leaching of ions from metal alloys fabricated to have specific biomechanical properties and where the ions can be toxic to the local tissue or the body. Cells might be able to sense different conditions of the surfaces such as texture orientation and morphology; isotropic and anisotropy; and mechanical, physical, and chemical signals that translate them into stimuli to promote cell motility, alignment, and others functions. Cell shape and phenotypic responses seem most pronounced when the scale of the surface feature is some fraction of the cell size, (e.g., from tens to hundreds of nanometers) [57]. In addition, physical properties that can interfere with surface modification are strength and flexibility. Therefore, Young's moduli that are close in magnitude can introduce adequate transition between materials with different

features avoiding stress shielding [58]. Furthermore, signals can mediate the histological response in the surrounding structures. Identifying the relationship of these key factors and tissue reconstruction and treatment can have a decisive implication on success or failure of implantation and device/tissue interactions. From this context, the immune response and the blood-material interactions play a critical role in multiscale interactions of the implant foreign body material and the body. With respect to blood-material complications related to implant integration in orthopedics, they can include blood clotting, bleeding, poor wound healing, infection in the wound and near prosthesis, damage to nerves and blood vessels, and pulmonary embolism. Understanding cell-surface interactions with implants can someday result in smarter biomaterials that enable faster healing/fixation, lower infection risk, and more adaptive function.

11.3.1.2 Surface free energy and the biointerface

The surface free energy of a material can be defined as the change or variation of interatomic or intermolecular bonds to form a surface. The surface energy could also be defined as the excess energy at the material surface compared with its bulk. Vogler, for example, defines surface energy as "an intensive thermodynamic property of a material that arises from the loss of nearest-neighbor interactions among atoms or molecules at the boundary. This excess energy most prominently manifests itself in adhesion and adsorption reactions at the surface" [57]. The surface in a material is a two-dimensional defect and thus atomic and defect mobility can be orders of magnitude higher than in the material bulk. Biomaterials are intrinsically dependent on surface free energy given that at this interface, living organisms can interact via complex biochemical bonding channels, for example, in the case of cell adhesion or in other cases such as blood plasma protein adsorption.

The biointerface of any biomaterial introduced in vivo will interact primarily with water given it's a major component of biological fluids. Consequently, the role of the biointerface and its interaction with the water molecule can dictate the design of a particular biomaterial interface and dictate the strategy in developing biomaterials around that particular dynamic medium. The surface energy of a biomaterial also is closely associated with the charge distribution on a surface. The combination of charge state and surface energy of a particular biomaterial surface (biointerface) can therefore dictate the surface wettability that ultimately influences protein adsorption. However, it is not intuitively obvious how wettability can control protein adsorption. Generally, hydrophilic surfaces can improve adhesion, but in the case of proteins, the probability for adhesion is largely determined by the local immunologic response at the biointerface. For example, conformational changes at a biointerface by processes such as inflammation, coagulation, and foreign body response can initiate reactions that bring tight adherence to hydrophobic biomaterial surfaces [59]. In addition to the characteristics of the surface and its effect on biocompatibility of a biomaterial is also its complex contact with body fluids in a region defined by Vogler as a "pseudo two-dimensional zone of water directly adjacent to the surface, referred to as interfacial or sometimes *vicinal* water" [57]. This region of water at the biomaterial surface can dictate how the surface chemistry influences the biomaterial effects on the body. The strong

coupling at this interface can also dictate the strategy for surface modification selected depending on what functional outcome is desired of the biomaterial. Moreover, the process-structure-property relationships dictating biomaterial design must also assess the dynamic environments where the biomaterial is exposed.

11.3.2 Techniques to modify metallic surfaces

Numerous techniques to modify metallic-based systems to improve hemocompatibility exist. In this section, we focus primarily on those techniques that enable a metallic surface to address issues with corrosion resistance and biocompatibility for a selected set of metals such nitinol and nickel-based metals. As discussed above, metallic implants can consist of a wide variety of materials including titanium, Ti alloys, stainless steel, and CoCr alloys. The processing of these materials will dictate their mechanical properties, and similarly, the surface modification properties may influence their surface functionality. The corrosion resistance of nitinol and nickel leaching rates depend strongly upon the surface characteristics of the implant [60]. A variety of surface passivation techniques have been explored on nitinol and other NiTi alloys to improve corrosion resistance and biocompatibility. These methods range from mechanical surface modification, to surface treatments with chemicals or ions, to deposition of corrosion resistant coatings on the surface of the implant. The following section will provide a review of some studies on these various techniques.

11.3.2.1 Mechanical modification

Mechanical polishing is the most common modification the NiTi alloy undergoes prior to implantation. For this reason, the performance of surfaces modified with the techniques discussed in this review will be compared with the performance of mechanically polished specimens. Mechanical polishing is not feasible for some devices with complex geometries, however [61]. Another mechanical modification that has been suggested is shot peening. Shot peening induces residual stresses in the material and produces an amorphous layer at the surface [61]. Topographical features have also been induced via shot peening, which may aid in cell adhesion and proliferation [62]. A study by Armitage et al. compared the roughness and hemocompatibility of samples modified by shot peening with those modified via other techniques [61]. Compared with the other modification techniques and comparable 316L and Ti samples, there was no significant difference in the hemolysis observed due to the shot-peened samples, though the roughness increased from 4.3 nm after mechanical polishing to 255 nm after shot peening [61].

11.3.2.2 Electropolishing

Electropolishing is commonly done on NiTi and other metals and alloys to improve corrosion resistance. Electropolishing removes the native oxide layer and forms a homogeneous TiO_2 layer at the surface, with uniform thickness and chemical composition. There is some inconsistency in the literature on how electropolishing affects the surface topography, with some studies reporting that electropolishing

results in nanometer size roughness, while other studies found the surface roughness to be comparable with that achieved with mechanical polishing [63]. This discrepancy may be caused by differences in the electropolishing conditions. Nanometer size surface roughness has been shown to improve blood compatibility [63]. For this reason, many endoluminal stent materials are electropolished prior to implantation [63]. Nickel content at the surface has also been shown to decrease as a result of electropolishing [64]. Thierry et al. found that the surface nickel concentration decreased from 11.5% to 1% as a result of electropolishing [65]. The breakdown potential was improved after electropolishing, as shown in Fig. 11.4, and significantly increased compared with stainless steel [63]. Trepanier et al. found that electropolishing increased the pitting corrosion potential (E_p) of NiTi stents in Hank's solution compared with untreated or heat-treated NiTi stents, thus improving the corrosion resistance [66]. The surface composition was examined through Auger electron spectroscopy (AES) depth profiling. The oxide layer formed through electropolishing was approximately 34 Å thick. The improved corrosion resistance might then be a result of a more uniform oxide layer with lower nickel content rather than a result of film thickness. The Ni-to-Ti ratio at the surface of the electropolished sample was low, around 0.05, prior to the corrosion tests and decreased slightly after immersion [66]. Nickel-leaching rates were not assessed in this study, so it is not clear how effective the oxide was in preventing nickel leaching, nor was surface roughness or biocompatibility assessed.

Armitage et al. electropolished mirror-finished NiTi disks in a 30% $HNO_3 + CH_3OH$ solution at 243 K, with a 15 V potential for 30 min and compared the surface topography and chemical composition, contact angle, and cell toxicity of these surfaces

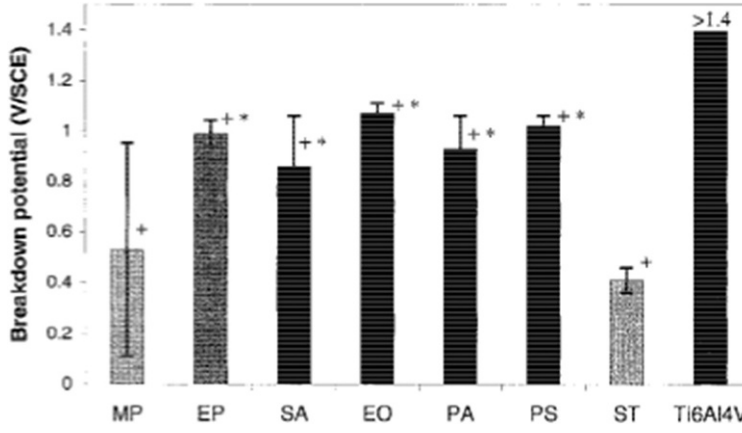
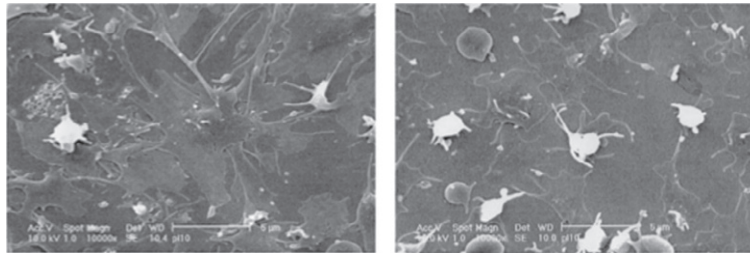


Fig. 11.4 Breakdown potential from cyclic polarization assays in Hank's solution. Data represent mean value ± standard deviations. *Significant versus stainless steel. $^{+}$Significant versus Ti6Al4V ($P<.05$).
Reproduced from C. Trepanier, M. Tabrizian, L. Yahia, L. Bilodeau, D.L. Piron, Effect of modification of oxide layer on NiTi stent corrosion resistance, J. Biomed. Mater. Res. 43 (4) (1998) 433–440.

with mechanically polished NiTi, 316L, and commercially pure titanium. X-ray photoelectron spectroscopy (XPS) results showed a decrease in the nickel concentration at the surface after electropolishing, while nickel hydroxide ($Ni(OH)_2$) was detected, which was not present on the mechanically polished specimen. Atomic force microscopy (AFM) showed an increase in surface roughness and an attendant increase in surface wettability, on the electropolished sample compared with the mechanically polished sample, which Armitage et al. attribute to the difficulty in obtaining optimal electropolishing conditions [61]. Cell testing with mouse fibroblasts and human venous endothelial cells revealed no cytotoxicity due to any of the examined specimens and no significant differences in cell morphologies between samples [61]. Armitage et al. showed with this study that the unmodified and electropolished NiTi surfaces are biocompatible, but there is no advantage to electropolishing in terms of hemocompatibility or cytotoxicity [61]. Fig. 11.5 shows the morphologies of platelets adhered to a mechanically polished sample compared with those on an electropolished sample [61]. This study did not include corrosion tests, so it is unclear whether this method of electropolishing affects corrosion resistance of Nitinol surfaces. The thickness of the oxide was not characterized in this study, nor was the ion release rate. This information is necessary in determining the utility of this treatment.

Navarro et al. electropolished NiTi disks in a 5:100 solution of CH_3COOH to $HClO_4$ for 135 s at 30 V, resulting in a surface predominantly composed of TiO_2 with a surface Ti/Ni ratio of 12.3 [67]. A sputtering depth profile with XPS revealed a Ni surface concentration of about 10 at%, increasing to 50 at% at a depth of 6 nm, compared with 15% at the surface of a sample simply mechanically polished, reaching equiatomic composition at 3 nm [67]. This study included surfaces treated by other methods, for which Ni release rate was measured, but the electropolished surface was not tested for Ni release. The surfaces were not tested for cytotoxicity, breakdown potential, or mechanical properties. These are important factors in determining the value of this technique.



(A) (B)

Fig. 11.5 Morphology of platelets from plasma incubated for 1 h at 37.C on (A) a mechanically polished NiTi surface and (B) on an electropolished NiTi surface.
Reproduced from D.A. Armitage, T.L. Parker, D.M. Grant, Biocompatibility and hemocompatibility of surface-modified NiTi alloys, J. Biomed. Mater. Res. Part A 66 (1) (2003) 129–137.

11.3.2.3 Thermal and hydrothermal treatments

In order to induce the shape-memory and superelastic properties of nitinol, thermal treatments must be applied. Some studies have examined how these thermal treatments affect the surface composition and corrosion resistance of the material, but the results are somewhat inconclusive. Michiardi et al. thermally treated NiTi disks at 400° and 3×10^{-2} mbar for 150 min [67]. The resultant surfaces had a Ti/Ni ratio of 14:1, and a sputtering depth profile with XPS showed the oxide layer to be 65 nm thick [67]. The nickel release rate in simulated body fluid (SBF) at 37°C for the thermally treated surface was approximately one quarter that of an untreated surface after 1 h, while after 48 h, the rates were comparable [67]. This oxide layer seems to be effective in blocking nickel release from NiTi in vitro, but it is unclear whether the oxide will affect the cytotoxicity and cell spreading or corrosion potential.

Shabalovskaya et al. treated NiTi alloys at 500°C for 15 min and compared the surface chemistry with the untreated alloys. The heat treatment resulted in a decrease in carbon content at the surface, but the nickel content increased by a factor of five, compared with the untreated sample [62]. Trépanier et al. treated electropolished NiTi stents in a standard nitrate salt bath at 500°C for a few minutes, until a dark-blue oxide was observed on the surface [66]. A sputtering depth profile with AES determined the oxide layer to be 91.1 ± 27.0 nm; however, the surface Ni-to-Ti ratio for the heat-treated sample was significantly higher than for electropolished or air-aged samples; this ratio further increased after potentiodynamic polarization tests in Hank's solution at 37°C, suggesting Ni diffusion to the surface during immersion in Hank's solution [66]. This is shown in Fig. 11.6 [66].

Autoclaving, which is a common sterilization technique, has been shown to affect the surface composition. Thierry and Tabrizian found that autoclaving contributed to localized corrosion by introducing surface defects and altering the energy of the surface [63]. This was a minor effect, however, and did not significantly reduce the corrosion resistance of the implant [63].

Shabalovskaya et al. boiled NiTi samples in water after chemical etching in $HF + HNO_3$ solution in order to induce diffusion of the Ni ions from the surface oxide into the solution, thus depleting the surface of Ni prior to implantation. The resultant surfaces were depleted in Ni as deep as 10 nm [62]. The boiling also resulted in a more uniform TiO_2 layer than chemical etching alone and is much more effective in oxidizing the surface than exposure to pure oxygen [62,68].

11.3.2.4 Chemical treatments

Many chemical treatments have been proposed for improving the surface of NiTi implants. These chemical treatments often involve the use of dangerous chemical agents. For example, chemical etching with HF has been proposed to remove the native oxide layer, allowing a new TiO_2 layer to form. Milosev and Kapun etched NiTi foils with a $HF + HNO_3$ solution for 5 min and examined the electrochemical, compositional, and topographical properties [60]. This treatment resulted in the formation of pits in the surface of up to 8 μm and an increased surface roughness compared with ground and polished samples. Despite this pit formation, the etched samples showed improved

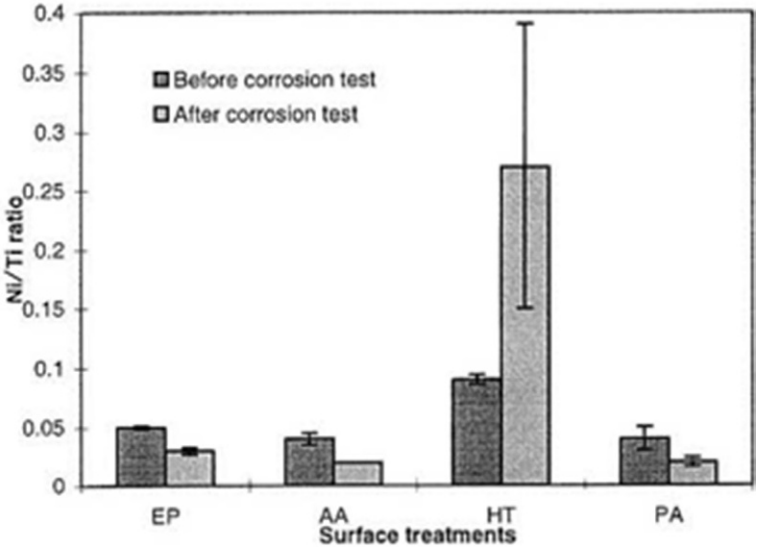


Fig. 11.6 Ni-to-Ti ratios of stents modified various surface treatments before and after corrosion potential experiments. *EP*, electropolished sample; *AA*, air-aged sample; *HT*, heat-treated sample; *PA*, nitric acid passivated sample.
Reproduced from C. Trepanier, M. Tabrizian, L. Yahia, L. Bilodeau, D.L. Piron, Effect of modification of oxide layer on NiTi stent corrosion resistance, J. Biomed. Mater. Res. 43 (4) (1998) 433–440.

resistance to localized corrosion compared with samples that were ground only [60]. The HF treatment decreased the surface Ni content compared with surface polishing, but grinding decreased the Ni concentration further [60]. Shabalovskaya et al. also examined the effect of chemical etching with $HF + HNO_3$ on NiTi wires and disks from various manufacturers [62]. The nickel content at the surface increased with etching time for NiTi plate samples, while the oxygen content decreased [62]. It is unclear, based on these results, whether the chemical etching treatment with $HF + HNO_3$ on NiTi improves the surface nickel content [62]. The discrepancy may be related to the previous surface conditions of the specimen.

Treatment in hydrogen peroxide (H_2O_2) solutions at low temperatures has been shown to improve the corrosion resistance of NiTi, but this treatment results in thick (~500 nm), brittle, porous TiO_2 layers with high Ni concentration at the surface [69]. These layers compromise the mechanical properties of the material [69]. Shabalovskaya et al. chemically etched NiTi disks and wires in order to remove the native oxide, then boiled the samples in H_2O_2 solutions for various lengths of time [69]. The resultant surfaces were examined using XPS, potentiostatic testing, and SEM[11]. Surface Ni concentrations on these hydrogen peroxide treated surfaces were 5 at% or higher compared with under 2 at% for surfaces that were only chemically etched, then boiled in water [69]. In the potentiostatic testing, breakdown potential was not shown in any of the disk samples in this study, but one of the two wire samples boiled in 30% H_2O_2 broke after 5 days with a current density of 17 nA/cm^2 [69]. The

resultant surfaces showed good resistance to pitting corrosion, but the samples boiled in 30% hydrogen peroxide for 2 h cracked extensively, as shown in Fig. 11.7 [69].

11.3.2.5 Ion implantation

The implantation of ions has been shown to increase the hardness and wear resistance of biomaterials [64]. A variety of ion species have been implanted into NiTi surfaces in order to improve its behavior in vivo. Oxygen is an attractive species for implantation, as it will form bond and form an oxide layer with the native Ti. Oxygen implantation is typically done via plasma immersion.

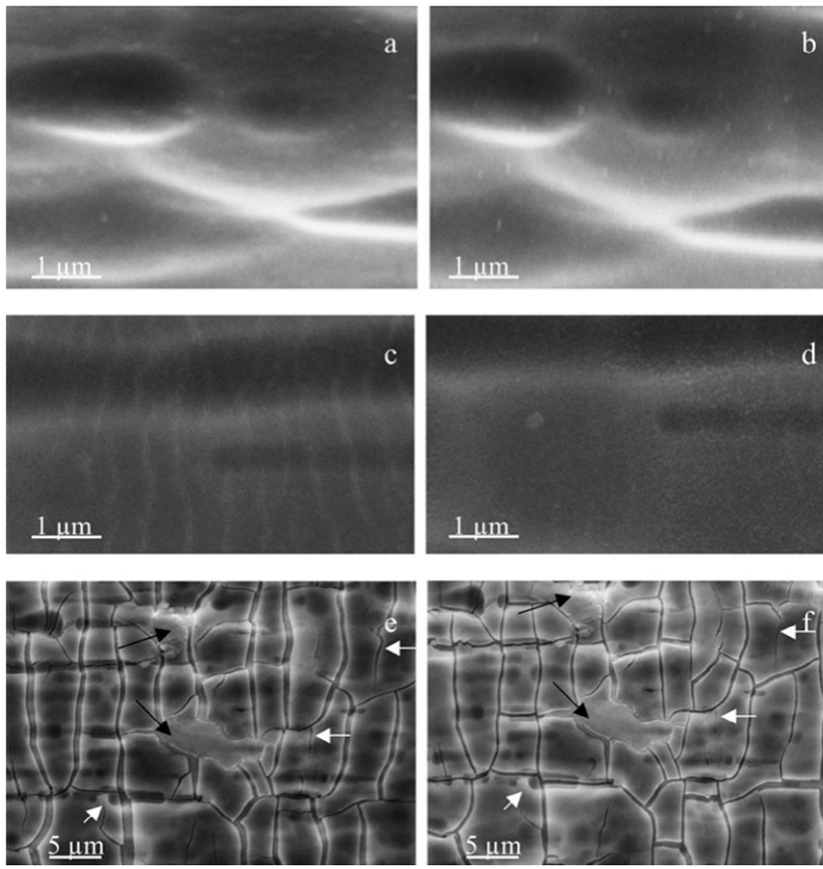


Fig. 11.7 SEM images of NiTi wires boiled in hydrogen peroxide solution at 30% for 15 min (A,B), 3% for 1 h (C,D), and 30% for 2 h (E,F). The left column shows the samples strained to ~7%, while the right column is unloaded. The samples boiled for 1 h in 30% hydrogen peroxide showed extensive cracking.
Reproduced from S.A. Shabalovskaya, J.W. Anderegg, A. Undisz, M. Rettenmayr, G.C. Rondelli, Corrosion resistance, chemistry, and mechanical aspects of Nitinol surfaces formed in hydrogen peroxide solutions, J. Biomed. Mater. Res. Part B Appl. Biomater. 100 (6) 1490–1499.

While oxygen is attractive for surface passivation, helium has also been considered in order to produce a nanoporous titanium oxide surface [70]. Maitz and Shevchenko implanted oxygen and helium ions into NiTi coupons via RF plasma immersion [72]. After plasma immersion, each sample was etched in 1% HF and ultrasonically cleaned in water and acetone. AES was coupled with Ar+ sputtering in order to produce a compositional depth profile of the surface [70]. Maitz and Shevchencho assessed hemocompatibility by examining fibrinogen adsorption and platelet adhesion and cytotoxicity with bovine aortic endothelial cells [70]. The cytotoxicity was determined by examining the metabolic rates cells cultured on the various specimen surfaces at various time points. Implantation of both ion species resulted in decreased nickel content at the surface, but the resultant nickel concentration was higher than that achieved by others using Ar+and N+ ions [70]. Only the oxygen implantation reduced the thrombogenic effects. While the helium implantation resulted in nanopores, the mechanical stability of the implant may be reduced compared with unmodified nitinol. Ideally, the nanoporous NiTi would be comparable mechanically with titanium [70].

Nitrogen (N) is also a useful ion species for implantation into NiTi, as it will form a TiN layer at the surface of the specimen, serving as a diffusion barrier to the Ni ions in the bulk. Carbon likewise can be implanted in order to create a TiC layer at the surface. Gorji et al. implanted annealed 2 μm NiTi thin films with carbon, argon, and nitrogen ions [71,72]. The ions were implanted with methane (for carbon) and nitrogen gases at energies of 80 keV to a fluence of $3 \times 10^{17}\,\mathrm{cm}^{-2}$. XPS was used to characterize the composition of the resultant surfaces, while the surface morphology was examined using AFM [71,72]. Nanoindentation was used to examine the mechanical properties of the films [71]. XPS revealed that the only N compound formed in the nitrogen-implanted specimens was TiN, and likewise the carbon implantation resulted in TiC as the only carbon compound [71]. Nitrogen implantation resulted in formation of Ni_4Ti_3 and Ni-enriched subsurface layer [71]. Implantation with N and C improved the corrosion potential of the NiTi films in Ringer's solution, while implantation of argon (Ar) under the same circumstances actually decreased the corrosion potential, as shown in Fig. 11.8 [71]. The TiN and TiC surfaces had higher nanohardness and decreased scratch coefficient and wear depth compared with the unmodified NiTi, suggesting the implanted surfaces will have better wear resistance [72]. Pelletier et al. also observed an increase in surface hardness of NiTi alloys implanted with N ions [73].

Plasma ion implantation can be combined with deposition in order to fabricate a variety of coatings on a specimen surface [74]. Recently, Shanaghi et al. passivated NiTi surfaces through plasma immersion ion implantation and deposition (PIII&D) of Ti and TiC films [74,75]. In this study, mechanically polished NiTi disks were magnetron sputter deposited with high purity Ti, followed by PIII&D of a TiC film of approximately 90–160 nm [74]. TiC is a good candidate for a ceramic film on NiTi as it is highly corrosion resistant, chemically inert, biocompatible, and has high hardness and low friction [74,75]. The resultant films were tested for chemical composition, corrosion resistance, and mechanical properties and compared with bare NiTi samples [74,75]. XPS and AES were used to determine the surface composition and perform a depth profile of the Ti/TiC films, revealing a Ti-to-C ratio near unity at the surface,

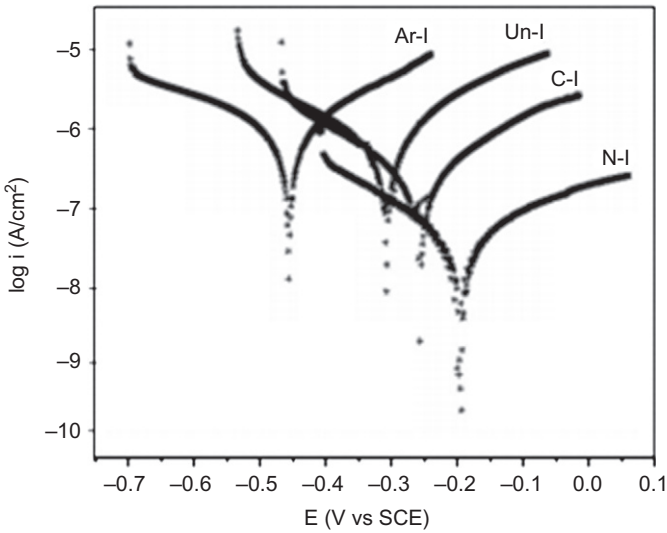


Fig. 11.8 Polarization curve of NiTi thin films implanted with nitrogen (N-1), carbon (C-1), and argon (Ar-1) compared with unmodified NiTi (Un-1).
Reproduced from T.M. Sridhar, S. Rajeswari, Biomaterials corrosion, Corros. Rev. 27 (Suppl.) (2009) 287–332.

with the C content decreasing gradually with depth [74]. This concentration gradient is a result of the energetic ion implantation into the TiC film; the implantation depth depends upon the energy of the deposited ions [74]. In corrosion tests in SBF, the TiC film had increased resistance compared with the native oxide, which Shanaghi et al. attributed to the decreased grain size caused by ion bombardment [75].

11.3.3 Materials used as coating in metallic stents to improve the biological response

Coating materials are used such as coatings on SS316 or nitinol for stents, Mg-based systems with anodized coatings (from review with Felix), and the use of metallic alloys (both permanent and bioresorbable). Another solution to improve corrosion resistance and to block nickel leaching is the deposition of a coating on the surface of the NiTi implant. This can prove challenging, as it is imperative that the coating adhere strongly to the bulk to prevent failure [67]. A number of different coatings have been applied to NiTi surfaces, varying from polymers to nitrides and carbides. Flamini and Saidman electrodeposited polypyrrole (PPy) films onto NiTi electrodes [76]. Ppy was chosen due to its good tissue compatibility, ease of fabrication, and high stability [76]. The PPy films adhered very poorly to the electrodes and were easily removed with Scotch tape [76]. The corrosion behavior and concentration of released ions was examined in chloride solution [76]. The impedance increased after the NiTi was coated with PPy, and the nickel release of the coated NiTi was half that of the uncoated

sample [76]. The adhesion of this coating must be improved in order to make it a viable candidate for surface treatment of NiTi. Polymeric coatings may also not be suitable for many orthopedic applications [67].

Some non-Ti-based ceramics have also been suggested for deposition onto NiTi surfaces. For example, silicon carbide has been investigated as a stent coating, designed to improve hemocompatibility, and reduced nickel leaching [75]. Nickel release was measured for 223 days in hydrous solution. Blood contact was assessed for both the coated and uncoated stents; the stents were placed in a modified chandler-loop system, in which human blood was circulated at 37°C for 120 min. After contact, the blood samples were assessed for thrombin-antithrombin (TAT) complex, beta-thromboglobulin (β-TG), and polymorphonuclear (PMN) elastase concentrations, which are factors in blood coagulation [75]. The nickel release was reduced by more than 90% after the SiC coating. With the exception of the PMN elastase, a significant decrease was seen in the blood coagulation factors in the sample in contact with the SiC coated stents versus the uncoated stents [75]. The stents were imaged before and after blood contact, as shown in Fig. 11.9. It is clear from these images that the thrombus formation was much more significant on the bare nitinol stent compared with the coated sample.

While the SiC coating showed good hemocompatibility and low nickel leaching, it is not clear from this study whether the corrosion resistance was significantly improved. Further investigation should be pursued in order to determine the efficacy of this method.

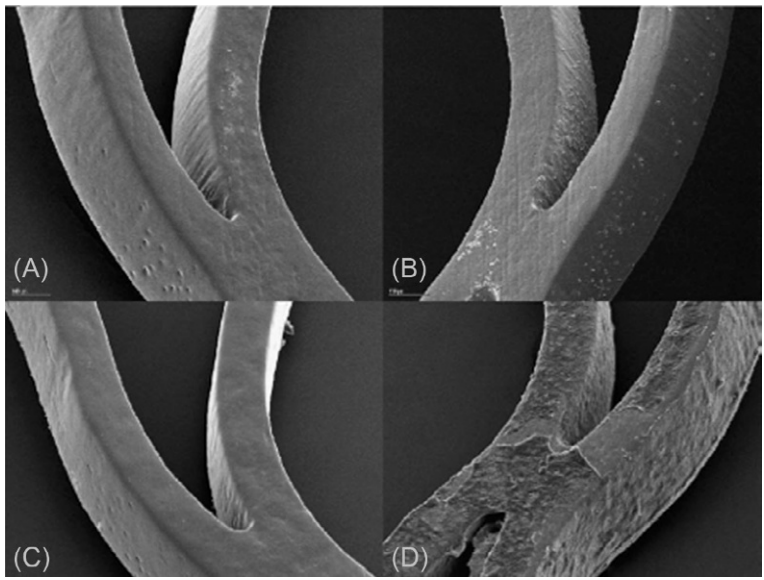


Fig. 11.9 SEM images of SiC/H-coated stent (A) before blood contact and (B) after 120 min of blood contact, showing no thrombus formation and bare nitinol stent (C) before blood contact and (D) after blood contact, showing an extensive fibrin network.
Reproduced from H. Pelletier, D. Muller, P. Mille, J.J. Grob, Structural and mechanical characterisation of boron and nitrogen implanted NiTi shape memory alloy, Surf. Coatings Technol. 158 (2002) 309–317.

11.4 Advanced hydrogels integrated with metallic nanoparticles and their hemocompatibility

This section will focus on the introduction of tailor-made hydrogels either natural or synthetic designed with metallic nanoparticles to induce specific bioactive functions such as antibactericidal, antithrombotic, increased endothelial adhesion, and increase of cell proliferation and differentiation for vascular reconstruction. This section would address fundamental factors on blood-surface interactions with hydrogels, examples in neuroendovascular applications and briefly move to more advanced interactions with nanostructured bioactive interfaces and in particular systems that integrate metallic nanoparticles (e.g., Fe_2O_3 for magnetic function, Ag for antibacterial, Au for biosensing, and other pharma-based approaches with NPs). This section is also a short case study on the use of metallic nanoparticles (e.g., metallic systems) that are integrated into natural or synthetic hydrogels for use as blood-contacting material. Here, we focus on bacterial nanocellulose (BNC) and chitosan as examples. This section also serves as background for Section 11.5 of this chapter focused on characterization and testing in *simulated environments* that mimic the in vivo characteristics driving design of the biomaterial.

11.4.1 Introduction to neuro-endovascular blood-material interactions

Stent technology since its introduction by Palmaz [77] in 1985 has mainly focused its benefit in maintaining the patency of the blood vessel or duct being treated. To a certain extent, as its utilization developed in the realm of neuroendovascular surgery, it has been used in opening up stenosed or occluded carotid arteries and to assist in the coiling of cerebrovascular aneurysms [78], especially wide-necked aneurysms, but not as its primary treatment. Endovascular coiling, the current first-line treatment for intracerebral aneurysms since 2002 [79], has shown mounting evidence of complications in the literature since its use, making revisions of aneurysmal coiling an accepted part of neuroendovascular practice [80–83]. The idea that stents can be used as a primary treatment for cerebral aneurysms had few adherents in the literature [84]. Reported cases of angiographically proven occlusion of difficult to clip or coil aneurysms after stenting [85] demonstrated a potential to induce closure of the aneurysmal sac through flow diversion (FD) techniques and progressive thrombosis giving rise to the pipeline embolization device (PED) (ev3, Plymouth, Minnesota) and the Silk FD (Montmorency, France). However, the unabated buildup of intra-aneurysmal thrombosis in these FD devices had been considered as a mitigating factor for delayed aneurysm rupture after FD treatment [86]. Wehman et al. illustrated a variable porosity stent in 2006 but could not follow-up with a fabricated prototype, much less its clinical application [87]. In 2009, Ionita et al. [88] in applying variable porosity stents (asymmetrical vascular stents) in rabbits indicated complete occlusion in all nine AVS cases but had three deaths during AVS treatment. Clearly, the approach in stenting aneurysms aside from lessening aneurysmal inflow through lessened stent porosity

should also safeguard against uncontrolled intra-aneurysmal thrombosis buildup or thrombogenic occlusion of the parent artery, for the endovascular strategy to be viable.

Although clinically used mainly for coronary stenosis/occlusion treatment, drug-eluting stents (DES) have previously been offered to counter stent thrombosis (ST), but recent studies [89,90] have shown DES to have a higher late onset ST risk with the same ST risk as bare-metal stents (BMS) [91]. Inversely but accurately stated, ST is an inherent consequence of stent placement and endoluminal manipulation. To use it for its original intention—which is to dilate a stenosed duct or vessel—is to accept varying degrees of ST, which can only be minimized but not totally removed as a complication. The major role of minimizing endoluminal manipulation in preventing intimal hyperplasia has not been better demonstrated with the comparison of postangioplasty occlusion versus a poststented minimal stenosis by Christen in porcine coronary arteries [92]. But what if stents were used to induce closure of aneurysms endoluminally? Would this inherent ST still solely be a "complication"? Is not the aim of the current first-line treatment for cerebral aneurysms the induction of endothelial proliferation through the introduction of thrombogenic coils within the sac? Thus, begins the first leg of the endovascular treatment strategy developed for the treatment of cerebral aneurysms: to use the *stent's inherent thrombogenicity* to induce hyperproliferative tissue closure at the aneurysm orifice. Within this answer comes the next question: With the stent's placement on the whole blood vessel lumen, how do we now confine the thrombogenic activity on just the blood vessel area encompassed by the aneurysm and orient further tissue growth extraluminally toward the aneurysmal sac?

11.4.1.1 Development of stent as scaffolds for functional hydrogel membranes

Aneurysms are defects within the arterial walls with failed attempts at vascular remodeling. The understanding of the hemodynamics on shear stress and arterial wall tension underlying aneurysm formation led to the first successful demonstration of cerebral aneurysm formation in primates in 1987 [92], an advancement from the previous glass models. By thinking of stents as a passive scaffold maintaining the patency of the parent artery to include the area of failed vascular remodeling (aneurysm) instead of utilizing it solely as a tool for endoluminal manipulation to coil the aneurysmal sac, one could readily appreciate its potential to repair the arterial wall defect. By repair, it means not only the thrombogenic induction of a weak neointimal film across the aneurysmal orifice, as has been repeatedly shown with coiling [93] or placement of variable porosity stents, but also the actual ingrowth of the missing arterial wall across the stent scaffold. Of special mention is the tunica media or vascular smooth muscle layer that will provide the resilience to counter the wall tension and shear stress created by hemodynamic forces and contribute to durability of treatment. The provision of a scaffold across the area of failed vascular remodeling (aneurysm orifice) would not be sufficient to induce repair across this defect. Therefore, an additional approach was developed to attract cells to the hydrogel membrane surface on the stent scaffold.

11.4.1.2 Confining induced thrombogenic activity extraluminally with a focal magnetic field

One of the challenges presented with the magnetic bacterial nanocellulose (MBNC) approach of Allain and Tigno was the spread of ST throughout the parent artery in the light of its radial placement within the blood vessel wall were myriad. As stated before, the ST consequence can only be minimized and not totally removed. A one-time placement of the stent is of course the least endoluminal manipulation possible. In fact, patients who underwent and continue to undergo stent placement harbor a certain degree of ST but are subclinical in significance for which antiplatelet therapy is routinely given. Other pharmaceutical options [94,95] were considered, but the complex biochemical interactions expected in pharmaceuticals were unpredictable when faced with an arterial wall radially stressed with bearing a stent and an aneurysmal orifice that needed closure. A bioabsorbable stent [96] was thought to basically provide no wall stress; however, the period of biodegradability had to be synchronized to the needs for adequate aneurysm closure, a feat that could open the aneurysm itself to risk of premature rupture should the overlapping of stent biodegradability and tunica media formation not be accurately sequenced. The concluding points therefore were first that the risk of early or late ST among BMS was clinically more acceptable when compared with that of DES, especially when stent placement is carried out with the least endoluminal manipulation and when the poststent coverage with antiplatelet therapy is carried out. Secondly, with the stent in place as a scaffold and MBNC integrated along the stent area covering the aneurysm orifice, the remaining element in the strategy was one that would confine tissue hyperproliferation. In selecting this inducing agent, a physical factor was considered more predictable than a biochemical one in initiating and redirecting thrombogenic endothelial proliferation extraluminally. Among the physical factors, studies on magnetic field activity with biological systems abound. Magnetic fields have been shown to affect cell cleavage in plants [97–99]. The field of Hematology had its beginnings with the blood banking system, which began when Waller [100] noted that older red blood cells had a different hemoglobin composition (methemoglobin). Molday [101] and Owen [105] later induced this ferric state (methemoglobin) by oxidizing the iron atoms and rendering them paramagnetic, leading to high gradient magnetic separation of erythrocytes from whole blood. In 2003, Berry et al. [103] demonstrated the ability of magnetic nanoparticles to induce fibroblastic growth and activity as seen in both comparative growth media and under the scanning electron microscope. *The retention of cells in the presence of blood flow using a magnetic field*, a requirement for tissue repair intravascularly formed the neuroendovascular treatment concept of Allain, Tigno, and Armonda. To ensure a directed path of growth extraluminally avoiding ST within the parent artery, the magnetic field was designed to emanate solely from the side of the stent facing the aneurysm. To address this challenge, a hierarchical biocompatible membrane was designed by Allain et al. taking advantage of novel nanostructured interfaces applied to conventional stent technology [102].

The role of nanotechnology in the endovascular treatment of cerebral aneurysms is increasingly becoming critical for localized, asymmetrical treatments (e.g., localized

treatment of cerebral aneurysms) as discussed in this chapter. One example where nanotechnology can have significant impact in the treatment of aneurysms and vascular disease is in the synthesis and manipulation of surfaces and interfaces of devices deployed for reconstruction and tissue repair (e.g., 3D scaffolds with commercial stents). The role of surface modification is critical due to the unique relationship between protein adsorption processes and how they are affected by a biomaterial's surface properties [103] at the nanoscale. Advanced coatings can be designed to induce functionality on 3D scaffolds. Multifunctional properties could be tailored with the use of *directed irradiation synthesis* pioneered by Allain et al. [102]. This method is a low-energy (below threshold damage) ion- and atom-beam modification technique that aids in the growth of thin films while inducing structure and topography at the nanoscale. Thus, one could envision coupling various functionalities (i.e., biocompatibility, hydrophilicity, magnetic attraction, surface chemistry, surface topography, and cell regulation) in one multicoating system deposited, for example, on stent surfaces. Ion-beam-induced nanopatterns can couple organic/inorganic systems and immiscible materials at the nanoscale. Advanced in situ synthesis methods have been recently developed by Allain et al. to elucidate ion-irradiation mechanisms that can manipulate surface chemistry and surface morphology to ultimately synthesize functional coatings for 3D scaffold systems.

Another study carried out by Kanda and Matsuda [104] who in showing the role carried out by pulsatile stress in creating hybrid muscle tissue that mimicked the molecular orientation and physiological function of native tunica media within a radial blood vessel wall, proved that *pulsatile stress is needed for an oriented growth of smooth muscle tissue*. Therefore, an essential requirement to the development of an advanced blood-material interaction medium was the design of *simulated* conditions that enable an understanding of both the resiliency and the hemocompatible activity of the proposed membrane hydrogel and to measure whether the placement of a rigid stent in a selected section of an elastic blood vessel would counter the pulsatile stress needed for an oriented smooth muscle growth.

11.5 Advanced in situ characterization of bioactive hemocompatible metallic surfaces

One of the most challenging knowledge gaps in the understanding of hemodynamic interactions with metallic interfaces is the mechanisms driving blood-material coupling in vivo and the lack of characterization of the same. Surrogate systems or experiments involving the realistic hemodynamic environment of the body and the material response is one of the emerging approaches at in situ characterization of hemocompatibility in *simulated environments* for metallic surfaces today. While static characterization experiments remain important, dynamic measurements are now driving deep understanding of the blood-contact material interactions that include complex behavior such as the hemodynamic effects of shear flow on adhesion and absorption of blood plasma proteins, cells and ultimate platelet and blood coagulation dynamics that affect the performance of biomedical implant and stent devices in the body.

11.5.1 Testing biomaterial properties of hemocompatible metallic systems under realistic conditions

Testing the properties of biomaterials and, in particular, their function in a hemodynamic environment can be challenging. The complexity and hierarchical interactions that occur from the biomolecular scale of tissue/biosurface interactions to blood-plasma platelet dynamics can render the assessment of biomaterial performance elusive. Biomaterials design must seek well-defined in vitro tests that can be translated to in vivo conditions. The latter is uniquely dependent on the highly complex environment of a living body and therefore identifying "simulated" conditions that can replicate some aspect of the living environment (e.g., hemodynamic pulsating flow) combined with appropriate in vitro protocols could elucidate biomaterial response and performance that can guide materials design. In this section, we will briefly cover three case studies that involve several levels of hierarchy and complexity to assess novel biomaterials for blood-contact case scenarios. The case studies are (1) testing the local hemodynamic flow around aneurysm models with a bioMEMS device coined "aneurysm-on-a-chip," (2) testing the local magnetic force dynamics on magnetized cells under simulated hemodynamic flow, and (3) in situ nanomechanical testing of a hydrated hydrogel membrane.

Before presenting these cases, we discuss one particular example that nicely illustrates the case in point. The work by Pham et al. consisted of examining the tissue response to a hemodynamic environment interacting with a microscale surface patterned biomaterial [37]. In their work, Pham et al. studied the potential of nano and microscale surface structures to influence the adhesion of platelets driving hemostasis locally on a biomaterial interface. This was accomplished by design of flow cell that mimics the hemodynamic environment of flow stress along the surface of the patterned polymer polydimethylsiloxane (PDMS) plate layer. The platelet adhesion measurements from flowing porcine blood in the test cell enabled were correlated to systematic parametric studies with finite element method (FEM) models. Results demonstrated about a 78% reduction of platelet adhesion compared with the control under simulated hemodynamic conditions. These results combined with static wetting angle measurements identified an inverse relationship between hydrophobicity and platelet adherence. These simple yet instructive experiments benefited from a well-designed *simulated* environment that enabled the measurement under closely realistic in vivo conditions providing more clues about the relationship of hemodynamic properties and surface nano- and microscale patterns on a biomaterial (Fig. 11.10).

11.5.1.1 Aneurysm-on-a-chip test cell for neuroendovascual reconstruction studies

The first case example is one that examines the local multiscale hemodynamic behavior near and around a brain aneurysm introduced earlier in this chapter by Allain, Reece, and Echeverry-Rendón [102,106]. An innovative bioMEMS device designed and developed by Lisa Reece and colleagues at Purdue University is briefly highlighted in this section [106]. The design of the Aneurysm-on-a-Chip by Dr. Lisa Reece

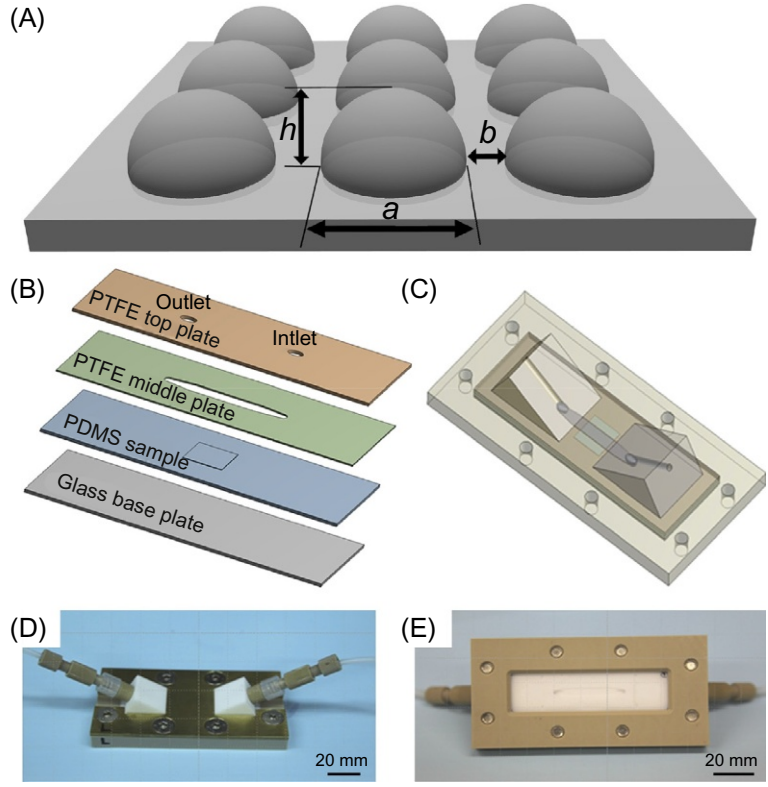


Fig. 11.10 The setup of experimental flow cell to test (A) surface patterns (i.e., regular arrays of hemispherical microstructures), (B) multiplate test stand system, (C) flow cell sketch, (D) photo, and (E) bottom side flow region photo.
From T.T. Pham, S. Wiedemeier, S. Maenz, G. Gastrock, U. Settmacher, K.D. Jandt, J. Zanow, C. Lüdecke, J. Bossert, Hemodynamic aspects of reduced platelet adhesion on bioinspired microstructured surfaces, Colloids Surf. B: Biointerfaces 145 (2016) 502–509.

focused on leveraging advantages of MEMS systems and capturing the essential flow-wall conditions found near the aneurysm wall to elucidate the hemodynamic complexity near and around brain aneurysm neck orifice. As discussed earlier, the premise behind a local focal magnetic region around a biocompatible membrane on a scaffold stent relied on mechanisms of hemodynamic flow and magnetized cell attachment to the MBNC surface.

One key aspect of this approach was an understanding of the local hemodynamic flow around various types of brain aneurysms. Reece and colleagues designed a bioMEMS device with the following characteristics: (1) the ability to provide simulated pulsating flow dynamics to mimic the hemodynamic shear forces along the aneurysm abluminal region, (2) the ability to provide in the same system a variety of aneurysm types and vessel flow configurations, and (3) the ability to handle relevant cell line and size as well as flow constraints.

Fig. 11.11 shows three different PDMS configurations of PDMS "aneurysms" that are used to flow material. In Fig. 11.11 panel A, the orange lines represent a bifurcated blood vessel with each microchannel at 25 µm diameter, while the blue line where the two channels converge to form a neck region is 50 µm across. The single microchannel on the opposite side of the aneurysm sac is 100 µm in width (yellow line). Finally, the vertical diameter of the aneurysm sac represented by the vertical purple line is 450 µm across, and the horizontal diameter represented by the green line is 800 µm in length. In panel B, the yellow line signifies an aneurysm neck that is 100 µm across, the blue line shows a microchannel that is 75 µm in diameter, and the purple and green lines for the 115 µm vertical and horizontal diameters across the sac are 350 µm wide. Looking at panel C, there are single microchannels leading into and out of the sac at about 75 µm in size (blue lines), while the vertical diameter of the sac is 300 µm (purple line) and the horizontal length is 800 µm. The oval shape of two of the "aneurysms"

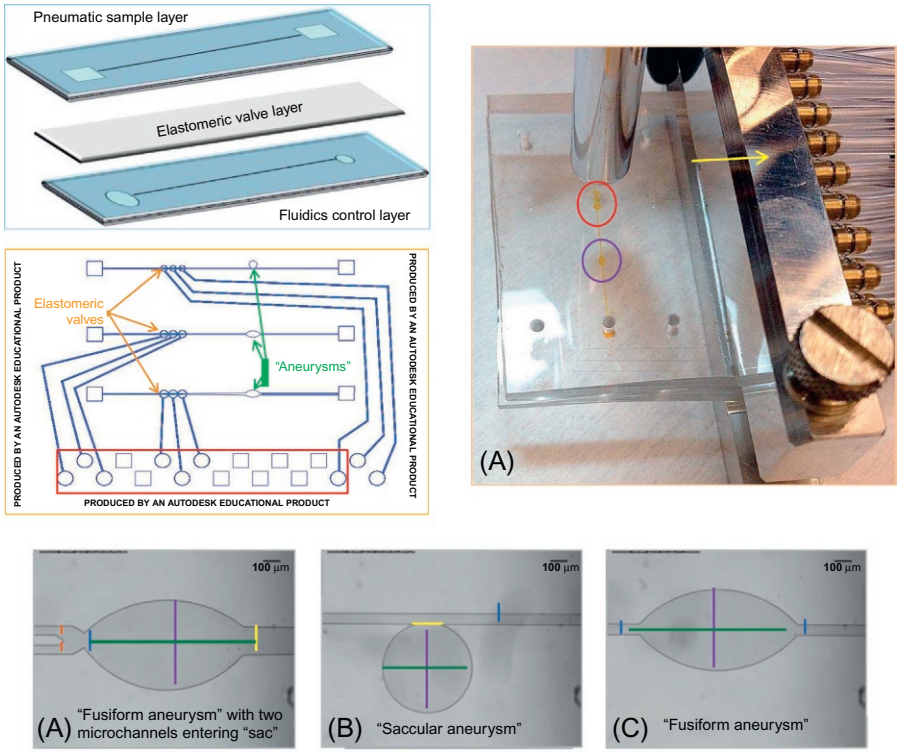


Fig. 11.11 Top left panels illustrate the multilayer system for the PDMS AOC bioMEMS chip system. Top right (panel A) shows *yellow* water inside device during a leak test: *red circle*—valves—and *purple circle*, aneurysm sac. Bottom panels A–C show the various microscale aneurysm models with fusiform and saccular aneurysm types.
From L. Reece PhD thesis, Purdue University, Copyright 2014; L.M. Reece, J.W. Khor, R. Thakur, A. Amin, S.T. Wereley, J.F. Leary, A microfabricated, microfluidic biomems device to model human brain aneurysms: the aneurysm-on-a-chip, Proc. SPIE 9320 (2015) 93200P-1.

seen in panels A and C is a mock-up of the fusiform aneurysms that have a gradual, progressive outpouching. The round "aneurysm" represents berry aneurysms. The dimensions for the AOC (Aneurysm-on-a-Chip) were designed to allow 10 µm cells to flow through the channels to simulate the actual live human blood vessel.

Results of the AOC bioMEMS device capture some unique flow dynamics around aneurysm models at the micron scale. Microbeads were designed in a series of trials to observe the overall flow through the bioMEMS device. The second set of trials involved the beads but three different pump speeds. Fig. 11.12 shows the 7 µm micro-

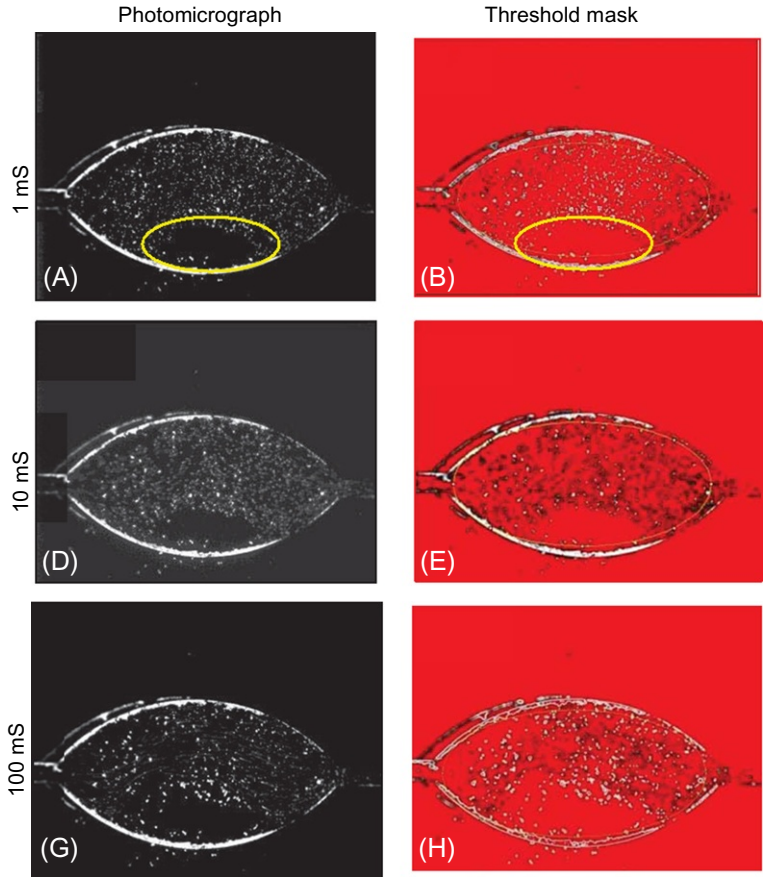


Fig. 11.12 Particle counts inside the "aneurysm sac." Panels A, D, and G are photomicrographs of microspheres flowing through aneurysm sac at pump speeds of 1, 10, and 100 mS, respectively. Panels B, E, and H are the threshold masks of the photomicrographs. Panels C, F, and I are the particle counts and statistics calculated from the threshold masks. *Yellow ovals* show bubbles in panels A and B.
From L. Reece PhD thesis, Purdue University, Copyright 2014; L.M. Reece, J.W. Khor, R. Thakur, A. Amin, S.T. Wereley, J.F. Leary, A microfabricated, microfluidic biomems device to model human brain aneurysms: the aneurysm-on-a-chip, Proc. SPIE 9320 (2015) 93200P-1.

spheres flowing through the sac of the AOC. Panel A is 1 mS pump speed, panel B is 10 mS, and panel C is 100 mS. The clear area seen at the bottom of each image is an air bubble (yellow ovals, panels A and B). The experiments were to see how well particles would flow with an obstruction (air bubble) and to determine how many particles could be contained within the sac.

Soft lithography methods were employed to generate the bioMEMS AOC prototype. A valve controller box and the software are applied where a software program can control all valves, allowing for forward and reverse flow, determining fluid flow speed. All components of the AOC are modular and can be assembled and reassembled with ease and swiftness. Low-resolution microscopes can be accommodated to capture real-time images of the flow. Different PDMS chips can be interchanged easily, and the PDMS chips, manifold, and tubing can all be autoclaved for sterility. Results provided proof of fluid flow properties for human aortic smooth muscle cells (HASMC) mixed with polystyrene microspheres within the device. The mixture was integrated in the flow and movies and images captured. Particle image velocimetry vector graphs were generated and analyzed to provide graphic evidence of the particle movement entering the "sac" region, exiting the "sac," and flowing through the "aneurysm sac." The images taken showed that during pulsatile flow, the sample particles did not agglomerate or stick together and remained monodispersed. Further, the wall shear stress (WSS) quiver plots reflected that there was back or reverse flow of the particles. This is a very important piece of information since it is flow patterns such as this that can be detrimental to a weakened blood vessel in the human body. The unique design of the bioMEMS AOC device is yet another example of in situ simulated testing of hemodynamic behavior.

11.5.1.2 Parallel-plate flow chamber cell for neuro-endovascular flow and magnetic attraction of MBNC hydrogels

The second case consists of a parallel-plate flow cell chamber to evaluate the magnetic attraction of MBNC hydrogels on magnetized HASMC cells to mimic the hemodynamic environment near the vessel wall, shown in Fig. 11.13. While the AOC bioMEMS cell examined the multiscale behavior of flow in and around various types of aneurysms, the design did not incorporate magnetic attraction and flow dynamic shear forces in one system. In this section, we briefly examine a flow test cell to demonstrate the efficacy of a magnetic field gradient established by the combination of an external magnetic field on superparamagnetic behavior of a magnetized hydrogel attracting magnetized cells. Earlier in the chapter, we discussed the concept invented by Allain, Tigno, and Armonda whereby a localized focal magnetic force would attract endothelial cells to a region along a scaffold membrane facing the cerebral aneurysm defect to regenerate the tunica media. The premise of this concept was that hemodynamic flow and the localized conditions around the aneurysm orifice would provide the conditions for a magnetic force to attract magnetized cells to the membrane surface. Providing other growth factors along the membrane surface such as porcine smooth muscle cells or similar nidus elements, an endothelial layer would be regenerated and grown to seal the aneurysm sac shut. To test the hypothesis that MBNC can locally target SPION-loaded

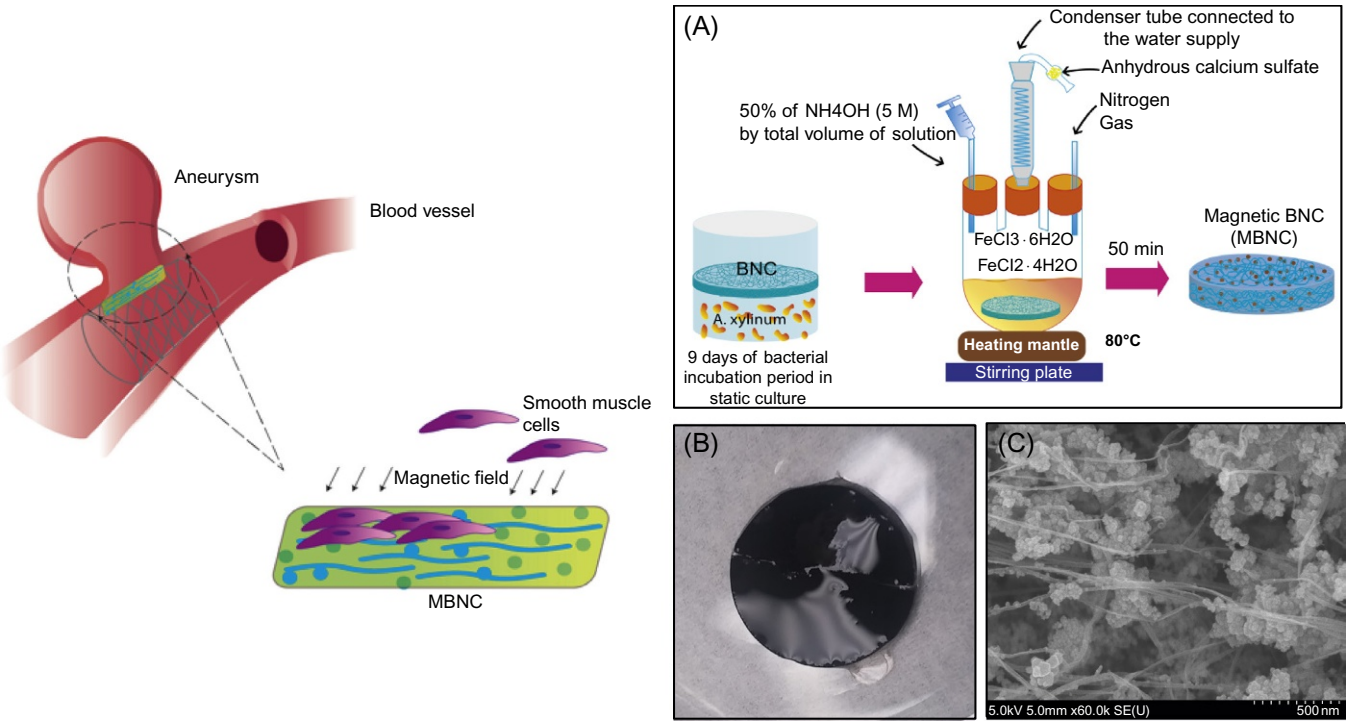


Fig. 11.13 Left panel includes a schematic of the local magnetic force concept by Allain and Tigno whereby magnetized cells are attracted locally to a membrane along a stent scaffold placed and oriented toward the cerebral aneurysm orifice. On right panels: (A) synthesis approach by Allain and Arias designed to synthesize SPIONs of ferrous oxide in bacterial nanocellulose (BNC) resulting in magnetic BNC. (B) Photograph of MBNC and (C) micrograph of NPs on BNC micro and nanofibrils.

cells by creating a strong magnetic field gradient across its surface, Arias et al. designed a parallel-plate flow system to test the capture of magnetically functionalized circulating cells toward the magnetic surface of MBNC. A chamber perpendicular to the gravity force so the effect of cell retention could be only due to the magnetic force applied to the SPION-loaded cells. The results of cell capture by the MBNC with (Mag^+) and without (Mag^-) an external magnetic field are presented in Fig. 11.14.

To create the external magnetic field, two neodymium magnets with a maximum magnetic strength of 0.3 T measured at its surface were placed facing one another, and in between them, the parallel-plate flow chamber was positioned. The neodymium magnets create a uniform magnetic field that is used to excite the SPION embedded in the MBNC and, therefore, produce a gradient magnetic field across the hydrogel. This gradient magnetic field exerts the force to target SPION-loaded cells to the MBNC surface. We observed higher cell retention for magnetically excited MBNC compared with MBNC without exposure to an external magnetic field (Fig. 11.14). The results were comparable between MBNC with different SPION concentrations, showing that even with the 50 mM MBNC, cell targeting can be achieved. This case in addition to examining the magnetic properties of the natural hydrogel also had to address an important question within the context of neuroendovascular reconstruction. The local hemodynamic behavior near and around the aneurysmal sac can exhibit extreme localized shear forces due to stagnant flow at the aneurysm orifice. When applying these magnetized hydrogels to locally attract magnetized cells, one clear challenge is how to overcome hemodynamic flow that induces not only a shear force driving blood plasma along the luminal side of vessel wall but also forces due to turbulence near the aneurysm sac. These hemodynamic forces pose serious challenges to the viability of magnetic attraction locally near the aneurysmal sac orifice.

Even though cell coverage was not large, this may stem from (1) a lower concentration of circulating cells, (2) a shorter time of cell capture, and (3) the pulsatile nature of the fluidic system. Pulsatile fluid flow may result in higher shear stresses at the surface of the MBNC; therefore, the peak WSS might be higher than that based on prior calculations. However, cell capture was improved when the collagen-conjugated MBNC was employed when using the same fluidic configuration and timing described before (Fig. 11.15).

Because the MBNC is not a completely smooth surface but instead, it is rough, there is a high probability of bubble formation, which affects accuracy of the cell capture system and may contribute to cell capture in nonmagnetized MBNC (Fig. 11.15). To the best of our knowledge, this is the first work using a magnetic hydrogel based on bacterial cellulose to physically target cells to its surface and that has been specifically designed for aneurysmal wall reconstruction. Other authors such as Pislaru and coworkers (2006) used permanent magnets that were applied on the outside surface of a vascular graft (Dacron) to rapidly capture and retain endothelial cells on the prosthetic material. Even though Pislaru's approach was able to magnetically capture cells, which is especially crucial for speeding up the reendothelization in small-diameter arteries, the magnetic material used in this approach was not biocompatible and, thus, not suitable for long-term experiments.

Continuing the example of applying a thin hydrogel membrane as a scaffold interface with a cerebral aneurysm defect, we examine the measurement of the membrane

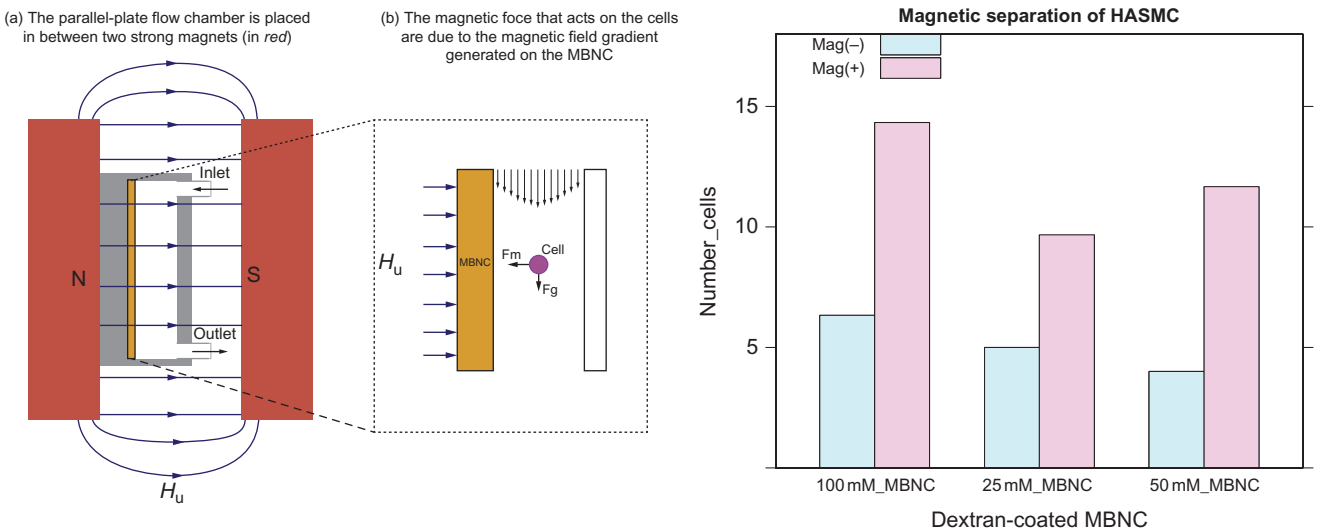


Fig. 11.14 (Left panel) SPION-loaded HASMC are taken up due to the magnetic field gradient created by the MBNC when it is placed in an external magnetic field H_u. (Right panel) Number of cells capture on the MBNC under pulsatile flow conditions. Comparisons are made between MBNC with different SPION concentrations and with Mag(+) and without Mag(–) exposure to an external magnetic field.

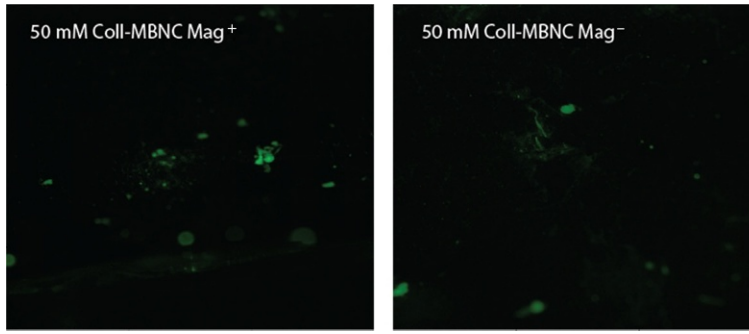


Fig. 11.15 Collagen-conjugated MBNC evaluated for HASMC targeting with (Mag^+) and without (Mag^-) external magnetic field exposure.

nano- to macroscale mechanical properties in a realistic aqueous environment. One of the key questions for the membrane design is its resilience against the complex hemodynamic flow in and out of the aneurysm sac. Here, we describe a unique in situ facility that measures the multiscale mechanical properties of a magnetic natural hydrogel known as MBNC in an aqueous state. We describe the unique experimental setup design by Tomar et al. and expand on its use to capture the elastic and creep properties of this complex biomaterial.

In comparison with crystalline cellulose (at nano- and microscales), bacterial cellulose hydrogels are quite different in their mechanical properties [107]. The elastic modulus of our BNC is consistent with mechanical properties of a hemicellulose structure, both flexible and amorphous with effectively lower tensile mechanical properties [108]. The work presented here is the first one to address nanomechanical properties of hydrated BNC under in operando realistic conditions. In this context, the results are reasonably consistent with those previously reported by Astley et al. [109] in which they studied mechanical properties of bacterial cellulose composites. These composite samples were tested using uniaxial deformation testing for stretching the strips in the wet state (typically 95% water by weight). Young's modulus measurements in Astley et al. [109] were between 0.05 and 1.00 MPa, with the highest values for pure BC samples; these results are in agreement with those extracted measured in the work by Pavon and Allain.

Mechanical properties of vascular tissue have been a topic of interest given the creep behavior of blood vessel walls and have been reported extensively [110,111]. However, blood vessels are able to maintain their stability and contain the pressure and flow of blood under a variety of physiological conditions. Cerebral blood vessels form part of the composite structure of the brain and, because of their relative stiffness in comparison with brain tissue, play an important role in the overall response of the brain to loading [112]. Previous studies of the mechanical properties of cerebral arteries have revealed some of the fundamental characteristics of these vessels, including observations that they are stiffer in both the axial [113,114] and circumferential [113,115] directions than most extracranial arteries and are stiffer than cerebral veins [115].

Here, we want to strongly highlight the importance of in operando nanomechanical properties of both BNC and MBNC presented in this work using in situ nanoindentation

measurements under aqueous state (i.e., hydrated state). Within this context, if we compare our estimations of BNC Young's modulus by nanoindentation (0.0025 and 0.04 GPa), the following observations can be made. The stiffness range of our BNC matches values measured for both large arteries and veins of human cerebral vessels as studied in detail by Monson et al. [116]. Therefore, if we consider that BNC is highly biocompatible and nondegradable, this elastic match with cerebral blood vessel tissue is critical given our intention to integrate our BNC and MBNC membranes along surfaces of arterial stents used as scaffolds interfacing cerebral aneurysm neck defects to induce tunica media reconstruction locally. Additionally, the elastic match with blood vessel tissue will also ensure the required compliance of vessel walls during healing around the cerebral aneurysm orifice. From the corresponding *P-h* curves (see example in Fig. 11.16) of MBNC, we observed that loading response (residual stress indicator) is similar to that exhibited by BNC samples. However, the same indentation load produced different maximum penetration depths; this is a consequence of some residual elastic deformation that can be sensed when the next indentation is performed within a short difference in time. The observed residual elastic straining effect is well-known in several biological tissues like cartilage, tendons, and ligaments [117] and in blood vessels. Normal loading-unloading nanoindentation tests were performed through a Berkovich indenter by using a multimodule mechanical tester (Micro Materials Ltd., the United Kingdom) shown in Fig. 11.16 (left panel). The tip of the radius of nanoindenter is approximately 20 nm. A Berkovich diamond indenter was used in this experiment, for which the contact area as a function of indenting depth was calibrated using fused silica and tungsten reference samples at room temperature. During the tests, the samples were mounted on the indentation stage using glue. The indenter approached the sample in its thickness direction. Indentation locations were selected randomly on sample surfaces. In the case of each chosen location, tests were performed with spacing of approximately 200–300 μm between each indentation spot (45 for BNC and 35 for MBNC).

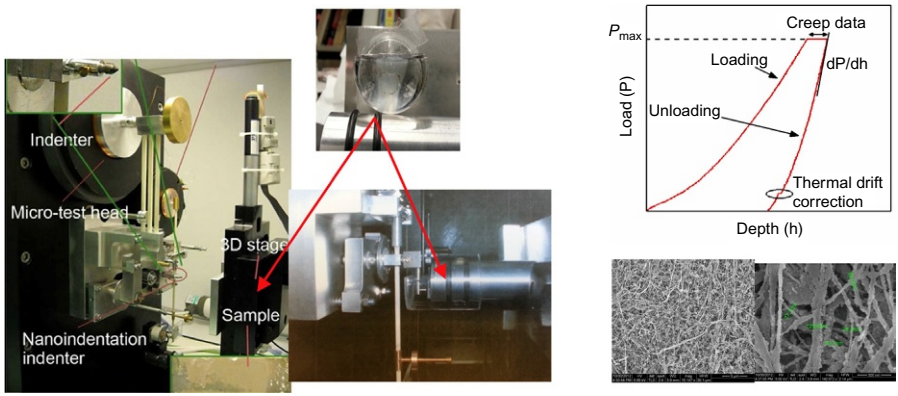


Fig. 11.16 Left panel: mechanical setup to perform in situ nanoindentation tests of BNC and MBNC samples in contact with fluid (DI water). Note that *red arrows* indicate location of the samples. Right panel: (top) a typical nanoindentation profile showing the source of both creep data and thermal drift rate. (bottom) SEM of magnetic bacterial nanocellulose.

11.5.1.3 *In situ nanomechanical testing on hydrated MBNC membranes*

Load was applied to the samples in steps and the corresponding displacement of the indenter was recorded. The plot of load versus depth is then analyzed to find the hardness and Young's modulus of the samples. Nanoindentation tests of the samples described above were all carried out in presence of deionized water (DI water), and they were tested by applying load rates between 0.001 and 0.005 mN/s, with peak loads between 0.01 and 0.60 mN. A liquid cell was used, and samples were kept under liquid during the experiment. This unique setup for nanomechanical characterization immersed in a fluid environment is ideal to effectively simulate the real biomechanical functionality of the BNC and MBNC membranes; in the context of the extreme environment, they are to encounter in the pulsating hemodynamic activity near and around the cerebral aneurysm defect. The mechanical setup used for testing the samples is presented in Fig. 11.16 (left panel). The creep behavior of samples was also evaluated. Figs. 11.16 and 11.17 show an example of the procedure used to extract the indentation creep data. The creep deformation profile is extracted from the dwell period at the peak load; dwell period may affect the creep data. A number of dwell periods were tried, and a dwell period of 20 s was decided based on convergence in the measurements.

In the case of highly viscoelastic polymers and porous hydrogels, plastic or inelastic deformation under nanoindentation creep is controlled by shear slipping events between both fibers and/or particles that are characterized by a horizontal constant load line on the *P-h* (load-depth) curve. In this case, holding the load below the shear slipping critical value during prolonged time will lead to indentation creep. Therefore, the creep investigations have to be performed at different peak indentation loads. This is the approach adopted in the present work. The modulus and hardness were calculated using the well-known Oliver-Pharr method [118,119]. A typical indentation loading-unloading curve is shown in Fig. 11.13, which can be described by the Oliver-Pharr method as

$$P = A\left(h - h^{\text{final}}\right)^{m} \tag{11.1}$$

In the above equation, A and m are material constants. Parameter h_{final} is the indentation depth after complete unloading. The contact depth h_c at the peak load, $P_{\max}$, that corresponds to the total indentation depth, $h_{\max}$, is expressed as

$$h_c = h_{\max} - \varepsilon\left(\frac{P_{\max}}{S}\right) \tag{11.2}$$

where S is the stiffness, and in the context of these measurements on a cellulose-based structure, stiffness is the initial unloading stiffness. The parameter ε is a correction factor, with $\varepsilon = 1$ for a spherical tip and $\varepsilon = 0.75$ for a Berkovich tip. The area of contact is calculated as a function of contact depth for Berkovich indenter as

$$A_c = 3\sqrt{3}h_c^2 \tan^2\theta \approx 24.5h_c^2 \tag{11.3}$$

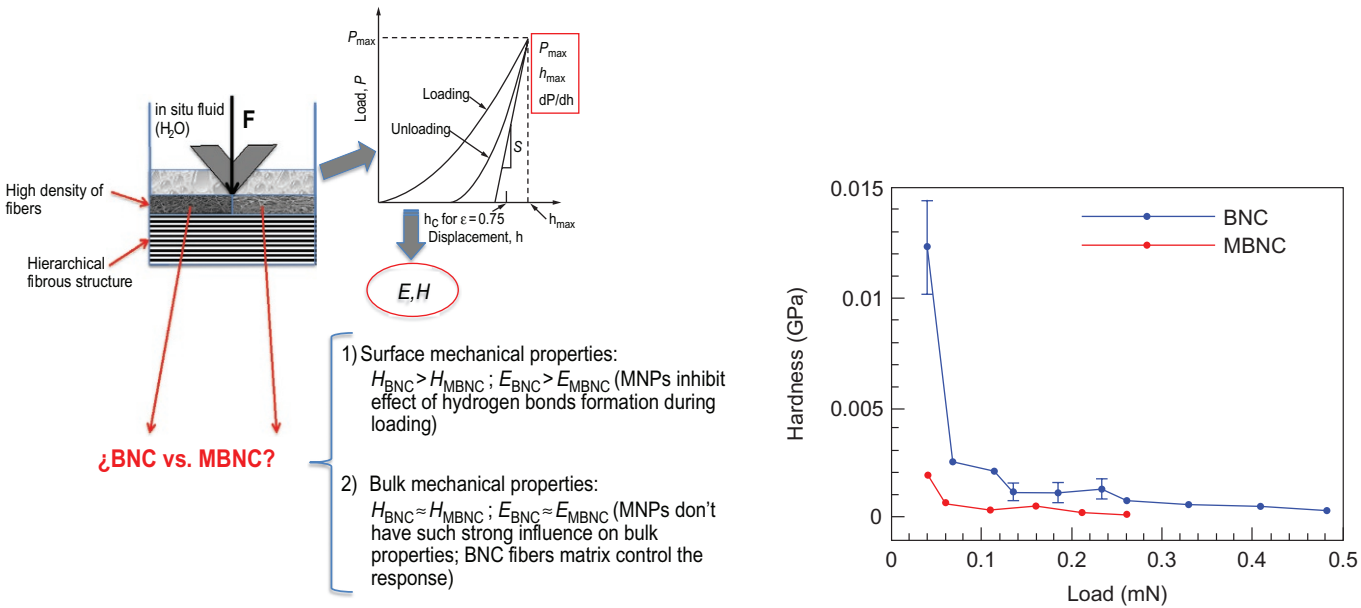


Fig. 11.17 Overall schematic of nanomechanical setup for in situ study of BNC and MBNC hydrogel membranes and their bionanomechanics details (e.g., *P-h* curve), with different responses and associated mechanisms. (Right panel) The hardness values of BNC versus MBNC measured in situ with applied load design from left panel.

with $\theta \sim 65.3°$. The reduced modulus, E_r, is given by

$$\left(\frac{1}{E_r}\right)=\left(\frac{1-\nu_i^2}{E_i}\right)+\left(\frac{1-\nu_s^2}{E_s}\right) \tag{11.4}$$

where ν is the Poisson's ratio, and E is the elastic modulus. Subscripts i and s represent the indenter tip and specimen (for the diamond tip, $\nu_i = 0.07$, and $E_i = 1141$ GPa), respectively. E_r is calculated using the formula derived from Sneddon's solution [120]:

$$E_r = \left(\frac{\sqrt{\pi}}{2}\right)\left(\frac{S}{\sqrt{A_c}}\right) \tag{11.5}$$

In the Oliver-Pharr scheme, the stiffness S is calculated as follows:

$$S = \frac{dP}{dh} \tag{11.6}$$

where P is the applied load and h is the displacement of the indenter. S corresponds to the slope of the indentation curve upon unloading. However, the elastic modulus calculated in this way can be highly affected by creep [121,122] especially when the material is soft (such as the case for cellulose-based structural materials), the holding time is short, the unloading rate is slow, or the peak load is large [122]. Ngan et al. have developed a correction formula to compensate the creep effect by calculating the correct elastic stiffness S_e as follows [121,122]:

$$\frac{1}{S_c} = \left(\frac{1}{S} - \frac{h_h'}{P_u'}\right)\left(\frac{1}{1-\left(P_h'/P_u'\right)}\right) \tag{11.7}$$

where S is calculated by Eq. (11.6), h_h is the creep rate at the end of load holding, P_h' is the load decaying rate at the end of the load holding, and P_u' is the unloading rate. For our experiments, constant load was applied in the load-holding period, so P_h' is zero in this case. The effect of creep on the elastic modulus and hardness can be evaluated by a creep factor proposed by Feng and Ngan [121]:

$$C = \frac{h_h' S_e}{\left|P_u'\right|} \tag{11.8}$$

This serves as an indicative of how much the indentation was affected by creep. Replacing S with S_e in Eqs. (11.2), (11.5), the elastic modulus of the sample can be calculated by Eq. (11.4) with the creep effect being taken into account. Hardness H is given as

$$H = \frac{P_{max}}{24.5h_c^2} \tag{11.9}$$

It must be noticed that the creep effect has been compensated here by the calculation of h_c using S_e.

Creep is a recognized mechanical phenomenon, which can affect blood vessels, and it has been widely studied, especially in animal models [123]. Besides the creep behavior of veins, they also suffer a residual stress and strain effect that is typically reflected in that they are known to retract both longitudinally and circumferentially after excision. Circumferential retraction of medium-caliber blood vessels, such as the carotid, iliac, and brachial arteries, can exceed 70% following reduction of internal blood pressure to zero. In that sense, it is reasonable to assume that blood vessels are in a nearly stress-free state when they are fully retracted and free of external loads. However, this ignores residual stress and strain effects that have been the subject of research [124–127]. In regard to creep effect results, several in vivo studies have shown important increments of percentage variation in diameter (PVD) with the time of the studied subjects [128]. This work was performed by ultrasonically determining systolic and diastolic pressures for diameter and wall thickness for several peripheral vessels as a function of age and to calculate mechanical parameters, including circumferential stiffness. For all arteries examined, the physiological parameters were observed to generally increase as a function of increasing age. However, variation in diameter (PVD) exhibited a decreasing trend with increasing age. This confirms that increasing the deformation of the blood vessels with time (age), leads to the decay of velocity or rate trends with time as is typically reflected in any creep curve.

Indentation creep experiments with typical holding times of 500 s are used to characterize such creep deformation. Correspondingly, nominal pressure during nanoindentation can easily reach a few percent of Young's modulus of materials resulting in an ideal strength situation. Nanoscale investigations of creep deformation can also provide important insights into achieving control of creep in materials such as soft hierarchical nanocellulose matter studied here (i.e., BNC and MBNC).

Comparison of creep of hydrated *Acetobacter xylinus* cellulose with creep of plant material also suggests that, although it is much less extensible than cell walls from growing tissue, the rheological behavior of pure BNC exhibits the same type of rheological elements as the plant cell wall [129]. Creep of BNC was measured as for tomato fruit epidermis [129]. The model found to correspond most closely was composed of a log-time function, two Kelvin elements, and a viscous flow element. This is identical to the model that was found to provide the best fit to extension of tomato fruit epidermis [129], pea leaves [130], tomato leaf rachis, wheat seed coats, and sunflower hypocotyls. Retardation and relaxation times are often interpreted as being specific to a particular type of process, with shorter times being associated with smaller scale events such as rotation of polymer segments relative to one another and longer times associated with larger-scale events such as relative movement of polymer chains.

11.5.2 Challenges and limitations of in situ characterization of blood-material interactions

The process of tissue healing and reconstruction through blood-contact interactions between the body and the implant material is a complex phenomenon. In particular, for metals, numerous chemical, physical, and biological elements combine to dictate the fate of tissue regeneration and reconstruction. Understanding the efficacy of candidate

metallic materials for novel biomedical devices designed as prosthetics, orthopedics, sensors, actuators, or local drug-eluting systems all must contend with the complex response of the local hemodynamic and immune response of the tissue. Simulating this process in order to provide in situ and pseudo in vivo characterization involves understanding the specific process to be simulated and the specific performance attribute to be examined. The holistic response of the body when presented by an initial wound and introduction of a foreign body is designed to provide localized self-healing processes coded in our genes. Understanding blood-material interactions can help elucidate novel biomedical device interfaces that can work together with the body in complementing healing and in some cases even accelerating the same. Hemodynamic flow, hemostasis, and local self-healing can be successfully studied and intervened by correlating the immune response pathways with the bioactive design of metallic biomaterials that enable tissue regenerative pathways.

References

[1] V. Goriainov, R. Cook, J.M. Latham, D.G. Dunlop, R.O.C. Oreffo, Bone and metal: an orthopaedic perspective on osseointegration of metals, Acta Biomater. 10 (10) (2014) 4043–4057.
[2] X. Wang, S. Xu, S. Zhou, W. Xu, M. Leary, P. Choong, M. Qian, M. Brandt, Y.M. Xie, Topological design and additive manufacturing of porous metals for bone scaffolds and orthopaedic implants: a review, Biomaterials 83 (2016) 127–141.
[3] D. Tahal, K. Madhavan, L.O. Chieng, G.M. Ghobrial, M.Y. Wang, Metals in spine, World Neurosurg. 100 (2017) 619–627.
[4] H. Hermawan, Biodegradable Metals, 2012. Springer, Heidelberg.
[5] M. Niinomi, M. Nakai, J. Hieda, Development of new metallic alloys for biomedical applications, Acta Biomater. 8 (11) (2012) 3888–3903.
[6] S. Ramcharitar, P.W. Serruys, Fully biodegradable coronary stents: progress to date, Am. J. Cardiovasc. Drugs 8 (5) (2008) 305–314.
[7] J. Foerst, M. Vorpahl, M. Engelhardt, T. Koehler, K. Tiroch, R. Wessely, Evolution of coronary stents: from bare-metal stents to fully biodegradable, drug-eluting stents, Comb. Prod. Ther. 3 (1–2) (2013) 9–24.
[8] J.P. Allain, M. Echeverry-Rendón, J.J. Pavón, S.L. Arias, Nanostructured biointerfaces, Nanopatterning and Nanoscale Devices for Biological Applications, CRC Press, Boca Raton, FL, 2014, pp. 41–67.
[9] G. Manivasagam, D. Dhinasekaran, A. Rajamanickam, Biomedical implants: corrosion and its prevention-a review, Corros. Sci. 2 (2010) 40–54.
[10] K. Neailey, R.C. Pond, Metal implants, Mater. Des. 3 (3) (1982) 470–478.
[11] W. Cao, L.L. Hench, Bioactive materials, Ceram. Int. 22 (6) (1996) 493–507.
[12] A.F. Mavrogenis, R. Dimitriou, J. Parvizi, G.C. Babis, Biology of implant osseointegration, J. Musculoskelet. Neuronal Interact. 9 (2) (2009) 61–71.
[13] M. Müller, F.F. Hennig, T. Hothorn, R. Stangl, Bone-implant interface shear modulus and ultimate stress in a transcortical rabbit model of open-pore Ti6Al4V implants, J. Biomech. 39 (2006) 2123–2132.
[14] D. Stoeckel, A. Pelton, T. Duerig, Self-expanding nitinol stents: material and design considerations, Eur. Radiol. 14 (2) (2004) 292–301.

[15] K. Hanada, K. Matsuzaki, X. Huang, Y. Chino, Fabrication of Mg alloy tubes for biodegradable stent application, Mater. Sci. Eng. C Mater. Biol. Appl. 33 (8) (2013) 4746–4750.
[16] J. Ma, M. Thompson, N. Zhao, D. Zhu, Similarities and differences in coatings for magnesium-based stents and orthopaedic implants, J. Orthop. Transl. 2 (3) (2014) 118–130.
[17] F. Witte, Reprint of: the history of biodegradable magnesium implants: a review, Acta Biomater. 23 (2015) S28–S40.
[18] M. Heiden, E. Walker, E. Nauman, L. Stanciu, Evolution of novel bioresorbable iron-manganese implant surfaces and their degradation behaviors in vitro, J. Biomed. Mater. Res. A 103 (1) (2015) 185–193.
[19] S. Franz, S. Rammelt, D. Scharnweber, J.C. Simon, Immune responses to implants—a review of the implications for the design of immunomodulatory biomaterials, Biomaterials 32 (28) (2011) 6692–6709.
[20] D.E. Packham, Surface energy, surface topography and adhesion, Int. J. Adhes. Adhes. 23 (6) (2003) 437–448.
[21] J.C. Doloff, O. Veiseh, A.J. Vegas, H.H. Tam, S. Farah, M. Ma, J. Li, A. Bader, A. Chiu, A. Sadraei, et al., Colony stimulating factor-1 receptor is a central component of the foreign body response to biomaterial implants in rodents and non-human primates, Nat. Mater. 16 (6) (2017) 671–680.
[22] B.N. Brown, B.D. Ratner, S.B. Goodman, S. Amar, S.F. Badylak, Macrophage polarization: an opportunity for improved outcomes in biomaterials and regenerative medicine, Biomaterials 33 (15) (2012) 3792–3802.
[23] D.C. Hansen, Metal corrosion in the human body: the ultimate bio-corrosion scenario, Electrochem. Soc. Interface 17 (2) (2008) 31.
[24] N. Hallab, K. Merritt, J.J. Jacobs, Metal sensitivity in patients with orthopaedic implants, JBJS 83 (3) (2001) 428.
[25] A. Balamurugan, S. Rajeswari, G. Balossier, A.H.S. Rebelo, J.M.F. Ferreira, Corrosion aspects of metallic implants—an overview, Mater. Corros. 59 (11) (2008) 855–869.
[26] H. Kalb, A. Rzany, B. Hensel, Impact of microgalvanic corrosion on the degradation morphology of WE43 and pure magnesium under exposure to simulated body fluid, Corros. Sci. 57 (2012) 122–130.
[27] M. Ascencio, M. Pekguleryuz, S. Omanovic, An investigation of the corrosion mechanisms of WE43 Mg alloy in a modified simulated body fluid solution: the influence of immersion time, Corros. Sci. 87 (October) (2014) 489–503.
[28] H.A. Videla, Manual of Biocorrosion, CRC Press, Boca Raton, FL, 1996.
[29] G. Mani, M.D. Feldman, D. Patel, C.M. Agrawal, Coronary stents: a materials perspective, Biomaterials 28 (9) (2007) 1689–1710.
[30] K.E. Robertson, R.A. McDonald, K.G. Oldroyd, S.A. Nicklin, A.H. Baker, Prevention of coronary in-stent restenosis and vein graft failure: does vascular gene therapy have a role? Pharmacol. Ther. 136 (1) (2012) 23–34.
[31] L. Milo, V. Antoli, A. Cör, S. Herman, V. Pavlov, Extensive metallosis and necrosis in failed prostheses with cemented titanium-alloy stems and ceramic heads, J. Bone Joint Surg. (Br.) 82 (3) (2000) 352–357.
[32] F. Lux, R. Zeisler, Investigations of the corrosive deposition of components of metal implants and of the behaviour of biological trace elements in metallosis tissue by means of instrumental multi-element activation analysis, J. Radioanal. Nucl. Chem. 19 (2) (1974) 289–297.
[33] C.G. Fraga, Relevance, essentiality and toxicity of trace elements in human health, Mol. Asp. Med. 26 (4–5) (2005) 235–244.

[34] D.F. Williams, Corrosion of implant materials, Annu. Rev. Mater. Sci. 6 (1) (1976) 237–266.
[35] J.M. Courtney, N.M.K. Lamba, S. Sundaram, C.D. Forbes, Biomaterials for blood-contacting applications, Biomaterials 15 (10) (1994) 737–744.
[36] US Food and Drug Administration (FDA), Implants and Prosthetics definition, 2015, www.fda.gov.
[37] T.T. Pham, S. Wiedemeier, S. Maenz, G. Gastrock, U. Settmacher, K.D. Jandt, J. Zanow, C. Lüdecke, J. Bossert, Hemodynamic aspects of reduced platelet adhesion on bioinspired microstructured surfaces, Colloids Surf. B: Biointerfaces 145 (2016) 502–509.
[38] I.-H. Kim, S.-H. Kim, Effects of ion beam irradiation on the properties and epitaxial growth of aluminium nitride film by the ion beam assisted deposition process, Thin Solid Films 253 (1) (1994) 47–52.
[39] C.A. Mullan, C.J. Kiely, A. Rockett, M. Imanieh, M.V. Yakushev, R.D. Tomlinson, Studies of the effects of ion-implantation and electron beam irradiation on CuInSe 2 single crystals, in: MRS Proceedings, vol. 262, 1992, pp. 1097.
[40] Y. Serruys, M.-O. Ruault, P. Trocellier, S. Henry, O. Kaïtasov, P. Trouslard, Multiple ion beam irradiation and implantation: JANNUS project, Nucl. Instrum. Methods Phys. Res., Sect. B 240 (1) (2005) 124–127.
[41] H. Yamashita, M. Harada, J. Misaka, M. Takeuchi, Y. Ichihashi, F. Goto, M. Ishida, T. Sasaki, M. Anpo, Application of ion beam techniques for preparation of metal ion-implanted TiO2 thin film photocatalyst available under visible light irradiation: metal ion-implantation and ionized cluster beam method, J. Synchrotron Radiat. 8 (2) (2001) 569–571.
[42] I. Yamada, A short review of ionized cluster beam technology, Nucl. Instrum. Methods Phys. Res., Sect. B 99 (1) (1995) 240–243.
[43] I. Yamada, J. Matsuo, N. Toyoda, et al., Cluster ion beam process technology, Nucl. Instrum. Methods Phys. Res., Sect. B 206 (2003) 820–829.
[44] I. Yamada, N. Toyoda, Nano-scale surface modification using gas cluster ion beams—a development history and review of the Japanese nano-technology program, Surf. Coat. Technol. 201 (19) (2007) 8579–8587.
[45] A.A. Rogachev, S. Tamulevičius, A.V. Rogachev, I. Prosycevas, M. Andrulevičius, Features of Polytetrafluoroethylene Coating Growth on Activated Surfaces from Gas Phase, in Interface Controlled Organic Thin Films, Springer, Berlin, Heidelberg, 2009, pp. 85–89.
[46] G.H. Takaoka, H. Ryuto, R. Araki, T. Yakushiji, Surface modification of polymer substrates by oxygen ion irradiation, in: Ion Implantation Technology: 17th International Conference on Ion Implantation Technology, vol. 1066, 2008, pp. 240–243.
[47] X. Li, Z. He, J. Yuan, G. Zeng, Y. He, M. Lei, Long-term results of permanent metallic stent implantation in the treatment of benign upper urinary tract occlusion, Int. J. Urol. 14 (8) (2007) 693–698.
[48] C. Lüdecke, M. Roth, W. Yu, U. Horn, J. Bossert, K.D. Jandt, Nanorough titanium surfaces reduce adhesion of Escherichia coli and Staphylococcus aureus via nano adhesion points, Colloids Surf. B: Biointerfaces 145 (2016) 617–625.
[49] P. Parhi, A. Golas, E.A. Vogler, Role of proteins and water in the initial attachment of mammalian cells to biomedical surfaces: a review, J. Adhes. Sci. Technol. 24 (5) (2010) 853–888.
[50] P. Koegler, A. Clayton, H. Thissen, G.N.C. Santos, P. Kingshott, The influence of nanostructured materials on biointerfacial interactions, Adv. Drug Deliv. Rev. 64 (15) (2012) 1820–1839.

[51] S.T. Mindaye, M. Ra, J. Lo Surdo, S.R. Bauer, M.A. Alterman, Improved proteomic profiling of the cell surface of culture-expanded human bone marrow multipotent stromal cells, J. Proteome 78 (January) (2013) 1–14.
[52] D.D. Deligianni, N. Katsala, S. Ladas, D. Sotiropoulou, J. Amedee, Y.F. Missirlis, Effect of surface roughness of the titanium alloy Ti-6Al-4V on human bone marrow cell response and on protein adsorption, Biomaterials 22 (2001) 1241–1251.
[53] H.-H. Huang, C.-T. Ho, T.-H. Lee, T.-L. Lee, K.-K. Liao, F.-L. Chen, Effect of surface roughness of ground titanium on initial cell adhesion, Biomol. Eng. 21 (3) (2004) 93–97.
[54] X. Liu, P.K. Chu, C. Ding, Surface nano-functionalization of biomaterials, Mater. Sci. Eng. R. Rep. 70 (3) (2010) 275–302.
[55] H. Senta, H. Park, E. Bergeron, O. Drevelle, D. Fong, E. Leblanc, F. Cabana, S. Roux, G. Grenier, N. Faucheux, Cell responses to bone morphogenetic proteins and peptides derived from them: biomedical applications and limitations, Cytokine Growth Factor Rev. 20 (3) (2009) 213–222.
[56] M. Kazemzadeh-Narbat, J. Kindrachuk, K. Duan, H. Jenssen, R.E.W. Hancock, R. Wang, Antimicrobial peptides on calcium phosphate-coated titanium for the prevention of implant-associated infections, Biomaterials 31 (36) (2010) 9519–9526.
[57] E.A. Vogler, L. Akhlesh, M.P. Raúl José, Surface Modification for Biocompatibility. Engineered Biomimicry, Elsevier, Boston, MA, 2013.
[58] S. Bauer, P. Schmuki, K. von der Mark, J. Park, Engineering biocompatible implant surfaces: part I: materials and surfaces, Prog. Mater. Sci. 58 (3) (2013) 261–326.
[59] L. Tang, P. Thevenot, W. Hu, Surface chemistry influences implant biocompatibility, Curr. Top. Med. Chem. 8 (4) (2008) 270–280.
[60] I. Milošev, B. Kapun, The corrosion resistance of nitinol alloy in simulated physiological solutions: part 1: the effect of surface preparation, Mater. Sci. Eng. C 32 (5) (2012) 1087–1096.
[61] D.A. Armitage, T.L. Parker, D.M. Grant, Biocompatibility and hemocompatibility of surface-modified NiTi alloys, J. Biomed. Mater. Res. A 66 (1) (2003) 129–137.
[62] S. Shabalovskaya, J. Anderegg, J. Van Humbeeck, Critical overview of Nitinol surfaces and their modifications for medical applications, Acta Biomater. 4 (3) (2008) 447–467.
[63] B. Thierry, M. Tabrizian, Biocompatibility and biostability of metallic endovascular implants: state of the art and perspectives, J. Endovasc. Ther. 10 (4) (2003) 807–824.
[64] Z.D. Cui, H.C. Man, X.J. Yang, The corrosion and nickel release behavior of laser surface-melted NiTi shape memory alloy in Hanks' solution, Surf. Coat. Technol. 192 (2) (2005) 347–353.
[65] B. Thierry, M. Tabrizian, C. Trepanier, O. Savadogo, L. Yahia, Effect of surface treatment and sterilization processes on the corrosion behavior of NiTi shape memory alloy, J. Biomed. Mater. Res. A 51 (4) (2000) 685–693.
[66] C. Trepanier, M. Tabrizian, L. Yahia, L. Bilodeau, D.L. Piron, Effect of modification of oxide layer on NiTi stent corrosion resistance, J. Biomed. Mater. Res. 43 (4) (1998) 433–440.
[67] M. Navarro, A. Michiardi, O. Castano, J.A. Planell, Biomaterials in orthopaedics, J. R. Soc. Interface. 5 (2008) 1137–1158.
[68] J.M. Schmehl, C. Harder, H.P. Wendel, C.D. Claussen, G. Tepe, Silicon carbide coating of nitinol stents to increase antithrombogenic properties and reduce nickel release, Cardiovasc. Revasc. Med. 9 (4) (2008) 255–262.
[69] S.A. Shabalovskaya, J.W. Anderegg, A. Undisz, M. Rettenmayr, G.C. Rondelli, Corrosion resistance, chemistry, and mechanical aspects of Nitinol surfaces formed in hydrogen peroxide solutions, J. Biomed. Mater. Res. B Appl. Biomater. 100 (6) (2012) 1490–1499.

[70] S.A. Shabalovskaya, J. Anderegg, F. Laab, P.A. Thiel, G. Rondelli, Surface conditions of Nitinol wires, tubing, and as-cast alloys. The effect of chemical etching, aging in boiling water, and heat treatment, J. Biomed. Mater. Res. B Appl. Biomater. 65 (1) (2003) 193–203.
[71] T.M. Sridhar, S. Rajeswari, Biomaterials corrosion, Corros. Rev. 27 (2009) 287–332.
[72] M.F. Maitz, N. Shevchenko, Plasma-immersion ion-implanted nitinol surface with depressed nickel concentration for implants in blood, J. Biomed. Mater. Res. A 76 (2) (2006) 356–365.
[73] M.R. Gorji, S. Sanjabi, Corrosion behavior of ion implanted NiTi shape memory alloy thin films, Mater. Lett. 73 (2012) 179–182.
[74] M.R. Gorji, S. Sanjabi, Z.H. Barber, Improving the wear resistance of NiTi shape memory alloy thin films by nitrogen and carbon ion implantation, Nano Lett. 7 (7) (2012) 641–645.
[75] H. Pelletier, D. Muller, P. Mille, J.J. Grob, Structural and mechanical characterisation of boron and nitrogen implanted NiTi shape memory alloy, Surf. Coat. Technol. 158 (2002) 309–317.
[76] A. Shanaghi, P.K. Chu, R. Xu, T. Hu, Structure and properties of TiC/Ti coatings fabricated on NiTi by plasma immersion ion implantation and deposition, Vacuum 89 (2013) 238–243.
[77] J.C. Palmaz, R.R. Sibbitt, S.R. Reuter, F. Garcia, F.O. Tio, Expandable intrahepatic portacaval shunt stents: early experience in the dog, Am. J. Roentgenol. 145 (4) (1985) 821–825.
[78] Y.-J. Lee, D.J. Kim, S.H. Suh, S.-K. Lee, J. Kim, D.I. Kim, Stent-assisted coil embolization of intracranial wide-necked aneurysms, Neuroradiology 47 (9) (2005) 680–689.
[79] C.J. Koebbe, E. Veznedaroglu, P. Jabbour, R.H. Rosenwasser, Endovascular management of intracranial aneurysms: current experience and future advances, Neurosurgery 59 (5) (2006) S3–S93.
[80] H.J. Cloft, D.F. Kallmes, Cerebral aneurysm perforations complicating therapy with Guglielmi detachable coils: a meta-analysis, Am. J. Neuroradiol. 23 (10) (2002) 1706–1709.
[81] S.K. Natarajan, L.N. Sekhar, B. Ghodke, G.W. Britz, D. Bhagawati, N. Temkin, Outcomes of ruptured intracranial aneurysms treated by microsurgical clipping and endovascular coiling in a high-volume center, Am. J. Neuroradiol. 29 (4) (2008) 753–759.
[82] S. Nishimura, T. Fujita, H. Sakata, E. Hori, M. Mino, M. Nishijima, H. Midorikawa, Choice of intentional partial coiling for a ruptured intracranial aneurysm in the acute stage followed by clipping in the chronic stage, No Shinkei Geka 37 (8) (2009) 757–763.
[83] A. Doerfler, I. Wanke, T. Egelhof, U. Dietrich, S. Asgari, D. Stolke, M. Forsting, Aneurysmal rupture during embolization with Guglielmi detachable coils: causes, management, and outcome, Am. J. Neuroradiol. 22 (10) (2001) 1825–1832.
[84] R.A. Hanel, A.S. Boulos, E.G. Sauvageau, E.I. Levy, L.R. Guterman, L.N. Hopkins, Stent placement for the treatment of nonsaccular aneurysms of the vertebrobasilar system, Neurosurg. Focus. 18 (2) (2005) 1–9.
[85] G. Lanzino, A.K. Wakhloo, R.D. Fessler, M.L. Hartney, L.R. Guterman, L.N. Hopkins, Efficacy and current limitations of intravascular stents for intracranial internal carotid, vertebral, and basilar artery aneurysms, J. Neurosurg. 91 (4) (1999) 538–546.
[86] Z. Kulcsár, E. Houdart, A. Bonafe, G. Parker, J. Millar, A.J.P. Goddard, S. Renowden, G. Gal, B. Turowski, K. Mitchell, et al., Intra-aneurysmal thrombosis as a possible cause of delayed aneurysm rupture after flow-diversion treatment, Am. J. Neuroradiol. 32 (1) (2011) 20–25.

[87] J.C. Wehman, R.A. Hanel, E.I. Levy, L.N. Hopkins, Giant cerebral aneurysms: endovascular challenges, Neurosurgery 59 (5) (2006) S3–S125.
[88] C.N. Ionita, A.M. Paciorek, A. Dohatcu, K.R. Hoffmann, D.R. Bednarek, J. Kolega, E.I. Levy, L.N. Hopkins, S. Rudin, J.D. Mocco, The asymmetric vascular stent, Stroke 40 (3) (2009) 959–965.
[89] I. Ferreira-González, J.R. Marsal, A. Ribera, G. Permanyer-Miralda, B. García-Del Blanco, G. Martí, P. Cascant, V. Martín-Yuste, S. Brugaletta, M. Sabaté, et al., Background, incidence, and predictors of antiplatelet therapy discontinuation during the first year after drug-eluting stent implantation, Circulation 122 (10) (2010) 1017–1025.
[90] D.-W. Park, S.-C. Yun, S.-W. Lee, Y.-H. Kim, C.W. Lee, M.-K. Hong, S.-S. Cheong, J.-J. Kim, S.-W. Park, S.-J. Park, Stent thrombosis, clinical events, and influence of prolonged clopidogrel use after placement of drug-eluting stent: data from an observational cohort study of drug-eluting versus bare-metal stents, J. Am. Coll. Cardiol. Intv. 1 (5) (2008) 494–503.
[91] P. Serruys, A. Ong, Drug-eluting stents: current issues, Tex. Heart Inst. J. 32 (3) (2005) 372–377.
[92] T. Christen, V. Verin, M.-L. Bochaton-Piallat, Y. Popowski, F. Ramaekers, P. Debruyne, E. Camenzind, G. Van Eys, G. Gabbiani, Mechanisms of neointima formation and remodeling in the porcine coronary artery, Circulation 103 (6) (2001) 882–888.
[93] J.M. Abrahams, M.S. Forman, M.S. Grady, S.L. Diamond, Delivery of human vascular endothelial growth factor with platinum coils enhances wall thickening and coil impregnation in a rat aneurysm model, Am. J. Neuroradiol. 22 (7) (2001) 1410–1417.
[94] Y. Tintut, Z. Alfonso, T. Saini, K. Radcliff, K. Watson, K. Boström, L.L. Demer, Multilineage potential of cells from the artery wall, Circulation 108 (20) (2003) 2505–2510.
[95] S.V. Pislaru, A. Harbuzariu, R. Gulati, T. Witt, N.P. Sandhu, R.D. Simari, G.S. Sandhu, Magnetically targeted endothelial cell localization in stented vessels, J. Am. Coll. Cardiol. 48 (9) (2006) 1839–1845.
[96] M.H. Koo, J.J. Nawarskas, W.H. Frishman, Prasugrel: a new antiplatelet drug for the prevention and treatment of cardiovascular disease, Cardiol. Rev. 16 (6) (2008) 314–318.
[97] R.V. Jeger, H.P. Brunner-La Rocca, P.R. Hunziker, D.A. Tsakiris, C.A. Kaiser, M.E. Pfisterer, B. Investigators, et al., Drug-eluting stents and glycoprotein IIb/IIIa inhibitors in vessels at low anatomic risk: a retrospective analysis of previously published data from the Basel stent kosten effektivit{ä}ts trial, Clin. Ther. 31 (12) (2009) 2886–2893.
[98] M.W. Krucoff, D.J. Kereiakes, J.L. Petersen, R. Mehran, V. Hasselblad, A.J. Lansky, P.J. Fitzgerald, J. Garg, M.A. Turco, C.A. Simonton, et al., A novel bioresorbable polymer paclitaxel-eluting stent for the treatment of single and multivessel coronary disease: primary results of the COSTAR (cobalt chromium stent with antiproliferative for restenosis) II study, J. Am. Coll. Cardiol. 51 (16) (2008) 1543–1552.
[99] M. Rochalska, The influence of electromagnetic fields on flora and fauna (Wplyw pól elektromagnetycznych na flore I faune), Med. Pr. 60 (1) (2009) 43.
[100] H.D. Waller, B. Schlegel, A.A. Müller, G.W. Löhr, Der H{ä}miglobingehalt in alternden erythrocyten, J. Mol. Med. 37 (17) (1959) 898–900.
[101] R.S. Molday, S.P.S. Yen, A. Rembaum, Application of magnetic microspheres in labelling and separation of cells, Nature 268 (5619) (1977) 437–438.
[102] M. Echeverry-Rendon, L.M. Reece, F. Pastrana, S.L. Arias, A.R. Shetty, J.J. Pavón, J.P. Allain, Bacterial nanocellulose magnetically functionalized for neuro-endovascular treatment, Macromol. Biosci. 17 (6) (2017) 1600382.

[103] C.C. Berry, S. Wells, S. Charles, A.S.G. Curtis, Dextran and albumin derivatised iron oxide nanoparticles: influence on fibroblasts in vitro, Biomaterials 24 (25) (2003) 4551–4557.
[104] K. Kanda, T. Matsuda, In vitro reconstruction of hybrid arterial media with molecular and cellular orientations, Cell Transplant. 3 (6) (1994) 537–545.
[105] C.S. Owen, High gradient magnetic separation of erythrocytes, Biophys. J. 22 (2) (1978) 171–178.
[106] L.M. Reece, J.W. Khor, R. Thakur, A. Amin, S.T. Wereley, J.F. Leary, A microfabricated, microfluidic biomems device to model human brain aneurysms: the aneurysm-on-a-chip, Proc. SPIE 9320 (2015) 93200P-1.
[107] S.J. Eichhorn, R.J. Young, The Young's modulus of a microcrystalline cellulose, Cellulose 8 (3) (2001) 197–207.
[108] H. Zhu, W. Luo, P.N. Ciesielski, Z. Fang, J.Y. Zhu, G. Henriksson, M.E. Himmel, L. Hu, Wood-derived materials for green electronics, biological devices, and energy applications, Chem. Rev. 116 (16) (2016) 9305–9374.
[109] O.M. Astley, E. Chanliaud, A.M. Donald, M.J. Gidley, Tensile deformation of bacterial cellulose composites, Int. J. Biol. Macromol. 32 (1) (2003) 28–35.
[110] D.H. Bergel, The static elastic properties of the arterial wall, J. Physiol. 156 (3) (1961) 445–457.
[111] Y.C. Fung, K. Fronek, P. Patitucci, Pseudoelasticity of arteries and the choice of its mathematical expression, Am. J. Physiol. Heart Circ. Physiol. 237 (5) (1979) H620–H631.
[112] L. Zhang, J. Bae, W.N. Hardy, K.L. Monson, G.T. Manley, W. Goldsmith, K.H. Yang, A.I. King, Computational study of the contribution of the vasculature on the dynamic response of the brain, in: SAE Conference Proceedings, 2002, pp. 145–164.
[113] D.E. Busby, A.C. Burton, The effect of age on the elasticity of the major brain arteries, Can. J. Physiol. Pharmacol. 43 (2) (1965) 185–202.
[114] K.L. Monson, W. Goldsmith, N.M. Barbaro, G.T. Manley, Axial mechanical properties of fresh human cerebral blood vessels, J. Biomech. Eng. 125 (2) (2003) 288–294.
[115] K. Hayashi, H. Handa, S. Nagasawa, A. Okumura, K. Moritake, Stiffness and elastic behavior of human intracranial and extracranial arteries, J. Biomech. 13 (2) (1980) 175181–179184.
[116] K.L. Monson, W. Goldsmith, N.M. Barbaro, G.T. Manley, Significance of source and size in the mechanical response of human cerebral blood vessels, J. Biomech. 38 (4) (2005) 737–744.
[117] M. Ding, M. Dalstra, F. Linde, I. Hvid, Mechanical properties of the normal human tibial cartilage-bone complex in relation to age, Clin. Biomech. 13 (4–5) (1998) 351–358.
[118] W.C. Oliver, G.M. Pharr, Measurement of hardness and elastic modulus by instrumented indentation: advances in understanding and refinements to methodology, J. Mater. Res. 19 (1) (2004) 3–20.
[119] W.C. Oliver, G.M. Pharr, An improved technique for determining hardness and elastic modulus using load and displacement sensing indentation experiments, J. Mater. Res. 7 (6) (1992) 1564–1583.
[120] I.N. Sneddon, The relation between load and penetration in the axisymmetric boussinesq problem for a punch of arbitrary profile, Int. J. Eng. Sci. 3 (1) (1965) 47–57.
[121] G. Feng, A.H.W. Ngan, Effects of creep and thermal drift on modulus measurement using depth-sensing indentation, J. Mater. Res. 17 (3) (2002) 660–668.
[122] A.J. Svagan, M.A.S. Azizi Samir, L.A. Berglund, Biomimetic polysaccharide nanocomposites of high cellulose content and high toughness, Biomacromolecules 8 (8) (2007) 2556–2563.

[123] J.D. Bronzino, Biomedical Engineering Handbook, vol. 2, CRC Press, Boca Raton, FL, 1999.
[124] A. Rachev, S. Greenwald, T. Kane, J. Moore, J.J. Meister, Effects of age-related changes in the residual strains on the stress distribution in the arterial wall, in: Proceedings of the Thirteenth Society of Biomedical Engineering Recent Developments, 1994, pp. 409–412.
[125] K. Takamizawa, K. Hayashi, Strain energy density function and uniform strain hypothesis for arterial mechanics, J. Biomech. 20 (1) (1987) 7–17.
[126] J. Vossoughi, Longitudinal residual strains in arteries, in: Proceedings of the 11th Southern Biomedical Engineering Conference, Memphis, TN, 1992, pp. 17–19.
[127] R.N. Vaishnav, J. Vossoughi, Estimation of residual strains in aortic segments, Biomedical Engineering II: Recent Development, Pergamon Press, New York, 1983, pp. 330–333.
[128] C.M. Buntin, F.H. Silver, Noninvasive assessment of mechanical properties of peripheral arteries, Ann. Biomed. Eng. 18 (5) (1990) 549–566.
[129] D.S. Thompson, Extensiometric determination of the rheological properties of the epidermis of growing tomato fruit, J. Exp. Bot. 52 (359) (2001) 1291–1301.
[130] E.M. Stam-Bolink, Causes of Leaf Area Reduction and Implications of Acclimation to UV-B Radiation in PISUM Sativum L (Ph.D. thesis), Groningen: s.n., 2003.

Bioinspired thin film materials designed for blood contact

12

R. Major[*], *M. Sanak*[†], *J.M. Lackner*[‡], *F. Bruckert*[§], *J. Marczak*[¶], *B. Major*[*]
[*]Institute of Metallurgy and Materials Science, Polish Academy of Sciences, Krakow, Poland, [†]Jagiellonian University Medical College, Cracow, Poland, [‡]Institute of Surface Technologies and Photonics, Functional Surfaces, Niklasdorf, Austria, [§]Grenoble Institute of Technology, Grenoble, France, [¶]Military University of Technology, Warsaw, Poland

12.1 Introduction

The work was defined to meet the pressing medical need of increasing effectiveness in heart insufficiency treatment. The surfaces, depending on the application were optimized to improve blood flow with the effective "washing" effect of all surfaces with sufficiently high shear stress. Thus, the main goal of this project is to develop novel blood-contacting materials to provide design rules for application of the composite materials for the blood pumps (ReligaHeart) [1]. The studies led us to consider several different problems associated with the proper blood flow in the system. The general assumption was to elaborate materials having properties similar to blood vessels in micro-scale and mechanical stability on the macro-scale. Thus, this concept focused on antithrombogenic construction by reduction of turbulence and sufficient washing of surfaces. Materials were subjected to biomimetic fluid-dynamic tests leading to their mechanical properties development. The aim was highly hemocompatible materials, hemocompatible tough coatings for low-friction sealing surfaces. The aim was gained by the chemical, mechanical, rheological, tribological, and biocompatibility characterization, including the application of the artificial biophysical models. A progress in the field of cardiac support systems is attributed to the use of advanced material solutions. The best solutions however, to design the appropriate blood-contacting material, could be found in nature. The paper presents new biomimetic solutions for the construction of cardiac support chamber. Depending on the place for the construction of the pump, various problems associated with the direct influence of artificial devices for life processes of the surrounding tissue occur.

12.2 Materials and methods

12.2.1 Blood-contacting materials dedicated to withstand the high shear stress

Inflow conduit system design and the levitation rotor cause the high risk of blood cell damage as well as platelet activation. The blood cells in this case are exposed to a high value of the shear stress. The surface of these elements should prevent a blood

Hemocompatibility of Biomaterials for Clinical Applications. https://doi.org/10.1016/B978-0-08-100497-5.00009-4
© 2018 Elsevier Ltd. All rights reserved.

cell damage and clotting. Materials proposed to this specific application were tested and selected based on the shear stress analysis between the blood cells and surfaces. The surfaces were optimized based on the radial flow chamber [2]. The analysis involves the specific cell response to the engagement of its adhesion molecules into noncovalent complexes, which in turn, actively modifies the adhesion process. At the molecular level, the formation of adhesive bonds between a cell and external molecules is directly controlled by the different cytoskeleton networks and by the membrane traffic of the adhesion proteins. Considering various physiological task(s), cells require localized reinforcement or reduction of cell adhesion strength. It is therefore not surprising that changes in cell adhesion accompany many cellular processes. From a physicochemical point of view, the bioadhesion involves three components: cells, solid substrate, and liquid medium [3]. The relevant microorganism properties are the cell surface hydrophobicity and charge and cell size [4,5].

For this purpose a series of materials in the form of thin coatings were prepared using physical vapor deposition technique. Materials were selected based on the previous analysis and experience presented elsewhere [6–9].

In order to analyze the effect of residual stress on the vital processes of cells, radial flow chamber was suggested. The test was normalized according to the standard 10993 and its exact description can be found in other publications [10].

A radial hydrodynamic flow is generated between the stainless steel disk and the examined surface on which cells adhere.

An important step in properly conducted experiment is suitable dilution of the concentrate cells. Concentrate should not be too dense, it would prevent the observation of a single cell. At the same time the dilution should not be too high, in this case the analysis of the intercellular interactions would be prevented. The selection of dilution is normally done using a Neubauer chamber. For the test, red blood cells were selected as the most reliable representatives. The erythrocytes are the most abundant blood cells. They are of the extremely high count of 4 mln/1 μL which states over 40% of the total blood volume which is occupied by the red blood cells. These cells are the most rigid and prone to rupture leading to subsequent hemolysis.

After selecting an appropriate blood cell for the adjusting experiment, it was necessary to provide the osmotic pressure equalization between the internal and external environment of the cell. Too high-pressure differences would result in immediate damage of the cell (Table 12.1).

Table 12.1 The deposited materials in order of the blood cell adhesion minimatin

Material	Composition	Thickness (nm)
C170_2	a-C:H	100
C170_4	Si-DLC	500
C170_5	Si-DLC	300
C170_6	Si-DLC	200
C170_7	Si-DLC	125
C170_8	Si-DLC	15

Table 12.2 The most common composition of PBS (1X)

Salt	Concentration (mmol/L)	Concentration (g/L)
NaCl	137	8.0
KCl	2.7	0.2
Na_2HPO_4	10	1.44
KH_2PO_4	1.8	0.24

The experimentally chosen coupling medium was determined to be at pH 7.4. The composition is presented in the Table 12.2.

Finally the cells were spread evenly at a density of 300 cells/mm^2. The shear stress induced by the flow on the plate decreases as $1/r$. The layout of the experimental system is presented in Fig. 12.1. Deposited cell are illustrated in Fig. 12.2.

For a given cell, detachment occurs for values of the applied hydrodynamic stress above a threshold. Cells are removed from the substrate with an apparent first-order kinetics strongly depending on the applied stress. The stress threshold depends on the cell size and the physicochemical properties of the substrate, but it is not affected by depolymerization of the actin and tubulin cytoskeleton. In contrast, the kinetics of cell detachment is almost independent of the cell size, but it is strongly affected by modification of the substrate and the presence of an intact actin cytoskeleton.

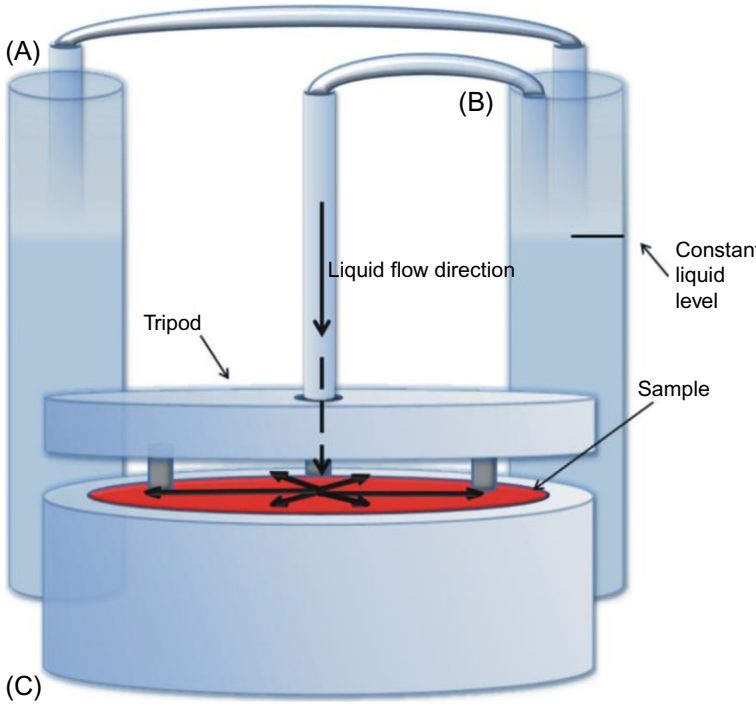


Fig. 12.1 The scheme of radial flow chamber.

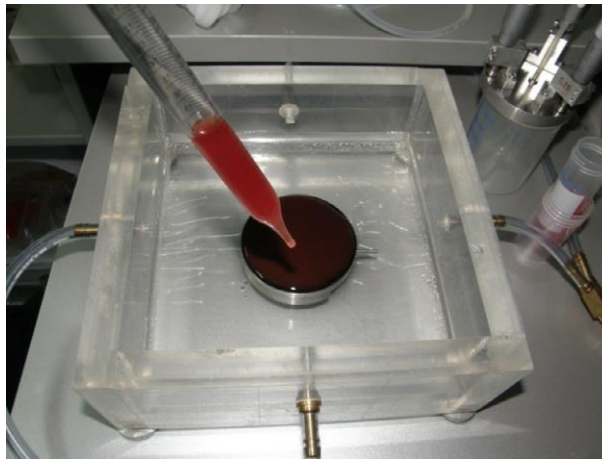


Fig. 12.2 Red blood cells deposited on the surface.

After the test, samples were given under the confocal microscopy observation confocal laser scanning microscopy (CLSM) Carl Zeiss Exciter 5.

The efficiency of the cell detachment was illustrated by the cell detachment in the function of the applied stress (Fig. 12.3).

The total cell washout at low values of stress proves the weak cell-to-substrate interactions. The final material classification was done on the basis of threshold stress analysis. The threshold stress is defined as the stress when the probability of the cell detachment and remaining on the surface is the same as marked as $\sigma_{50\%}$. This relationship was described by Eq. (12.1).

$$\sigma_{50\%} = \frac{3D\eta}{\pi r_{50\%} e^2} \tag{12.1}$$

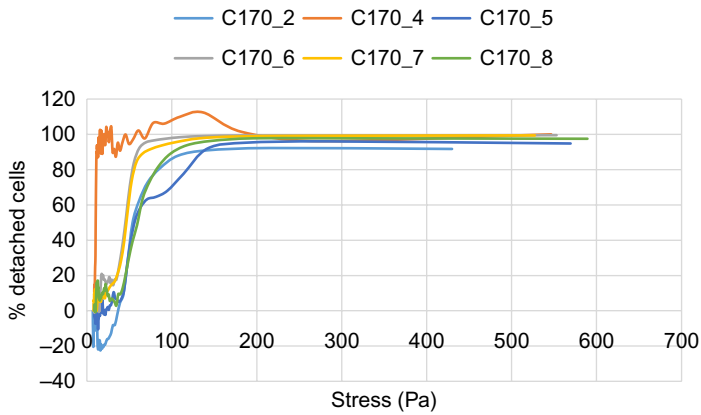


Fig. 12.3 Detached cells in the function of applied shear stress.

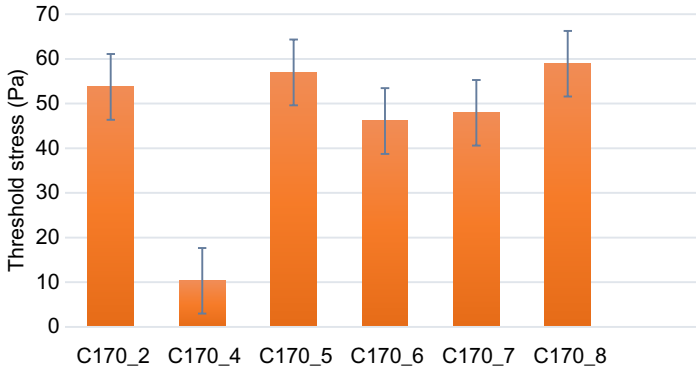


Fig. 12.4 The threshold stress in relation to the tested material.

where

D is the medium flow rate s^{-1}.
η is the medium viscosity.
e is the distance between the surface of the sample and the surface of the working disk. The threshold stress in relation to the tested material is shown in Fig. 12.4.

In a next step determining the quality of the surface dedicated to work under high shear stress, the detachment rate in the function of the applied stress was calculated. The experimental points were fitted by the exponential function. The diagram has strong value from the technological point of view. It delivers illustrative information regarding the cell-material interaction. The more the vertical nature of the graph, the weaker is the cell-material interaction. The more the spread character of the exponential function, the stronger the cell-material interaction (Fig. 12.5).

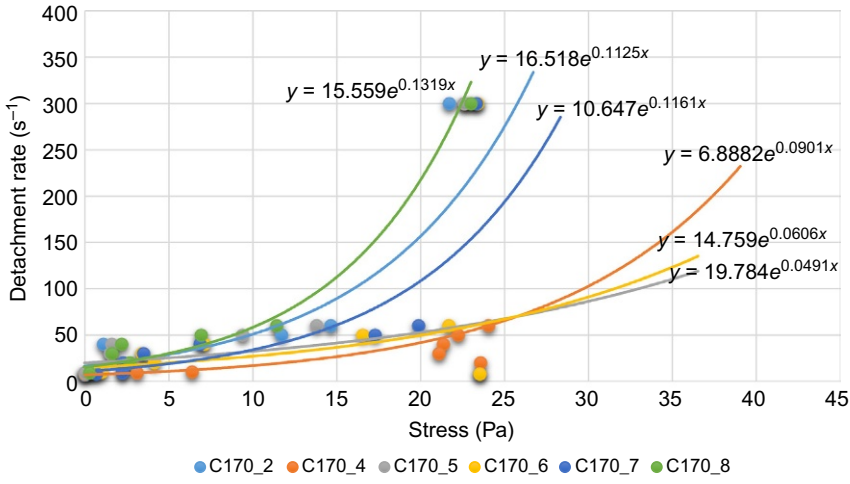


Fig. 12.5 Red blood cell detachment efficiency.

Table 12.3 Spontaneous shear rate

Material	Spontaneous shear rate (s^{-1})
C170_2	16.5
C170_4	6.9
C170_5	19.8
C170_6	14.8
C170_7	10.6
C170_8	15.6

For the surface dedicated for the impeller, the weaker interaction is more expected. A strong cell-material interaction could cause rapid degradation of the cell. The additional information was received when extrapolating the function to the value 0 of the stress. This situation meets the requirements of the absence of external forces acting on the cell. This analysis determines the rate of spontaneous detachment of cells from the substrate (Table 12.3).

12.2.2 Tissue like structures

The second key issue is related to the design and implementation of surface for the internal side of the inflow cannula. The work was related to the development of alternatives to existing solutions in the form of biomimetic surfaces. The surface properties were borrowed from the luminal side of the natural blood vessel (Fig. 12.6).

The idea was to elaborate extracellular matrix (ECM)-like surface structure to stimulate endothelium cell to grow and to form stable and dense monolayer. Endothelium is the most efficient inhibitor of the blood-clotting cascade activation. Bioactive

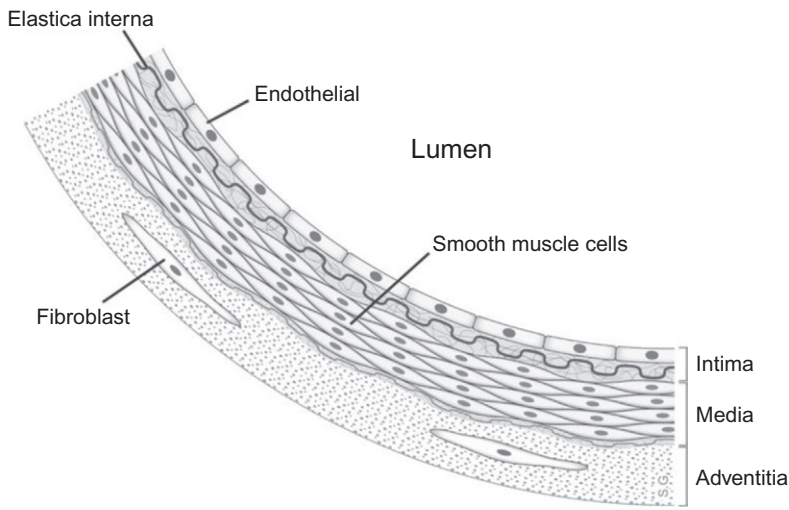


Fig. 12.6 The scheme of the cross section of blood vessel [11].

materials should assist the body in regeneration of the natural hierarchical systems of cells to rebuild tissues. The problem of designing and implementing an appropriate biomaterial dedicated to blood contact is complicated. Many attempts and solutions, in some cases controversial, were done so far. The paper [11] describes the blood-contacting materials, which are characterized by a strong roughness. The roughness influence the properties of biocompatible implant, in particular when contact with blood, seems to be in general negative. The rough surfaces are not expected and the more smooth the surface the better. The rough surfaces have been however, taken into account. The clots formation was induced on the introduced material surface. The surface was optimized to have the blood cells attached strictly to it and not cause congestion [12,13]. The cells may form part of the ECM which was the indirect step of the natural anticoagulation layer formation. The effect was observed on the laboratory scale. Its implementation was danger. Thus in the subsequent years a change was observed. The latest World's trend is the tissue analogs. Proofs of these statements are presented in the presented publications [14–23]. The idea consider the scaffolding of cell repopulation.

Tissue analogs allow better and longer use in the treatment of cardiovascular diseases. The material proposed reveals the implementation of porous materials, porous coatings, and surface nanofunctionalization. For this reason the well-known laboratory process had to be automatized in order to produce repetitive quality of the coatings. Therefore the originally designed system for the repetitive surface modification was built (Fig. 12.7A–D).

12.2.2.1 Automatization of the surface modification

The elaborated automatic system for the polymer coating deposition is under control of the originally written software responsible for the communication between the device and computer [24,25]. The program was dedicated especially to control its movements. The information related to the way of movement and time of the porous, synthetic coating elaboration was sent as a sequence of bits (SDU Serial Data Unit), from computer's USB port to FT232RL component (Future Technology Devices International Limited). FT232RL is an interface which converts the information to UART (Universal Asynchronous Receiver and Transmitter) form. Subsequently, the signal was translated from parallel to serial form by FT232RL interface and sent to microcontroller ATmega16. The ATmega16 is a low-power CMOS (Complementary Metal-Oxide-Semiconductor) 8-bit microcontroller based on AVR (Automatic Voltage Regulator) enhanced by RISC (Reduced Instruction Set Computing) architecture. It provided 16 Kb of In-System Programmable Flash Program memory and highly flexible and cost-effective solution for the process control. The ATmega16 AVR was supported by the C compiler tool. The commands that have been written separated the single bits from the achieved information and translated them to high or low signals, depending on the need, which controlled the functioning of the engines responsible for the movements of the biorobot arms. The microcontroller was responsible for manipulation via three-axis, micro-step driver STC102 manufactured by WObit company. The controller STC102 and device created consisted of two independent systems

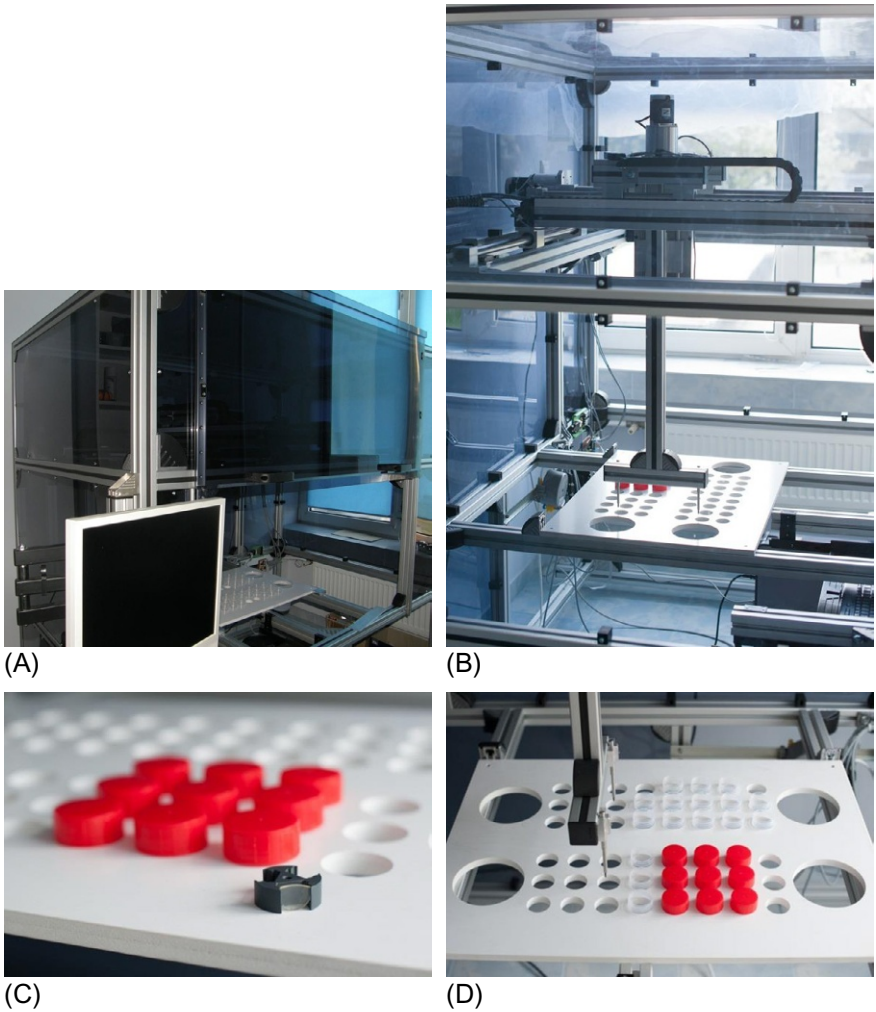


Fig. 12.7 (A) The overview of the system dedicated to deposit polymer-based porous coatings. (B) The moving arm of the system dedicated to depositing polymer-based porous coatings. (C) The matrix with containers of the system dedicated to depositing polymer-based porous coatings. (D) The working zone arm with matrix of the system dedicated to depositing polymer-based porous coatings.

operated separately. A galvanic barrier used for this purpose effectively separated both systems. The program was written using the Java programming language. The detailed description of the software prepared could be found elsewhere [26].

12.2.2.2 The design of the ECM-like coating

Following the information given elsewhere [27], the nonthrombogenic surface for vascular grafts/artificial hearts was prepared so as to consist of an intact luminal

endothelial cell layer. Before porous coating the initial step of the substrate preparation considered thin hemocompatibile coating deposition using physical vapor deposition. Ultrathin coatings were deposited to form the appropriate surface charge as well as to ensure hemocompatibility. For this reason a-C:H:N:Ti coatings were considered. Porous materials in the form of porous coatings were the key issue. In the performed experiments porous coatings were deposited using the "layer-by-layer" method using oppositely charged polyelectrolytes. The surface was immobilized by small molecular domains to promote endothelium cells' growth. For the top polyethylene glycol (PEG) was deposited. The PEG surface was modified using tripeptide Arg-Gly-Asp (RGD) protein sequence that is responsible for binding proteins to cell surfaces. The goal of the RGD incorporation into a surface was to promote the cell growth on the hydrophilic PEG containing surfaces [27]. The RGD motif was initially identified in fibronectin as the sequence motif that mediates the cell attachment. To promote the RGD association with the surface, it was necessary to stimulate the binding of an activated surface carboxylic acid group with the nucleophilic N-terminus of the peptide. Carboxylic acid groups can be activated with a peptide coupling reagent, e.g., 1-ethyl-3-(3-dimethylaminopropyl)- carbodiimide (EDC, also referred to as water-soluble carbodiimide) [28]. By forming brush-like structures, PEG-creates a "stealth effect," repelling proteins, cells, and bacteria [29]. Biofunctional ligands, such as small peptide sequences, can be added to the (PLL-g-PEG) chains to induce specific interactions between cells and the surfaces of the biomaterial. The RGD incorporation process is described elsewhere in detail [30].

To reconstitute vascular-like properties the small molecular domains were adsorbed under the final HUVEC layer. The steps of the appropriate confluence formation are shown in Fig. 12.8A–D. The blood-material interactions of the coatings with natural endothelium monolayer were examined.

Impact-R chosen for the experiment and material selection, is a simplified method to assess hemocompatibility under high-shear-stress conditions [31–39]. This study was designed to evaluate the performance of an alternative in vitro dynamic test for hemocompatibility. Material selection was performed based on several aspects of the blood response, like the amount of activated platelets and the influence on the aggregates formation. Results are presented as the amount of platelet aggregates formed in the function of the tested material. Among the platelet aggregates small (2 platelets) and big (more than 2 platelets) were taken under consideration. For the experiment the following samples were prepared:

The As the base line was determined bas.
Polystyrene (PS) reference material.
Ti(C,N)-a-C:H:N:Ti layer deposited on the polyurethane (PU) substrate.
PLL + HUVEC-porous 12 bilayer coatings PLL/HA deposited on the PU substrate with a-C:H:N:Ti thin coating deposited in the initial stage, cross-linked with EDC and NHS. As the final step PLL was deposited and HUVEC monolayer was formed in the incubation conditions.
PEG + RGD + HUVEC-porous 12 bi-layer coating PLL/HA deposited on the PU substrate with Ti(C,N) thin coating deposited in the initial stage, cross-linked with EDC and NHS. As the final step PEG was deposited. On the PEG surface small molecular domains were

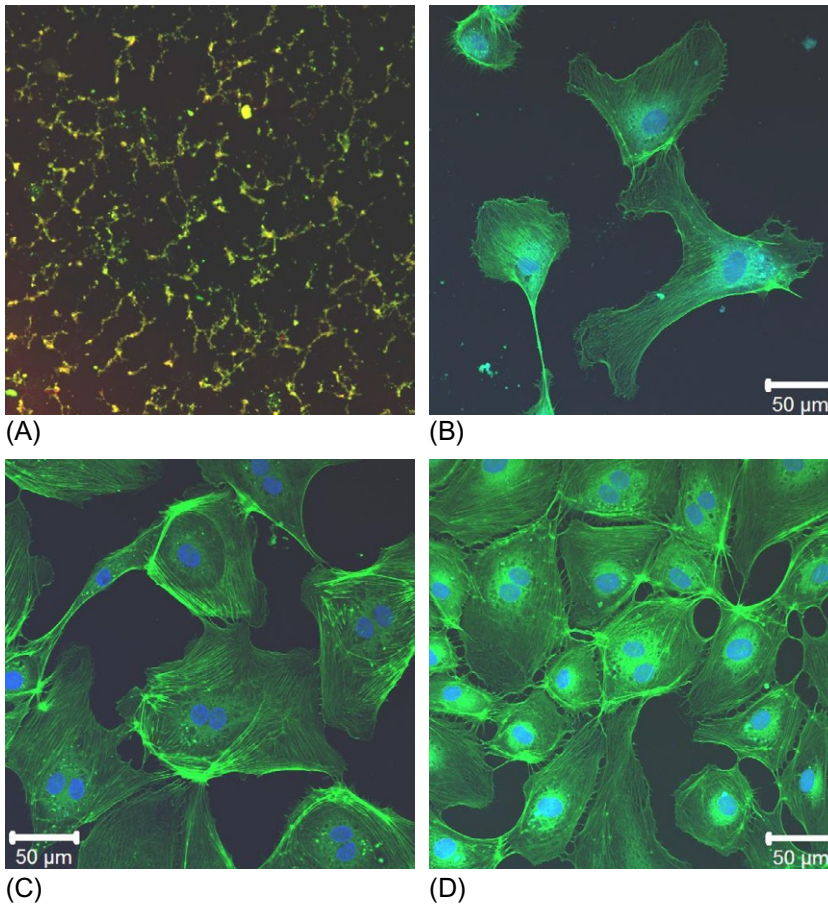


Fig. 12.8 (A) Plane view of the porous coating. (B) Plane view of the porous coating with endothelium cells after 0.5 day of incubation. (C) Plane view of the porous coating with endothelium cells after 1 day of incubation. (D) Plane view of the porous coating with endothelium cells after 3 days of incubation.

immobilized to activate mezenchymal origin cells to grow. Finally HUVEC monolayer was formed.
Adenosine-di-phosphate (ADP), it was positive control. Platelets were activated by ADP.

The results are presented in Fig. 12.9. All solutions presented the appropriate blood-material interaction in the dynamic conditions. The most promising results were observed for a-C:H:N:Ti, PEG, RGD, and HUVEC modified PU surface.

12.2.2.3 The design of the niche-like structures

The different challenging solutions dedicated to the design and implementation of surface for the internal side of the inflow cannula, seems to be with regard to reproducing the cellular niches. Currently, most attention is given to the stem cells. Stem cells

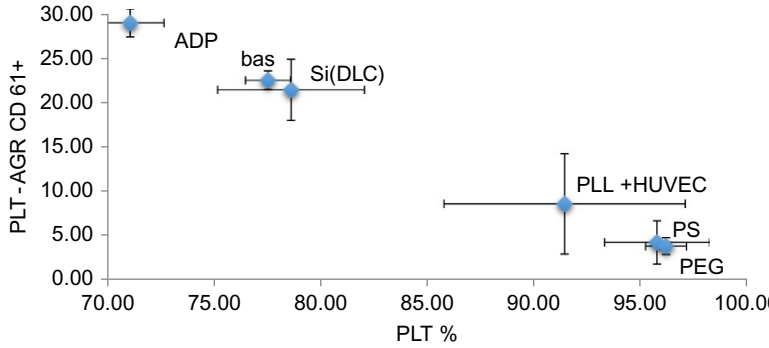


Fig. 12.9 Platelet aggregate formation in the function of used platelets.

are of great interest because of their biological properties and clinical application. Stem cells are capable of self-renewal, they have a high potential to differentiate into other cell types. The selected stem cells isolated from the early embryo can develop into an embryo. Pluripotent stem cells, isolated from the body, have the potential to differentiate into all tissue types. In the near future treatment associated with stem cells will allow incubating cells in vitro for transplantation. Stem cells are defined as self-renewable and producing differentiated, specialized cells [40–42]. Each stem cell is capable of proliferation, self-renewal, and differentiation through divisions, which are asymmetrical and therefore give rise to two derived cells, which differ from each other. One of them is the same as the original stem cell, so that supports the population, while the other goes into more mature. Each cell, which grows and matures, has its own niche. Each niche is a spatial structure of cells and extracellular material. It forms a microenvironment that keeps the cells and gives signals to the main cell proliferation, maturation, or to self-renewal. Stem cell niche refers to an anatomical and functional structure, including cellular and extracellular components, local and systemic factors that are integrated to regulate stem cell proliferation, differentiation, survival, and localization [43–45]. In 1978, Schofield proposed the concept of "stem cell niche" in studies of the hematopoietic stem cells [46]. Since then, this hypothesis has been validated by a number of studies. The in vivo evidence of the existence of stem cell niche was first provided in studies using invertebrate models [47] and in the Drosophila germline stem cells [48,49]. In mammals, stem cell niches have been identified in different tissues over the past several years, including bone marrow, brain, hair follicles, intestines, and teeth [50–55]. Theoretically, a stem cell niche is composed of the stem cells themselves; stromal support cells; extra cellular matrix proteins; and blood vessels and neural inputs. The interaction of the biomaterial with the stem cells is described in the literature [56–61,41]. Scaffolds are manufactured from suitable biocompatible materials which will allow disintegration and absorption in the body [62]. There are three theoretical models which could be adopted for the surface modification in order to reconstruct niche like structures (Fig. 12.10).

For the work, the third model was chosen based on the modular substrate stiffness. Surface modification of polymers by the use of thin layers allows forming new features of the material while maintaining or slightly changing the physical properties

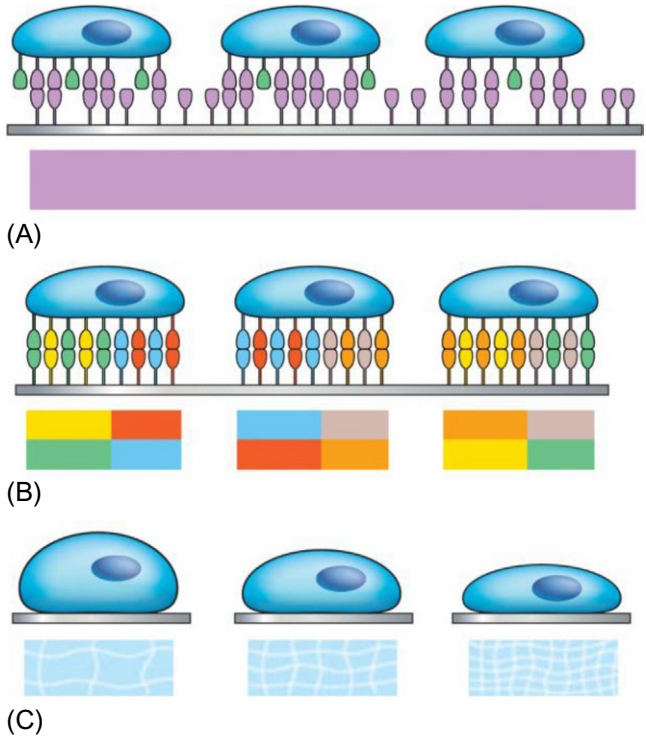


Fig. 12.10 Possible models of the niche like structures reconstruction [62]: (A) individual signals, (B) combinatorial signal mixtures, and (C) modular substrate stiffness.

of the polymer [63–65]. The main attention of the surface modification of medically used polymers is on improving the stability of the material in direct contact with tissue. Adhesion of the layer to the substrate is one of the most important factors which classify material for the biomedical engineering. In order to reconstruct the niche-like structures the surface wrinkling is considered (Fig. 12.11A–C).

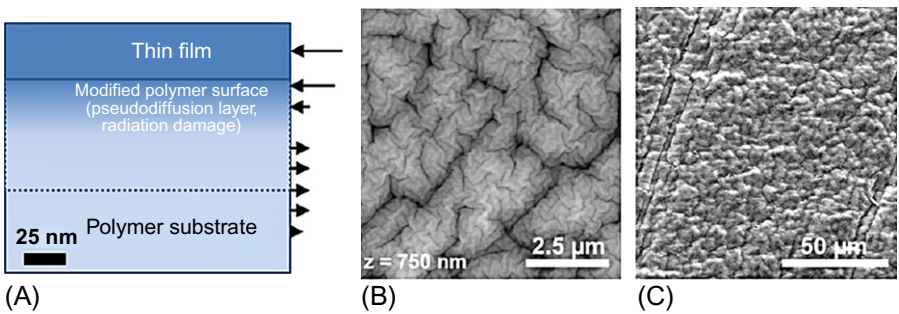


Fig. 12.11 (A) Theoretical explanation of the wrinkles origin [28]. (B) Plane view of the wrinkles (high magnification). (C) Plane view of the wrinkles (low magnification).

Reducing the overall strain energy in the layers subjected to compressive stress, so-called surface "Wrinkling" appears. The suggested explanation considers a common deformation of the substrate surface and the layer [28]. "Wrinkling" is described as the forming of sinusoidal elevations on the surface which do not cause the loss of adhesion to the substrate.

$$\lambda_c = 2\pi h \left[\frac{\left(1-\nu_f^2\right)E_s}{3\left(1-\nu_s^2\right)E_f} \right]^{1/3} \tag{12.2}$$

- The wavelength of wrinkles depends on the material properties of the surface layer (s) and the foundation (substrate, f).
- Poisson ratios (ν_s, ν_f).
- Elastic moduli (E_s, E_f).
- The thickness of the surface layer (h).

The main mechanism of wrinkling is the substrate or subsurface areas of the substrate with the applied layer uplifting. The reason for the folding of the deposited layer comes from the mechanical instability. This can be compared to the problem of instability of elastic layer on a flexible substrate medium. In this model, both the base layer and the substrate have a biaxial stress. The result of compressive stress relaxation is the formation of the wavy structure of the surface [66,67].

The idea concerns a novel approach of the surface modification. As a substrate, clinically used polymers were used. The intended target of the developed materials is surface modification which could lead to the effective capture of stem cells. The stem cells should exhibit self-differentiation process through proper shape and stiffness of the surface, to endothelium. Endothelium is the most effective inhibitor of the blood clotting process. The scientific issues taken in the frame of the work project are of particular importance in the design and development of new components dedicated to the regeneration of the blood circular system.

The presented work related to the development of materials in the form of thin films, with a modified surface in the form of wrinkles, in the aspect of inhibiting coagulation process and the potential for the endothelium monolayer formation.

For this purpose carbon based coatings were proposed. The details are presented in Table 12.4.

Table 12.4 List of the coatings prepared as niche like structures

Sample	Coating	Thickness (nm)
C154_3	a-C:H (sputtered)	110
C154_4	a-C:H (sputtered)	105
C154_6	a-C:H (lower gas flow; sputtered)	100
C154_7	a-C:N (sputtered)	60
B334_7	DLC (with ALS)	85
B334_8	DLC (with ALS)	43
B334_10	DLC (with ALS)	65
B334_12	DLC (with ALS)	86

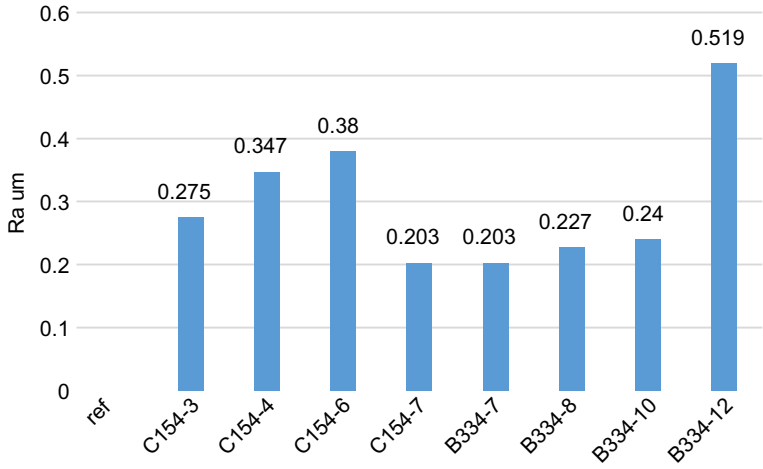


Fig. 12.12 Composition and thickness dependent surface roughness.

Depending on the phase composition and thickness different surface roughness was detected. The surface topography analysis is shown in Fig. 12.12.

The surface roughness as well as the phase composition have significant influence on the endothelialization as well as the blood-material interaction. The three dimensional fluorescent image of endothelial cells (HUVEC) in association with differential interference contrast (DIC) analysis of the substrate surface in the form of wrinkles done using CLSM is shown in Fig. 12.13.

On the basis of the results shown in Fig. 12.14A–I, it is possible to determine the degree of endothelialization. The samples are defined according to Table 12.4. It can be seen that the materials based on amorphous carbon are better than materials considered as diamond like carbon. Statistically more cells were found on the surface of a-C:H based materials. Such materials better prognosis for the next stage, that is, to differentiate progenitor cells into the endothelial and eventually capture progenitor cells from whole blood and their spontaneous differentiation.

Simultaneously, separately to endothelialization determination, blood-material interaction in the dynamic conditions was performed. When exposed to physiological-like conditions, blood components are activated, which may result in platelet and leukocyte adhesion to the biomaterial surface. This process is preceded by coagulation of blood above the surface. Blood coagulation, followed by increasing platelet aggregate density in the blood could initiate thrombus formation. Physiological shear stress promotes all of these processes and induces the immune response of the organism. Shear forces can also destroy platelets, resulting in microparticle formation. After the dynamic test on blood the surface of each material was analyzed in order of the immune response as well as the blood clotting activation using confocal scanning laser microscopy. For this analysis fluorophore labeled antibodies were applied. Immuneresponse was defined by the anti-CD45. Platelet activation was defined by the anti-CD62P. For the analysis, the coating of the extreme parameters of each group was selected according to the Table 12.4. The blood-material interaction results are shown in Fig. 12.15.

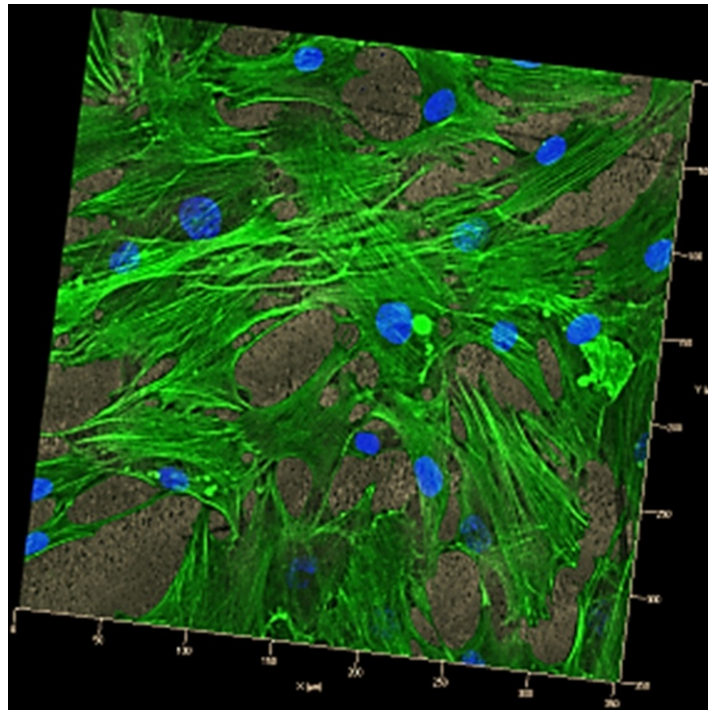


Fig. 12.13 3D CLSM fluorescence and DIC analysis of the HUVEC deposited on the wrinkled surfaces.

For the diamond like carbon coatings, designated as B334 (Table 12.4) the dominance of the immune response for B334_7 was exchanged for the dominance of the coagulation system activation for B334_12. For the coating a-C:H any change was found. In general, stronger immune response was observed. It means that the coatings of a-C:H are stable with phase. They also exhibit high potential for the endothelialization which was already illustrated and described (Fig. 12.14B–E).

Evaluation of the quality of the blood that was collected from the surface was evaluated using flow cytometry techniques. As a negative control full uncoagulated human blood with salt citrate and heparin was assumed. For the preparation of the positive control, ADP was used. It is a very strong platelet activator. The analysis considered the formation of platelet aggregates. The formation of large and small platelet aggregates was studied. Small platelet aggregates were described as two platelets, large platelets aggregates were described as over two platelets. The platelet aggregate formation function is shown in Fig 12.16. In general for all coatings, lower amount of platelets is formed compared to the clinically used PU and hemocompatibile PS.

Activation of coagulation was evaluated in terms of the diagnosis of membrane receptors of platelets. Activation of Selectin P and IIb/IIIa was tested (Fig 12.17). Strong blood activation is the result of the applied dynamic conditions simulating arterial flow conditions.

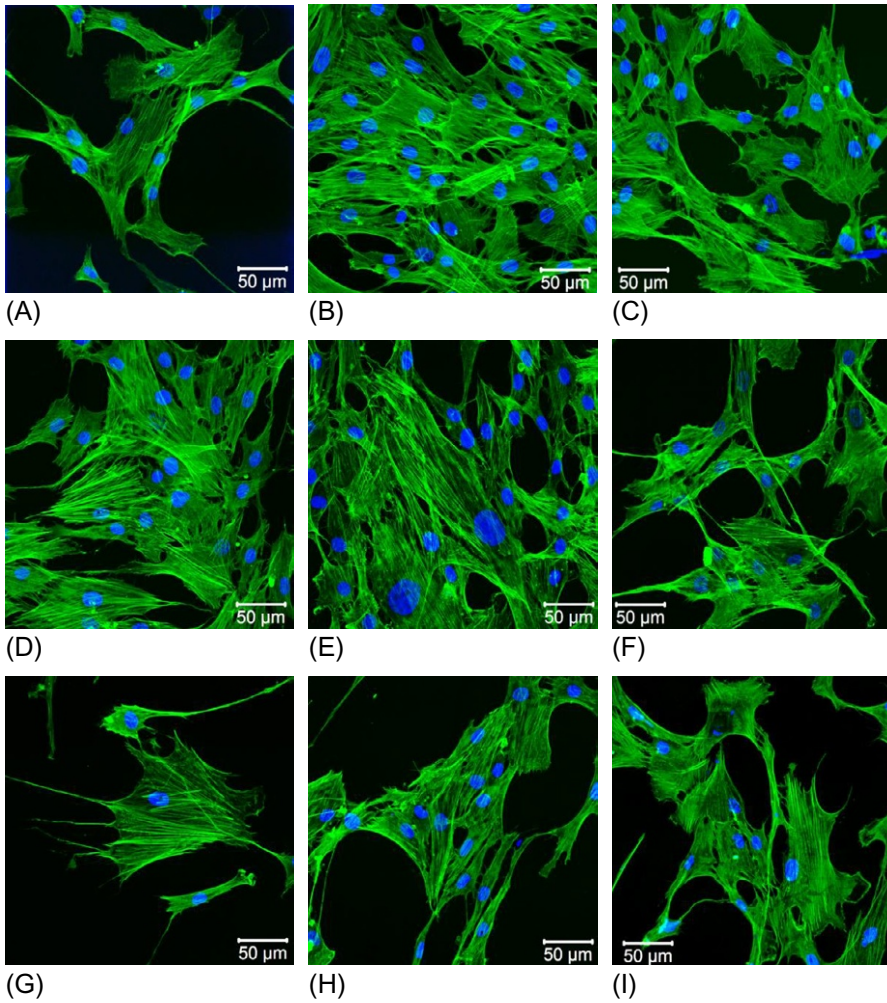


Fig. 12.14 (A) Reference substrate without coating. (B) C154_3. (C) C154_4. (D) C154_6. (E) C154_7. (F) B334_7. (G) B334_8. (H) B334_10. (I) B334_12.

The final material selection was done based on the phospholipid rich microparticle analysis. Microparticles are derived from the cellular membrane and are detected by the anexin V. Fig. 12.18 presents microparticle concentration as a function of the remaining platelets after the test.

Generally the closer the results of the tested material to the positive control (ADP) the worse. Promising results should oscillate close to the negative control (bas). Thus the most promising materials are a-C:H.

12.2.3 Controlled smooth muscle formation-migration channels

The third part of the surface modification was considered for the external side of the inflow cannula. The heart assist chamber is introduced into the left side of the heart

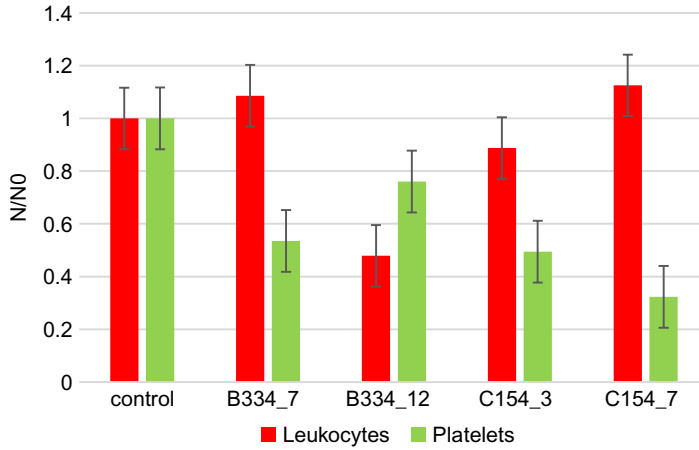


Fig. 12.15 Blood-material interaction analysis. Active leucocytes and platelets attached on the surface analyzed by CLSM using anti CD45 for leucocytes and anti-CD62P for platelets.

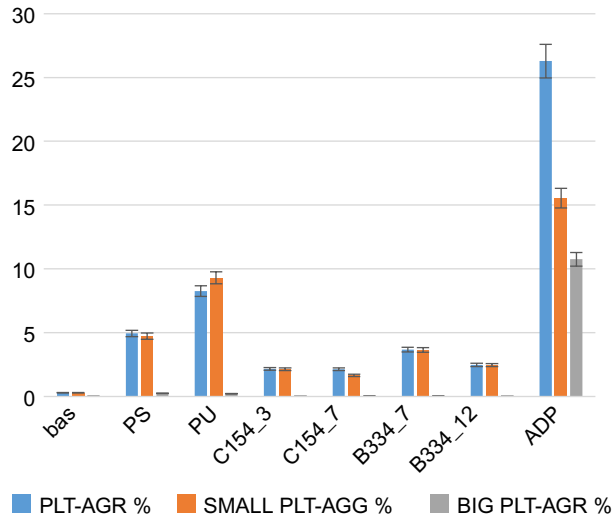


Fig. 12.16 The platelet aggregate formation in the blood above the sample analyzed by flow cytometry.

through the apex cordis. The external side of the cannula is then in direct contact with the cardiac muscle cells. The surface in direct contact with the myocardium should stimulate integration to a certain height of the inflow cannula. The surface without the surface modification, would induce the process of the biofilm formation which finally could result with the artificial blood vessel conduit closure. For this reason the method of surface modification was proposed. The surface functionalization was regarded in the form of migration channels [68]. A local environment creates a crucial influence on cells' behavior, their shape, alignment, and orientation. The chemical composition and topography of a substrate affect cellular functions like: adhesion, growth, locomotion,

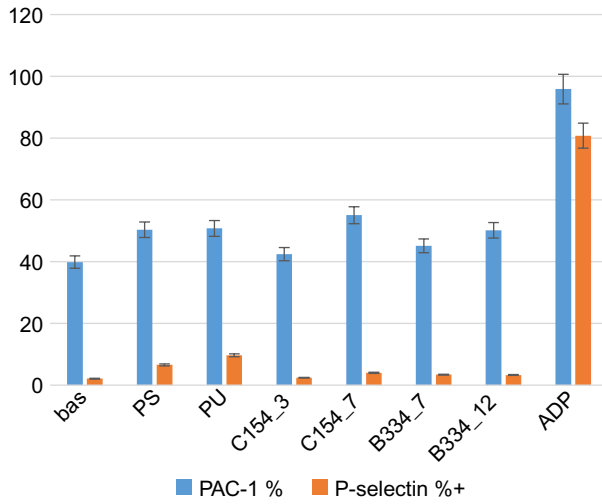


Fig. 12.17 The activation of coagulation evaluated in terms of the diagnosis of membrane receptors of platelets. Selectin P and IIb/IIIa.

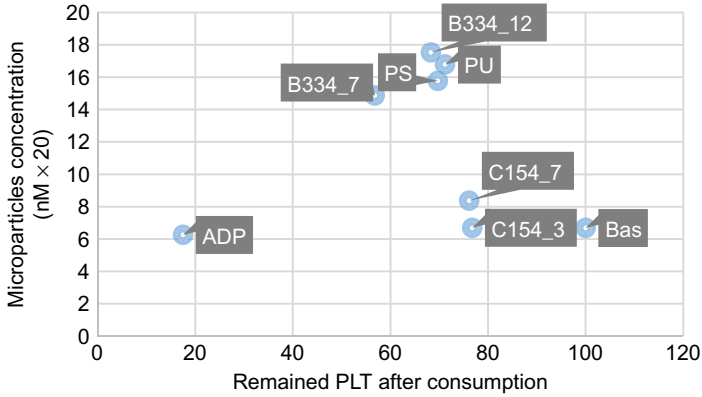


Fig. 12.18 Microparticle concentration as a function of the remaining platelets after the test.

gene expression, and apoptosis. Control of the biological environment through suitable scaffold properties is the essential task for tissue engineering [69]. Proper physical and chemical properties promote cell adhesion. Channels and ridges in a surface structure guide cells' migration and their orientation, providing healthy tissue organization [70]. In the study, the laser ablation technique was used. Advantages of this approach are as follow: high resolution (down to 25 nm [71]), noncontact interaction and applicability to any substrate. The thermal and mechanical propagation occur during irradiation by nanosecond and longer laser pulses, causing melting and vaporization far from the absorption site and resolidification of the melt zone [72].

The most important aspects of surface functionalization in the form of channels, was predicted using finite element modeling. The simulation concerns the work associated

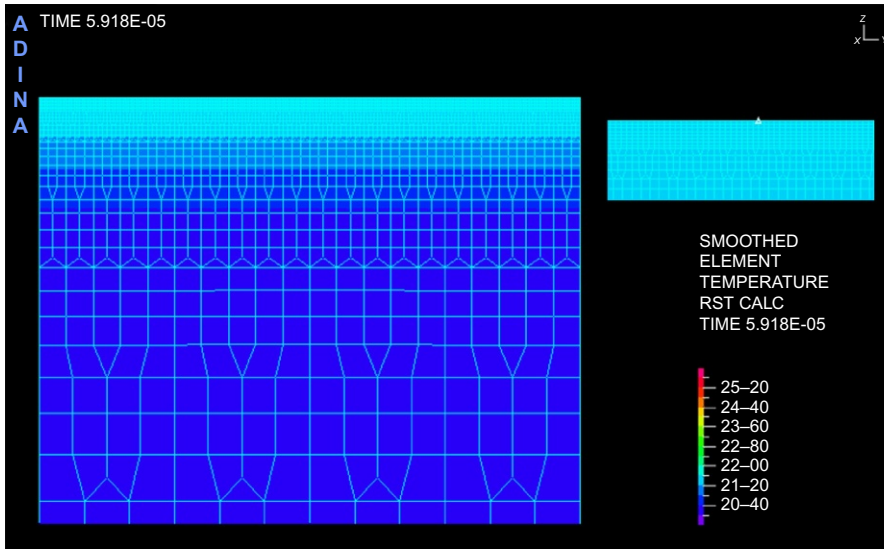


Fig. 12.19 Finite element simulation of the temperature distribution in the thin coating structure during deposition process.

with the theoretical determination of the optimal structure of the elaborated channel, temperature optimization, and renucleation after evaporation. Fig. 12.19 presents the finite element simulation of the temperature distribution in the thin coating structure during deposition process.

During the initial stages of evaporation, followed by uniform temperature distribution in the substrate, the local thermal decomposition occurs (Fig. 12.20). In such places, the vibrations of the atoms in the structure networks are the strongest and evaporation process is most likely to occur. Local laser pulse energy conversion causes lattice vibration. The threshold energy defines vaporized creation within the channel formation. Part of the energy of vibration is transformed into heat which cause heat affected zone formation.

On the simulation results, the dark blue color is cut off from the light blue. This indicates the nonuniform temperature distribution. It may prove the possible local increase of temperature. Numerical analysis considers partial evaporation effect, the effect of resputtering and the influence of the heat affected zone. These elements are the key parameters of the interaction of cells with the material. The numerical analysis was verified experimentally.

Based on the preliminary studies, the following materials in the form of thin layers were selected for further analysis: amorphous carbon (a-C:H), titanium carbo-nitride (a-C:H:Ti:N), titanium oxide (Ti:O), carbon doped silicon (a-C:H:Si), and carbon-doped titanium (a-C:H:Ti). These coatings were chosen because of their biocompatibility.

Carbon coatings were obtained by application of variable energy conditions in the direct current method (DC) and magnetron pulse method. Titanium oxide and titanium-carbo nitride were deposited by applying a hybrid method pulsed laser deposition using a Nd; YAG laser, 1064 nm, ablation of a pure source of Ti (>99%), assisted magnetron sputtering method under an atmosphere of argon, nitrogen, and atmospheric oxygen.

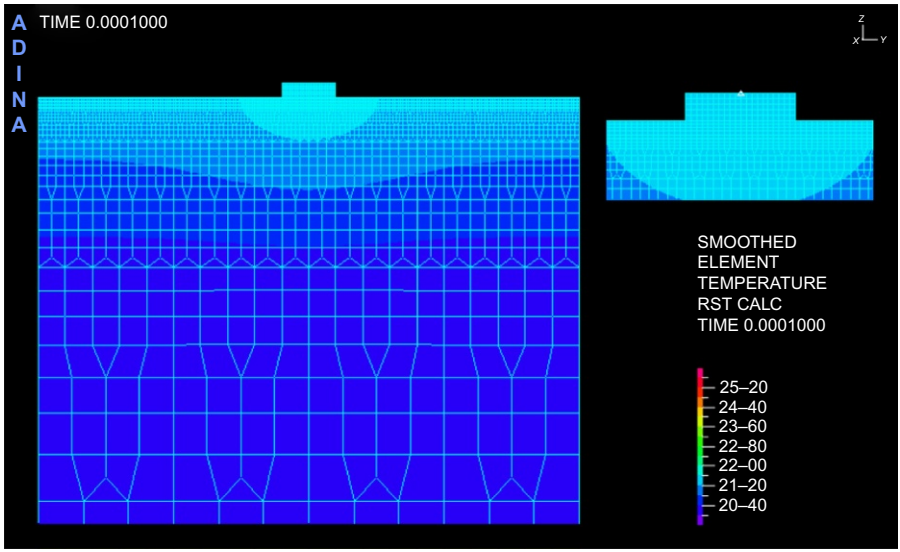


Fig. 12.20 Finite element simulation of the local temperature concentration during partial coating evaporation.

a-C:H was obtained using magnetron sputtering in an inert atmosphere of argon. Doped carbon with Si or Ti, respectively were obtained by evaporating silicon or titanium under an atmosphere of acetylene (C_2H_2). The coatings were obtained in the room temperature. A detailed description of the method is described elsewhere [6].

The work concerned the optimization of the surface by creating migration channels for controlled cell proliferation. Channels migration were prepared by laser ablation on a depth equal to half the thickness of the coatings. The microstructure in the boundary region between the processed and unprocessed material was analyzed by transmission electron microscope techniques. For the analysis of the cell-material interaction smooth muscle cells (SMCs) were used. The interaction between the cells and the surface of the material was analyzed using CLSM. The applied parameters include the refractive index ν and extinction coefficient κ for the modified coatings (Table 12.5 and Fig. 12.21).

The controlled growth of muscle cells was prepared with two different migration channel geometries. Migration channels were prepared in the form of lines and wells (Fig. 12.21).

The microstructure was analyzed using transmission electron microscopy (TEM). Thin foils for the TEM were prepared from the border between the migration channel migration and the unmodified part of the material (Fig. 12.22, step I). Observation of

Table 12.5 **Refractive index ν and extinction coefficient κ**

Refractive index	Extinction coefficient
ν for the wavelength 1064 nm = 1.86	κ for the wavelength 1064 nm = 0.025
ν for the wavelength 523 nm = 1.92	κ for the wavelength 532 nm = 0.05
ν for the wavelength 355 nm = 1.96	κ for the wavelength 355 nm = 0.3

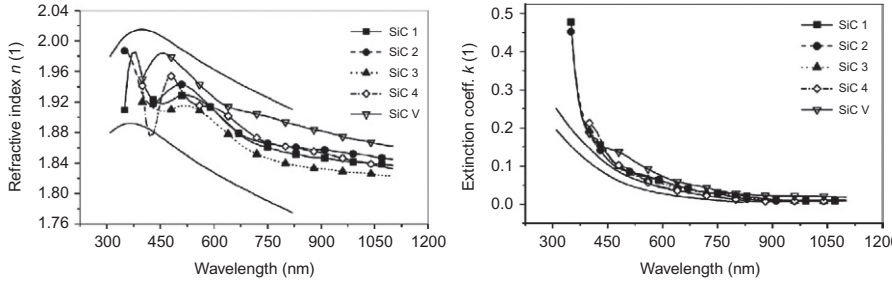


Fig. 12.21 Refractive index and extinction coefficient in the function of wavelength.

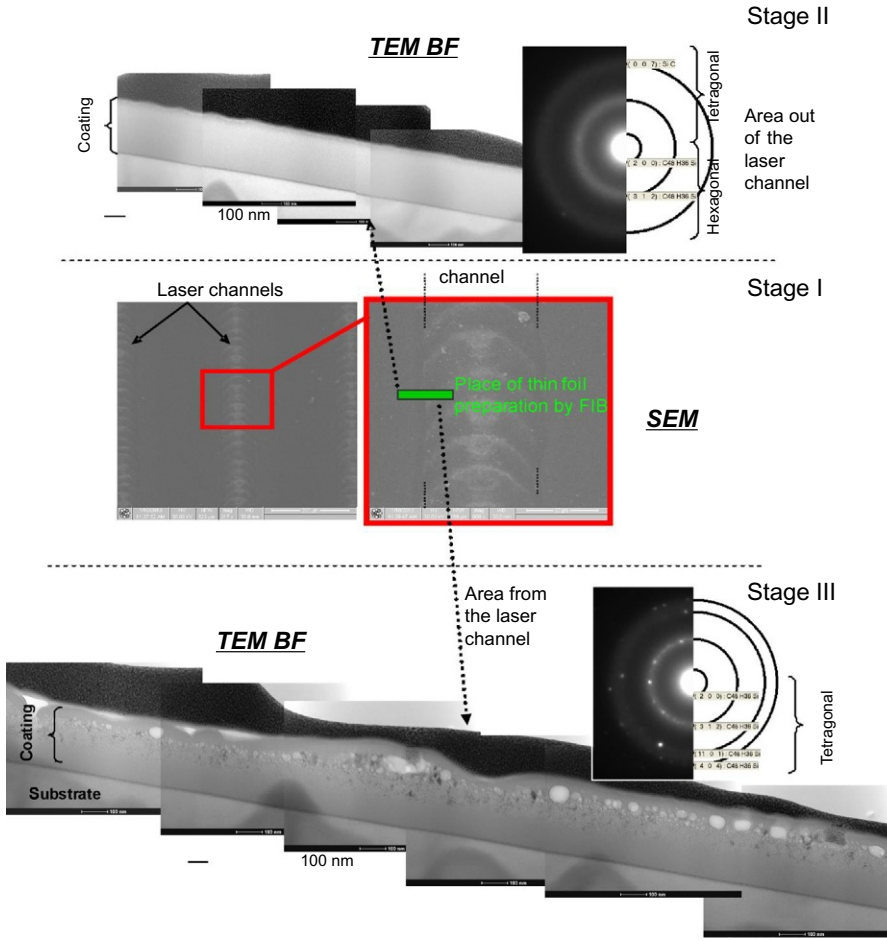


Fig. 12.22 TEM cross section analysis of the migration channel. Step I-selection of the surface to prepare thin foil for analysis using a transmission electron microscope, step II-sectional analysis of unmodified part, and step III analysis of the section with modified surface.

cross section was undertaken under bright-field. Microstructure analysis of the nonmodified part (Fig. 12.22, step II) showed amorphous structure, which was confirmed by electron diffraction. The cross-section of a modified part is shown in Fig. 12.22, step III.

TEM analysis showed nonuniform microstructure in the migration channels (Fig. 12.22, step III). The material from the migration channel has been partly removed and the substrate has not been completely exposed. Grains of a modified part of the coating showed a larger size than the area without modification. This was confirmed by electron diffraction image. Diffraction rings of processed area (migration channels) were less blurred than that in the area of the unmodified part. Phase analysis was carried out using high-resolution transmission electron microscopy technique (HREM) (Fig. 12.23). The protective gas used during the evaporation of migration channels influenced the formation of bubbles during recrystallization below the surface.

12.2.3.1 SMC deposition

Depending on the geometry of the formed channels, a different behavior of SMCs was observed. Fig. 12.24 shows the effect of surface modification in the form of linear channels (as paths) to maintain the cells.

Heat affected zone is formed on the border of the migration canal. The cells were grown on the surface of a-C:H:Si and have been positioned along the direction of migration channels. The difficulties in the build-up of cells were observed in the heat affected zone. The formation of the characteristic junctions caused by the heat affected zone was observed. In the channel which was prepared in the form of wells, heat affected zone played a significant role in the interaction of cells to the surface. This zone has been produced around the wells. The overlapping of the areas of the heat affected zones have been observed. This area is an obstacle to the growth and proliferation of cells (Fig. 12.25).

12.2.3.2 The channel shape optimization by the direct laser interference lithography

Recently a periodical modifying the surface of all solid materials, a method of direct interference lithography applying a laser of high power density, from several MW/cm^2 to several GW/cm^2 is used. This method allows a direct modification of surface structures on a scale of micrometer and submicrometer with well-defined long-range ordering. A full field $\vec{E}$ of multiple interfering beams is obtained by superposition of each individual field $\vec{E}_j$ of each laser beam. This is described by the following equation:

$$\vec{E} = \sum_{j=1}^{n} \vec{E}_j = \sum_{j=1}^{n} \vec{E}_{j_0} \cdot \exp\left[-i\left(\vec{k} \cdot \vec{r} - \omega \cdot t\right)\right] \tag{12.3}$$

For two laser beams the strength of interference field can be described in the form of

$$I = 4I_0 \cos^2\left(kx \sin\theta\right) \tag{12.4}$$

for which the period of the field is

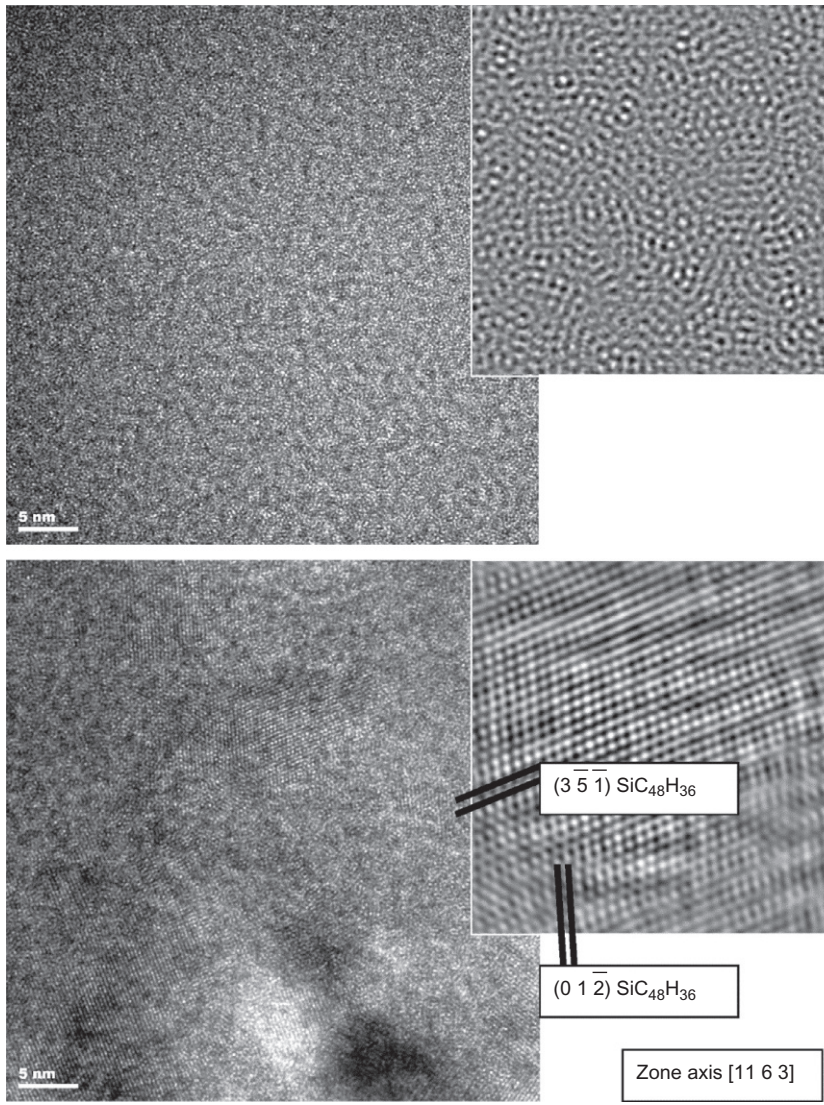


Fig. 12.23 Phase analysis carried out using high-resolution transmission electron microscopy technique (HREM).

$$d = \frac{\lambda}{2\sin\theta} \tag{12.5}$$

Fig. 12.26 illustrates the geometry and resulting interference images using two and three laser beams. As a result of the process, spatial structure of linear and point-shape structures were obtained.

The preliminary results of SMC cultures on a periodic linear structure are shown in images taken using CLSM Zeiss Exciter 5 (Fig. 12.27).

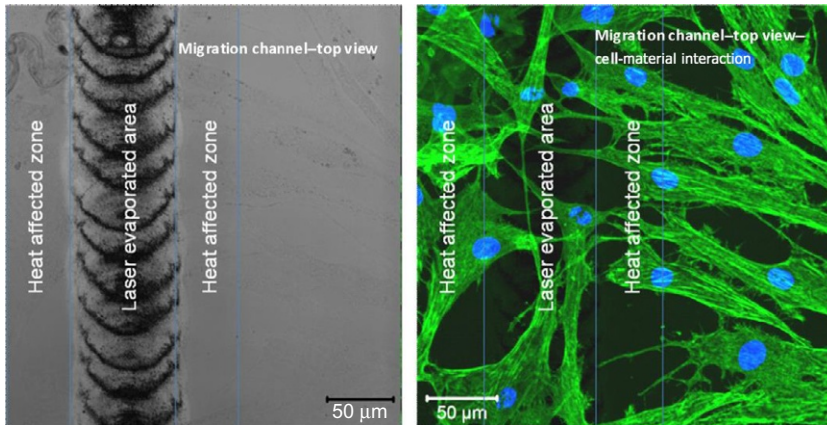


Fig. 12.24 Effect of surface modification in the form of linear channels on the muscle cell behavior.

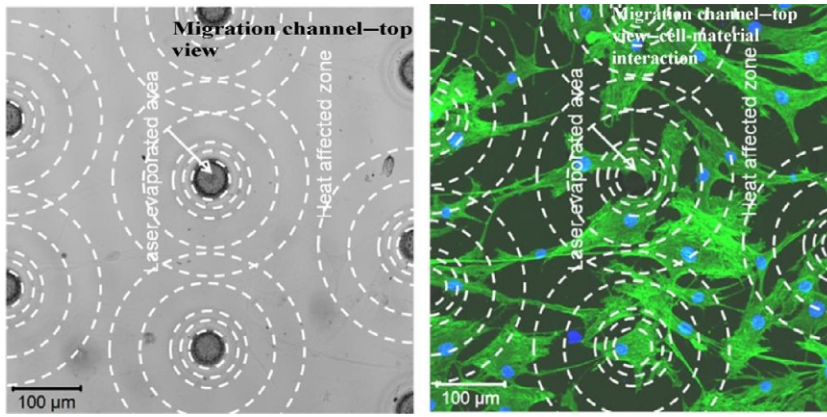


Fig. 12.25 Effect of heat affected zone on the growth and proliferation of the smooth muscle cells.

Further work related to studying the impact of structural parameters: the distance between the interference fringes and their depth on the behavior of the cells (Fig. 12.28).

12.3 Concluding remarks

The alternative functional coatings pumps assist in the contents of the surface engineering were developed separately for each component. The surface function has been developed according to the destination. In the case of the rotor surface, large shear forces endanger the viability of the morphotic elements of blood. For this reason, surfaces were developed in order to minimize the destructive effect of the high shear stress on blood cellular components. Coatings dedicated to internal elements of the inflow

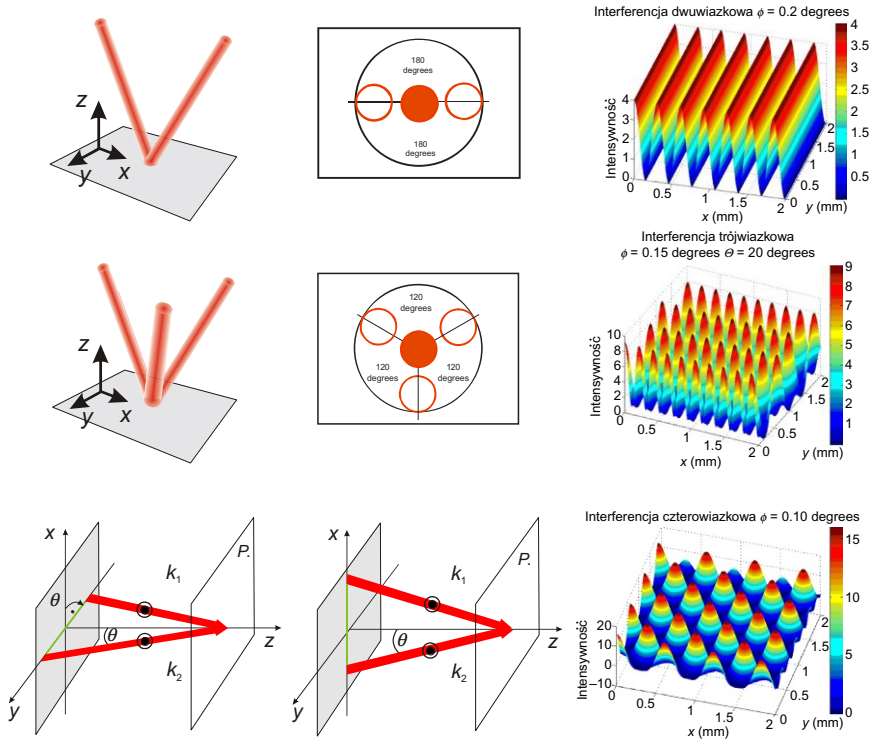


Fig. 12.26 Interference pattern created by a series of coherent laser beams.

cannula, the surfaces were developed considering the opportunity of the endothelial tissue formation which should effectively inhibit the clotting process. Considering the porous, ECM-like coatings the initial surface modification plays a significant role. For this reason layer-by-layer technique associated with polyelectrolyte deposition seemed to be the appropriate one to reconstitute ECM structure. Blood clotting cascade inhibition was the most efficient with the endothelium cell layer support.

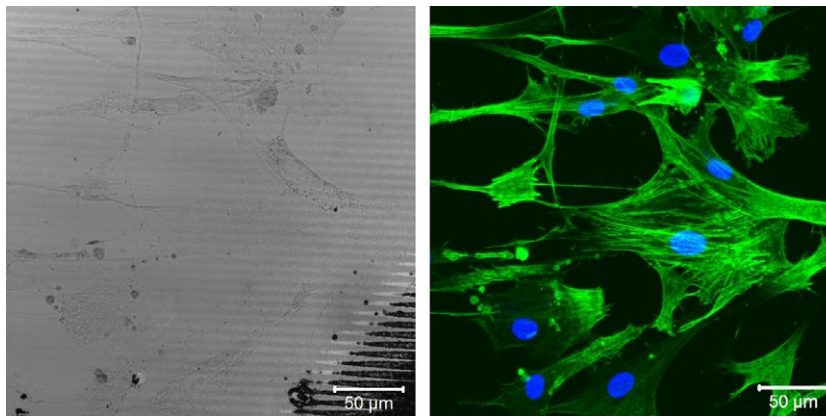


Fig. 12.27 Smooth muscle cell cultures on a periodic linear structure.

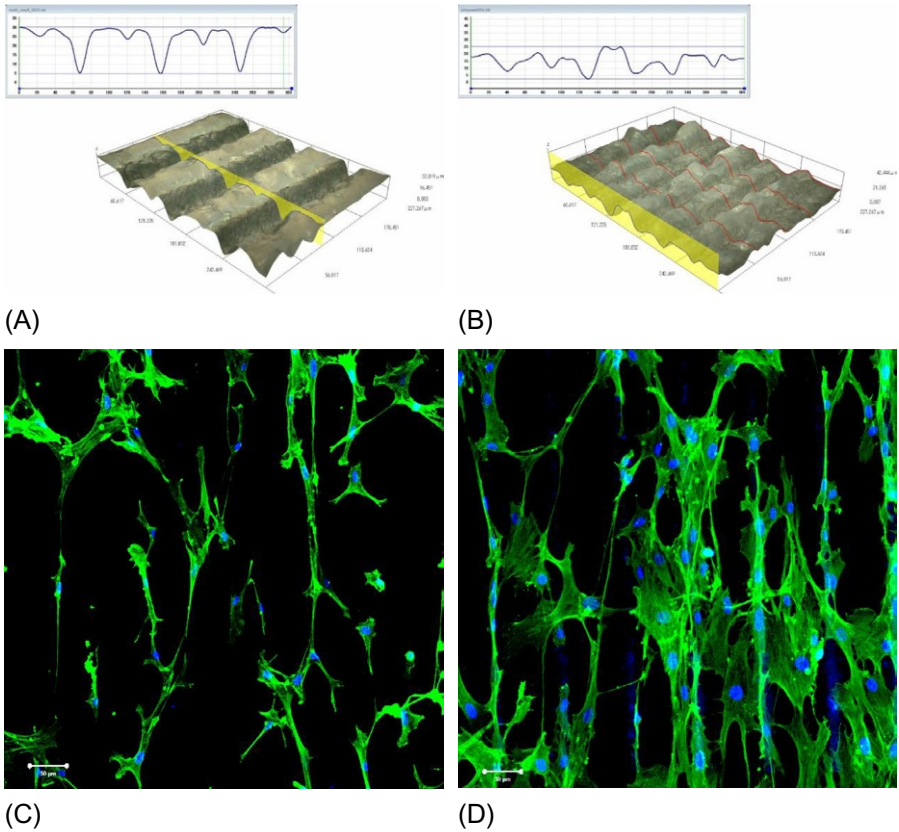


Fig. 12.28 (A) Channels prepared with period 100 μm. (B) Channels prepared with period 500 μm. (C) Smooth muscle cell cultured on a periodic linear structure (period 100 μm). (D) Smooth muscle cell cultured on a periodic linear structure (period 50 μm).

Wrinkling as the most suitable model occurs on the micro to millimeter scale for tissue and on the nano to micrometer scale for polymers with inorganic thin coatings. Mechanically, the wrinkles were found to have high impact on the elongation. Finally, the last part of the surface modification considered appropriate integration of artificial surface with muscle cells. The surfaces were modified with ablation technique. The several experiments enabled us to refine the coating. At present, we are able to control the migration of muscle cells and even their density. Generally it can be stated that the best dedicated solutions for biomaterials can be found in nature. The more the material is inspired by the anatomical built, the better.

Acknowledgments

The research was financially supported by the Project no. 2014/13/B/ST8/04287 “Bio-inspired thin film materials with the controlled contribution of the residual stress in terms of

the restoration of stem cells microenvironment" of the Polish National Centre of Science and 2011/03/D/ST8/04103 "Self-assembling, biomimetic porous scaffolds in terms of inhibiting the Activation of the coagulation system" of the Polish National Center of Science.

References

[1] A. Kapis, M. Czak, R. Kustosz, M. Gawlikowski, New extracorporeal cardiac support system ReligaHeart EXT, in: R. Kustosz, M. Gonsior, A. Jarosz (Eds.), Polish Artificial Heart, the Development of Design, Qualification, Preclinical and Clinical Tests, Epigraf s.c, ISBN: 978-83-63310-12-7, 2013, pp. 22–77 (in Polish).

[2] R. Major, F. Bruckert, J.M. Lackner, W. Waldhauser, M. Pietrzyk, B. Major, Kinetics of eukaryote cells adhesion under shear flow detachment on the PLD deposited surfaces, Bull. Acad. Pol. Sci. Tech. Sci. 56 (3) (2008) 223–228.

[3] M. Demilly, Y. Brechet, F. Bruckert, L. Boulang'e, Kinetics of yeast detachment from controlled stainless steel surfaces, Colloids Surf. B Biointerfaces 51 (2006) 71–79.

[4] M.C. van Loosdrecht, W. Norde, A.J. Zehnder, Physical chemical description of bacterial adhesion, J. Biomater. Appl. 5 (1990) 91–106.

[5] S. Vatanyoopaisarn, A. Nazli, C.E. Dodd, C.E. Rees, Effect of flagella on initial attachment of Listeria monocytogenes to stainless steel, Appl. Environ. Microbiol. 66 (2000) 860–863.

[6] J.M. Lackner, R. Major, L. Major, T. Schoberl, W. Waldhauser, RF deposition of soft hydrogenated amorphous carbon coatings for adhesive interfaces on highly elastic polymer materials, Surf. Coat. Technol. 203 (16) (2009) 2243–2248.

[7] J. Sarna, R. Kustosz, R. Major, J.M. Lackner, B. Major, Polish artificial heart—new coatings, technology, diagnostics, Bull. Acad. Pol. Sci. 58 (2) (2010) 329–335.

[8] J.M. Lackner, W. Waldhauser, R. Major, B. Major, F. Bruckert, Hemocompatible, pulsed laser deposited coatings on polymers, Biomed. Tech. 55 (2010) 57–64.

[9] R. Major, M. Sanak, P. Wilczek, J.M. Lackner, M. Kot, B. Major, Nanostructural materials for implants and cardiovascular biomedical devices, (chapter in book ImplantExpert) M Studia Zabrze, 2011, pp. 67-90.

[10] E. Decave, D. Garrivier, Y. Brechet, B. Fourcade, F. Bruckert, Shear flow-induced detachment kinetics of dictyostelium discoideum cells from solid substrate, Biophys. J. 82 (2002) 2383–2395.

[11] A. Nicholas, in: B.D. Ratner, A.S. Hoffman, F.J. Shoen, J.E. Lemons (Eds.), Biomaterials Science. An Introduction to Materials in Medicine, second ed., Elsevier, Oxford, UK, 2004, pp. 100–106.

[12] S. Rafii, M.C. Oz, J.A. Seldomridge, B. Ferris, A.S. Asch, R.L. Nachman, F. Shapiro, E.A. Rose, H.R. Levin, Characterization of hematopoetic cells arising on the textured surface of left ventricular assist devices, Ann. Thorac. Surg. 60 (1995) 1627–1632.

[13] H.O. Frazier, R.T. Baldwin, S.G. Eskin, J.M. Duncan, Immunochemical identification of human endothelial cells on the lining of a ventricular assist device, Tex. Heart Inst. J. 20 (1993) 78–82.

[14] Y. Ohta, C. Otsuka, H. Okamoto, Changes in surface roughness of erythrocytes due to shear stress: atomic force microscopic visualization of the surface microstructure, J. Artif. Organs 6 (2003) 101–105.

[15] T. Tsyganov, M.F. Maitz, E. Wieser, E. Richter, H. Reuther, Correlation between blood compatibility and physical surface properties of titanium-based coatings, Surf. Coat. Technol. 200 (2005) 1041–1044.

[16] K. Cai, J. Bossert, K.D. Jandt, Does the nanometre scale topography of titanium influence protein adsorption and cell proliferation? Colloids Surf. B: Biointerfaces 49 (2006) 136–144.
[17] N.B. Naduvinamani, P.S. Hiremath, G. Gurubasavaraj, Effect of surface roughness on the couple-stress squeeze film between a sphere and a flat plate, Tribol. Int. 38 (2005) 451–458.
[18] T.-W. Chung, D.-Z. Liu, S.-Y. Wang, S.-S. Wang, Enhancement of the growth of human endothelial cells by surface roughness at nanometer scale, Biomaterials 24 (2003) 4655–4661.
[19] N. Mirhosseini, P.L. Crouse, M.J.J. Schmidth, L. Li, D. Garrod, Laser surface micro- texturing of Ti–6Al–4 V substrates for improved cell integration, Appl. Surf. Sci. 253 (2007) 7738–7743.
[20] F. Rupp, L. Scheideler, D. Rehbein, D. Axmann, J. Geis-Gerstorfer, Roughness induced dynamic changes of wettability of acid etched titanium implant modifications, Biomaterials 25 (2004) 1429–1438.
[21] B. Chehroudi, D. Maxwell Brunette, Subcutaneous microfabricated surfaces inhibit epithelial recession and promote long-term survival of percutaneous implants, Biomaterials 23 (2002) 229–237.
[22] M. Trtica, B. Gakovic, D. Batani, T. Desai, P. Panjan, B. Radak, Surface modifications of a titanium implant by a picosecond Nd:YAG laser operating at 1064 and 532 nm, Appl. Surf. Sci. 253 (2006) 2551–2556.
[23] D. Khang, J. Lu, C. Yao, K.M. Haberstroh, T.J. Webster, The role of nanometer and sub-micron surface features on vascular and bone cell adhesion on titanium, Biomaterials 29 (2008) 970–983.
[24] A. Gasparetto, V. Zanotto, Optimal trajectory planning for industrial robots, Adv. Eng. Softw. 41 (2010) 548–556.
[25] E. Gambao, C. Balaguer, F. Gebhart, Robot assembly system for computer-integrated construction, Autom. Constr. 9 (2000) 479–487.
[26] K. Trembecka-Wojciga, R. Major, F. Bruckert, J.M. Lackner, P. Lacki, M. Sanak, B. Major, A Computer engineering in designing and fabrication of tissue analogue-type coating dedicated for the cardiovascular regeneration, Arch. Civ. Mech. Eng. 15 (2015) 621–630.
[27] M.V. Sefton, C.H. Gemmel, Nonthrombogenic treatments and strategies, in: B.D. Ratner, A.S. Hoffman, F.J. Schoen, J.E. Lemons (Eds.), Biomaterials Science. An Introduction to Materials in Medicine, Elsevier Academic, San Diego, CA, 2004, pp. 456–470.
[28] U. Hersel, C. Dahmen, H. Kessler, RGD modified polymers: biomaterials for stimulated cell adhesion and beyond, Biomaterials 24 (2003) 4385–4415.
[29] Y. Germanier, S. Tosatti, N. Broggini, M. Textor, D. Buser, Enhanced bone apposition around bio-functionalized sandblasted and acidetched titanium implant surfaces. A histomorphometric study in miniature pigs, Clin. Oral Implants Res. 17 (3) (2006) 251–257.
[30] R. Major, Self-assembling surfaces of blood-contacting materials, J. Mater. Sci. Mater. Med. 24 (2013) 725–733.
[31] S. Sbrana, F. Della Pina, A. Rizza, M. Buffa, R. De Filippis, J. Gianetti, A. Clerico, Relationships between optical aggregometry (type born) and flow cytometry in evaluating ADPinduced platelet activation, Cytometry B Clin. Cytom. 74 (1) (2008) 30–39.
[32] S. Nomura, A. Shouzu, K. Tamoto, Y. Togane, S. Goto, S. Uchiyama, Y. Ikeda, Assessment of an ELISA kit for platelet-derived microparticles by joint research at many institutes in Japan, J. Atheroscler. Thromb. 16 (2009) 878–887.
[33] P. Harrison, Progress in the assessment of platelet function, Br. J. Haematol. 111 (3) (2000) 733–744.

[34] B. Shenkman, N. Savion, R. Dardik, I. Tamarin, D. Varon, Testing of platelet deposition on polystyrene surface under plow conditions by the cone and plate(let) analyser: role of platelet activation, fibrinogen and von Willebrand factor, Thromb. Res. 99 (4) (2000) 353–362.
[35] C.H. Gemmel, Activation of platelets by in vitro whole blood contact with materials: increases in microparticle procoagulant activity, and soluble P-selectin blood levels, J. Biomater. Sci. Polym. Ed. 12 (8) (2001) 933–934.
[36] D. Varon, I. Lashevski, B. Brenner, R. Beyar, N. Lanir, I. Tamarin, N. Savion, Cone and plate(let) analyzer: monitoring glycoprotein IIb/IIIa antagonists and von Willebrand disease replacement therapy by testing platelet deposition under flow conditions, Am. Heart J. 135 (5 Pt 2 Su) (1998) 187–193.
[37] S. Nomura, Y. Ozaki, Y. Ikeda, Function and role of microparticles in various clinical settings, Thromb. Res. 123 (1) (2008) 8–23.
[38] A. Blann, E. Shantsila, A. Shantsila, Microparticles and arterial disease, Semin. Thromb. Hemost. 35 (5) (2009) 488–496.
[39] C.H. Gemmel, S.M. Ramirez, E.L. Yeo, M.V. Sefton, Platelet activation in whole blood by artificial surfaces: identification of platelet-derived microparticles and activated platelet binding to leukocytes as material-induced activation events, J. Lab. Clin. Med. 125 (2) (1995) 276–287.
[40] M.P. Lutolf, P.M. Gilbert, H.M. Blau, Designing materials to direct stem-cell fate, Nature 462 (7272) (2009) 433–441.
[41] H.M. Blau, A. Sacco, P.M. Gilbert, Essentials of Stem Cell Biology. 2, in: R. Lanza, et al. (Eds.) Academic, pp. 249–257 (in press), ISBN: 978-0-12 374729-7.
[42] H.M. Blau, A. Sacco, P.M. Gilbert, Encyclopedia of Stem Cell Research, in: C. Svendsen, A. Ebert (Eds.), Sage (in press), ISBN: 141295908X.
[43] D.T. Scadden, The stem-cell niche as an entity of action, Nature 441 (7097) (2006) 1075–1079.
[44] D.L. Jones, A.J. Wagers, No place like home: anatomy and function of the stem cell niche, Nat. Rev. Mol. Cell Biol. 9 (1) (2008) 11–21.
[45] E. Fuchs, T. Tumbar, G. Guasch, Socializing with the neighbors: stem cells and their niche, Cell 116 (6) (2004) 769–778.
[46] R. Schofield, The relationship between the spleen colony-forming cell and the haemopoietic stem cell, Blood Cells 4 (1–2) (1978) 7–25.
[47] D. Nie, Cancer stem cell and niche, Front. Biosci. (Schol. Ed.) 2 (1) (2010) 184–193.
[48] F.J. King, H. Lin, Somatic signaling mediated by fs(1)Yb is essential for germline stem cell maintenance during Drosophila oogenesis, Development 126 (9) (1999) 1833–1844.
[49] T. Xie, A.C. Spradling, A niche maintaining germ line stem cells in the Drosophila ovary, Science 290 (5490) (2000) 328–330.
[50] T. Tumbar, G. Guasch, V. Greco, C. Blanpain, W.E. Lowry, M. Rendl, E. Fuchs, Defining the epithelial stem cell niche in skin, Science 303 (5656) (2004) 359–363.
[51] T.H. Yen, N.A. Wright, The gastrointestinal tract stem cell niche, Stem Cell Rev. 2 (3) (2006) 203–212.
[52] J.C. Conover, R.Q. Notti, The neural stem cell niche, Cell Tissue Res. 331 (1) (2008) 211–224.
[53] T.A. Mitsiadis, O. Barrandon, A. Rochat, Y. Barrandon, C. De Bari, Stem cell niches in mammals, Exp. Cell Res. 313 (16) (2007) 3377–3385.
[54] H. Ohshima, N. Nakasone, E. Hashimoto, H. Sakai, K. Nakakura-Ohshima, H. Harada, The eternal tooth germ is formed at the apical end of continuously growing teeth, Arch. Oral Biol. 50 (2) (2005) 153–157.

[55] A. Wilson, A. Trumpp, Bone-marrow haematopoietic-stem-cell niches, Nat. Rev. Immunol. 6 (2) (2006) 93–106.
[56] C. Chai, K.W. Leong, Biomaterials approach to expand and direct differentiation of stem cells, Mol. Ther. 15 (2007) 467–480.
[57] K. Saha, J.F. Pollock, D.V. Schaffer, K.E. Healy, Designing synthetic materials to control stem cell phenotype, Curr. Opin. Chem. Biol. 11 (2007) 381–387.
[58] N.S. Hwang, S. Varghese, J. Elisseeff, Controlled differentiation of stem cells, Adv. Drug Deliv. Rev. 60 (2008) 199–214.
[59] E. Dawson, G. Mapili, K. Erickson, S. Taqvi, K. Roy, Biomaterials for stem cell differentiation, Adv. Drug Deliv. Rev. 60 (2008) 215–228.
[60] S.M. Dellatore, A.S. Garcia, W.M. Miller, Mimicking stem cell niches to increase stem cell expansion, Curr. Opin. Biotechnol. 19 (2008) 534–540.
[61] N. Evans, E. Gentelman, J. Polak, Scaffolds for stem cells, Mater. Today 9 (12) (2006) 26–33.
[62] H.M. Blau, A. Sacco, P.M. Gilbert, Encyclopedia of Stem Cell Research, in: C. Svendsen, A. Ebert, (Eds.), Sage (in press), ISBN: 978-0-12-374729-7.
[63] H. Sächtling, Kunststoff-Handbuch, Hanser, München, 1992.
[64] D.S. Rickerby, G. Eckold, K.T. Scott, I.M. Buckley-Golder, The interrelation between internal stress, processing parameters and microstructure of physically vapour deposited and thermally sprayed coatings, Thin Solid Films 154 (1987) 125.
[65] Y.P. Cao, X.-P. Zheng, F. Jia, X.Q. Feng, Wrinkling and creasing of a compressed elastoplastic film resting on a soft substrate, Comput. Mater. Sci. 57 (2012) 111.
[66] R. Huang, Z. Suo, Wrinkling of an elastic film on a viscous layer, J. Appl. Phys. 91 (2002) 1135.
[67] Z. Huang, W. Hong, Z. Suo, Evolution of wrinkles in hard films on soft substrates, Phys. Rev. E Stat. Phys. Plasmas Fluids Relat. Interdiscip. Topics 70 (2004) 030601.
[68] R. Major, K. Maksymow, J. Marczak, J.M. Lackner, M. Kot, B. Major, Migration channels produced by laser ablation for substrate endothelialization, Bull. Pol. Acad. Sci. Chem. Techn. Sci. 60 (2) (2012) 337–342.
[69] S. Yang, K. Leong, Z. Du, C. Chua, The design of scaffolds for use in tissue engineering, part I, traditional factors, Tissue Eng. 7 (2001) 679–689.
[70] J.H. Wang, F. Jia, T.W. Gilbert, S.L. Woo, Cell orientation determines the alignment of cell-produced collagenous matrix, J. Biomech. 36 (1) (2003) 97–102.
[71] A.P. Joglekar, H. Liu, G.J. Spooner, E. Meyhofer, G. Mourou, A.J. Hunt, A study of the deterministic character of optical damage by femtosecond laser pulses and applications to nanomachining, Appl. Phys. Lasers Opt. B 77 (2003) 25–30.
[72] Y. Liua, S. Sunb, S. Singhaa, M.R. Chob, R.J. Gordon, 3D femtosecond laser patterning of collagen for directed cell attachment, Biomaterials 26 (22) (2005) 4597–4605.

Improving the hemocompatibility of biomedical composites

13

G. Voskerician
Case Western Reserve University, Cleveland, OH, United States

13.1 Introduction

This chapter introduces current developments in improving the hemocompatibility of biomedical composites in contact with the circulating blood. The technological advances will be introduced in the context of the clinical problem and relevant pathology. Three clinical applications will be addressed: heart valves, vascular grafts, and stents.

To ensure clarity and purpose, two fundamental definitions applicable to this chapter are introduced: biomedical composite and hemocompatibility.

The active debate in defining a composite material continues. The source of the debate is the perception in the context of a specific field, be materials science, composite engineering, biomedical engineering, or clinical science. While the community agrees to disagree on the definition of what a composite material means, it must be stated that none of the definitions are incorrect. Each definition is correctly applied in the context in which it is used. For the purpose of this chapter, a biomedical composite is defined as consisting of two or more distributed active components with overall tailored properties not depicted by any of the components in isolation. The tailored properties meet a specific functional need dictated by the particular composite biomedical application(s).

The debate further extends to defining hemocompatibility. In this case, the challenge is compounded as refined understanding of blood contacting performance requirements still lack. The fundamental requirements currently establishing the blood-compatibility "grade" of a biomaterial (composite or otherwise) include functionality within the cardiovascular system + a set of specific "do not's": (1) no platelet adhesion, (2) no thrombogenicity, (3) no pro-inflammatory, and a "do": (4) pro-healing.

The field of biomedical material and device development (composite or otherwise) has ushered an explosion of technological innovations over the past several decades. Yet, the bedside adoption certainly does not reflect the innovative boom. Two particular obstacles deserve attention: (1) absence of translational research focus in academic research (the main hotbed of innovation), and (2) cautious, sluggish, and expensive regulatory pathways, with (at times) unrealistic/confusing demands on validation. Such demands, more often than not, are the result of a regulatory infrastructure that keeps playing "catch-up" to the ongoing innovation wave.

The roadmap of this chapter takes the reader through each clinical application device category (heart valves, vascular grafts, and stents). Within each category, the clinical burden and associated pathophysiological problem are stated. Then, the current innovation towards more effective blood-surface interactions is introduced.

Hemocompatibility of Biomaterials for Clinical Applications. https://doi.org/10.1016/B978-0-08-100497-5.00010-0
© 2018 Elsevier Ltd. All rights reserved.

13.2 Design criteria of blood contacting devices

The design criteria for the ideal hemocompatible device must address both structural and functional requirements. The structural requirements refer to meeting the anatomy of the diseased structure being replaced/augmented in terms of placement, size, and macro/micro-architecture, while the functional requirements address the appropriate flow/blood pressure needs across the valve with its inherent hemocompatibility behavior. While for the purpose of providing some categorization context, it might be useful to separate the design criteria as described above, device design must consider their symbiotic action. For example, hemcompatibility is dependent on physiological forces across the device, its functional characteristics, as well as the type of structural materials being used, their size and aspect. Simply put, each category heavily depends on the other, in a vicious cycle that appears to defy the human capacity to achieve the perfect replacement (as good as the original at all levels of structure and function).

This is the point where the "design compromise" comes into play, and the debate on which parameters are more important stirs the scientific and clinical communities. Ultimately, the debate is settled by its most limiting decision body, the regulatory guidelines that ask (in this specific order): (1) is the device safe, (2) is the device effective in addressing the clinical need, and (3) does the device (reasonably) meet patient's life-style needs (what are the complications the patient hopes to minimize/eliminate—a gray area that remains quite subjective and very much device and disease stage dependent).

Therefore, hemocompatibility is not limited to blood-material surface interaction. It is not solely characterized by blood-surface interaction, but emerges from a symbiotic blend of structural and functional design criteria. It must be recognized that the limiting factor in qualifying the device as hemocompatible is its blood-surface behavior. If the surface is not hemocompatible, then irrespective of function and macro/micro-architecture, the device will fail. While recognizing the multidimensional and symbiotic relationship between surface and bulk, the material introduced will strictly address blood-surface solutions.

The general principles of preparing a surface for a particular interaction remain the same whether the interaction is with circulating blood or in an in situ static environment (where blood is present). The intention is to control the deposition of proteins, the generation of thrombin leading to blood coagulation, the platelet adhesion followed by aggregation and activation, and the surrounding tissue environment response to the presence of the replacement (cellular migration/inhibition, scar formation, etc.). Physical, chemical, and biofunctional methods have been developed to (theoretically) achieve various degrees of hemocompatibility. The goal of these techniques is to present a less "foreign" surface to the circulating blood and stimulate a close-to-natural process of healing/integration within the native environment.

Physical techniques help modify the surface topography. Manipulating surface topography can provide a selective method of including/excluding the surface binding of various blood entities based on size. While perhaps crude, this physical technique provides a venue to manipulate surface roughness in meeting particular inclusion/exclusion criteria. One practical aspect of this approach is manipulating the surface

porosity to allow the absorption of smaller structures (such as proteins) but ensure that larger structures (cells) are not trapped within its pores. Surface roughness also impacts the possibility of blood cells navigating over its surface. A rough surface will lead to high shear of the circulating blood and its components resulting in undesirable (especially) cellular damage, as these components come in contact with the surface. Some of the more advanced physical modification techniques include deposition of polymer films/islands, nanoparticles, metallographic paper or diamond paste polishing, sand blasting, photolithography, and e-beam etching.

Physical techniques expand beyond surface roughness and into physical immobilization intended to enhance the inherent material properties towards an improved degree of hemocompatibility. Some of these methods include polymer gelling (addition of growth factor cocktails in the liquid state of the material; addition of components that modify the inherent pH/chemical balance leading to the formation of controlled nano-pores) emulsion techniques (addition of factors insoluble in aqueous solutions) or high pressure gas foaming (incorporation of growth factors into porous scaffolds, without the use of solvents).

Chemical techniques help manipulate the manner in which blood bound components "see" the device surface. One established example is surface wettability (measure using contact angle methods). The method that achieves various levels of wettability directly modulates the hydrophobicity/hydrophilicity of the surface to meet specific blood contacting requirements. Techniques include ion bombardment, UV irradiation, or exposure to plasma discharge. In addition, given the nonfouling degree of the material used, its hemocompatibility can be enhanced through the process a "passivation" to achieve a nonadhesive, nonbiofouling surfaces. Polymers such as PEG (polyethylene glycol), hydrogels (containing dextran), and PEO (polyethylene oxide) have been recognized to enhance overall hemocompatibility of the original material.

Chemical functionalization is also used to improve the degree of hemocompatibility. Covalent modifications that include surface and bulk distribution of ligands have been proven useful. Additionally, passive adsorption driven by secondary interactions between the native surface chemistry and targeted proteins has led to modulating blood interaction behavior. Self-assembled monolayers adsorption of a specific peptide (typically designed with hydrophobic tail and a spacer) from solution have also led to modulating the manner in which blood proteins and cells interact with the device surface. The direct protein patterning techniques (drop dispersing, microfluidic patterning) play a growing role in modulating blood-surface interactions. Finally, direct and chemical surface crosslinking add to the battery of methods used to improve hemocompatibility.

Biofunctionalization techniques refer to methods that allow material functionalization using cells. The intent is to create a structure that closely resembles the native tissue and/or improves its integration within the local environment. This particular drive is championed by the field of stem cell technology. Here, progenitor stem cells are employed for the purpose of recreating anatomically and functionally the healthy native human environment. Then, diseased tissues are replaced with healthy native tissues readily functional and integratable within the replacement environment. The use of cellular entities has also led to recognition of providing a fairly familiar

environment for these cells to populate the material and thrive. Extensive research has been performed on the importance of the extracellular matrix (ECM) common to any biological structure, its architecture, and biological reservoir of cell signaling motifs and growth factors, critical to cradling the correct development of progenitor stem cells toward biologically relevant and appropriate morphology and function.

13.3 Heart valves

13.3.1 The problem

Heart valve disease is ranked high among the leading causes of death worldwide [1]. Every year almost 300,000 patients undergo valve replacement surgery, with a projected 850,000 procedures being performed annually by 2050 [2]. The structure and function of the normal heart ensures that blood is pumped from each atrium to the respective ventricle, as well as from the ventricles into the circulatory system. The aortic valve is particularly important, as it directs blood through the aorta and coronary arteries. The efficiency of valve performance is controlled by its complex anatomical geometry and heterogeneous tissue biomechanics [3]. As a result of congenital malformations and/or acquired valve disease, the valve shape and/or tissue mechanics are compromised, leading to the narrowing of valve orifice area (stenosis) or leaking back into the immediate upper chamber(s) of the heart (regurgitation). This results in impaired cardiac function by blood leaking back into the atria or by requiring the heart chambers to contract above the normal range to move blood across a narrowed valve. It has been recognized that valve disease (and especially aortic valve disease) is a significant cause of morbidity and mortality [4]. In rare cases, the valve can be repaired, but for the majority of patients the only option is valve replacement [5].

The cause of valvular heart disease varies. The presence of chronic disease due to aging represents a major cause of defective valves. Investigation of clinical mechanisms of disease has linked valve disease to a triggering event of the past, for example rheumatic fever. The anatomy and physiology of the heart is affected by a number of changes such as bacterial and viral infections, or inflammatory disease (endocarditis). These events lead to the stiffening of the valve leaflets, therefore impairing normal function. An additional cause of valvular disease stems from congenital defect in the embryologic development of the heart. This aspect usually manifests in young individuals. Valvular disease also manifests as a developing comorbidity to a primary chronic disease, such as coronary artery disease (CAD), cardiac hypertrophy, and cardiac dilation.

Valvular defects belong to one of the following categories: stenosis or insufficiency. It is typical to see in a patient a combination of the two, with various contributions. Valvular stenosis is characterized by reduced cross-section area of the opened valve resulting from thickening and increased rigidity of the valve leaflets. Clinical investigation has often associated stenosis with an ongoing process of leaflet calcification. The result is reflected in abnormally high blood pressure in the proximal chamber, and abnormally low blood pressure in the distal chamber, in reference to the valve.

Valvular insufficiency is manifested when the leaflets do not completely seal when the valve is closed. The result is leakage of the blood into the proximal chamber (also known as blood regurgitation).

13.3.2 Pathology

The hemocompatiblity of heart valves is pathologically evaluated based on the presence or absence of thrombi. The event could be examined from two perspectives: (a) role of the prosthetic valve design in inducing thrombi formation; and (b) role of the environment in driving thrombi formation.

When addressing the design of the prosthetic valve, the first requirement that emerges is the behavior of the material (composite) in contact with blood, itself, as well as at the suture site. The traditional phenomena of the inflammatory and wound healing response help explain the behavior. The molecular components' interactions between the plasma proteins and the prosthesis itself lead the natural progression towards healing in the presence of what is recognized by the body as “foreign.” The body's response attempts to wall-off/repair the “foreign” presence, as it is programmed to do. The less “foreign” the material surface appears to the body, the less aggressive the inflammatory and wound healing mechanisms tends to be. Hence, the challenge of achieving acceptable bio/hemocompatibility emerges. Another valve design parameter affecting thrombus formation is the hemodynamic characteristics of the prosthesis. The hemodynamic profile of the prosthesis is designed to minimize/eliminate turbulent flow, yet the uniqueness of each patient (hemodynamic flow, severity of the condition, geometry of the implant location, etc.) does lead to an impossibility in perfectly designing an off-the-shelf valve for that one patient, instead, the closest fit prosthetic valve is used.

When considering the role of the prosthetic valve design parameters, the environmental factors must be considered in evaluating the overall hemocompatibility efficacy. Specifically, low flow or reduced cardiac output leads to the formation of thrombi. This phenomenon results from the extended exposure of proteins and platelets with the surface of the prosthesis. Further, hemostatic factors come into play as a result of the prescribed anticoagulation treatment. The risks are life-impacting: (a) overanticoagulation therapy could lead to life threatening hemorrhagic complications, while (b) underanticoagulation could lead to early thrombosis.

Roudaut et al. report that thrombi are a subacute or chronic phenomenon. They are the result of dynamic formation and maturation of various clot layers with individual levels of organization. The authors further signal the connection between fibrous pannus formation at the suture site and thrombus presence in 45%–75% of prosthetic valve replacement cases.

13.3.3 Improving overall hemocompatibilty

Hemocompatibility is a direct extension of the overall prosthetic valve design. As previously introduced, each valve design parameter will affect to some extent the response of the blood when contacting the surface of the prosthesis. Some of the most

innovative approaches to building prosthetic valves are discussed, with direct reference to improving overall hemocompatibility.

Duan et al. report on the preparation of an aortic valve using 3D printing of a composite alginate/hydrogel heterogeneous structure, with subsequent addition of pertinent cells to the structure [6]. Their primary goal is to offer a more hemocompatible solution to the mechanical valve design that requires life-long anticoagulation therapy to control thrombus formation. The advent of 3D printing had entered the field of biomedical engineering almost a decade ago. The field had moved from simple bioprinting of hydrogel "slabs" [7–9] to that of high resolution geometric structures, featuring rapid prototyping techniques capable of generating intricate constructs, using specific anatomical blueprints [10–12].

Duan et al. have taken advantage of these advancements to develop an interesting prosthetic valve manufacturing protocol using 3D bioprinting, layer-by-layer of custom gelatin/hydrogel formulations and cells. The aortic valve conduits were bioprinted with smooth muscle cells (SMCs) in the valve root, and valve leaflet interstitial cells (VIC) in the leaflets [6]. The goal was to fabricate a living heterogeneous aortic valve conduit free of thrombi formation. This proof-of-concept demonstrated that the composite material maintained its mechanical properties at the early 7 days time point for which they were evaluated. Additionally, the embedded cells displayed normal function and viability. In a subsequent work [13], the group was able to demonstrate the human VIC viability over time and the subsequent deposition of a human native matrix by these cells. These encouraging results indicate the potential of the native valve cells to reestablish the macro and micro frame within which they survive and function.

The fabrication of live aortic valve conduits that display correct anatomical and functional properties is expected to lead efforts in bringing valve replacement design one step closer to the structure and function of a normal human heart valve. A concern here is the in situ behavior, especially sustaining the appropriate functional properties over time (especially dynamic mechanical stress). It is possible that the intent here is to create a live in vitro prosthetic valve "made to order" for each patient that when fully functional would be ready to be implanted as a replacement to the diseased counterpart. While for the scientific community this approach is far from being qualified as Sci-Fi, the current regulatory venues to endorse such a product for clinical use are virtually nonexistent.

Eslami et al. maintain that hydrogels are not mechanically suitable to withstand dynamic mechanical stress therefore, a fiber reinforced hydrogel scaffold would be a more realistic solution to heart valve replacement [14]. The research group increases the "stakes" in prosthetic valve replacement by acknowledging the current thrombi formation/anticoagulation therapy problem, along with failure characteristics of the current bioprosthetic heart valves such as calcification and mechanical failure [2,5].

The research group recognizes the importance of replicating the micro and macro environments within which the specialized cells pertinent to the anatomical and functional properties of the valve reside and thrive [14]. This approach opens the door to shifting the solution from an inanimate valve replacement to a valve replacement that grows "along with the patient." Especially for the pediatric patient population such

approach could lead to eliminating the need of recurring replacements. This design is specifically concerned with the long-term mechanical performance of the valve along with ensuring that the cellular environment resembles that of a normally functioning valve. Here, the implanted valve is expected to mature over time, in sync with the body's natural growth and development.

Masoumi et al., of the same Harvard research group (Eslami et al.) proposed a tri-layered elastomeric scaffold for engineering heart valve leaflets. While the ultimate goal remained the same, eliminating thrombi formation, the solution approached the problem from a slightly different perspective [15]. In this case the group intended to address the problem of mimicking the structural as well as the anisotropic mechanical characteristics of the native valve leaflets. As in the previous report, a combination of biodegradable (co)polymers was selected to provide the original matrix for the seeding and survival of VIC and mesenchymal stem cells. In addition, the individual layers were carefully designed and oriented along anisotropic axes in an effort to resemble the native leaflet. The complexity of the regulatory path is evident, very much in line with that associated with the group's previous work [14].

13.4 Vascular grafts

13.4.1 The problem

Atherosclerosis, including CAD, cerebrovascular disease, and peripheral arterial disease, is one of the most common causes of death and disability in the United States and throughout the world [16,17]. More than 25 million people in the United States have at least one clinical manifestation of atherosclerosis, and in many more individuals, atherosclerosis remains a latent precursor of significant CVD events, including MI and stroke [16,17].

Although advanced pharmacological and minimally-invasive techniques offer a growing therapy option [18], a surgical bypass of blood vessels on the heart or on a lower extremity remains the procedure of choice in a number of patients [19]. Over decades of clinical application, it was found that this approach is also more cost-effective, and in particular preserves the quality of the patient's life better than primary amputation of a limb. A synthetic tube or a vascular prosthesis has to be implanted when the patient's own artery or vein is not available. After more than half a century of development work, the results achieved with currently available materials are not optimal in terms of healing and tissue regeneration.

Arterial prostheses procedures are performed in 1.4 million Americans every year [20]. The vascular graft replacement options offer limited clinical success, with an annual price-tag to the healthcare system of $25 billion [20]. The clinical success “bottle-neck” is the result of vascular replacements of medium and small diameter vascular grafts, associated with the highest incidence of death [21,22]. The currently available options are: autologous grafts (e.g. coronary artery bypass graft with autologous mammary arteries and saphenous veins), allografts (donor/cadaveric), xenografts (e.g., bovine or porcine pulmonary valve conduit), and artificial prostheses

or synthetic vascular grafts made of expanded polytetrafluroethylene (ePTFE) and polyethylene terephthalate (PET) [23].

The major impediment to the use of autografts and allografts is the lack of tissue donors, previous autologous harvesting, or anatomical variability [24]. Xenografts have been reported to offer limited patency. Significant concerns related to the long-term functionality are specifically related to the current protocols of decellularization, in addition to limited control over physical and mechanical properties, inflammation, and calcification [25]. Especially in pediatric procedures, the limited life-span offered by current xenografts indicate the need of a subsequent procedure. Synthetic vascular grafts, especially those <6 mm in diameter are rejected by the body within a few months from graft replacement. Reocclusion as a result of thrombosis aneurysm, and intimal hyperplasia due to mismatch of compliance (compliance is the opposite of stiffness, measured as the strain/expansion or contraction of the graft with force) represent the primary modes of failure [24–27].

13.4.2 Pathology

Atherosclerosis is a disease process that is triggered by sometimes subtle physical or chemical insults to the endothelial cell (EC) layer of arteries. The "Response to Injury Theory" now has widespread acceptance among scientific and medical scholars [16,17]. This theory holds that the earliest event in atherogenesis is injury to the endothelium, which can be triggered by any number of insults, either alone or in combination. These include [17,28]:

- Physical injury or stress as a result of direct trauma or hypertension.
- Turbulent blood flow, for example, where arteries branch.
- Circulation of reactive oxygen species (free radicals), e.g., from smoking or air pollutants.
- Hyperlipidemia (high blood concentrations of low-density lipoprotein (LDL) or very low-density lipoprotein (VLDL)).
- Chronically elevated blood glucose levels.
- Homocysteinemia, which results from an inherited metabolic defect that leads to very high levels of the homocysteine, a metabolite of methionine; high concentrations are toxic to the endothelium.

The injured endothelium leads to the initiation of an inflammatory response. Specifically, the injured endothelium initiates the production of cell surface adhesion molecules such as VCAM-1, causing monocytes and T-lymphocytes to adhere to the endothelium. In a subsequent stage, the inflammatory populations are able to infiltrate the vascular construct by literally squeezing between the endothelial junctions.

This process leads to EC morphological changes, and loosening of the EC tight junctions, therefore increasing the permeability to fluid, lipids, and leukocytes. Lipoprotein particles, and especially LDL, enter the arterial wall and undergo oxidation. Oxidation of LDL in the arterial wall occurs as a result of its exposure to nitric oxide, macrophages, and some enzymes such as lipoxygenase. Once they have migrated into the intima, monocytes differentiate into macrophages and begin to take up oxidized LDL now present in the intima. Macrophages retain the lipid they take up, and as they become more lipid-laden, they are referred to as "foam cells." Eventually, the foam cell will undergo apoptosis and die, but the lipid will accumulate in the intima. This process leads to the formation of macroscopically identifiable "fatty streaks."

13.4.3 Improving overall hemocompatibilty through in vitro and in situ endothelialization

ECs create a thromboprotective surface at the interface between the substrate (native or engineered vessel) and the circulating blood. The thromboprotective behavior manifests itself through the expression of anticoagulant, and fibrinolytic agents [29,30]. Thrombomodulin, heparan sulfate, nitric oxide (NO), and prostacyclin (PGI2) have all been established as antithrombotic factors modulating coagulation. Further, the endothelium gates and controls the exchange of macromolecules across its layer, therefore modulating the activity of the SMCs contraction and influencing vascular remodeling [29,30].

Biofunctionalization of a scaffold (decellularized vessel conduit, biodegradable as well as nonbiodegradable material) can be performed via the "usual suspects" methods: surface adsorption of molecules and chemical immobilization.

De Visscher et al. used simple adsorption protocols to coat Gelsoft and Polymaille C (knitted polyester precoated with collagen) with fibronectin and stem cell homing factor SDF-1α [31]. The outcomes showed improved EC coverage and adherence, as well as reduced intimal hyperplasia and thrombotic material aggregation. It is however recognized that surface adsorption is typically temporary, especially under conditions of shear stress, and adsorption, in general lacks control over ligand orientation [31].

Therefore, when possible, chemical functionalization is preferred. Covalent linkage offers control over the distribution and orientation of bioactive molecules on surfaces. It has been shown to be effective in improving EC retention of various polymers. For example, Krijgsman et al. enhanced EC retention of a poly(carbonate-urea) urethane graft with arginylglycylaspartic acid (RGD peptide) and heparin [32]. Chemical functionalization relies on the affinity between the polymer and the ligand. This type of specificity leads to the development of unique polymer-ligand protocols to ensure covalent immobilization and retainment of ligand activity [33].

The local hemostatic environment is therefore influenced by the presence of native ECs. In 1997, Asahara et al. isolated circulating endothelial progenitor cells (EPCs). The group was able to differentiate the isolated EPCs into an endothelial-like phenotype therefore establishing a new source of autologous ECs [34]. Among the phenotypically and functionally diverse EPCs family, a population termed endothelial outgrowth cells (EOCs) have shown promise in regulating thrombosis by controlling several components of the hemostatic environment [35–44]. Two primary strategies have been employed in an attempt to improve the thromboprotective role of EOCs, preconditioning under shear stress and thrombomodulin overexpression through genetic modification [37,42,44–47].

The success of a substrate-EOC composite builds on the seeded EOCs behavior. Consequently, the role of the substrate is essential. It has been recognized that synthetic materials lack the instructional biological cues inherent to the native ECM. As outlined by Glynn et al, examples of such cues include 3D topography instrumental in cell alignment and adhesion, in addition to biochemical signals such as growth factors [48]. Two specific strategies have shown reasonable success in sustaining the EOCs thromboprotective role—blood vessel decellularization followed by in vitro

reseeding, and SMC seeding on biodegradable scaffolds to create a de novo tubular conduit, thereafter seeded with EOCs [49–52].

However, what if the multiple steps associated with the ECs/EOCs seeding could be eliminated, to be replaced with an implantable material capable of recruiting circulating ECs/EPCs?

EPCs levels in circulation are considered relatively low, especially in the patients who need bypass grafts and elderly [53]. Therefore, the first step in improving in situ endothelialization led to the development of strategies that increase the number of circulating EPCs [54]. Research has identified a number of factors active in increasing the number of circulating EPCs, such as vascular endothelial growth factor [55], stromal cell-derived factor-1 (SDF-1) [56], granulocyte-colony stimulating factor (G-CSF) [57], HMG-CoA reductase inhibitors (statins) [58], erythropoietin (EPO) [59], and angiotensin II antagonists (e.g., Irbesartan) [60]. These, along with other factors, can be released systemically or at location (biocomposite controlled release) to achieve the set goal.

After ensuring that the number of circulating EPCs is increased, the biocomposite must provide the suitable exposed blood-surface chemistry to attract EPCs adhesion. An extensive review of various functionalization and mechanical modification methods for in situ EPCs adhesion has been recently published by Goh et al. [61].

The currently active investigations in surface immobilization include antibodies, nucleic acid sequences, oligosaccharides, and magnetic homing protocols. The immobilization of antibodies strategy takes advantage of the affinity between the surface-antibody biocomposite and the EPC or EC specialized cell marker that recognizes it. EPCs surface markers that can potentially be used as a target for antibody-immobilized grafts are: CD133, kinase insert domain receptor (KDR), and CD34 [62]. Further, ECs marker targets for antibody immobilized surfaces include: CD31 and KDR [63,64]. The functionalization of DNA sequences with specific groups via chemical coupling has gained attraction and success recently [61]. Schleicher et al. reported success in biofunctionalizing polystyrene and ePTFE to attract EPCs and ECs adhesion [65]. One oligosaccharide that has been evaluated for its potential to enhance surface endothelialization is hyaluronic acid (HA). Studies accomplishing incorporation of HA into the PU backbone or being used as surface-modified hydrogels reported promising results [66,67]. Ruiz et al. further reported on the thromboprotective behavior of low molecular weight HA in surface endothelialization [67]. Magnetic homing represents a relatively incipient development in attracting EPCs/ECs surface adhesion. Fayol et al. reported on the development of a continuous endothelium as a result of EPC labeled iron oxide nanoparticles [68]. As more investigations are performed, concerns related to the potentially harmful activity of magnetic nanoparticles in the proliferation and metabolism of ECs and associated cell families will require to be further addressed [69]. The active research in the field of biofunctionalization shows great potential as a viable venue of promoting endothelialization in cardiovascular grafts.

Micropatterning and nanopatterning has been employed for decades in an attempt to enhance “surface presentation” to the biologic environment. Specific to vascular grafts, the physical and mechanical properties of graft surfaces represent determining factors in the process of endothelialization. Interestingly, stem cells have been

reported to respond to topographical cues independent of the surface chemistry [70]. The micro- versus nano-scale research brings together investigations on the relevance of each patterning venue, with its advantages and disadvantages [71]. A balance between the practicality of micropatterning and the biological relevance of nanopatterning is yet to be achieved.

13.5 Stents

13.5.1 The problem

CAD is the leading cause of death in the world, and was responsible for 7.4 million deaths in 2012 [72]. Major advances in treatment and technology have led to a reduction in age-related cardiovascular deaths over the past several decades [73]. However, the prevalence of CAD is projected to further increase as a result of the growing epidemic of obesity and its consequences, including hypertension, dyslipidemia, and diabetes [73].

Dr. Andreas Grüntzig performed the first balloon angioplasty to correct [known as percutaneous coronary intervention (PCI)] in 1977. The limitations of balloon angioplasty however included an acute vessel closure and a relatively high rate of restenosis at the site of the lesion. This outcome led to the development of stent technology. Stent implantation led to stabilization of the disrupted plaque leading to less vessel thrombosis [74]. As the advantages of stent implantation experienced its evolution from a "bail out" procedure after complicated balloon angioplasty to a standard treatment strategy, two important limitations were recognized: early acute vessel closure due to stent thrombosis (ST), and the onset of late stent failure due to in-stent restenosis [74].

ST is one of the most serious complications of PCI. The majority of ST occurs within the first 30 days after PCI. The expected rate of early ST is ~1%, and beyond 30 days it is 0.2%–0.6% compounded annually [75].

First-generation drug eluting stents (DES) have led to a steady annual rate of 0.4%–0.6% of thrombosis for up to 4 years [76]. Unfortunately, the incidence of thrombosis associated with bare metal stents (BMS) has been poorly characterized and documented, with some literature suggesting a compounded 2% predicted thrombosis at 10 years [77]. Metaanalyses of existing clinical trial outcomes have led to assigning incidence of thrombus formation to each type of stent. Specifically, it was found that DES average a 0.1%–0.4% incidence of thrombosis compared to BMS category found to induce thrombosis in 1% of cases [78]. While the rate of ST appears seemingly low, the alarming fact remains that its incidence is responsible for 20%–45% mortality, and 50%–70% myocardial infarction [79,80]. Kirtane et al. also reported that approximately 20% of patients who have ST will have a recurrent episode within 2 years [80].

13.5.2 Pathology

The pathogenesis of ST is led by the manner in which the vascular injury affects the endothelium. Vascular injuries result in typical response of neointimal formation characterized by intimal thickening as a result of SMC proliferation [81]. An autopsy

registry study found that the external elastic lamina, plaque area, and stent area were significantly greater in lesions with thrombus presence [82]. In the case of incidence of ST 1 year after vascular positioning, the DES category leads the incidence of failure. A multifactorial etiology has been proposed, submitting that the outcome is likely associated with an abnormal vascular response, such as hypersensitivity reaction, excessive fibrin deposit, or neoatherosclerosis [83,84].

Recently, a new term has been coined—neoatherosclerosis, or atherosclerosis within the neointima. Neoatherosclerosis is described as a macrophage clusters with or without calcification, thin-cap fibroatheromas, and plaque ruptures without communication with the underlying native atherosclerotic plaque [83]. Autopsy registries have helped determine that in the case of late onset of ST neoatherosclerosis was significantly more prevalent in the DES category (31%) than the BMS counterpart (16%) [85]. It has also been recognized that neoatherosclerosis accompanied by neointimal rupture represent an important factor of DES thrombosis [86].

13.5.3 Improving overall hemocompatibilty

Stents can generally be described as tubular scaffolds manufactured from a wire mesh or a slotted tube. They are either self-expanding or balloon-expandable. The "high-traction" used in stent manufacturing are stainless steel and cobalt-chromium alloys for balloon-expandable stents, and nickel-titanium alloys (nitinol) for self-expanding stents [87]. Despite their efficacy, the occurrence of stent restenosis led to advancements in stent design through the introduction of the DES. Beyond DES, biodegradable and DES biodegradable stents have subsequently been developed.

In a recent pathological study, Otsuka et al. indicated that the newer generation durable polymers continue to be a source of inflammation, neoatherosclerosis, and thrombosis risk [88]. Additional findings have reported that damage to the polymer in a DES can cause polymer embolization in cases undergoing complex procedures [89–91]. Therefore, it is expected that the use of polymer-free DES would eliminate this current DES shortcoming. Designing a polymer-free DES requires a solution that would replace the current controlled drug delivery profile supported by the polymer substrate of the DES. Aoki recommends several approaches, currently in various stages of development [92]:

- using nonpolymeric drug carriers, such as hydroxyapatite, coated onto the surface of the stent
- using the stent surface nanopatterning to pack the drug
- using sophisticated chemistry to attach the drug covalently onto the surface of the stent
- using hollow stent struts to contain the drug filling the drug

The increased strength of the relatively recently manufactured metal alloys has allowed for abluminal reservoirs to be made without affecting overall stent strength [93]. Several similar designs utilizing different drugs have recently been tested against prior and current generation DES, and in early studies have demonstrated noninferiority with up to 1-year follow-up [94,95]. McGinty et al. recently modeled drug elution from polymer-free arterial drug-eluting stents [96]. The algorithm can be customized to modeling drug elution from a number of polymer-free systems.

Drug eluting metal stents are currently considered the "gold standard," with the recognized limitations: chronic local inflammatory reaction due to permanent implantation of a foreign body, restriction of vascular vasomotion due to a metal cage, and the risk of late and very late ST [97,98]. The introduction of the biodegradable stent design has been initiated to circumvent those limitations. Theoretically, the design goal is to ensure short-term scaffolding support and basis for drug release, then dissolve, therefore, alleviating the limitations of the drug eluting metal stents. Specifically, due to stent degradation, the long-term presence of a foreign body in the vessel is minimized. Consequently, the occurrence of late and very late ST is minimized/eliminated [98]. The biodegradable materials being considered reflect the primary understanding and performance evaluation status of established biodegradable polymers, especially the polylactic acid family [97,98]. Other biodegradable stent design materials being investigated include magnesium, tyrosine polycarbonate, and polylactic anhydride-*co*-salicylic acid [98].

13.6 Conclusion

The design criteria of blood contacting devices are expected to preferably promote endothelial adhesion but resist other local mechanisms that can give rise to thrombosis and intimal hyperplasia. A greater understanding of the pathophysiology of disease dynamics as well as postimplantation/repair interactions of blood proteins with material surfaces will enable better designing of surfaces for blood contact. With the advent of innovation in manufacturing, current limitations in surface and bulk processing unable to meet specific biological criteria will be minimized and subsequently eliminated. However, for the solutions to reach bedside, two fundamental components must symbiotically merge. First, the process of design and product development to the stage of Phase I clinical trials must be accelerated. This phase, known as translational research, performed in majority by academic centers is often unfocused and punctuated in its cadence. Second, the regulatory infrastructure necessary to evaluate safety and efficacy of such devices must be enhanced and streamlined to be prepared to move at a reasonable pace a device towards approval and market release. Currently, the regulatory bodies, unfortunately, focus on "reacting" to a product submission rather than being prepared to address the novel technology. In this continuum of obstacles, unfortunately, often the patient and his need is lost in the intricate folding of biocompatible composite design and validation.

References

[1] D.T. Simionescu, J. Chen, M. Jaeggli, B. Wang, J. Liao, Form follows function: advances in trilayered structure replication for aortic heart valve tissue engineering, J. Health Care Eng. 3 (2012) 179–202.

[2] M.K.S. Loftin, Y.W. Chun, A. Khademhosseini, W.D. Merryman, EMT inducing biomaterials for heart valve engineering: taking cues from developmental biology, J. Cardiovasc. Transl. Res. 4 (2011) 658–671.

[3] J.T. Butcher, G.J. Mahler, L.A. Hockaday, Aortic valve disease and treatment: the need for naturally engineered solutions, Adv. Drug Deliv. Rev. 63 (2011) 242–268.
[4] R.B. Hinton, K.E. Yutzey, Heart valve structure and function in development and disease, Annu. Rev. Physiol. 73 (2011) 29–46.
[5] E. Filova, F. Straka, T. Mirejovsky, J. Masin, L. Bacakova, Tissue-engineered heart valves, Physiol. Res. 58 (2009) S141–S158.
[6] B. Duan, L.A. Hockaday, K.H. Kang, J.T. Butcher, 3D bioprinting of heterogeneous aortic valve conduits with alginate/gelatin hydrogels, J. Biomed. Mater. Res. A 101 (5) (2013) 1255–1264.
[7] S.J. Li, Z. Xiong, X.H. Wang, Y.N. Yan, H.X. Liu, R.J. Zhang, Direct fabrication of a hybrid cell/hydrogel construct by a double-nozzle assembling technology, J. Bioact. Compat. Polym. 24 (2009) 249–265.
[8] L. Pescosolido, W. Schuurman, J. Malda, P. Matricardi, F. Alhaique, T. Coviello, P.R. van Weeren, W.J.A. Dhert, W.E. Hennink, T. Vermonden, Hyaluronic acid and dextran-based semi-IPN hydrogels as biomaterials for bioprinting, Biomacromolecules 12 (2011) 1831–1838.
[9] A. Skardal, J.X. Zhang, G.D. Prestwich, Bioprinting vessel-like constructs using hyaluronan hydrogels crosslinked with tetrahedral polyethylene glycol tetracrylates, Biomaterials 31 (2010) 6173–6181.
[10] C.C. Chang, E.D. Boland, S.K. Williams, J.B. Hoying, Direct-write bioprinting three-dimensional biohybrid systems for future regenerative therapies, J. Biomed. Mater. Res. Part B 98B (2011) 160–170.
[11] B. Guillotin, F. Guillemot, Cell patterning technologies for organotypic tissue fabrication, Trends Biotechnol. 29 (2011) 183–190.
[12] V. Mironov, N. Reis, B. Derby, Bioprinting: a beginning, Tissue Eng. 12 (2006) 631–634.
[13] B. Duan, L.A. Hockaday, K.H. Kang, J.T. Butcher, 3D printed trileaflet valve conduits using biological hydrogels and human valve interstitial cells, Acta Biomater. 10 (5) (2014) 1836–1846.
[14] M. Eslami, N.E. Vrana, P. Zorlutuna, S. Sant, S. Jung, M. Masoumi, R.A. Khavari-Nejad, G. Javadi, A. Khademhosseini, Fiber-reinforced hydrogel scaffolds for heart valve tissue engineering, J. Biomater. Appl. 29 (3) (2014) 399–410.
[15] N. Masoumi, N. Annabia, A. Assmanna, B.L. Larsone, J. Hjortnaesa, N. Alemdara, M. Kharazihaa, K.B. Manningc, J.E. Mayer Jr., A. Khademhosseinia, Tri-layered elastomeric scaffolds for engineering heart valve leaflets, Biomaterials 35 (27) (2014) 7774–7785.
[16] D.P. Faxon, M.A. Creager, S.C. Smith Jr., R.C. Pasternak, J.W. Olin, M.A. Bettmann, M.H. Criqui, R.V. Milani, J. Loscalzo, J.A. Kaufman, D.W. Jones, W.H. Pearce, American Heart Association, Atherosclerotic vascular disease conference: executive summary: atherosclerotic vascular disease conference proceeding for healthcare professionals from a special writing group of the American Heart Association, Circulation 109 (21) (2004) 2595–2604.
[17] D.P. Faxon, V. Fuster, P. Libby, J.A. Beckman, W.R. Hiatt, R.W. Thompson, J.N. Topper, B.H. Annex, J.H. Rundback, R.P. Fabunmi, R.M. Robertson, J. Loscalzo, American Heart Association, Atherosclerotic vascular disease conference: writing group III: pathophysiology, Circulation 109 (21) (2004) 2617–2625.
[18] R. Met, K.P. Van Lienden, M.J. Koelemay, S. Bipat, D.A. Legemate, J.A. Reekers, Subintimal angioplasty for peripheral arterial occlusive disease: a systematic review, Cardiovasc. Intervent. Radiol. 31 (2008) 687–697.
[19] L. Norgren, W.R. Hiatt, J.A. Dormandy, M.R. Nehler, K.A. Harris, F.G. Fowkes, TASC II working group. Inter-society consensus for the management of peripheral arterial disease (TASC II), J. Vasc. Surg. 45 (2007) S5–S67.

[20] M.B. Browning, D. Dempsey, V. Guiza, S. Becerra, J. Rivera, B. Russell, et al., Multilayer vascular grafts based on collagen-mimetic proteins, Acta Biomater. 8 (2011) 1010–1021.
[21] A. Ratcliffe, Tissue engineering of vascular grafts, Matrix Biol. 19 (2000) 353–357.
[22] J.V. Tu, C.L. Pashos, C.D. Naylor, E.L. Chen, S.L. Normand, J.P. Newhouse, et al., Use of cardiac procedures and outcomes in elderly patients with myocardial infarction in the united states and Canada, N. Engl. J. Med. 336 (1997) 1500–1505.
[23] C.V.C. Bouten, P.Y.W. Dankers, A. Driessen-Mol, S. Pedron, A.M.A. Brizard, F.P.T. Baaijens, Substrates for cardiovascular tissue engineering, Adv. Drug Deliv. Rev. 63 (2011) 221–241.
[24] S.G. Wise, M.J. Byrom, A. Waterhouse, P.G. Bannon, M.K.C. Ng, A.S. Weiss, A multilayered synthetic human elastin/polycaprolactone hybrid vascular graft with tailored mechanical properties, Acta Biomater. 7 (2011) 295–303.
[25] K.A. McKenna, M.T. Hinds, R.C. Sarao, P.-C. Wu, C.L. Maslen, R.W. Glanville, et al., Mechanical property characterization of electrospun recombinant human tropoelastin for vascular graft biomaterials, Acta Biomater. 8 (2011) 225–233.
[26] S.E. Greenwald, C.L. Berry, Improving vascular grafts: the importance of mechanical and haemodynamic properties, J. Pathol. 190 (2000) 292–299.
[27] P. Klinkert, P.N. Post, P.J. Breslau, J.H. van Bocke, Saphenous vein versus PTFE for above-knee femoropopliteal bypass. A review of the literature, Eur. J. Vasc. Endovasc. Surg. 27 (2004) 357–362.
[28] D. Wolf, A. Zirlik, K. Ley, Beyond vascular inflammation—recent advances in understanding atherosclerosis, Cell. Mol. Life Sci. 72 (20) (2015) 853–869.
[29] K.S. Cunningham, A.I. Gotlieb, The role of shear stress in the pathogenesis of atherosclerosis, Lab. Investig. 85 (2005) 9–23.
[30] Y.S. Li, et al., Molecular basis of the effects of shear stress on vascular endothelial cells, J. Biomech. 38 (2005) 1949–1971.
[31] G. De Visscher, L. Mesure, B. Meuris, A. Ivanova, W. Flameng, Improved endothelialization and reduced thrombosis by coating a synthetic vascular graft with fibronectin and stem cell homing factor SDF-1α, Acta Biomater. 8 (2012) 1330–1338.
[32] B. Krijgsman, A.M. Seifalian, H.J. Salacinski, N.R. Tai, G. Punshon, B.J. Fuller, G. Hamilton, An assessment of covalent grafting of RGD peptides to the surface of a compliant poly(carbonate-urea)urethane vascular conduit versus conventional biological coatings: its role in enhancing cellular retention, Tissue Eng. 8 (2002) 673–680.
[33] K. Wulf, M. Teske, M. Lobler, F. Luderer, K.P. Schmitz, K. Sternberg, Surface functionalization of poly(epsilon-caprolactone) improves its biocompatibility as scaffold material for bioartificial vessel prostheses, J. Biomed. Mater. Res. Part B 98 (2011) 89–100.
[34] T. Asahara, T. Murohara, A. Sullivan, M. Silver, R. Van Der Zee, T. Li, et al., Isolation of putative progenitor endothelial cells for angiogenesis, Science 275 (1997) 964.
[35] K.A. Ahmann, S.L. Johnson, R.P. Hebbel, R.T. Tranquillo, Shear stress responses of adult blood outgrowth endothelial cells seeded on bioartificial tissue, Tissue Eng. A 17 (2011) 2511.
[36] J.B. Allen, S. Khan, K.A. Lapidos, G.A. Ameer, Toward engineering a human neoendothelium with circulating progenitor cells, Stem Cells 28 (2010) 318.
[37] A.E. Ensley, R.M. Nerem, D.E.J. Anderson, S.R. Hanson, M.T. Hinds, Fluid shear stress alters the hemostatic properties of endothelial outgrowth cells, Tissue Eng. A 18 (2012) 127.
[38] M.T. Hinds, M. Ma, N. Tran, A.E. Ensley, S.M. Kladakis, K.B. Vartanian, et al., Potential of baboon endothelial progenitor cells for tissue engineered vascular grafts, J. Biomed. Mater. Res. A 86A (2008) 804.

[39] S. Kaushal, G.E. Amiel, K.J. Guleserian, O.M. Shapira, T. Perry, F.W. Sutherland, et al., Functional small-diameter neovessels created using endothelial progenitor cells expanded ex vivo, Nat. Med. 7 (2001) 1035.
[40] C. Quint, Y. Kondo, R.J. Manson, J.H. Lawson, A. Dardik, L.E. Niklason, Decellularized tissue-engineered blood vessel as an arterial conduit, Proc. Natl. Acad. Sci. USA 108 (2011) 9214.
[41] T. Shirota, H. He, H. Yasui, T. Matsuda, Human endothelial progenitor cell-seeded hybrid graft: proliferative and antithrombogenic potentials in vitro and fabrication processing, Tissue Eng. 9 (2003) 127.
[42] J.D. Stroncek, Y. Xue, N. Haque, J.H. Lawson, W.M. Reichert, In vitro functional testing of endothelial progenitor cells that overexpress thrombomodulin, Tissue Eng. A 17 (2011) 2091.
[43] A.N. Veleva, D.E. Heath, J.K. Johnson, J. Nam, C. Patterson, J.J. Lannutti, et al., Interactions between endothelial cells and electrospun methacrylic terpolymer fibers for engineered vascular replacements, J. Biomed. Mater. Res. A 91 (2009) 1131.
[44] C. Zhu, D. Ying, J. Mi, L. Li, W. Zeng, C. Hou, et al., Development of anti-atherosclerotic tissue-engineered blood vessel by A20-regulated endothelial progenitor cells seeding decellularized vascular matrix, Biomaterials 29 (2008) 2628.
[45] R.F. Ankeny, M.T. Hinds, R.M. Nerem, Dynamic shear stress regulation of inflammatory and thrombotic pathways in baboon endothelial outgrowth cells, Tissue Eng. A 19 (2013) 1573.
[46] D. Kong, L.G. Melo, A.A. Mangi, L. Zhang, M. Lopez-Ilasaca, M.A. Perrella, et al., Enhanced inhibition of neointimal hyperplasia by genetically engineered endothelial progenitor cells, Circulation 109 (2004) 1769.
[47] T. Lund, S.E. Hermansen, T.V. Andreasen, J.O. Olsen, B. Østerud, T. Myrmel, et al., Shear stress regulates inflammatory and thrombogenic gene transcripts in cultured human endothelial progenitor cells, Thromb. Haemost. 104 (2010) 582.
[48] J.J. Glynn, M.T. Hinds, Endothelial outgrowth cells: function and performance in vascular grafts, Tissue Eng. B Rev. 20 (4) (2014) 294–303.
[49] G.E. Amiel, M. Komura, O. Shapira, J.J. Yoo, S. Yazdani, J. Berry, et al., Engineering of blood vessels from acellular collagen matrices coated with human endothelial cells, Tissue Eng. 12 (2006) 2355.
[50] A. Bader, G. Steinhoff, A. Haverich, Tissue engineering of vascular grafts: human cell seeding of decellularised porcine matrix, Eur. J. Vasc. Endovasc. Surg. 19 (2000) 381.
[51] S.F. Badylak, The extracellular matrix as a biologic scaffold material, Biomaterials 28 (2007) 3587.
[52] S.-W. Cho, H.J. Park, J.H. Ryu, S.H. Kim, Y.H. Kim, C.Y. Choi, et al., Vascular patches tissue-engineered with autologous bone marrow-derived cells and decellularized tissue matrices, Biomaterials 26 (2005) 1915.
[53] Q. Xiao, S. Kiechl, S. Patel, F. Oberhollenzer, S. Weger, A. Mayr, B. Metzler, M. Reindl, Y. Hu, J. Willeit, et al., Endothelial progenitor cells, cardiovascular risk factors, cytokine levels and atherosclerosis—results from a large population-based study, PLoS One 2 (2007) e975.
[54] A. Aicher, A.M. Zeiher, S. Dimmeler, Mobilizing endothelial progenitor cells, Hypertension 45 (2005) 321–325.
[55] K. Hattori, S. Dias, B. Heissig, N.R. Hackett, D. Lyden, M. Tateno, D.J. Hicklin, Z. Zhu, L. Witte, R.G. Crystal, et al., Vascular endothelial growth factor and angiopoietin-1 stimulate postnatal hematopoiesis by recruitment of vasculogenic and hematopoietic stem cells, J. Exp. Med. 193 (2001) 1005–1014.
[56] T. Sobrino, M. Perez-Mato, D. Brea, M. Rodriguez-Yanez, M. Blanco, J. Castillo, Temporal profile of molecular signatures associated with circulating endothelial progenitor cells in human ischemic stroke, J. Neurosci. Res. 90 (2012) 1788–1793.

[57] J.F. Liu, Z.D. Du, Z. Chen, Z.C. Han, Z.X. He, Granulocyte colony-stimulating factor attenuates monocrotaline-induced pulmonary hypertension by upregulating endothelial progenitor cells via the nitric oxide system, Exp. Ther. Med. 6 (2013) 1402–1408.
[58] B. Hibbert, T. Simard, F.D. Ramirez, A. Pourdjabbar, J.E. Raizman, R. Maze, K.R. Wilson, S. Hawken, E.R. O'Brien, The effect of statins on circulating endothelial progenitor cells in humans: a systematic review, J. Cardiovasc. Pharmacol. 62 (2013) 491–496.
[59] C. Heeschen, Erythropoietin is a potent physiologic stimulus for endothelial progenitor cell mobilization, Blood 102 (2003) 1340–1346.
[60] A. Georgescu, N. Alexandru, M. Nemecz, I. Titorencu, D. Popov, Irbesartan administration therapeutically influences circulating endothelial progenitor cell and microparticle mobilization by involvement of pro-inflammatory cytokines, Eur. J. Pharmacol. 711 (2013) 27–35.
[61] E.T. Goh, E. Wong, Y. Farhatnia, A. Tan, A.M. Seifalian, Accelerating in situ endothelialisation of cardiovascular bypass grafts, Int. J. Mol. Sci. 16 (2015) 597–627.
[62] M. Avci-Adali, G. Ziemer, H.P. Wendel, Induction of EPC homing on biofunctionalized vascular grafts for rapid in vivo self-endothelialization—a review of current strategies, Biotechnol. Adv. 28 (2010) 119–129.
[63] B.D. Markway, O.J. McCarty, U.M. Marzec, D.W. Courtman, S.R. Hanson, M.T. Hinds, Capture of flowing endothelial cells using surface-immobilized anti-kinase insert domain receptor antibody, Tissue Eng. Part C 14 (2008) 97–105.
[64] M. Zhang, Z. Wang, Z. Wang, S. Feng, H. Xu, Q. Zhao, S. Wang, J. Fang, M. Qiao, D. Kong, Immobilization of anti-CD31 antibody on electrospun poly(varepsilon-caprolactone) scaffolds through hydrophobins for specific adhesion of endothelial cells, Colloids Surf. B 85 (2011) 32–39.
[65] M. Schleicher, J. Hansmann, B. Elkin, P.J. Kluger, S. Liebscher, A.J. Huber, O. Fritze, C. Schille, M. Muller, K. Schenke-Layland, et al., Oligonucleotide and parylene surface coating of polystyrene and ePTFE for improved endothelial cell attachment and hemocompatibility. Int. J. Biomater. 2012 (2012), https://doi.org/10.1155/2012/397813.
[66] G. Camci-Unal, H. Aubin, A.F. Ahari, H. Bae, J.W. Nichol, A. Khademhosseini, Surface-modified hyaluronic acid hydrogels to capture endothelial progenitor cells, Soft Matter 6 (2010) 5120–5126.
[67] A. Ruiz, C.E. Flanagan, K.S. Masters, Differential support of cell adhesion and growth by copolymers of polyurethane with hyaluronic acid, J. Biomed. Mater. Res. A 101 (2013) 2870–2882.
[68] D. Fayol, C. Le Visage, J. Ino, F. Gazeau, D. Letourneur, C. Wilhelm, Design of biomimetic vascular grafts with magnetic endothelial patterning, Cell Transplant. 22 (2013) 2105–2118.
[69] A. Tiwari, G. Punshon, A. Kidane, G. Hamilton, A.M. Seifalian, Magnetic beads (Dynabead) toxicity to endothelial cells at high bead concentration: implication for tissue engineering of vascular prosthesis, Cell Biol. Toxicol. 19 (2003) 265–272.
[70] F. Nazneen, G. Herzog, D.W.M. Arrigan, N. Caplice, P. Benvenuto, P. Galvin, M. Thompson, Surface chemical and physical modification in stent technology for the treatment of coronary artery disease, J. Biomed. Mater. Res. Part B 100B (2012) 1989–2014.
[71] D.S. Chong, B. Lindsey, M.J. Dalby, N. Gadegaard, A.M. Seifalian, G. Hamilton, Luminal surface engineering, "micro and nanopatterning": potential for self endothelialising vascular grafts? Eur. J. Vasc. Endovasc. Surg. 47 (2014) 566–576.
[72] WHO (World Health Organization), The Top Ten Causes of Death Fact Sheet 2012, Available from: http:/www.who.int/mediacentre/factsheets/fs310/en/, 2015 (accessed 10 January 2016).

[73] V. Fuster, B.M. Mearns, The CVD paradox: mortality vs prevalence, Nat. Rev. Cardiol. 6 (11) (2009) 669.
[74] R.A. Byrne, M. Joner, A. Kastrati, Stent thrombosis and restenosis: what have we learned and where are we going? Eur. Heart J. 36 (2015) 3320–3331, https://doi.org/10.1093/eurheartj/ehv511.
[75] G.N. Levine, E.R. Bates, J.C. Blankenship, et al., 2011 ACCF/AHA/SCAI guideline for percutaneous coronary intervention: a report of the American college of cardiology foundation/American heart association task force on practice guidelines and the society for cardiovascular angiography and interventions, J. Am. Coll. Cardiol. 58 (2011) e44–e122.
[76] P. Wenaweser, J. Daemen, M. Zwahlen, et al., Incidence and correlates of drug-eluting stent thrombosis in routine clinical practice. 4-year results from a large 2-institutional cohort study, J. Am. Coll. Cardiol. 52 (2008) 1134–1140.
[77] R. Reejhsinghani, A.S. Lotfi, Prevention of stent thrombosis: challenges and solutions, Vasc. Health Risk Manag. 11 (2015) 93–106.
[78] L. Mauri, W.H. Hsieh, J.M. Massaro, K.K. Ho, R. D'Agostino, D.E. Cutlip, Stent thrombosis in randomized clinical trials of drug-eluting stents, N. Engl. J. Med. 356 (2007) 1020–1029.
[79] D.R. Holmes Jr., D.J. Kereiakes, S. Garg, et al., Stent thrombosis, J. Am. Coll. Cardiol. 56 (2010) 1357–1365.
[80] A.J. Kirtane, G.W. Stone, How to minimize stent thrombosis, Circulation 124 (2011) 1283–1287.
[81] S.L. Robbins, V. Kumar, R.S. Cotran, Robbins and Cotran Pathologic Basis of Disease, eighth ed., Saunders/Elsevier, Philadelphia, PA, 2010.
[82] A.V. Finn, M. Joner, G. Nakazawa, et al., Pathological correlates of late drug-eluting stent thrombosis: strut coverage as a marker of endothelialization, Circulation 115 (2007) 2435–2441.
[83] G. Nakazawa, Stent thrombosis of drug eluting stent: pathological perspective, J. Cardiol. 58 (2011) 84–91.
[84] K. Nishihira, A. Yamashita, T. Ishikawa, K. Hatakeyama, Y. Shibata, Y. Asada, Composition of thrombi in late drug-eluting stent thrombosis versus de novo acute myocardial infarction, Thromb. Res. 126 (2010) 254–257.
[85] G. Nakazawa, F. Otsuka, M. Nakano, et al., The pathology of neoatherosclerosis in human coronary implants: bare-metal and drug-eluting stents, J. Am. Coll. Cardiol. 57 (2011) 1314–1322.
[86] A.V. Finn, F. Otsuka, Neoatherosclerosis: a culprit in very late stent thrombosis, Circ. Cardiovasc. Interv. 5 (2012) 6–9.
[87] T. Hanawa, Materials for metallic stents, J. Artif. Organs 12 (2009) 73.
[88] F. Otsuka, M. Vorpahl, M. Nakano, et al., Pathology of secondgeneration everolimus-eluting stents versus first-generation sirolimus- and paclitaxel-eluting stents in humans, Circulation 129 (2014) 211–223.
[89] Y. Fujimoto, Y. Kobayashi, M. Yamaguchi, Delamination of abluminal polymer of biolimus-eluting stent, J. Am. Coll. Cardiol. Intv. 5 (2012) e5–e6.
[90] H. Kitahara, Y. Kobayashi, M. Yamaguchi, et al., Damage to polymer of paclitaxel-eluting stent, Circ. J. 72 (2008) 1907–1908.
[91] N. Kuriyama, Y. Kobayashi, M. Yamaguchi, Y. Shibata, Usefulness of rotational atherectomy in preventing polymer damage of everolimus-eluting stent in calcified coronary artery, J. Am. Coll. Cardiol. Intv. 4 (2011) 588–589.
[92] J. Aoki, Complications of polymers on drug-eluting stents: looking toward polymer-free drug-eluting stents, Intern. Med. 54 (2015) 549–550.

[93] B. O'Brien, W. Carroll, The evolution of cardiovascular stent materials and surfaces in response to clinical drivers: a review, Acta Biomater. 5 (4) (2009) 945–958.
[94] D. Carrie, A next prospective, randomized trial comparing Cre8, a polymer-free stent eluting sirolimus, to a paclitaxel-eluting stent, in: Paper Presented at the Transcatheter Cardiovascular Therapeutics 23rd Annual Scientific Symposium, San Francisco, CA, November 7–11, 2011.
[95] E. Grube, BioFreedom: a prospective randomized trial of polymer-free bioliums A9-eluting stents and paclitaxel-eluting stents in patients with coronary artery disease, in: Paper Presented at the Transcatheter Cardiovascular Therapeutics 22rd Annual Scientific Symposium, September 23–25, Washington, DC, 2010.
[96] S. McGinty, T.T. Vo, M. Meere, S. McKee, C. McCormick, Some design considerations for polymer-free drug-eluting stents: a mathematical approach, Acta Biomater. 18 (2015) 213–225.
[97] N. Nikam, T.B. Steinberg, D.H. Steinberg, Advances in stent technologies and their effect on clinical efficacy and safety, J. Med. Devices 3 (7) (2014) 165–178.
[98] J. Wiebe, H.M. Nef, C.W. Hamm, Current status of bioresorbable scaffolds in the treatment of coronary artery disease, J. Am. Coll. Cardiol. 64 (23) (2014) 2541–2551.

This page intentionally left blank

Part Four

Biomedical applications of hemocompatible biomaterials

This page intentionally left blank

Improving the hemocompatibility of stents

14

H.Q. Liu
Chengdu University of Technology, Chengdu, China

14.1 Introduction

During the implanting of the vessel stent, the materials come into direct contact with the blood, the hemocompatibility of stent would be related to thrombus formation, inflammatory response, and restenosis in clinical application [1]. As a result of the contact of blood with nonendothelial surfaces, several humoral and cellular systems can be activated. Exposure of blood proteins and cells to blood contacting stent materials can activate plasma proteolytic systems, fibrinolysis, complement cascade, and at least three cellular elements (leukocytes, endothelial cells, and platelets). Activation of these systems by various stent materials can result in nonlocalized systemic reactions, it also relates to the section on both improving hemocompatibility method and materials selection.

14.2 Stent materials

The stents are of three types, based on the material's deformation or status: self-expanding stent, balloon dilated stent, and absorbable stent. Balloon expandable stents should have the ability to undergo plastic deformation and then maintain the required size once deployed [2]. Self-expanding stents should have sufficient elasticity to be compressed for delivery and then expand in the target area. Generally, the metals used for manufacturing stents are 316L stainless steel (316L SS), platinum-iridium (Pt-Ir) alloy, tantalum (Ta), nitinol (Ni-Ti), cobalt-chromium alloy(605L), and titanium (Ti) etc.

Fully biodegradable stent represents the most ambitious emerging stent technology. The rationale is to provide a stable supporting force in the short term; the stent materials will disappear with the degradation in vivo, thus biodegradable stent is provided with minimizing restenosis due to vascular recoil, constrictive remodeling, and loose intimal dissection flaps [3]. The materials of biodegradable stent include absorbable polymer (Table 14.1) and degradable metal, the metal maintains pure iron (Fe) and magnesium (Mg) alloys.

A variety of coating materials are commonly used in an attempt to improve the performance of stents; including inorganic materials, polymers, and porous ceramics. The materials and the coating techniques used in commercially available drug eluting stent (DES) are described in surface modification of stent materials.

Hemocompatibility of Biomaterials for Clinical Applications. https://doi.org/10.1016/B978-0-08-100497-5.00011-2
© 2018 Elsevier Ltd. All rights reserved.

Table 14.1 Fully biodegradable stent

Stent	Manufacture	Materials	Coating	Strut thickness (μm)	Trials
ABSORB BVS	Abbott	PLLA	PDLLA + Everolimus	150	ABSORB A,B,Extend,II
Igaki-Tamai	Kyoto Medical	PLLA	Nil	170	Igaki-Tamai
DESolveNx	Elixir	PLLA	PLA + Novolimus	150	DESolveFIM,Nx
ReZolve	Reva	Tyrosine polycarbonate	Sirolimus	200	RESORB,RESTORE
DREAMS	Biotronik	Magnesium alloy	PLGA + Paclitaxel	125	BIOSOLVE-1

PLLA, poly-L-lactic acid; PDLLA, poly-D-L-lactide; PLGA, polylactin-co-glycolic acid; PLA, polulactide derivative.

14.3 The consequence induced by hemocompatibility

14.3.1 Inflammatory response

As a result of exposure to a blood contacting stent, blood may initiate the production of proteolytic substances. This will result in the production of thrombin, plasmin, and proinflammatory cleavage products, C3a and C5a [4]. Although the production of proteolytic substances is initiated by proteins present in plasma, its amplification results are mainly from the contribution of cellular elements. As mentioned, the cellular reaction of blood to stent is not limited to platelet activation and aggregation. This will lead to more cells being available for interaction when vessel walls are wounded by the intervention of the stent. These cellular elements will bind to surfaces (both endothelial and nonendothelial) and adhesion of leukocytes will be followed by degranulation and release of factors that further contribute to reduced hemocompatibility. Endothelial cells will also respond to humoral signals to increase leukocyte adhesion and procoagulant activity. These alterations in cellular activity, will result in an inflammatory response that may have consequences beyond those tests of stent in vitro.

14.3.2 Thrombus formation

Thrombus formation is the result of two interdependent mechanisms; platelets and protein clotting factors. It is well known that blood contact with stent surfaces can elicit platelet activation by a variety of mechanisms [5], including materials related alteration in blood flow that trigger shear-related platelet activation [6], and due to direct platelet adherence to the deposited protein layer on the stent surfaces, an event largely attributed to adsorption of fibrinogen [7]. Activated platelets undergo dramatic shape changes which promote aggregation with other platelets, and release platelet and pro-coagulant agonists [8]. The phospholipids of the platelet membrane also serve as the substrate for activated clotting factors, resulting in local amplification of the coagulation cascade. Aggregation of platelets, together with explosive activation of protein clotting factors, may result in significant thrombus accumulation in-stent.

The protein clotting factors are a set of structurally similar serineproteases that circulate in the plasma as inactive proenzymes. After vascular injury during stent implanting, or through the introduction of foreign materials into the circulatory system, clotting factors are triggered and undergo activation in a sequential cascade-like fashion that culminates in the formation of a fibrin clot. This cascade consists of two pathways during stent implanting, tissue factor that is released due to vascular injury is the primary initiator of the extrinsic pathway [9]. The intrinsic pathway is considered the most critical pathway in biomaterial-associated thrombosis.

14.3.3 In-stent restenosis

Restenosis of coronary stent is a complex process that an vascular injury induces triggers increasing platelet deposition and inflammatory response within the vessel wall, which lead to the release of growth factors and cytokines activating smooth muscle cells and to neointimal hyperplasia [10,11]. On the other side, whether it is a bare

stent or with a surface modified stent; 316LSS, nitinol, and cobalt-chromium alloy are the most commonly used metals for stents. Allergic reactions to the release of nickel can occur among stent implants [12]. In particular, the release of nickel, chromate, and molybdenum ions from stent materials may trigger local immune response and inflammatory reactions, which in turn may induce intimal hyperplasia and in-stent restenosis [13].

14.4 The assess method of hemocompatibility

14.4.1 The hemolysis

Hemolysis can be evaluated via exposure of stent materials under in vitro, in vivo, and ex vivo conditions. In vitro conditions are used to evaluate materials as well as stents. Hemolysis experiments were conducted in accordance with ISO 10993-4:2009 and ASTMF756-00 [1,14].

In vivo and ex vivo assessments in animal models or during clinical trials are possible. Justification can be made for either of the following study designs. The test stent is compared to reference stent materials with known acceptable levels of hemolysis; furthermore the significant consequences was evaluated according to clinical application.

14.4.2 The adherence of platelets

Various methods have been designed to measure the adhesion of platelets to stent surfaces [15]. Most of these methods are based on the observation that a certain proportion of platelets are removed from normal whole blood under controlled conditions of flow or pressure. This principle has been adapted to the quantification of the adhesion of other blood cells to materials surface. An alternative method is the direct counting of platelets adherent to a sample surface. Following exposure to blood or platelet-rich plasma under standardized conditions, the stent surface is rinsed to remove nonadherent platelets, fixed and prepared for either light or scanning electron microscopy. The number of adherent platelets per unit area is directly counted and their morphology is evaluated. The lactate dehydrogenase (LDH) activity and the P-selectin (CD62P, GMP-140) are also used to determine the amount of adhesion platelets and the activation level of adherent platelets respectively.

14.4.3 The adherence and activation of fibrinolysis

Dysfibrinogenaemia, afibrinogenaemia, and hypofibrinogenaemia will maybe prolonged prothrombin time (PT), activated partial thromboplastin time (APTT), and thromboplastin time (TT) [16]. Normal physiological fibrinolysis yields the FDPs X, Y, C, D, and E in concentrations below 2 mg/mL of plasma. The normally low level of FDPs is maintained by the low rate of the degradation reaction, and the high rate of clearance of FDPs from the circulation. Pathologic degradation of fibrin and

fibrinogen, a result of increased plasminogen activation, yields FDP of 2–40 mg/mL or more. The test is useful for evaluating implant materials only. The use of commercially available methods is recommended [17,18].

14.4.4 Coagulation factors

The consequences of the interaction of material's surfaces with the blood can range from gross thrombosis and embolization to subtle effects such as accelerated consumption of hemostatic elements; the latter may be compensated or lead to depletion of platelets or plasma coagulation factors. Some coagulation factors were activated when the samples were immersed in platelet-poor plasma (PPP). Under the combined action of tissue thromboplastin and Ca2, factor X is activated and transformed to factor Xa; factor Xa then activates prothrombin(factor II) to form thrombin (factor IIa) [19].

14.4.5 The contact systems

Surface characteristics of a stent material, which influence thrombosis and neointimal hyperplasia, include surface energy, surface texture, surface potential, and the stability of the surface oxide layer [20,21]. In many circumstances a combination of one or more of these listed factors predicts the outcome. The surface properties of stent largely depend on the surface treatment. Structure of stent also influences the surface area and level of trauma that the blood encounters. Surface tension, the residual binding capability of the exposed surface, can affect the hemocompatibility of a material. Blood cells and vessels are negatively charged an isoelectric point between pH 4.8 and 5. The vessel wall being negatively charged causes platelets to be repelled and helps reduce thrombogenic potential. Distribution of charged sites and surface polarity will affect plasma protein absorption to the material. Modification of stent materials in one area may not solve all issues with regard to hemocompatibility. For example, hydrophilic substituents have a stimulatory effect on the complement cascade, but simultaneously have negligible effect on platelet activation. However, hydrophobic substituents show a reduced complement activation, but stimulate platelet adhesion. Generally, blending or mosaics are used to balance hydrophilic/hydrophobic properties to improve hemocompatibility.

14.5 The improving approach of hemocompatibility

The surface modification of stent materials is a simple and effective approach to improving the hemocompatibility [22].Surface films, such as inorganic film and drug-eluting coating have been widely applied to increase the biocompatibility of stents [23,24]. The coating materials for stents can be broadly classified into three types: inorganic materials, DES, and surface biological modification. Inorganic materials and surface biological modification are exclusively used as coating materials, while the DES are used as both, a coating material as well as the sole stent material.

14.5.1 The surface modification of stent materials

Surface modification technique has been identified as an effective approach to overcome and improve the hemocompatibility. Researchers have focused on improving various surfaces to impart well with biofunctional surface. The techniques used for this purpose include deposition of a thin uniform coating, development of stable passivation oxide layer, ion beam processing for surface modification, and surface texturing.

Ti-O film modified stents have shown good hemocompatibility and antithombosis property, and the outcome in clinic was also accepted. Huang [25] reported that the nonstoichiometrical titanium oxide films were obtained by ion beam deposition system. Hemocompatibility of the films was evaluated by clotting time, platelet adhesion and hemolysis analyses separately. The results revealed that hemocompatibility of the stent materials was improved by titanium oxide films (Fig. 14.1A1–A3). Semiconductor property of nonstoichiometric titanium oxide films might be responsible for the improvement of hemocompatibility.

Titanium nitride (TiN) films were deposited on AISI 316L stainless steel substrates by reactive magnetron sputtering using a Ti target [26]. Platelet adhesion experiments were done to examine the interaction between blood and the materials in vitro. The properties of TiNx films were correlated with their thrombogenicity involving platelet adhesion, activation, and protein clustering mechanisms. It was found that the stoichiometry of TiNx films and surface roughness affect the platelet response(Fig. 14.2).

Diamond-like carbon (DLC) films offer numerous functional characteristics that make them particularly attractive as potential wear-resistant coatings for biomedical applications. The hemocompatibility of various forms of doped DLCs was reported in past ten years, and the possible correlations with film structure and surface properties was investigated [27].Unalloyed DLC thin films did not exhibit fibrin or platelet aggregation in platelet rich plasma testing. On the other hand, DLC-metal composite films exhibited low time constants and significant in vitro thrombosis. These results indicate that a functionally gradient DLC-metal composite film, which there is a reduction of metal atom concentration from the substrate/film interface to the film surface, may provide the positive attributes of unalloyed and alloyed films.

Liu [28,29] reported a simple approach to fabricate a copper-titanium film with the aim of imparting the stent with good hemocompatibility and accelerating endothelialization. In this work, copper-titanium films exhibited good hemocompatibility in vitro; however, the increase of Cu/Ti ratio could lead to increasing hemolysis ratio. Furthermore, the investigation of various copper-titanium coated stents in vivo was used to assess hemocompatibility. After the 1st week of implantation, the lumen of the vascular vessel remained unobstructed, but slight tissue adhered to lower copper coated stent (Fig. 14.3D). In contrast, no other tissues adhered on the strut surface of 316L SS stents or higher copper coated stents (Fig. 14.3A and G). In the 2nd week, transparent tissues nearly covered lower copper-containing coated stents (Fig. 14.3E). In the 3rd week, all of the stents implanted in the abdominal aorta remained thrombus-free, most stent struts were covered with proliferated tissue, but the lower copper-containing film (Fig. 14.3F) contained a more complete tissue layer than higher

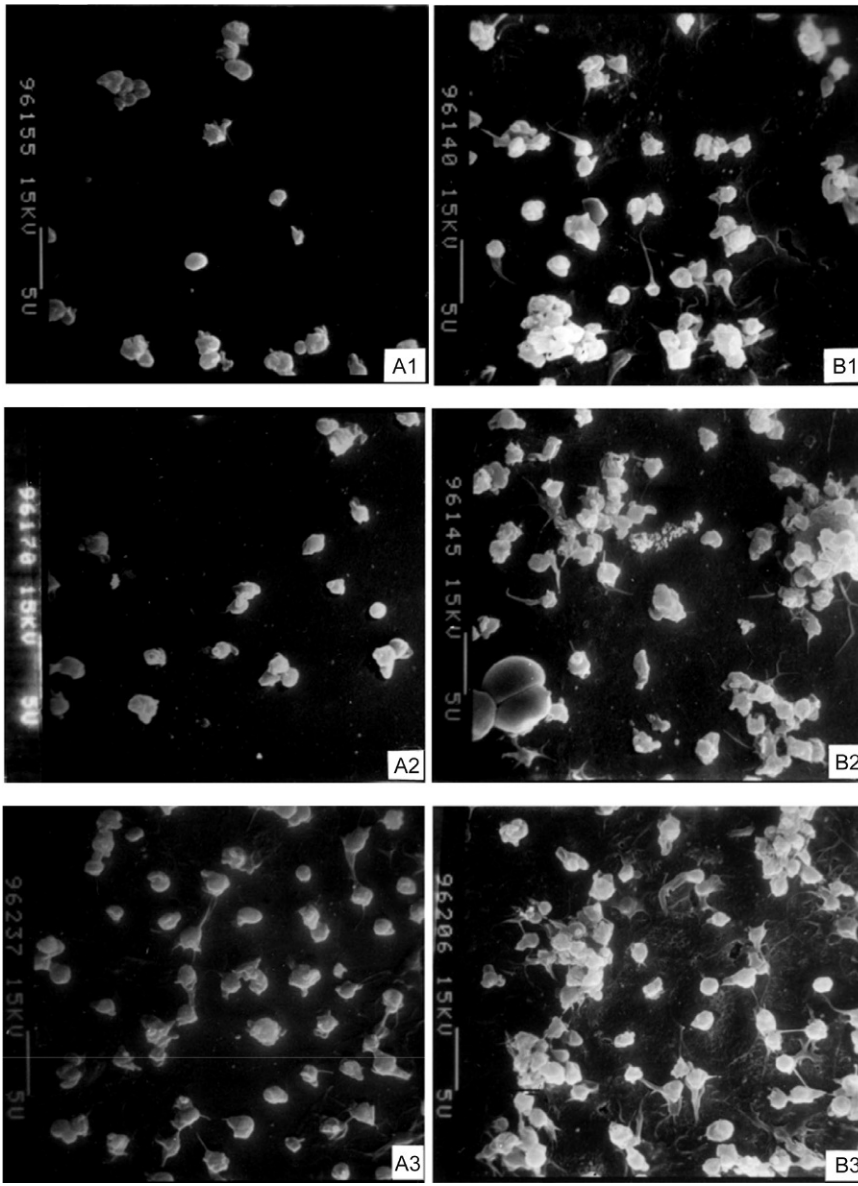


Fig. 14.1 The morphology of adherent platelet on the material's surface. (A1) $TiO_{2\sim x}$ film, incubation time: 10 min. (A2) $TiO_{2\sim x}$ film, incubation time: 60 min. (A3) $TiO_{2\sim x}$, the comparing sample is 316L SS (B1, B2, B3).

copper-containing film and 316L SS did (Fig. 14.3C and I), which indicates that the copper-titanium film increases the hemocompatibility of stent.

Amorphous hydrogenated SiC, a semiconductor, has been well known for its anti-thrombogenic properties [30]. The reduction in the deposition of platelets, leukocytes,

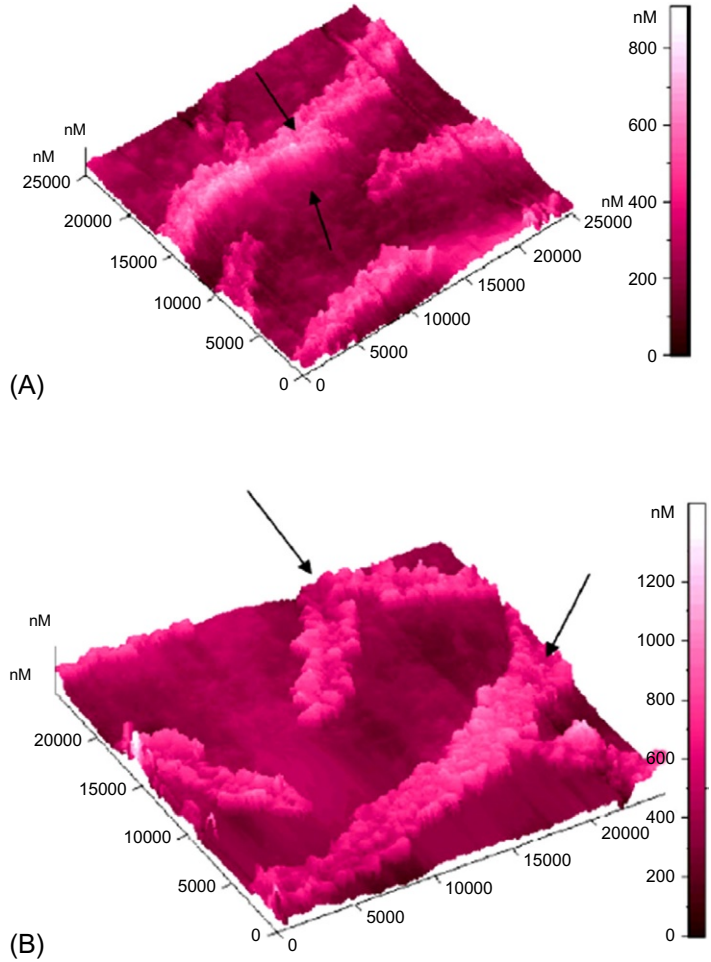


Fig. 14.2 The 3D image of AFM topography. (A) Platelets on stoichiometric TiN film after 1 h incubation time; (B) platelets on stoichiometric TiN film after 2 h incubation time. *Arrows* indicate the platelets' aggregation (island-like).

and monocytes over a stent made of SiC offers a promising coating material for reducing restenosis [31,32]. Although in-vitro studies [33] provided encouraging results, the outcomes from the various human trials produced contradictory results. For instance, the presence of endothelialization was reported in a 6-month clinical follow-up of the Tenax coronary stent [34]. In contrast, results showing greater neointimal hyperplasia were observed in a 6-month clinical follow-up for SiC-coated stents in another study [35]. A clinical trial compared the SiC-coated stents (Biotronik, Germany) with 316L NIR stents (Boston Scientific, USA) and concluded that both stents had a low rate of major adverse coronary events at 12 weeks of follow-up, with no definite superiority [36]. These mixed results indicate the need for further research in this area.

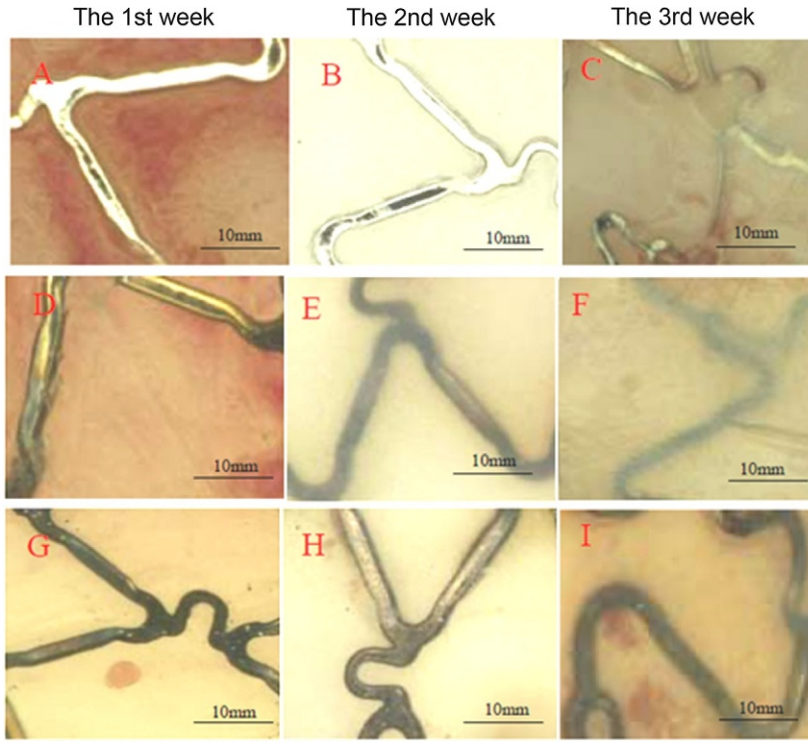


Fig. 14.3 The optical microscope images of implanted stent's surface. Where A, B, and C are the bare stents (316L SS) implantation with 1st, 2nd, and 3rd week respectively; where D, E, and F are lower copper-containing film coated stents implanted for 1, 2, and 3 weeks, respectively; where G, H, and I are higher copper-containing film coated stents implantation with 1st, 2nd, and 3rd week separately.

The C-N films were synthesized on Si (111) wafers by means of ion beam assisted deposition (IBAD). In vitro measurements of contact angle, dynamic clotting time, and platelet consumption rate were used to evaluate the hemocompatibility of C-N film in comparison with that of TiNi and 316L SS [37]. Nitrogen content, types of C/N bonds, and roughness of C-N films play important role in clotting time and amount of adhered platelets(Fig. 14.4). Hemocompatibility of C-N film betters with the increase in N/C atomic composition ratio and decrease in surface roughness.

Yang [38] reported plasma deposited PEO-like films that were investigated as surface modifications of stent, this kind of PEO-like films had good stability in phosphate buffer solution. In vitro hemocompatibility revealed low platelet adhesion, platelet activation, and fibrinogen adhesion (Fig. 14.5). This made it a potential candidate for the applications in antifouling surfaces of blood-contacting biomedical devices.

Chen [39] dealt with improving the hemocompatibility and enhancing EPC colonization of titanium by covalently bonding PEG600 or PEG4000, then end-grafting of an anti-CD34 antibody. For this, a chemically hydroxylated titanium surface was

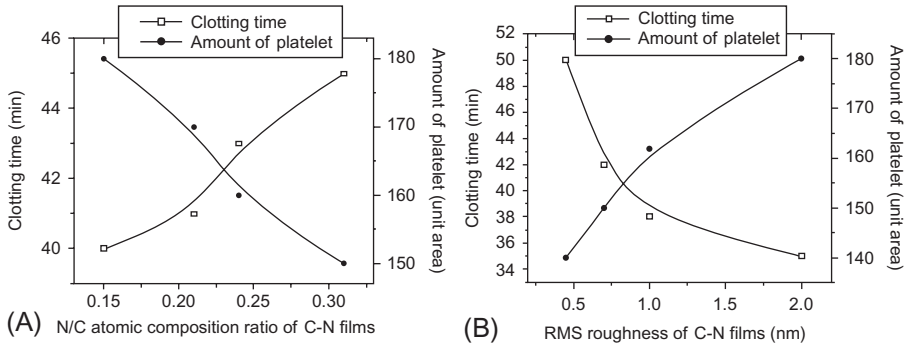


Fig. 14.4 Influence of C-N films with various character. (A) N/C atomic composition ratio, (B) RMS roughness on hemocompatibility of C-N films.

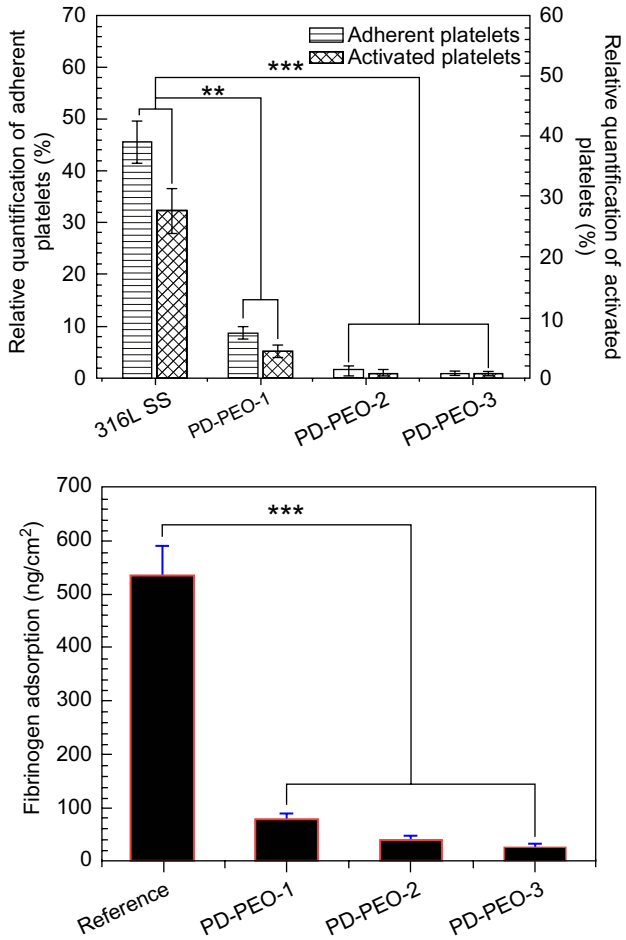


Fig. 14.5 Relative quantification of adherent platelets (results obtained by LDH assay, 45 min incubation in PRP, initial nondilute concentration of platelets that used to make standard curve is taken as 100%.), and relative quantification of activated platelets (results obtained by GMP-140 assay, initial nondilute concentration of HRP labeled antibody that used to make standard curve is taken as 100%.) of 316L SS and plasma deposited PEG-like films.

aminosilanized, which was further used for covalent grafting of polyethylene glycol and the antibody. The grafting efficiency was verified in each step. In vitro platelet adhesion analysis con- firmed superior hemocompatibility of the modified surface over the control. A long chain PEG4000 grafted the anti-CD34 antibody was shown the superior antifouling and thromboresistant properties, it also presents the good affinity to EPC in vivo.

14.5.2 The drug eluting stent

Numerous clinical studies have compared heparin-coated versus noncoated vascular stent. The coating is considered to improve patient safety by reducing the adherence of blood components and by inhibiting blood clotting. Heparin coated stent showed lessened humoral and cellular activation, in particular a reduced complement activation and enhanced platelet protection. This surface modification has led to a decrease in healthcare costs and an increase in patient safety owing to increased hemocompatibility of vessel stent.

Endothelial and smooth muscle cells (SMCs) damage, unavoidable in PTCA and stent placement, is a cause of restenosis [40]. The main reason for the failure of systemic pharmacological therapy is the inability to deliver an adequate drug dose at the site of injury [41].The concept of delivering medications at the injury site has evolved from paclitaxel-coated stents, in which loaded drugs will inhibit neointimal hyperplasia. The rapamycin coating of stent surface can also prevent SMCs hyperplasia, an appropriate drug concentration has to be delivered for at least 30 days during which the biology of restenosis is known to occur.

Pharmacological inhibition of the key enzymes responsible for the consecutive activation of cascade of reactions, including aprotinin, tranexamic acid, aminocapron acid, C1-esterase inhibitor, antioxidants, and free radical scavengers are also under evaluation to improve hemocompatibility. Research into the modification of surfaces with integrin fragments, such as peptides with RGD amino acid sequence has been conducted to increase hemocompatibility and biocompatibility. Further research into the improvement of stent function by the local modification of the stent surface is ongoing and may prove to be one of the most exciting areas of research in this field.

14.5.3 Developing novel stent materials

In the past decade, the evolution of biodegradable stents has become one of the biggest topics of discussion in stent materials field. Due to relocking or a process of a permanent stent becoming inactive, there is a high chance that the patient is not receiving the proper care needed for the area of their body that is in need of a stent. Scientists have also found that biodegradable metallic material for stents may be more beneficial in the body than permanent metal due to a problem-causing agent called late stent thrombosis.

Mg-based biodegradable material has the key advantage to reduce or even eliminate the late restenosis [42]. Besides, Mg has attracted most attention because of its

role in many important biological functions and its hemocompatibility. Mg-based stents are tailored to benefit the body and allow cell proliferation. The main problem of Mg for stent application is its rather rapid biodegradation, which occurs in the form of corrosion. This rapid corrosion could lead to loss of mechanical integrity and release of high concentration of degradation products. The first biodegradable magnesium alloy stent was created by Biotronik, which was made from WE43 [43].The stent demonstrated good biocompatibility and clinical trial has shown very promising results [44].

Pure Fe is the major component in degradable Fe stents [45]. Fe has superior radial strength because of its higher elastic modulus, and has good biocompatibility owing to essential trace elements of human body. The biodegradation involves the oxidation of Fe into ferrous and ferric ions and these ions dissolve into biological media [46]. Ferrous ions reduce the proliferation of SMCs in in vitro conditions, and thus may inhibit neointimal hyperplasia. Thrombogenicity and neointimal proliferation were reduced and no local toxicity was observed [45,47]. Endothelialization of Fe stents was also observed in animal models.

Biodegradable polymers have been considered as an option of stent materials. Stack et al. [48] developed the first biodegradable stent made of PLLA and deployed it in canine model. The initial results showed the occurrence of limited thrombosis and minimal neointimal proliferationin the short term. However, the implantation of biodegradable polymers in a porcine model showed extensive inflammation and neointimal proliferation [49]. But subsequent studies showed that molecular weight of polymer also has an impact on neointimal hyperplasia. Though it has been speculated that biodegradable polymers induce inflammatory reactions because of an immune response to degradation products and nonreacted monomer compounds [158], the basic mechanism is still not completely understood.

14.5.4 Therapeutic approach

It is necessary in most patients undergoing coronary stent to continue the combination therapy of oral anticoagulation and antiplatelet drugs [50]. Aspirin (ASP), the most common antiplatelet medication, has been extensively evaluated for prevention of platelet aggregation through the inhibition of thromboxane production [51]. However, the lack of clinical outcomes with aspirin monotherapy recommended dual antiplatelet therapy with the association of thienopyridines whose active metabolites irreversibly bind to P2Y12 receptor on platelet and thereby inhibit platelet function [52]. One such agent, prasugrel (PRAS), a third generation thienopyridine, was recently approved for use in patients with atherosclerotic vascular disease to reduce the incidence of ischemic events as well as in-stent restenosis [53]. Propolis (PROP) is a natural extract produced by the honeybee and widely used in native medicine as an antibiotic agent. Similarly, several studies have reported the potential of propolis to inhibit platelet aggregation and to be antiinflammatory [12]. These antiplatelet drugs such as ASP, PRAS, and PROP might affect inflammatory responses as well as platelet function because thrombotic and inflammatory pathways share common signaling cascades [54].

14.6 Summary

The hemocompatibility of stent materials and improving methods were stated in this chapter. The hemocompatibility directly influence inflammatory, thrombus formation and in-stent restenosis, and the types of stent materials would be related to the hemolysis rate, adhesion of platelets, activation of fibrinolysis and coagulation factors. The surface modification is an effective approach to improve hemocompatibility of stent, the coating or films coved on stent surface will enhance surface characteristics, which show suitable biocompatibility, including reducing complement activation, platelet adhesion, and improving anticoagulant properties.

Acknowledgments

This work was sponsored by Natasha Welford, Christopher Siedlecki of Penn State University, USA. This work was jointly and financially supported by Training plan for young and middle-aged core teachers of Chengdu University of Technology (Grant No. KYGG201708). This study was supported by the Open Fund Project (Grant No. jr1603) supported by the Jiangsu Provincial Key Laboratory for Interventional Medical Devices. This study was also supported by Open Fund Project supported by the Key Laboratory of Advanced Technology of Materials, Ministry of Education of the People's Republic of China. The authors earnestly thank the review and revision by Guicai Li of Nantong University.

References

[1] Biological evaluation of medical devices Part 4: Selection of tests for interactions with blood. ISO 10993–4:2009.
[2] A. Taylor, Metals, in: U. Sigwart (Ed.), Endoluminal Stenting, W.B. Saunders Company Ltd, London, 1996, pp. 28–33.
[3] P.W. Serruys, M.J.B. Kutryk, A.T.L. Ong, Coronary-artery stents, N. Engl. J. Med. 354 (2006) 483–495.
[4] B.D. Ratner, Blood compatibility—a perspective, J. Biomater. Sci. Polym. Ed. 11 (2000) 1107–1119.
[5] M.B. Gorbet, M.V. Sefton, Biomaterial-associated thrombosis: roles of coagulation factors, complement, platelets and leukocytes, Biomaterials 25 (2004) 5681–5703.
[6] H.T. Spijker, R. Graaff, P.W. Boonstra, H.J. Busscher, W. van Oeveren, On the influence of flow conditions and wettability on blood material interactions, Biomaterials 24 (2003) 4717–4727.
[7] I.H. Jaffer, J.C. Fredenburgh, J. Hirsh, J.I. Weitz, Medical device-induced thrombosis: what causes it and how can we prevent it? J. Thromb. Haemost. 13 (Suppl. 1) (2015) S72–S81.
[8] D. Blockmans, H. Deckmyn, J. Vermylen, Platelet activation, Blood Rev. 9 (1995) 143–156.
[9] R. Bach, Y. Nemerson, W. Konigsberg, Purification and characterization of bovine tissue factor, J. Biol. Chem. 256 (1981) 8324–8331.

[10] A.K. Mitra, D.K. Agrawal, In stent restenosis: bane of the stent era, J. Clin. Pathol. 59 (2006) 232.
[11] C.J. Pan, J. Wang, N. Huang, Preparation, characterization and in vitro anticoagulation of emodin-eluting controlled biodegradable stent coatings, Colloids Surf. B: Biointerfaces 77 (2010) 155.
[12] R.O. Orsi, J.M. Sforcin, S.R.C. Funari, J.C. Gomes, Effect of propolis extract on guinea pig lung mast cell, J. Venom. Anim. Toxins Incl. Trop. Dis. 11 (2005) 76.
[13] R. Koster, M. Sommerauer, J. Kahler, S. Baldus, T. Meinertz, C.W. Hamm, et al., Nickel and molybdenum contact allergies in patients with coronary in-stent restenosis, Lancet 356 (9245) (2000) 1895–1897.
[14] Standard Practice for Assessment of Hemolytic Properties of Materials. ASTMF756-2000.
[15] T.J. Kunicki, M. Tucelli, G.A. Becker, R.H. Aster, A study of variables affecting the quality of platelets stored at room temperature, Transfusion 15 (1975) 414–421.
[16] D.M. Corriveau, G.A. Fritsma, Hemostasis and thrombosis in the clinical laboratory, J.B. Lippincott, Philadelphia, PA, 1988. p. 443.
[17] K.H. Grotemeyer, R. Viand, K. Beykirch, Thrombozytenfunktion bei vasomotorischen Kopfschmerzen und Migränekopfschmerzen, Dtsch. Med. Wschr. 108 (1983) 775–778.
[18] K.K. Wu, J.C. Hoak, A new method for the quantitative detection of platelet aggregates in patients with arterial insufficiency, Lancet 2 (1974) 924.
[19] M.B. Gorbet, M.V. Sefton, Biomaterial associated thrombosis: roles of coagulation factors platelets and leukocytes, Biomaterials 25 (2004) 5681–5703.
[20] J. Palmaz, New advances in endovascular technology, Tex. Heart Inst. J. 24 (3) (1997) 156–159.
[21] Y. Huang, E. Verbeke, E. Schacht, I.D. Scheerder, Local drug delivery using drug-eluting stents, in: P.W. Serruys, M.B. Leon, A. Colombo, M.J. Kutryk (Eds.), Coronary lesions a pragmatic approach, Martin Dunitz Ltd, London, 2002, pp. 319–335.
[22] X.J. Zhou, Y.X. Leng, H. Sun, et al., The structure and adhesion of hydrogenated amorphous carbon (a-C:H) films synthesized on CoCrMo alloy by plasma immersion ion implantation and deposition at different flow ratios of acetylene to argon, Surf. Coat. Technol. 206 (2011) 994.
[23] I. Menow, R. Lowe, I. Penn, Passive stent coatings in the drug-eluting era, Invasive Cardiol. 17 (2005) 222.
[24] M. Avci-Adali, A. Paul, G. Ziemer, H.P. Wendel, New strategies for in vivo tissue engineering by mimicry of homing factors for self-endothelialisation of blood contacting materials, Biomaterials 29 (2008) 3936.
[25] N. Huang, P. Yang, Y.X. Leng, et al., Hemocompatibility of titanium oxide films, Biomaterials 24 (13) (2003) 2177–2187.
[26] K.M.D. Varvara, M.S.L. Stergios, K. Nikolaos, et al., Atomic force microscopy probing platelet activation behavior on titanium nitride nanocoatings for biomedical applications, Nanomedicine 5 (2009) 64–72.
[27] A. Melanie, A. Arvind, S. Dirk, A. Rosario, et al., Hemocompatibility of diamond like carbon–metal composite thin films, Diam. Relat. Mater. 15 (2006) 1941–1948.
[28] H.Q. Liu, C.J. Pan, S.J. Zhou, J.F. Li, N. Huang, et al., Improving hemocompatibility and accelerating endothelialization of vascular stents by a copper-titanium film, Mater. Sci. Eng. C 69 (2016) 1175–1182.
[29] H.Q. Liu, J.F. Li, S.J. Zhou, J.P. Long, L.H. Dong, G.X. Wei, Mechanical behavior and blood compatibility of copper-containing films as potential biomaterials, Bio-Med. Mater. Eng. 26 (1-2) (2015) 39–47.
[30] A. Bolz, M. Schaldach, Artificial heart valves: improved blood compatibility by PECVD a-SiC:H coating, Artif. Organs 14 (4) (1990) 260–269.

[31] M. Unverdorben, B. Sippel, R. Degenhardt, K. Sattler, R. Fries, B. Abt, et al., Comparison of a silicon carbide-coated stent versus a noncoated stent in human beings: the Tenax versus Nir stent study's long-term outcome, Am. Heart J. 145 (4) (2003) E17.
[32] P. Schuler, D. Assefa, J. Ylanne, N. Basler, M. Olschewski, I. Ahrens, et al., Adhesion of monocytes to medical steel as used for vascular stents is mediated by the integrin receptor Mac-1 (CD11b/CD18; alphaM beta2) and can be inhibited by semiconductor coating, Cell Commun. Adhes. 10 (1) (2003) 17–26.
[33] S.H. Monnink, A.J. van Boven, H.O. Peels, I. Tigchelaar, P.J. de Kam, H.J. Crijns, et al., Silicon-carbide coated coronary stents have low platelet and leukocyte adhesion during platelet activation, J. Investig. Med. 47 (6) (1999) 304–310.
[34] U. Kalnins, A. Erglis, I. Dinne, I. Kumsars, S. Jegere, Clinical outcomes of silicon carbide coated stents in patients with coronary artery disease, Med. Sci. Monit. 8 (2) (2002) 116–120.
[35] L.F. Tanajura, A.A. Abizaid, F. Feres, I. Pinto, L. Mattos, R. Staico, et al., Randomized intravascular ultrasound comparison between patients that underwent amorphous hydrogenated silicon-carbide coated stent deployment versus uncoated stent, JACC (2003). Abstracts—Angiography & Interventional Cardiology: 58A.
[36] M. Unverdorben, K. Sattler, R. Degenhardt, R. Fries, B. Abt, et al., Comparison of silicon carbide coated stent versus a noncoated stent in humans: the Tenax-versus Nir-stent study, J. Interv. Cardiol. 16 (4) (2003) 325–333.
[37] C.L. Zheng, F.Z. Cui, B. Meng, J. Ge, D.P. Liu, et al., Hemocompatibility of C–N films fabricated by ion beam assisted deposition, Surf. Coat. Technol. 193 (2005) 361–365.
[38] Z.L. Yang, J. Wang, X. Li, Q.F. Tu, H. Sun, et al., Interaction of platelets, fibrinogen and endothelial cells with plasma deposited PEO-like films, Appl. Surf. Sci. 258 (2012) 3378–3385.
[39] J.L. Chen, J.J. Cao, J. Wang, M.F. Maitz, et al., Biofunctionalization of titanium with PEG and anti-CD34 for hemocompatibility and stimulated endothelialization, J. Colloid Interface Sci. 368 (2012) 636–647.
[40] R.K. Myler, S.H. Stertzer, Coronary and peripheral angioplasty: historical perspective, in: E.J. Topol (Ed.), Textbook of Interventional Cardiology, second ed., W.B. Saunders Company, Philadelphia, PA, 1994, pp. 171–185.
[41] R.L. Wilensky, K.L. March, I. Gradus-Pizlo, A.J. Spaedy, D.R. Hathaway, Methods and devices for local drug delivery in coronary andperipheral arteries, Trends Cardiovasc. Med. 3 (5) (1993) 163–170.
[42] N. Zhao, N. Watson, Z. Xu, Y. Chen, J. Waterman, J. Sankar, D. Zhu, In vitro biocompatibility and endothelialization of novel magnesium-rare Earth alloys for improved stent applications, PLoS ONE 9 (2014) e98674.
[43] H. Gong, K. Wang, R. Strich, et al., In vitro biodegradation behavior, mechanical properties, and cytotoxicity of biodegradable Zn–Mg alloy, J. Biomed. Mater. Res. Part B 103 (2015) 1632–1640.
[44] R. Erbel, C. Di Mario, J. Bartunek, J. Bonnier, B. de Bruyne, F.R. Eberli, P. Erne, M. Haude, B. Heublein, M. Horrigan, Temporary scaffolding of coronary arteries with bioabsorbable magnesium stents: a prospective, non-randomised multicentretrial, Lancet 369 (2007) 1869–1875.
[45] M. Peuster, P. Wohlsein, M. Brugmann, M. Ehlerding, K. Seidler, C. Fink, et al., A novel approach to temporary stenting: degradable cardiovascular stents produced from corrodible metal-results 6-18months after implantation into new zealand white rabbits, Heart 86 (5) (2001) 563–569.
[46] P.P. Mueller, T. May, A. Perz, H. Hauser, M. Peuster, Control of smooth muscle cell proliferation by ferrous iron, Biomaterials 27 (10) (2006) 2193–2200.

[47] M. Peuster, C. Hesse, T. Schloo, C. Fink, P. Beerbaum, C.V. Schnakenburg, Long-term biocompatibility of a corrodible peripheral iron stentin the porcine descending aorta, Biomaterials 27 (28) (2006) 4955–4962.
[48] R. Stack, R. Califf, H. Phillips, D. Pryor, P. Quigley, R. Bauman, et al., Interventional cardiac catheterization at Duke medical center, Am. J. Cardiol. 62 (1988) 3F–24F.
[49] A.M. Lincoff, R.S. Schwartz, W.J.V.D. Giessen, H.M.M.V. Beusekom, P.W. Serruys, D.R. Holmes, et al., Biodegradable polymers can evoke a unique inflammatory response when implanted in the coronary artery, Circulation 86 (Suppl. 4) (1992) I–801.
[50] J.W. Eikelboom, J. Hirsh, Combined antiplatelet and anticoagulant therapy: clinical benefits and risks, J. Thromb. Haemost. 5 (2007) 255.
[51] A.T. Cohen, S. Imfeld, J. Markham, S. Granziera, The use of aspirin for primary and secondary prevention in venous thromboembolism and other cardiovascular disorders, Thromb. Res. 135 (2015) 217.
[52] J. John, S.K. Koshy, Current oral antiplatelets: focus update on prasugrel, J. Am. Board Fam. Med. 25 (2012) 343.
[53] S.D. Wiviott, E.M. Antman, E. Braunwald, Prasugrel, Circulation 122 (2010) 394.
[54] T. Inoue, K. Croce, T. Morooka, M. Sakuma, K. Node, D.I. Simon, Vascular inflammation and repair: implications for re-endothelialization, restenosis, and stent thrombosis, JACC Cardiovasc. Interv. 4 (2011) 1057.

Improving the hemocompatibility of heart valves

15

T. Gourlay, M. Rozeik
University of Strathclyde, Glasgow, United Kingdom

Abbreviations

a-C	nonhydrogenated amorphous carbon
a-C:H	hydrogenated amorphous carbon
AS	aortic stenosis
BPV	bovine pericardial valve
DLC	diamond like carbon
EC	endothelial cell
EOA	effective orifice area
Fng	fibrinogen
HSA	human serum albumin
INR	international normalized ratio
LTI	low temperature isotropic
LVAD	left ventricular assist device
MH	medtronic hall
MHV	mechanical heart valve
MR	mitral regurgitation
PAV	porcine aortic valve
PHV	prosthetic heart valve
PIII and D	plasma ion implantation and deposition
PPM	patient prosthesis mismatch
PVT	prosthetic valve thrombosis
PyC	pyrolytic carbon
RNS	Reynolds normal stress
RSS	Reynolds shear stress
SIBS	poly (styrene-block-isobutylene-block-styrene)
SJM	St. Jude Medical
ta-C	tetrahedral amorphous carbon
TAVI	transcatheter aortic valve implantation
TEHV	tissue engineered heart valves
TiN	titanium nitride
TiO	titanium oxide
TPG	transvalvular pressure gradient
TPU	thermoplastic polyurethane

Hemocompatibility of Biomaterials for Clinical Applications. https://doi.org/10.1016/B978-0-08-100497-5.00012-4
© 2018 Elsevier Ltd. All rights reserved.

15.1 Introduction

Heart valve replacement with a prosthetic heart valve (PHV) remains the most effective treatment for valvular diseases such as aortic stenosis (AS) and mitral regurgitation (MR); where degeneration is the most common etiology followed by rheumatic disease [1–4]. These relatively simple mechanical devices have considerably prolonged the lives of patients affected with morbidity associated with angina, syncope, dyspnoea, hypertension, ventricular dysfunction, and heart failure. Without replacement, prognosis worsens with increased disease severity and time. The survival rate of patients with AS over the age of 80 years is currently 52%, 40%, and 22% at 1, 2, and 5 years respectively [5].

Despite improvements in materials such as pyrolytic carbon (PyC) which is widely considered hemocompatible, PHVs still experience hemolysis, thrombosis, calcification, and pannus tissue growth occasionally leading to thromboembolism and mechanical obstruction which can be fatal. The ideal biocompatible heart valve would be bioinert and not recognized by the body as a foreign material, which would ameliorate many of these complications. This ideology has spurned excitement surrounding tissue engineering heart valves (TEHV) in recent years but these have currently failed to live up to expectations, sometimes with disastrous consequences [6,7]. Similarly, attempts to fashion PHVs from autografts fell drastically short of meeting the dynamic demands placed by the heart [8]. Despite these examples, the ideal PHV could one day be attainable, but may be some way off. However, until such technology is available for patients to obtain their own regenerative tissue valve, the more realistic goal would be to minimize the bioincompatibility of PHVs.

With blood contacting artificial devices, the first significant biological response is the rapid adsorption of serum proteins to the surface of the material (the Vroman effect). The effect of interactions between the proteins and the surface depends on the protein and the surface energy, wettability, charge, size, and many other factors. For example, the most abundant of these proteins, human serum albumin (HSA) has been linked to increased hemocompatibility through surface passivation, reducing platelet adhesion. However, activation of fibrinogen (Fng) leads to the formation of fibrin and a stable clot. In addition, diversion from the normal physiological blood flow leads to disruption to hemostasis. The physiological flow through the native undamaged valve is laminar, has virtually no pressure gradient, resulting in minimal shearing, hemolysis, and thromboembolism. Clear unobstructed flow in artificial heart valves however, is limited due to the unavoidable necessity for the occluding mechanism and supporting structures.

Thus although it is imperative to understand the relationship between PHV materials and the activation of coagulation factors, the fundamental mechanical design and its impact on blood flow, must also be considered. Valve design has improved significantly over the last 50 years, from the lateral flow profiles produced by ball and cage prosthesis to the more central flow types of tilting disk and bi-leaflet mechanical valves. These changes have introduced other hemocompatibility considerations, for example, the hinge region of bi-leaflet heart valves is susceptible to flow stagnation which could consequently lead to a local thrombus formation. In addition,

with improved access to new technology, the future of prosthetic valves is diverting towards transcatheter heart valve implantation (TAVI) and TEHV. Both these relatively modern technologies will open up more avenues for the drive towards improved valve hemocompatibility. The development of PHVs to the present day has been a complex journey, often driven by failure to join the loop between mechanical design and physiological requirements. This journey can be characterized by the following three phases; the pioneering phase, the development phase, and the refinement phase.

15.2 Valve pioneering era

Early PHVs deviated substantially from native valve design and focused primarily on applying a mechanical solution to a mechanical problem. One of the earliest mechanical prosthetic heart valves (MHVs) dates back to 1952 when Dr. Charles Hufnagel fitted a Plexiglas housing containing a silicone coated nylon ball into the descending aorta of patients with aortic insufficiency [9–11]. The increase in blood pressure during systole would cause the ball to displace distally and return when pressures drop in diastole. At the clamped edge of the prosthesis, a cul-de-sac which earlier contributed to thrombus formation, was eliminated by wrapping an Orlon mesh around the aortic wall [12–14]. Although the valve had an operative survival rate of 80%, incidence of thrombosis were high and prolonged aortic clamping times resulted in the death of some patients [15].

15.2.1 Mechanical heart valves

The advent of cardiopulmonary bypass facilitated the development of the next generation of caged ball valve prosthesis, which could be surgically implanted in the anatomical position without the time constraints faced by Hufnagel. In 1962 Albert Starr and Lowell Edwards, developed a silastic (silicone) ball within a Stellite cage valve inspired by an 18th century bottle stopper patent (Fig. 15.1). Ball variance, defined as "damage or change in structure of the poppet due to fatty infiltration of the silicone rubber ball," was a common phenomenon and caused hemolytic anemia from blood flow occlusion and thromboembolism from ball fractures [16–18]. This facilitated a material change from silastic (models 1000, 1200-1260) to a hollow Stellite ball (aortic and mitral models 2300 and 6300), although ball variance was eventually resolved with improved curing techniques in later models. In an attempt to promote endothelial growth and reduce thromboembolism, models 2300 and 6300 incorporated Dacron covered struts but no effective change to the platelet survival time was noted compared to model 1200 [19]. In addition, model 2300 and 6300 suffered high rates of intravascular hemolysis attributed to the Stellite material, a reduced effective orifice area (EOA), higher pressure gradients, exposed regions of the struts, and paravalvular leakage [20–23]. Explanted aortic and mitral cloth covered valves showed no tissue incorporation on the struts. On the contrary, cloth wear and pannus tissue growth on the orifice were noted, contributing to hemolysis from high pressure gradients, turbulence, and insufficiency [24–26].

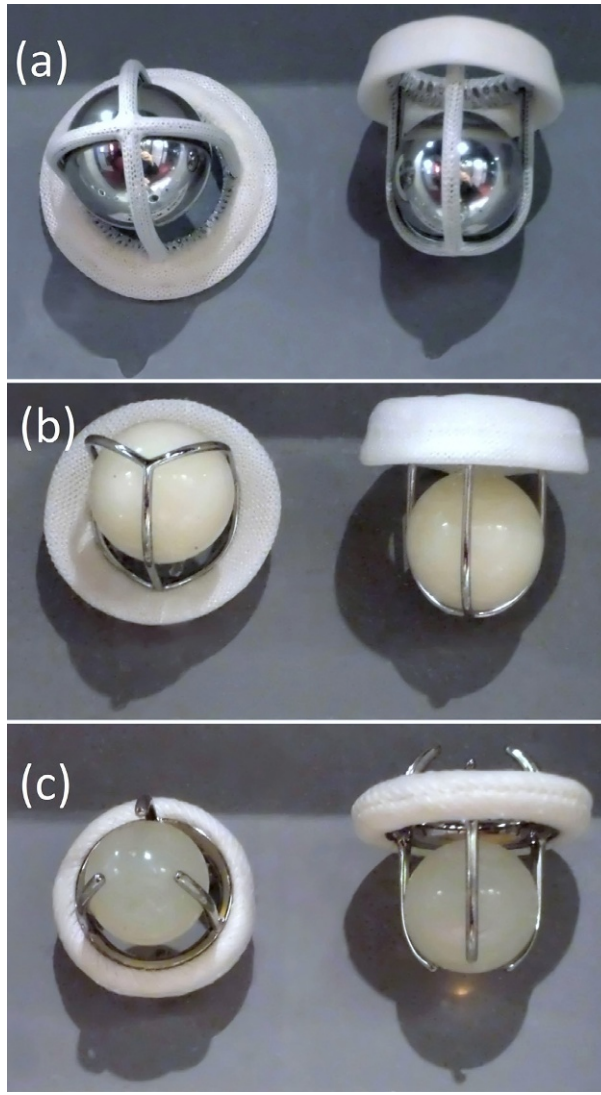


Fig. 15.1 Types of ball valve prostheses: (A) Starr-Edwards mitral valve with a Stellite poppet and cloth covered struts, (B) Starr-Edwards aortic valve model 1260 with a silicone poppet, and (C) Smelhoff-Cutter ball valve with a silicone poppet.
Courtesy of Dr Mirko Junge, CC BY 3.0.

Open caged designs such as the Smelhoff-Cutter ball valve allowed the ball to sit in the outflow cage rather than at the suture ring. This had many benefits in relation to the Starr-Edwards prosthesis, including a larger EOA and a washing away of stagnant blood between the ball and suture ring. The valve also experienced so little thrombosis that anticoagulation treatment was not administered to patients [27,28]. However, ball variance remained an issue and the valve was discontinued. Many of the failed ball

valves were replaced with homografts made from the patient's dura mater or pericardium which had low rates of thrombosis and hemolysis but, at that time, these bioprostheses performed poorly against the complex dynamic demands of the heart.

Around the mid-1960's, the high profile caged ball valves were swapped for low profile caged disk valves which had some benefits including a decreased risk of myocardial impingement and reduced opening and closing times [29]. However, the long-term outcomes such as severe disk wear leading to embolism, disk dislodgement, and large energy losses caused by lateral blood flow eventually led to their discontinuation [30]. Despite their short lifetime, they paved the way for the development of the tilting disk valves which allowed for a more central flow profile. One of the first successful tilting disk valves was the Björk-Shiley valve which could tilt to 50 degrees, reducing the pressure gradient significantly compared to the Starr-Edwards valves. The valve initially used a Delrin disk with Stellite struts and a Teflon sewing ring oriented so that the downward portion of the disk aligned with the noncoronary cusp of the aortic valve [31]. Shortly after their initial design, the opening angle was increased to 60 degrees and the disk was replaced with low temperature isotropic PyC carbon (LTI-carbon) as it demonstrated improved durability and hemocompatibility compared to Delrin which tended to expand [32,33]. LTI-carbon became the gold standard material for MHVs and is discussed in greater detail in the next section.

Attempts to improve the hemocompatibility of the Björk-Shiley valve led to the development of a convexo-concave disk held in place with an inlet and welded outflow strut (Fig. 15.2A). The changes created a 70 degrees opening and a gap between the disk and struts, eliminating regions of low flow. Although this increased the valve orifice area and reduced thromboembolism, the high pressures caused the outlet struts to fracture at the weld lines. This resulted in catastrophic failure from disk embolism, severe regurgitation and sudden cardiac death, forcing the manufacturers to recall the valve in 1986 [34]. Acknowledging the failure of the convexo-concave design, a monostrut valve was later developed, machined from a single piece of Hynes 25 to eliminate weld lines [35]. The valve had lower rates of structural failure and nill to

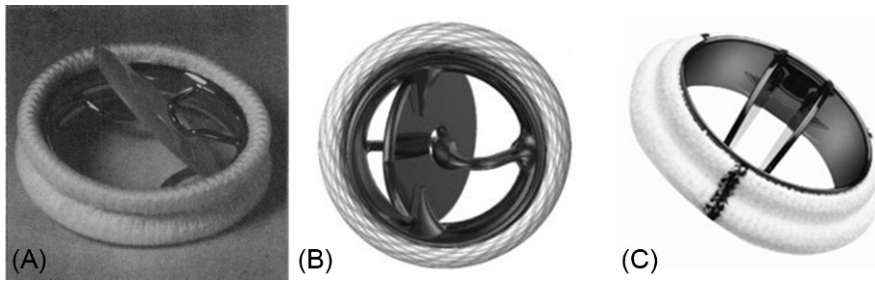


Fig. 15.2 Mechanical heart valves: (A) Björk-Shiley tilting disc valve with Delrin disk tilted open to a 60 degrees angle in a Stellite cage, [31], (B) Medtronic Hall tilting disc valve, and (C) Medtronic ATS Open Pivot bi-leaflet valve.
(A) Reproduced with permission from BMJ Publishing Group Ltd and (B,C) Reproduced with permission from Medtronic, Inc.

low rates of valve thrombosis though the incidence of thromboembolism was slightly higher than that of other mechanical valves [36–38].

The most successful tilting disk valve was the medtronic hall (MH) valve which first entered clinical use in 1977 as the Hall-Kaster valve (Fig. 15.2B). It used a perforated disk mounted on a central guide rod, enabling the disk to freely rotate to prevent thrombus formation whilst also increasing the tilting angle [39]. Results for the valve have shown very low rates of valve thrombosis (<0.2% per patient-year) and low rates of thromboembolism (1.1%–2.1% per patient-year), although it was slightly higher in the mitral position [39–42].

The search for a more central blood flow to reduce large pressure drops and increase the EOA, led to the development of the bi-leaflet mechanical valve which was first implanted in 1977. Blood flows through three orifices; a small middle and two larger lateral openings. The most common of these valves to date is the St Jude Medical (SJM) Masters valve with LTI-carbon leaflets and housing. Several bi-leaflet valve designs have since been developed including the SJM Regent, CarboMedic, Medtronic Parallel, Medtronic ATS Open Pivot (Fig. 15.2C), and the On-X all-carbon valves. The implications of their designs on hemocompatibility will be discussed later on in this chapter.

Blood compatibility complications are more prevalent in MHVs for two reasons; they produce nonphysiological blood flows which cause turbulence and shearing of red blood cells and their foreign surface can encourage Fng adsorption. Incidence of thrombolytic complications in MHVs is estimated to be between 0.6% and 6% per patient year (Table 15.1) [61,62]. Consequently, patients fitted with a mechanical prosthetic valve need to be on continuous anticoagulation therapy, increasing the likelihood of hemorrhagic complications. Obstruction of MHVs is mainly due to thrombus formation (Fig. 15.3) but pannus formation, although infrequent, can also occur [63] (Tables 15.2 and 15.3).

15.2.2 Bioprosthetic valves

Around the mid-1960s, the increased desire for a more physiological blood flow generated interest in bioprosthetic valves. More encouragingly, their native collagenous structure reduced the propensity for thrombus formation, eliminating the need for chronic anticoagulation treatment. Like MHVs, bioprosthetic valves underwent several design modifications to improve their hemodynamic performance. This included reducing their profile, changing from rigid to flexible stent posts, eliminating commissural sutures, and increasing the EOA [75,83–85]. In an attempt to increase hemocompatibility and eliminate immunogenicity issues, autologous heart valves were developed using the patient's own tissue which included fascia lata, dura mater, pericardium, peritoneum, and superior vena cava [86–90]. Inspired by the hemocompatibility of homografts used in the Ross Procedure, Ionescu pioneered the use of autologous fascia lata tissue sutured around a Dacron covered titanium stent, which he prepared in the operating theater [88]. Early results with autologous heart valves were positive; reporting freedom from infection, nill to low pressure gradients and good viability following implantation [89,91–93]. However despite their biostability,

Table 15.1 **Percentage rates per patient year of prosthetic valve thrombosis and thromboembolism for various mechanical heart valves**

Valve	Type	PV Thrombosis		Thromboembolism		References
		Aortic	Mitral	Aortic	Mitral	
ATS Open Pivot	Bi-leaflet	0.00	0.40			Emery et al. (2004)
Björk-Shiley	Tilting-disc	0.18	0.79			Ryder et al. (1984)
BS-Monostrut	Tilting-disc	0.00	0.00	0.60	2.60	Björk and Lindblom (1985)
CarboMedics	Bi-leaflet	0.30	0.63-1.00	0.50	0.80-4.40	Kuwaki et al. (2002), Nazarov et al. (2014), Jamieson et al. (1999)
CarboMedics*	Bi-leaflet	2.60	6.50	0.00	1.40	Williams et al. (2004)
CardiaMed	Bi-leaflet		0.63			Nazarov et al. (2014)
Edwards MIRA	Bi-leaflet	0.34-2.81		1.00		De Feo et al. (2003), Driever et al. (2004), Verhoye et al. (2007)
Medtronic Hall	Tilting-disc	0.00-0.10	0.20	1.30-1.47	1.70-2.10	Hall et al. (1985), Akins (1996), Svennevig et al. (2007)
Medtronic Hall*	Tilting-disc	0.00	2.90	1.60	1.10	Williams et al. (2004)
Omnicarbon	Tilting-disc		0.30			Carrier et al. (2004)
On-X	Bi-leaflet	0.00-0.11	0.10-0.35	0.60-0.88	1.00-1.76	Ozyurda et al. (2005), Williams and van Riet (2006), Palatianos et al. (2007), Chambers et al. (2013)
On-X *	Bi-leaflet	0.00	0.00	1.80	0.00	Williams et al. (2004)
Sorin BiCarbon	Bi-leaflet			1.33		Spiliopoulos et al. (2009)
St Jude Medical	Bi-leaflet	0.20		1.30	2.30-5.40	Chaux et al. (1984), Silber et al. (1993), Jamieson et al. (1999)
Starr-Edwards (Silastic ball)	Ball and Cage	0.10	0.40			Metzdorff et al. (1984)

* Inadequate anti-coagulation used.

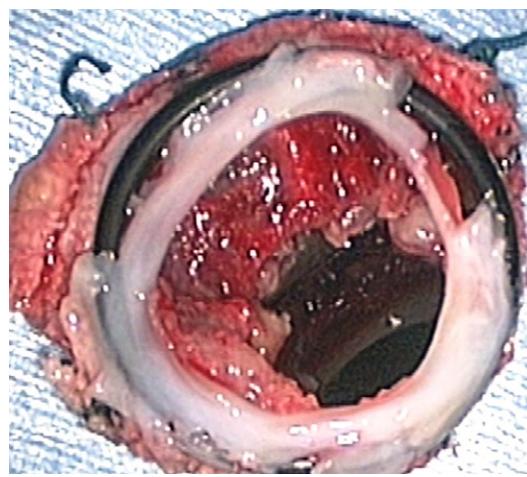


Fig. 15.3 An explanted thrombosed mechanical mitral valve.
Courtesy of Mr. Prakash Punjabi, Dept. Cardiothoracic Surgery, Imperial College London.

Table 15.2 Percentage rates per patient year of prosthetic valve thrombosis and thromboembolism for various bioprosthetic heart valves

Valve	Type	PV Thrombosis		Thromboembolism		References
		Aortic	Mitral	Aortic	Mitral	
Biocor	Porcine valve	1.26	-	1.25	1.82	Brown et al. (2012), Mykén (2005)
Carpentier-Edwards (CE)	Porcine valve	0.03	-	2.60	-	Gao et al. (2004)
	Bovine pericardium	0.00	-	1.30	-	Gao et al. (2004)
CE Perimount	Bovine pericardium	-	-	-	1.10	Marchand et al. (2001)
Hancock	Porcine valve	0.84	-	-	-	Brown et al. (2012)
Medtronic Freestyle	Aortic root	-	n/a	2.10	n/a	Doty et al. (1998)
Mosaic	Porcine valve	0.37	-	-	-	Brown et al. (2012)
SJM Trifecta	Bovine pericardium	-	-	1.90	-	Bavaria et al. (2014)

accumulation of plasma proteins and erythrocytes on the surface of the leaflets led to collagen fiber disintegration [8].

With the advent of glutaraldehyde fixation to reduce immunogenicity, the development of biological xenografts rapidly expanded. Two of the most common types to date are porcine aortic valves (PAV) and bovine pericardial valves (BPVs). With the latter, early results with the Ionescu-Shiley pericardial valve reported very low rates of thromboembolism without the need for chronic anticoagulation but the long-term outcomes included cuspal tearing, leaflet thickening, and calcification [76–78]. Early failure of BPVs shelved their use until the mid-1980s when they were revived by the Carpentier Edwards pericardial valve (Fig. 15.4A and B) and focus instead went to the use of native stented PAVs. These valves appeal as their native structures allow for elastic radial deformation to facilitate coaptation with minimal strain on the commissures. However, their glutaraldehyde treatment at high fixation pressures of 80–100 mmHg, considerably stiffened the leaflets and contributed to high rates of calcification and structural degradation. This prompted a change to significantly lower pressures of 0–4 mmHg and reduced concentrations of glutaraldehyde to increase durability [83]. A disadvantage of PAVs is their limited design flexibility compared to BPVs and the presence of a stent significantly compromises their EOA. Around the mid-1990's stentless PAVs were introduced having superior EOAs and hemocompatibility (Fig. 15.4C). Yet they remain within a niche market due to the longer cross-clamp times and increased technical difficulty to implant surgically.

In addition to conventional bioprosthetic valves, pericardium has been utilized in TAVI which rapidly took off after the first human implantation in 2002 [94]. The common components of the technology are comprised of pericardial leaflets sutured onto a collapsible stent and a delivery catheter to facilitate percutaneous valve

Table 15.3 Valve related complications and their impact on hemocompatibility

Property	Complication	Description	Paravalvular Leakage	Increased TPG	Flow Turbulence	Thrombosis	Haemolysis	Thromboembolism
Valve Positioning and Sizing	Valve Migration	Migration is more likely to occur with TAVI valves. This may occur if valves are inadequately expanded, non-uniformity of calcific annulus or mal-positioning (Cao et al., 2012; Pang et al., 2012).	×			×	×	×
	Patient prosthesis mismatch (PPM)	PPM can occur from an underestimation of the valve annulus, leading to a lower EOA relative to the patient's body surface area (Bakhtiary et al., 2007; Lund et al., 1997).		×	×	×	×	×
	Mal-positioning	Incorrect positioning of the valve can occur through either poor commissural alignment or poor annular seating (Webb et al., 2007).	×	×	×	×	×	×
Valve Material	Cloth cover wear	Wear from the occluder on cloth covered sewing rings and struts (Schottenfeld et al., 1971; Shah et al., 1978; Shiono et al., 2005).				×	×	×
	Disc Wear	Valve occluder wear from constant rubbing against the valve housing (Edgett et al., 1967).				×		
	Leaflet calcification	Calcification commonly occurs with glutaraldehyde treated bioprosthetic valves leading to leaflet thickening, stiffness and stenosis (Vesely, 2003).		×				
	Leaflet tear	Leaflet tears can be associated with calcification through stress regions on calcific nodules, through suture regions or along the leaflet free edge (García-Bengochea et al., 1982; Schoen et al., 1987; Walley et al., 1992).	×	×			×	
	Disc lipid adsorption	Common with silicone poppets of Starr-Edwards valves and Björk-Shiley Delrin tilting disc valve (Garcia et al., 1968; Hylen, 1970; Joyce et al., 1978).		×		×	×	×
Valve Design	Strut Failure/Fracture	Strut fracture can occur due to mal-positioning or poor sizing, subjecting the housing to increased stress (Blot et al., 2005; Von Der Emde J et al., 1990).				×	×	×
	Disc immobilization	Occluder can become immobilized secondary to other complications such as strut fractures (Edgett et al., 1967).		×	×			
	Low EOA	A low EOA can result from PPM, valve migration, or leaflet calcification.		×	×			
	Flow obstruction	Obstruction to flow can occur due to the presence of the annular sewing ring or through thrombus formation (Roudaut et al., 2007).		×	×	×		
	Recirculating flow	Low flow regions can occur around the hinge mechanism of bi-leaflet MHVs or further downstream of the valve (Ellis et al., 1996; Gross et al., 1996; Leo et al., 2002).				×		×
Surface Properties	High surface roughness	Increased affinity for protein adsorption (Alves et al., 2014).				×	×	×
	High surface energy	Increased affinity for protein adsorption (Alves et al., 2014).				×	×	×



Fig. 15.4 Bioprosthetic heart valves: (A) Medtronic Hancock porcine valve, (B) Carpentier-Edwards MAGNA pericardial aortic bioprosthesis, and (C) Medtronic Freestyle aortic root prosthesis.
Reproduced with permission from Medtronic, Inc. and Edwards Lifesciences LLC, Irvine, CA.

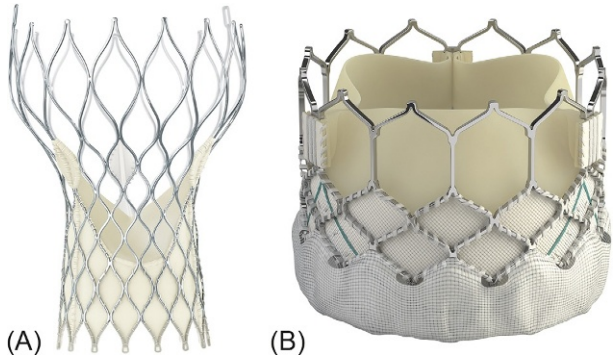


Fig. 15.5 Transcatheter aortic heart valves: (A) Medtronic CoreValve Evolut and (B) Edwards SAPIEN valve.
Reproduced with permission from Medtronic, Inc. and Edwards Lifesciences LLC, Irvine, CA.

deployment through the arteries and over the native diseased valve. The two leading valve technologies in this field are the Medtronic CoreValve (Fig. 15.5A); a porcine pericardial valve with a self-expandable Nitinol stent, and the Edwards SAPIEN heart valve (Fig. 15.5B); a BPV with a cobalt-chromium stent. Delivery routes have evolved from the gold standard retrograde trans-femoral approach to other routes including trans-apical, trans-axillary, trans-aortic and trans-carotid [95–99]. The technology has progressed rapidly from being initially limited to high-risk elderly patients denied conventional surgical valve replacement towards implantation in low and intermediate risk patients and continues to make strides in state-of-the-art valve technologies [100].

The long-term freedom from thromboembolism in pericardial valves in the absence of anticoagulant treatment is considered to be a significant benefit [76,101,102]. In a study of 1751 patients receiving aortic valve replacement with a mean follow up period of 3.4 years, PAVs were reported to be independent predictors of obstruction, with a thrombosis rate of 2.3% compared to none in BPVs [103]. However, both types of bioprosthesis have a high propensity for calcification, reducing their durability and making them unsuitable in younger patients. Calcification can be intrinsic (calcific nodules forming on the surface of an intact leaflet) or extrinsic (calcification formed

at site of lesion or crack on surface of leaflet). Conversely, tearing can be caused by localized calcific nodules on the surface of the leaflet. Apart from leading to structural degradation, leaflet tears can lead to hemolysis due to the increased shearing of blood through these gaps [104]. This has promoted a drive for alternative fixation methods to reduce leaflet calcification.

15.2.3 Polymeric materials

Polymeric heart valves combine the durability of MHVs with the biocompatibility of bioprosthetic valves [105]. Valve leaflets can be manufactured from a wide variety of polymers including thermoplastic polyurethane (TPU), silicone, polyvinyl acetate, polytetrafluoroethylene, and poly(styrene-block-isobutylene-block-styrene) (SIBS) [106–110]. TPUs in particular, are a popular choice due to their composition of alternating blocks of soft and hard segments, providing a good compromise between compatibility and mechanical strength. Early TPUs such as polyester urethane and polyether urethane suffered from hydrolysis, oxidation, and calcification, subjecting them to surface cracking and limiting their use to short term applications such as left ventricular assist devices. Polymeric heart valves have also been prone to thrombogenicity and calcification [105,111]. Significant advancements in material science have improved polymer resistance to hydrolysis and oxidation. Recently, a polyether urethane elastomer marketed as Elast-Eon with a poly(dimethylsiloxane) to poly(hexamethylene oxide) ratio of 80:20 was shown to have increased biostability compared to standard polyether urethane and has demonstrated potential use in PHVs [112,113]. The surface properties of polymeric heart valves can be modified to increase their resistance to platelet attachment. This is discussed in further detail below.

15.3 Advancements in valve development

Despite the advances made in the development of PHVs, hemocompatibility issues including prosthetic valve thrombosis (PVT), hemolysis, pannus tissue growth, and calcification remain a concern. PVT is particularly prevalent in MHVs, with incidences as high as 20% in the tri-cuspid position [114]. It is influenced through a range of factors including inadequate anticoagulation treatment, valve material, blood-surface interactions, and prosthetic valve hemodynamics. The design considerations for improving valve hemocompatibility are discussed in depth below.

15.3.1 Hemocompatible coatings

15.3.1.1 Low temperature isotropic pyrolytic carbon

Since the introduction of low temperature isotropic pyrolytic carbon (LTI-carbon), most mechanical valves have utilized it for its superior hemocompatibility, durability, and resistance to crack growth. Initially, used for nuclear fuel particle coatings before finding use in biological applications by Bokros and colleagues in 1969, LTI-carbon

differs from graphite in that the graphene layers are disorderedly stacked against each another; giving it increased flexibility and durability [115]. It is applied as a thick coating over a suitable substrate using fluidized bed chemical vapor deposition. Substrates of graphite or titanium or cobalt-chromium alloys can be used and could be machined off afterwards to leave a monolithic substrate. The Debakey Surgitool was the first valve to utilize this material for their ball occluder although the superior toughness of the ball contributed to strut fracture [116]. The improved blood compatibility of LTI-carbon valves independent of valve design was demonstrated in a study comparing two tilting disk valves identical in form but which differed in composition. The incidence of thromboembolism was reduced in the all-LTI-carbon Omnicarbon valve compared to the Omniscience valve which had a titanium housing and LTI-carbon disk (0.5% vs. 1.7% per patient year in the aortic position) [117].

LTI-carbon is widely acknowledged to have a strong affinity for all plasma proteins to its surface, implying that blood compatibility is achieved through surface passivation [118–120]. Feng and Andrade hypothesized four stages for protein surface conditioning: diffusion of protein (collision with the surface), adsorption (mainly albumin, as it is the most abundant), denaturation (adsorbed protein denatures and a protective film of protein forms), and modification (the film prevents activation of the coagulation cascade) [121]. In one study, high levels of Fng adsorption on LTI-carbon were noted to have undergone conformational changes upon adsorption, leading to a loss of platelet binding sites [119]. This may suggest that the active state of the protein adsorbed rather than its affinity is the contributing factor for surface passivation [118].

Early MHVs incorporated silicon carbide (SiC) into the structure of PyC to improve its mechanical properties such as hardness and wear resistance. With improved processing techniques it was eventually possible to develop pure LTI-carbon with improved toughness and deformation, facilitating development of more complex designs previously not possible with silicon alloyed LTI-carbon [122]. Despite this, Goodman et al. found no evidence that a pure LTI-carbon improved hemocompatibility compared to silicon alloyed valves as long as the amount of SiC was within a reasonable range (0.54–13.5 wt%) [123].

One example of a pure LTI-carbon valve is the On-X bi-leaflet heart valve, having a highly polished surface and a 90 degrees opening angle. These valves had very low rates of PVT ($\leq$0.11% and $\leq$0.35% per patient year in aortic and mitral positions) and thromboembolism (0.88% and 1.76% per patient year for aortic and mitral positions) [53,55,124]. The Prospective Randomized On-X Anticoagulation Clinical Trial (PROACT) observed that patients with the On-X valve could take a lower dose of warfarin (international normalized ratio (INR), 1.5–2.0) compared to the standard treatment (INR, 2.0–3.0) 3 months after aortic valve replacement, which would reduce the rate of bleeding complications without significantly impacting thromboembolism [125]. It is possible that the design and highly polished surface of these valves rather than their pure carbon content is the contributing factor to its increased hemocompatibility.

Despite the improved hemocompatibility of LTI-carbon compared to titanium and other earlier mechanical valve materials, they are still prone to thromboembolism. Although, a high adsorption of HSA is attributed to increased blood compatibility, platelet activation even in the presence of HSA was shown on CarboMedic and SJM LTI-carbon valves [126]. In addition, their brittle nature makes them prone to

fracturing. This has encouraged some research into the use of ceramics as alternative coating materials for MHVs. Surface coating techniques such as plasma-enhanced chemical vapor deposition (PECVD), ion beam enhanced deposition, and plasma immersion ion implantation, and deposition (PIII and D) have facilitated the deposition of titanium oxide (TiO), titanium nitride (TiN), and diamond-like carbon (DLC) coatings on the irregular surfaces of MHVs [127–132].

15.3.1.2 Titanium alloyed coatings

One of the earlier studies investigating the use of titanium alloyed coatings developed a tilting disk valve made from a single crystal alumina disk with a titanium ring coated with TiN using ion plating [133]. Titanium alloyed coatings have reduced platelet adhesion, protein denaturing, Fng activation, and longer clotting times making them promising alternatives to LTI-carbon [132,134–136]. Both the surface energy and semiconductivity of these coatings play a vital role in improving the hemocompatibility of heart valves. Chen et al. found that n-type doping titanium oxide films with tantalum raised the films' Fermi energy level which facilitated electron transfer from the inner regions to the outer surface. This made it more difficult to transfer charge from the protein to the surface, inhibiting the decomposition of Fng [134]. Improved hemocompatibility has also been observed through this reduction in the work function (the energy required to move an electron from the highest Fermi level of a solid to a vacuum) of Ti^{2+} and Ti^{3+} in TiO_2 coatings [132]. Huang et al. found that changing from an amorphous to a crystalline TiO structure reduced platelet adhesion even further [135].

The techniques that could be applied to deposit titanium alloyed coatings are limited due to the complexity and nonplanar surfaces of MHVs. Leng et al. used titanium metal and oxygen PIII to deposit films of titanium oxide on the surface of titanium alloy Ti6Al4V, demonstrating good wear resistance although plastic deformation was an issue due to an inadequate film thickness [130].

15.3.1.3 Diamond like carbon coatings

DLC are a class of amorphous carbons having similar properties to diamond, containing a mixture of both sp^2 and sp^3 carbon-carbon interatomic bonds. Their classification include tetrahedral amorphous carbon (ta-C), hydrogenated amorphous carbon (a-C:H), and nonhydrogenated amorphous carbon (a-C). DLC coatings have generated recent interest due to their chemical inertness, low coefficient of friction, high resistance to wear, and biocompatibility. They have reported high ratios of HSA to Fng adsorption and reduced platelet adhesion [137–139]. The improved blood compatibility of titanium incorporated a-C:H films compared to TiN and (titanium carbide) TiC coatings was shown to be due to their increased hydrophobicity [139]. There is also evidence of DLC coatings inhibiting the activation of clotting factors irrespective of affinity for protein adsorption. Although ta-C films and LTI-carbon had identical protein adsorption, the reduced effective work function of the surface of the ta-C film (1.0 eV) compared with LTI-carbon (5.5 eV), made it harder to transfer charge from the inactive state of Fng to the surface (Fig. 15.6) [140].

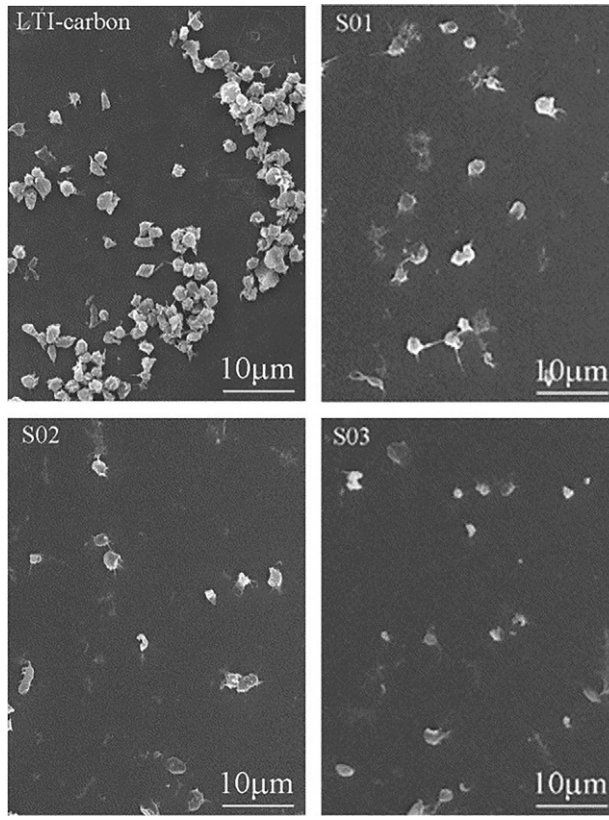


Fig. 15.6 Platelet adherence on samples of LTI-carbon and DLC coatings [140].

DLC coatings can be doped with other elements such as silicon, fluorine, and chromium to improve its hemocompatibility. Nitrogen doped hydrogen-free DLC coatings using PIII and D reported decreased adhesion and activation of platelets compared to LTI-carbon, although this deteriorated at higher nitrogen concentrations [141]. Silicon doping of a-C:H films reduced platelet aggregation compared to as-deposited DLC films and lowered its electrical resistivity, work function, and surface energy which increased adhesion of endothelial cells (ECs) [142–144]. Chromium modified DLC films deposited on silicon wafers using magnetron sputtering found a positive correlation between an increase in the disordered graphitic phase and enhanced EC attachment [145,146].

More studies are needed to determine the long-term environmental effects on the tribological properties of DLC coatings. Hydrogenated DLC samples aged for three years had a higher coefficient of friction, age-induced surface oxidization, and reduced hydrophobicity compared to as-deposited samples [147]. In addition, the adhesion between the coating and the substrate can be poor due to high intrinsic compressive stresses [148]. One of the more promising methods to improve stability of DLC coatings is through the incorporation of silicon. This has shown reduced environmental

and thermal effects, reduced internal stresses, stabile sp^3 bonds, and inhibited sp^2 hybridization [148]. The deposition method could also improve DLC stability. Pulsed DC PECVD was shown to improve stability and recommended as an alternative to RF (radio frequency) PECVD due to its deeper penetration into the substrate [149].

15.3.2 Surface engineering

It has been suggested that an increased understanding of the relationship between the surface of the prosthesis and attachment of plasma will facilitate development of materials with improved blood compatibility [33,150]. This has created a cascade of surface treatments through the application of anticoagulant coatings or by modifying the surface energy and roughness.

15.3.2.1 Anticoagulant coatings to inhibit thrombin formation

The ability of heparin and other anticoagulant coatings to inhibit thrombin relies on the immobilization techniques and durability of the coating on the surface of the heart valve. One of the first studies on anticoagulant coated surfaces used a cationic surface active agent to bond heparin to graphite, demonstrating freedom from coagulation in the 10 h time limit of the study compared to rinsed heparin treated graphite which experienced coagulation within an hour [151]. Following this, rings of heparin bound graphite reported little to no sign of thrombosis following implantation studies after a year. Immobilization of heparin oligosaccharides on surface modified LTI-carbon coated graphite found some evidence of protein resistance and anticoagulant activity particularly with cleaved, low affinity heparin with factor Xa inhibition activity [152]. Heparin coatings have also found antithrombogenic potential with tissue valves using a heparin-vascular endothelial growth factor multilayer film [153]. The durability of immobilized heparin following exposure to plasma at a high shear rate however remains an issue, with studies showing a shearing of the top layer of the coating in combination with a loss of heparin conjugate and some plasma deposition [153,154]. In addition, there has been some indication of heparin adsorption into the blood stream which may limit its anticoagulant potential with time [151]. Bokros and colleagues speculated that the amount of heparin may have little effect on the thrombogenicity of LTI-carbon heart valves whereas surface roughness and oxygen may play a greater role [115].

Hirudin is a small protein with thrombin inhibition properties which has also been examined for use as a potential antithrombogenic coating. Covalent binding of hirudin on the surface of Dacron, for sewing rings, was found to reduce the rate of platelet adhesion and activation as well as a reduced conformational change to Fng [155].

15.3.2.2 Surface modification to inhibit platelet adhesion

Surface energy plays a crucial role in platelet adhesion. It was noted that materials with either a low critical (20–30 dyne/cm) or high surface tension, could prevent thrombus formation through different mechanisms [150]. A low surface tension was associated with an increased dynamic clotting time and a weak adherence of protein, allowing

any attached platelets to wash away with the shearing rate of blood. For example, the surface tension of the Stellite 21 struts of the Starr-Edwards ball-valves was reduced through a coating of Teflon. Conversely, a high surface tension would promote a strong cellular attachment, forming a protective biological barrier.

Surface modification of polymeric heart valves have shown some reduction in platelet adhesion. Park et al. measured an increase in proteolytic activity and a lack of thrombus formation on polyurethane heart valves with lumbrokinase (a fibrinolytic enzyme) immobilized on their surface by photoreaction [156]. The surface modification of a SIBS polymeric heart valve with phospholipids has shown to reduce platelet adhesion by a factor of 10 [157]. When these valves were compared against the Carpentier-Edwards PERIMOUNT Magna Aortic bioprosthetic valve, the platelet activation rate was five times lower using a platelet activity state assay [158]. Surface grafting 2-hydroxyethylmethacrylate on TPU films by plasma treatment was shown to decrease surface roughness and increase hydrophilicity. The higher polar component of its surface energy created a low affinity for proteins adsorption, thereby reducing thrombus formation [82].

15.3.2.3 Surface endothelization

Native heart valves are protected through the endocardium, a protective nonthrombogenic layer of ECs surrounding the myocardium and heart valves. Utilizing this feature, ECs can be grown on artificial surfaces to provide a hemocompatible layer. The success of developing a confluent layer depends on the surface type and roughness. For instance, EC growth on PyC coated knitted Dacron and Teflon was reportedly greater compared to uncoated fabrics [159]. Conversely, increasing surface roughness can improve attachment. Endothelium grown on polished LTI-carbon surfaces of bi-leaflet and mono-cusp MHVs were found to detach an hour after they were implanted in the mitral position of a pig [160]. Micro-channels to increase the surface area of mechanical bi-leaflet valves, reduced local shear stress and enabled ECs to remain confluent even following exposure to shear rates of up to 600 dyn/cm^2 [161]. Incremental seeding of ECs at a volume flow rate of 2 L/min using a computer-assisted bioreactor system allowed uniform endothelization with reduced platelet adhesion (6200 ± 1352 platelets compared to $39{,}200 \pm 4249$ platelets on nonseeded constructs) on decullularized porcine pulmonary valve tissue [162].

15.3.3 Valve design

15.3.3.1 Introduction

Despite improved material and surface blood compatibility, the nonphysiological flow behavior through prosthetic valves, particularly in MHVs, are associated with high jet velocities, flow divergence, and regions of recirculating flow. These disturbances lead to high shear stresses which contribute to hemolysis, platelet activation, and thrombus formation. High wall shear stresses can also damage the endothelium of surrounding structures, promoting thrombus and calcific plaque formation [163]. The impact of valve design on flow and accordingly the hemocompatibility was highly evident when

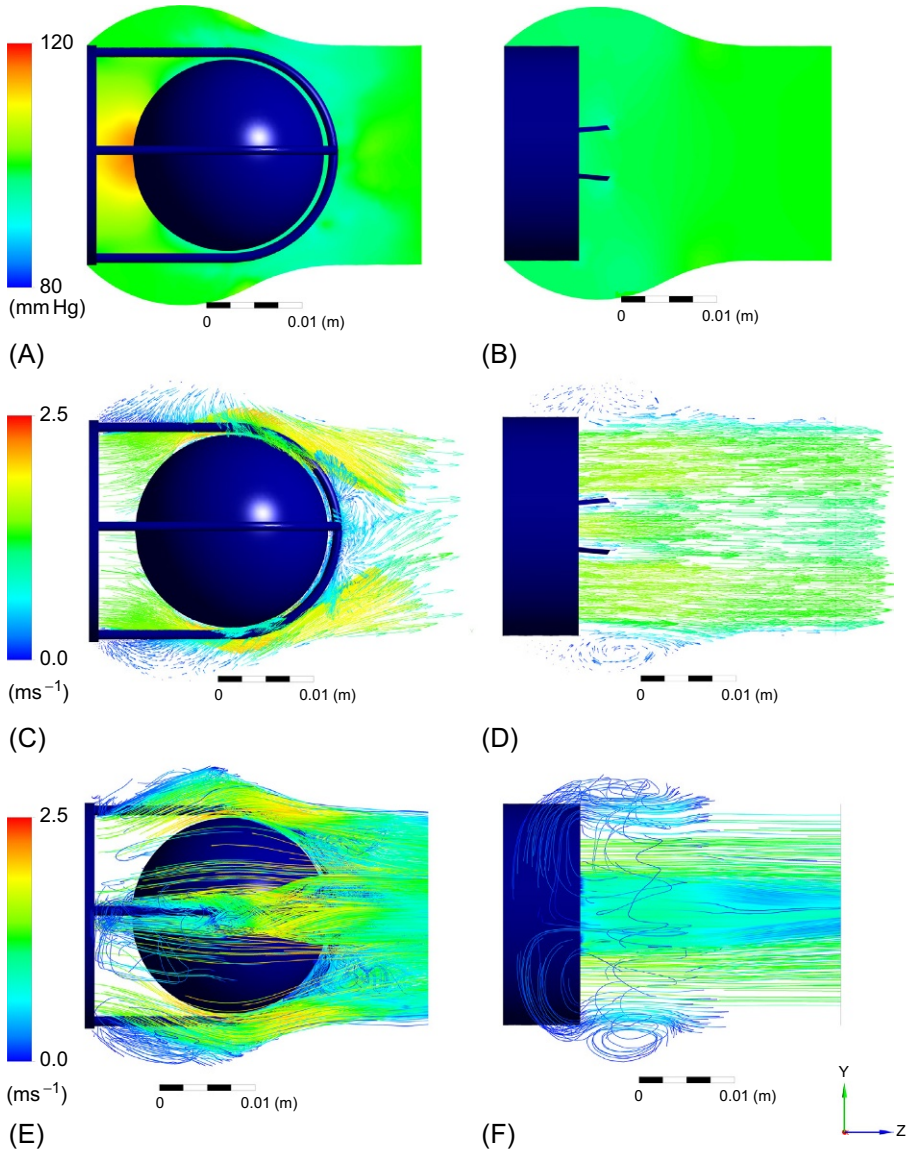


Fig. 15.7 Impact of mechanical valve design on flow parameters within an aortic annulus in a (A,C,E) ball valve prosthesis and a (B,D,F) flat bi-leaflet valve. Images (A,B) are of the pressure across valve, (C,D) of their velocity profiles—a wake can be observed downstream of the ball and cage valve, and (E,F) their flow streamlines.

blood flow switched from lateral to central (Fig. 15.7). For instance, the incidence of intravascular hemolysis in the Björk-Shiley tilting disk valve was approximately a third that of the Starr-Edwards prosthesis [23]. Similarly, relative to bi-leaflet MHVs, both the Starr-Edwards and the Björk-Shiley valves demonstrated higher average systolic Reynolds normal stress (RNS) values. This correlated with increased endothelial damage two diameters downstream of the blood flow although the maximum RNS valves reported were not high enough to cause hemolysis [164].

In silico and in vitro circulatory flow models have improved understanding of the relationship between flow patterns and valve design. These models can closely predict hemodynamic parameters such as shear stress, transvalvular pressure gradients (TPGs), leakage, and hemolysis which can be benchmarked against threshold values to gauge the hemocompatibility of different valve designs. For example, Reynolds shear stress (RSS) thresholds of 4000–8000 dyn/cm^2 have been reported as critical levels below which no damage to the blood elements is observed [165–167]. Thus gradual improvements to the valve could be made through an iterative process of design development and testing. This section will focus on the refinements made to existing prosthetic valves to improve their flow profiles. Although these issues are largely associated with mechanical bi-leaflet valves and thus will be the primary focus in the following paragraphs, the influence of design on flow through other valves will also be discussed.

15.3.3.2 Maximizing valve opening area

As minimizing flow obstruction is a key requirement to reducing flow disturbance, there is a need for leaflets to rapidly open as wide as possible. Exceptionally high EOAs are attainable with stentless aortic bioprostheses which concomitantly contribute to lower trans-aortic velocities and lower TPG values [168]. The impact of eliminating the stent was evident through earlier left ventricular regression in stentless valves, particularly in patients with reduced LV function [145,146,168,169]. In stented bioprostheses, BPVs have a greater degree of design flexibility in maximizing their EOA than PAVs. For example, the pericardium can be wrapped around the exterior of the stent to minimize flow obstruction and provide a larger opening angle. However, structural valve deterioration could develop as it did with the Sorin Mitroflow valve, associated with tissue abrasion, commissural tearing, and calcification, particularly in younger patient populations [170–173]. Tissue abrasion can be reduced by covering the stent with pericardium, as is the case with the SJM Trifecta valve, ensuring tissue on tissue contact [174].

MHVs have optimized their EOA by increasing the leaflet opening angle. The MH tilting disk valve achieved this through incorporation of a central guide rod and a small clearance between the rod and the disk perforation which facilitated rapid closure and minimized regurgitation. In smaller valves of the same size, the areas were notably larger with the MH valves compared to the Björk-Shiley and Lillehei-Kaster tilting-disk valves [39]. Most bi-leaflet valves have opening angles in the range of 78 to 85 degrees to ensure leaflets are able to tilt back to their closed position during diastole. The On-X bi-leaflet MHV enabled leaflets to open to 90 degrees without af-

fecting closure by incorporating an "actuated pivot design" which ensured leaflets tilt back following reversal of blood flow [175]. Though optimizing valves to have larger opening angles is desirable, increased traverse angles (from a fully open to a fully closed position) could increase closure time, closing velocity magnitude, and shear stress, promoting higher potential for platelet activation [176].

Simply increasing the valve opening area, however, would alone not be sufficient to physiologically mimic the flow through native valves. Despite improvements towards a more central blood flow and decreased wake when the leaflet opening angle of bi-leaflet MHVs increased from 78 to 85 degrees, the shear rates and maximum flow velocities were reportedly higher [177]. These finding highlighted two additional design features with bi-leaflet MHVs that can influence hemocompatibility; the leading edge of leaflets where vortices were seen to form, and the valve housing where higher shear stresses and a slower flow of blood can lead to clot formation.

15.3.3.3 Reducing flow recirculation

Regions of recirculating blood and low flow velocities can accumulate with blood and eventually contribute to thrombus formation. One of the more problematic hemocompatible regions are the hinges of bi-leaflet MHVs, where blood can recirculate over several cardiac cycles before washing away with the flow. Studies around the inflow channel of the hinge of the Medtronic Parallel bi-leaflet heart valve identified vortical flow combined with high turbulent stresses, flow stagnation, and disturbed flow patterns as the cause of thrombus formation [79,80]. Similarly, the sharper angles of the hinge of CarboMedics valve contributed to higher turbulent shear stresses and leakage velocities than the SJM valve [81,178]. The high thrombotic complications associated with the Medtronic Parallel valves eventually led to their withdrawal. The On-X bi-leaflet valve reduced these complications by developing a more streamlined pivot recess and a gap between the leaflet hinge and pivot, enabling blood to channel through. The Medtronic ATS Open-Pivot valve has a spherical convex pivot guide to enable blood to wash away rather than pool around the hinges. These improvements led to low thromboembolic rates of 1.25% per patient year and encouraged a reduction in anticoagulation treatment to an INR of 1.5 to 2.5 in isolated aortic valve replacement cases [179].

Blood can also pool around the valve housing. The Jyros bi-leaflet MHV attempted to reduce flow stagnation by allowing the leaflets to freely rotate around the central axis of the housing. However, studies found no evidence of valve rotation in 0%–50% of cases and reported high rates of PVT [180–182]. The valve was discontinued but resurfaced in 2003 as the CardiaMed heart valve, made from a single piece of LTI-carbon which also allowed the leaflets to rotate about the central axis. Mid-term results of a multicenter trial of 420 patients found PVT occurring in 0.63% per patient year in the mitral position, and thromboembolism occurring in 0.5% and 0.8% per patient year in the respective aortic and mitral positions [46].

Leaflet rotation had also been attempted in the CarboMedic valve, although it was considered to be "only useful when the native valve is preserved or for repeat valve replacements" [183]. Incidences of PVT were relatively high in comparison

to other valves, with rates of 0.3% and 1.0% per patient year for aortic and mitral valves respectively. A study in a poorly anticoagulated patient population found that the CarboMedic valve in the mitral position had higher PVT rates (6.5% per patient year) compared to the MH tilting disk and On-X heart valve, attributed to its hinge design [54].

As the design of polymeric valves is more flexible, gap channels can be created at the commissures to allow washing away of stagnant blood. However, leakage jets through the commissures during diastole contributed to high rates of RSS which could lead to hemolysis and thrombus formation from the damaged blood elements [184].

15.3.3.4 Improving leaflet shape

Whilst most bi-leaflet mechanical valves utilize a flat leaflet, the Sorin Bicarbon valve was developed with curved leaflets in an attempt to improve the TPG. The impact on flow within an aortic root across two identical bi-leaflet valves with the exception of the curvature of their leaflets, is shown in Fig. 15.8. Larger vortices and turbulence were observed with the curved bi-leaflet valve in the lateral regions compared to the flat leaflets. Similarly observations were made by Grigioni et al. who noted increased turbulence within the inner curvature of the Sorin Bicarbon leaflets compared to an SJM valve reaching turbulent shear stress peak (TSS_{max}) values over 500 N/m^2. However, they argued that this value was still within the accepted threshold value for hemolysis [185]. A nonrandomized clinical study in single mitral or double mitral and aortic valve replacement found no significant difference in the Sorin Bicarbon valve compared to the SJM valve [186].

There is great flexibility in design with polymeric valves which can be developed with leaflets having either flat, cylindrical, conical, hyperbolic, elliptical, or a multitude of these features. This can allow optimization for a more streamlined approach.

15.3.3.5 Supra-annular valve seating

As a large part of the geometric orifice areas of PHVs is taken up by the stent or housing, many valves are designed to be seated supra-annularly, allowing the prosthesis to be positioned completely within the bloodstream. This design feature was initially incorporated in bioprostheses but many mechanical valves are now being designed with this seating in mind. Supra-annular implantation with bioprosthesis have shown improved hemodynamics compared to intraannular seating, although this improvement is more significant in larger annuli [187,188]. The Carpentier Edwards PERIMOUNT Magna valve designed for supra-annular seating was observed to have a larger EOA and a reduced transvalvular peak gradient compared to both the standard Carpentier Edwards PERIMOUNT and the stentless Edwards Prima Plus valve [189].

The On-X bi-leaflet valve incorporated a flared inlet to enable parallel streaming of flow through the valve and eliminating the development of a vena contracta downstream of the valve. A supra-annular version of the CarboMedics valve known as the "Top Hat" has the sewing cuff positioned at the inlet of the valve rather than around the

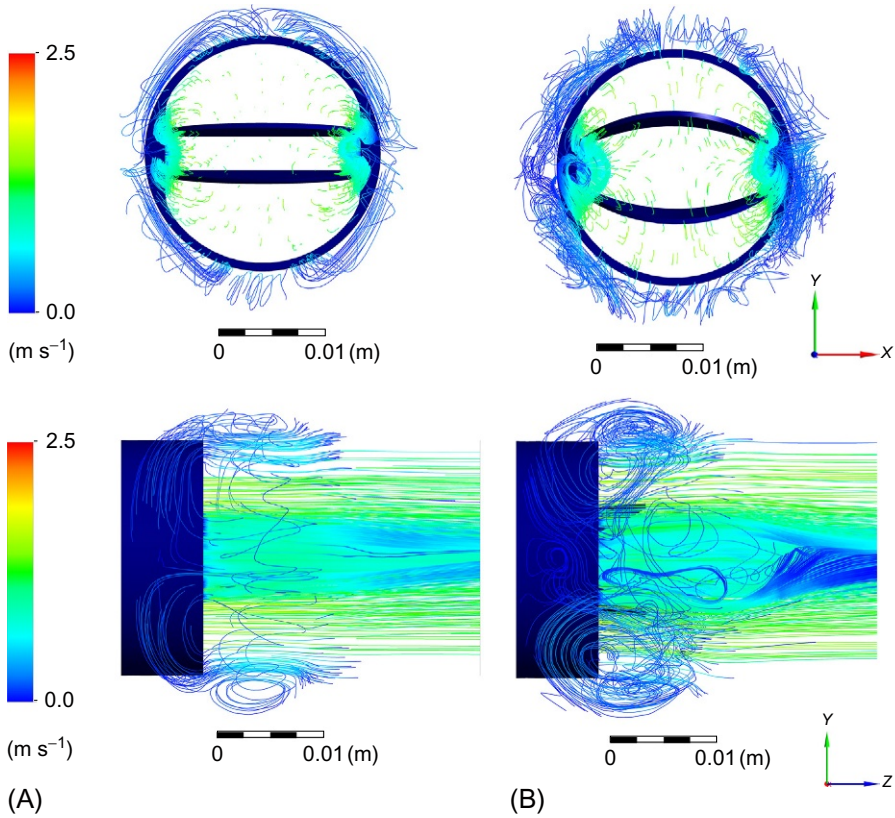


Fig. 15.8 Streamlines formed within the annulus with (A) flat and (B) curved bi-leaflet MHVs. Larger vortices and a wake downstream are observed with the curved bi-leaflet valve.

housing, with low rates of thrombosis reported [190]. This valve enabled an implantation of a larger prosthesis compared to the standard intraannular CarboMedics valve, which was particularly beneficial in patients with small aortic root sizes [191–193].

15.3.3.6 Effect of valve orientation on flow profile

As the normal physiological flow profile through the valve is eccentric, valve orientation has an impact on the velocity profile downstream of the valve. Valves developed to rotate within their housing such as the CardiaMed and Cardiomedic valves, may resolve some of the issues with flow turbulence. However, correctly aligning the valve may avoid turbulence, regions of flow stasis or reverse flow irrespective of valve design. Chandran et al. observed that valve orientation of the tilting disk valve impacted flow downstream in the mid arch and brachiocephalic arterial branch regions. Flow reversal was observed in the mid-arch region and regions for flow stasis when the valve was tilted towards the inner wall of curvature [194].

An antianatomical orientation (90 degrees rotation to the anatomical location) has been found to be the optimal orientation for mitral valve replacement [195,196]. Positioning the valve in an anatomical location led to divergent flow patterns until peak flow was reached, low velocity regions and turbulent stresses downstream of the valve. In an antianatomical position, flow diversion is absent and a single circulatory flow in the ventricle is observed, ameliorating the risk of hemolysis [197]. Although bi-leaflet valves have been widely accepted to be hemodynamically superior to tilting disk valves, optimally aligning the latter was shown to achieve superior hemodynamics, with maximum flow identified along the noncoronary leaflet of the aortic valve. Thus the larger orifice of the tilting disk valve and one lateral portion with all three orifices of the bi-leaflet valve were aligned with the noncoronary cusp to achieve optimal hemodynamic performance [198,199].

15.4 Future

History has taught us that the relationship between valve design and hemocompatibility has a significant impact on clinical outcomes. Research continues focused on the development of the "ideal" heart valve apparatus. This research is currently taking two discrete directions. Firstly, continued development of conventional tissue and mechanical valves that, using state-of-the-art simulation techniques are addressing the hemodynamic challenges that impact valve durability and device/patient interaction. These new, advanced modeling techniques enable the multitude of fluid and environmental factors be simulated in an effort to design an ideal technology but in terms of the functional (leaflet) apparatus and the anchorage (sewing rings) apparatus to meet the complex hemodynamic challenges associated with the valve when deployed in the heart.

In addition, work on conventional valve apparatus, particularly in consideration of mechanical valves is focused on the materials being utilized for the blood interaction components. New materials and coatings are constantly being developed based on feedback from clinicians associated with valve durability. Valve design both in terms of structure and materials, remains a focus of ongoing research and will continue to do so until the "ideal" configuration for this traditional valve type is derived, whether for conventional or percutaneous heart valve deployment devices.

The second direction is through continued research and development in TEHV technology which promises tissue regeneration and repair. This is an attractive route for both pediatric and adult valve development technologies by mitigating the problems of thrombogenicity, immunogenicity, and valvular degeneration. The basic principle behind TEHV is to seed cells on a suitable scaffold through several approaches including seeding decellularized valves, biodegradable scaffolds, protein based, in vivo, and hybrid TEHVs [162,200–202]. Despite their anticipated advantages, TEHVs have struggled to take off largely due to the technical challenges faced in their production including incomplete initial decellularization, cellular leaching, and weaker structural properties of the substrate [7,203]. In addition, TEHV will not be a viable option for

patients requiring emergency surgical valve replacement procedures. However, the future will see continued investment and research in tissue engineering technology towards the development of a regenerative living tissue valve. This will advance knowledge and understanding towards the development of TEHVs and address some of the challenges that lay ahead.

References

[1] B. Iung, A prospective survey of patients with valvular heart disease in Europe: the Euro Heart Survey on Valvular Heart Disease, Eur. Heart J. 24 (2003) 1231–1243, https://doi.org/10.1016/S0195-668X(03)00201-X.

[2] B. Iung, G. Baron, P. Tornos, C. Gohlke-Bärwolf, E.G. Butchart, A. Vahanian, Valvular heart disease in the community: a European experience, Curr. Probl. Cardiol. 32 (2007) 609–661, https://doi.org/10.1016/j.cpcardiol.2007.07.002.

[3] B. Iung, A. Vahanian, Epidemiology of valvular heart disease in the adult, Nat. Rev. Cardiol. 8 (2011) 162–172, https://doi.org/10.1038/nrcardio.2010.202.

[4] V.T. Nkomo, J.M. Gardin, T.N. Skelton, J.S. Gottdiener, C.G. Scott, M. Enriquez-Sarano, Burden of valvular heart diseases: a population-based study, Lancet 368 (2006) 1005–1011, https://doi.org/10.1016/S0140-6736(06)69208-8.

[5] P. Varadarajan, N. Kapoor, R.C. Bansal, R.G. Pai, Survival in elderly patients with severe aortic stenosis is dramatically improved by aortic valve replacement: results from a cohort of 277 patients aged > or =80 years, Eur. J. Cardiothorac. Surg. 30 (2006) 722–727, https://doi.org/10.1016/j.ejcts.2006.07.028.

[6] G. Perri, A. Polito, C. Esposito, S.B. Albanese, P. Francalanci, G. Pongiglione, A. Carotti, Early and late failure of tissue-engineered pulmonary valve conduits used for right ventricular outflow tract reconstruction in patients with congenital heart disease, Eur. J. Cardiothorac. Surg. 41 (2012) 1320–1325, https://doi.org/10.1093/ejcts/ezr221.

[7] P. Simon, Early failure of the tissue engineered porcine heart valve SYNERGRAFT™ in pediatric patients, Eur. J. Cardio-Thoracic Surg. 23 (2003) 1002–1006, https://doi.org/10.1016/S1010-7940(03)00094-0.

[8] M. Grabenwöger, F. Fitzal, C. Gross, D. Hutschala, P. Böck, P. Brucke, E. Wolner, Different modes of degeneration in autologous and heterologous heart valve prostheses, J. Heart Valve Dis. 9 (2000) 104–109.

[9] J.A. Gravel, Surgical treatment of aortic insufficiency, Can. Med. Assoc. J. 72 (1955) 599–601.

[10] C.A. Hufnagel, Aortic plastic valvular prosthesis, Bull. Georgetown Univ. Med. Cent. 4 (1951) 128–130.

[11] J.C. Rose, C.A. Hufnagel, E.D. Freis, W.P. Harvey, E.A. Partenope, The hemodynamic alterations produced by a plastic valvular prosthesis for severe aortic insufficiency in man, J. Clin. Invest. 33 (1954) 891–900, https://doi.org/10.1172/JCI102962.

[12] J. Butany, M.S. Ahluwalia, C. Fayet, C. Munroe, P. Blit, C. Ahn, Hufnagel valve, Cardiovasc. Pathol. 11 (2002) 351–353, https://doi.org/10.1016/S1054-8807(02)00132-1.

[13] D.M. French, C.C. Sampson, Thrombosis of a Hufnagel valve. A case report, J. Natl. Med. Assoc. 53 (1961) 144–147.

[14] C.A. Hufnagel, P.D. Villegas, H. Nahas, Experiences with new types of aortic valvular prostheses, Ann. Surg. 147 (1958) 636–644.

[15] B.S. Dhillon, A.W. Fawcett, Treatment of aortic insufficiency by the Hufnagel valve with four illustrative cases, Postgrad. Med. J. 32 (1956) 438–443.
[16] M.C. Garcia, A.M. Clarysse, C.S. Alexander, Y. Sako, W.R. Swaim, Hemolytic anemia due to progressive enlargement of silastic ball component of aortic prosthesis, Circulation 38 (1968) 505–513.
[17] J.C. Hylen, Aortic ball variance: diagnosis and treatment, Ann. Intern. Med. 72 (1970) 1, https://doi.org/10.7326/0003-4819-72-1-1.
[18] L.D. Joyce, R.W. Emery, D.M. Nicoloff, Ball variance and fracture of mitral valve prosthesis causing recurrent thromboemboli, J. Thorac. Cardiovasc. Surg. 75 (1978) 309–312.
[19] P. Steele, H. Weily, H. Davies, G. Ppppas, E. Genton, Platelet survival time following aortic valve replacement, Circulation 51 (1975) 358–362.
[20] C. Crexells, N. Aerichide, Y. Bonny, G. Lepage, L. Campeau, Factors influencing hemolysis in valve prosthesis, Am. Heart J. 84 (1972) 161–170, https://doi.org/10.1016/0002-8703(72)90330-4.
[21] J.T. Santinga, M.M. Kirsh, Hemolytic anemia in series 2300 and 2310 Starr-Edwards prosthetic valves, Ann. Thorac. Surg. 14 (1972) 539–544, https://doi.org/10.1016/S0003-4975(10)65264-2.
[22] J.T. Santinga, M.M. Kirsh, J.G. Batsakis, Hemolysis in the Starr-Edwards aortic prostheses, Am. J. Cardiol. 31 (1973) 156, https://doi.org/10.1016/0002-9149(73)90988-0.
[23] S.D. Slater, I.A. Sallam, W.H. Bain, M.A. Turner, T.D. Lawrie, Haemolysis with Björk-Shiley and Starr-Edwards prosthetic heart valves: a comparative study, Thorax 29 (1974) 624–632.
[24] M. Schottenfeld, J.D. Wisheart, J.K. Ross, J.C.R. Lincoln, D.N. Ross, Cloth destruction and haemolysis with totally cloth-covered Starr-Edwards prostheses, Thorax 26 (1971) 159–162, https://doi.org/10.1136/thx.26.2.159.
[25] A. Shah, M. Dolgin, D.A. Tice, N. Trehan, Complications due to cloth wear in cloth-covered Starr-Edwards aortic and mitral valve prostheses—and their management, Am. Heart J. 96 (1978) 407–414.
[26] M. Shiono, Y. Sezai, A. Sezai, M. Hata, M. Iida, N. Negishi, Long-term results of the cloth-covered Starr-Edwards ball valve. Ann. Thorac. Surg. 80 (2005) 204–209, https://doi.org/10.1016/j.athoracsur.2005.02.003.
[27] B. Gometza, C.M. Duran, Ball valve (Smeloff-Cutter) aortic valve replacement without anticoagulation, Ann. Thorac. Surg. 60 (1995) 1312–1316, https://doi.org/10.1016/0003-4975(95)00757-C.
[28] M. Nakajima, K. Tsuchiya, Y. Ichihara, S. Amenomori, H. Koshiyama, Y. Kaku, Forty-year durability of a Smeloff-Cutter ball valve prosthesis in the mitral position, Gen. Thorac. Cardiovasc. Surg. 59 (2011) 809–811, https://doi.org/10.1007/s11748-010-0755-z.
[29] F.S. Cross, R.D. Jones, A caged-lens prosthesis for replacement of the aortic and mitral valves, Ann. Thorac. Surg. 2 (1966) 499–507, https://doi.org/10.1016/S0003-4975(10)66609-X.
[30] J.W. Edgett, W.P. Nelson, R.J. Hall, E.J.J. Col, G.V. Aaby, A complication of valve replacement by a Caged-Lens prosthesis, Circulation 36 (1967) 422–426, https://doi.org/10.1161/01.CIR.36.3.422.
[31] V.O. Björk, Aortic valve replacement with the Björk-Shiley tilting disc valve prosthesis, Br. Heart J. 33 (Suppl.) (1971) 42–46.
[32] V.O. Björk, The pyrolytic carbon occluder for the Björk-Shiley tilting disc valve prosthesis, Scand. J. Thorac. Cardiovasc. Surg. 6 (2) (2009) 109–113.
[33] T. Gourlay, R.A. Black, Biomaterials and Devices for the Circulatory System, Woodhead Publishing, Cambridge, 2010.

[34] W.J. Blot, M.A. Ibrahim, T.D. Ivey, D.E. Acheson, R. Brookmeyer, A. Weyman, J. Defauw, J.K. Smith, D. Harrison, Twenty-five-year experience with the Björk-Shiley convexoconcave heart valve: a continuing clinical concern, Circulation 111 (2005) 2850–2857, https://doi.org/10.1161/CIRCULATIONAHA.104.511659.
[35] V.O. Björk, D. Lindblom, The monostrut Björk-Shiley heart valve, J. Am. Coll. Cardiol. 6 (1985) 1142–1148, https://doi.org/10.1016/S0735-1097(85)80322-3.
[36] H. Ahn, K.H. Kim, D.J. Kim, D.S. Jeong, Long-term experience with the Bjork-Shiley Monostrut tilting disc valve, J. Korean Med. Sci. 22 (2007) 1060–1064.
[37] A. Aris, J.M. Padró, M.L. Cámara, O. Lapiedra, J.M. Caralps, X. Borrás, F. Carreras, G. Pons-Lladó, The Monostrut Björk-Shiley valve. Seven years' experience, J. Thorac. Cardiovasc. Surg. 103 (1992) 1074–1082.
[38] D. Lindblom, U. Lindblom, A. Henze, V.O. Björk, B.K. Semb, Three-year clinical results with the Monostrut Björk-Shiley prosthesis, J. Thorac. Cardiovasc. Surg. 94 (1987) 34–43.
[39] K.V. Hall, S. Nitter-Hauge, M. Abdelnoor, Seven and one-half years' experience with the Medtronic-Hall valve, J. Am. Coll. Cardiol. 6 (1985) 1417–1421, https://doi.org/10.1016/S0735-1097(85)80234-5.
[40] G.W. Akins, Long-term results with the medtronic-hall valvular prosthesis, Ann. Thorac. Surg. 61 (1996) 806–813, https://doi.org/10.1016/0003-4975(95)01115-3.
[41] E.G. Butchart, H.H. Li, N. Payne, K. Buchan, G.L. Grunkemeier, Twenty years' experience with the Medtronic Hall valve, J. Thorac. Cardiovasc. Surg. 121 (2001) 1090–1100, https://doi.org/10.1067/mtc.2001.113754.
[42] J.L. Svennevig, M. Abdelnoor, S. Nitter-Hauge, Twenty-five-year experience with the Medtronic-Hall valve prosthesis in the aortic position: a follow-up cohort study of 816 consecutive patients, Circulation 116 (2007) 1795–1800, https://doi.org/10.1161/CIRCULATIONAHA.106.677773.
[43] R.W. Emery, C.C. Krogh, D.J. Jones, D.M. Nicoloff, D.P. Blake, K.V. Arom, Five-year follow up of the ATS mechanical heart valve, J. Heart Valve Dis. 13 (2004) 231–238.
[44] S.J. Ryder, H. Bradley, J.J. Brannan, M.A. Turner, W.H. Bain, Thrombotic obstruction of the Björk-Shiley valve: the Glasgow experience, Thorax 39 (1984) 487–492.
[45] K. Kuwaki, M. Tsukamoto, K. Komatsu, J. Sakata, T. Abe, Ten year clinical experience with the CarboMedics heart valve implants, Artif. Organs 26 (2002) 695–702, https://doi.org/10.1046/j.1525-1594.2002.06964.x.
[46] V.M. Nazarov, S.I. Zheleznev, A.V. Bogachev-Prokophiev, A.V. Afanasyev, E.V. Nemchenko, Y.V. Jeltovskiy, S.O. Lavinyukov, CardiaMed mechanical valve: mid-term results of a multicenter clinical trial, Asian Cardiovasc. Thorac. Ann. 22 (2014) 9–17, https://doi.org/10.1177/0218492312464035.
[47] W.R. Jamieson, R.T. Miyagishima, G.L. Grunkemeier, E. Germann, C. Henderson, G.J. Fradet, L.H. Burr, S.V. Lichtenstein, Bileaflet mechanical prostheses performance in mitral position, Eur. J. Cardiothorac. Surg. 15 (1999) 786–794.
[48] M.A. Williams, L. Crause, S. Van Riet, A comparison of mechanical valve performance in a poorly anticoagulated community, J. Card. Surg. 19 (2004) 410–414, https://doi.org/10.1111/j.0886-0440.2004.04084.x.
[49] M. De Feo, A. Renzulli, F. Onorati, A. Della Corte, G. Dialetto, F.E. Covino, M. Cotrufo, Initial clinical and hemodynamic experience with Edwards MIRA mechanical bileaflet valve, J. Cardiovasc. Surg. (Torino) 44 (2003) 25–30.
[50] R. Driever, S. Fuchs, M. Meissner, E. Schmitz, H.O. Vetter, The Edwards MIRA heart valve prosthesis: a 2-year study, J. Card. Surg. 19 (2004) 226–231, https://doi.org/10.1111/j.0886-0440.2004.04060.x.

[51] J.-P. Verhoye, I. Abouliatim, B. Lelong, A. Ingels, X. Roques, J. Pierre Villemot, T. Langanay, A. Leguerrier, Edwards Mira bileaflet prosthesis in aortic position: mid-term results of a prospective multi-centre study, Interact. Cardiovasc. Thorac. Surg. 6 (2007) 458–461, https://doi.org/10.1510/icvts.2006.135533.

[52] J. Carrier, J. Teijeira, D. Greentree, S. Gagnon, M.-C. Brochu, C. Paulin, S. Lepage, M. Côté, A six-year experience with the omnicarbon valve in North American patients, J. Card. Surg. 19 (2004) 432–437, https://doi.org/10.1111/j.0886-0440.2004.04086.x.

[53] U. Ozyurda, A.R. Akar, O. Uymaz, M. Oguz, M. Ozkan, C. Yildirim, A. Aslan, R. Tasoz, Early clinical experience with the On-X prosthetic heart valve, Interact. Cardiovasc. Thorac. Surg. 4 (2005) 588–594, https://doi.org/10.1510/icvts.2005.114843.

[54] M.A. Williams, S. van Riet, The On-X heart valve: mid-term results in a poorly anticoagulated population, J. Heart Valve Dis. 15 (2006) 80–86.

[55] G.M. Palatianos, A.M. Laczkovics, P. Simon, J.L. Pomar, D.E. Birnbaum, H.H. Greve, A. Haverich, Multicentered European study on safety and effectiveness of the On-X prosthetic heart valve: intermediate follow-up, Ann. Thorac. Surg. 83 (2007) 40–46, https://doi.org/10.1016/j.athoracsur.2006.08.010.

[56] J.B. Chambers, J.L. Pomar, C.A. Mestres, G.M. Palatianos, Clinical event rates with the On-X bileaflet mechanical heart valve: a multicenter experience with follow-up to 12 years, J. Thorac. Cardiovasc. Surg. 145 (2013) 420–424, https://doi.org/10.1016/j.jtcvs.2011.12.059.

[57] K. Spiliopoulos, A. Haschemi, P. Parasiris, B.M. Kemkes, Sorin Bicarbon bileaflet valve: a 9.8-year experience. Clinical performance of the prosthesis after heart valve replacement in 587 patients, Interact. Cardiovasc. Thorac. Surg. 8 (2009) 252–259, https://doi.org/10.1510/icvts.2008.183590.

[58] A. Chaux, L.S. Czer, J.M. Matloff, M.A. DeRobertis, M.E. Stewart, T.M. Bateman, R.M. Kass, M.E. Lee, R.J. Gray, The St. Jude Medical bileaflet valve prosthesis. A 5 year experience, J. Thorac. Cardiovasc. Surg. 88 (1984) 706–717.

[59] H. Silber, S.S. Khan, J.M. Matloff, A. Chaux, M. DeRobertis, R. Gray, The St. Jude valve. Thrombolysis as the first line of therapy for cardiac valve thrombosis, Circulation 87 (1993) 30–37, https://doi.org/10.1161/01.CIR.87.1.30.

[60] M.T. Metzdorff, G.L. Grunkemeier, C.W. Pinson, A. Starr, Thrombosis of mechanical cardiac valves: a qualitative comparison of the silastic ball valve and the tilting disc valve, J. Am. Coll. Cardiol. 4 (1984) 50–53.

[61] R. Roudaut, K. Serri, S. Lafitte, Thrombosis of prosthetic heart valves: diagnosis and therapeutic considerations, Heart 93 (2007) 137–142, https://doi.org/10.1136/hrt.2005.071183.

[62] J.M. Vesey, C.M. Otto, Complications of prosthetic heart valves, Curr. Cardiol. Rep. 6 (2004) 106–111, https://doi.org/10.1007/s11886-004-0007-x.

[63] E. Deviri, P. Sareli, T. Wisenbaugh, S.L. Cronje, Obstruction of mechanical heart valve prostheses: clinical aspects and surgical management, J. Am. Coll. Cardiol. 17 (1991) 646–650.

[64] M.L. Brown, S.J. Park, T.M. Sundt, H.V. Schaff, Early thrombosis risk in patients with biologic valves in the aortic position, J. Thorac. Cardiovasc. Surg. 144 (2012) 108–111, https://doi.org/10.1016/j.jtcvs.2011.05.032.

[65] P.S. Mykén, Seventeen-year experience with the St. Jude medical biocor porcine bioprosthesis, J. Heart Valve Dis. 14 (2005) 486–492.

[66] G. Gao, Y. Wu, G.L. Grunkemeier, A.P. Furnary, A. Starr, Durability of pericardial versus porcine aortic valves, J. Am. Coll. Cardiol. 44 (2004) 384–388, https://doi.org/10.1016/j.jacc.2004.01.053.

[67] M.A. Marchand, M.R. Aupart, R. Norton, I.R. Goldsmith, L.C. Pelletier, M. Pellerin, T. Dubiel, W.J. Daenen, P. Herijgers, F.P. Casselman, M.P. Holden, T.E. David, Fifteen-year experience with the mitral Carpentier-Edwards PERIMOUNT pericardial bioprosthesis, Ann. Thorac. Surg. 71 (2001) S236–S239.

[68] D.B. Doty, A. Cafferty, N.D. Kon, H.A. Huysmans, A.H. Krause, S. Westaby, Medtronic Freestyle aortic root bioprosthesis: implant techniques, J. Card. Surg. 13 (1998) 369–375.

[69] J.E. Bavaria, N.D. Desai, A. Cheung, M.R. Petracek, M.A. Groh, M.A. Borger, H.V. Schaff, The St Jude Medical Trifecta aortic pericardial valve: results from a global, multicenter, prospective clinical study, J. Thorac. Cardiovasc. Surg. 147 (2014) 590–597, https://doi.org/10.1016/j.jtcvs.2012.12.087.

[70] C. Cao, S.C. Ang, M.P. Vallely, M. Ng, M. Adams, M. Wilson, Migration of the transcatheter valve into the left ventricle, Ann. Cardiothorac. Surg. 1 (2012) 243–244, https://doi.org/10.3978/509.

[71] P.Y.K. Pang, P.T.L. Chiam, Y.L. Chua, Y.K. Sin, A survivor of late prosthesis migration and rotation following percutaneous transcatheter aortic valve implantation, Eur. J. Cardiothorac. Surg. 41 (2012) 1195–1196, https://doi.org/10.1093/ejcts/ezr195.

[72] F. Bakhtiary, M. Schiemann, O. Dzemali, S. Dogan, V. Schächinger, H. Ackermann, A. Moritz, P. Kleine, Impact of patient-prosthesis mismatch and aortic valve design on coronary flow reserve after aortic valve replacement, J. Am. Coll. Cardiol. 49 (2007) 790–796, https://doi.org/10.1016/j.jacc.2006.10.052.

[73] O. Lund, K. Emmertsen, T.T. Nielsen, F.T. Jensen, C. Flø, H.K. Pilegaard, B.S. Rasmussen, O.K. Hansen, L.H. Kristensen, Impact of size mismatch and left ventricular function on performance of the St. Jude disc valve after aortic valve replacement, Ann. Thorac. Surg. 63 (1997) 1227–1234, https://doi.org/10.1016/S0003-4975(97)00313-5.

[74] J.G. Webb, S. Pasupati, K. Humphries, C. Thompson, L. Altwegg, R. Moss, A. Sinhal, R.G. Carere, B. Munt, D. Ricci, J. Ye, A. Cheung, S.V. Lichtenstein, Percutaneous transarterial aortic valve replacement in selected high-risk patients with aortic stenosis, Circulation 116 (2007) 755–763.

[75] I. Vesely, The evolution of bioprosthetic heart valve design and its impact on durability, Cardiovasc. Pathol. 12 (2003) 277–286.

[76] J.B. García-Bengochea, M.F. Siebert, C.I. Carreño, A.A. Cendon, J.R. Alvarez, Clinical experience with the Ionescu-Shiley xenograft valve: four to five-year follow-up, Tex. Heart Inst. J. 9 (1982) 285–292.

[77] F.J. Schoen, J. Fernandez, L. Gonzalez-Lavin, A. Cernaianu, Causes of failure and pathologic findings in surgically removed Ionescu-Shiley standard bovine pericardial heart valve bioprostheses: emphasis on progressive structural deterioration, Circulation 76 (1987) 618–627, https://doi.org/10.1161/01.CIR.76.3.618.

[78] V.M. Walley, C.A. Keon, M. Khalili, D. Moher, M. Campagna, W.J. Keon, Ionescu-Shiley valve failure. I: experience with 125 standard-profile explants, Ann. Thorac. Surg. 54 (1992) 111–116.

[79] J.T. Ellis, T.M. Healy, A.A. Fontaine, R. Saxena, A.P. Yoganathan, Velocity measurements and flow patterns within the hinge region of a Medtronic Parallel bileaflet mechanical valve with clear housing, J. Heart Valve Dis. 5 (1996) 591–599.

[80] J.M. Gross, M.C. Shu, F.F. Dai, J. Ellis, A.P. Yoganathan, A microstructural flow analysis within a bileaflet mechanical heart valve hinge, J. Heart Valve Dis. 5 (1996) 581–590.

[81] H.-L. Leo, Z. He, J.T. Ellis, A.P. Yoganathan, Microflow fields in the hinge region of the CarboMedics bileaflet mechanical heart valve design, J. Thorac. Cardiovasc. Surg. 124 (2002) 561–574, https://doi.org/10.1067/mtc.2002.125206.

[82] P. Alves, R. Cardoso, T.R. Correia, B.P. Antunes, I.J. Correia, P. Ferreira, Surface modification of polyurethane films by plasma and ultraviolet light to improve haemocompatibility for artificial heart valves, Colloids Surf. B: Biointerfaces 113 (2014) 25–32, https://doi.org/10.1016/j.colsurfb.2013.08.039.
[83] N.D. Broom, F.J. Thomson, Influence of fixation conditions on the performance of glutaraldehyde-treated porcine aortic valves: towards a more scientific basis, Thorax 34 (1979) 166–176, https://doi.org/10.1136/thx.34.2.166.
[84] G.W. Christie, B.G. Barratt-Boyes, On stress reduction in bioprosthetic heart valve leaflets by the use of a flexible stent, J. Card. Surg. 6 (1991) 476–481.
[85] S. Krucinski, I. Vesely, M.A. Dokainish, G. Campbell, Numerical simulation of leaflet flexure in bioprosthetic valves mounted on rigid and expansile stents, J. Biomech. 26 (1993) 929–943.
[86] C.M. Duran, B. Gometza, N. Kumar, R. Gallo, R. Martin-Duran, Aortic valve replacement with freehand autologous pericardium, J. Thorac. Cardiovasc. Surg. 110 (1995) 511–516.
[87] A.M. Fadali, M.D. Ramos, S.R. Topaz, V.L. Gott, The use of autogenous peritoneum for heart valve replacement, J. Thorac. Cardiovasc. Surg. 60 (1970) 188–195.
[88] M.I. Ionescu, D.N. Ross, R. Deac, V.A. Grimshaw, S.H. Taylor, W. Whitaker, G.H. Wooler, Autologous fascia lata for heart valve replacement, Thorax 25 (1970) 46–56.
[89] V. Martelli, W.H. Wain, E. Bodnar, D.N. Ross, Mitral valve replacement with dura mater bioprostheses, Artif. Organs 4 (1980) 163–166.
[90] B.T. Williams, B.J. Bellhouse, F. Ashton, Autologous superior vena cava as a material for valve replacement, J. Thorac. Cardiovasc. Surg. 66 (1973) 952–958.
[91] W.T. Dubiel, L. Johansson, R. Willén, Postoperative changes in autologous fascia lata heart valve grafts. A pathological study, Ann. Thorac. Surg. 15 (1973) 140–155, https://doi.org/10.1016/S0003-4975(10)64947-8.
[92] L.B. Puig, G. Verginelli, K. Iryia, L. Kawabe, G. Bellotti, E. Sosa, F. Pilleggi, E.J. Zerbini, Homologous dura mater cardiac valves. Study of 533 surgical cases, J. Thorac. Cardiovasc. Surg. 69 (1975) 722–728.
[93] R. Willén, W.T. Dubiel, L. Johansson, Viability and surface properties of autologous fascia lata heart valve grafts: a radioautographic and scanning electron microscopical study, Ann. Thorac. Surg. 18 (1974) 597–607, https://doi.org/10.1016/S0003-4975(10)64407-4.
[94] A. Cribier, H. Eltchaninoff, A. Bash, N. Borenstein, C. Tron, F. Bauer, G. Derumeaux, F. Anselme, F. Laborde, M.B. Leon, Percutaneous transcatheter implantation of an aortic valve prosthesis for calcific aortic stenosis—first human case description, Circulation 106 (2002) 3006–3008.
[95] J.A. Lardizabal, B.P. O'Neill, H.V. Desai, C.J. Macon, A.P. Rodriguez, C.A. Martinez, C.E. Alfonso, M.S. Bilsker, R.G. Carillo, M.G. Cohen, A.W. Heldman, W.W. O'Neill, D.B. Williams, The transaortic approach for transcatheter aortic valve replacement: initial clinical experience in the United States, J. Am. Coll. Cardiol. 61 (2013) 2341–2345, https://doi.org/10.1016/j.jacc.2013.02.076.
[96] S.V. Lichtenstein, A. Cheung, J. Ye, C.R. Thompson, R.G. Carere, S. Pasupati, J.G. Webb, Transapical transcatheter aortic valve implantation in humans—initial clinical experience, Circulation 114 (2006) 591–596, https://doi.org/10.1161/CIRCULATIONAHA.106.632927.
[97] U. Schäfer, Y. Ho, C. Frerker, D. Schewel, D. Sanchez-Quintana, J. Schofer, K. Bijuklic, F. Meincke, T. Thielsen, F. Kreidel, K.-H. Kuck, Direct percutaneous access technique for transaxillary transcatheter aortic valve implantation, JACC Cardiovasc. Interv. 5 (2012) 477–486, https://doi.org/10.1016/j.jcin.2011.11.014.

[98] V.H. Thourani, R.L. Gunter, S. Neravetla, P. Block, R.A. Guyton, P. Kilgo, S. Lerakis, C. Devireddy, B. Leshnower, K. Mavromatis, J. Stewart, A. Simone, P. Keegan, T.C. Nguyen, J. Merlino, V. Babaliaros, Use of transaortic, transapical, and transcarotid transcatheter aortic valve replacement in inoperable patients, Ann. Thorac. Surg. 96 (2013) 1349–1357, https://doi.org/10.1016/j.athoracsur.2013.05.068.

[99] T. Walther, T. Dewey, M.A. Borger, J. Kempfert, A. Linke, R. Becht, V. Falk, G. Schuler, F.W. Mohr, M. Mack, Transapical aortic valve implantation: step by step, Ann. Thorac. Surg. 87 (2009) 276–283, https://doi.org/10.1016/j.athoracsur.2008.08.017.

[100] M.M.M. Rozeik, D.J.D. Wheatley, T. Gourlay, Percutaneous heart valves; past, present and future, Perfusion 29 (2014) 397–410, https://doi.org/10.1177/0267659114523464.

[101] J.B. García-Bengoechea, J.R. González-Juanatey, J. Rubio, D. Durán, J. Sierra, Thromboembolism in patients with pericardial valves in the absence of chronic anticoagulation: 12 years' experience, Eur. J. Cardiothorac. Surg. 5 (1991) 592–597.

[102] N.C. Poirier, L.C. Pelletier, M. Pellerin, M. Carrier, 15-year experience with the Carpentier-Edwards pericardial bioprosthesis, Ann. Thorac. Surg. 66 (1998) S57–S61, https://doi.org/10.1016/S0003-4975(98)01110-2.

[103] N. Jander, H. Sommer, C. Pingpoh, R.-P. Kienzle, G. Martin, W. Zeh, G. Pache, M. Siepe, F. Beyersdorf, M. Schumacher, F.-J. Neumann, J. Minners, The porcine valve type predicts obstructive thrombosis beyond the first three postoperative months in bioprostheses in the aortic position, Int. J. Cardiol. 199 (2015) 90–95, https://doi.org/10.1016/j.ijcard.2015.07.022.

[104] R. Maraj, L.E. Jacobs, A. Ioli, M.N. Kotler, Evaluation of hemolysis in patients with prosthetic heart valves, Clin. Cardiol. 21 (1998) 387–392, https://doi.org/10.1002/clc.4960210604.

[105] D.J. Wheatley, L. Raco, G.M. Bernacca, I. Sim, P.R. Belcher, J.S. Boyd, Polyurethane: material for the next generation of heart valve prostheses? Eur. J. Cardiothorac. Surg. 17 (2000) 440–448.

[106] N.S. Braunwald, It will work: the first successful mitral valve replacement, Ann. Thorac. Surg. 48 (1989) S1–S3, https://doi.org/10.1016/0003-4975(89)90615-2.

[107] T.E. Claiborne, M.J. Slepian, S. Hossainy, D. Bluestein, Polymeric trileaflet prosthetic heart valves: evolution and path to clinical reality, Expert Rev. Med. Devices 9 (2012) 577–594, https://doi.org/10.1586/erd.12.51.

[108] H. Jiang, G. Campbell, D. Boughner, W.-K. Wan, M. Quantz, Design and manufacture of a polyvinyl alcohol (PVA) cryogel tri-leaflet heart valve prosthesis, Med. Eng. Phys. 26 (2004) 269–277, https://doi.org/10.1016/j.medengphy.2003.10.007.

[109] T.G. Mackay, D.J. Wheatley, G.M. Bernacca, A.C. Fisher, C.S. Hindle, New polyurethane heart valve prosthesis: design, manufacture and evaluation, Biomaterials 17 (1996) 1857–1863.

[110] Q. Wang, A.J. McGoron, R. Bianco, Y. Kato, L. Pinchuk, R.T. Schoephoerster, In-vivo assessment of a novel polymer (SIBS) trileaflet heart valve, J. Heart Valve Dis. 19 (2010) 499–505.

[111] K. Imachi, Y. Abe, T. Chinzei, K. Mabuchi, K. Baba, H. Matsuura, A. Kouno, T. Ono, S. Mochizuki, Y.-P. Son, K. Imanishi, I. Fujimasa, Calcification and thrombus formation on polymer surfaces of an artificial heart, in: T. Akutsu, H. Koyanagi (Eds.), Heart Replacement SE-16, Springer, Tokyo, 1998, pp. 110–117, https://doi.org/10.1007/978-4-431-65921-1_16.

[112] P.A. Gunatillake, G.F. Meijs, S.J. Mccarthy, R. Adhikari, Poly(dimethylsiloxane)/poly(hexamethylene oxide) mixed macrodiol based polyurethane elastomers. I. Synthesis and properties, J. Appl. Polym. Sci. 76 (2000) 2026–2040, https://doi.org/10.1002/(SICI)1097-4628(20000628)76:14<2026::AID-APP5>3.0.CO;2-X.

[113] A. Simmons, J. Hyvarinen, R.A. Odell, D.J. Martin, P.A. Gunatillake, K.R. Noble, L.A. Poole-Warren, Long-term in vivo biostability of poly(dimethylsiloxane)/poly(hexamethylene oxide) mixed macrodiol-based polyurethane elastomers, Biomaterials 25 (2004) 4887–4900, https://doi.org/10.1016/j.biomaterials.2004.01.004.
[114] C.W. Thorburn, J.J. Morgan, M.X. Shanahan, V.P. Chang, Long-term results of tricuspid valve replacement and the problem of prosthetic valve thrombosis, Am. J. Cardiol. 51 (1983) 1128–1132.
[115] J.C. Bokros, V.L. Gott, L.D. La Grange, A.M. Fadall, K.D. Vos, M.D. Ramos, Correlations between blood compatibility and heparin adsorptivity for an impermeable isotropic pyrolytic carbon, J. Biomed. Mater. Res. 3 (1969) 497–528, https://doi.org/10.1002/jbm.820030311.
[116] J.J. Von Der Emde, U. Eberlein, J.J. Breme, Asymptomatic strut fracture in DeBakey-Surgitool aortic valves: incidence, management, and metallurgic aspects, Tex. Heart Inst. J. 17 (1990) 223–227.
[117] S.J. Phillips, Thrombogenic influence of biomaterials in patients with the Omni series heart valve: pyrolytic carbon versus titanium, ASAIO J. 47 (1992) 429–431.
[118] J.A. Chinn, R.E. Phillips Jr., K.R. Lew, T.A. Horbett, Tenacious binding of fibrinogen and albumin to pyrolite carbon and biomer, J. Colloid Interface Sci. 184 (1996) 11–19, https://doi.org/10.1006/jcis.1996.0592.
[119] S. Forti, L. Lunelli, C. Della Volpe, S. Siboni, L. Pasquardini, A. Lui, R. Canteri, L. Vanzetti, C. Potrich, M. Vinante, C. Pederzolli, M. Anderle, Hemocompatibility of pyrolytic carbon in comparison with other biomaterials, Diam. Relat. Mater. 20 (2011) 762–769, https://doi.org/10.1016/j.diamond.2011.03.026.
[120] S.L. Goodman, Sheep, pig, and human platelet-material interactions with model cardiovascular biomaterials, J. Biomed. Mater. Res. 45 (1999) 240–250.
[121] L. Feng, J.D. Andrade, Protein adsorption on low temperature isotropic carbon: V. How is it related to its blood compatibility? J. Biomater. Sci. Polym. Ed. 7 (1996) 439–452, https://doi.org/10.1163/156856295X00445.
[122] J.L. Ely, M.R. Emken, J.A. Accuntius, D.S. Wilde, A.D. Haubold, R.B. More, J.C. Bokros, Pure pyrolytic carbon: preparation and properties of a new material, On-X carbon for mechanical heart valve prostheses, J. Heart Valve Dis. 7 (1998) 626–632.
[123] S.L. Goodman, V.L. Scranton, A.M. Brendzel, Platelet responses to silicon-alloyed pyrolytic carbons, J. Biomed. Mater. Res. A 83 (2007) 64–69, https://doi.org/10.1002/jbm.a.31206.
[124] R. Moidl, P. Simon, E. Wolner, The On-X prosthetic heart valve at five years, Ann. Thorac. Surg. 74 (2002) S1312–S1317.
[125] J. Puskas, M. Gerdisch, D. Nichols, R. Quinn, C. Anderson, B. Rhenman, L. Fermin, M. McGrath, B. Kong, C. Hughes, G. Sethi, M. Wait, T. Martin, A. Graeve, Reduced anticoagulation after mechanical aortic valve replacement: interim results from the prospective randomized on-X valve anticoagulation clinical trial randomized Food and Drug Administration investigational device exemption trial, J. Thorac. Cardiovasc. Surg. 147 (2014) 1202–1210, https://doi.org/10.1016/j.jtcvs.2014.01.004.
[126] S.L. Goodman, K.S. Tweden, R.M. Albrecht, Platelet interaction with pyrolytic carbon heart-valve leaflets, J. Biomed. Mater. Res. 32 (1996) 249–258, https://doi.org/10.1002/(SICI)1097-4636(199610)32:2<249::AID-JBM15>3.0.CO;2-E.
[127] A. Bolz, M. Schaldach, Artificial heart valves: improved blood compatibility by PECVD a-SiC:H coating, Artif. Organs 14 (1990) 260–269, https://doi.org/10.1111/j.1525-1594.1990.tb02967.x.

[128] N. Huang, Y.X. Leng, P. Yang, J.Y. Chen, H. Sun, J. Wang, G.J. Wan, In vivo blood compatibility of titanium oxide film coated artificial heart valves prepared by plasma immersion ion implantation and deposition, in: The 30th International Conference on Plasma Science, 2003. ICOPS 2003. IEEE Conference Record—Abstracts. IEEE, 2003, https://doi.org/10.1109/PLASMA.2003.1228827. p. 280.

[129] M.J. Jackson, G.M. Robinson, N. Ali, Y. Kousar, S. Mei, J. Gracio, H. Taylor, W. Ahmed, Surface engineering of artificial heart valve disks using nanostructured thin films deposited by chemical vapour deposition and sol–gel methods, J. Med. Eng. Technol. 30 (2006) 323–329, https://doi.org/10.1080/03091900500441287.

[130] Y.X. Leng, J.Y. Chen, Z.M. Zeng, X.B. Tian, P. Yang, N. Huang, Z.R. Zhou, P.K. Chu, Properties of titanium oxide biomaterials synthesized by titanium plasma immersion ion implantation and reactive ion oxidation, Thin Solid Films 377–378 (2000) 573–577, https://doi.org/10.1016/S0040-6090(00)01306-7.

[131] H.S. Tran, M.M. Puc, C.W. Hewitt, D.B. Soll, S.W. Marra, V.A. Simonetti, J.H. Cilley, A.J. DelRossi, Diamond-like carbon coating and plasma or glow discharge treatment of mechanical heart valves, J. Investig. Surg. 12 (1999) 133–140, https://doi.org/10.1080/089419399272520.

[132] F. Zhang, X. Liu, Y. Mao, N. Huang, Y. Chen, Z. Zheng, Z. Zhou, A. Chen, Z. Jiang, Artificial heart valves: improved hemocompatibility by titanium oxide coatings prepared by ion beam assisted deposition, Surf. Coat. Technol. 103–104 (1998) 146–150, https://doi.org/10.1016/S0257-8972(98)00434-4.

[133] Y. Mitamura, T. Mikami, T. Yuta, T. Matsumoto, T. Shimooka, E. Okamoto, N. Eizuka, K. Yamaguchi, Development of a fine ceramic heart valve for use as a cardiac prosthesis, ASAIO Trans. 32 (1986) 444–448.

[134] J. Chen, Y. Leng, X. Tian, L. Wang, N. Huang, P. Chu, P. Yang, Antithrombogenic investigation of surface energy and optical bandgap and hemocompatibility mechanism of Ti(Ta + 5)O2 thin films, Biomaterials 23 (2002) 2545–2552, https://doi.org/10.1016/S0142-9612(01)00389-1.

[135] N. Huang, P. Yang, Y.X. Leng, J.Y. Chen, H. Sun, J. Wang, G.J. Wang, P.D. Ding, T.F. Xi, Y. Leng, Hemocompatibility of titanium oxide films, Biomaterials 24 (2003) 2177–2187, https://doi.org/10.1016/S0142-9612(03)00046-2.

[136] X. Wang, F. Zhang, C. Li, Z. Zheng, X. Wang, X. Liu, A. Chen, Z. Jiang, Improvement of blood compatibility of artificial heart valves via titanium oxide film coated on low temperature isotropic carbon, Surf. Coat. Technol. 128–129 (2000) 36–42, https://doi.org/10.1016/S0257-8972(00)00659-9.

[137] A. Alanazi, C. Nojiri, T. Noguchi, T. Kido, Y. Komatsu, K. Hirakuri, A. Funakubo, K. Sakai, Y. Fukui, Improved blood compatibility of DLC coated polymeric material, ASAIO J. 46 (2000) 440–443.

[138] M. Fedel, A. Motta, D. Maniglio, C. Migliaresi, Surface properties and blood compatibility of commercially available diamond-like carbon coatings for cardiovascular devices, J. Biomed. Mater. Res. B Appl. Biomater. 90 (2009) 338–349, https://doi.org/10.1002/jbm.b.31291.

[139] M.I. Jones, I.R. McColl, D.M. Grant, K.G. Parker, T.L. Parker, Protein adsorption and platelet attachment and activation, on TiN, TiC, and DLC coatings on titanium for cardiovascular applications, J. Biomed. Mater. Res. 52 (2000) 413–421.

[140] L. Yu, X. Wang, X. Wang, X. Liu, Haemocompatibility of tetrahedral amorphous carbon films, Surf. Coat. Technol. 128–129 (2000) 484–488, https://doi.org/10.1016/S0257-8972(00)00626-5.

[141] S.C.H. Kwok, P. Yang, J. Wang, X. Liu, P.K. Chu, Hemocompatibility of nitrogen-doped, hydrogen-free diamond-like carbon prepared by nitrogen plasma immersion ion implantation-deposition, J. Biomed. Mater. Res. A 70 (2004) 107–114, https://doi.org/10.1002/jbm.a.30070.

[142] A.A. Ogwu, T.I.T. Okpalugo, N. Ali, P.D. Maguire, J.A.D. McLaughlin, Endothelial cell growth on silicon modified hydrogenated amorphous carbon thin films, J. Biomed. Mater. Res. B Appl. Biomater. 85 (2008) 105–113, https://doi.org/10.1002/jbm.b.30922.

[143] T.I.T. Okpalugo, A.A. Ogwu, P.D. Maguire, J.A.D. McLaughlin, Platelet adhesion on silicon modified hydrogenated amorphous carbon films, Biomaterials 25 (2004) 239–245.

[144] T.I.T. Okpalugo, A.A. Ogwu, P.D. Maguire, J.A.D. McLaughlin, D.G. Hirst, In-vitro blood compatibility of a-C:H:Si and a-C:H thin films, Diam. Relat. Mater. 13 (2004) 1088–1092, https://doi.org/10.1016/j.diamond.2003.10.064.

[145] A. Ali, J.C. Halstead, F. Cafferty, L. Sharples, F. Rose, R. Coulden, E. Lee, J. Dunning, V. Argano, S. Tsui, Are stentless valves superior to modern stented valves? A prospective randomized trial, Circulation 114 (2006) I535–I540, https://doi.org/10.1161/CIRCULATIONAHA.105.000950.

[146] N. Ali, Y. Kousar, T.I. Okpalugo, V. Singh, M. Pease, A.A. Ogwu, J. Gracio, E. Titus, E.I. Meletis, M.J. Jackson, Human micro-vascular endothelial cell seeding on Cr-DLC thin films for mechanical heart valve applications, Thin Solid Films 515 (2006) 59–65, https://doi.org/10.1016/j.tsf.2005.12.023.

[147] M. Cloutier, C. Harnagea, P. Hale, O. Seddiki, F. Rosei, D. Mantovani, Long-term stability of hydrogenated DLC coatings: effects of aging on the structural, chemical and mechanical properties, Diam. Relat. Mater. 48 (2014) 65–72, https://doi.org/10.1016/j.diamond.2014.07.002.

[148] N. Moolsradoo, S. Abe, S. Watanabe, Thermal stability and tribological performance of DLC-Si–O films, Adv. Mater. Sci. Eng. 2011 (2011) 1–7, https://doi.org/10.1155/2011/483437.

[149] A. Bendavid, P.J. Martin, C. Comte, E.W. Preston, A.J. Haq, F.S. Magdon Ismail, R.K. Singh, The mechanical and biocompatibility properties of DLC-Si films prepared by pulsed DC plasma activated chemical vapor deposition, Diam. Relat. Mater. 16 (2007) 1616–1622, https://doi.org/10.1016/j.diamond.2007.02.006.

[150] R.E. Baier, The role of surface energy in thrombogenesis, Bull. N. Y. Acad. Med. 48 (1972) 257–272.

[151] V.L. Gott, J.D. Whiffen, R.C. Dutton, Heparin bonding on colloidal graphite surfaces, Science 142 (1963) 1297–1298.

[152] S. Yuan, W. Cai, G. Szakalas-Gratzl, K. Kottke-Marchant, K. Tweden, R.E. Marchant, Immobilization of heparin oligosaccharides onto radiofrequency plasma modified pyrolytic carbon-coated graphite, J. Appl. Biomater. 6 (1995) 259–266, https://doi.org/10.1002/jab.770060407.

[153] X. Ye, H. Wang, J. Zhou, H. Li, J. Liu, Z. Wang, A. Chen, Q. Zhao, The effect of Heparin-VEGF multilayer on the biocompatibility of decellularized aortic valve with platelet and endothelial progenitor cells, PLoS One 8 (2013), https://doi.org/10.1371/journal.pone.0054622. e54622.

[154] E.M.E. Kristensen, R. Larsson, J. Sánchez, H. Rensmo, U. Gelius, H. Siegbahn, Heparin coating durability on artificial heart valves studied by XPS and antithrombin binding capacity, Colloids Surf. B: Biointerfaces 49 (2006) 1–7, https://doi.org/10.1016/j.colsurfb.2006.02.007.

[155] F. Li, J. Wang, N. Huang, In vitro blood compatibility of polyethylene terephthalate with covalently bounded hirudin on surface, J. Wuhan Univ. Technol. Sci. Ed. 26 (2011) 950–954, https://doi.org/10.1007/s11595-011-0343-9.

[156] Y. Park, E. Ryu, H. Kim, J. Jeong, J. Kim, J. Shim, S. Jeon, Y. Jo, W. Kim, B. Min, Characterization of antithrombotic activity of lumbrokinase-immobilized polyurethane valves in the total artificial heart, Artif. Organs 23 (1999) 210–214.
[157] N. Duraiswamy, T.D. Choksi, L. Pinchuk, R.T. Schoephoerster, A phospholipid-modified polystyrene-polyisobutylene-polystyrene (SIBS) triblock polymer for enhanced hemocompatibility and potential use in artificial heart valves, J. Biomater. Appl. 23 (2009) 367–379, https://doi.org/10.1177/0885328208093854.
[158] T.E. Claiborne, G. Girdhar, S. Gallocher-Lowe, J. Sheriff, Y.P. Kato, L. Pinchuk, R.T. Schoephoerster, J. Jesty, D. Bluestein, Thrombogenic potential of Innovia polymer valves versus Carpentier-Edwards Perimount Magna aortic bioprosthetic valves, ASAIO J. 57 (2011) 26–31, https://doi.org/10.1097/MAT.0b013e3181fcbd86.
[159] R. Sbarbati, D. Giannessi, M.C. Cenni, G. Lazzerini, F. Verni, R. De Caterina, Pyrolytic carbon coating enhances Teflon and Dacron fabric compatibility with endothelial cell growth, Int. J. Artif. Organs 14 (1991) 491–498.
[160] L.A. Bengtsson, A.N. Haegerstrand, Endothelialization of mechanical heart valves in vitro with cultured adult human cells, J. Heart Valve Dis. 2 (1993) 352–356.
[161] C.M. Frendl, S.M. Tucker, N.A. Khan, M.B. Esch, S. Kanduru, T.M. Cao, A.J. García, M.R. King, J.T. Butcher, Endothelial retention and phenotype on carbonized cardiovascular implant surfaces, Biomaterials 35 (2014) 7714–7723, https://doi.org/10.1016/j.biomaterials.2014.05.075.
[162] D.J. Lee, J. Steen, J.E. Jordan, E.H. Kincaid, N.D. Kon, A. Atala, J. Berry, J.J. Yoo, Endothelialization of heart valve matrix using a computer-assisted pulsatile bioreactor, Tissue Eng. Part A 15 (2009) 807–814, https://doi.org/10.1089/ten.tea.2008.0250.
[163] R.S. Figliola, T.J. Mueller, On the hemolytic and thrombogenic potential of occluder prosthetic heart valves from in-vitro measurements, J. Biomech. Eng. 103 (1981) 83, https://doi.org/10.1115/1.3138265.
[164] J.M. Hasenkam, H. Nygaard, M. Giersiepen, H. Reul, H. Stødkilde-Jørgensen, Turbulent stress measurements downstream of six mechanical aortic valves in a pulsatile flow model, J. Biomech. 21 (1988) 631–645.
[165] M. Grigioni, C. Daniele, G. D'Avenio, V. Barbaro, A discussion on the threshold limit for hemolysis related to Reynolds shear stress, J. Biomech. 32 (1999) 1107–1112.
[166] P.C. Lu, H.C. Lai, J.S. Liu, A reevaluation and discussion on the threshold limit for hemolysis in a turbulent shear flow, J. Biomech. 34 (2001) 1361–1364.
[167] A.M. Sallam, N.H. Hwang, Human red blood cell hemolysis in a turbulent shear flow: contribution of Reynolds shear stresses, Biorheology 21 (1984) 783–797.
[168] T. Walther, V. Falk, G. Langebartels, M. Kruger, U. Bernhardt, A. Diegeler, J. Gummert, R. Autschbach, F.W. Mohr, Prospectively randomized evaluation of stentless versus conventional biological aortic valves : impact on early regression of left ventricular hypertrophy, Circulation 100 (1999) II-6–II-10, https://doi.org/10.1161/01.CIR.100.suppl_2.II-6.
[169] J. Dunning, R.J. Graham, J. Thambyrajah, M.J. Stewart, S.W.H. Kendall, S. Hunter, Stentless vs. stented aortic valve bioprostheses: a prospective randomized controlled trial, Eur. Heart J. 28 (2007) 2369–2374, https://doi.org/10.1093/eurheartj/ehm327.
[170] J.R. Alvarez, J. Sierra, M. Vega, B. Adrio, J. Martinez-Comendador, F. Gude, J. Martinez-Cereijo, J. Garcia, Early calcification of the aortic Mitroflow pericardial bioprosthesis in the elderly, Interact. Cardiovasc. Thorac. Surg. 9 (2009) 842–846, https://doi.org/10.1510/icvts.2009.204958.
[171] J. Butany, T. Feng, A. Luk, K. Law, R. Suri, V. Nair, Modes of failure in explanted mitroflow pericardial valves, Ann. Thorac. Surg. 92 (2011) 1621–1627, https://doi.org/10.1016/j.athoracsur.2011.06.092.

[172] J. Leandri, P. Bertrand, J.P. Mazzucotelli, D. Loisance, Mode of failure of the Mitroflow pericardial valve, J. Heart Valve Dis. 1 (1992) 225–231.
[173] J.L. Pomar, W.R. Eric Jamieson, L. Conrad Pelletier, A.N. Gerein, M. Castellá, R.T. Brownlee, Mitroflow pericardial bioprosthesis: clinical performance to ten years, Ann. Thorac. Surg. 60 (1995) S305–S310, https://doi.org/10.1016/0003-4975(95)00307-7.
[174] E. Permanyer, A.-J. Estigarribia, A. Ysasi, E. Herrero, O. Semper, R. Llorens, St. Jude Medical Trifecta™ aortic valve perioperative performance in 200 patients, Interact. Cardiovasc. Thorac. Surg. 17 (2013) 669–672, https://doi.org/10.1093/icvts/ivt270.
[175] J.C. Bokros, M.R. Emken, A.D. Haubold, T.S. Peters, J.C. Stupka, Inventors; Onx Inc., applicant. Heart valve prosthesis, Patent WO1994002085 A1, 1994.
[176] V. Govindarajan, H.S. Udaykumar, L.H. Herbertson, S. Deutsch, K.B. Manning, K.B. Chandran, Impact of design parameters on bileaflet mechanical heart valve flow dynamics, J. Heart Valve Dis. 18 (2009) 535–545.
[177] M.J. King, T. David, J. Fisher, Three-dimensional study of the effect of two leaflet opening angles on the time-dependent flow through a bileaflet mechanical heart valve, Med. Eng. Phys. 19 (1997) 235–241, https://doi.org/10.1016/S1350-4533(96)00066-5.
[178] H.A. Simon, H.-L. Leo, J. Carberry, A.P. Yoganathan, Comparison of the hinge flow fields of two bileaflet mechanical heart valves under aortic and mitral conditions, Ann. Biomed. Eng. 32 (2004) 1607–1617.
[179] S. Westaby, G. Van Nooten, H. Sharif, R. Pillai, F. Caes, Valve replacement with the ATS open pivot bileaflet prosthesis, Eur. J. Cardiothorac. Surg. 10 (1996) 660–665.
[180] W.C. Dihmis, P. Wilde, J.A. Hutter, Early experience with the Jyros bileaflet valve. Is leaflet rotation clinically important? J. Heart Valve Dis. 3 (1994) 191–196.
[181] K. Onoda, F. Yasuda, T. Komada, B. Pagoada-Cruz, Y. Katayama, T. Shimono, H. Shimpo, I. Yada, Five-year follow-up of valve replacement with the Jyros bileaflet mechanical valve, Artif. Organs 24 (2000) 70–78, https://doi.org/10.1046/j.1525-1594.2000.06339-2.x.
[182] R.K. Walesby, C. Di Salvo, M.M. Black, One hundred patients' experience with the Jyros valve, J. Cardiovasc. Surg. (Torino) 37 (1996) 37–41.
[183] J.M. Bernal, J.M. Rabasa, F. Gutierrez-Garcia, C. Morales, J.F. Nistal, J.M. Revuelta, The CarboMedics valve: experience with 1,049 implants, Ann. Thorac. Surg. 65 (1998) 137–143, https://doi.org/10.1016/S0003-4975(97)01238-1.
[184] H.L. Leo, L.P. Dasi, J. Carberry, H.A. Simon, A.P. Yoganathan, Fluid dynamic assessment of three polymeric heart valves using particle image velocimetry, Ann. Biomed. Eng. 34 (2006) 936–952, https://doi.org/10.1007/s10439-006-9117-5.
[185] M. Grigioni, C. Daniele, G. D'Avenio, V. Barbaro, The influence of the leaflets' curvature on the flow field in two bileaflet prosthetic heart valves, J. Biomech. 34 (2001) 613–621, https://doi.org/10.1016/S0021-9290(00)00240-2.
[186] L. Camilleri, Mitral and mitro-aortic valve replacement with Sorin Bicarbon valves compared with St. Jude Medical valves, Cardiovasc. Surg. 9 (2001) 272–280, https://doi.org/10.1016/S0967-2109(00)00136-8.
[187] L.P. Badano, D. Pavoni, S. Musumeci, R. Frassani, P. Gianfagna, M. Baldassi, V. Tursi, E. Mazzaro, E. Zakja, P.M. Fioretti, U. Livi, Stented bioprosthetic valve hemodynamics: is the supra-annular implant better than the intra-annular? J. Heart Valve Dis. 15 (2006) 238–246.
[188] F. Botzenhardt, W.B. Eichinger, S. Bleiziffer, R. Guenzinger, I.M. Wagner, R. Bauernschmitt, R. Lange, Hemodynamic comparison of bioprostheses for complete supra-annular position in patients with small aortic annulus, J. Am. Coll. Cardiol. 45 (2005) 2054–2060, https://doi.org/10.1016/j.jacc.2005.03.039.

[189] P. Totaro, N. Degno, A. Zaidi, A. Youhana, V. Argano, Carpentier-Edwards Perimount Magna bioprosthesis: a stented valve with stentless performance? J. Thorac. Cardiovasc. Surg. 130 (2005) 1668–1674, https://doi.org/10.1016/j.jtcvs.2005.07.011.
[190] J. Aagaard, The Carbomedics aortic heart valve prosthesis: a review, J. Cardiovasc. Surg. (Torino) 45 (2004) 531–534.
[191] J.M. Bernal, J. Lorca, D. Prieto-Salceda, I. Pulitani, A. Pontón, I. García, J.M. Revuelta, Performance at 10 years of the CarboMedics "Top-Hat" valve. Postclamping time is a predictor of mortality, Eur. J. Cardiothorac. Surg. 29 (2006) 144–149, https://doi.org/10.1016/j.ejcts.2005.10.044.
[192] J.M. Bernal, R. Martin-Duran, J.M. Rabasa, J.M. Revuelta, The CarboMedics "Top-Hat" supraannular prosthesis, Ann. Thorac. Surg. 67 (1999) 1299–1303, https://doi.org/10.1016/S0003-4975(99)00170-8.
[193] A.M. Gillinov, E.H. Blackstone, J.M. Alster, J.M. Craver, W.A. Baumgartner, S.A. Brewster, L.H. Kleinman, N.G. Smedira, The CarboMedics Top Hat supraannular aortic valve: a multicenter study, Ann. Thorac. Surg. 75 (2003) 1175–1180, https://doi.org/10.1016/S0003-4975(02)03991-7.
[194] K.B. Chandran, B. Khalighi, C.-J. Chen, Experimental study of physiological pulsatile flow past valve prostheses in a model of human aorta—II. Tilting disc valves and the effect of orientation, J. Biomech. 18 (1985) 773–780, https://doi.org/10.1016/0021-9290(85)90052-1.
[195] H. Mächler, M. Perthel, G. Reiter, U. Reiter, M. Zink, P. Bergmann, A. Waltensdorfer, J. Laas, Influence of bileaflet prosthetic mitral valve orientation on left ventricular flow—an experimental in vivo magnetic resonance imaging study, Eur. J. Cardiothorac. Surg. 26 (2004) 747–753, https://doi.org/10.1016/j.ejcts.2004.06.019.
[196] G.L. Van Rijk-Zwikker, B.J. Delemarre, H.A. Huysmans, The orientation of the bileaflet CarboMedics valve in the mitral position determines left ventricular spatial flow patterns, Eur. J. Cardiothorac. Surg. 10 (1996) 513–520.
[197] T. Akutsu, D. Higuchi, Flow analysis of the bileaflet mechanical prosthetic heart valves using laser Doppler anemometer: effect of the valve designs and installed orientations to the flow inside the simulated left ventricle, J. Artif. Organs 4 (2001) 113–125, https://doi.org/10.1007/BF02481421.
[198] P. Kleine, M.J. Hasenkam, H. Nygaard, M. Perthel, D. Wesemeyer, J. Laas, Tilting disc versus bileaflet aortic valve substitutes: intraoperative and postoperative hemodynamic performance in humans, J. Heart Valve Dis. 9 (2000) 308–311.
[199] J. Laas, P. Kleine, M.J. Hasenkam, H. Nygaard, Orientation of tilting disc and bileaflet aortic valve substitutes for optimal hemodynamics, Ann. Thorac. Surg. 68 (1999) 1096–1099, https://doi.org/10.1016/S0003-4975(99)00780-8.
[200] C. Del Gaudio, M. Grigioni, A. Bianco, G. De Angelis, Electrospun bioresorbable heart valve scaffold for tissue engineering, Int. J. Artif. Organs 31 (2008) 68–75.
[201] N. Masoumi, N. Annabi, A. Assmann, B.L. Larson, J. Hjortnaes, N. Alemdar, M. Kharaziha, K.B. Manning, J.E. Mayer, A. Khademhosseini, Tri-layered elastomeric scaffolds for engineering heart valve leaflets, Biomaterials 35 (2014) 7774–7785, https://doi.org/10.1016/j.biomaterials.2014.04.039.
[202] N. Masoumi, K.L. Johnson, M.C. Howell, G.C. Engelmayr, Valvular interstitial cell seeded poly(glycerol sebacate) scaffolds: toward a biomimetic in vitro model for heart valve tissue engineering, Acta Biomater. 9 (2013) 5974–5988, https://doi.org/10.1016/j.actbio.2013.01.001.
[203] D. van Geemen, A. Driessen-Mol, L.G.M. Grootzwagers, R.S. Soekhradj-Soechit, P.W. Riem Vis, F.P.T. Baaijens, C.V.C. Bouten, Variation in tissue outcome of ovine and human engineered heart valve constructs: relevance for tissue engineering, Regen. Med. 7 (2012) 59–70, https://doi.org/10.2217/rme.11.100.

This page intentionally left blank

Improving the hemocompatibility of catheters via NO release/generation

16

Y. Wo, E.J. Brisbois, R.H. Bartlett, M.E. Meyerhoff
University of Michigan, Ann Arbor, MI, United States

16.1 The need for hemocompatible polymeric surfaces

Vascular access through use of intravascular (IV) catheters is a very common practice in hospitals and outpatient settings and is essential for patient diagnosis, monitoring, and treatment [1,2]. In 1929, Forssmann introduced the first cardiac catheterization technique for drug administration and shared the 1956 Nobel Prize for Medicine along with two other scientists for pioneering work in this important field [3]. IV catheters are indispensable in modern-day medical practice and an estimated 150 million IV devices are used in the United States annually [4]. Catheters are typically classified by their functional lifetime (short-term or long-term), the catheter's intended location/use (e.g., peripherally inserted central catheter), the catheterization methodology (e.g., tunneled), number of lumens, or other characteristics (e.g., presence/inclusion of anticoagulants or antibiotics) [5].

Two of the major challenges associated with catheters include thrombosis and infection (Fig. 16.1) [1,5–14]. When foreign surfaces are in contact with blood, plasma proteins such as fibrinogen, Factor XII, and Factor XI, adsorb on the device surfaces. The adsorbed proteins activate the platelet surface membrane receptor GPIIb/IIIa, which has the capacity to bind with fibrinogen, von Willebrand Factor, fibronectin, and vitronectin [15]. This platelet activation process leads to conformational changes, subsequent release of intracellular agents (e.g., Factor V, VIII and Ca^{2+}, etc.), and platelet aggregation (intrinsic coagulation pathway) [15–20]. If the homeostasis of the blood is disrupted by surgery or trauma, tissue factor will be released into the blood (extrinsic pathway) [19]. Both the intrinsic and the extrinsic coagulation pathways will trigger the activation of Factor X and formation of thrombin (Factor II), that converts fibrinogen monomer into fibrin polymer and ultimately leads to thrombus formation [15,17–19].

Thrombus formation on IV catheter surfaces not only causes device malfunction, but can also result in extended hospital stays and higher healthcare costs. If a detachment of the thrombosis travels to the leg or the lungs, it can cause potentially life-threatening conditions, such as deep vein thrombus or pulmonary embolism [21–23]. In order to prevent these complications, some patients are treated with anticoagulant agents, such as heparin or warfarin [15,22]. Ideally, it is desirable to have localized anticoagulant activity only in regions immediately close to the catheter surfaces.

Hemocompatibility of Biomaterials for Clinical Applications. https://doi.org/10.1016/B978-0-08-100497-5.00013-6
© 2018 Elsevier Ltd. All rights reserved.

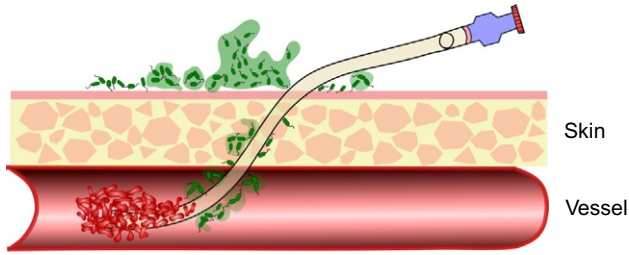


Fig. 16.1 Thrombus formation (*red*) and bacterial infection (*green*) on surface of intravascular catheters.

This has led to the use of immobilized or slow heparin releasing catheters [24,25], or the routine use of catheter lock solutions [26,27] containing heparin that can leak out the distal end of the catheter and prevent thrombus formation at that site, thereby preventing catheter occlusion. If this approach fails, the only solution to clot formation on indwelling devices is replacement, which can lead to further risk of infection [15,17].

Bloodstream infections are another major and growing problem associated with IV catheters. Indeed, common nosocomial infections can cause lengthy hospital stays, increased healthcare costs, and an increased mortality rate as high as 23% in hospitalized patients [9,28,29]. With the increasing use of IV catheters, catheter related bloods stream infections (CRBSIs) continue to pose a threat to hospitalized patients, particularly in intensive care units (ICUs) [2,7,8,10,29–38], with an estimated attributed cost ranging from $670 million to $2.68 billion annually in the United States alone [3]. Of note, the combination of peripheral vein blood cultures and semiquantitative superficial cultures are a more accurate screening method for patients with CRBSIs, compared to using blood drawn from IV catheters for microbial culturing which can potentially yield false-negative results because of the frequent withdraws from those sites [39].

Several microorganisms are commonly responsible for CRBSIs, including *Staphylococcus epidermidis*, *Staphylococcus aureus*, and *Pseudomonas aeruginosa* [40,41]. The first step of bacterial infection is bacteria colonization via nonspecific interactions with the catheter surface, followed by bacteria proliferation and ultimately biofilm formation [42]. Biofilm formation on biomedical devices is extremely difficult to treat because of the presence of extracellular polysaccharide substances (EPS) produced by the bacteria that decreases the ability of antibiotics to penetrate this layer, reducing antibiotic efficacy, that can further lead to bacterial genetic mutations [43–47]. One additional growing concern has been the expanding population of antibiotics resistant bacteria species, such as methicillin-resistant *Staphylococcus aureus* (MRSA). The *S. aureus* isolates with methicillin resistance increased from 22% in 1995 to 57% in 2001 [48,49]. The Centers for Disease Control and Prevention (CDC) has published "Guidelines for Prevention of Intravascular Catheter-Related Infections," which emphasizes the importance of training healthcare personnel who place catheters into patients and mandating that maximal sterile precautions be taken during catheter insertion (e.g., antiseptic skin preparation, avoiding unnecessary routine replacements, etc.) [5].

Vascular access is essential in medical practice and in addition to following the existing CDC guidelines, considerable research has focused on developing more hemocompatible and antiseptic materials for blood-contacting biomedical devices to reduce the rates of thrombosis and infection. The requirements of biomedical devices set by the International Standards Organization (ISO) are that they be nontoxic, nonthrombogenic, noncarcinogenic, nonantigenic, and nonmutanenic [16]. However, an ideal device material should also encourage a positive healing process and the formation of healthy, normal tissue around the device. The most common polymers used to prepare catheters are silicone (polydimethylsiloxane, PDMS), polyurethane (PU), poly(vinylchloride) (PVC), polytetrafluoroethylene (PTFE), and natural latex rubber [50]. This chapter provides an overview of the current approaches being studied to create more thromboresistant and antibacterial surfaces for use in creating IV catheters, with an extra focus on nitric oxide (NO) releasing/generating catheters.

16.2 Catheter lock solutions

Currently, various catheter lock solutions are used as one approach to reduce clotting and infection complications. To prevent catheter occlusion due to thrombosis, flushing and locking of the IV catheters is performed with anticoagulant lock solution (e.g., heparin or citrate [27,51]) or a thrombolytic lock solution (e.g., urokinase) [52]. Heparin lock solutions play a key role in preventing catheter induced thrombosis [53]. Concentrated heparin solutions are inserted into catheter lumens, and it is very important to use the right concentration of heparin to reduce the risk of systemic bleeding or HIT. Ivan et al. compared the catheter patency between two concentrations of heparin lock solutions, 1000 and 5000 U/mL, among 105 patients with newly placed tunneled hemodialysis catheters [54]. There was no significant difference between catheter survival in the two groups (71% vs. 73% over 120 days in low and high-concentration heparin lock solution groups, respectively), but the overall drug cost for maintaining catheter patency was 23% lower with the lower concentration lock group. Moran et al. suggested that the low concentration heparin lock solution (1000 U/mL with 4% sodium citrate) should be used for most patients because of its effectiveness and low risk of complications, while high concentrations of heparin lock should be reserved for patients who have evidence of catheter occlusion or thrombosis [27]. Of note, the effectiveness of using a thrombolytic agent (urokinase) in the lock solution when compared to heparin has generated mixed results, depending on the dose of urokinase or heparin given during each use [55,56]. Still, the most effective antithrombotic locking solution will depend on the catheter type and the patient's condition [53].

Catheter lock solutions are also used to deliver antibacterial agents such as antibiotics [57], ethanol [58], or biofilm dispersing agents [59,60]. This intraluminal antibacterial therapy, using a catheter lock solution in which a high concentration of antibacterial agents are instilled in the catheter in situ for a sufficient time, is used to prevent or eliminate biofilm formation [59–61]. *N*-Acetylcysteine (NAC) is a mucolytic agent that interferes with the EPS formation, inhibits the biofilm production, and disrupts mature biofilm [44,60,62]. Darouiche and coworkers conducted in vivo rabbit

experiments that showed that a NAC lock solution (80 mg/mL) could successfully prevent catheter-associated bacteremia [60]. The same authors have also demonstrated that the combination of NAC with the antibiotic tigecycline could greatly reduce the biofilm formation on the surfaces of central venous catheters (CVCs) [63]. The catheters were first incubated in Trypticase soy broth that contained 10^5 colony forming units (CFU)/mL of bacteria for 24 h at 37°C for biofilm development and then later suspended in treatment solutions for 4 or 12 h. The results showed that the NAC and tigecycline were synergistic against MRSA and methicillin-resistant *Staphylococcus epidermidis* (MRSE). The authors suggest that it is possible that NAC disrupts the biofilm and makes the bacteria more susceptible to tigecycline.

Many researchers have also utilized IV catheter lock solutions containing both antibiotics and heparin [26,59]. For example, Aslam et al. used lock solutions with heparin (2000 U/mL), NAC (80 mg/mL), and tigecycline (1 mg/mL) to treat patients with hemodialysis catheter-associated bacteremia [59]. All patients in this study were already receiving systemic antibiotic therapy; however, hemodialysis catheter-associated bacteremia is reportedly refractory to systemic antibiotic treatment. The catheter lock solution was incorporated into the catheter lumen daily and then three times a week after patient discharge for 14 days. The results showed that 15 out of 18 patients (83%) were treated successfully within a 90-day follow up period, in which their blood drawn cultures showed no sign of persistent or recurrent bacteremia of the original pathogen. This novel lock solution has a higher success rate of eradicating biofilm-based bacteremia caused by catheter colonization than the previous studies of catheter lock solutions that contain heparin and various antibiotics (40%–70%) [59]. Further, Filippi et al. prepared a fusidic acid (4 mg/mL) and heparin (10 IU/mL) lock solution for prevention of CRBSIs in critically ill neonates ($n = 100$) who were already treated with systemic antibiotics. The solution was infused once a day up to 39 days and was maintained within the catheter for 30–60 min each time. The results demonstrated significantly lower incidences of CRBSIs (6.6 vs. 24.9 per 1000 catheter days), and no staphylococcal infections occurred in the treatment group whereas it still remained the main cause of infections in the control group [26]. Although the use of various catheter lock solutions have demonstrated effectiveness in the clinical setting, the development of catheters made from polymers with inherent properties that can prevent thrombosis and infection locally, is another viable and more attractive strategy to pursue.

16.3 Thromboresistant catheters

Several different approaches have been pursued to develop thromboresistant polymeric surfaces. First, passive surfaces can be created to reduce protein or cell adsorption by various surface modifications such as creating submicron textured surfaces that minimize surface contacting area [41] or by chemical surface modifications with hydrophilic polymers such as poly(ethylene oxide) or poly(ethylene glycol) (PEG), or other biocompatible polymers that reduce adhesion [17,64]. Krishna et al. reported a method in which they covalently grafted a phospholipid monolayer onto medical grade silicone catheters that resulted in excellent water retention properties and

enhanced biocompatibility based on in vitro and in vivo studies [65,66]. The highly hydrated polymer coating exhibits a large exclusion volume effect that inhibits protein and cell adhesion [62,67]. Plasma polymerization of allyl alcohol was employed for silicone catheter surface hydroxylation, which was then chemically anchored using in situ polymerization with mono-acrylated phospholipid. The phospholipid-modified silicone catheters demonstrated a sharp decrease in water contact angle compared to the silicone controls (58 vs. 112 degrees). Based on in vitro studies, the changes in the levels of platelet adhesion to the material surfaces represent the relative thrombogenic potential of the material [68]. Both grafted and ungrafted silicone catheters were hydrated in phosphate buffer saline (PBS) for 1 h before incubation in rabbit platelet-rich plasma for 3 h at 37°C. Scanning electron microscope (SEM) images showed that the majority of the platelets on the ungrafted catheters were in the spread dendritic stages with protruded pseudopodes while the platelets maintained a round morphology (not activated) on the phospholipid-grafted catheters. The number of platelets adhered on the treated catheter surface was reduced by approximately 81% as compared to the controls [65]. Passive surfaces without functional active agents being delivered at the polymer/blood interface over time are probably not ideal for long-term applications because these surfaces may eventually become deteriorated in the complex physiological media [20,69].

Active polymer surfaces can be fabricated by modifying the polymer with active molecules, such as anticoagulants (e.g., heparin) [70], thrombomodulin [71], direct thrombin inhibitors (such as hirudin [15] or argatroban [72]), or antiplatelet drugs (e.g., prostacyclin (PGI2) or prostaglandin (PGE1 and PGD2)) [15] in order to disrupt thrombin and fibrin formation. Specifically, heparin has been commonly used to develop thromboresistant catheter surfaces. Two general approaches have been pursued: (1) heparin-releasing surfaces, where heparin is released over a short period of time in free form with high bioactivitiy [73–76]; and (2) heparin-immobilized surfaces, where heparin is bound onto a polymer surface via either covalent [71,77–79] or ionic bonding [80–82], providing a long-lasting antithrombogenic effect. For example, Gutowska et al. developed a thermosensitive poly(*N*-isopropylacrylamide) (poly (NiPAAm)), which has temperature dependent polymer-water and polymer-polymer interactions [24,83]. Poly(NiPAAm) has a lower critical solution temperature (LCST) of 32°C, which enables it to swell when immersed in a heparin solution at low temperature (e.g., room temperature, RT) and uptake the polyanionic drug [24]. When the temperature is higher than LCST, the swollen coating will collapse dramatically and release heparin. The thermosensitive hydrogel coating holds promise for loading relatively large amounts of heparin without the use of organic solvents, which may affect the bioactivity of the loaded heparin. When a commercial PU intravenous catheter (Vialon) was first dip-coated with the poly(NiPAAm) and the dried catheters were immersed in the heparin loading solution at RT, the maximum loading of heparin (1.5 ± 0.3 wt%) was attained after 1 h. The in vitro heparin release rate was tested in PBS at 37°C, and 70% of the loaded heparin was released over 15 min (100 µg/h per cm^2), followed by a slower release (1.0 µg/h per cm^2) of up to 6 h. The short-term antithrombogenicity of the heparin-releasing PU catheters were evaluated in a canine animal model [24]. Both the heparin-coated and control PU catheter were inserted into

the saphenous veins for 1.5 h, and the heparin-releasing PU catheter surfaces demonstrated a significant reduction in thrombus formation while in contact with venous blood as demonstrated by the SEM images (compared to the controls). Lee et al. also used canine model to demonstrate the thromboresistant effects of heparin-coated angiographic catheters with three different heparin release profiles [25]. The catheters were inserted into dog arteries for 30 min and then carefully removed to compare the weight of dry thrombi inside. The results showed that the rapid-heparin-release coating, that released 64% of loaded heparin within 12 h in the in vitro study, had the least amount of clot (52.0 ± 12.6 vs. 374.6 ± 11.6 mg for controls). This approach is suitable for angiographic catheters since angiography procedures are usually completed within hours and the rapid free heparin release exhibits maximized bioactivity during such periods [25].

There are also several commercially available heparin coated PU CVCs currently on the market, sold by Cook Medical or Harvard Apparatus, which are designed for treatment of critically ill patients. Such catheters enable continuous or intermittent drug infusions, central venous blood pressure monitoring, and blood sampling. Harvard Apparatus developed CBAS (Carmeda BioActive Surface), a longer-lasting heparin coating by end-point covalent attachment of heparin onto a PU catheter surface. It acts by repeatedly binding to activated antithrombin to prevent clot formation. The advantage of this technique is that only the thrombin-antithrombin complex is washed away, and the active heparin moiety does not elute into the bloodstream and remains active for a relatively longer period of time.

16.4 Antibacterial catheters

The commonly studied antibacterial material surfaces are divided into the following four categories: (1) surfaces that prevent cell adhesion, such as hydrogel modified surfaces [84] or submicron textured surfaces [41]; (2) surfaces that contains small molecules or enzymes that are able to interfere with biofilm formation or disperse existing biofilms, including *cis*-2-decenoic acid, d-amino, NAC, chelating agents, and dispersin B [1,42,44,45,59,60,63,85–87]; (3) surfaces that are able to kill bacteria based on contact, such as zwitterion [88], quaternary ammonium compounds [89,90], and chitosan containing surfaces [91–93]; and (4) surfaces that release bactericidal agents such as silver ions [94–97], superoxide radicals [98], alcohol [58], and bacteriophages [45,99–101] or antibiotics [5,63]. However, the most commonly used approaches for fabricating antibacterial catheters are focused on biomaterials that can contain and release bactericidal agents or species that interfere with biofilm formation.

It has been well demonstrated that silver-coated [97] or silver nanoparticles [94–96] embedded in a polymeric medical device can slowly release Ag^+ ions and provide promising strategies to combat bacterial infections related to such indwelling devices [44,69]. Silver ions bind to bacterial DNA and further interfere with important enzyme/protein functions, eventually leading to cell death [61,69]. Usually, silver nanoparticles (AgNP) are formed on the surface of the catheters through a reduction reaction involving a silver salt solution and a reducing agent [94] or photo-reduction [95]

process. Roe et al. coated polyamide catheters with a thin (~100 nm) layer of AgNP from radioactive $AgNO_3$ ($^{111m}Ag^{+}$) and demonstrated sustained silver release over a 10 days period [94]. The catheters exhibited significant antibacterial activities against bacteria commonly associated with CRBSIs, such as *S. aureus*, *P. aeruginosa,* and *Escherichia coli*, for at least 72 h. In vivo experiments were conducted to study the silver release and distribution in male mice, in which the AgNP coated catheters were implanted subcutaneously under the dorsal skin for 10 days. After the organ and tissue collection at the end of the experiments, silver distribution was measured by radioactivity. Silver was predominantly excreted in feces (more than 55%) and a significant amount was retained in the tissue in direct contact with the catheter (~20%), but minimal organ accumulation (<0.6%) was noted [94]. Lin and coworkers recently reported a mussel-inspired method to induce AgNPs formation by using a thin polydopamine layer without additional reductants. However, the antibacterial activity of the AgNPs coated catheters was concentration dependent, where a higher dose of the AgNPs showed excellent antibacterial activity, but also had increased cytotoxicity against human cells [96]. It has also been reported that silver-loaded catheters are effective in preventing early-onset catheter-related infections, but are limited in providing long lasting protection [64,102]. Additionally, silver-containing PU catheters have been demonstrated to trigger greater platelet activation and adhesion on the catheter surfaces than the controls when in contact with blood, where platelets can become activated after coming in contact with the silver particles on the surface and this actually accelerates the coagulation process [68,103]. Therefore, most commercially available silver-based catheters on the market (e.g., Bardex I.C. by Bard Medical) are silver alloy coated urinary Foley catheters, not blood-contacting devices.

Coating or impregnating the catheters with antibiotics has also become a standard of care to reduce risk of infections associated with the use of catheters [104–106]. Cook Medical is one of the companies that manufactures commercial antibiotic impregnated CVCs, such as the Cook Spectrum line, that release the antibiotics minocycline and rifampin. CVCs are central lines that are inserted through veins and terminate within the thorax [107], and they are essential devices for the care of critically ill patients who require hemodialysis or total parenteral nutrition [108]. Raad et al. recently developed a new generation of antibiotic impregnated CVCs [106]. A combination of chlorhexidine-minocycline-rifampin (CHX-M/R) was used to impregnate CVCs and their efficacy was compared with previously developed M/R catheters, CHX catheters, and CHX-silver sulfadiazine releasing catheters against MRSA, vancomycin-resistant *Enterococcus faecium* (VRE), and other microbes in vitro [106]. The results showed that only CHS-M/R impregnated CVCs had complete inhibition and antibacterial activity against MRSA and VRE for up to 3 weeks. However, even though antibiotic-releasing catheters have been shown in the laboratory to reduce bacterial adhesion and inhibit bacterial growth with some success [109,110], clinical results and efficiency with such devices has been less than satisfactory owing to the biofilm matrix that protects the bacteria from antibiotics as well as an increased level of microbial mutations that contribute to the survival of biofilms [104,111].

Curtin et al. has investigated the use of bacteriophages for prevention of biofilm formation on indwelling catheters [101]. Hydrogel-coated silicone catheters were

used to represent CVCs to help adsorb and maintain the bacteriophage culture within the catheter lumen. The experimental hydrogel coated catheters were pretreated with phages by exposing the catheter lumen to Mueller-Hinton broth (MHB) containing 10^{10} plaque-forming units (PFU)/mL phage 456 for 1 h at 37°C before biofilm formation. Experiments were also conducted using MHB containing $MgCl_2$ and $CaCl_2$ in order to assess the effect of divalent cations on the growth and multiplication of the phages. Catheters pretreated with heat-inactivated phages were used as a control group. The antibiofilm effect of phage-treated catheters was evaluated by culturing *S. epidermidis* biofilm on the catheter surfaces for 24 h at 37°C. The results showed a reduction of viable cell count on both bacteriophage-treated catheters (with or without divalent cation supplements) by 4.47 and 2.34 in log CFU/cm^2, respectively, as compared to the controls (7.01 ± 0.47 log CFU/cm^2) [101]. This in vitro model system suggests the potential of bacteriophages for mitigating biofilm formation on IV catheters and reducing rates of CRBSIs, particularly as the problem of antibiotic resistance continues to grow and traditional antibacterial agents become less effective. However, further research efforts, particularly in vivo studies, are necessary before such phage-treated catheters can be considered as viable devices to resolve the catheter associated infection problem.

16.5 Antithrombotic and antibacterial nitric oxide releasing/generating catheters

In order to better combat thrombus formation and bacterial infection on IV catheters, new strategies are still needed. Some researchers have tried to combine the individual approaches mentioned above to create multifunctional antithrombotic and antibacterial surfaces. For example, studies have combined heparin or hydrophilic polymer brush modified surfaces with embedded antibacterial quaternary compounds or silver nanoparticles [64,112–114]. Fischer et al. prepared multilayered silver-containing PEG-heparin hydrogel coated PU disks [64]. Heparin was covalently attached to PEG forming a hydrogel network, which was later modified with AgNPs via immersion into acetate buffer containing $AgNO_3$. A second Ag-free hydrogel layer was coated on top of the AgNP containing layer as a diffusion barrier for prolonged silver release and to avoid direct cellular interactions with AgNPs at the coating-blood interface. This coating, loaded with 4000 ppm AgNPs, showed a concentration-dependent zone inhibition effect for both *E. coli* and *S. epidermidis* for up to 6 days. In the hemolysis assay testing, multilayer functionalized PU disk did not induce hemolysis, as determined by a colorimetric assay, when incubated with heparinized whole blood for 2 h at 37°C, whereas the 4000 ppm free silver triggered 5.6% hemolysis. Although this technique offers promise as a versatile surface that combines both antiseptic and enhanced blood compatibility properties, the complex surface modification process has not yet been adapted for improving the hemocompatibility of catheters [64]. Hence, the need for novel combination thromboresistant/antibacterial surfaces has driven further research using other approaches, including the use of nitric oxide (NO) releasing or generating polymers to reduce the possibility of both thrombus and infection.

NO was identified as the endothelium-derived relaxation factor by Ignarro, Furchgott, and Murad in 1987, who were later awarded the Nobel Prize in Physiology or Medicine for their discovery in 1998 [115,116]. The human body synthesizes large quantities of bioregulatory NO from the amino acid L-arginine via three distinct isoforms of nitric oxide synthases (NOS): endothelial NOS (eNOS), neuronal NOS (nNOS), and inducible NOS (iNOS) [117–119]. Nitric oxide has been extensively studied for its various important physiological functions including prevention of platelet activation and adhesion, inhibiting bacteria colonization and proliferation, promoting endothelization, and enhancing wound healing process [115,116,120–123]. NO is produced by the endothelial cells that line the inner wall of all blood vessels at a low flux rate ($0.5–4.0\times10^{-10}$ mol cm^{-2} min^{-1}) [117] to control the balance between thrombosis and hemorrhage [118]. Additionally, NO has been reported to kill both gram-positive and gram-negative bacteria [43,124–126]. It has also been reported that NO can modulate biofilm metabolism and make it more susceptible to antibiotics [127].

Nitric oxide has a very short half-life (a few seconds) and short diffusion distance (~100 μm) [115] in blood due to its rapid reactions with hemoglobin, oxygen, and thiols. Therefore, many NO donor compounds have been studied for targeted NO release and therapeutic effects including organic nitrates, metal nitrosyls, inorganic nitrite and nitrate, *N*-diazeniumdiolates (NONOates), and *S*-nitrosothiols (RSNOs) (Fig. 16.2)

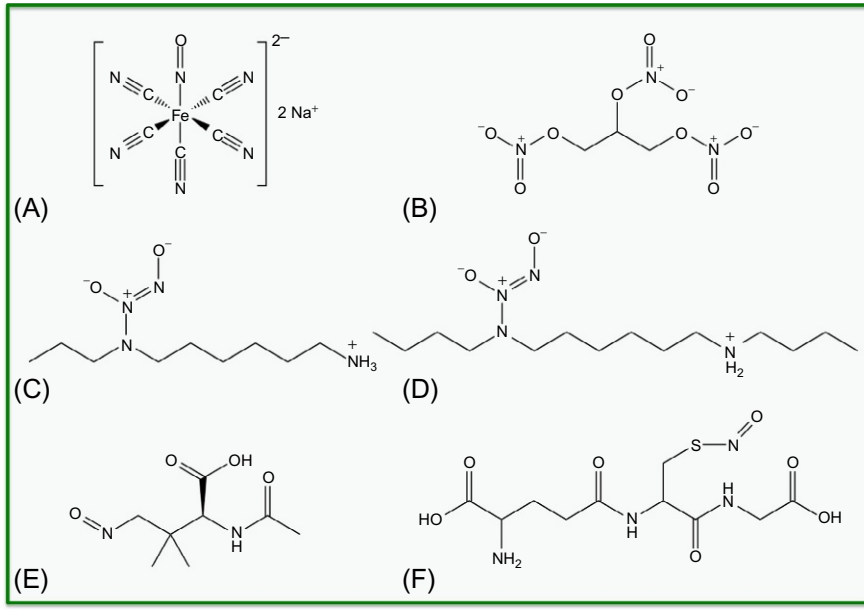


Fig. 16.2 Representative NO donor structures, including (A) sodium nitroprusside; (B) nitroglycerin; (C) diazeniumdiolated *N*-(6-aminohexyl)aminopropane (DACA/N_2O_2); (D) diazeniumdiolated dibutylhexyldiamine (DBHD/N_2O_2); (E) *S*-nitroso-*N*-acetylpenicillamine (SNAP); and (F) *S*-nitrosoglutathione (GSNO).

[128–134]. Nitroglycerin, also known as glyceryl trinitrate (GTN) is a precursor to NO and is the most commonly used organic nitrate for treating angina pain. However, patients often developed tolerance to the drug and the enzyme (mitochondrial aldehyde dehydrogenase, mtALDH) can be oxidized over time by the generated reactive oxygen species, lowering its functionality and bioavailability for converting nitroglycerin to NO [135–138]. Sodium nitroprusside ($Na_2[Fe(CN)_5NO$, SNP) also generates NO in vivo and has been used as vasodilator for treating hypertension, but its cytotoxicity from potential byproducts cyanide and peroxynitrite has limited its use in the clinical setting [139].

N-Diazeniumdiolates (NONOates) are one of the most well studied NO donors. They are synthesized by reacting secondary amines with high pressurized NO in the presence of base [130]. Such donors release two molar equivalents of NO per mole of NONOate and an amine byproduct via a proton and thermally driven reaction in the presence of buffer, tissue fluids, or blood [130]. However, when NONOates like DBHD/NONO are incorporated in hydrophobic polymers, the NO release lifetime is short due to a gradual increase in pH within the organic polymer phase. Various additives, such as tetraphenylborate or other borates [78,135,140] have been incorporated into the organic polymer phase to serve as counter ions for organic ammonium cations and this helps prevent an increase of the pH within the organic phase to prolong the NO release lifetime. However, the borate additives are not ideal because of their inability to extend the NO release to no more than a few days and their potential cytotoxicity toward endothelial cells [141,142]. More recently, poly(lactic-*co*-glycolic) acid (PLGA) was used as the additive for NONOates in polymers to provide the protons needed to generate NO continuously [141,143]. PLGA is a biocompatible and biodegradable polymer that forms lactic acid and glycolic acid, which can serve as proton sources in the polymer matrix. Moreover, PLGA is already approved for use by the FDA for the development of devices for controlled delivery of small molecule drugs, proteins, and other macromolecules [144]. One drawback associated with the use of NONOates is their potential formation of carcinogenic nitrosamine byproducts [145,146]. Therefore, many researchers have developed more lipophilic NONOates [140] or have covalently attached NONOate functionalities onto polymer fillers [147] or polymer backbones [148] to reduce donor leaching from polymeric phases.

S-Nitrosothiols (RSNOs) are considered one of the most potentially biocompatible NO donors because of the existence of many endogenous RSNOs as natural NO reservoirs and transporters in tissues and blood [119,149]. Endogenous RSNOs include *S*-nitrosoalbumin (SNO-Alb), *S*-nitrosohemoglobin (SNO-Hb), *S*-nitrosocysteine (SNO-Cys), and *S*-nitrosoglutathione (GSNO) [150]. Many other RSNOs have also been synthesized, such as *S*-nitroso-*N*-acetylpenicillamine (SNAP), via a nitrosation reaction between the parent thiol *N*-acetylpenicillamine (NAP) and acidified nitrite solution [151]. SNAP is considered biocompatible because NAP and its ultimate degradation product, penicillamine, have been used as chelators to treat heavy metal poisoning, such as Wilson's disease in humans, for many years [152–156]. RSNOs can release NO and form the corresponding byproduct disulfide (RSSR) via metal ion catalysis reactions (such as cuprous or ferrous ions, etc.) [157–160], thermal decomposition, photodecomposition at the RSNO characteristic absorption wavelengths

(330–350 or 550–600 nm [134,161]), or in the presence of ascorbate [160,162,163]. RSNOs can react with ascorbate to generate NO via two pathways. In one, ascorbate at low concentration, acts as a reducing agent generating Cu^+ from copper ion impurities in solution and the Cu^+ species reduced the RSNO to produce NO and a thiolate anion. At higher concentrations of ascorbate, the ascorbate acts as a nucleophile, attacking the nitroso group and generates a thiolate and dehydroascorbate [163–165].

Many organoselenium species that mimic enzymes such as glutathione peroxidase can also be utilized to covert RSNOs into NO in the presence of thiols or other reducing agents [166,167]. Similarly, many copper containing species (such as copper nanoparticles [168], copper(II) cyclen [158], and molecular organic frameworks (MOFs) created with Cu(II) ions [169–172], or copper zinc superoxide dismutase (CuZn-SOD) [134,173]) have proven to be catalysts in generating NO from RSNOs, in which the true reactive species is Cu(I) ion generated in the presence of suitable oxidizing or reducing agents [134]. RSNOs have also been doped into [151,174] or covalently attached [175–177] to polymeric materials for localized NO release. Furthermore, RSNOs and NONOates can decompose and release NO independent from enzymes, thus making them less likely to provoke tolerance over time, which is appealing in the medical field [128,178].

Besides NO release from various NO donors or NO generation via metal catalysis, another promising approach for NO production involves using electrochemical (e-chem) NO generation from an inorganic nitrite solution. The e-chem NO generation is based on generating transient levels of Cu(I) species at the electrode surface from Cu^0 or from suitable Cu(II)-ligand complexes when applying given potentials to an electrode surface. The Cu(I) species can then reduce nitrite to NO. This method is unique because of its ability to modulate the rate of NO production merely by controlling the potentials applied to the electrodes [179–181].

Many different polymers, including PVC, PTFE, dendrimers, chitosan, polysaccharides, PLGA, polyester, PU, and silicone rubber (PDMS) have been used for localized NO release for various biomedical applications [91–93,125,141,182–187]. Nitric oxide releasing/generating materials have demonstrated experimental success as coating materials for IV catheters [167,170,174,180,181,188–190], implantable sensors [191–199], vascular grafts [178,183], stents [118,131,178,200], extracorporeal circulation (ECC) tubing [72,141,142,147,151,168,201–203], as well as antibacterial wound healing dressings [93,143,204–209]. For IV catheters specifically, NO release/generation has dramatically improved the antithrombotic and antibacterial properties of indwelling catheters in many in vitro and in vivo experiments. Below we summarize experimental results with the three different types of NO releasing/generating catheters, including chemical-based NO releasing catheters, catalyst-based NO generating catheters, and electrochemical-based NO generating catheters (see Fig. 16.3).

16.5.1 Chemical-based NO releasing catheters

Amoako et al. developed extruded trilaminar NO-releasing silicone catheters and tested their thrombogenicity in a 4 h rabbit model [189]. An extruded trilayer catheter configuration was used, with the base and top layer consisting of silicone resin and

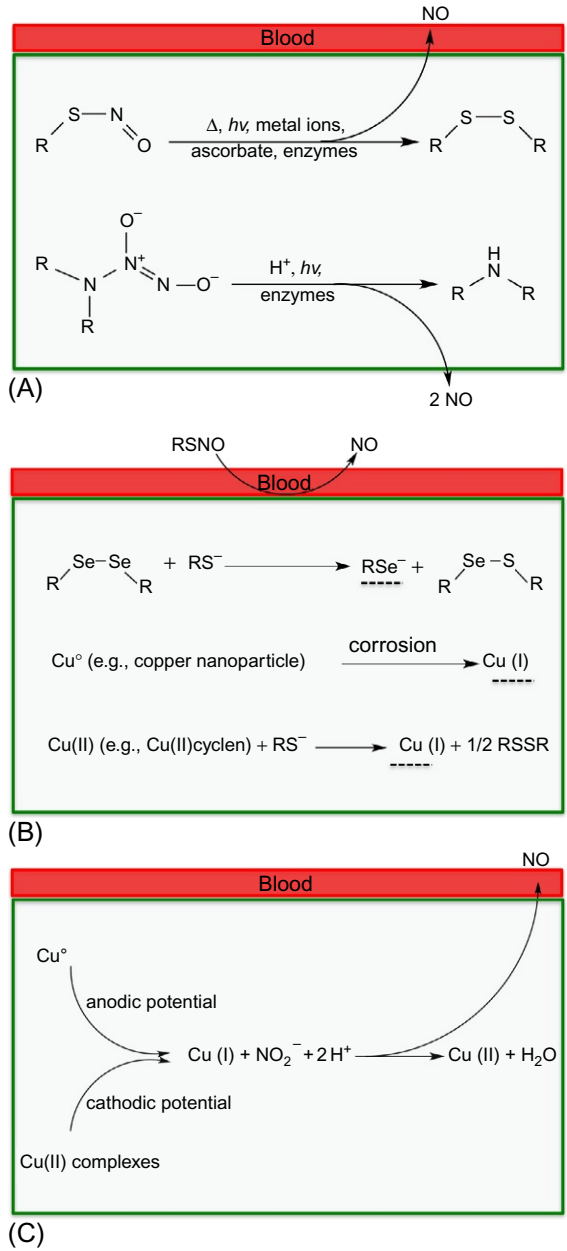


Fig. 16.3 Three types of NO releasing/generating catheters, where (A) NO is released from the NO donors (e.g., NONOates and RSNOs) embedded in the polymer via thermal, photo, or catalytic decomposition; (B) NO is generated from the endogenous RSNOs in blood via catalytic sites (e.g., Cu^{+}, RSe^{-}) within the polymer; and (C) NO is generated electrochemically at the electrode surfaces (e.g., Cu or Pt) by creating Cu(I) species via application of appropriate potentials to the working electrode in the presence of an inner reservoir of nitrite ions.

the active layer containing silicone resin with 15 wt% *N*-(6-aminohexyl)aminopropyl trimethoxysiloxane (DACA-6/SR) and 11 wt% potassium tetrakis (4-chlorophenyl) borate as additives. The catheters were exposed to high pressure of NO (80 psi) to form DACA/NONOate using a NO reactor. The catheters released NO at approximately $6 \pm 0.92 \times 10^{-10}$ mol cm^{-2} min^{-1} under physiological conditions for the first 4 h of testing. However, after storing the catheters dry for 24 h at −20°C the NO release rate dropped 66.7%, suggesting that this type of NO releasing catheter is not stable enough for long-term storage. Nonetheless, the catheters were implanted in rabbit veins for 4 h, and the average functioning time was 2.3 ± 0.7 h for control catheter (with 4 of 6 occluded), and 4 ± 0 h for the NO release catheters, which all catheters remained patent for this time period [189].

GSNO and SNAP are the two most commonly used RSNOs for therapeutic applications, and the stability of RSNO-based polymeric materials during storage is a very important factor for their further development into clinically useful catheter devices [151,210,211]. Recently, Brisbois et al. discovered that SNAP is exceptionally stable in several low water uptake biomedical grade PU-based copolymers, such as Elast-eon E2As [151] and CarboSil [174], with more than 80% of the initial SNAP remaining after 2 months of storage at 37°C [151]. Wo et al. used Raman spectroscopy and powder X-ray diffraction (PXRD) to further investigate the enhanced stability and NO release mechanism of SNAP-based polymers, such as SNAP-doped Carbosil [174]. A polymer-crystal composite forms during the solvent evaporation process if the SNAP exceeds its solubility in the polymer CarboSil (3.4–4.0 wt%). The SNAP that exceeds the solubility limit exists in stable orthorhombic crystal form within the bulk of the polymer. The proposed mechanism for sustained NO release comes from the slow dissolution process of the SNAP within the bulk of the polymer, initially in the water-rich regions of the polymer, which ultimately leads to stable, continuous NO release over a 3-week period in PBS buffer at 37°C.

Meyerhoff and coworkers have also conducted studies with SNAP [43] or lipophilic SNAP analogs [212] impregnated into existing commercial silicone catheter tubing. SNAP or the analogs were dissolved in organic solvents (e.g., tetrahydrofuran or chloroform), and the catheter tubing was soaked for a given time period to impregnate the SNAP species within the catheter wall at RT. This impregnation process is beneficial because many NO donors are not stable at the high temperatures used during the industrial catheter extrusion processes [43]. The NO released from these impregnated catheters can last for more than 30 days above 0.5×10^{-10} mol cm^{-2} min^{-1}, which is at the lower end of physiological NO released from endothelial cells. These catheters exhibited exceptional antibacterial effects toward several microorganisms (e.g., *S. epidermis* and *S. aureus*) [43,212]. This approach provides an excitingly new opportunity of transforming existing commercial biomedical catheters into NO releasing devices with enhanced hemocompatibility, both with respect to decrease in thrombosis as well as microbial infection/biofilm formation.

SNAP-based polymers have been used to fabricate catheters that have already been evaluated in vivo for their hemocompatibility [151,174]. The SNAP/E2As catheters tested in vivo had a trilayer configuration, with plain E2As as base and top layer to reduce SNAP leaching and 10 wt% SNAP/E2As as a NO releasing layer in the middle.

These catheters were prepared by a dip-coating method using a suitable mandrel, not the new solvent impregnation method described above. The SNAP/E2As catheters were able to continuously release NO for 20 days under physiological conditions above 0.5×10^{-10} mol cm^{-2} min^{-1}. The SNAP/E2As catheters also retained $88.8 \pm 1.7\%$ of original SNAP after ethylene oxide sterilization. After 7 days of implantation within sheep veins, the SNAP/E2As catheters exhibited a significant reduction in thrombus formation when compared to the controls (1.56 ± 0.76 vs. 5.06 ± 1.44 cm^2 clot area per catheter). The viable bacteria count on the surfaces of SNAP/E2As catheters were also 90% less than on the controls [188]. Similarly, SNAP/CarboSil catheters were fabricated and evaluated for antimicrobial activity against *S. aureus* in a drip-flow bioreactor. After 7 days, a 5 logarithmic unit reduction in viable cell count was observed on the surfaces of the SNAP/Carbosil catheters when compared to the controls [174]. These studies demonstrate the potential of SNAP-doped biomedical grade polymeric material for improving the hemocompatibility and antibacterial properties of IV catheters.

16.5.2 Catalyst-based NO generating catheters

Another approach to enhance IV catheter hemocompatibility is to use catalyst-mediated NO generation, in which a catalyst in or on the surface of the catheter walls converts endogenous RNSOs in blood (e.g., *S*-nitrosoglutathione) into NO when in contact with blood. Organoselenium molecules (such as 3.3′-dipropionicdiselenide, SeDPA) that mimic the selenium-containing enzyme glutathione peroxidase (GPx), can be covalently attached to polyethyleneimine (PEI) to form selenium-containing PEI (SePEI) [166]. Such organoselenium-derivatized polymers are converted to their corresponding selenolates in the presence of reducing agents (e.g., glutathione), which are the key intermediates that generate NO from a range of RSNO species known to exist in blood. Yang et al. utilized a layer-by-layer (LbL) deposition method to immobilize sodium alginate (Alg) and SePEI on PU catheters [190]. The PEI can absorb on the PU surfaces via hydrophobic interaction to introduce the cationic amine groups and initialize the LbL process. The resulting catheters with 10 bilayers generated NO at 1.8×10^{-10} mol cm^{-2} min^{-1} when in contact with solution containing 50 μM GSNO and 50 μM GSH. The catalytic polyelectrolyte multilayer exhibited sufficient permeability for GSNO and GSH to access the catalytic sites. Hence, the amount of NO generated at the catheter surface could be altered by changing the number of catalytic bilayers or the concentration of RSNOs and free thiol that the catheter was in contact with. The catheters maintained catalytic activity even after prolonged contact with blood, indicating that covalent attachment reduces catalyst leaching [190]. However, aliphatic selenium species are known to trigger thiol mediated reduction of cytochrome C enzyme, and can also react very fast with oxygen and produce superoxide and selenenyl radicals, which both contribute to its toxicity [213,214]. Studies have shown that aromatic selenium compounds are less toxic than aliphatic ones because the Se-C (aromatic) bond can help reduce selenium release [213]. Therefore, more recently, Cai et al. used the LbL technique to coat commercial PU catheters with an aromatic organoselenium catalyst (carboxyl-ebselen) and alginate [167]. The resulting catheter with

the LbL e-PEI/Alg coating can generate NO between 3 to 5×10^{-10} mol cm^{-2} min^{-1} in the presence of 10 μM SNO-Cys, 20 μM cysteine, and 100 μM EDTA, after soaking in PBS buffer, sheep plasma, or sheep blood for 24 h.

Metal organic frameworks (MOFs) offer another means to create NO generating surfaces. These species are a class of hybrid network solid materials comprised of organized organic linkers and metal cations and are widely regarded as promising materials for applications in catalysis and gas storage [215,216]. The crystalline MOF compounds are typically rigid and thermally stable with large pores and surface area that provides accessibility of species to open metal ion centers that can serve as active NO catalyst sites [216]. However, MOFs have inherent water instability, thus the use of MOFs in biological environments often necessitates MOFs being incorporated into polymer matrices [217,218]. Reynolds and coworkers have demonstrated the feasibility of extruding PU tubing by a conventional industrial extrusion process with embedded copper(II) benzenetricarboxylate (Cu-BTC) MOF complexes as catalysts for NO generation from endogenous RSNOs [170]. The MOFs embedded in the catheter walls maintain their reactivity after extrusion, and the tubing can generate NO for 1 to 15 h in the presence of 1 μmol RSNO, depending on the type of RSNO that it is in contact with. This novel design of sustained NO generation from a catalyst containing composite material offers a very promising approach for fabricating new hemocompatible catheters in the medical industry.

16.5.3 Electrochemical-based NO generating catheters

Electrochemically modulated NO generation from catheters in which one lumen is filled with inorganic nitrite solution is a cost-effective, controllable approach for generating NO at desired levels. Initially, to demonstrate the concept, a copper wire working electrode was used within a single lumen silicone rubber catheter that contained a nitrite reservoir [179,181]. Nitric oxide is released on demand by "turning on" the electrochemical pulse sequence, and the flux of NO can be modulated by applying different voltages to the Cu^0 working electrode. The anodic pulse provides a transient level of Cu(I) ions that are capable of reducing nitrite to NO, as described in the following reaction:

$$\mathrm{Cu(I)} + \mathrm{NO_2^-} + 2\mathrm{H^+} \rightarrow \mathrm{Cu(II)} + \mathrm{NO} + \mathrm{H_2O}$$

However, the oxidation of the copper electrode surfaces forms oxides of copper that passivate the electrode surface, requiring an additional cathodic pulse to regenerate a clean Cu^0 surface and reducing the overall NO generation efficiency [181]. In order to facilitate potential clinical applications, multilumen catheters are required, where one lumen is dedicated to the electrochemical NO generation and the other lumen(s) remain available for clinical use (see Fig. 16.4). Ren et al. demonstrated electrochemical NO generation from dual-lumen catheters using copper(II)-tri(2-pyridylmethyl) amine (Cu(II)TPMA) to mediate the reduction of nitrite, where the Cu(II)-ligand complex is reduced to the Cu(I)-ligand by applying a cathodic potential at the Pt working electrode [180]. The Cu(I)-ligand complex then reacts to reduce nitrite to NO. The modified catheters can continuously release NO for more than 7 days, while the

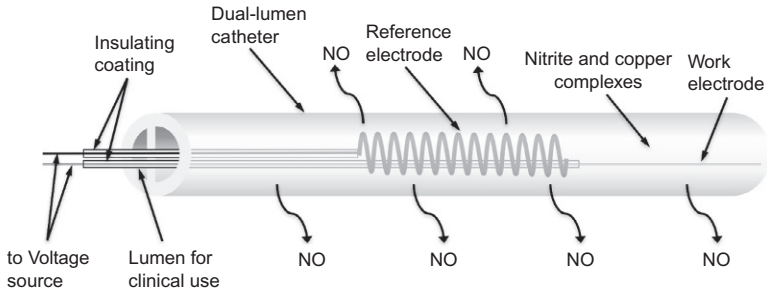


Fig. 16.4 Schematic of a dual-lumen catheter configuration, with one lumen dedicated to electrochemical NO generation from a reservoir of nitrite ions and one lumen for clinical usage.

temporal profile of NO release can be modulated readily by applying different levels of cathodic voltage to the working Pt wire electrode [180]. Finite element analysis simulations confirmed that similar concentrations of NO are found near the external surfaces of both lumens after 2 h of NO generation, due to the very high solubility and mobility of lipophilic NO in silicone rubber material as well as its high partition coefficient in silicone over water [180,219,220]. This catheter design demonstrated reduced thrombus formation after 7 h implantation in rabbit veins, with $83 \pm 12\%$ of clot area reduction when compared to control catheters. In a 3 day in vitro antibacterial experiment against *E. coli* biofilm formation using a drip-flow bioreactor where the NO release was only "turned on" for 3 h in each day, the catheters still exhibited more than 100-fold decrease in the amount of live bacteria on the catheter surfaces [180]. More importantly, this Cu(II)TPMA mediated NO generation from a multilumen catheter has a couple of important advantages. First, it has the potential to be used in actual clinical practice because it has an unoccupied lumen available for blood withdrawal, or infusion of drugs or other agents. Additionally, owing to its ability to generate NO at constant levels with one single applied cathodic potential, this approach is not only more efficient but also more practical, since it is possible to use a miniaturized battery as the power supply for the NO generation similar to many small low energy biomedical devices (e.g., pacemakers) already used in patients.

Another potential use of IV catheters is for continuous monitoring of many important chemical species in blood (such as blood gases (pO_2, pH and pCO_2), electrolytes (Na^+, K^+, Ca^{2+}), glucose, and lactate [164,193–199,221,222], which can provide invaluable information for patient diagnosis and treatment [223]. Since patient measurements in the hospital are currently done with point-of-care devices intermittently with large gaps of information between each blood draw [221,224], it would be beneficial to develop IV chemical sensors that can monitor key chemical species in real time [225]. However, sensors in contact with blood trigger the coagulation cascade. The resulting clot can isolate the chemical sensing area from the bulk of the blood, leading to false analytical signals, and also increase the risk of developing life-threatening emboli or stroke [11,164].

To overcome these problems, there have been many catheter-style IV sensors developed that combine NO release/generating capability to increase their

hemocompatibility for continuous in vivo chemical monitoring, especially IV oxygen sensors. Several NO delivery approaches have been used for developing in vivo IV oxygen sensors, including coating the catheter surface with polymers containing NONOates [197,198], covalently attaching NONOates to catheter polymer surface [199], catalytically generating NO in situ from endogenous RSNOs using embedded copper particles [164,196], and electrochemically modulating NO generation from nitrite [221]. These oxygen sensors as well as glucose [191–193,222,226], pH [193,227], and CO_2 [193,194] sensors using various NO donors have all demonstrated significantly improved accuracy in comparison to the corresponding control sensors when placed in the arteries or veins of rabbits and pigs.

16.6 Conclusion

Over the past decade, significant advances have been made by industrial and academic researchers to improve the hemocompatibility of IV catheters. Many traditional approaches to reduce thrombus formation on catheter surfaces focus on using anticoagulants and modified surface structures. To fight against catheter-associated infections, catheters have been modified with antibiotics, silver nanoparticles, or biofilm dispersing agents to inhibit biofilm formation or dissemble mature biofilm thereby making the bacteria more susceptible to antibiotics. Catheter lock solutions containing anticoagulants and/or antiseptics have also been widely examined, and implemented in the hospital setting to achieve the same goals. While these methods have all shown promise in vitro and/or in vivo, due to the complexity of blood-material interactions, surfaces with combined anticoagulant and antibacterial functionalities would be more efficient and attractive. Nitric oxide has such dual functionality and its chemical simplicity has made it a promising therapeutic agent for modifying catheter surfaces to provide simultaneous antiplatelet and antimicrobial activities. Both chemical and electrochemical methods have been used to generate/release NO from catheter surfaces at physiologically relevant fluxes, and such devices have exhibited promising antithrombotic and antibacterial effects in many in vitro and in vivo experiments. Moving forward, it is essential to develop standardized in vivo testing methods (e.g., catheter occlusion time, thrombus area, catheter retention time, incidents of infection per 1000 catheter days, etc.) to fully evaluate each new material before they can be used in clinical applications. Further, medical device manufacturers will need to develop methods that will enable the incorporation of NO release/generating chemistries into IV catheter products in a cost-effective and stable manner so that such devices become commercially available for use in hospitalized patients in the not too distant future.

References

[1] H. Shah, W. Bosch, K.M. Thompson, W.C. Hellinger, Neurohospitalist 3 (2013) 144–151.
[2] M.A. Almuneef, Z.A. Memish, H.H. Balkhy, O. Hijazi, G. Cunningham, C. Francis, J. Hosp. Infect. 62 (2006) 207–213.

[3] P. Sette, R.M. Dorizzi, A.M. Azzini, J. Vasc. Access 13 (2012) 137–144.
[4] L.A. Mermel, M. Allon, E. Bouza, D.E. Craven, P. Flynn, N.P. O'Grady, I.I. Raad, B.J. Rijnders, R.J. Sherertz, D.K. Warren, Clin. Infect. Dis. 49 (2009) 1–45.
[5] N.P. O'Grady, M. Alexander, L.A. Burns, E.P. Dellinger, J. Garland, S.O. Heard, P.A. Lipsett, H. Masur, L.A. Mermel, M.L. Pearson, I.I. Raad, A.G. Randolph, M.E. Rupp, S. Saint, Clin. Infect. Dis. 52 (2011) e162–e193.
[6] C. Abad, N. Safdar, Infect Dis. Spec. Ed. 14 (2011) 84–98.
[7] S. Fletcher, Contin. Educ. Anaesth. Crit. Care Pain 5 (2005) 49–51.
[8] A. Sitges-Serra, M. Girvent, World J. Surg. 23 (1999) 589–595.
[9] M.R. Goede, C.M. Coopersmith, Surg. Clin. North Am. 89 (2009) 463–474.
[10] R. Gahlot, C. Nigam, V. Kumar, G. Yadav, S. Anupurba, Int. J. Crit. Illn. Inj. Sci. 4 (2014) 162–167.
[11] K.E.A. Burns, A. McLaren, Can. Respir. J. 16 (2009) 163–165.
[12] E. Venturini, L. Becuzzi, L. Magni, Case Rep. Vasc. Med. 2012 (2012) 469619.
[13] P.W. Kamphuisen, A.Y.Y. Lee, Hematology Am. Soc. Hematol. Educ. Program 2012 (2012) 638–644.
[14] M.L. Linenberger, J. Natl. Compr. Canc. Netw. 4 (2006) 889–901.
[15] A.G. Kidane, H. Salacinski, A. Tiwari, K.R. Bruckdorfer, A.M. Seifalian, Biomacromolecules 5 (2004) 798–813.
[16] M.N. Helmus, D.F. Gibbons, D. Cebon, Toxicol. Pathol. 36 (2008) 70–80.
[17] S.W. Jordan, E.L. Chaikof, J. Vasc. Surg. 45 (2007) 104–115.
[18] E.J. Brisbois, H. Handa, M.E. Meyerhoff, in: F. Puoci (Ed.), Advanced Polymers in Medicine, Springer International Publishing, Cham, 2015, pp. 481–511.
[19] M.B. Gorbet, M.V. Sefton, Biomaterials 25 (2004) 5681–5703.
[20] M.V. Sefton, C.H. Gemmell, M.B. Gorbet, J. Biomater. Sci. Polym. Ed. 11 (2000) 1165–1182.
[21] S.Z. Goldhaber, J. Fanikos, Circulation 110 (2004) e445–e447.
[22] J. Hirsh, J. Hoak, Circulation 93 (1996) 2212–2245.
[23] S.Z. Goldhaber, R.B. Morrison, Circulation 106 (2002) 1436–1438.
[24] A. Gutowska, Y.H. Bae, H. Jacobs, F. Mohammad, D. Mix, J. Feijen, S.W. Kim, J. Biomed. Mater. Res. 29 (1995) 811–821.
[25] K.H. Lee, J.K. Han, Y. Byun, H.T. Moon, C.J. Yoon, S.J. Kim, B.I. Choi, Cardiovasc. Intervent. Radiol. 27 (2004) 507–511.
[26] L. Filippi, M. Pezzati, S. Di Amario, C. Poggi, P. Pecile, Pediatr. Crit. Care Med. 8 (2007) 556–562.
[27] J.E. Moran, S.R. Ash, Semin. Dial. 21 (2008) 490–492.
[28] B. Digiovine, C. Chenoweth, C. Watts, M. Higgins, Am. J. Respir. Crit. Care Med. 160 (1999) 976–981.
[29] X. Zhang, M. Tong, M. Zhang, H. Zhu, Int. J. Clin. Exp. Med. 8 (2015) 16682–16687.
[30] I. Raad, S. Davis, A. Khan, J. Tarrand, L. Elting, G.P. Bodey, Infect. Control Hosp. Epidemiol. 13 (1992) 215–221.
[31] P. Pronovost, D. Needham, S. Berenholtz, D. Sinopoli, H. Chu, S. Cosgrove, B. Sexton, R. Hyzy, R. Welsh, G. Roth, J. Bander, J. Kepros, C. Goeschel, N. Engl. J. Med. 355 (2006) 2725–2732.
[32] B.B. Drews, R. Sanghavi, J.D. Siegel, P. Metcalf, N.K. Mittal, Gastroenterol. Nurs. 32 (2009) 385–390 (quiz 391–392).
[33] S. Cicalini, F. Palmieri, N. Petrosillo, Crit. Care 8 (2004) 157–162.
[34] H. Wu, C. Moser, H.-Z. Wang, N. Høiby, Z.-J. Song, Int. J. Oral Sci. 7 (2015) 1–7.
[35] A.B. Seabra, D. Martins, M.M.S.G. Simões, R. Da Silva, M. Brocchi, M.G. De Oliveira, Artif. Organs 34 (2010) 204–214.

[36] M. Pawar, Y. Mehta, P. Kapoor, J. Sharma, A. Gupta, N. Trehan, J. Cardiothorac. Vasc. Anesth. 18 (2004) 304–308.
[37] R. Parameswaran, J.B. Sherchan, D. Muralidhar Varma, C. Mukhopadhyay, S. Vidyasagar, J. Infect. Dev. Ctries. 5 (2011) 452–458.
[38] L. Lorente, A. Jiménez, M. Santana, J.L. Iribarren, J.J. Jiménez, M.M. Martín, M.L. Mora, Crit. Care Med. 35 (2007) 2424–2427.
[39] E. Bouza, N. Alvarado, L. Alcalá, M.J. Pérez, C. Rincón, P. Muñoz, Clin. Infect. Dis. 44 (2007) 820–826.
[40] M.R. Kiedrowski, A.R. Horswill, Ann. N. Y. Acad. Sci. 1241 (2011) 104–121.
[41] L.C. Xu, C.A. Siedlecki, Acta Biomater. 8 (2012) 72–81.
[42] S.R. Shah, A.M. Tatara, R.N. D'Souza, A.G. Mikos, F.K. Kasper, Mater. Today 16 (2013) 177–182.
[43] A. Colletta, J. Wu, Y. Wo, M. Kappler, H. Chen, C. Xi, M.E. Meyerhoff, ACS Biomater. Sci. Eng. 1 (2015) 416–424.
[44] M. Chen, Q. Yu, H. Sun, Int. J. Mol. Sci. 14 (2013) 18488–18501.
[45] R.M. Donlan, Clin. Infect. Dis. 52 (2011) 1038–1045.
[46] R.M. Donlan, Emerg. Infect. Dis. 7 (2001) 277–281.
[47] R.M. Donlan, Clin. Infect. Dis. 33 (2001) 1387–1392.
[48] J.M. Walz, S.G. Memtsoudis, S.O. Heard, J. Intensive Care Med. 25 (2010) 131–138.
[49] H. Wisplinghoff, T. Bischoff, S.M. Tallent, H. Seifert, R.P. Wenzel, M.B. Edmond, Clin. Infect. Dis. 39 (2004) 309–317.
[50] M.F. Maitz, Biosurf. Biotribol. 1 (2015) 161–176.
[51] T. Lee, C. Lok, M. Vazquez, L. Moist, I. Maya, M. Mokrzycki, Int. J. Nephrol. 2012 (2012) Article ID: 170857.
[52] C.P. Shrivastava, S. Devgarha, Asian Cardiovasc. Thorac. Ann. 15 (2007) 405–407.
[53] G.A. Goossens, Nurs. Res. Pract. 2015 (2015) Article ID: 985686.
[54] D.M. Ivan, T. Smith, M. Allon, Clin. J. Am. Soc. Nephrol. 5 (2010) 1458–1462.
[55] P.W. Dillon, G.R. Jones, H.A. Bagnall-Reeb, J.D. Buckley, E.S. Wiener, G.M. Haase, J. Clin. Oncol. 22 (2004) 2718–2723.
[56] B. Solomon, J. Moore, C. Arthur, H.M. Prince, Eur. J. Cancer 37 (2016) 2379–2384.
[57] N. Fernandez-Hidalgo, B. Almirante, R. Calleja, I. Ruiz, A.M. Planes, D. Rodriguez, C. Pigrau, A. Pahissa, J. Antimicrob. Chemother. 57 (2006) 1172–1180.
[58] P.W. Wales, C. Kosar, M. Carricato, N. De Silva, K. Lang, Y. Avitzur, J. Pediatr. Surg. 46 (2011) 951–956.
[59] S. Aslam, B.W. Trautner, V. Ramanathan, R.O. Darouiche, Infect. Control Hosp. Epidemiol. 29 (2008) 894–897.
[60] S. Aslam, K. Jenne, S. Reed, M. Ghannoum, R. Mehta, R. Darouiche, Int. J. Artif. Organs 35 (2012) 893–897.
[61] C. Sousa, M. Henriques, R. Oliveira, Biofouling 27 (2011) 609–620.
[62] C.R. Arciola, D. Campoccia, P. Speziale, L. Montanaro, J.W. Costerton, Biomaterials 33 (2012) 5967–5982.
[63] S. Aslam, B.W. Trautner, V. Ramanathan, R.O. Darouiche, Antimicrob. Agents Chemother. 51 (2007) 1556–1558.
[64] M. Fischer, M. Vahdatzadeh, R. Konradi, J. Friedrichs, M.F. Maitz, U. Freudenberg, C. Werner, Biomaterials 56 (2015) 198–205.
[65] O.D. Krishna, K. Kim, Y. Byun, Biomaterials 26 (2005) 7115–7123.
[66] M.N. Babapulle, M.J. Eisenberg, Circulation 106 (2002) 2734–2740.
[67] K.G. Neoh, E.T. Kang, ACS Appl. Mater. Interfaces 3 (2011) 2808–2819.

[68] S.M. Peckham, V.T. Turitto, J. Glantz, H. Puryear, S.M. Slack, J. Biomater. Sci. Polym. Ed. 8 (1997) 847–858.
[69] Q. Yu, Z. Wu, H. Chen, Acta Biomater. 16 (2015) 1–13.
[70] J. Hirsh, N. Engl. J. Med 324 (1991) 1565–1574.
[71] B. Wu, B. Gerlitz, B.W. Grinnell, M.E. Meyerhoff, Biomaterials 28 (2007) 4047–4055.
[72] T.C. Major, E.J. Brisbois, A.M. Jones, M.E. Zanetti, G.M. Annich, R.H. Bartlett, H. Handa, Biomaterials 35 (2014) 7271–7285.
[73] C.A. Hufnagel, P.W. Conrad, J.F. Gillespie, R. Pifarre, A. Llano, T. Yokoyama, Ann. N. Y. Acad. Sci. 146 (1968) 262–270.
[74] J.Y. Lin, C. Nojiri, T. Okano, S.W. Kim, ASAIO Trans. 33 (1987) 602–605.
[75] P.W. Heyman, C.S. Cho, J.C. McRea, D.B. Olsen, S.W. Kim, J. Biomed. Mater. Res. 19 (1985) 419–436.
[76] C. Ebert, J. McRea, S.W. Kim, in: Controlled Release of Bioactive Materials, Academic Press, New York, 1980, pp. 107–122.
[77] N. Ayres, D.J. Holt, C.F. Jones, L.E. Corum, D.W. Grainger, J. Polym. Sci. A Polym. Chem. 46 (2008) 7713–7724.
[78] K.A. Mowery, M.H. Schoenfisch, J.E. Saavedra, L.K. Keefer, M.E. Meyerhoff, Polymer (Guildf) 21 (2000) 9–21.
[79] Z. Zhou, M.E. Meyerhoff, Biomaterials 26 (2005) 6506–6517.
[80] H. Tanzawa, Y. Mori, N. Harumiya, H. Miyama, M. Hori, N. Ohshima, Y. Idezuki, ASAIO J. 19 (1973) 188–194.
[81] V.L. Gott, J.D. Whiffen, R.C. Dutton, Science 142 (1963) 1297–1298.
[82] R. Shibuta, M. Tanaka, M. Sisido, Y. Imanishi, J. Biomed. Mater. Res. 20 (1986) 971–987.
[83] A. Gutowska, Y.H. Bae, J. Feijen, S.W. Kim, J. Control. Release 22 (1992) 95–105.
[84] N.A. Peppas, Y. Huang, M. Torres-Lugo, J.H. Ward, J. Zhang, Annu. Rev. Biomed. Eng. 2 (2000) 9–29.
[85] N. Barraud, M.V. Storey, Z.P. Moore, J.S. Webb, S.A. Rice, S. Kjelleberg, Microb. Biotechnol. 2 (2009) 370–378.
[86] N. Barraud, M.J. Kelso, S.A. Rice, S. Kjelleberg, Nitric oxide: a key mediator of biofilm dispersal with applications in infectious diseases, Curr. Pharm. Des. 21 (2015) 31–42.
[87] J.B. Kaplan, J. Dent. Res. 89 (2010) 205–218.
[88] A. Vaterrodt, B. Thallinger, K. Daumann, D. Koch, G.M. Guebitz, M. Ulbricht, Langmuir 32 (2016) 1347–1359.
[89] M.C. Jennings, L.E. Ator, T.J. Paniak, K.P.C. Minbiole, W.M. Wuest, Chembiochem 15 (2014) 2211–2215.
[90] M.C. Jennings, K.P.C. Minbiole, W.M. Wuest, ACS Infect. Dis. 1 (7) (2015) 288–303.
[91] K.P. Reighard, M.H. Schoenfisch, Antimicrob. Agents Chemother. 59 (2015) 6506–6513.
[92] K.P. Reighard, D.B. Hill, G.A. Dixon, B.V. Worley, M.H. Schoenfisch, Biofouling 31 (2015) 775–787.
[93] J.O. Kim, J.K. Noh, R.K. Thapa, N. Hasan, M. Choi, J.H. Kim, J.H. Lee, S.K. Ku, J.W. Yoo, Int. J. Biol. Macromol. 79 (2015) 217–225.
[94] D. Roe, B. Karandikar, N. Bonn-Savage, B. Gibbins, J.B. Roullet, J. Antimicrob. Chemother. 61 (2008) 869–876.
[95] M. Pollini, F. Paladini, M. Catalano, A. Taurino, A. Licciulli, A. Maffezzoli, A. Sannino, J. Mater. Sci. Mater. Med. 22 (2011) 2005–2012.
[96] K. Wu, Y. Yang, Y. Zhang, J. Deng, C. Lin, Int. J. Nanomedicine 10 (2015) 7241–7252.
[97] B. Jansen, M. Rinck, P. Wolbring, A. Strohmeier, T. Jahns, J. Biomater. Appl. 9 (1994) 55–70.
[98] P.L. Tran, N. Lowry, T. Campbell, T.W. Reid, D.R. Webster, E. Tobin, A. Aslani, T. Mosley, J. Dertien, J.A. Colmer-Hamood, A.N. Hamood, Antimicrob. Agents Chemother. 56 (2012) 972–978.

[99] W. Fu, T. Forster, O. Mayer, J.J. Curtin, S.M. Lehman, R.M. Donlan, Antimicrob. Agents Chemother. 54 (2010) 397–404.
[100] T.K. Lu, J.J. Collins, Proc. Natl. Acad. Sci. 104 (2007) 11197–11202.
[101] J. Curtin, R. Donlan, Antimicrob. Agents Chemother. 50 (2006) 1268–1275.
[102] N. Gatter, W. Kohnen, B. Jansen, Zentralbl. Bakteriol. 287 (1998) 157–169.
[103] K.N.J. Stevens, O. Crespo-Biel, E.E.M. van den Bosch, A.A. Dias, M.L.W. Knetsch, Y.B.J. Aldenhoff, F.H. van der Veen, J.G. Maessen, E.E. Stobberingh, L.H. Koole, Biomaterials 30 (2009) 3682–3690.
[104] P. Ramritu, K. Halton, P. Collignon, D. Cook, D. Fraenkel, D. Battistutta, M. Whitby, N. Graves, Am. J. Infect. Control 36 (2008) 104–117.
[105] J.C. Hockenhull, K.M. Dwan, G.W. Smith, C.L. Gamble, A. Boland, T.J. Walley, R.C. Dickson, Crit. Care Med. 37 (2009) 702–712.
[106] I. Raad, J.A. Mohamed, R.A. Reitzel, Y. Jiang, S. Raad, M. Al Shuaibi, A.M. Chaftari, R.Y. Hachem, Antimicrob. Agents Chemother. 56 (2012) 935–941.
[107] E. Cheung, M.O. Baerlocher, M. Asch, A. Myers, Can. Fam. Physician 55 (2009) 494–496.
[108] I. Raad, H. Hanna, D. Maki, Lancet Infect. Dis. 7 (2007) 645–657.
[109] S. Rossi, A.O. Azghani, A. Omri, J. Antimicrob. Chemother. 54 (2004) 1013–1018.
[110] N.D. Allan, K. Giare-Patel, M.E. Olson, J. Biomed. Biotechnol. 2012 (2012) Article ID: 921617.
[111] N. Høiby, T. Bjarnsholt, M. Givskov, S. Molin, O. Ciofu, Int. J. Antimicrob. Agents 35 (2010) 322–332.
[112] L. Wang, H. Li, S. Chen, C. Nie, C. Cheng, C. Zhao, ACS Biomater. Sci. Eng. 1 (2015) 1183–1193.
[113] J. Deng, L. Ma, X. Liu, C. Cheng, C. Nie, C. Zhao, Adv. Mater. Interfaces 3 (2016) 1500473.
[114] Z.-Q. Shi, H.-F. Ji, H.-C. Yu, X.-L. Huang, W.-F. Zhao, S.-D. Sun, C.-S. Zhao, Colloid Polym. Sci. 294 (2016) 441–453.
[115] A.W. Carpenter, M.H. Schoenfisch, Chem. Soc. Rev. 41 (2012) 3742–3752.
[116] L. Ignarro, G. Buga, Proc. Natl. Acad. Sci. U. S. A. 84 (1987) 9265–9269.
[117] M. Vaughn, L. Kuo, J. Liao, Am. J. Physiol. 274 (1998) 2163–2176.
[118] K.M. Vural, M. Bayazit, Eur. J. Vasc. Endovasc. Surg. 22 (2001) 285–293.
[119] M.C. Jen, M.C. Serrano, R. van Lith, G.A. Ameer, Adv. Funct. Mater. 22 (2012) 239–260.
[120] M. Rosselli, P.J. Keller, R.K. Dubey, Hum. Reprod. Update 4 (1998) 3–24.
[121] D. Tousoulis, A.-M. Kampoli, C. Tentolouris, N. Papageorgiou, C. Stefanadis, Curr. Vasc. Pharmacol. 10 (2012) 4–18.
[122] A.B. Seabra, in: R. Beck, S. Guterres, A. Pohlmann (Eds.), Nanocosmetics and Nanomedicines, Springer, Berlin, Heidelberg, 2011, pp. 253–268.
[123] E.M. Hetrick, M.H. Schoenfisch, Annu Rev Anal Chem (Palo Alto, Calif) 2 (2009) 409–433.
[124] B.B. McMullin, D.R. Chittock, D.L. Roscoe, H. Garcha, L. Wang, C.C. Miller, Respir. Care 50 (2005) 1451–1456.
[125] A. Pegalajar-Jurado, K.A. Wold, J.M. Joslin, B.H. Neufeld, K.A. Arabea, L.A. Suazo, S.L. McDaniel, R.A. Bowen, M.M. Reynolds, J. Control. Release 220 (2015) 617–623.
[126] Y. Lu, D. Slomberg, B. Sun, M. Schoenfisch, Small 9 (2013) 2189–2198.
[127] R.N. Allan, S. Morgan, S. Brito-Mutunayagam, P. Skipp, M. Feelisch, S.M. Hayes, W. Hellier, S.C. Clarke, P. Stoodley, A. Burgess, H. Ismail-Koch, R.J. Salib, J.S. Webb, S.N. Faust, L. Hall-Stoodley, Antimicrob. Agents Chemother. 60 (2016) 2456–2466.
[128] G. Richardson, N. Benjamin, Clin. Sci. (Lond.) 102 (1) (2002) 99–105.

[129] R. Scatena, P. Bottoni, G. Martorana, B. Giardina, Expert Opin. Invest. Drugs 14 (7) (2005) 835–846.
[130] J.A. Hrabie, L.K. Keefer, Chem. Rev. 102 (2002) 1135–1154.
[131] V.N. Varu, N.D. Tsihlis, M.R. Kibbe, Vasc. Endovascular Surg. 43 (2009) 121–131.
[132] J. Saraiva, S.S. Marotta-Oliveira, S.A. Cicillini, J.D.O. Eloy, J.M. Marchetti, J. Drug Deliv. 2011 (2011) Article ID: 936438.
[133] S. Sortino, Chem. Soc. Rev. 39 (2010) 2903–2913.
[134] P.G. Wang, M. Xian, X. Tang, X. Wu, Z. Wen, T. Cai, A.J. Janczuk, Chem. Rev. 102 (2002) 1091–1134.
[135] M.M. Reynolds, M.C. Frost, M.E. Meyerhoff, Free Radic. Biol. Med. 37 (2004) 926–936.
[136] K. Sydow, A. Daiber, M. Oelze, Z. Chen, M. August, M. Wendt, V. Ullrich, A. Mülsch, E. Schulz, J.F. Keaney, J.S. Stamler, T. Münzel, J. Clin. Invest. 113 (2004) 482–489.
[137] A. Daiber, M. Oelze, M. Coldewey, M. Bachschmid, P. Wenzel, K. Sydow, M. Wendt, A.L. Kleschyov, D. Stalleicken, V. Ullrich, A. Mulsch, T. Munzel, Mol. Pharmacol. 66 (2004) 1372–1382.
[138] T. Münzel, A. Daiber, A. Mülsch, Circ. Res. 97 (2005) 618–628.
[139] L. Grossi, S.J. D'Angelo, Med. Chem. 48 (2005) 2622–2626.
[140] M.M. Batchelor, S.L. Reoma, P.S. Fleser, V.K. Nuthakki, R.E. Callahan, C.J. Shanley, J.K. Politis, J. Elmore, S.I. Merz, M.E. Meyerhoff, J. Med. Chem. 46 (2003) 5153–5161.
[141] H. Handa, E.J. Brisbois, T.C. Major, J. Mater. Chem. B 1 (2013) 3578–3587.
[142] H. Handa, T.C. Major, E.J. Brisbois, K.A. Amoako, M.E. Meyerhoff, R.H. Bartlett, J. Mater. Chem. B 2 (2014) 1059–1067.
[143] E.J. Brisbois, J. Bayliss, J. Wu, T.C. Major, C. Xi, S.C. Wang, R.H. Bartlett, H. Handa, M.E. Meyerhoff, Optimized polymeric film-based nitric oxide delivery inhibits bacterial growth in a mouse burn wound model, Acta Biomater. 10 (2014) 4136–4142.
[144] H.K. Makadia, S.J. Siegel, Polymers (Basel) 3 (2011) 1377–1397.
[145] L.K. Keefer, R.W. Nims, K.M. Davies, D.A. Wink, Methods Enzymol. 268 (1996) 281–293.
[146] C.M. Maragos, D. Morley, D.A. Wink, T.M. Dunams, J.E. Saavedra, A. Hoffman, A.A. Bove, L. Isaac, J.A. Hrabie, L.K. Keefer, J. Med. Chem. 34 (1991) 3242–3247.
[147] H. Zhang, G.M. Annich, J. Miskulin, K. Stankiewicz, K. Osterholzer, S.I. Merz, R.H. Bartlett, M.E. Meyerhoff, J. Am. Chem. Soc. 125 (2003) 5015–5024.
[148] H. Zhang, G.M. Annich, J. Miskulin, K. Osterholzer, S.I. Merz, R.H. Bartlett, M.E. Meyerhoff, Biomaterials 23 (2002) 1485–1494.
[149] J.S. Stamler, O. Jaraki, J. Osborne, D.I. Simon, J. Keaney, J. Vita, D. Singel, C.R. Valeri, J. Loscalzo, Proc. Natl. Acad. Sci. U. S. A. 89 (1992) 7674–7677.
[150] D. Giustarini, A. Milzani, R. Colombo, I. Dalle-Donne, R. Rossi, Clin. Chim. Acta 330 (2003) 85–98.
[151] E.J. Brisbois, H. Handa, T.C. Major, R.H. Bartlett, M.E. Meyerhoff, Biomaterials 34 (2013) 6957–6966.
[152] W.H. Lyle, J. Rheumatol. Suppl. 7 (1981) 96–99.
[153] V. Parameshvara, Br. J. Ind. Med. 24 (1967) 73–76.
[154] K.A. Graeme, C.V. Pollack, Heavy metal toxicity, part I: arsenic and mercury, J. Emerg. Med. 16 (1998) 45–56.
[155] M.M. Jones, A.D. Weaver, W.L. Weller, Res. Commun. Chem. Pathol. Pharmacol. 22 (1978) 581–588.
[156] G. Lautner, M.E. Meyerhoff, S.P. Schwendeman, J. Control. Release 225 (2016) 133–139.
[157] J. McAninly, D.L.H. Williams, S.C. Askew, A.R. Butler, C. Russell, J. Chem. Soc. Chem. Commun. 23 (1993) 1758–1759.

[158] S. Hwang, M.E. Meyerhoff, Biomaterials 29 (2008) 2443–2452.
[159] D.L.H. Williams, Transit. Met. Chem. 21 (1996) 189–191.
[160] D.L.H. Williams, Chem. Commun. 10 (1996) 1085–1091.
[161] R.J. Singh, N. Hogg, J. Joseph, B. Kalyanaraman, J. Biol. Chem. 271 (1996) 18596–18603.
[162] S.P. Singh, J.S. Wishnok, M. Keshive, W.M. Deen, S.R. Tannenbaum, Proc. Natl. Acad. Sci. U. S. A. 93 (1996) 14428–14433.
[163] A.J. Holmes, D.L.H. Williams, Chem. Commun. (1998) 1711–1712.
[164] Y. Wu, M.E. Meyerhoff, Talanta 75 (2008) 642–650.
[165] A.J. Holmes, D.L.H. Williams, J. Chem. Soc. Trans. 2 (2000) 1639–1644.
[166] W. Cha, M.E. Meyerhoff, Biomaterials 28 (2007) 19–27.
[167] W. Cai, J. Wu, C. Xi, A.J. Ashe, M.E. Meyerhoff, Biomaterials 32 (2011) 7774–7784.
[168] T.C. Major, D.O. Brant, C.P. Burney, K.A. Amoako, G.M. Annich, M.E. Meyerhoff, H. Handa, R.H. Bartlett, Biomaterials 32 (2011) 5957–5969.
[169] J.L. Harding, M.M. Reynolds, J. Am. Chem. Soc. 134 (2012) 3330–3333.
[170] J.L. Harding, M.M. Reynolds, J. Mater. Chem. B 2 (2014) 2530–2536.
[171] J.L. Harding, J.M. Metz, M.M. Reynolds, Adv. Funct. Mater. 24 (2014) 7503–7509.
[172] M.J. Neufeld, J.L. Harding, M.M. Reynolds, ACS Appl. Mater. Interfaces 7 (2015) 26742–26750.
[173] D. Jourd'Heuil, F.S. Laroux, A.M. Miles, D.A. Wink, M.B. Grisham, Arch. Biochem. Biophys. 361 (1999) 323–330.
[174] Y. Wo, Z. Li, E.J. Brisbois, A. Colletta, J. Wu, T.C. Major, C. Xi, R.H. Bartlett, A.J. Matzger, M.E. Meyerhoff, ACS Appl. Mater. Interfaces 7 (2015) 22218–22227.
[175] M.C. Frost, M.E. Meyerhoff, J. Am. Chem. Soc. 126 (2004) 1348–1349.
[176] G.E. Gierke, M. Nielsen, M.C. Frost, S-Nitroso-N-acetyl-D-penicillamine covalently linked to polydimethylsiloxane (SNAP–PDMS) for use as a controlled photoinitiated nitric oxide release polymer, Sci. Technol. Adv. Mater. 12 (2011). 055007.
[177] C.W. McCarthy, J. Goldman, M.C. Frost, ACS Appl. Mater. Interfaces 8 (16) (2016) 10128–10135.
[178] N. Naghavi, A. De Mel, O.S. Alavijeh, B.G. Cousins, A.M. Seifalian, Small 9 (2013) 22–35.
[179] L. Höfler, D. Koley, J. Wu, C. Xi, M.E. Meyerhoff, RSC Adv. 2 (2012) 6765–6767.
[180] H. Ren, J. Wu, C. Xi, N. Lehnert, T. Major, R.H. Bartlett, M.E. Meyerhoff, ACS Appl. Mater. Interfaces 6 (2014) 3779–3783.
[181] H. Ren, A. Colletta, D. Koley, J. Wu, C. Xi, T.C. Major, R.H. Bartlett, M.E. Meyerhoff, Bioelectrochemistry 104 (2015) 10–16.
[182] C.J. Backlund, B.V. Worley, M.H. Schoenfisch, Acta Biomater. 29 (2016) 198–205.
[183] D.J. Smith, D. Chakravarthy, S. Pulfer, M.L. Simmons, J.A. Hrabie, M.L. Citro, J.E. Saavedra, K.M. Davies, T.C. Hutsell, D.L. Mooradian, S.R. Hanson, L.K.J. Keefer, J. Med. Chem. 39 (1996) 1148–1156.
[184] J.-W. Yoo, H. Nurhasni, J. Cao, M. Choi, I. Kim, B. Luel Lee, Y. Jung, Int. J. Nanomedicine 10 (2015) 3065–3080.
[185] N.A. Stasko, M.H. Schoenfisch, J. Am. Chem. Soc. 128 (2006) 8265–8271.
[186] N.A. Stasko, T.H. Fischer, M.H. Schoenfisch, Biomacromolecules 9 (2008) 834–841.
[187] J.P. Yapor, A. Lutzke, A. Pegalajar-Jurado, B.H. Neufeld, V.B. Damodaran, M.M. Reynolds, J. Mater. Chem. B 3 (2015) 9233–9241.
[188] E.J. Brisbois, R.P. Davis, A.M. Jones, T.C. Major, R.H. Bartlett, M.E. Meyerhoff, H. Handa, J. Mater. Chem. B 3 (2015) 1639–1645.
[189] K.A. Amoako, C. Archangeli, H. Handa, T. Major, M.E. Meyerhoff, G.M. Annich, R.H. Bartlett, ASAIO J. 58 (2012) 238–246.

[190] J. Yang, J.L. Welby, M.E. Meyerhoff, Langmuir 24 (2008) 10265–10272.
[191] Q. Yan, T.C. Major, R.H. Bartlett, M.E. Meyerhoff, Biosens. Bioelectron. 26 (2011) 4276–4282.
[192] A.K. Wolf, Y. Qin, T.C. Major, M.E. Meyerhoff, Chin. Chem. Lett. 26 (2015) 464–468.
[193] R.K. Meruva, M.E. Meyerhoff, Biosens. Bioelectron. 13 (1998) 201–212.
[194] M.C. Frost, M.M. Batchelor, Y. Lee, H. Zhang, Y. Kang, B. Oh, G.S. Wilson, R. Gifford, S.M. Rudich, M.E. Meyerhoff, Microchem. J. 74 (2003) 277–288.
[195] S.M. Marxer, M.E. Robbins, M.H. Schoenfisch, Analyst 130 (2005) 206–212.
[196] Y. Wu, A.P. Rojas, G.W. Griffith, A.M. Skrzypchak, N. Lafayette, R.H. Bartlett, M.E. Meyerhoff, Sensors Actuators B Chem. 121 (2007) 36–46.
[197] K.A. Mowery, M.H. Schoenfisch, N. Baliga, J.A. Wahr, M.E. Meyerhoff, Electroanalysis 11 (1999) 681–686.
[198] M.H. Schoenfisch, K.A. Mowery, M.V. Rader, N. Baliga, J.A. Wahr, M.E. Meyerhoff, Anal. Chem. 72 (2000) 1119–1126.
[199] M.C. Frost, S.M. Rudich, H. Zhang, M.A. Maraschio, M.E. Meyerhoff, Anal. Chem. 74 (2002) 5942–5947.
[200] A.B. Seabra, R. Da Silva, G.F.P. De Souza, M.G. De Oliveira, Artif. Organs 32 (2008) 262–267.
[201] T.C. Major, D.O. Brant, M.M. Reynolds, R.H. Bartlett, M.E. Meyerhoff, H. Handa, G.M. Annich, Biomaterials 31 (2010) 2736–2745.
[202] A.M. Skrzypchak, N.G. Lafayette, R.H. Bartlett, Z. Zhou, M.C. Frost, M.E. Meyerhoff, M.M. Reynolds, G.M. Annich, Perfusion 22 (2007) 193–200.
[203] T.C. Major, H. Handa, G.M. Annich, R.H. Bartlett, J. Biomater. Appl. 29 (2014) 479–501.
[204] R. Vercelino, T.M. Cunha, E.S. Ferreira, F.Q. Cunha, S.H. Ferreira, M.G. De Oliveira, J. Mater. Sci. Mater. Med. 24 (2013) 2157–2169.
[205] F.S. Schanuel, K.S. Raggio Santos, A. Monte-Alto-Costa, M.G. De Oliveira, Colloids Surf. B Biointerfaces 130 (2015) 182–191.
[206] T.P. Amadeu, A.B. Seabra, M.G. de Oliveira, A.M.A. Costa, J. Eur. Acad. Dermatol. Venereol. 21 (2007) 629–637.
[207] K. Masters, S. Leibovich, P. Belem, J.L. West, L. Poole-Warren, Wound Repair Regen. 10 (2002) 286–294.
[208] Y. Kang, J. Kim, Y.M. Lee, S. Im, H. Park, W.J. Kim, J. Control. Release 220 (2015) 624–630.
[209] M. Neidrauer, U.K. Ercan, A. Bhattacharyya, J. Samuels, J. Sedlak, R. Trikha, K.A. Barbee, M.S. Weingarten, S.G. Joshi, J. Med. Microbiol. 63 (2014) 203–209.
[210] A.B. Seabra, G.F.P. de Souza, L.L. da Rocha, M.N. Eberlin, M.G. de Oliveira, Nitric Oxide 11 (2004) 263–272.
[211] M.M. Simões, M.G. de Oliveira, J. Biomed. Mater. Res. B Appl. Biomater. 93 (2010) 416–424.
[212] A. Ketchum, M. Kappler, J. Wu, C. Xi, M.E. Meyerhoff, J. Mater. Chem. B 4 (2015) 422–430.
[213] G. Mugesh, H.B. Singh, Chem. Soc. Rev. 29 (2000) 347–357.
[214] G. Mugesh, W.W. du Mont, H. Sies, Chem. Rev. 101 (2001) 2125–2179.
[215] C. Dey, T. Kundu, B.P. Biswal, A. Mallick, R. Banerjee, Acta Crystallogr. Sect. B: Struct. Sci. Cryst. Eng. Mater. 70 (2014) 3–10.
[216] H. Li, M. Eddaoudi, M. O'Keeffe, O.M. Yaghi, Nature 402 (1999) 276–279.
[217] A. Dhakshinamoorthy, A.M. Asiri, H. Garcia, Chem. Commun. 50 (2014) 12800–12814.
[218] P. Guo, D. Dutta, A.G. Wong-Foy, D.W. Gidley, A.J. Matzger, J. Am. Chem. Soc. 137 (2015) 2651–2657.

[219] K.A. Mowery, M.E. Meyerhoff, Polymer (Guildf) 40 (1999) 6203–6207.
[220] M.H. Abraham, J.M.R. Gola, J.E. Cometto-Muniz, W.S. Cain, J. Chem. Soc. Perkin Trans. 2 (2000) 2067–2070.
[221] H. Ren, M.A. Coughlin, T.C. Major, S. Aiello, A. Rojas Pena, R.H. Bartlett, M.E. Meyerhoff, Anal. Chem. 87 (16) (2015) 8067–8072.
[222] M.C. Frost, A.K. Wolf, M.E. Meyerhoff, in: Detection Challenges in Clinical Diagnostics, The Royal Society of Chemistry, Cambridge, 2013, pp. 129–155.
[223] B.M. Bloom, J. Grundlingh, J.P. Bestwick, T. Harris, Eur. J. Emerg. Med. 21 (2014) 81–88.
[224] D.S. Martin, M.P.W. Grocott, Crit. Care Med. 41 (2) (2013) 423–432.
[225] The Juvenile Diabetes Research Foundation Continuous Glucose Monitoring Study Group, N. Engl. J. Med. 359 (2008) 1464–1476.
[226] J.H. Shin, S.M. Marxer, M.H. Schoenfisch, Anal. Chem. 76 (2004) 4543–4549.
[227] K.P. Dobmeier, G.W. Charville, M.H. Schoenfisch, Anal. Chem. 78 (2006) 7461–7466.

This page intentionally left blank

Index

Note: Page numbers followed by *f* indicate figures, and *t* indicate tables.

A

Activated clotting time (ACT), 237
Activated FIX (FIXa), 30–31
Activated neutrophils, 33–34, 33*f*
Activated partial thromboplastin time (APTT), 55–56, 201–202
Activated platelets, 17–20, 94
Active polymer surfaces, 435–436
Adenosine diphosphate (ADP), 20, 131–132
Adhesive glycoproteins (Gp), 125
Adverse foreign body reactions, 29
Air bubbles, 166
Albumin, 169–170
Alginate, 256
Allografts, 364
Alternative pathway (AP), 40–41
Amidolytic activity, 5
Analytical parameters
  cellular activation, 94–96
  clotting times, of blood plasma, 90
  humoral markers, 91–94, 91*t*
  microscopic and gravimetric analysis, 91
  surrogate markers, 89–90
  thrombin formation, 90
  thromboelastography, 90
Anaphylatoxins, 282
Aneurysm-on-a-chip test cell, 305–309, 307–308*f*
Antibacterial catheters, 436–438
Anticoagulant coatings, 409
Anticoagulation, 54–55
  citrate, 81
  corn trypsin inhibitor (CTI), 82
  heparin, 81–82, 82*f*
  hirudin, 82
  in vitro blood incubation test systems, 81, 81*t*
  work, 247
Antiinflammatory material, 235
Antiinflammatory M2 phenotype, 282
Antiplatelet agents, 175
Antiproliferative agents, 175–176
Antithrombin (AT), 34–35
Antithrombotic/antibacterial nitric oxide, 438–447, 439*f*
Antithrombotics, 31
Argon (Ar), 298
Arterial prostheses procedures, 363–364
Aspirin (ASP), 238, 390
AT. *See* Antithrombin (AT)
Atherosclerosis, 363
ATmega16, 333–334
Atom transfer radical polymerization (ATRP), 137–138, 210
Auger electron spectroscopy (AES), 292–293
Autoclaving, 295
Autografts, 364

B

Bacterial infection, 432*f*
Bare metal stents (BMS), 367
Bioactive coatings
  anticoagulants
    direct thrombin inhibitors, 173
    hirudin and derivatives, 173
    indirect thrombin inhibitors, 170–173, 174*f*
    small synthetic inhibitors, 173
    thrombomodulin, 173–175
  antiplatelet agents, 175
  antiproliferative agents, 175–176
  bioactive component, surface modification, 170, 171*t*
  fibrinolytic agents, 176
  gene elution, 176–177
  nitric oxide (NO), 175
Bioactive glass, 265
Bioceramics, 264–265
Biocompatible system, 191–192
Biocorrosion, 282–283
Biodegradable biomaterials

alginate, 256
biodegradable polymeric materials, 254–264
biomaterial hemocompatibility, 254
blood-contacting materials, 255*f*
chitosan, 256–258
collagen, 259–260
foreign body response (FBR), 253
hemocompatible surface coatings, 268–270
hyaluronic acid (HA), 258
hybrid biodegradable biomaterials, 264–268
immunomodulating cells, 253
inorganic/organic (I/O) hybrid materials, 266–268
nanocomposite materials, 266*f*, 267–268
natural polymers, 254–260
pharmaceutically active materials, 268–270
heparin and heparin-like molecules, 269–270
heparin binding peptides, 270
nitric oxide, 270
polymer hybrids, 268
silk, 258–259
substrate materials, 264–265
bioactive glass, 265
bioceramics, 264–265
calcium phosphates, 265
synthetic biodegradable polymers, 260–264
poly (vinyl alcohol), 264
polycaprolactone, 262–263
polyesters, 260–263
polylactic acid, 260–262
poly lactic-co-glycolide, 262
polyurethane, 263
Biodegradable polymeric materials, 254–264
Bioinspired thin film materials, 350–352
blood-contacting materials, high shear stress
adhesive bonds formation, 327–328
cell-material interaction, 331
confocal microscopy observation, 330
deposited materials, blood cell adhesion minimatin, 328, 328*t*
detached cells function, applied shear stress, 330, 330*f*
dilution, 328
PBS (1X) composition, 329, 329*t*
physical vapor deposition technique, 328
radial flow chamber, 329, 329*f*
radial hydrodynamic flow, 328
red blood cell detachment efficiency, 331, 331*f*
red blood cells deposition, surface, 329, 330*f*
spontaneous shear rate, 332, 332*t*
stress threshold, 329, 331*f*
total cell washout, 330
overview, 327
smooth muscle formation-migration channels
carbon coatings, 345–346
channel shape optimization, direct laser interference lithography, 348–350, 351–352*f*
channels migration, 346
finite element simulation, 344–345, 345–346*f*
heart assist chamber, 342–344
local laser pulse energy conversion, 345
phase analysis, 348, 349*f*
refractive index and extinction coefficient, 346, 346*t*, 347*f*
SMC deposition, 348, 350*f*
surface functionalization, 342–344
thermal and mechanical propagation, 342–344
transmission electron microscopy (TEM), 346–348, 347*f*
tissue like structures
automatization, surface modification, 333–334
blood contact, 332–333
blood vessel cross section, 332, 332*f*
clots formation, 332–333
depositing polymer-based porous coatings, 333, 334*f*
ECM-like coating, 334–336, 336–337*f*
endothelium, 332–333
niche-like structure (*see* Niche-like structures)
rough surfaces, 332–333
tissue analogs, 333
Biointerface, 291–292
Biomaterial-associated thrombosis, 41, 42*f*

Biomaterial coatings
bioactive coatings, 170–177
endothelialization promotion, 177–178
inorganic passive coatings, 167
organic passive coatings
hydrophilic coatings/polymer brushes, 168–169
passivating proteins, 169–170, 170*f*
protein resistant surfaces, 167–168
surface passivation, 167–168
zwitterionic materials, 169
overview, 163–165, 164*f*, 164*t*
physicochemical properties, 165
air bubbles, 166
roughness/topography, 166
specific surface functional groups, 166
wettability, 165
Biomaterial hemocompatibility, 254
Biomaterial modification techniques, 193*f*
atom transfer radical polymerization (ATRP), 210
biocompatible material, 191–192
blood-biomaterials interactions, 193–197, 195*f*, 196*t*
cellular methods, 207–210, 208–209*f*
chemical methods
covalent crosslinking approaches, 205–207, 205–206*f*
functional groups, 199–202, 200–201*f*
physical immobilization approaches, 202–203, 202*f*, 204*f*
endothelial outgrowth cells (EOCs), 208–210
future prospects, 211–213
human umbilical vein endothelial cells (HUVECs), 197–198
physical methods, 197–199, 198*f*
plasma treatment, 198–199, 199*f*
poly(2-hydroxyethyl methacrylate) (PolyHEMA), 210
poly(ethylene oxide) (PEO), 210
poly(methyl methacrylate), 191–192
Biomaterial surfaces
blood cells and proteins
adhesion and activation, platelets, 37–39
endothelium role, 39, 40*f*
organic and inorganic molecules, 36
protein adsorption, 37
blood coagulation, 3
hemocompatibility property, 120
quaternary ammonium groups, 8–9
Biomedical composites, 369
blood contacting devices
biofunctionalization techniques, 359–360
chemical functionalization, 359
chemical techniques, 359
physical techniques, 358–359
polymers, 359
surface porosity, 358–359
surface roughness, 358–359
surface wettability, 359
heart valves (*see* Heart valves)
overview, 357
stents
overall hemocompatibilty improvement, 368–369
pathology, 367–368
problem, 367
vascular grafts
overall hemocompatibilty improvement, in vitro/in situ endothelialization, 365–367
pathology, 364
problem, 363–364
Biomedical devices
biofilm formation, 432
foreign body response (FBR), 253
metallic materials used, 279–281, 280*f*, 280*t*
requirements of, 433
roles, 120
Biomedical polymers
activated clotting time (ACT), 237
anticoagulation work, 247
antiinflammatory material, 235
aspirin, 238
biomaterial surface, 225–231, 226*f*, 235
blood-contacting devices, 223–224, 224*f*
blood interaction, 225–230, 226*f*
colocalizing multiple anticlotting mechanisms, 241–243, 242*t*
complement activation, 229–230, 246
direct thrombin inhibitors (DTIs), 239
hemolysis testing, 245–246
heparin, 237
hydrophilic coatings, 235
intrinsic and extrinsic pathways, 227–228

Biomedical polymers *(Continued)*
ISO 10993-Part 4 standard, 245
limitations, 231–236, 232*t*
local surface anticoagulation, 239–243
multimodal biomaterial surface-focused anticoagulation, 241*f*
new oral anticoagulants (NOACs), 239
partial thromboplastin time (PTT), 246
platelet activation, 228–229, 229*t*
prelude, 223
pyrolytic-carbon coating, 236
surface anticoagulation approaches, 231–236
systemic anticoagulation, 236–239
thrombosis, 246
vitamin K epoxide reductase complex (VKORC1), 237–238
in vitro/in vivo test protocols, 243–246, 244*f*
warfarin, 237
zymogens FXII, 227*f*
Bioprosthetic valves, 400–405, 404*f*
Björk-Shiley valve, 399–400, 399*f*
Bleeding disorders, 31
Blood-biomaterial interactions, 51–52, 193–197, 195*f*, 196*t*
Blood clotting (thrombosis), 36
blood cells and proteins
adhesion and activation, platelets, 37–39
endothelium role, 39, 40*f*
organic and inorganic molecules, 36
protein adsorption, 37
complement system activation, 40–41
and physiological inhibitors
extrinsic clotting pathway, 30–31
intrinsic (contact) clotting pathway, 31
physiological inhibition, 34–36, 35*f*
prothrombotic biomolecules, 32–34
Blood compatibility, 124
Blood components, 119
Blood contacting devices, 163–164, 223–224, 224*f*
biofunctionalization techniques, 359–360
chemical functionalization, 359
chemical techniques, 359
physical techniques, 358–359
polymers, 359
surface porosity, 358–359
surface roughness, 358–359
surface wettability, 359
Blood-contacting materials, 255*f*
Blood interaction, 225–230, 226*f*
Blood plasma
clotting times, 90
composition, 119–120
contact activation
activators, 7
coagulation time (CT), 7
fibrin oligomerization, 7–8
Michaelis-Menten enzyme kinetics, 8–9
procoagulant catalytic potential, 8–9, 8*t*
surface area titration curves (SAT), 7, 7*f*
surface-induced FXII activation, 7
Blood regurgitation, 360–361
Bloodstream, 126
infections, 432
Blood-surface interactions
brain vasculature system, 108*f*, 107
Chandler's loop, 110, 110*f*
design, 110–111
dynamic hemocompatibllity, 114*f*
flow dynamics, 110
materials, 110, 111*f*
methods, 112–113
platelet rich plasma preparation, 112–113, 112*f*
static hemocompatibility experiment, 113–114, 114*f*
thrombosis model, 107–108
Brain vasculature system, 107

C

Calcium phosphates, 265
Carbon-based inorganic coatings, 167
Carboxylic acid groups, 334–335
Cardiovascular disease, 121–122
Cardiovascular technology, 163–164, 164*t*
Catalyst-based NO generating catheters, 444–445
CD11b (Mac-1), 63–64
Cell-free nucleic acids (cfNAs), 34
Cell-free plasma layer, 126
Cell surface adhesion molecules, 364
Cell-surface interactions
antimicrobial activity, 290
cell shape and phenotypic responses, 290–291
primary effects, 289
surface topography, 290

Cellular activation
granulocytes/monocytes, 96
material-induced blood cell activation, 94, 94*t*
platelets, 94–96, 95*f*
suspended cells, 94
Cellular methods, 207–210, 208*f*
Centers for Disease Control and Prevention (CDC), 432
Central venous catheters (CVCs), 433–434
Ceramics, 121
cfNAs. *See* Cell-free nucleic acids (cfNAs)
Chandler's loop, 87–88, 87*f*, 110, 110*f*
Chemical-based NO releasing catheters, 441–444
Chemical crosslinking, 205
Chitosan, 256–258
Chlorhexidine-minocycline-rifampin (CHX-M/R), 437–438
Circular dichroism (CD) spectroscopy, 14
Citrate, 81
Classical pathways (CP), 40–41
Clots, 39, 40*f*
Coagulation factors, deficiency, 31
Coagulation factor (F) XII (FXII), 29
Coagulation time (CT), 7
Collagen, 259–260
Complement activation, 93–94
Complement system, 40–41
Cone-plate-incubation, 89
Contact activation, 15, 52, 62–63
blood plasma
activators, 7
coagulation time (CT), 7
fibrin oligomerization, 7–8
Michaelis-Menten enzyme kinetics, 8–9
procoagulant catalytic potential, 8–9, 8*t*
surface area titration curves (SAT), 7, 7*f*
surface-induced FXII activation, 7
FXII, neat-buffer
amidolytic activity, 9
autoactivation, 9–11, 10*f*
FXII-derived products, surface energy and surface area, 13–14, 13*t*
molecular events, FXII contact activation, 14
procoagulant activity, 9
suppressive effects, 9
surface area dependence, FXII autoactivation, 11–12, 11*f*
surface charge, FXII autoactivation, 12–13, 12*f*
Copper(II) benzenetricarboxylate (Cu-BTC), 445
Copper-titanium film, 384–385
Corn trypsin inhibitor (CTI), 82
Coronary artery disease (CAD), 367
Corrosion, 282–283
Covalent crosslinking approaches, 205–207, 205–206*f*
Covalent modifications, 359
C-reactive protein, 80
CTI. *See* Corn trypsin inhibitor (CTI)
Cyclic adenosine monophosphate (cAMP), 131–132
Cytotoxicity, 298

D

Debakey Surgitool valve, 405–406
Diamond-like carbon (DLC), 167, 384, 407–409, 408*f*
N-Diazeniumdiolates (NONOates), 440, 442*f*, 446–447
Dihydrorhodamine-123, 63–64
DIN/EN/ISO 10993-4 standard, 77
Direct adsorption approach, 202–203
Direct thrombin inhibitors (DTIs), 173, 239
DNA-histone complexes, 34
Donor selection/stratification, 55–56, 57*t*
3D printing, 361–363
Drug eluting stent (DES), 369, 379
DTIs. *See* Direct thrombin inhibitors (DTIs)

E

EDTA. *See* Ethylene diamine tetra-acetic acid (EDTA)
Edwards SAPIEN valve, 402–404, 404*f*
Electrochemical-based NO generating catheters, 445–447, 446*f*
Electropolishing, 292–294, 293–294*f*
Ellipsometry
advantages, 145
disadvantages, 145–146
dry thickness of layers, 146
Endothelial and smooth muscle cells (SMCs), 389
Endothelial cell adhesion, 286

Endothelial cells (ECs), 39, 207–208
adhesion, 286
Endothelial glycocalyx lining, 135
Endothelial injury, 39
Endothelial outgrowth cells (EOCs), 208–210, 365
Endothelial progenitor cells (EPCs), 177, 365
Endothelium, 332–333, 339
Erythrocytes, 64
Ethylene diamine tetra-acetic acid (EDTA), 54–55
European Medicines Agency (EMA), 284
Extrinsic clotting pathway, 30–31, 30*f*

F

Factor XII, 3–4
Fibrin formation, 92
Fibrinogen, 124
Fibrinolysis, 382–383
Fibrinolytic agents, 176
Flow cytometry, 61
Fluorescence microscopy, 136
Foam cells, 364
Food and Drug Administration (FDA), 284
Foreign body response (FBR), 253
FT232RL, 333–334
FVIIa, 30–31
active kallikrein, 31
corn trypsin inhibitor (CTI), 82
plasma kallikrein (PK), 31
FVII-activating protease (FSAP), 41
αFXIIa, 6–7
βFXIIa, 6–7
FXII activation, 4–5
activated platelets, 20
biochemical pathways, 5
efficiency of, 5
enzymatic cleavage, 6–7
plasma coagulation, 5
polyP, 33–34
FXII autoactivation
plasma proteins
kallikrein-mediated amplification, 17, 19*f*
not related to intrinsic pathway, 15–17, 16*f*, 18*f*
surface area dependence, 11–12, 11*f*
surface charge, 12–13, 12*f*
surface wettability, 10–11

G

Galvanic corrosion, 283
Gelatin, 130
Gene elution, 176–177
Glutaraldehyde (GA), 205
Glycoclyx, 193–194
Granulocytes, 96

H

Hageman factor (HF), 3–4, 225
contact activation, 62–63
structural analysis
concentration, 5
FXII activation, 6–7
kallikrein and FXIIa, 6–7, 6*f*
monoclonal antibody KOK5, 5–6
Heart valves
advancements, 405–416
disease, 405–416
future research, 416–417
hemocompatible coatings, 405–409
Debakey Surgitool valve, 405–406
diamond like carbon coatings, 407–409, 408*f*
low temperature isotropic pyrolytic carbon (LTI-carbon), 405–407
plasma-enhanced chemical vapor deposition (PECVD), 406–407
Prospective Randomized On-X Anticoagulation Clinical Trial (PROACT), 406–407
titanium alloyed coatings, 407
human serum albumin (HSA), 396
overall hemocompatibilty improvement, 361–363
pathology, 361
problem, 360–361
prosthetic heart valve (PHV), 396
surface engineering, 409–410
anticoagulant coatings, 409
platelet adhesion, 409–410
surface endothelization, 410
surface modification, 409–410
tissue engineering heart valves (TEHV), 396
transcatheter heart valve implantation (TAVI), 396
valve design, 410–412, 411*f*
actuated pivot design, 412–413

CarboMedic valve, 413–414
flow profile valve orientation, 415–416
leaflet shape, 414, 415*f*
maximizing valve opening area, 412–413
reducing flow recirculation, 413–414
in silico and in vitro circulatory flow models, 412
supra-annular valve seating, 414–415
valve pioneering era, 397–405
bioprosthetic valves, 400–405, 404*f*
Björk-Shiley valve, 399–400, 399*f*
Edwards SAPIEN valve, 402–404, 404*f*
mechanical heart valves, 397–400, 398–399*f*, 401–402*t*, 401*f*
Medtronic Core Valve, 402–404, 404*f*
polymeric materials, 405
Smelhoff-Cutter ball valve, 398–399
Starr-Edwards aortic valve model, 398*f*
Starr-Edwards mitral valve, 398*f*
thermoplastic polyurethane (TPU), 405
transcatheter aortic heart valves, 402–404, 404*f*
Hemocompatible molecules, 191–192
Hemocompatible polymeric surfaces, 431–433
Hemocompatible surface coatings, 268–270
Hemolysis, 93, 119
testing, 245–246
Hemophilia, 31
Hemostasis, 30, 34
Heparan sulfate, 34–35
Heparin and heparin-like molecules, 269–270
Heparin-based hydrogels, 172–173
Heparin binding peptides, 270
Heparins, 34–35, 54–55, 81–82, 170–173, 237
Hermansky-Pudlak syndrome, 33–34
HF. *See* Hageman factor (HF)
Hirudin, 54–55, 82
and derivatives, 173
Human serum albumin (HSA), 396
Human umbilical vein endothelial cells (HUVECs), 197–198
Humoral markers, 91–94, 91*t*
Hyaluronic acid (HA), 258
Hybrid biodegradable biomaterials, 264–268
Hydrogel-coated silicone catheters, 437–438
Hydrophilic coatings/polymer brushes, 168–169, 235
Hydrophilicity, 165

I

Immune response, 281–282
Immunomodulating cells, 253
Incubation settings, 82
closed, agitated systems, 85–86, 86*f*
duration, 83–84, 83*f*
overview, 84–85, 84*t*
reference materials, 84
with stagnant blood, 85, 85*f*
with streaming blood, 86–89
Indirect anticoagulants, 34–35
Indirect thrombin inhibitors, 170–173, 174*f*
Inflammatory response, 282
Inorganic/organic (I/O) hybrid materials, 266–268
Inorganic passive coatings, 167
In situ ellipsometry, 146–147
In-stent restenosis, 381–382
Intravascular catheters
N-acetylcysteine (NAC), 433–434
active polymer surfaces, 435–436
antibacterial catheters, 436–438
antithrombotic and antibacterial nitric oxide, 438–447, 439*f*
bacterial infection, 432*f*
bloodstream infections, 432
catalyst-based NO generating catheters, 444–445
catheter lock solutions, 433–434
Centers for Disease Control and Prevention (CDC), 432
central venous catheters (CVCs), 433–434, 437
chemical-based NO releasing catheters, 441–444
chlorhexidine-minocycline-rifampin (CHX-M/R), 437–438
copper(II) benzenetricarboxylate (Cu-BTC), 445
N-diazeniumdiolates, 440
electrochemical-based NO generating catheters, 445–447, 446*f*
Escherichia coli, 438
hemocompatible polymeric surfaces, 431–433
hydrogel-coated silicone catheters, 437–438
lower critical solution temperature (LCST), 435–436

Intravascular catheters *(Continued)*
metal organic frameworks (MOFs), 445
Mueller-Hinton broth (MHB), 437–438
nitroglycerin, 438–447, 439*f*
S-nitrosothiols (RSNOs), 440–441
phosphate buffer saline (PBS), 434–435
poly(*N*-isopropylacrylamide) (poly (NiPAAm), 435–436
polyethyleneimine (PEI), 444–445
Pseudomonas aeruginosa, 432
scanning electron microscope (SEM), 434–435
selenium-containing PEI (SePEI), 444–445
silver nanoparticles (AgNP), 436–437
SNAP/E2As catheters, 443–444
Staphylococcus aureus, 432
Staphylococcus epidermidis, 432, 438
thermosensitive hydrogel coating, 435–436
thromboresistant catheters, 434–436
thrombus formation, 432*f*
vancomycin-resistant *Enterococcus faecium* (VRE), 437
vascular access, 433
Intrinsic (contact) clotting pathway, 31, 32*f*
Intrinsic tenase complex, 31
In vitro test protocols, 243–246, 244*f*
In vivo test protocols, 243–246, 244*f*
Ion beam assisted deposition (IBAD), 387
Ion implantation, 297–299, 299*f*
Ion irradiation, 287–288
IR-spectroscopy, 153
ISO 10993-4 norm, 53–54
ISO 10993-5 norm, 53
ISO 10993-Part 4 standard, 245

K

Kallikrein, 17

L

Lectin pathway (LP), 40–41
Leukocyte activation, 93
Leukocytes, 38
Lipoprotein particles, 364
Lower critical solution temperature (LCST), 435–436
Low-temperature isotropic pyrolytic carbon (LTIC) coatings, 167, 405–407

M

Macrophages, 38–39, 282
Magnetic bacterial nanocellulose (MBNC) hydrogels, 309–314
Mean platelet volume (MPV), 54–55
Mechanical heart valves, 397–400, 398–399*f*, 401–402*t*, 401*f*
Mechanical modification, 292
Medicines and Healthcare products Regulatory Agency (MHRA), 284
Medtronic Core Valve, 402–404, 404*f*
Megakaryocytes, 51–52
Metallic biomaterials, surface treatment
advanced hydrogels, metallic nanoparticles, 301–304
advanced in situ characterization, hemocompatible metallic surfaces, 304, 306*f*
aneurysm-on-a-chip test cell, 305–309, 307–308*f*
bioMEMS device, 305
challenges and limitations, 318–319
parallel-plate flow chamber cell, 309–314, 310*f*, 312–313*f*
in situ nanomechanical testing, 314*f*, 315–318
hemo and biocompatibility evaluation, 283–284
irradiation-driven synthesis and modification
blood-material interface, 286, 287*f*
endothelial cell adhesion, 286
metallic stents, biological response, 299–300
modify metallic surfaces, 292–299
surface properties, 286–292
vascular tissue, 286
multiscale interaction, blood and metals
biocorrosion, 282–283
biomedical devices, 279–281, 280*f*, 280*t*
immune response and metals, 281–282
regulation and safety aspects, 284, 285*t*
Metallic surfaces modification
chemical treatments, 295–297, 297*f*
electropolishing, 292–294, 293–294*f*
ion implantation, 297–299, 299*f*
mechanical modification, 292

nitinol and nickel-based metals, 292
thermal and hydrothermal treatments, 295, 296*f*
Metal-nitrides, 167
Metal organic frameworks (MOFs), 445
Metal-oxides, 167
Metals, 121
Michaelis-Menten enzyme kinetics, 8–9
Micropatterning, 366–367
Model miniature hemodialyzer, 89
Monocytes, 38–39, 96
MSN nanoparticles, 127–128
Mueller-Hinton broth (MHB), 437–438
Multi-Link PIXEL stent, 203

N

N-Acetylcysteine (NAC), 433–434
Nano-biomaterials, 123
hemocompatibility/blood compatibility, 124
hemocompatibility test
nanofibers, 130–135, 131–134*f*
nanofilms, 137–141, 139–140*f*, 142–143*f*
nanoparticles, 126–129, 127–130*f*
nanotubes, 135–136, 135–137*f*
platelet activation and adhesion, 125–126
protein adsorption, 124–125
Nanocomposite materials, 266*f*, 267–268
Nanopatterning, 366–367
Natural anticoagulant proteins, 34
Natural polymers, 254–260
Neoatherosclerosis, 368
NETosis, 33–34, 33*f*
NETs. *See* Neutrophil extracellular traps (NETs)
Neuro-endovascular blood-material interactions
bare-metal stents (BMS), 302
confining induced thrombogenic activity, 303–304
coronary stenosis/occlusion treatment, 302
drug-eluting stents (DES), 302
endovascular coiling, 301–302
flow diversion (FD) techniques, 301–302
functional hydrogel membranes, 302
Neutrophil adhesion, 96
Neutrophil extracellular traps (NETs), 33–34, 33*f*
Neutrophils, 38
New oral anticoagulants (NOACs), 239
Niche-like structures, 342*f*
blood coagulation, 340
blood-material interaction analysis, 340, 343*f*
coagulation activation, 341, 344*f*
coatings preparation, 339, 339*t*
combinatorial signal mixtures, 336–337, 338*f*
composition and thickness, surface roughness, 340, 340*f*
3D CLSM fluorescence and DIC analysis, 340, 341*f*
endothelium, 339
individual signals, 336–337, 338*f*
microparticle concentration, 342, 344*f*
modular substrate stiffness, 336–337, 338*f*
physiological shear stress, 340
platelet activation, 340
platelet aggregate formation, 341, 343*f*
pluripotent stem cells, 336–337
stem cell niche, 336–337
wrinkling
mechanism, 339
origin, 337–338, 338*f*
plane view, 337–338, 338*f*
Nitric oxide (NO), 39, 175, 270
Nitrogen (N), 298
Nitroglycerin, 438–447, 439*f*
Nonactivated platelets, 125

O

Oliver-Pharr method, 315
OMT ellipsometer, 146
Organic passive coatings
hydrophilic coatings/polymer brushes, 168–169
passivating proteins, 169–170, 170*f*
protein resistant surfaces, 167–168
surface passivation, 167–168
zwitterionic materials, 169
Oxygen, 298

P

Parallel-plate flow chamber cell, 88, 88*f*, 314*f*
collagen-conjugated MBNC, 311, 313*f*
external magnetic field, 311

Parallel-plate flow chamber cell *(Continued)*
local magnetic force concept, 309–311, 310*f*
Pislaru's approach, 311
SPION-loaded HASMC, 309–311, 312*f*
vascular tissue, mechanical properties, 313
Partial thromboplastin time (PTT), 246
Passivating proteins, 169–170, 170*f*
PECVD. *See* Plasma-enhanced chemical vapor deposition (PECVD)
PEO-like films, 387
Percentage variation in diameter (PVD), 318
Percutaneous coronary intervention (PCI), 367
Phosphate-buffered saline (PBS), 128–129
Phosphate buffer saline (PBS), 434–435
Phosphorylcholine methacrylate (MPC), 169
Physical immobilization approaches, 202–203, 202*f*, 204*f*
Plasma coagulation cascade, 3
extrinsic pathway, 3–4, 4*f*
intensity of, 9
intrinsic pathway, 3–4, 4*f*
Plasma-enhanced chemical vapor deposition (PECVD), 406–407
Plasma immersion ion implantation and deposition (PIII&D), 298–299
Plasma ion implantation, 298–299
Plasma oscillations, 148
Plasma proteins
kallikrein-mediated amplification, 17, 19*f*
not related, intrinsic pathway, 15–17, 16*f*, 18*f*
Plasma treatment, 198–199, 199*f*
Plasminogen activator inhibitor-1 (PAI-1), 39
Platelet activation, 92–93, 228–229, 229*t*
and adhesion, 125–126
anti-CD62P, 340
and markers, 94, 95*f*
Platelet adhesion, 141, 409–410
Platelet aggregation, 3
formation, 336, 337*f*
Platelet deposition, 131
Platelet P-selectin, 95
Platelet rich plasma preparation, 112–113
Platelets, 36, 51–52
adhesion and activation, 37–39, 136
FXII contact activation
activated platelets, 17–20
activated platelet titration, human platelet-poor plasma (PPP), 20, 21*f*
adenosine diphosphate (ADP), 20
coagulation time assay, 20, 21*f*
coagulation time, human plasma, 19*f*, 20
collagen, 20–22
FXII activation and intrinsic coagulation pathway, 20
kallikrein and high-molecular-weight kininoge, 20–22
PolyP, 22–23
role of, 17–20
GPIIb/IIIa receptor, 54–55
material-induced activation, 52
Pluripotent stem cells, 336–337
Poly(2-hydroxyethyl methacrylate) (PolyHEMA), 210
Poly(caprolactone) (PCL), 199–200
Poly(ethersulfone) (PES), 203
Poly(ethylene oxide) (PEO), 210
Poly(ethylene terephthalate) (PET), 197–198
Poly(MEOEGMA), 147
Poly(methyl methacrylate), 191–192
Poly(*N*-isopropylacrylamide) (poly (NiPAAm)), 435–436
Poly(vinyl alcohol) (PVA), 130
Polyanions, 137–138
Polycaprolactone (PCL), 122–123, 262–263
Polycations, 137–138
Polydimethylsiloxane, 37
Polyesters, 260–263
Polyethylene glycol (PEG), 168, 334–335
Polylactic acid, 260–262
Poly lactic-co-glycolide, 262
Polymer hybrids, 268
Polymeric grafts, 51
Polymeric materials, 405
Polymers, 121
Polymorphonuclear (PMN) elastase, 300
Polymorphonuclear (PMN) granulocytes, 63–64
Poly (ethylene) oxide (PEO), 168–169
Polyphosphate (polyP), 22–23, 32–34, 33*f*
Polypyrrole (PPy) films, 299–300
Polyurethane (PU), 37, 263
Prasugrel (PRAS), 390

PROACT. *See* Prospective Randomized On-X Anticoagulation Clinical Trial (PROACT)
Procoagulant activity, 5
Pro-inflammatory M1 phenotype, 282
Propolis (PROP), 390
Prospective Randomized On-X Anticoagulation Clinical Trial (PROACT), 406–407
Prostacyclin, 39
Prosthetic heart valve (PHV), 396
Protein adsorption, 37, 124–125, 165
  flow conditions, 166
  nanoscaled roughness, 166
Protein C activation, 35–36
Proteoglycans, 34–35
Prothrombin time (PT), 55–56
Pyrolytic-carbon coating, 236

Q

Quartz crystal microbalance (QCM), 148–149

R

Reactive oxygen species (ROS), 63–64
Red blood cells (RBCs), 119, 128–129
Reference materials, 53–54, 84
Reproducible/standardized in vitro testing, 52
  anticoagulation, 54–55
  blood collection, 56–59, 60*f*
  donor selection and stratification, 55–56, 57*t*
  materials preparation, 52–53, 53*f*
  preparation and storage, 56–59, 60*f*
  reference materials, 53–54
Rhodamin-123, 63–64

S

Sauerbrey equation, 149
Secondary-ion mass spectroscopy (SIMS), 152
Shear rate, 126
Shear stress, 126
Silk, 258–259
Silver nanoparticles (AgNP), 436–437
Small synthetic inhibitors, 173
Smelhoff-Cutter ball valve, 398–399
Smooth muscle cells (SMCs), 389
s-MSN nanoparticles, 128–129
SNAP/E2As catheters, 443–444
Sodium periodate, 145
Soft lithography methods, 309
Specific surface functional groups, 166
Staphylococcus aureus, 432
Staphylococcus epidermidis, 432
Starr-Edwards aortic valve model, 398*f*
Starr-Edwards mitral valve, 398*f*
Static hemocompatibility experiment, 113–114, 114*f*
Stealth effect, 334–335
Stem cell niche, 336–337
Stent materials
  adherent platelets, 388*f*
  amorphous hydrogenated SiC, 385–386
  assess method, 382–383
    adherence of platelets, 382
    coagulation factors, 383
    contact systems, 383
    fibrinolysis, 382–383
  biodegradable stent, 379, 380*t*
  biomedical composites
    overall hemocompatibilty improvement, 368–369
    pathology, 367–368
    problem, 367
  C-N films, 387, 388*f*
  consequences, 381–382
    inflammatory response, 381
    in-stent restenosis, 381–382
    thrombus formation, 381
  definition, 379
  diamond-like carbon (DLC), 384
  drug eluting stent (DES), 379, 389
  endothelial and smooth muscle cells (SMCs), 389
  improving approach, 383–390
  ion beam assisted deposition (IBAD), 387
  Mg-based biodegradable material, 389–390
  novel stent materials, 389–390
  PEO-like films, 387
  surface modification, 384–389, 385–387*f*
  therapeutic approach, 390
  titanium nitride (TiN) films, 384
Stent thrombosis (ST), 367
Sterilization materials, 53
Substrate materials, 264–265

Surface analysis technique, 119–120
biomaterials
cardiovascular disease, 121–122
ceramics, 121
3-D scaffold, 120–121
ellipsometry, 145–146
implanted, 122
IRRAS spectroscopy, 154
IR-spectroscopy, 153
metals, 121
nanowires and nanofibers, 122–123
PM-IRRAS technique, 154
polycaprolactone (PCL), 122–123
polymers, 121
quartz crystal microbalance (QCM), 148–150
surface characterization techniques, 144–145
surface-enhanced Raman scattering (SERS), 155
surface plasmon resonance (SPR), 148, 150
swelling behavior using in situ ellipsometry, 146–147
time-of-flight secondary ion mass spectrometry (ToF-SIMS), 152
tissue response, 144
X-ray photoelectron spectroscopy (XPS), 150–151
nano-biomaterials, 123
hemocompatibility/blood compatibility, 124
hemocompatibility test, 126–141
platelet activation and adhesion, 125–126
protein adsorption, 124–125
Surface area dependence, 11–12, 11*f*
Surface area titration curves (SAT), 7, 7*f*
Surface endothelization, 410
Surface-enhanced Raman scattering (SERS), 155
Surface free energy, 291–292
Surface modification, 409–410
Surface plasmon resonance (SPR), 148
Surface properties, biomaterials
advanced tailored tools, 287–288
biomaterial interface, 288
cell-surface interactions
antimicrobial activity, 290
cell shape and phenotypic responses, 290–291
primary effects, 289
surface topography, 290
hydrophobicity/hydrophilicity, 288, 289*f*
ion implantation, 288
ion irradiation, 287–288
surface free energy and biointerface, 291–292
surface wettability, 288
thin-film deposition, 288
thrombus formation, 286–287
Surface roughness, 340, 340*f*, 358–359
Surface wettability, 288, 359
Synthetic biodegradable polymers, 260–264
poly (vinyl alcohol), 264
Synthetic vascular grafts, 364
Systemic anticoagulation, 236–239

T

Test methods/protocols, 77–78, 96–97
analytical parameters
cellular activation, 94–96
clotting times of blood plasma, 90
humoral markers, 91–94, 91*t*
microscopic and gravimetric analysis, 91
surrogate markers, 89–90
thrombin formation, 90
thromboelastography, 90
hemocompatibility, 62–64, 63*f*
incubation settings, 82
closed, agitated systems, 85–86, 86*f*
duration, 83–84, 83*f*
overview, 84–85, 84*t*
reference materials, 84
with stagnant blood, 85, 85*f*
with streaming blood, 86–89
microscopic air bubbles, 61
platelet-leukocyte aggregation, 61
static tests, 59
thrombogenicity, 61, 62–63*f*
whole blood *vs.* blood fractions
blood anticoagulation, 80–82, 82*f*
blood defense systems, 78, 78*f*
material-blood interaction, 78–79
sequential protein adsorption, 78–79
valid incubation results, 79–80
in vitro incubation, 79, 79*f*, 80*t*

Thermoplastic polyurethane (TPU), 405
Thermosensitive hydrogel coating, 435–436
Thrombin, 92
  formation, 90
Thrombin-thrombomodulin complex (T-TM complex), 35–36
Thromboelastography, 90
Thrombogenicity, 51–52, 61, 62–63*f*
Thrombomodulin (TM), 35–36, 173–175
Thromboresistant catheters, 434–436
Thrombosis, 119–120, 246
  model, 107–108
Thrombus formation, 381, 432*f*
Time-of-flight secondary ion mass spectrometry (ToF-SIMS), 152
Tissue engineering heart valves (TEHV), 396
Tissue factor pathway inhibitor (TFPI), 33–34
Tissue like structures
  automatization, surface modification, 333–334
  blood contact, 332–333
  blood vessel cross section, 332, 332*f*
  clots formation, 332–333
  depositing polymer-based porous coatings, 333, 334*f*
  ECM-like coating, 334–336, 336–337*f*
  endothelium, 332–333
  niche-like structure (*see* Niche-like structures)
  rough surfaces, 332–333
  tissue analogs, 333
Tissue plasminogen activator (tPA), 39
Tissue response, 144
Titanium alloyed coatings, 407
Titanium nitride (TiN) films, 384
Titanium oxide, 167
Transcatheter aortic heart valves, 402–404, 404*f*
Transcatheter heart valve implantation (TAVI), 396
Tri-sodium citrate, 54–55

V

Valve design, 410–412, 411*f*
  actuated pivot design, 412–413
  CarboMedic valve, 413–414
  flow profile valve orientation, 415–416
  leaflet shape, 414, 415*f*
  maximizing valve opening area, 412–413
  reducing flow recirculation, 413–414
  in silico and in vitro circulatory flow models, 412
  supra-annular valve seating, 414–415
Valve leaflets, 360–361
Valvular insufficiency, 360–361
Valvular stenosis, 360–361
Vancomycin-resistant *Enterococcus faecium* (VRE), 437
Vascular access, 433
Vascular endothelial growth factor (VEGF), 208–210
Vascular grafts
  overall hemocompatibilty improvement, in vitro/in situ endothelialization, 365–367
  pathology, 364
  problem, 363–364
Venipuncture, 56–59
VisuEl software version 3.4.1, 146
Vitamin K, 81
Vitamin K epoxide reductase complex (VKORC1), 237–238
Vroman effect, 15

W

Warfarin, 237
Wettability, 165
White clot, 51–52
Wrinkling, 352
  mechanism, 339
  origin, 337–338, 338*f*
  plane view, 337–338, 338*f*

X

Xenografts, 364
X-ray photoelectron spectroscopy (XPS), 150–151

Y

Young's moduli, 290–291

Z

Zwitterionic materials, 169
Zymogens FXII, 227*f*

This page intentionally left blank

WOODHEAD PUBLISHING SERIES IN BIOMATERIALS

Establishing if biomaterials are hemocompatible has been a challenge for the biomaterial community. Blood is highly complex. As a result, developing materials that do not trigger thrombosis, inflammation, or fibrinolysis and establishing reliable hemocompatibility standards and test methods remain active areas of research.

This book summarizes the state of the art in this important subject. The first part of the book reviews the fundamentals and latest research on blood composition and response, mechanisms of coagulation, and test standards and methods. The second part of the book assesses techniques for modifying biomaterial surfaces and developing coatings to improve hemocompatibility.

The third part of the book reviews ways of improving the hemocompatibility of particular classes of biomaterials, while the final part reviews particular applications of hemocompatible biomaterials for medical devices. The book will provide a standard reference for researchers in the field.

Christopher A. Siedlecki is a professor of Surgery and Bioengineering at The Pennsylvania State University, the United States. He has a PhD from Case Western Reserve University. Dr. Siedlecki has authored over 70 journal articles and has an h-index of 25. His teaching and research interests comprise physical and chemical properties of synthetic and natural surfaces, protein structure/function relationships, and the development of novel strategies for synthesis and modification of biomaterials.

ELSEVIER
WP
WOODHEAD PUBLISHING
An imprint of Elsevier
elsevier.com/books-and-journals

ISBN 978-0-08-100497-5
9 780081 004975